LEABHARLANN CHOLÁISTE NA TRÍONÓIDE, BAILE ÁTHA CLIATH | TRINITY COLLEGE LIBRARY DUBLIN
Ollscoil Átha Cliath | The University of Dublin

Terms and Conditions of Use of Digitised Theses from Trinity College Library Dublin

Copyright statement

All material supplied by Trinity College Library is protected by copyright (under the Copyright and Related Rights Act, 2000 as amended) and other relevant Intellectual Property Rights. By accessing and using a Digitised Thesis from Trinity College Library you acknowledge that all Intellectual Property Rights in any Works supplied are the sole and exclusive property of the copyright and/or other IPR holder. Specific copyright holders may not be explicitly identified. Use of materials from other sources within a thesis should not be construed as a claim over them.

A non-exclusive, non-transferable licence is hereby granted to those using or reproducing, in whole or in part, the material for valid purposes, providing the copyright owners are acknowledged using the normal conventions. Where specific permission to use material is required, this is identified and such permission must be sought from the copyright holder or agency cited.

Liability statement

By using a Digitised Thesis, I accept that Trinity College Dublin bears no legal responsibility for the accuracy, legality or comprehensiveness of materials contained within the thesis, and that Trinity College Dublin accepts no liability for indirect, consequential, or incidental, damages or losses arising from use of the thesis for whatever reason. Information located in a thesis may be subject to specific use constraints, details of which may not be explicitly described. It is the responsibility of potential and actual users to be aware of such constraints and to abide by them. By making use of material from a digitised thesis, you accept these copyright and disclaimer provisions. Where it is brought to the attention of Trinity College Library that there may be a breach of copyright or other restraint, it is the policy to withdraw or take down access to a thesis while the issue is being resolved.

Access Agreement

By using a Digitised Thesis from Trinity College Library you are bound by the following Terms & Conditions. Please read them carefully.

I have read and I understand the following statement: All material supplied via a Digitised Thesis from Trinity College Library is protected by copyright and other intellectual property rights, and duplication or sale of all or part of any of a thesis is not permitted, except that material may be duplicated by you for your research use or for educational purposes in electronic or print form providing the copyright owners are acknowledged using the normal conventions. You must obtain permission for any other use. Electronic or print copies may not be offered, whether for sale or otherwise to anyone. This copy has been supplied on the understanding that it is copyright material and that no quotation from the thesis may be published without proper acknowledgement.

Synthetic, photophysical and biological studies into new tools for investigating bile acid disposition and toxicity

Ferenc Májer M.Sc.

A thesis presented to the University of Dublin for the degree of Doctor of Philosophy in Pharmaceutical Chemistry



Based on research carried out under the supervision of
John Gilmer B.A. (Mod), Ph.D.

at

The School of Pharmacy and Pharmaceutical Sciences,
Trinity College,
Dublin.

2013

TRINITY COLLEGE
2 4 MAY 2013
LIBRARY DUBLIN

Thesis 9938

DECLARATION

I declare that this thesis has not been submitted as an exercise for a degree at this or any other university and it is entirely my own work except where duly acknowledged.

I agree to deposit this thesis in the University's open access institutional repository or allow the library to do so on my behalf, subject to Irish Copyright Legislation and Trinity College Library conditions of use and acknowledgement.

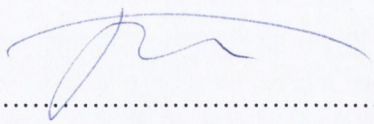

.....

Ferenc Májer

SUMMARY

The overall objective of this thesis was to use synthetic chemistry to provide tools to understand problems in bile acid research including their disposition and mechanism of toxicity. Fluorescent reporter groups are very widely used for probing problems of biochemical distribution and mechanism especially in the bile acid field. This area is reviewed here, structured by fluorescent derivatizing agent.

Our group has a particular interest in how bile acids induce cell death (this is particularly important in the case of deoxycholic acid (DCA), lithocholic acid (LCA) and chenodeoxycholic acid (CDCA)). There are many questions about the biochemistry, physiology and pharmacology of these bile acids connected in some way to their disposition and especially cellular localization that suitable fluorescent reporters could help answer. To answer questions we designed and synthesized ursodeoxycholic acid (UDCA) and DCA analogues with a reporter group (dansyl or 7-nitrobenzofurazan 2-oxa-1,3-diazole (NBD)) incorporated in the A ring and we also synthesized the appropriate control substances.

The prepared fluorescent bile acids are highly suitable for determining the disposition of bile acids in cell-based assays, for detecting active transport processes affecting bile acids and for investigating the many questions about these compounds. Our work showed that oesophageal cells have the capacity to actively take up bile acids and that this is positively regulated by bile acid exposure. Meanwhile, work of colleagues demonstrated that the transport of these compounds is sensitive to the orientation of the fluorescent reporter group. The work described here can only be the beginnings of investigations with these fascinating substances which are now in widespread use in numerous laboratories interested in anionic transport, the oesophagus and the effects of bile acids.

Additionally we produced several highly potent new bile acids. The purpose of the work was to prepare and study new bile acids integrating structural features of bile acids that were associated with inhibition of cell viability in previous work from our lab. In this process we conducted some preliminary investigations into the mechanism of action of these substances in order to characterize apoptosis versus necrosis and to try to define some of the pathways involved. In total we prepared and studied 23 new bile acids starting from LCA, DCA, and CDCA featuring 3-alpha and beta azido groups with optional further substitution at C-24 with parallel amides.

ACKNOWLEDGEMENTS

I would like to express my sincerest gratitude to my supervisor, Dr. John Gilmer for his never-ending patience and persistence and for his constant support through my work. During the three years he has given me an incredible amount of his knowledge and has helped me to perfect my English language skill.

Special thanks to Dr. Aideen Long for the opportunity to work in the IMM and for her advices and suggestions that were very useful for me.

I would also like to thank Dr. Ruchika Sharma for teaching me the basics of cell work and for her constant help and advice.

A special group, Dr. Jun Wang, Dr. Shona Harmon, Dr. Paul O'Byrne and Johanna Salomon deserves big thanks, as well.

Thanks to all the post docs and post grads in the IMM, Mike, David, Fiona, Annemarie, Conor, Christine, and Sinead for being always helpful.

Special thanks to you, Patrick Kelly and Dr. Michael Jones for being my friends and also my flat mates.

Thanks to Fran, Tadhg, Gábor, and Keith for the proof reading of my thesis.

To all the post docs and post grads in the School of Pharmacy in the past three years and the guys, for the unbelievable soccer matches.

Thanks to Dr. John O'Brien and Dr. Manuel Ruether for NMRs, Dr. Martin Feeney and Dilip Rai for mass specs and Ray Keaveney for HPLC work.

I would like to thank my Hungarian friends, Gábor, Barna, Patri and Szabolcs for being with me if I have desired for a little Hungarian speech.

Thanks to my mother-in-law to be and my father-in-law to be for their sacrifice for us.

Thanks to my father, mother and brothers for their patience and for their understanding during the time when they rarely saw me.

And last, but not least my special thanks belongs to my fiancée, who has waited for me over three years with faith, love and support, what was needed for this work and for her help and kindness, especially through all the hard times.

ABBREVIATIONS

Abs	Absorbance
Ac_2O	Acetic anhydride
AcCl	Acetyl chloride
AIF	Apoptosis initiating factor
AP-1	Activator protein-1
aromatic-C	Aromatic Carbon
aromatic-H	Aromatic Hydrogen
BA	Bile acid
BABP	Bile acid binding protein
BAs	Bile acids
BOC	tert-Butyloxycarbonyl
Boc_2O	Di-tert-butyl dicarbonate
BSEP	Bile salt export pump
CA	Cholic acid
CamF	Cholylamidofluorescein
CC_{50}	Concentration of 50% cellular cytotoxicity
CDCA	Chenodeoxycholic acid
$CDCl_3$	Deuterated chloroform
CGamF	Cholylglycylamido-fluorescein
CGN	*cis*-Golgi network
$CHCl_3$	Chloroform
Cholyl-lys-F	Cholyl-lysine-fluorescein
C-L-F	Cholyl-lysine-fluorescein
CMC	Critical micellar concentration
CO_2	Carbon Dioxide
CPA	Cyclopropylamine
CTX	Cerebrotendinous xanthomatosis
d	Day(s)
d	Doublet
DBU	1,8-Diazabicyclo[5.4.0]undec-7-ene
DCA	Deoxycholic acid
DCC	Dicyclohexylcarbodiimide
DCM	Dichloromethane
DDQ	2,3-dichloro-5,6-dicyano-benzoquinone
DIAD	Diisopropyl azodicarboxylate
DIPEA	Di-isopropylethylamine
DMEM	Dulbecco's modified Eagle's medium

DMF	Dimethylformamide
DMPU	1,3-dimethyl-3,4,5,6-tetrahydro-2(1H)-pyrimidinone
DMSO	Dimethyl sulfoxide
DMSO-d6	Deuterated dimethyl sulfoxide
DNA	Deoxyribonucleic acid
DNSC	Dansyl chloride
E_{0-0}	Singlet energy
EC_{50}	Half maximal effective concentration
EDC	1-[3-(Dimethylamino)propyl]-3-ethylcarbodiimide
EEDQ	*N*-Ethoxycarbonyl-2-ethoxy-1,2-dihydroquinoline
ER	Endoplasmic reticulum
ERKs	Extracellular signal regulated kinases
ESI-MS	Electrospray ionization mass spectrometry
Et_3N	Triethylamine
Ether	Diethyl ether
EtOAc	Ethyl acetate
EtOH	Ethanol
FBAs	Fluorescent BAs
FBS	Fetal bovine serum
FCS	Fetal calf serum
FITC	Fluorescein isothiocyanate
FITC-GC	Cholylglycylamido-fluorescein
FT-IR	Fourier transform infrared spectroscopy
FXR	Farnesoid X receptor
GC	Glycocholate
GR	Glucocorticoid receptor
h	Hour
H_2	Hydrogen gas
hASBT	Ileal bile acid transporter
HBPC	Heptane-buffer partition coefficient
HCl	Hydrochloric acid
$HClO_4$	Perchloric acid
HCOOEt	Ethyl formate
HCOOH	Formic acid
HOBt	Hydroxybenzotriazole
HPLC	High performance liquid chromatography
HRMS	High-resolution mass spectrometry
IC_{50}	The half maximal inhibitory concentration
IR	Infrared
KBr	Potassium bromide

K_M	Michaelis constant
KOH	Potassium hydroxide
KRB	Krebs-Ringer Bicarbonate Buffer
LCA	Lithocholic acid
LC-MS	Liquid chromatography–mass spectrometry
Li_2CO_3	Lithium carbonate
$LiAlH_4$	Lithium aluminium hydride
LiBr	Lithium bromide
L-L-F	Lithocholyl lysylfluorescein
M	Molar
m	Multiplet
m.p.	Melting point
mCPBA	m-chloroperbenzoic acid
MeCN	Acetonitrile
MeOD	Deuterated methanol
MeOH	Methanol
MeONa	Sodium methoxide
mg	Milligramme
$MgSO_4$	Magnesium sulfate
ml	Milliliter
µl	Microliter
mm	Millimeter
MsCl	Methanesulfonyl chloride
MTT	3-(4,5-dimethylthiazol-2-yl)-2,5-diphenyltetrazolium bromide
N_2	Nitrogen gas
Na_2SO_4	Sodium sulfate
$NaHCO_3$	Sodium bicarbonate
NaN_3	Sodium azide
NaOH	Sodium hydroxide
NBD	7-nitrobenzofurazan 2-oxa-1,3-diazole
NBD-F	4-fluoro-7-nitrobenzo-2-oxa-1,3-diazole
NBS	N-bromosuccinimide
N-HO-Su	N-hydrosuccinimide ester
nm	Nanometer
NMR	Nuclear magnetic resonance
ns	Nanosecond
NTCP	Na-taurocholate co-transporting polypeptide
OATP	Organic anion transporting polypeptide
PBS	Phosphate buffered saline
PCC	Pyridinium chlorochromate

Pd/C	Palladium on carbon
PET	Photoinduced electron transfer
PI	Propidium iodide
PKC	Protein kinase C
$POCl_3$	Phosphorus oxychloride
PPh_3	Triphenylphosphine
ppm	Parts per million
PS	Phosphatidylserine
q	Quartet
QSAR	Quantitative structure–activity relationship
R_f	Retention Factor
RMSD	Root mean square deviation
ROS	Reactive oxygen species
RPM	Revolutions per minute
rt	Room temperature
s	Singlet
SAR	Structure–Activity Relationship
sex	Sextet
SLCA	Sulpho-lithocholic acid
t	Triplet
TCA	Taurocholic acid
TFA	Trifluoroacetic acid
THF	Tetrahydrofuran
TLC	Thin layer chromatography
TNF	Tumour necrosis factor
UDCA	Ursodeoxycholic acid
UDCamF	Ursodeoxycholylamidofluorescein
UV	Ultraviolet
v/v	Volume per volume
w/v	Weight per volume
w/w	Weight per weight
WOPC	Water:octanol partition coefficient
XTT	2,3-bis-(2-methoxy-4-nitro-5-sulfophenyl)-2H-tetrazolium-5-carboxanilide
µg	Microgramme
µM	Micromolar

TABLE OF CONTENTS

CHAPTER 1 **1**

1.1. General introduction **2**

1.1.1. Classification and chemical structure of bile acids 2

1.1.2. Conjugation of bile acids 4

1.1.3. Biosynthesis of bile acids 5

1.1.4. Physiological functions of bile acids 7

1.1.5. Bile acids and disease 7

1.2. Fluorescent reporter compounds and labels for bile acids **9**

1.2.1. NBD as fluorophore 9

1.2.2. NBD labelled cholic acid derivatives 10

1.2.3. Other NBD bile acids 13

1.2.4. Biological uses of NBD labelled bile acids 13

1.2.5. Dansyl as fluorophore 19

1.2.6. Dansyl labelled bile acid derivatives 20

1.2.7. Biological uses of dansyl labelled bile acids 24

1.2.8. Fluorescein as fluorophore 26

1.2.9. Fluorescein labelled bile acids 27

1.2.10 Biological uses of fluorescein labelled bile acids 33

1.2.11. Other fluorophores: synthesis, characterization and biological uses 37

CHAPTER 2 **42**

2.1 Aims and objectives **43**

2.2. Design and synthesis of A-ring fluorescent reporter bile acids **45**

2.2.1. Synthetic discussions 45

2.2.2. Protection of UDCA (**7**) 46

2.2.3. Selective deprotection of **55** 48

2.2.4. Design of 2Δ–alkene derivative 49

2.2.5. Elimination of 3α-hydroxyl with $POCl_3$ 50

2.2.6. Elimination of 3α-hydroxyl with methanesulfonyl chloride 51
2.2.7. Synthesis of 3α-mesylate 52
2.2.8. Cleavage of 3α-mesylate 52
2.2.9. Synthesis of epoxide isomers 54
2.2.10. Development of 2- or 4-fluorescence derivatives *via* ketone derivative 56
2.2.10.1. Synthesis of 3-keto derivative 56
2.2.10.2. Attempt for 2-hydroxymethylene derivative 56
2.2.11. Design of 4-fluorescent derivatives *via* haloketones 57
2.2.11.1. Preparation of 4-bromo ketone 58
2.2.11.2. Attempt for 4-azido ketone 59
2.3. Design and synthesis of 3-fluorescent bile acids and non-bile acid controls 60
2.3.1. Introduction 60
2.3.2. Design of 3-dansyl derivatives and intermediates 61
2.3.3. Protection of DCA (**4**) 63
2.3.4. Synthesis of 3α-dansyl UDCA and 3α-dansyl DCA derivatives 65
2.3.4.1. Synthesis of 3β-bromo derivatives 65
2.3.4.2. Synthesis of 3α–azido derivatives 66
2.3.4.3. Reduction of 3α-azido derivatives 68
2.3.4.4. Synthesis of 3α-dansyl derivatives 69
2.3.4.5. Hydrolysis of **76** and **77** 70
2.3.4.6. Hydrolysis of azido intermediates 71
2.3.4.7. Deprotection of **74** and **75** 72
2.3.5. Synthesis of 3β-amino-dansyl UDCA and 3β-amino-dansyl DCA and hydrolysis of the protecting groups 73
2.3.6. Design and synthesis of the dansyl control compound 75
2.3.7. Design and synthesis of 3-NBD derivatives 76
2.3.7.1. Introduction 76
2.3.7.2. Experiments towards synthesis of 3α-amino-NBD DCA 77
2.3.7.3. Experiments for the synthesis of 3β-amino-NBD UDCA 78
2.3.7.4. Protection of **54** and **67** with formic acid 79

2.3.7.5. Selective deprotection of **102** and **103** 80
2.3.7.6. Preparation of 3β-NBD derivative of UDCA 81
2.3.7.7. Investigation into deprotection of **109** 82
2.3.7.8. Selective deprotection of **74** and **84** 83
2.3.7.9. Synthesis of 3β-NBD, 7β-hydroxy-5β-cholanoate 84
2.3.7.10. Synthesis of 3β-NBD DCA 86
2.3.7.11. Synthesis of 3β-azido DCA derivative 88
2.3.7.12. Synthesis of 3α-NBD derivatives 88
2.4. Design and synthesis of 24-amino-NBD derivative of UDCA and cyclohexyl-NBD 91
2.4.1. Introduction 91
2.4.2. Synthesis of 24-amide 91
2.4.3. Reduction of **132** 92
2.4.4. Synthesis of 24-amino-NBD derivative 92
2.4.5. Synthesis of cyclohexyl-NBD derivative 92
2.5. Synthesis of cyclopropyl-amide derivatives of 99 and 126 93
2.5.1. Introduction 93
2.5.2. Design and synthesis of NBD labelled UDCA and DCA CPA 94
CHAPTER 3 95
3.1. Aims and Objectives 96
3.2. Absorption and emission study of fluorescent derivatives 97
3.2.1. Introduction and methods 97
3.2.2. Absorption and emission measurements of the fluorescent bile acids and control compounds 99
3.3. Fluorescence quantum yield of the NBD derivatives 102
3.3.1 Introduction 102
3.3.2 Fluorescence quantum yield measurements and results. 103
3.4. Stability study of 3β-NBD UDCA (101) and 3β-NBD DCA (119) 105
3.4.1. Stability study of **101** 105
3.4.2. Stability study of **119** 106

3.5. Cytotoxicity of the fluorescent bile acids **107**
3.5.1. The MTT assay 107
3.5.2. Introduction 108
3.5.3. Cytotoxicity of the parent bile acids 109
3.5.4. Cytotoxicity of the NBD compounds in different cell lines 110
3.5.5. Cytotoxicity of the dansyl compounds in different cell lines 113
3.5.6. Conclusion 115
3.6. Uptake studies with in cell and confocal microscopy **116**
3.6.1. Introduction 116
3.6.2. Disposition of NBD-bile acids within live cell environment 117
3.6.3. Examination of NBD-bile acids using confocal microscopy 118
3.6.4. The presence of the NBD derivatives in HET1A cells after 4 h 121
3.6.5. Experiments for inhibiting the vesicular transport process 122
3.6.6. Competition experiments 123
3.6.7. Examination of the relationship between the NBD derivatives and the Golgi apparatus 124
3.6.7.1. Organelle staining in fixed cells 124
3.6.7.2. Organelle staining in live cells 126
3.6.8. Examination of the uptake of dansyl bile acids using confocal microscopy 127
3.6.8.1. Uptake study of 3α-dansyl UDCA (**78**) 128
3.6.8.2. Uptake study of 3α-dansyl DCA (**79**) 131
3.6.8.3. Uptake study of the 3β-dansyl bile acids (**87** and **94**) 132
3.6.9. Effect of cytochalasin D on intracellular distribution of the fluorescent bile acids 134
3.7. Examination of stability and uptake of the fluorescently labelled bile acids in HET1A cell line by HPLC. **135**
3.7.1. Development of the HPLC method. 135
3.7. 2. Stability study of the fluorescent compounds in live cell environment. 138
3.7. 3. Uptake of 3α-dansyl bile acids (**78** and **79**). 142
3.7. 4. The uptake of 3α-dansyl bile acids (**78** and **79**) in competition experiments. 145
3.8. The uptake of NBD-bile acids by Caco-2 cell line. **148**

3.8.1. Cytotxicity of the NBD-bile acids in Caco-2 cell line. 148
3.8.2. The bicinchoninic assay. 148
3.8.3. Examination of NBD-bile acid uptake in Caco-2 cell line. 149
3.9. Conclusions **154**
CHAPTER 4 **155**
4.1. Introduction **156**
4.2. Synthetic chemistry **162**
4.2.1. Synthesis of 3β-azido CDCA derivatives 162
4.2.2. Experiments to afford 7β-azido CDCA 165
4.2.3. Synthesis of 3β-azido, 7α-hydroxyl CDCA derivatives 167
4.2.4. Synthesis of 3β-azido DCA derivatives 169
4.2.5. Synthesis of compound **176–181** 171
4.2.6. Synthesis of compound **182** and **183** 174
4.2.7. Synthesis of compound **186** 176
4.2.8. Summary of synthesis: a new panel of toxic bile acid derivatives 176
4.3. Cytotoxic bile acid effects on cell viability of Caco-2 and HT1080 cells **178**
4.4. Cell Viability - Flow Cytometry **181**
4.5. Cell viability effects on oesophageal normal and cancer cells **184**
4.6. Preliminary mechanistic studies in the toxic bile acid 169 **185**
4.6.1. Extrinsic pathways and bile acids 186
4.6.2. Mitochondrial/intrinsic pathways of apoptosis and bile acids 187
4.6.3. ER stress and bile acids 188
CHAPTER 5 **192**
5.1. Chapter 2 **193**
5.1.1. General synthetic methods 193
5.1.2. Methods for TLC visualization 193
5.1.3. Synthesis 194
5.2. Chapter 3 Methods **242**
5.2.1. Absorption measurements 242

5.2.2. Fluorescence measurements 243
5.2.3. Fluorescence quantum yield 243
5.2.4. Stability study of 3β-NBD UDCA (**101**) and 3β-NBD DCA (**119**) by HPLC 243
5.2.5. Cell cultures 244
5.2.5.1. HET1A 244
5.2.5.2. SKGT4 244
5.2.5.3. HUH7 245
5.2.6. The MTT assay 245
5.2.7. InCell measurements 245
5.2.8. Confocal measurements 246
5.2.8.1. Uptake study 246
5.2.8.2. Inhibition of vesicular transport 246
5.2.8.3. Competition experiments 247
5.2.8.4. Organelle staining in fixed cells 247
5.2.8.5. Live cell Golgi staining 248
5.2.9. Analysis of biological samples by HPLC 248
5.2.10. Uptake studies in Caco-2 cell line 249
5.2.11. Kinetics 249
5.2.12. Molecular modelling 250
5.3. Chapter 4 **250**
5.3.1. Chemistry 250
5.3.2. MTT assay 270
5.3.3. Flow cytometry 270
REFERENCES **271**
APPENDIX **291**

Chapter 1

Introduction

1.1. General introduction

1.1.1. Classification and chemical structure of bile acids

Bile acids are steroidal compounds biosynthesized from cholesterol (**1**) in the liver and stored in the gall bladder. They serve a number of important physiological functions such as generation of bile flow that helps in the extraction and recirculation of drugs and vitamins and cholesterol homeostasis [1]. The nomenclature of bile acids is complex, because of the high number of naturally occurring derivatives. These compounds can be divided into two great groups depending on the number of carbons, thus we can distinguish "cholanoids" and "cholestanoids". Cholanoids consist of all C_{24} compounds, while cholestanoids encompass the all C_{27} compounds including the C_{27} bile acids and C_{27} bile alcohols. Bile acids are classified into primary, secondary and tertiary bile acids. The primary bile acids, as cholic acid (CA, **2**) and chenodeoxycholic acid (CDCA, **3**) are synthesized from cholesterol enzymatically in the hepatocyte. These primary bile acids are modified by anaerobic bacterial flora to form the secondary bile acids, deoxycholic acid (DCA, **4**) and lithocholic acid (LCA, **5**). The tertiary bile acids ursodeoxycholic acid (UDCA, **7**) and sulfo-LCA (SLCA, **6**) are derived from **3** with epimerisation and from **5** with sulfation, respectively *(Figure 1.1)*.

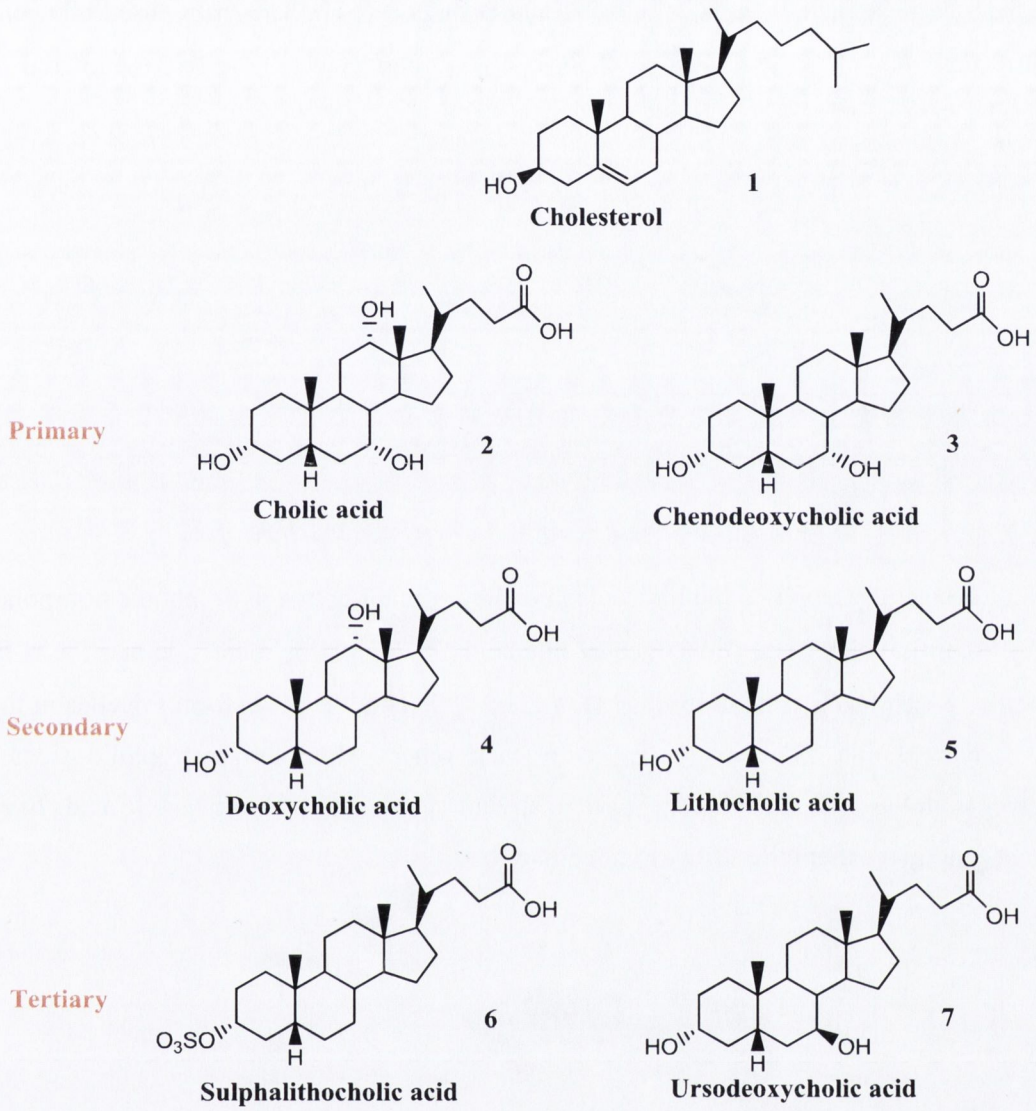

Figure 1.1: Classification of bile acids

The structure of bile acids can be divided into two components, a rigid steroid `nucleus` and an aliphatic side chain. In the case of cholestanoids, the side chain contains eight carbons, while the side chain of cholanoids contains only five carbons. The steroid nucleus of bile acid is saturated and contains three six-member hydrocarbon rings (A, B and C) and a five-member ring (D). In addition, there are two angular methyl groups at positions C-18 and C-19 [2]. Bile acids can be flat or curved molecules depending on the fusion between A and B rings. In the higher vertebrates, the bile acids are curved, thus the A and B rings are in a *cis*-fused configuration (The hydrogen is in β-orientation at position C-5). The bile acids of lower vertebrates are usually flat

compounds, because of the *trans*-fusion of A and B rings (5α-H). The *trans*-fused bile acids are also known as *allo*-bile acids. The side chain is always connected to the five-membered ring at position C-17 *(Figure 1.2)*.

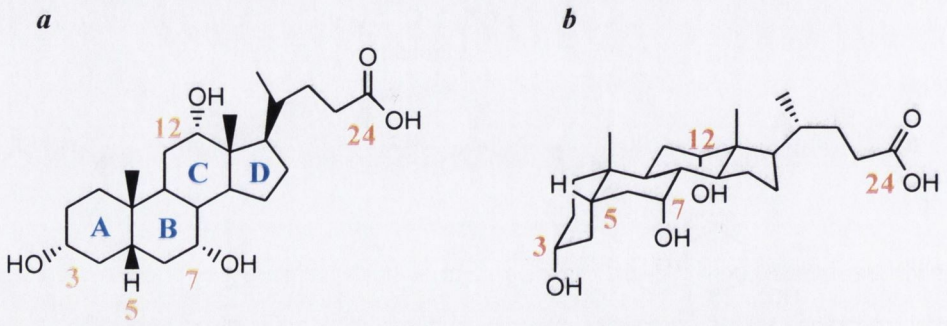

*Figure 1.2: **a** Structure of **2**, **b** Chemical structure of **2***

Bile acids are facially amphipathic molecules i.e. they contain both a hydrophobic non-polar face and a hydrophilic polar face. The β-face of bile acids is the hydrophobic side and the α-face is hydrophilic, which has hydroxyl groups [3] *(Figure 1.3)*. The bile acids form micelles in the gut, with the hydrophobic sides in contact with each other, while the hydrophilic sides align themselves with the aqueous solution. It is this structural property that allows bile acids to acts as surfactants and gives them the ability to micellise.

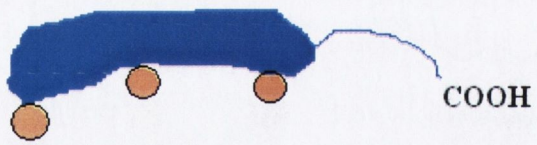

*Figure 1.3: Cartoon representation of **2** (introduced by Small)*

1.1.2. Conjugation of bile acids

After their biosynthesis bile acids are conjugated, and this conjugation increases their water-solubility [3]. Bile acids can be conjugated at C-24 or via the hydroxyl groups of the steroid nucleus. They can be N-acyl amidated with either glycine or taurine at C-24, where the carboxyl group of the bile acid is linked to the amino group of the amino acid to form an amide bond *(Figure 1.4)*. This conjugation changes the acidity of bile acids resulting in increased solubility

and ionisation at the pH conditions during the digestive process. The carboxyl group also undergoes sulfation and ester glucuronidation. The hydroxyl group at C-3 can be conjugated with sulfate, which prevents absorption in the intestine and the rapid elimination of the compound. Bile acids with 7β-hydroxyl group (e.g. **7**) can be conjugated with N-acetylglucosamination at C-7. Conjugation of bile acids on both the steroid nucleus and the side chain can occur simultaneously [4].

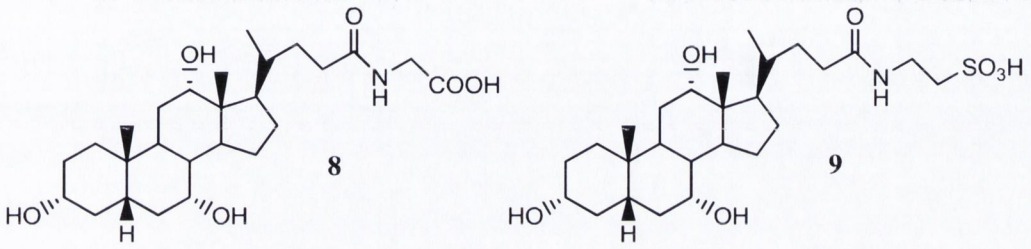

Figure 1.4: Structures of conjugated bile acids. ***8****: Glycocholic acid;* ***9****: Taurocholic acid*

1.1.3. Biosynthesis of bile acids

Bile acids are synthesized from **1** via a number of complex steps in both the side chain and steroid nucleus [5-7] *(Figure 1.5.)*. In the first step of biosynthesis the cholesterol 7α-hydroxylase enzyme oxidizes the cholesterol to a 7α-hydroxycholesterol intermediate (**10**), which is converted to cholest-7α-hydroxy-Δ^4-3-one (**11**) in the next step by isomerase and oxidase enzymes giving the key intermediate of the biosynthetic route. At this point the biosynthesis branches out causing the formation of the primary bile acids, cholic and chenodeoxycholic acid. The unsaturated oxo derivative undergoes a hydroxylation at C-12 forming the backbone of cholic acid. This step is followed by side chain oxidation to afford the C_{27} acid (**13**). This step is believed to occur in the mitochondria mediated by a P-450 hydroxylase. In the next two steps **13** is stereoselectively reduced to form the A/B *cis* bile acid skeleton, and then the 3-oxo group is reduced to 3α-hydroxyl (**14**). The formed C_{27} acid undergoes an oxidative cleavage of the side chain for the mature C_{24} bile acid in the last step, which is catalysed by peroxisomal enzymes. For the formation of **3** the key oxo intermediate undergoes the same transformations except for the hydroxylation step. These biosynthesized bile acids are conjugated with glycine and taurine by an acyltransferase enzyme in an amidation reaction [8].

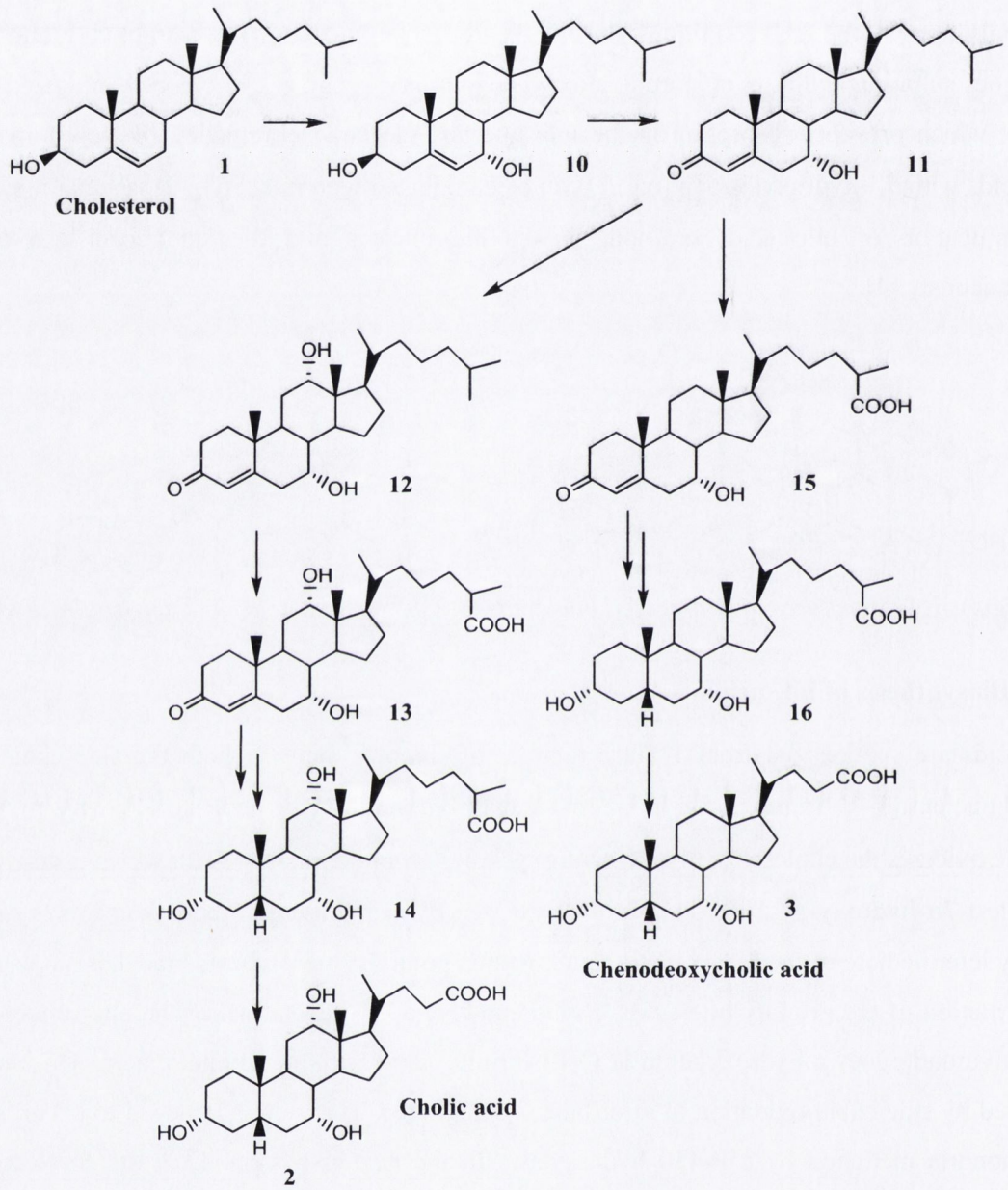

Figure 1.5: Biosynthesis of cholic and chenodeoxycholic acid from cholesterol.

The biosynthesis of secondary bile acids from **2** and **3** takes place in the intestine by bacterial enzymes [9]. On the side chain, bacteria deconjugate the bile salt to form bile acids, taurine and glycine. Some of these deconjugated bile acids are sent back to the liver and reconjugated during the transit through the hepatocyte [10]. The 7α-hydroxyl group on the nucleus is removed by anaerobic bacteria to form secondary bile acids. In the case of **2**, the dehydroxylation results in **4**, which has two hydroxyl groups on the steroid nucleus at C-3 and C-12. The bacterial

dehydroxylation of **3** results in **5,** which contains only one OH-group at C-3. Both of **4** and **5** are absorbed in the colon and returned to the hepatocyte. The epimerisation of 7α-hydroxyl group of **3** or the sulfation of 3-OH of **5** leads to the tertiary bile acids, **7** and **6**. Compound **7** is currently used for cholesterol gallstone dissolution therapy and in the treatment of cholestatic liver diseases.

1.1.4. Physiological functions of bile acids

The physiological functions of bile acids can be divided into five major established parts [9]. The most important is the elimination of cholesterol (**1**) from the body by converting to bile acid or micellar solubilisation in bile, which allows the moving of cholesterol to the intestine and the elimination *via* the faecal route. Bile acids also take part in lipid transport in the form of mixed micelles. They function to promote lipid solubilisation in the small intestine and accelerate the lipid transport through the intestine. A lack of bile acids results in deficiency of the fat soluble vitamins (A, D, E and K_1) as they are not absorbed. Micelle formation can also promote cholesterol elimination and the solubilisation of phospholipids.

Bile acids also function as secratogues increasing biliary phospholipid secretion and inducing the flow of bile. One of the most important functions of bile acids is in maintaining cholesterol homeostasis through negative feedback regulation of cholesterol. Indeed excessive intake of cholesterol in high fatty western diets also results in increased accumulation of bile acids in the liver and intestine. It is thought that these high concentrations of bile acids are involved in the initiation and progression of colon cancer [11].

Bile acids have additional functions in the intestine apart from these principal functions [9]. They promote the solubilisation of polyvalent metals e.g. iron and calcium in the duodenum or stimulate the release of motilin, which coordinates the interdigestive migrating motility complex. Bile acids can also stimulate mucin secretion in the small intestine and affect the absorption of electrolytes and water.

1.1.5. Bile acids and disease

Despite bile acids being essential components of normal body function, they are important in hepatic, biliary and intestinal disease [9]. Mutations in biosynthesis of bile acids can cause a number of identified hepato-biliary diseases such as cerebrotendinous xanthomatosis (CTX) or

Zellweger`s syndrome [2]. The concentration of bile acids can also take part in the development of different disease.

It is also generally accepted that increased concentrations of secondary hydrophobic bile acids results in cytotoxicity either intracellularly or extracellularly [9]. Hydrophobic bile salts have been shown to be cytotoxic against a variety of different cell types including hepatocytes [12], erythrocytes [13], mast cells [14] and gastric or intestinal cells [15]. The toxicity of bile acids strongly depends on their structure. While the hydrophobic components, such as **3** and **4** show high cytotoxicity, **7** is hydrophilic and devoid of the cytotoxic properties in most model systems [14, 16]. As a result bile acids significantly contribute to the development of a number of hepatobiliary cholestatic disorders such as primary biliary cirrhosis and primary sclerosing cholangitis. It is commonly thought, that the retention of bile acids in the hepatocytes leads to all forms of cholestasis. The high concentration of cytotoxic bile acids can result in cellular membrane damage and induce apoptosis or necrosis of hepatocytes, which leads to a chronic cholestatic liver disease. The leakage of bile acids into the peribiliary space causes portal inflammation and fibrosis [9, 17, 18].

It has been documented that bile acids take part in the development of intestinal cancer [19]. Cook and Kenway have described bile acids first as carcinogens in 1939 and 1940 [20]. Studies have shown that dietary habits affect bile acid metabolism and the ingestion of large amount of fats is an important element responsible for intestinal cancer. *In vitro* a number of carcinogenic cascades have been found to be upregulated by bile acids, these include activator protein-1 (AP-1), extracellular signal regulated kinases (ERKs) and protein kinase C (PKC) [21]. Bile acids have also been identified as causative agents in the development of liver and colon cancer in number epidemiological studies [22].

1.2. Fluorescent reporter compounds and labels for bile acids

The overall objective of this thesis was to use synthetic chemistry to provide tools to understand problems in bile acid research including their disposition and mechanism of toxicity. Fluorescent reporter groups are very widely used for probing problems of biochemical distribution and mechanism especially in the bile acid field. This area is reviewed here, structured by fluorescent derivatizing agent.

1.2.1. NBD as fluorophore

The NBD group, 7-nitrobenzofurazan 2-oxa-1,3-diazole is widely used to label peptides, drugs, proteins and other biomolecules. It may be introduced by electrophilic substitution onto its chloride **17** or fluoride **18** (Figure 1.6). It is also commonly used in HPLC analysis as a pre-labeling compound for amino acids and low molecular weight amines [23]. NBD chloride (**17**) is a pale yellow powder, which is not fluorescent itself, but reacting with primary, secondary amines or thiols it forms exceedingly fluorescent adducts as an orange solid. The fluorescence spectra of these derivatives are highly environment-sensitive; the fluorescence intensity of the NBD-labelled compounds is higher in organic solvents than in aqueous solutions. The NBD-amine adducts have λ_{ex} around 464 nm and λ_{em} around 512 nm in aqueous solutions [24]. NBD chloride was first prepared by Boulton *et al.* by nitration of 4-chlorobenzofurazan at position-7 in 1966 [25].

The fluoro derivative of NBD (4-fluoro-7-nitrobenzo-2-oxa-1,3-diazole, NBD-F) **18** is also used to label amines and thiols giving the same NBD labelled products as NBD-Cl. NBD-F is also non-fluorescent itself but much more reactive in forming the NBD-amine adducts than the chlorinated derivative. It was firstly synthesized by Di Nunno *et al.* by nitration of 4-Fluoro-2,1,3-benzoaxadiazole [26]. It is also used as derivatization reagent for HPLC analysis of amino acids and low molecular weight amines [23].

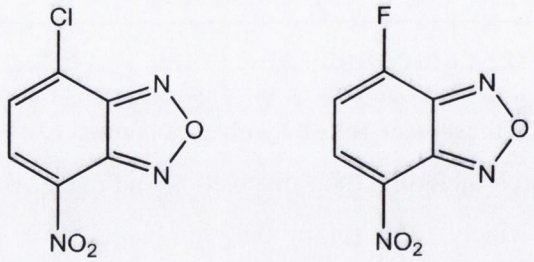

17 **18**

Figure 1.6: Chemical structures of NBD chloride and NBD fluoride

The favorable fluorescent features, the highly reactive halogen derivatives and the relatively small molecular weight make the NBD fluorophore popular for labeling drugs and other biologically active molecules.

1.2.2. NBD labelled cholic acid derivatives

Cholic acid presents several possible points of introduction of a fluorescent reporter group. Preparation of stable *N*-substituted NBD analogs requires replacement of the hydroxyl or carboxyl functionality with amino group(s) or amidation at C24 with an amine bearing moiety. The necessary selective synthetic manipulation is facilitated by the long history of bile acid synthetic chemistry in the 20th Century.

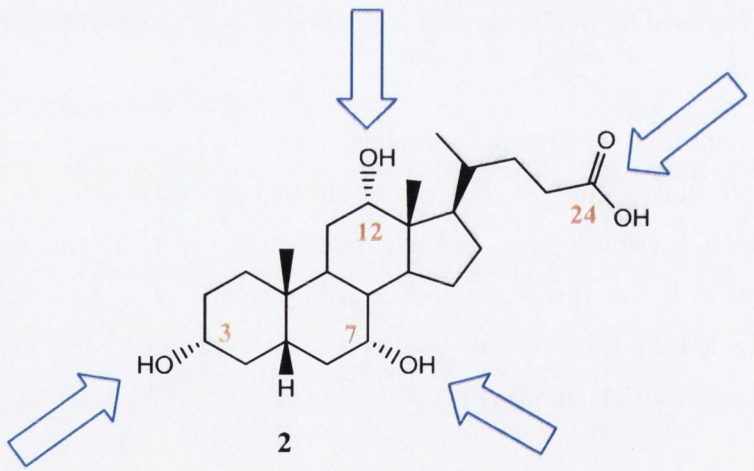

2

Figure 1.7: Positions to label cholic acid with NBD fluorophore

The first NBD-derivatives of cholic acid (**2**) were described by Schneider *et al.* in 1991 who introduced the fluorophore into the 3, 7 and 12 positions providing a complete set of

diastereomeric isomers, as well as their taurine conjugates (**19-21**) [27] (*Figure 1.8*). The fluorescent steroids were synthesized in four steps in the case of the unconjugated and in five steps in the case of the taurine conjugated cholic acid. In the first step the bile acid was oxidized to 3, 7 or 12-oxo derivative, followed by the conversion to oximo intermediate, which was reduced to amine. Finally the fluorophore was introduced, and the α- and β- isomers were separated. The authors described two options for conjugation. Taurine can be coupled to the carboxyl group after the selective oxidation of the corresponding hydroxyl group or the previously prepared NBD-cholic acid can be conjugated with taurine at the end. The spectroscopic properties of these NBD-labelled cholic acid compounds and salts were extensively characterized. The absorption spectra of all the derivatives are similar showing four absorption maxima in every case. The longest wavelength absorption band (between 460–500 nm) is strongly dependent on the solvent. Increasing the hydrophobicity of the solvent results in decreased absorption maxima (blue shifted), while the pH of the environment and the concentration of the compounds have no effect on the absorption properties. The emission maxima of all the derivatives are in the range between 540 and 570 nm depending on the polarity of the solvent. The more hydrophobic solvents result in higher emission maxima and greater quantum yield compared to the polar solvents (e.g. $\Phi = 0.025$ in water or pH = 7.4 phosphate buffer and $\Phi = 0.398$ in n-octanol). The quantum yield is temperature dependent, decreasing it on higher temperatures. However many fluorophores have strong pH dependence; in the case of NBD-labelled bile acids the variation of the pH does not significantly affect the wavelength of the emission maxima or the quantum yield.

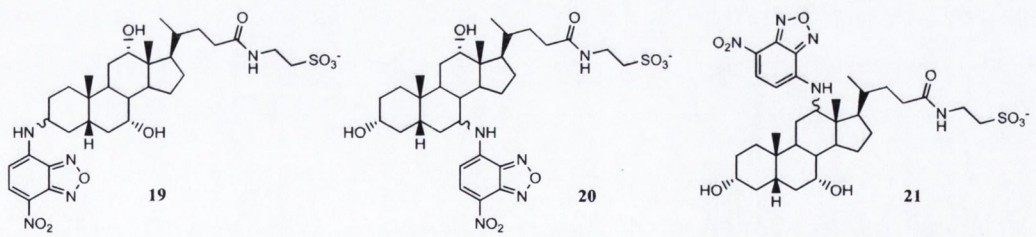

Figure 1.8: Chemical structures of the first NBD labelled taurocholates (Schneider et al., 1991)

Rohacova *et al.* used the previously described synthetic approach to prepare 3- and 7-NBD-labelled cholic acid in order to assess their suitability for detecting functional active uptake processes in hepatocytes by flow cytometry [28]. The absorption and emission properties of the compounds in ethanol (EtOH) were similar to the previously presented corresponding taurine-

conjugated NBD derivatives. The authors determined the fluorescence lifetimes ($\tau_s \sim 6$ ns) of the four fluorescent cholic acids in ethanol and estimated the singlet energy ($E_{0\text{-}0}$) values of ~ 242 kJ mol^{-1}.

Yan Zhao and Zhenqi Zhong introduced a different method to convert the 3-hydroxyl group of **2** to an amine using the obtained monomer to produce amide-linked oligomeric cholates [29]. They prepared NBD-amino adducts of cholate monomer, trimer, pentamer and heptamer to study the conformation of the foldamers in different solvents. To obtain the 3α-amino group first methyl cholate was converted 3β-mesylate using PPh_3 and diisopropyl azodicarboxylate (DIAD), followed by an S_N2 azide reaction. The azide group was then reduced to amine by PPh_3 in aqueous THF that was used together with the hydrolyzed form to produce oligomer cholates. The monomer ester and the oligomers were than labelled with NBD to study interactions between their helix structure and different solvents using fluorescent techniques.

An NBD attached cholic acid derivative, linking the fluorophore to the side chain via a lysine conjugate was described by Maglova *et al.* in 1995 [30].

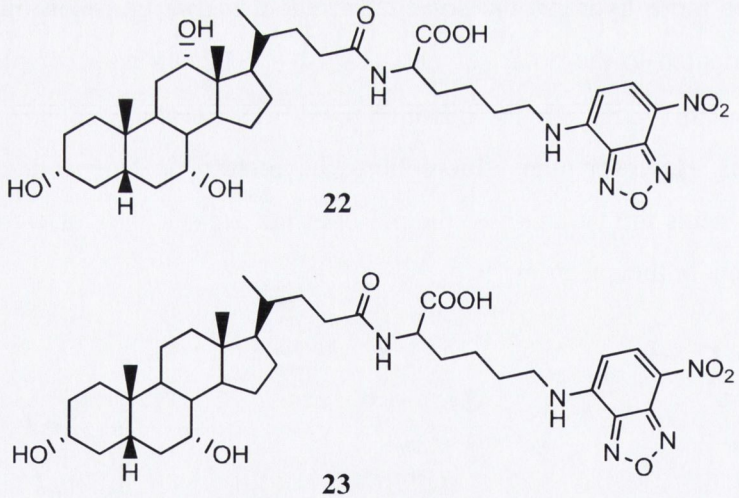

Figure 1.9: Cholyl-(Nε-NBD)-lysine and Chenodeoxycholyl-(Nε-NBD)-lysine

Cholyl-(N~-nitrobenzoxadiazolyl [NBD])-lysine (**22**) was prepared using lysine conjugated cholic acid that was already coupled with the NBD-group [31]. The absorption and emission maxima of the compound were consistent in different solvents ($A_{max.}$ = 468–469 nm, $Em_{max.}$ = 523–532 nm), while the quantum yield was much lower in aqueous solutions than in organic

solvents. As expected the fluorescent properties of the NBD-cholic acid conjugate did not exhibit pH dependence.

1.2.3. Other NBD bile acids

In the previous study the authors also described the first NBD derivative of CDCA (**23**) (*Figure 1.9*). This was produced by coupling the fluorophore to the ε-amino group of the lysine conjugated CDCA [30]. This was followed by reports of the preparation of NBD-labelled secondary and tertiary bile acid derivatives, such as ursodeoxycholyl- [31, 32], deoxycholyl- and lithocholyl-(Nε-NBD)-lysine [32] by other groups. There is little spectroscopic information available about these materials. The corresponding 3/7/12 amino NBD analogs of CDCA, UDCA and DCA have not been reported.

1.2.4. Biological uses of NBD labelled bile acids

Attachment of a fluorophore reporter can be expected to have a large impact on the biological activity of a small molecule. Hence when synthesizing fluorescent compounds it is essential that a fluorophore is introduced at a position which has been proven in SAR studies to have minimal effect on biological activity. It also follows that introduction of large bulky fluorophores is less desirable than a smaller more discrete fluorescent group. For the latter reason, the NBD group has gained increased popularity for probing the distribution and mechanism of bile acids as it is a relatively small fluorophore and has favourable optical properties.

The most obvious biological application of fluorescent bile acids is in the study of bile acid and organic anion transporter systems. Bile acid transporters have been reviewed in depth in a number of recent reviews [33-35]. More than 95% of total bile acids in humans secreted from the liver are absorbed by active or passive mechanisms in the intestine and returned to the liver for re-secretion [36]. In order for the process of enterohepatic recirculation to function efficiently, the presence of bile acid transporters at the hepatocyte and ileal enterocyte is required. These are outlined in *Figure 1.10.*

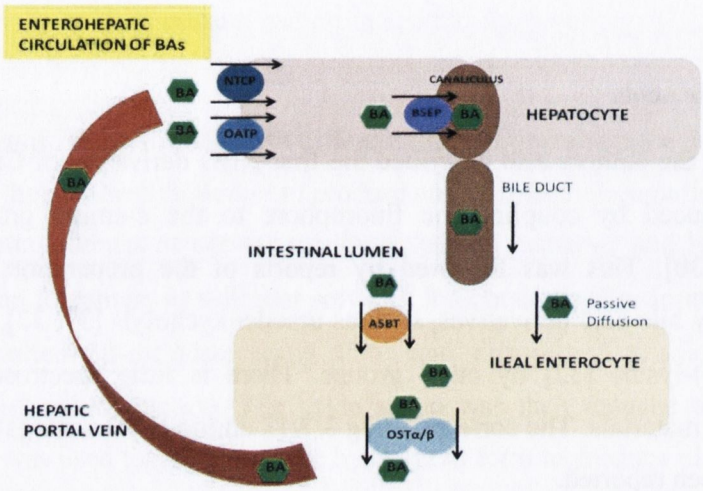

Figure 1.10: Enterohepatic circulation of bile acids. Bile acid uptake at the hepatocyte is mediated by the Na-taurocholate co-transporting polypeptide (NTCP) and the organic anion transporting polypeptide family (OATP). The bile salt export pump (BSEP) is involved in secreting bile acids out of the hepatocyte into the canaliculus where the bile duct then transports bile in to the intestinal lumen. The apical sodium dependent bile salt transporter (ASBT) is the principal transporter involved in uptake at the ileal enterocyte, although passive uptake is also known to occur in the intestine. Finally the transporters OSTα/β are involved in basolateral secretion out of the enterocyte where the hepatic portal vein can then return bile acids back to the liver. In portal venous blood bile acids are predominantly bound to albumin. Figure is adapted from [37]

A number of researchers are currently involved in investigating the interaction of bile acids and other molecules with these transporters in the intestine and liver. These research efforts have greatly increased in recent years with the realization that these transporters are ideal drug targets. For example, blockade of bile acid uptake at ileal enterocyte level promotes cholesterol metabolism and reduction in plasma total cholesterol, a favourable outcome in clinical management of patients with lipid abnormality. Currently functional studies involving characterization of the uptake and transport of natural and synthetic substrates rely on the use of radiolabelled ligands. The dangers of radioactivity and the expense of radioactive waste disposal are obvious drawbacks for these experiments and hence the use of fluorescent bile acids as a substitute for radiolabelled ligands in these experiments would be highly favourable. Furthermore fluorescent bile acids allow investigators to study transport at the cellular and organ level actually visualizing bile acid transport through fluorescence microscopy techniques potentially in real

time. The latter opportunities arise because of the increasing availability of high resolution confocal and associated high content techniques [38].

To this end, the suitability of NBD labelled fluorescent bile acids for assessment of substrate uptake in transport studies has been investigated. Some of the earliest work was carried out by the Kurz group in the early nineties. This group introduced the NBD amino group in 3-, 7- or -12-positions of CA with alpha or beta orientations. They also synthesized the corresponding taurine conjugates for each diastereomer (**19-21**) [27]. The group then investigated the suitability of the different compounds for the study of bile acid transport by fluorescence microscopy by examining their interaction with bile acid binding proteins and their behaviour in hepatic metabolism in the course of their transport from blood to bile [39]. The compounds could bind to albumin, to varying degrees, depending upon the position and orientation of the NBD group. This was detected by a small hypsochromic shift of the emission maxima and increase in the fluorescence quantum yield suggesting binding through hydrophobic interactions. The greatest increase was observed with the 3-β NBD-TCA derivatives whereas with the 7-α NBD TCA this increase was insignificant. Furthermore, the different fluorescent bile acids were metabolized differently in liver infusion experiments performed in rats. The unconjugated 3β- NBD was completely transformed to its taurine conjugate and secreted as such, whereas the 3α- compound produced a metabolite even more polar than 3α NBD TCA. The unconjugated 7α- and 7β- NBD CA underwent about 15% conjugation to taurine but were mainly secreted unmetabolised. The 12α and 12β isomers were secreted predominantly unconjugated, with 15% metabolized to a fluorescent compound, which was less polarized. All the taurine conjugated compounds were secreted into bile unmetabolised, and, with the exception of the 3β NBD TCA, more than 95% of the applied compound could be detected in bile within 30 minutes. Only 40% of the 3α-NBD TCA appeared in bile within this timeframe. All of the fluorescent TCA derivatives interfered with the secretion of radiolabelled TCA, again with the exception of the 3α-NBD derivative. Photoaffinity labelling studies revealed that in hepatocytes the fluorescent bile acids interacted with the same polypeptides as natural bile acids [39]. In the third part of this series of publications the group kinetically characterized the uptake of TCA and the 7β-NBD TCA derivative and demonstrated that the two compounds were taken up into isolated rat hepatocytes by similar mechanisms involving two transport systems. The authors conclude that the 7β-NBD derivative is a true analogue of TCA and hence is suitable for study of hepatobiliary transport

[38]. This derivative was subsequently used to investigate the transport of 3α, 7α, 12α-trihydroxy-24-nor-5 β-cholan-23-sulfonate (*Figure 1.11*) into isolated rat hepatocytes (**24**) [40].

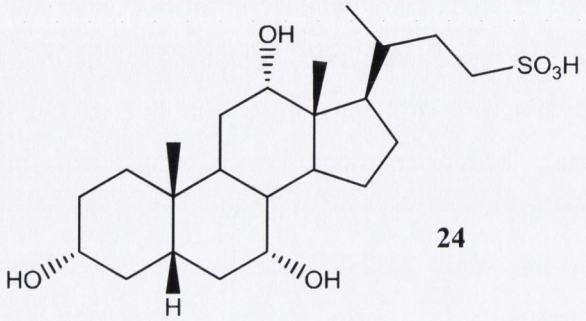

24

Figure 1.11: Chemical structure of 3α, 7α, 12α-trihydroxy-24-nor-5 β-cholan-23-sulfonic acid

Alpha and beta derivatives of CA at the 3 and 7 positions (**25-28**) have since appeared in a variety of studies. Rohacova *et al.* showed uptake of these compounds (*Figure 1.12*) into isolated rat hepatocytes using flow cytometry [28]. In this set of experiments the efficiency of the uptake of the NBD CA derivatives was in the order: **25** > **26** > **27** > **28**. Treatment with troglitazone, an inhibitor of the NTCP decreased fluorescent bile acid uptake indicating the specificity of the uptake. The cholestatic compounds chlorpromazine and cyclosporine A also decreased the uptake of compound **25**.

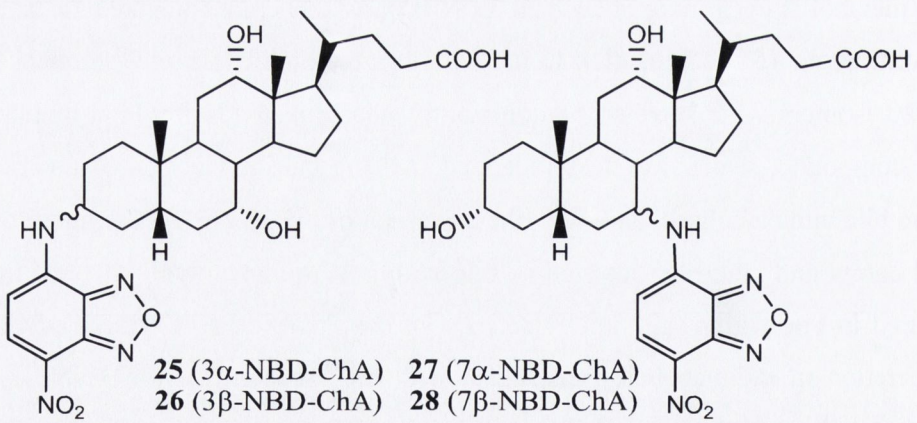

25 (3α-NBD-ChA) **27** (7α-NBD-ChA)
26 (3β-NBD-ChA) **28** (7β-NBD-ChA)

Figure 1.12: NBD-substituted cholic acid derivatives used by Rohacova et al. in transport studies.

Rohacova *et al.* went on to investigate the interaction between these fluorescent bile acids and human serum albumin. Incubation with albumin resulted in enhancement of fluorescence emission, which was used to estimate the binding constants for the fluorescent bile acids-albumin

interaction. The 3- and 7- NBD-CA isomers as well as a 3β-NBD TCA and cyclohexyl NBD derivative complexed with albumin with a 1:1 stoichiometry and with apparent binding constants in the 10^4 M^{-1} range. Albumin is known to have two binding sites. Warfarin binds to site 1 and ibuprofen to site 2. Titration experiments with warfarin and ibuprofen showed a significant decrease in the emission intensity with warfarin whereas only a minor change was observed with ibuprofen indicating that the CA derivatives bind to albumin at site 1. Interestingly, the cyclohexyl NBD group was displaced by ibuprofen and not warfarin showing that the steroidal skeleton as opposed to the NBD moiety determines the binding site [41]. Similar experiments have been performed using dansyl labelled CA derivatives. These are discussed later in this chapter.

Fluorescent bile acids incorporating the NBD group at the side chain have also been prepared. These compounds tend to be conjugated to the bile acid carboxyl group via a linker such as lysine. Kida *et al.* used [3H]-TCA and **22** to show that intrahepatic bile duct cells transport bile acids from the apical to the basolateral side which is the opposite direction of transport to that seen in hepatocytes [42].

Yamaguchi *et al.* used CDCA-NBD lysine (**23**) to characterize the contributions of OATP polypeptides, specifically OATP1B1 and OATP1B3, to the liver uptake of CDCA. Compound **23** was efficiently transported with high affinity by HepG2 cells expressing OATP1B1 or OATP1B3. Confocal imaging showed that the compound accumulated in the cytoplasm of the cells. Interestingly the apparent K_M values for 3 uptake by OATP1B1 and OATP1B3 were 1.45 μM and 0.54 μM. The group also reported the uptake values for **22** by OATP1B1 and OATP1B3 as 0.67 μM and 16.2 μM which they report as being much lower than those reported for radiolabelled CA uptake by OATP1B1 and OATP1B3 (11.4 μM and 85.3 μM respectively). Hence conjugation with an NBD group may alter the affinity of bile acids for transporters. Inhibitors of the OATPs significantly inhibited the transport of CDCA-NBD. The study also presented a comparison between CDCA-NBD (**23**), CA-NBD (**22**), DCA-NBD, LCA-NBD and UDCA-NBD (all conjugated at the 24 position) and showed that the CDCA derivative was transported most efficiently in these cell lines and that OATP1B1 and OATP1B3 have different substrate specificities that depend upon the native bile acid chemical structure [32].

The uptake of **23** by OATP1B3 was later utilized by Yamaguchi *et al.* to establish a high content screening assay for identifying antineoplastic substrates of OATP1B3. Using **23** as a fluorescent

probe in an immunofluorescence screening assay identified docetaxel, actinoymycin D, mitoxantrone, paclitaxel and SN-38 as potential OATP1B3 substrates. However subsequent uptake studies revealed that SN-38 was the only agent transported to a significant extent [43].

Holzinger *et al.* used a biliary fistula rat model to assess the hepatic transport, biotransformation and choleretic activity of six different fluorescent bile acids including **22** and UDCA-NBD-lysine. They also assessed intestinal absorption using jejunal or ileal perfusion studies. Fluorescent bile acids did not undergo extensive biotransformation during hepatocyte transport. In contrast to the fluorescein labelled bile acids, which were also used during the study, **22** and UDCA-NBD-lysine were actively transported by the intestine (ileum > jejunum). Steric bulk has been shown in recent studies to influence hASBT (ileal bile acid transporter) mediated transport [44]. Neither compound displayed passive intestinal permeability. However they underwent complete biotransformation during jejunal transport. Very interestingly the UDC-L-NBD was a cholestatic agent and displayed pulmonary toxicity. This was surprising as UDCA and TUDCA are non-toxic and are used for treatment of hepatic inflammatory conditions [31].

In a subsequent study, Holzinger *et al.* used isolated rat liver perfusion experiments on the same set of fluorescent bile acids. They found that **22** and UDCA-NBD-lysine were efficiently taken up by the isolated rat liver. However the two compounds were recovered to varying extents in bile due to hepatic sequestration which is not seen for natural bile acids (81% recovery for **22** and 13% recovery for UDCA-NBD after 60 min). Possibilities for the nature of hepatic sequestration include binding to cytosolic proteins and/or organelles such as microsomes, mitochondria, pericanalicular vesicles and nuclei. Interestingly it was found that confusion of conjugated bile acids resulted in mobilization of UDCA-L-NBD from the hepatocyte. This observation with fluorescent UDCA led the authors to the hypothesis that the cytoprotective effects of UDCA observed in hepatocytes could be explained by UDCA preventing hepatic sequestration of cytotoxic bile acids in organelles. Hence the use of fluorescent bile acids can provide valuable insight into potential mechanisms of action [45].

Murray *et al.*, tested 7 β NBD CA (**28**) and found that the compound could accumulate in isolated rat hepatocytes but was preferentially transported by HeLa cells expressing OATP1A1 as opposed to HeLa cells expressing NTCP [46].

UDCA-NBD-lysine and **28** were have also been evaluated for uptake, transport and excretion across NTCP and BSEP co-expressing LLC-PK1 cells. In this system however there was no detectable transport of these NBD labelled fluorescent bile acids [47].

Compounds **22** and **23** were also studied by Maglova *et al.* for uptake into isolated rat hepatocytes and the hepatocyte couplets. Uptake was found to be time and concentration dependent and was saturable. K_M values were estimated to be 3.8 and 3.0 μM for **22** and **23,** respectively. Interestingly in this report although uptake decreased by 38% for **22** in the absence of Na^+, there was no change in the uptake of **23** suggesting that its uptake is Na^+-independent. Furthermore Na^+-dependent and Na^+-independent uptake of **22** was inhibited by **2**, **8**, and dehydrocholyltaurine but these unlabelled compounds had no effect on the uptake of **23**. Both of the fluorescent bile acids were secreted into the canalicular space of 50–60% of hepatocyte couplets [30]. Hepatocyte couplets consist of two nondissociated hepatocytes enclosing a sealed canalicular space [48].

Grüne *et al.* showed that uptake of **22** into whole cell patch-clamped hepatocytes was electrogenic and incubation with 8-bromo c-AMP increased the uptake rate of this fluorescent bile acid by 25%. Uptake of CGamF was shown to be neutral and 8-bromo c-AMP had no effect on its uptake rate. This work also showed that the cAMP-induced stimulation of C-NBD-lysine is due to membrane hyperpolarisation [49].

1.2.5. Dansyl as fluorophore

Dansyl chloride (DNSC) or 5-(dimethylamino)naphthalene-1-sulfonyl chloride (**29**) is commonly used fluorescent labelling agent in amino acid analysis, and protein sequencing. It reacts with aliphatic or aromatic primary amines to produce stable blue- or blue-green-fluorescent sulfonamide adducts. It can also be used to label hydroxyl and carboxylic acid groups. **29** was prepared and used to label proteins first by Weber in 1952 and it was synthesized by reacting the corresponding sulfonic acid derivative with phosphorus pentachloride (PCl_5) [50].

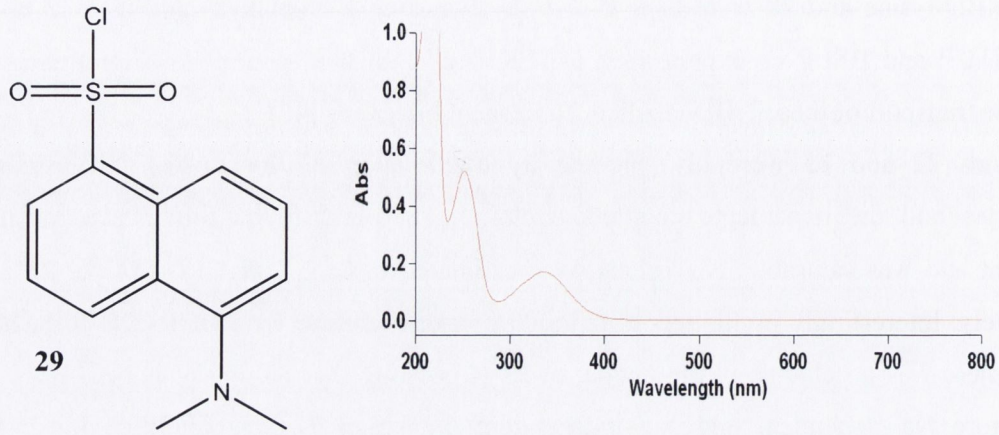

*Figure 1.13: Chemical structure of dansyl-chloride (**29**) and Absorption spectra of 3α-dansyl UDCA in EtOH.*

Compound **29** is nonfluorescent until it reacts with amines forming fluorescent dansyl amides that exhibit large Stokes shifts. The quantum yield and the emission maxima of the dansyl amides are highly environment-sensitive, a property that makes **29** an important tool for biophysical studies.

1.2.6. Dansyl labelled bile acid derivatives

As we have seen above, labelling bile acids with the NBD fluorophore is very prevalent in transport and other related bile acid studies. However, the dansyl group also has quite minor sterical impact and very good fluorescent properties, but there are only a few publications based on bile acid – dansyl adducts. In these papers, as in the case of NBD derivatives, the dansyl fluorophore is coupled to the bile acid via an amino group connected to the steroidal nucleus or to the side chain of the bile acid or bile salt.

The first dansyl labelled bile acid derivatives were described by Crawford *et al.* in 1991 [51]. They prepared five fluorescent bile salts to explore the role of hydroxyl groups of steroid ring in hepatocellular transport and biliary extraction. In their study, dansyl fluorophore was coupled to taurocholates using ethylenediamine as a linker (**30**) (*Figure 1.14*). The dansyl labelled tauro bile salts were synthesized in five steps. First α-phthalimidoethanesulfonyl chloride and the dansyl-ethylenediamine adduct were prepared, then these molecules were covalently linked to obtain the dansyl-tauro intermediate. This was followed by the conversion of the phthalimido group to free amine and finally this precursor was conjugated to the 24-carboxyl group of CA, DCA, UDCA,

CDCA and the triketo DHCA. The physicochemical properties of these derivatives are well described. The analysis showed that the fluorescent bile salts have greater aqueous solubility and water/octanol partitioning than the parent compounds, but these values are consistent. The HPLC study demonstrated that the dansyl derivatives were significantly more hydrophobic than the original bile salts. Unfortunately the photophysical characterization of these dansyl-bile salt adducts are not published.

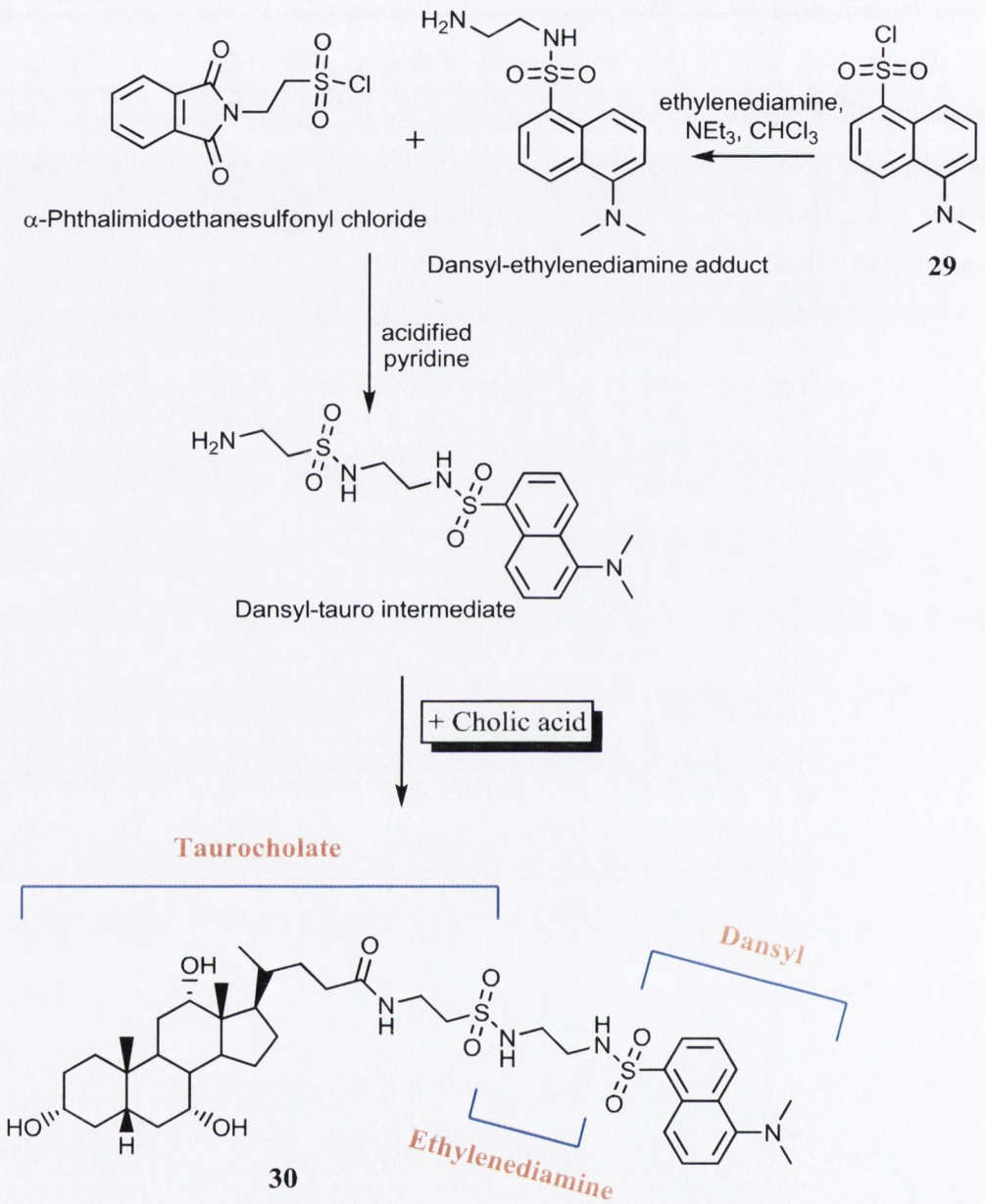

*Figure 1.14: The key intermediates of the synthetic route and the chemical structure of the prepared dansyl labelled taurocholate (**30**) developed by Crawford et al. [51]*

Introduction of the dansyl group at the functionalized positions of the steroid ring system was described by Rohacova *et al.* in 2009 [52]. They synthesized four fluorescent derivatives of cholic acid incorporating an amino dansyl moiety at 3α-, 3β-, 7α- and 7β-positions (**31-34**) to study the kinetics of bile acid transport by flow cytometry. To obtain the desired dansylated cholates first the authors converted the corresponding hydroxyl group to amine with the required

orientation and then linked to the dansyl fluorophore. For the 3-amino cholic acid derivatives the carboxylic acid group was methylated in the first step. Providing the 3α-amino isomer, regioselective oxidation of the 3-hydroxyl group was carried out using Ag_2CO_3 supported on celite, followed by stereoselective amination of the carbonyl group with $NaBH_3CN/AcONH_4$. To obtain the β-epimer the 3-hydroxyl was converted to mesylate then to an azido intermediate in a substitution reaction, and then the azide was reduced to amine under $Pd/C/HCOONH_4$ conditions. For the 7-amino compounds, cholic acid was treated with NBS to obtain a 7-oxo intermediate which underwent reductive amination and esterification giving the 7α-isomer. The β-orientation was formed converting the 7-oxo derivative to oxime, followed by reduction using Na/1-BuOH and esterification giving the mixture of 7α- and 7β-epimers (30:70). These intermediates were then coupled with DNSC and deprotected to afford the desired dansyl-cholic acid adducts (*Figure 1.15*).

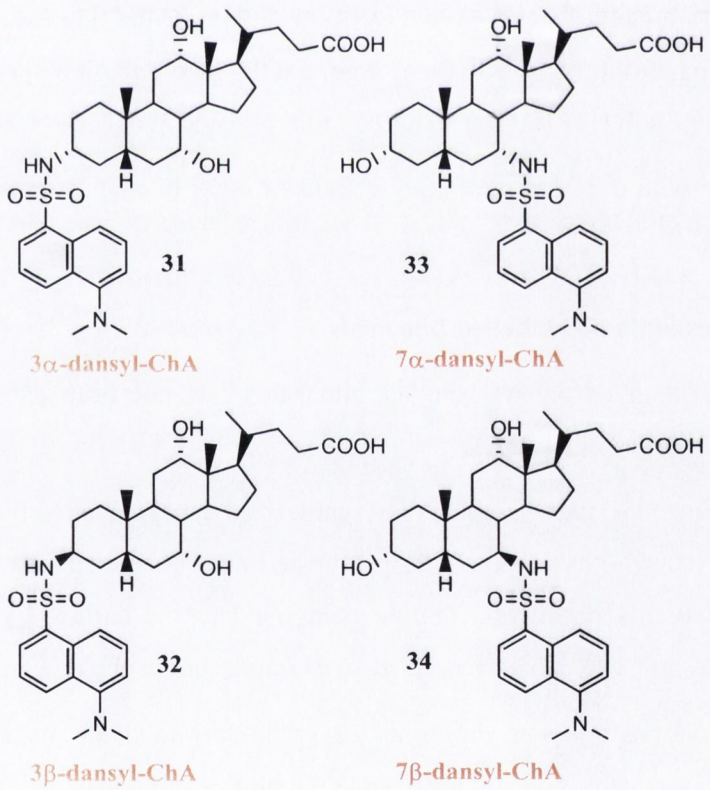

Figure 1.15: Dansyl labelled cholic acid derivatives developed by Rohacova et al. [52]

The photophysical properties of the four dansylated bile acids were examined. The compounds provided two absorption maxima in EtOH at 250 and 335 nm and the fluorescence spectra

showed maxima in the range 504–514 nm. Singlet energy values ($E_{0\text{-}0}$) were estimated about 286 kJ/mol and significant emission quenching by oxygen was observed (*Table 1.1*).

Dansyl-ChA	λ_{em} (nm)	ϕ_F*			τ_S (ns)		
		N_2	air	O_2	N_2	air	O_2
31	514	0.38	0.26	0.11	19.9	13.7	5.5
32	514	0.40	0.27	0.12	20.2	12.7	4.1
33	504	0.42	0.28	0.13	20.9	13.3	5.4
34	508	0.41	0.27	0.12	19.5	12.8	4.4

* standard solution: Coumarine30 in MeCN (air-saturated, $\phi_F = 0.67$, $\lambda_{exc} = 370$ nm)

Table 1.1: Photophysical properties of the dansyl-cholic acid derivatives, determined by Rohacova et al.[52]

In aqueous solution the fluorescent maxima shifted to 550 nm for C-3 and 540 nm for C-7 regioisomers (**33**, **34**), quantum yields were lower ($\phi_F \sim 0.05$) and the fluorescent lifetimes shorter (~ 4–5 ns) comparing to the obtained values from EtOH. The emission spectra exhibited blue fluorescence in organic solvents (EtOH) and green fluorescence in aqueous media.

Labeling cholic acid with dansyl fluorophore at C-12 or other bile acids on the steroid rings are not described to date.

1.2.7. Biological uses of dansyl labelled bile acids

The biological utilization of dansyl labelled bile acids has not been as widespread as the fluorescein or NBD labelled derivatives.

Crawford *et al.* conducted a study in which they synthesized dansyl labelled fluorescent bile acids derivatives using a dansyl-ethylene diamine precursor linked to the sulfonyl group of taurine. They then conjugated this fluorescent taurine compound to the carboxyl group of CA (**30**), UDCA, DCA, CDCA and also dehydrocholic acid, example shown above with dansyl TCA (**30**).

Modification at the 24 position was chosen as the group specifically wanted to retain an intact steroid ring structure so that they could investigate the impact of hydroxylation on bile acid-lipid interactions. Measurement of HPLC retention times revealed that although the dansylated derivatives were more hydrophobic than the native bile acids (as expected), they eluted in the same order as the native taurine conjugated bile acids with the dansylated dehydrocholic acid

being the most polar compound and the dansyl DCA being the most hydrophobic. This indicates that these compounds mirror the physicochemical relationships observed for the native bile acids. The dansylated derivatives inhibited radiolabelled taurocholate uptake into isolated hepatocytes. The study also found that in isolated perfused liver experiments excretion into bile followed the same rank order, indicative of the effect of the different hydroxylation pattern on the transcellular transport of these derivatives. Hence these compounds are still potential tools for defining the role of the steroid ring in the interaction of bile acids or other steroids with intracellular organelles and membrane transport systems [51].

In contrast to this work Rohacova *et al.*, have more recently described the synthesis of four compounds incorporating the dansyl group on the 3- and 7- position of CA (**31-34**) in both the alpha and beta orientations. These studies were conducted in parallel by this group with the NBD-CA derivatives (**25-28**) [28, 41]. In contrast to the NBD labelled bile acids, the dansyl compounds are both UV active and display green fluorescence. Furthermore these compounds were taken up in a time and concentration dependent manner into isolated rat hepatocytes, the **31** compound being taken up most efficiently. There was also regioselective uptake of **33** over **34**, although the difference was not as great as that observed between the 3-dansyl isomers. Pretreatment with troglitazone, an inhibitor of bile acid uptake through both the NTCP and OATP transporters, led to a reduction in the uptake of the four compounds confirming that the dansylated derivatives were accumulating in the cells using the same transporter systems as natural bile acids [52].

In a later study these compounds were investigated for their ability to bind to human serum albumin. Using a combination of steady state and time resolved fluorescence Rohacova *et al.* determined the binding constants for formation of the fluorescent bile acid-albumin complexes. Very interestingly the study illustrated a region-differentiation of the compounds in their relative affinity for the two known binding sites of albumin. Using titration experiments with warfarin and ibuprofen which are known to selectively bind to albumin at site 1 and site 2 respectively it was found that **31** and **32** binds to albumin at site 2 whereas the C-7 compounds (**33**, **34**) bind to albumin at site 1. The group then used this region-differentiation to assess the different binding affinities of the natural bile acids and found that the C-3 labelled compounds were displaced by LCA but not by CA indicating that LCA binds to albumin at site 2 [53]. It is worth noting however that this regio-differentiation was not observed in the 3 and 7 NBD-CA derivatives (**25-**

28) tested by this group, which all seemed to bind to site 1. Hence the position of the dansyl group influences the binding site, which is not the case with the NBD derivatives. This underlines the utility of different fluorophores in answering different biological questions.

1.2.8. Fluorescein as fluorophore

Fluorescein is a widely used fluorophore for many applications; it can be used in microscopy (as gain medium), in forensics and serology or in dye tracing. Fluorescein and its derivatives are amine reactive reagents for covalently labeling proteins with relatively high absorptivity, excellent fluorescence quantum yield and good water solubility. Its excitation (494 nm) and emission maxima (521 nm) in water [54] makes it an important labelling agent for confocal microscopy and flow cytometry. It is available as a dark orange/red powder and soluble in water and alcohol.

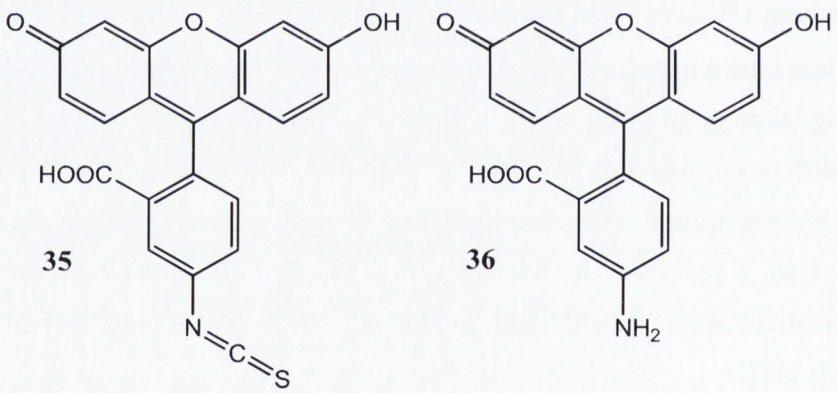

*Figure 1.16: Fluorescein isothiocyanate (**35**) and Aminofluorescein (**36**) are popular reagents to label biologically active molecules*

Fluorescein was first synthesized by Albert Baeyer in 1871 [55] and it has been used for decades to derivatize biomolecules. Several fluorescein derivatives are commercially available nowadays. Fluorescein isothiocyanate (FITC, **35**) or NHS-fluorescein (a succinimidyl ester group attached to the fluorescein core) are the most common amine active derivatives yielding stable amido adducts with biomolecules (e.g. intracellular proteins). Amino-fluorescein (**36**) is also used in many reactions to react with carbonyl groups to form amide bonds (*Figure 1.16*).

Beside its excellent fluorescent features, fluorescein has several significant drawbacks. First of all its fluorescence is pH sensitive [56, 57]; absorption and emission are significantly reduced below

pH 7 (pK_a~6.4). It also has broad emission spectrum which limit its utility in multicolor applications, together with a relatively high rate of photobleaching [58-60].

Although the molecular weight of this fluorophore is quite high, which affects the activity of the labelled compound; it is popular for labeling not just large molecules like proteins but also smaller bioactive molecules like bile acids. The high number of publications describing relevant applications shows that fluorescein is popular to label bile acids for studying distribution processes.

1.2.9. Fluorescein labelled bile acids

The first fluorescein tagged bile acid was described by Sherman and Fisher in 1986 [61]. To synthesize this the authors mixed equimolar amounts of **35** and sodium glycocholate (GC) in DMSO and stirred the mixture at 100 °C for 4 h. They proposed that the fluorescein moiety was linked to the A-ring of the bile salt at the C-3 position. This theory was disproved by *Schteingart et al.* in 1992 [62] and the correct structure of the adduct was assigned with the fluorescein coupled to the carbonyl group of the side chain giving fluorescent bile acid called cholylglycylamido-fluorescein (FITC-GC or CGamF, **37**) (*Figure 1.17*). This compound was resynthesized by Kitamura *et al.* [63] to determine biliary secretion in rats and by Briz *et al.* to study transport processes in rat liver [64]. In the latter publication the behavior and localization of **37** in live cells was followed by measuring fluorescence intensity, using 354 nm as the excitation, and 525 nm as the emission wavelengths. The limit of the detection was 0.2 μmol/l in this experiment. Further characterization of the fluorescent properties is not publically available.

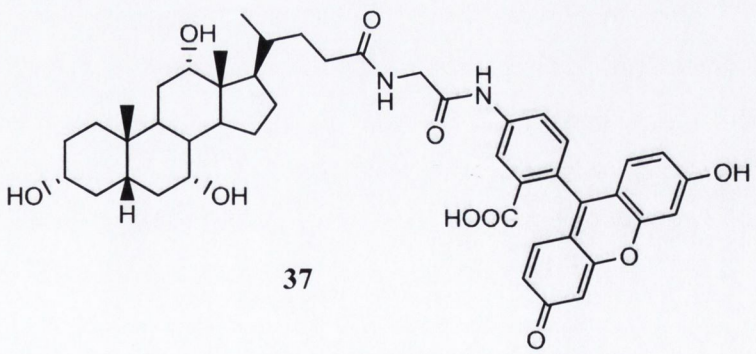

37

*Figure 1.17: Chemical structure of cholylglycylamido fluorescein (CGamF, **37**), the first fluorescein labelled bile acid*

Holzinger *et al.* prepared **37** coupling 5-aminofluorescein with the carboxylic acid group of CG in the presence of the coupling agent 1-(3-dimethylaminopropyl)-3-ethylcarbodiimide in a pyridine-hydrochloric acid buffer [31]. The absorbance of the compound does not change between pH 7.0 and 8.0, and it shows maxima at 492 nm at the latter pH value. This was measured in isotonic TRIS buffer. Quantum yield, emission maxima, fluorescent life time or other photo physical properties are not described. Mita *et al.* used the same method to prepare the corresponding CDCA derivative (CDCGamF) [47].

Mills and colleagues coupled fluorescein to the carbonyl group of the bile acid side chain via an amino acid linker [65]. The fluorescent bile salt was synthesized in two steps. Cholyl lysine was produced first using excess N-ε-CBZ-$_L$-lysine methyl ester (**38**) and **2** in the presence of *N*-Ethoxycarbonyl-2-ethoxy-1,2-dihydroquinoline (EEDQ). The benzyl protection of the adduct was removed and the compound was transformed to the sodium salt of cholyl-lysine (**39**) using 0.1M methanolic NaOH solution with a yield of 94%. Compound **39** was then reacted with equimolar amount of **35** in bicarbonate buffer (pH~9.5) yielding 70% cholyl-lysine-fluorescein (cholyl-lys-F or C-L-F, **40**) after purification (*Figure 1.18*). The structure of the product was proven by elemental analysis and IR spectroscopy.

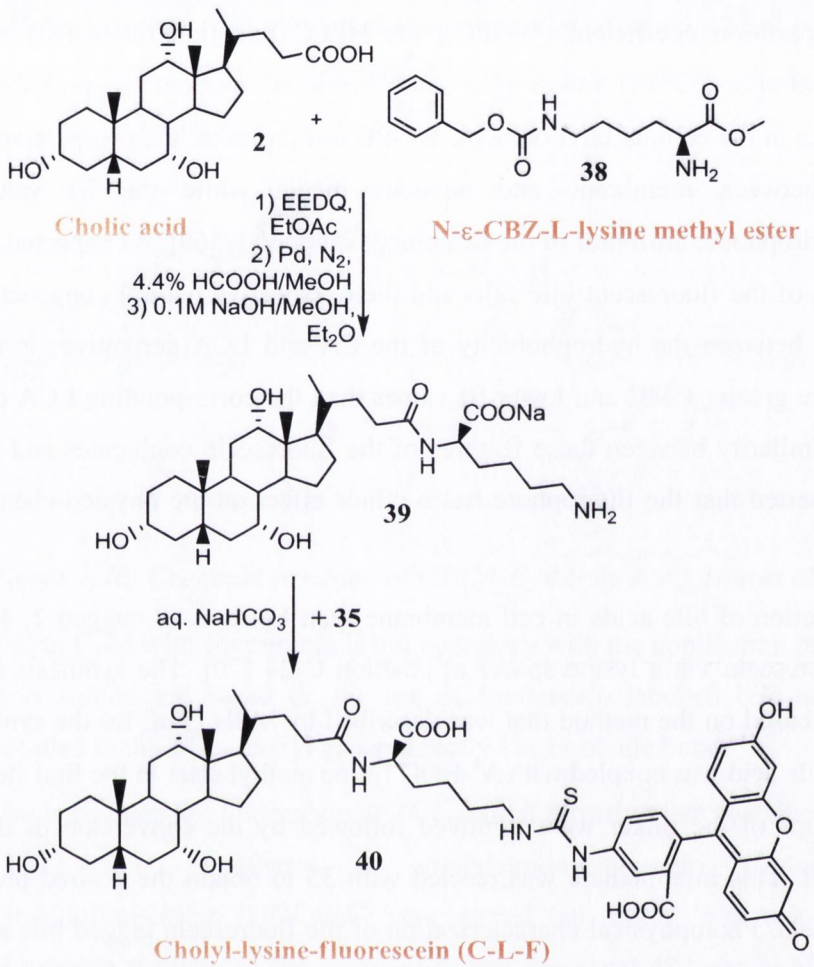

Figure 1.18: General synthetic approach to fluorescein labelled lysine conjugated bile acids

The heptane-buffer partition coefficient (HBPC), absorbance and emission maxima of **40** were determined. The HBPC was studied for three compounds ([^{14}C]glycocholic acid, **40** and F) at 500 μM concentration to evaluate solubility (the method was developed by Mills *et al.* in 1986 [66]). The means of the partition coefficients were 1.6×10^{-5} ([^{14}C]GC), 1.1×10^{-6} (**40**) and 1.8×10^{-5} (F). The absorption and emission maxima were similar to that of fluorescein with the values of λ_{abs}=490 nm and λ_{em}=520 nm.

In subsequent studies Mills *et al.* described some physical and biological properties of **40** and lithocholyl lysylfluorescein (L-L-F) [67, 68]. Lysyl fluorescein bile acid analogues can be compared to each other or to the parent compounds using various techniques. The authors used three parameters to describe the main physical properties of conjugated bile acids. The

water:octanol partition coefficient (WOPC), the HPLC retention times (Rt) and the critical micellar concentration (CMC) values give some information about the probable behaviour of these substances in the cellular environment. WOPC can represent the prospective distribution of a bile salt between membrane and aqueous media while the Rt values show the hydrophilic/hydrophobic attributes of the examined compounds [69]. As expected, the WOPC, Rt and CMC data of the fluorescent bile salts and their respective natural congeners were similar. The difference between the hydrophobicity of the CA and LCA derivatives is marked, as CA derivatives have greater CMC and lower Rt values than the corresponding LCA compounds. By virtue of the similarity between these features of the fluorescein conjugates and the related bile salts it was asserted that the fluorophore has a minor effect on the physico-chemical properties [67].

To study the action of bile acids in cell membrane Jean Louis *et al.* tagged **2**, **4** and **7** (*Figure 1.19*) with fluorescein via a lysine spacer at position C-24 [70]. The synthesis of DC-L-F and UDC-L-F was based on the method that was described by Mills *et al.* for the synthesis of C-L-F [65, 68]. The bile acid was coupled with N^{ε}-BOC lysine methyl ester in the first step, and then the protecting groups of the linker were removed followed by the conversion of the free acid to carboxylate salt. This intermediate was reacted with **35** to obtain the desired product with 35–37% overall yield. Photophysical characterization of the fluorescein tagged bile acid derivatives was not discussed in this publication.

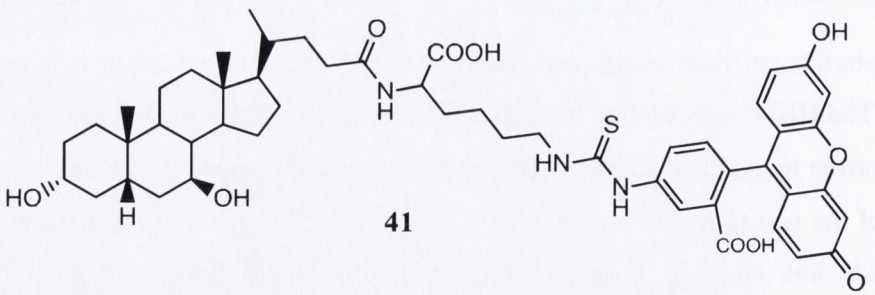

41

*Figure 1.19: Chemical structure of ursodeoxycholyl-lysine-fluorescein (UDC-L-F, **41**)*

Ki-Cheol Han and colleagues linked **35** to **3** at C-24 using ethylenediamine as spacer (*Figure 1.20*) and searched for inhibitors of CDCA interaction with the nuclear receptor FXR [71]. In this recent study the interaction between FXR and fluorescein labelled CDCA was detected directly using a fluorescence polarization method. The fluorescent bile acid was prepared in two simple

steps in which **35** was reacted with ethylenediamine then the obtained adduct was linked to **3**. The structure of the CDCA-F (**42**) was confirmed by mass spectrometry but the photophysical properties of the compound were not described.

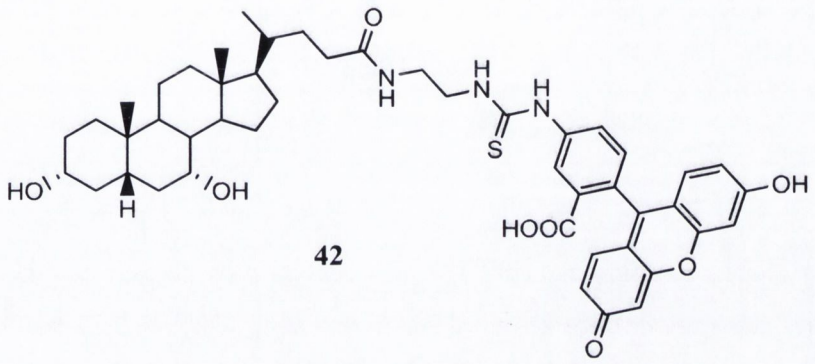

42

*Figure 1.20: Chemical structure of CDCA-F (**42**) by K.-C. Han et al.*

Tagging bile acids at C-24 with fluorescein is not necessary with the application of linkers. Many bile acid transport studies are based on the use of fluorescein labelled bile acids where the fluorophore is coupled to the 24-carbonyl group directly via an amide bond.

The first compounds coupled the fluorescein to 24-carbonyl directly were described by Holzinger *et al.* in 1997 [31]. Synthesis of cholylamidofluorescein (CamF, **45**) and ursodeoxycholylamidofluorescein (UDCamF) was carried out in one step using EDC·HCl in pyridine. The absorption maxima of the compounds was the usual 492 nm in pH = 8.0 buffer. These compounds were studied in live cell environment exploring bile acid transport processes [31, 45, 47].

Rohacova and colleagues worked out a different synthetic method to prepare **45**. They then studied the photophysical properties of this compound followed by as assessment of its potential flow cytometry applications [72]. The authors studied the absorption and emission wavelengths of the compound in different solvents using different pH conditions and described the fluorescence quantum yields and lifetimes.

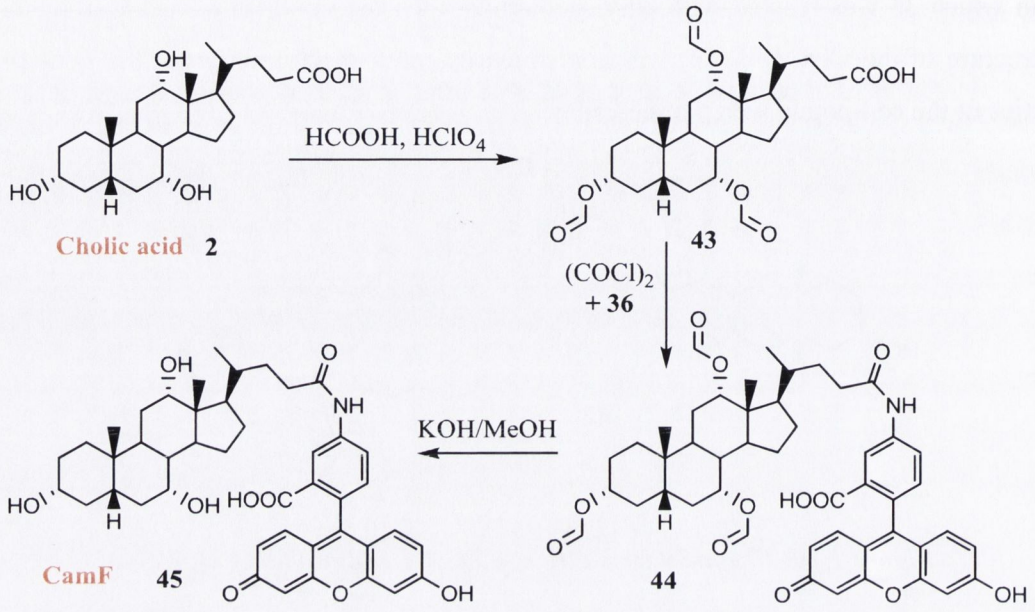

*Figure 1.21: Synthesis of cholylamidofluorescein (CamF, **45**) by Rohacova [72].*

Compound **45** was prepared in three steps with a good overall yield (49%). The synthetic route started with the formyl protection of the three hydroxyl groups followed by the coupling of **36** to the previously activated carbonyl group. The formyl groups were removed under basic conditions in the last step (*Figure 1.21*). This method is longer than the previously described, but it results in cleaner product that is important for photophysical studies.

The absorption and fluorescence properties of the molecule were examined under different conditions. In aqueous media the spectrum of **45** showed two absorption maxima at 450 and 490 nm. The intensity of these maxima changed dramatically within the employed pH range (between 2 and 12). In ethanolic solution the intensity of the absorption was examined in different atmosphere (air, CO_2, N_2,and O_2) and showed two maxima at 454 and 481 nm. The presence of O_2 and CO_2 significantly affected the spectroscopic features of the material.

The fluorescence spectrum of **45** was measured in EtOH (λ_{exc} = 481 nm) under N_2 atmosphere and showed the maximum at 518 nm. The quantum yield of the compound was determined in ethanolic solution (Φ = 0.67) using fluorescein as standard in 0.01 M NaOH solution under an atmosphere of N_2 (Φ = 0.85, λ = 490 nm).

Singlet lifetime (τ_s) of fluorescence was also measured in EtOH by means of time resolved fluorescence spectroscopy resulting in 4.8 ns.

Liu *et al.* examined the functional reestablishment of polarity in hepatocytes cultured between two layers of collagen [73]. To study the vectorial transport of organic anions and bile acids into this system they applied a fluorescein labelled taurocholate derivative (**46**). The fluorescent bile acid was stable under the experimental conditions and localized in the canalicular spaces after 10 minutes incubation.

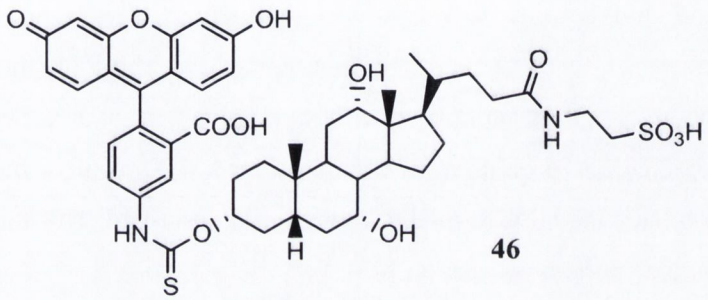

46

*Figure 1.22: Structure of fluorescein labelled taurocholate (**46**).*

However **46** is the only bile acid derivative where the fluorescein linked to the steroidal nucleus to date (*Figure 1.22*), the synthesis and photophysical properties of the molecule were not described.

1.2.10 Biological uses of fluorescein labelled bile acids

CamF **45** is taken up by live rat hepatocytes in a concentration-dependent fashion. However, CamF is much bulkier than **2** and lacks the negative charge at the side chain, which may affect its specific transport through the main bile acid transporters in the hepatocyte membrane-from [28].

Studies were performed by the Hofmann group to characterize the hepatic and intestinal transport, the biotransformation and the choleretic activity of fluorescent bile acids including cholyglycylaminofluuorescein (**37**), cholylysylfluorescein (**40**), cholylyaminofluorescein (**45**) and ursodeoxycholylaminofluorescein. Fluorescein was also used in these studies as a control. The biliary fistula rat model and jejunal and ileal perfusion studies were carried out. The fluorescent bile acids underwent <5% hepatic biotransformation during hepatocyte transport. CGamF was the only fluorescent bile acid which had normal choleretic activity and resembled the natural bile acids the best in terms of hepatic transport as well. Interestingly however the fluorescein compounds were not actively transported by the intestine [31].

Holzinger *et al.* characterized the transport of six fluorescent bile acids including cholyglycylaminofluorescein (**37**), cholylysylfluorescein (**40**), cholylyaminofluorescein (**45**) and ursodeoxycholylaminofluorescein. These were taken up efficiently by the isolated perfused rat liver but they were recovered to variable extents in bile due to hepatic sequestration. Recovery was 92.5%, 83.1%, 74.4% and 67.7% for **37**, **40**, **45** and UDCamF respectively. Recovery of cholylglycine (**8**) and cholyltaurine (**9**) was almost complete at 98%. Hence **37** and **40** resemble the natural bile acids best. Recovery of fluorescein by itself was 59.3%. Uptake of fluorescein is expected to occur passively at the hepatocyte without involvement of a carrier. It was also found that that sequestered UDCamF could be mobilized by a cAMP precursor but not by conjugated bile acids which mobilized the UDC-L-NBD as previously described. This indicates that there are two types of intracellular trapping occurring [45].

Martinez *et al.* reported that **37** was actively taken up in CHO cells expressing rat OATP1A1, human OATP1B1 or OATP1B3. This was done using flow cytometry and also using immunofluorescence [74].

In a recent study Murray *et al.* demonstrated that both CDCGamF and **37** accumulated rapidly in primary rat hepatocytes. Stably transfected HeLA cells expressing rat NTCP preferentially took up CDCGamF over those expressing rat OATP1A1. TCA and TDCA inhibited NTCP-mediated accumulation of CDCGamF by 98% and 95% respectively and depolymerisation by actin caused retraction of NTCP-GFP into a region surrounding the nucleus. The authors conclude that NTCP transporter activity can be affected by changes in its cellular distribution. Another interesting observation by this group was that accumulation of CDCGamF was variable and did not correlate with expression of NTCP in hepatocytes. In contrast to the work carried out by Martinez *et al.*, in this study there was no significant accumulation of **37** in cells expressing rat OATP1A1 or NTCP [46].

Work by Mita *et al.* illustrated that CDCGamF and **37** but **45** were substrates for both NTCP and BSEP in NTCP/BSEP coexpressing LLC-PK1 cells. The compounds were transported from the basolateral to apical side across the LLC monolayers at a rate 4.3-4.5 times that of the vector control. It is worth noting that these rates were smaller than those for radiolabelled TCA. As a result, the subsequent inhibition studies carried out by this group were conducted using radiolabelled instead of the fluorescent bile acids [47].

Rohacova *et al.* showed that **45** is specifically taken up by isolated rat hepatocyte suspensions in a flow cytometry based assay [72].

Maglova *et al.* also investigated the transport of **37** in isolated rat hepatocytes and hepatocyte couplets and reported a K_M value of 10 μM. In the absence of Na^+ the uptake rate of **37** was decreased by 50% and uptake was also inhibited by TCA. **37** was also secreted into the canalicular space of 50–60% of couplets screened [30].

Compound **40** is a fluorescent bile acid that is currently being developed for determining liver function *in vivo*. In a variety of cholestatic disorders the excretory capacity of BSEP and MRP2 in the hepatocyte is reduced. Bile acid levels can rise as a result and hence the transporters involved in bile acid uptake at the hepatocyte are downregulated. In primary biliary cirrhosis there is a decrease in the expression of the bile acid uptake transporters whereas the export systems are minimally affected. Therefore, determining the clearance of substrates of hepatocellular transport systems can be used as a measure of *in vivo* liver function. Traditionally agents such as sulfobromophthalein and indocyanine green have been used in the assessment of liver function however these compounds have disadvantages in terms of systemic reactions and allergy [75]. Over the past two decades, the Elias group have carried out a number of studies on the lysylfluorescein conjugated bile acids, with a focus on **40** and lithocholyl lysyl fluorescein [65, 67, 68, 76-79]. The synthesis and photophysical characterization of this compound was described in 1991 and its biliary kinetics and hepatic excretion were studied in Wistar rats and in the isolated perfused rat liver. Biliary output and hepatic extraction were found to be similar to the of **8** [65]. Subsequently synthesis of lithocholylysylfluorescein (LLF) was also described by this group [68]. Physicochemical properties of **40** and LLF including water:octanol partition coefficient, HPLC retention time and CMC were similar to those of GCA and GLCA respectively. Furthermore, in human and rat hepatocytes uptake of **40** and LLF closely resembled that of GCA and GCA in normal and multiorganic anion transporter knockout mice suggesting that **40** and LLF are substrates of the canalicular BSEP. The authors suggest that these similarities make the compounds potential useful tools for visualization of bile acid movement in various models of bile formation and secretion [67]. An experimental study was reported in which **40** was used to visualize the biliary tree of the rabbit in anatomic detail [80]. **40** and LLF have also been administered to rats to assess the fluorescent bile acids as tools for visualization of bile acid transport within liver tissue. After administration, serial liver biopsies were taken at

fixed intervals. The study found that both compounds were taken up from sinusoidal blood however **40** was rapidly transported into bile whereas LLF was slower, which resulted in greater bile duct fluorescence [79].

Compound **40** has been introduced as a potential alternative for measuring *in vivo* liver function [75]. A pilot study was conducted in which plasma clearance of **40** in six healthy humans was assessed. The volume of distribution and residual fluorescence of **40** after 60 min were similar to those of the natural or radiolabelled bile acids. The study also determined that **40** is safe at concentrations higher than 25 times the dose used (up to 0.02mg/kg body weight). Hence the study concluded that this compound may offer a new alternative for liver function assessment *in vivo* [77]. Subsequently a pilot study was conducted in 26 patients with liver cirrhosis using nine healthy volunteers as controls. It was found that plasma elimination of **40** was significantly impaired in patients with cirrhosis compared to healthy subjects. The test showed 100% sensitivity for liver cirrhosis when residual fluorescence was measured 30–60 min after injection and after 20 min it still showed greater sensitivity than routine liver function tests including bilirubin, total bile acids, aspartate aminotransferases, albumin and alkaline phosphatase [78].

In a recent study de Waart *et al.*, carried out a comprehensive investigation of the mechanisms of uptake and excretion of **40** by hepatocytes so that they could identify the proteins involved in its transport. Using *in vitro* studies in cell lines and plasma membrane vesicles and *in vivo* studies in mice, the group found that the NTCP and BSEP were incapable of transporting **40** and that transport of the fluorescent bile acid is mediated by OATP1B3 and ABCC2 [75].

Bile acids are synthesised by the fetal liver very early on in gestation and may be toxic when accumulated in blood and liver. Therefore transport of these compounds by the liver is of vital importance. In certain diseases including intrahepatic cholestasis of pregnancy the concentration of serum bile acids is elevated. Briz *et al.* used **37** in the search for new models for the study on the physiology and pathophysiology of this condition. The group measured the transfer of fluorescent bile acid given through the umbilical artery of *in situ* perfused rat placenta and collected this in the maternal bile in order to determine the usefulness of this model is evaluating the efficiency of the excretory pathway. The rate of FITC-GC output into bile was found to reflect the rate of transfer across the placenta of the rat. Therefore the authors suggest that the *in*

situ perfused rat placenta is a useful model to study the fetal excretion of cholephilic compounds [64].

Efficient transport of bile acids is lost in normal hepatocytes after some days in culture and also in most hepatoma cell lines. Bravo *et al.* used **37** to determine if polarized rat hepatoma-human fibroblast hydrid cell lines were able to perform vectorial transport of bile acids. It was found that two of the cell lines tested (WIF-B and WIF-B9) were able to accumulate **37** and that their transport was time, temperature and partly sodium dependent. The group used confocal microscopy to visualize the compound in the cytoplasm [81].

Lysyl fluorescein derivatives of CA (**40**), CDCA, UDCA and LCA have been used to visualize routes of transport across the hepatocyte and delivery to the canalicular vacuole of isolated hepatocyte couplets. **40** and CDCA-L-F were rapidly transported to the vacuole while the LCA and UDCA lysyl fluorescein derivatives accumulated more slowly with a punctuate fluorescence within the cell. Inhibition of vesicular transport by brefeldin A and colchicine dramatically impaired delivery of **5** and **7** to the vacuole [82].

1.2.11. Other fluorophores: synthesis, characterization and biological uses

As we have seen above dansyl, NBD and fluorescein are popular fluorophores used as reporter groups for bile acids especially in the study of their cellular transport and distribution. These components are usually linked to the 24-carboxyl group of the bile acid directly or via a spacer or they are coupled to the steroidal nucleus at position 3, 7 or 12. In this section there is a brief survey of less popular fluorophores used in the bile acid field.

Yamaguchi *et al.* recently published the synthesis and characterisation of a novel fluorescent bile acid derivative **47** (tauro-nor THCA-24-DBD) using 4-*N,N*-dimethylaminosulfonyl-2,1,3-benzoxadiazole (DBD) as a fluorophore [83]. This fluorophore was coupled at C-24 of tauro-conjugated nor-C27 bile acid derivative via an amino group (*Figure 1.23*). The sequence started with the production of the 3,7,12-triformate 24-oxo, 26-ethyl ester derivative. This intermediate was treated with ammonium acetate and $NaCNBH_3$ to afford the 24-amine which was coupled with DBD-F in the next step. The ethyl ester and formate groups were then hydrolysed and the free 26-carboxylic acid was conjugated with taurine to give the final fluorescent bile acid derivative (**47**). Its structure was provided by NMR and mass spectrometry and the absorption

and emission spectra of the compound were determined in acetonitrile showing the maxima at 454 and 570 nm.

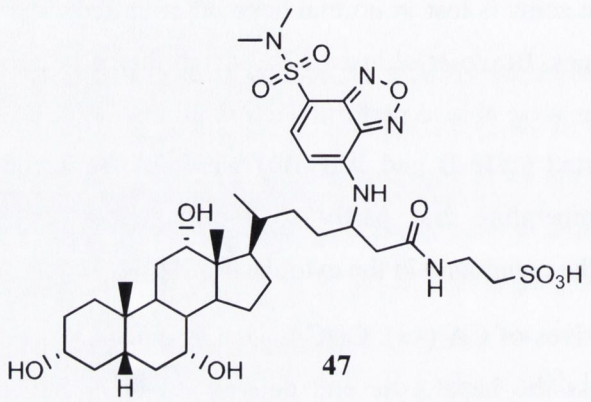

47

Figure 1.23: Chemical structure of tauro-nor THCA-24-DBD

Using membrane vesicles obtained from hBSEP-expressing Sf9 cells they found that **47** was taken up into the vesicles in an ATP dependent manner. A K_M value of 23.1 μM for the derivatives and a V_{max} of 632.2 pmol/min/mg protein was reported. These values are comparable to those found for **9** in this system. As the compound consisted of a mixture of diastereomers the group attempted to chromatographically separate the isomers under LC-MS conditions and concluded that since the peak area ratio of isomers in the chromatograms obtained from the incubation mixture were almost the same, the transport properties of the 24R and 24s isomer were identical. Inhibitory effects of various drugs on transport were also investigated. Rifampicin, glibenclamide, cyclosporine A, pravastatin and TLCA inhibited uptake of **47** with TLCA being the most potent and efficacious inhibitor [83].

In recent years there has been much interest in the development of fluorescent sensing probes which target biologically important substrates such as amino acids, as this can provide information for understanding the mechanism of molecular recognition in biological systems. The CA structure has been exploited in the design of fluorescent sensing probes. Fang *et al.* developed three anion sensors (*Figure 1.24*, compound **48-50**) introducing anthracene via a thiourea group at C-24 or C-3 [84]. Compound **48** was prepared in five steps linking the fluorophore to the 24-carbonyl group via an amidothiourea spacer. The synthetic sequence started with the preparation of 7-, 12-carbamate of the adequately protected cholic acid then the carboxyl

hydrazide was formed in three steps. 9-isothiocyanomethylantracene was reacted with the obtained intermediate giving the anion senor.

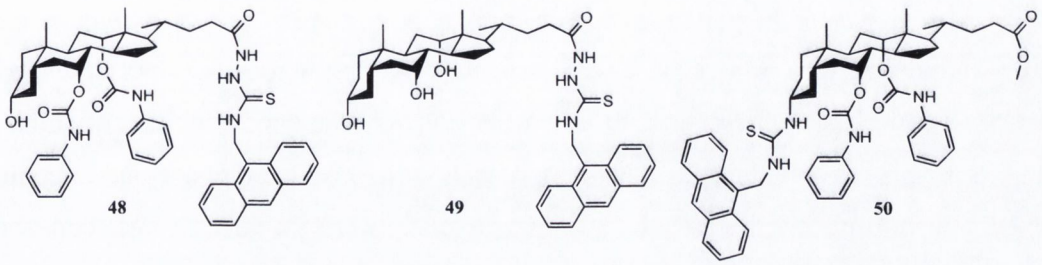

Figure 1.24: Anion sensors developed by Fang [84]

Compound **49** was prepared through a similar procedure without the addition of the carbamate groups leaving the 3, 7 and 12 hydroxyl groups free. To form compound **50** the 3-hydroxyl was converted to 3α-azide followed by introduction of the required carbamates. After the reduction of azide to amine the intermediate was reacted with the fluorophore giving the 3-anthracenylmethyl cholic acid derivative. The identity of each of the resulting compounds was proven by NMR, IR and HRMS and the absorption and emission maxima determined at 366 and 413 nm. The emission properties of the sensors can be quenched by different anions in the form of tetraalkylammonium salts. The fluorescence response of the compounds was examined in the presence of different anions using acetonitrile as medium.

In this work, the C7 and C12 hydroxyl groups were functionalized as carbamates serving as H-bond donors and amidothiourea group was introduced at C24 as an anion receptive site. The group introduced an anthracene moiety via the thiourea group as a typical emissive photoinduced electron transfer (PET) functional unit on the molecule. This resulted in a change in the fluorescence signal on interaction with guest molecules or ions. Collective studies on binding affinity towards carboxylates, dihydrogen phosphate and halides using compounds **48**, **49** and **50** illustrated that the amidothiourea moiety on the C17 side chain could work cooperatively with the H-bond donating groups on C7 and C12 to bind spherical halide anions.

If chirality can be introduced into the binding site then the resulting fluorescent host molecule may exhibit enantioselective recognition of chiral organic molecules. A sensor based in the CA structure has been used for enantioselective detection of tri-functional amino acids (*Figure 1.25*). The CA structure utilized consists of a chiral trans-1,2-diaminocyclohexane group attached at the 7- and 12- positions and an anthracene moiety at the 24 position which conferred fluorescence to

the molecule (**51**). The C24 side chain bearing the aminothiourea group was expected to strongly bind with a carboxylate group while the cyclic vicinal amino groups attached to C7 and C12 provide an additional binding site for hydroxyl and amino groups. The absorption and emission maxima were determined in MeCN (366 and 413 nm). Using fluorometric titration experiments in MeCN, in which the fluorescence of the sensors was quenched upon addition of amino acids, binding of the probes to the trifunctional amino acids serine, lysine, tyrosine and threonine was observed. Enantioselectivities (K_D/K_L) of up to 8.9 were achieved. The corresponding diastereomeric sensor **52** showed opposite enantioselectivity towards serine, threonine, lysine and tyrosine with comparable enantioselectivity between the two CA based compounds. This indicates that enantioselectivity of these compounds is due to the 1,2-diaminocyclohexane moiety [85].

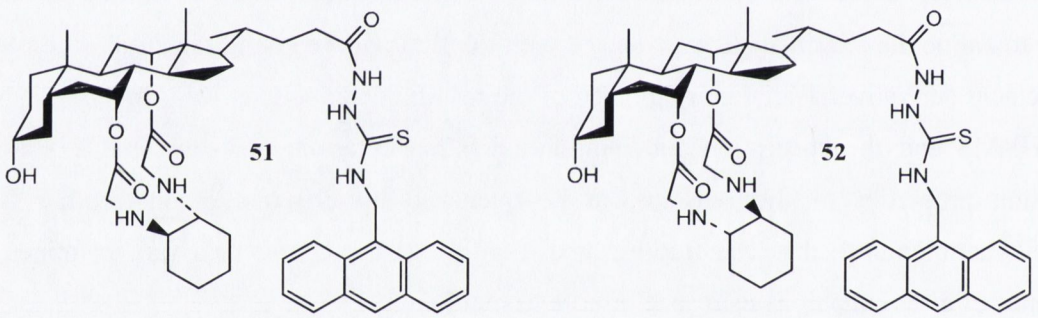

Figure 1.25: Sensors for trifunctional amino acids, developed by Wang et al. [85]

In a parallel study by this group compound **51** was used to detect interactions with a variety of phosphates and nucleotides including AMP, ADP, ATP, CTP, GTP, tetrabutylammonium dihydrogen phosphate and sodium pyrophosphate. The compound was selective towards ATP over other nucleotides. The authors suggest that this is due to a combination of electronic and spatial factors [86].

Cholic acid derivative containing two anthracene moiety (**53**) was developed by Liu *et al.* in 2005 as a chemosensor for dicarboxylates and acidic amino acids (Figure 1.26) together with the previously discussed 3-anthracenylmethyl cholic acid derivative [87]. The binding affinities of the probes were investigated in MeOH/water system at pH = 7.4 by fluorescence titration experiments. The synthesis of the compounds was as described above, while the excitation wavelength and the emission maxima was the same as in the case of the previous anthracene-containing compounds.

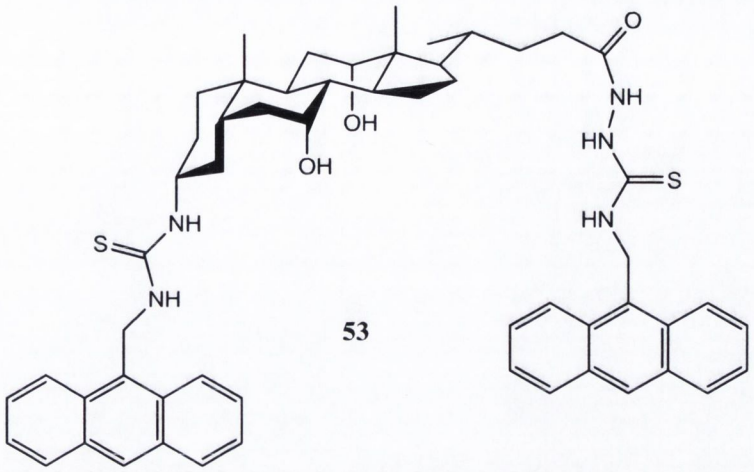

53

Figure 1.26: Chemical structure of dianthracenyl cholic acid derivative

The fluorescent intensity of **53** was measured in different solvents. Excitation wavelength was chosen at 366 nm and the solutions were prepared in 5.0×10^{-6} M concentration. It was found that the compound has high fluorescence intensity in chloroform ($CHCl_3$), while it is hardly fluorescent in acetonitrile. Mixing acetonitrile with HEBES buffer (1:1) or DMSO (0.04%) higher fluorescent intensity was observed, similar to the sensor in DMSO system. This compound showed good binding ability towards a variety of dicarboxylates and in particular towards glutamate.

Chapter 2

Design and Synthesis of Fluorescent Bile Acids

2.1 Aims and objectives

Applications of commonly used fluorescent reporter groups in bile acid research were reviewed in the previous chapter. The Gilmer group has been working for several years in collaboration with Aideen Long and Dermot Kelleher and others on some important questions in bile acid actions and pharmacology. Our group has a particular interest in how bile acids induce cell death (this is particularly important in the case of DCA, LCA and CDCA). Some of the events preceding cell death- organelle damage to the Golgi apparatus and ER area also unexplained. How does UDCA block some effects of DCA and CDCA? Does it require them to be co-localised? Are they cell surface mediated events or do the bile acids penetrate cells? At the outset of this work it was believed that the major feature of DCA and UDCA causing them to exhibit such markedly different effects was their relative polarity and differing cellular access. Cells without a transporter were believed to be impermeable to UDCA. Related to these questions of organelle damage and apoptosis were a set of unexplained effects of UDCA. This has been known for 20 years to activate the glucocorticoid receptor and cause its translocation to the nucleus [88, 89]. There is some evidence that UDCA's anti-inflammatory effects in hepatic disease are due to this and it may even explain its ability to prevent DCA induced Golgi fragmentation because a similar effect is observed with the classical glucocorticoid receptor (GR) agonist dexamethasone.

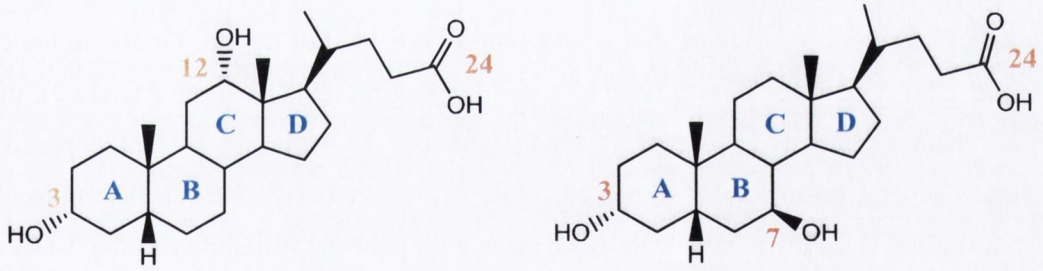

Figure 2.1. Structures of UDCA and DCA

In another collaborator lab (Stephen Keely, Royal College of Surgeons in Ireland at Beaumont), it has been shown that DCA causes ion secretion from monolayers of colorectal cancer cells (T84) and that it amplifies the effect of carbachol, an acetylcholine mimic [90]. Here too UDCA has an opposing effect, preventing ion secretion induced by carbachol. Here a mechanism

remains elusive, nor is it even clear whether it is cell surface mediated or an intracellular interaction. Another issue about disposition is that whereas it is possible to detect specific transporter proteins in cells and tissue, it remains difficult to detect functional transporter activity for bile acids. This is usually done with radiolabelled material which is difficult to handle and not suitable for high content analysis and live cell imaging of distribution. There are many questions about the biochemistry, physiology and pharmacology of these bile acids connected in some way to their disposition and especially cellular localization that suitable fluorescent reporters could help answer. However, when we examined the available or previously reported fluorescent derivatives of UDCA and DCA, none seemed suitable for our work. As already outlined a number of NBD substituted amino acid conjugates of the bile acids have been reported but these are relatively high in molecular weight, polar and probably not candidates for passive diffusion, which is likely to be an important contributor to the distribution of the free bile acids. Generally the amino acid conjugates substituted with NBD appear to be more suitable for investigating the glycine conjugates rather than the free bile acids. Similarly incorporation of a reporter group at either the C7 or C12 –OH groups appeared undesirable because these hydroxyl groups may be conferring on UDCA and DCA respectively the properties or interaction capabilities which account for their different effects. Incorporation of the fluorescent reporter group in the A ring appeared to use to optimal for investigating questions related to UDCA and DCA disposition. This would conserve the characteristic free acid side chain and 7- or 12- hydroxyl groups. There are a number of other observations that would support this kind of design. Firstly, in the crystal structure of UDCA with the intracellular bile acid binding protein (IBAP or AKR1C2), the bile acid side chain is buried deep in the protein with the 3-OH group solvent exposed [91]. Furthermore several groups have shown that bile acids can be used as carrier molecules to improve intestinal absorption by linking substances with poor bioavailability to the 3-OH of the bile acid [92-94]. This shows that the transporter proteins in this case can tolerate a mode of binding substrates with bulky 3-substituents. Surprisingly, given the activity in the area, 3- dansyl or NBD derivatives of UDCA or DCA had not been described previously (these might be called 3-deoxy-3-amino NBD or dansyl but for the sake of simplicity here will be referred to as 3-NBD or dansyl). The corresponding NBD derivatives of cholic acid have reported, as described in the previous chapter. Therefore the purpose of the work described in this Chapter was design and

synthesise UDCA and DCA analogues with a reporter group incorporated in the A ring (*Figure 2.2.*).

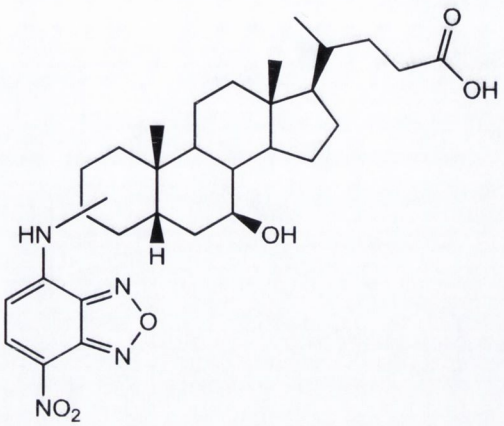

Figure 2.2. NBD-substituted UDCA derivative

2.2. Design and synthesis of A-ring fluorescent reporter bile acids

2.2.1. Synthetic discussions

The A-ring contains a hydroxyl group in the 3-position with alpha orientation, which permits reactions on the neighbour carbons at position 2 or 4. Initially our project focused on developing a fluorescent derivative of UDCA (7) attached the fluorophore at position-2. To obtain the desired compound we proposed a synthetic route *via* alkene- and epoxide-derivatives (*Scheme 2.1.*).

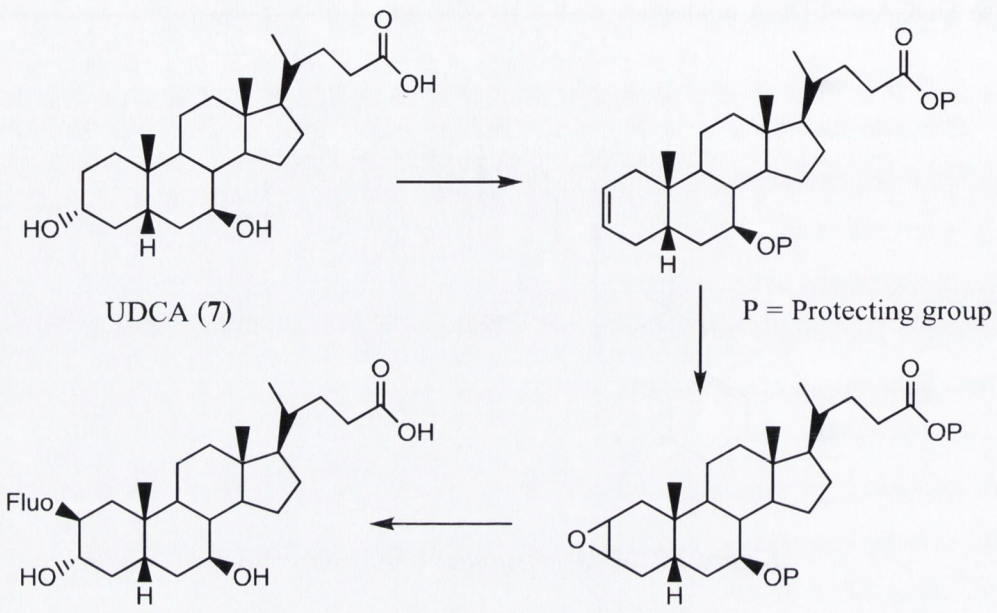

Scheme 2.1. Design of 2-fluorescent UDCA

As seen from *Scheme 2.1.*, the synthetic route proposes the introduction of the fluorophore at position 2 with β-orientation, while recovering the original 3α-hydroxyl, through opening of an epoxide ring. Also it includes necessary protection/deprotection steps. The scheme shows the intended route for the preparation of the fluorescent derivative of **7**.

2.2.2. Protection of UDCA (7)

The first step in the synthetic approach was the selective protection of the 24-carboxylic acid and the 7β-hydroxyl groups. Numerous studies can be found in the literature concerning the protection of bile acids [95-97]. The protection of the carboxylic acid was performed first. The most widely used approach to protect the carboxylic acid is esterification. Sebastien Gouin *et al.* obtained methyl esters in high yields from bile acids in an acid catalysed reaction [98]. We pursued this option. The formation of methyl ester **54** was carried out in MeOH by adding half an equivalent of 37% HCl at reflux. In this reaction, the solvent itself is the reactant and the mineral acid plays the part of the catalyst. After 1.5 h, TLC analysis did not show the presence of the starting material indicating that 100% conversion had been achieved. The TLC plate was developed in hexane – EtOAc 1:1 with vanillin solution used for detection. The lower polarity of the ester resulted in higher R_f value ($R_f \sim 0.25$), than the free carboxylic acid on the TLC plate.

After working up the reaction, the methyl ester was obtained as a white solid in high yield (91%). (*Scheme 2.2.*)

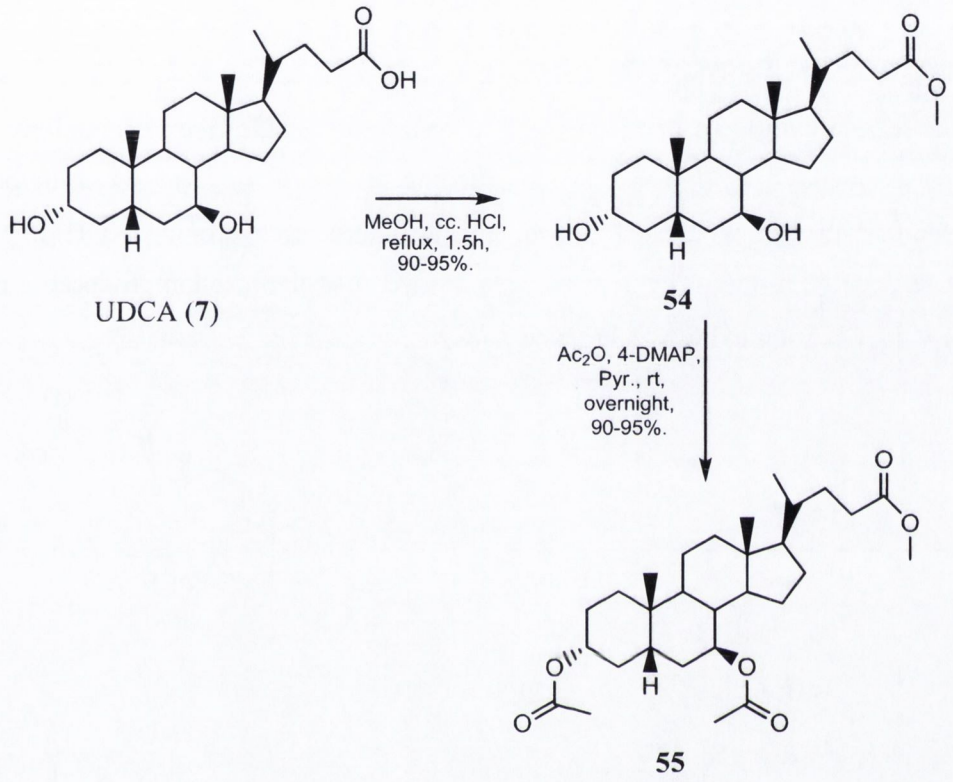

UDCA (7)

54

55

Scheme 2.2. Protection of compound 7

The selective protection of the 7β-hydroxyl at position-7 posed a challenging regioselectivity issue due to the α-hydroxyl at position 3 (both equatorial). Selective protection of the 7-hydroxyl group in methyl ursodeoxycholate is not possible in one step, because the 3-alcohol is more reactive than the 7, for steric reasons. Our approach was to protect both hydroxyl groups, followed by selective cleavage of the protecting group on the less hindered A-ring. Fieser and Rajagopalan acetylated cholic acid (**2**) on C3 and C7 selectively with acetic anhydride (Ac_2O) in pyridine to obtain 70% yield [99]. Bryson W. Katona *et al.* used 4-dimethylaminopyridine (4-DMAP) to catalyse this reaction to reach over 90% of the diacetyl product [100].

In our case, the esterification of both the 3- and 7-hydroxyl groups was successful with Ac_2O in pyridine with the use of 4-dimethylaminopyridine (4-DMAP) as a catalyst to yield diacetate **55** *(Scheme 2.2.)*. The formation of **55** was followed by TLC analysis using hexane – EtOAc 1:1 as

mobile phase. After stirring overnight the conversion was complete and the crude product was purified by flash chromatography to yield product **55** as white foam (89%).

2.2.3. Selective deprotection of 55

The regioselective hydrolysis of **55** on C-3 was attempted using different conditions. The most generally used method to achieve cleavage of the acetyl group is hydrolysis in the presence of base. In the first attempt, we treated **55** with aqueous potassium hydroxide (KOH) in MeOH and stirred at reflux for an hour. The TLC analysis showed that the reaction produced a mixture of UDCA **7** and UDCA methyl ester **54** *(Scheme 2.3.)*.

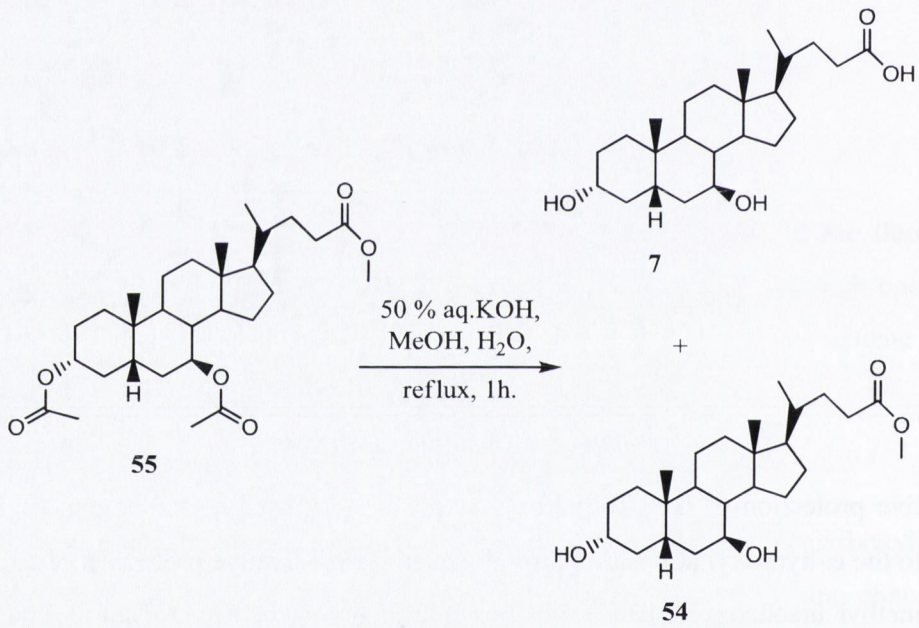

*Scheme 2.3. Attempted selective deprotection of **55***

Since the KOH was a too strong base in this case, we decided to use $NaHCO_3$ instead. The hydrolysis was carried out in MeOH at pH~10 at rt. After 2 d, the starting material had disappeared by TLC while the main spot of the three products was the expected compound. After working up and separating the mixture we obtained **56** in 65%. The reaction was then attempted on a larger scale. However in this case, the hydrolysis was not fully finished under the same conditions. After 9 d, the mixture was worked up to obtain **56** again in 65% yield. We recovered 21% starting material together with **54,** which appeared in a few percent *(Scheme 2.4.)*. It was not

logical to increase the reaction temperature to get a higher yield, because this was likely to reduce selectivity. The long reaction time did however require us to investigate an alternative approach.

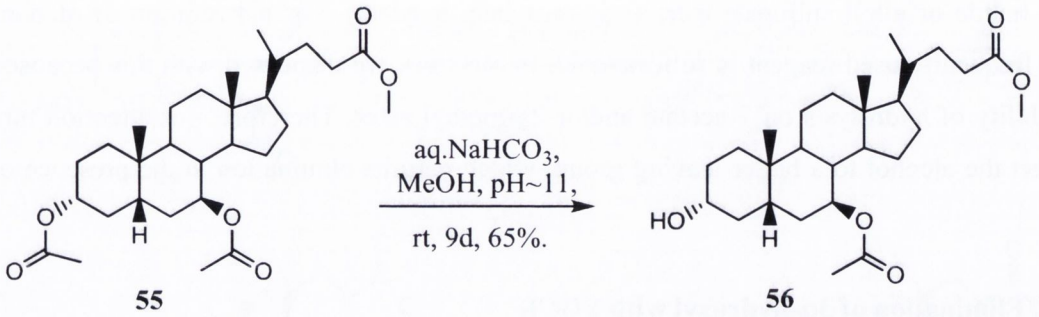

55 **56**

Scheme 2.4. Selective deprotection of ***55*** *with* $NaHCO_3$

A method for the selective deprotection of the 3α-alcohol was reported by Dias *et al.* [101]. They treated the triacetate derivative of cholic acid (**2**) with acetyl chloride (AcCl) in MeOH which led them to the deprotected diacetate at position-3. In our attempt, AcCl was added dropwise to **55** in anhydrous MeOH at 0 °C and left stirring overnight at rt. The TLC analysis showed that the conversion of starting material was complete and we obtained a mixture of **54** and **56** (approx. 2:3 ratio). The repeated reaction was monitored by TLC effected 75% yield of **56** and 12% yield of **54** after 6 h reaction time *(Scheme 2.5.)*. The formation of **54** and **56** did not show dependence on the scale of reaction.

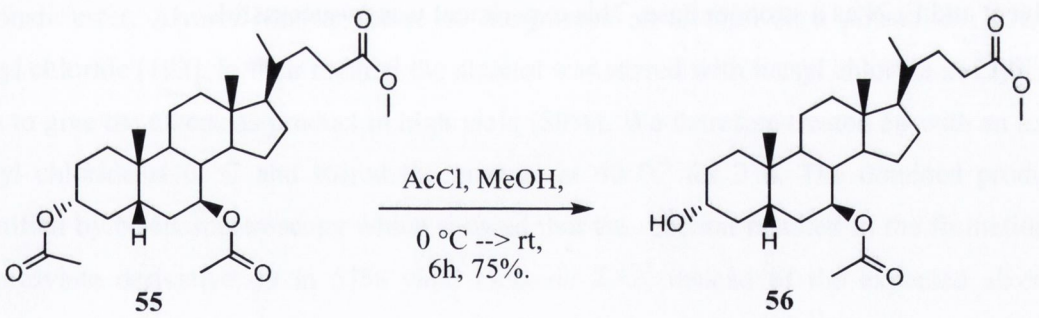

55 **56**

Scheme 2.5. Selective deprotection of ***55*** *with acetyl chloride*

2.2.4. Design of 2Δ–alkene derivative

After the preparation of the appropriately protected UDCA (**56**), the focus then shifted to the development of the 2Δ-alkene derivative. There are some well-known routes to synthesize an alkene derivative from the corresponding alcohol. Two common methods of elimination are

dehydrohalogenation of alkyl halides and more direct dehydration of the alcohol. In the dehydration reaction, water is lost *via* the E1 mechanism, while the E2 elimination starts with an alkyl halide or alkyl sulfonate ester (e.g. mesylate, tosylate). For dehydration of alcohols, the most frequently used reagent is sulfuric acid. In our case, we dispensed with this because of the possibility of hydrolysis on 7-acetate and/or 24-methyl ester. Therefore, our attention turned to convert the alcohol to a better leaving group, which permits elimination in the presence of mild base.

2.2.5. Elimination of 3α-hydroxyl with $POCl_3$

Yehuda Yanuka and Gideon Halperin treated 3,7- protected cholic acid (**2**) with phosphorus oxychloride ($POCl_3$) using pyridine as solvent to obtain the 11Δ-alkene [102]. The reaction mechanism begins with formation of phosphate ester, followed by E2 elimination, in which the pyridine acts as base. Our reaction was attempted under the same conditions. Upon dissolution of compound **56** in pyridine, 5.5 equivalents of $POCl_3$ were added and the resultant solution was stirred for 18 h at 40 °C. After the work up, the crude product was purified by flash chromatography to give the main product as light-yellow oil in 64% yield. NMR analysis showed that the main product was not the expected compound; instead, we obtained the 3β-chloro derivative (**57**) of **56**. *(Scheme 2.6.)*. The attempt was repeated at lower temperature using DCM as solvent and Et_3N as a stronger base. This experiment was unsuccessful.

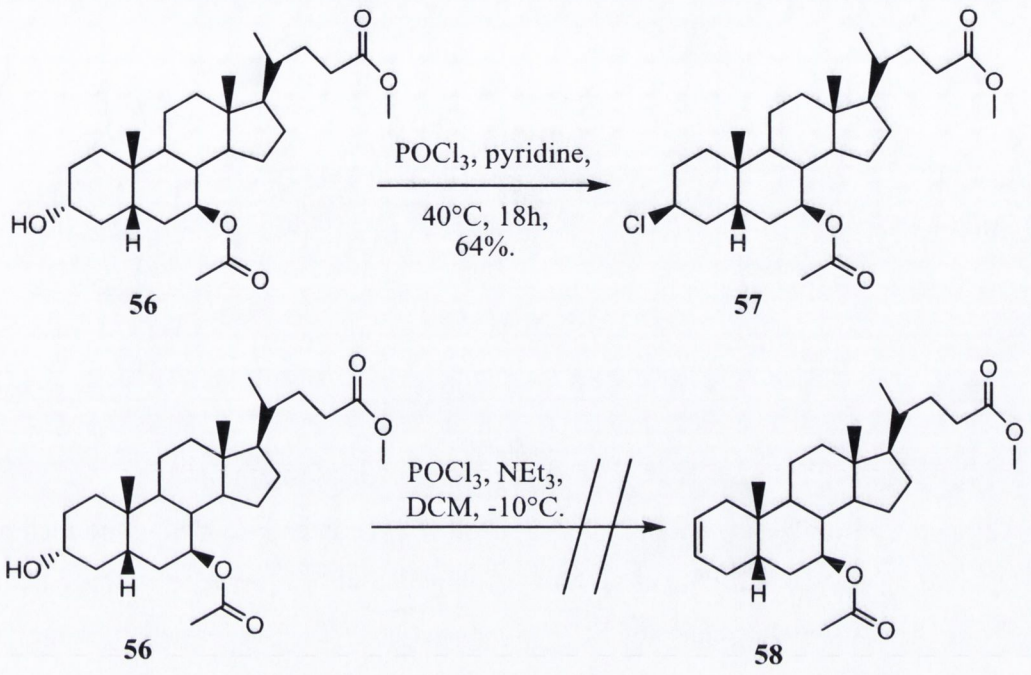

Scheme 2.6. Experiment for elimination of 3–hydroxyl with $POCl_3$

2.2.6. Elimination of 3α-hydroxyl with methanesulfonyl chloride

Another possible way to prepare alkenes is *via* alkyl sulfonate ester intermediates such as mesylate or tosylate. The elimination can be carried out in one step without isolating the sulfonate ester. Alvarez-Manzaneda *et al.* dehydrated an alcohol on a pinacol derivative with mesyl chloride [103]. In their method the alcohol was stirred with mesyl chloride in Et_3N at rt for 12 h to give the alkene as product in high yield (80%). We therefore treated **56** with an excess of mesyl chloride at 0 °C and stirred the mixture at 40 °C for 2 d. The obtained product was identified by NMR spectroscopy which showed that the reaction resulted in the formation of the 3α-mesylate derivative **59** in 57% yield *(Scheme 2.7.)*, instead of the expected alkene. The mesylate was therefore formed successfully during the reaction, but this was not followed by elimination. The success of this reaction is probably dependent of the type of base used.

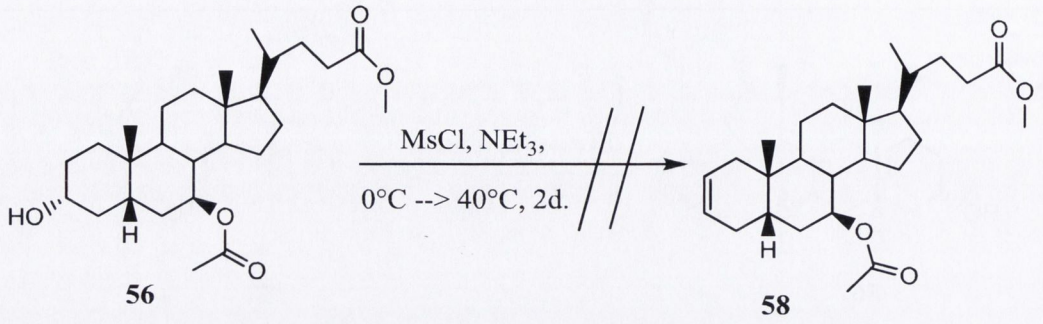

56 58

Scheme 2.7. Experiment for elimination of 3–hydroxyl with MsCl

2.2.7. Synthesis of 3α-mesylate

Hence, compound **59** was synthesized for the further experiments following the method which was reported by Vandana S. Pore *et al.* [104]. Compound **56** was treated with mesyl chloride in anhydrous DCM using 1.1 equiv. of Et_3N as catalyst at 0 °C. The formation of mesylate was carried out in 20 min furnishing **59** in 96% yield *(Scheme 2.8.)*.

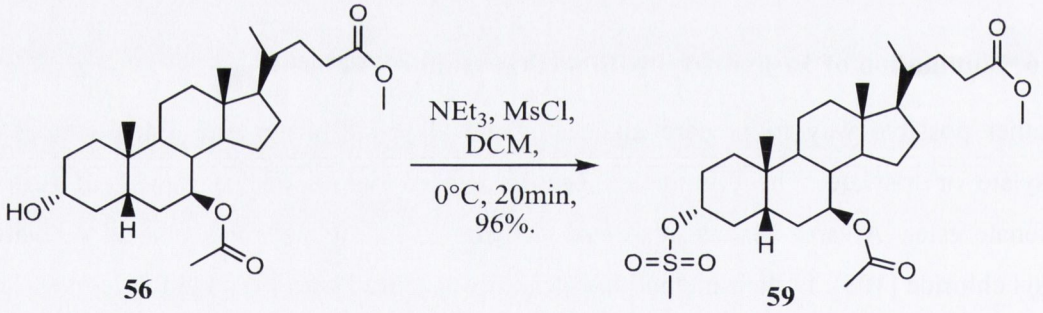

56 59

Scheme 2.8. Synthesis of ***59***

2.2.8. Cleavage of 3α-mesylate

Sulfonate esters are effective leaving groups in elimination reactions in the presence of base. 1,8-Diazabicyclo[5.4.0]undec-7-ene (DBU) is a commonly used catalyst to eliminate sulfonate esters. Hirota *et al.* applied this reagent on a quassinoid derivative with success [105]. In our next experiment, **59** was stirred with 5 equiv. of DBU in anhydrous tetrahydrofuran (THF) at rt. However, TLC analysis did not show any change after 24 h. Hence, 5 equiv. of DBU was added to the mixture again and the temperature of reaction increased to reflux. We did not observe any product on the TLC plate, so the reaction was stopped after 5 d *(Scheme 2.9.)*.

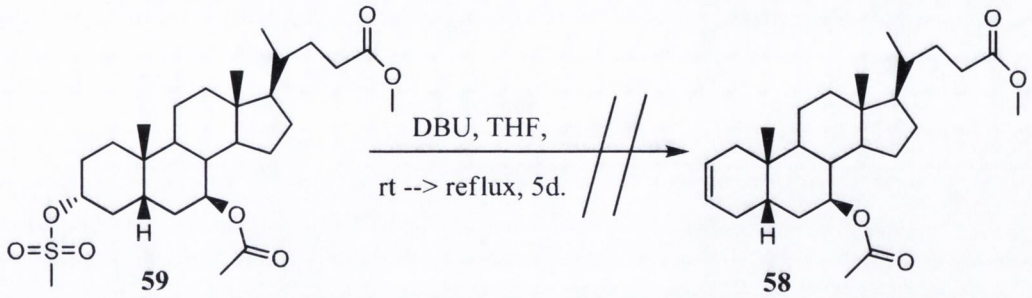

Scheme 2.9. Experiment for elimination of 3–mesylate with DBU

Gustavo A. Garrido Santos *et al.* carried out an E2 elimination on 3β-hydroxy-5α-cholestane tosylate with LiBr and lithium carbonate (Li_2CO_3) in dry DMF to obtain 5α-cholest-2-ene in high yield (85%) [106]. The same reaction conditions were used on **59** and all the starting material was consumed after 3.5 h. However, TLC analysis showed a high number of products with close R_f values and therefore this reaction route was abandoned *(Scheme 2.10.)*.

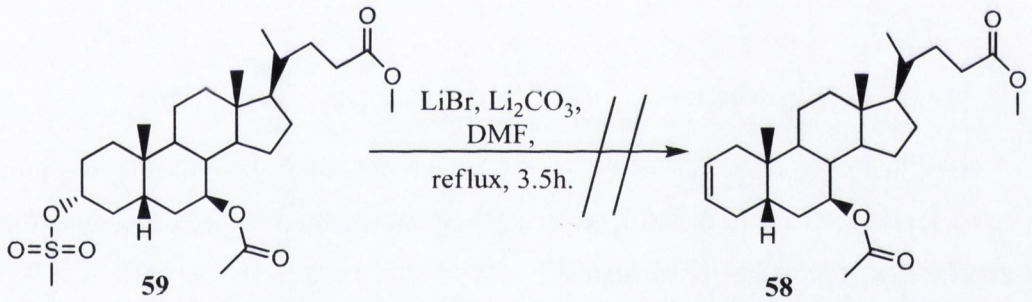

Scheme 2.10. Experiment for elimination of 3–mesylate with LiBr and Li_2CO_3

Holysz afforded the desired 2Δ-alkene [107] using similar conditions to above but without the Li_2CO_3. Using four equivalents of LiBr in our attempt, we found that the reaction did not work at rt. After 2 d, the temperature of the mixture was initially increased to 60 °C, then 120 °C. We noticed that some products appeared on the TLC plate after 7 d stirring, but some **59** was present also in the reaction mixture. TLC analysis showed a significant number of different products from which we concluded that different bromide derivatives were being formed. Hence, three equiv. of DBU was added to the mixture which was then stirred for 24 h at 120 °C, after which time the TLC analysis showed reaction progress. All of the starting material had been consumed and the product appeared as one spot on the TLC plate with higher R_f value (~0.72) than the intermediates after the treatment with lithium bromide (R_f~0.60-0.65) using hexane – EtOAc 5:1 as mobile phase. The higher R_f value indicates lower polarity and it appeared that the

intermediate might be a different bromide. After the work up procedure NMR analysis showed that the resulted product was the mixture of 2Δ-alkene **58** and 3Δ-alkene **60** approximately in 1:1 ratios *(Scheme 2.11.)*.

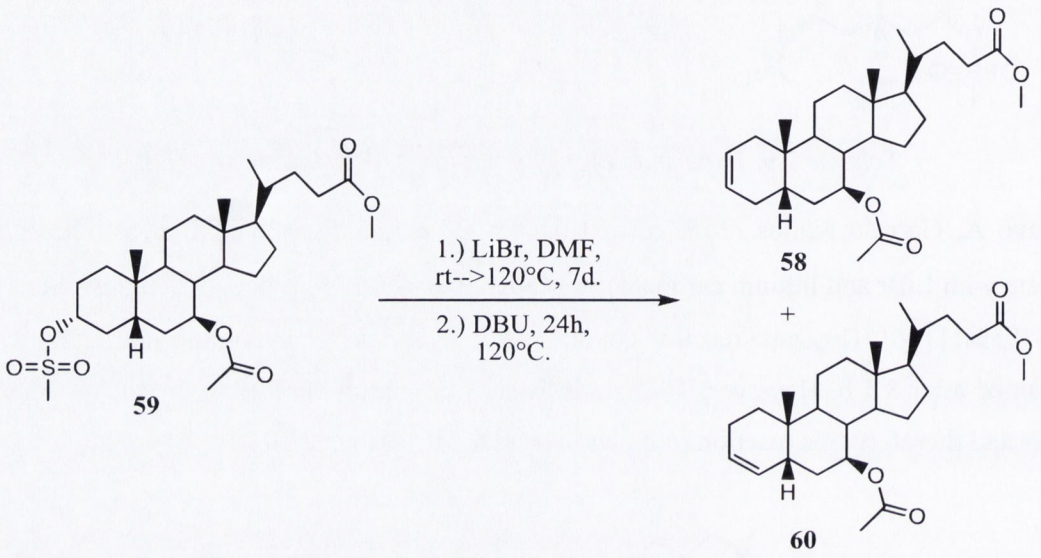

Scheme 2.11. Elimination of 3–mesylate with LiBr and DBU

Unfortunately the separation of the isomers was not possible; consequently we turned our attention to develop the epoxy-derivatives from **58** and **60** where we expected a bigger difference between polarities of products for separation.

2.2.9. Synthesis of epoxide isomers

Most epoxides are generated by treating an alkene with peroxide-containing reagents that donate single oxygen. Typical peroxide reagents include hydrogen peroxide, peroxycarboxylic acids and alkyl hydroperoxides. Typically for laboratory scale synthesis, the Prilezhaev reaction is employed [108]. This approach involves the oxidation of the alkene with a peroxyacid such as *m*-chloroperbenzoic acid (*m*CPBA). The reaction proceeds *via* what is commonly known as the "Butterfly Mechanism" [109]. The peroxide is viewed as an electrophile, and the alkene a nucleophile.

M. J. Comin *et al.* synthesized 2α-epoxy derivative from 5α-Pregn-2-en-20-one with *m*CPBA in 59% yield [110]. Our reaction was carried out under the same conditions. The mixture of **58** and **60** was dissolved in dichloromethane (DCM) and 2 equivalents of *m*CPBA was added in small

portions at 0 °C and then stirred at rt for 4.5 h. After this time, the TLC analysis showed that the starting material was converted into two products (R_f~ 0.42 and R_f~ 0.35 developed in hexane – EtOAc 5:1) *(Scheme 2.12.)*.

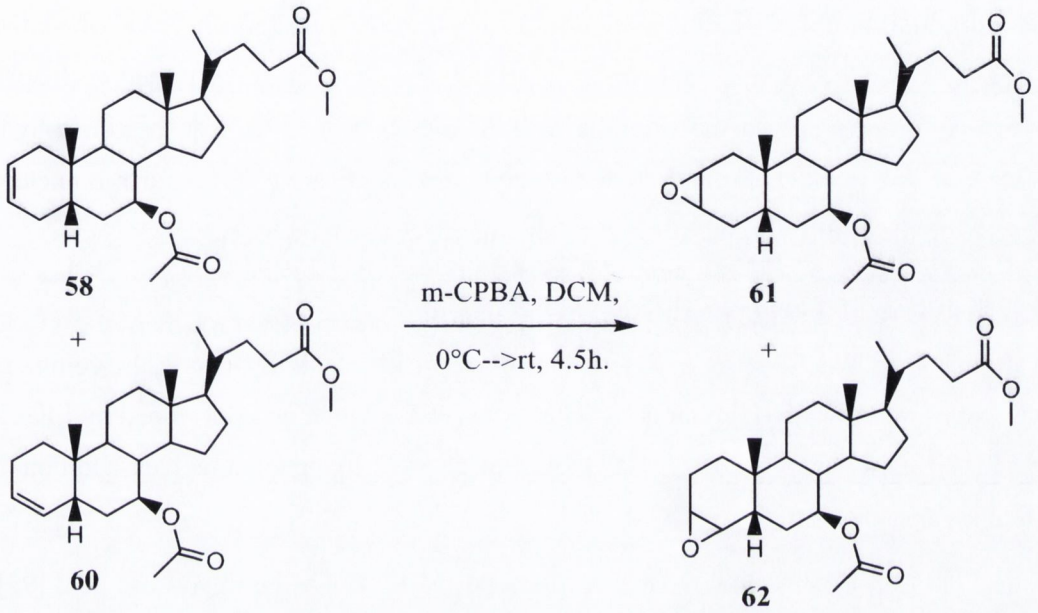

Scheme 2.12. Formation of epoxides

After separation by flash chromatography, NMR analysis showed that the reaction produced a mixture of α- and β-epoxides of **61** and **62** in low yields.

Although, some reports presented the preparation of 2Δ-alkenes then 2α-epoxides on *cis*-fused A-ring of steroids, we could not synthesize it selectively. In our case, the resultant product consisted of a mixture of 2Δ- and 3Δ-alkenes because of the mechanism of elimination. When the molecule is symmetric, the elimination reaction leads to a mixture of alkenes. The β-hydrogens on the carbon-2 and carbon-4 are equivalent from the aspect of elimination, where the most obvious potential influence would be the steric effect. However this did not lead us to success on *cis*-fused A-ring. In our experiments, the preparation of the epoxide derivative afforded numerous isomers and epimers. As a consequence of the high number of products, we did not proceed with further investigations along this line.

2.2.10. Development of 2- or 4-fluorescence derivatives *via* ketone derivative

Another possible way to allow the transformations on C-2 and C-4 is the development of 3-oxo-derivative from **56**. Ketones having α-hydrogen are in rapid equilibrium with their enol form, although this equilibrium is strongly shifted in the favor of the keto form in cases where the enol form is not stabilized. This keto-enol tautomerism is responsible for the increased nucleophilicity of the carbonyl oxygen and the electrophilicity of the α-carbon. As a consequence the α-hydrogen is relatively acidic, and ketones and other carbonyl compounds are able to undergo nucleophilic substitutions in the α position, with either stoichiometric or catalytic base.

2.2.10.1. Synthesis of 3-keto derivative

There are many options to generate ketones from secondary alcohols. One of the common used reagents in this regard is pyridinium chlorochromate (PCC) which was developed by Elias James Corey and William Suggs in 1975 [111]. A typical PCC oxidation involves addition of the alcohol to a suspension of PCC in DCM.

It was decided to use the sequence, which was reported by Bonar-Law with use of **2** [95]. The reaction was carried out in DCM using 1.2 equiv. of PCC at rt to obtain 3-keto compound **63** as product in 93% yield *(Scheme 2.13.)*.

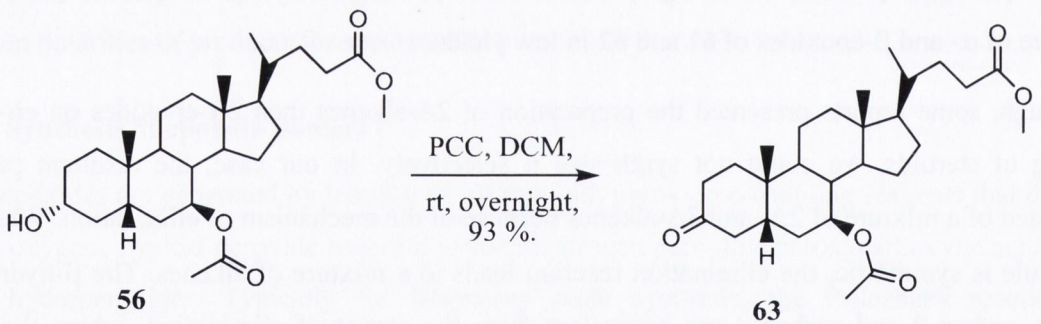

56 **63**

Scheme 2.13. Oxidation of 3-alcohol with PCC

2.2.10.2. Attempt for 2-hydroxymethylene derivative

For the preparation of 1-dehydro-3-keto steroids, we used a method developed by Shimizu *et al.* [112]. The 3-keto steroid would be first converted into the 2-hydroxymethylene derivative, **64**, using sodium methoxide (MeONa) and ethyl formate. This was then followed by dehydrogenation with 2,3-dichloro-5,6-dicyano-benzoquinone (DDQ), subsequent deformylation of the resulting 17β-hydroxy-5β-androst-l-en-3-one with chlorotris (triphenyl phosphine)

rhodium. However, the conditions reported by Shimizu *et al.* did not produce the expected product **64** from **63** (*Scheme 2.14.).*

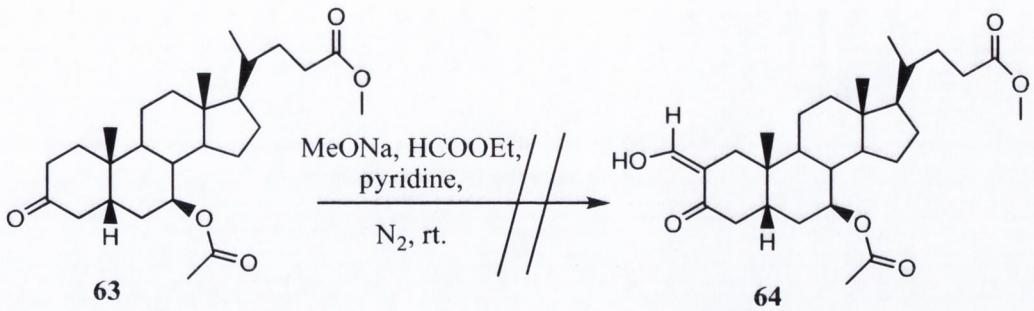

63 **64**

Scheme 2.14. Experiment for synthesis of 2-hydroxymethylene derivative

Although the authors could obtain the 2-hydroxymethylene derivative in over 90% yield, our attempt was unsuccessful.

2.2.11. Design of 4-fluorescent derivatives *via* haloketones

After this unsuccessful attempt, we turned our attention to synthesize the fluorescent derivative *via* α-haloketone intermediate. α-Haloketones can take part in nucleophilic substitutions in the activated α position, and we envisaged a synthetic route that would enable us to attach the fluorophore at position-4. We intended to synthesize the haloketone in the first step, and then convert the halo group into azide in a nucleophilic substitution reaction. Reduction of azide- and keto-groups would be carried out in the next step to obtain the corresponding 3-hydroxy and 4-amine derivatives, which would be followed by coupling the fluorophore to the amino-group *(Scheme 2.15.)*. An amine group seemed to be the ideal way to introduce a fluorescent group due to the high number of fluorophores available for amine labelling.

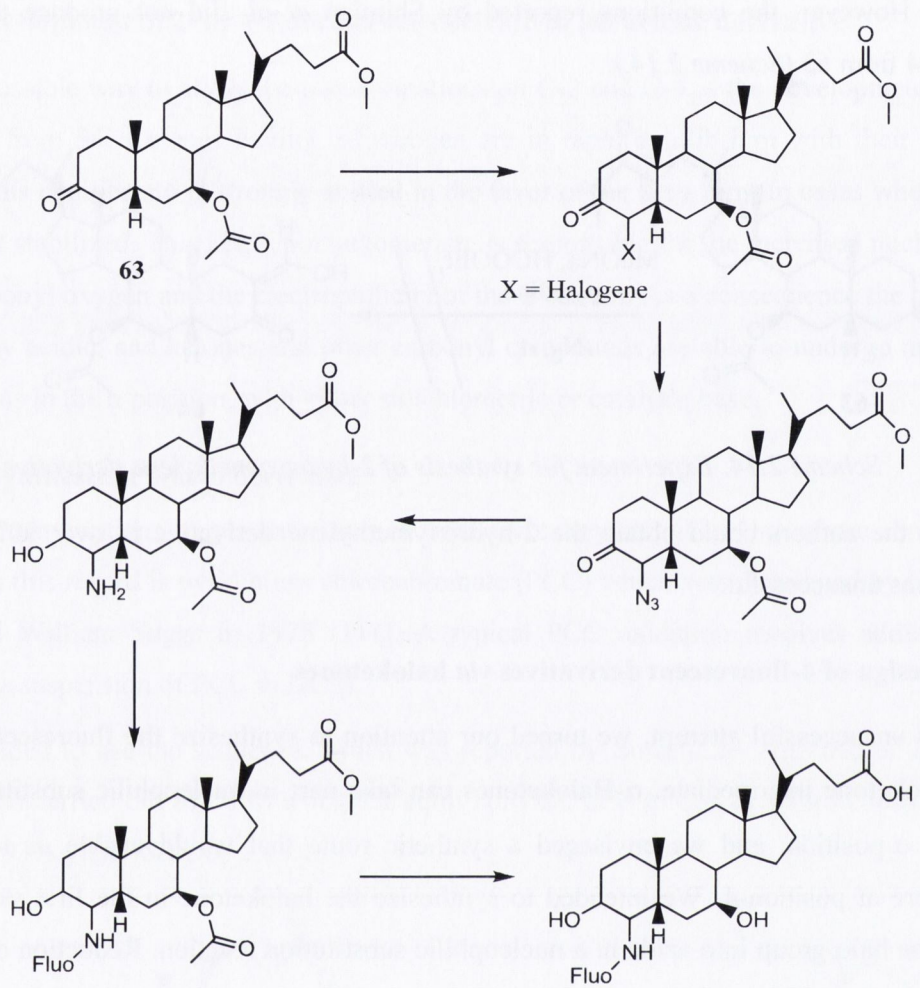

Scheme 2.15. Design of 4-amino-fluorescent derivative

Haloketones and halo carbonyl compounds in general are synthesized by the reaction of a carbonyl compound with a halogenation agent. For the synthesis of bromoketones such a halogenation agent can be bromine, tetrabutylammonium tribromide or *N*-bromosuccinimide (NBS).

2.2.11.1. Preparation of 4-bromo ketone

Several procedures can be found in the literature for the preparation of bromoketone steroids [113-115]. The solvent is acetic acid in most cases, but as bromine source, different reagents might be used. Bromine is a generally used reactant, which is sometimes applied together with hydrobromic acid. In our first synthetic attempt, **63** was dissolved in glacial acetic acid and bromine was added to the stirred solution at rt. The reaction was monitored by TLC analysis.

After 3 h, all starting material was consumed. The product was recovered as a white solid in high yield (89%). The structure was confirmed by NMR analysis as the 3-oxo-4β-bromo derivative **65** *(Scheme 2.16.)*.

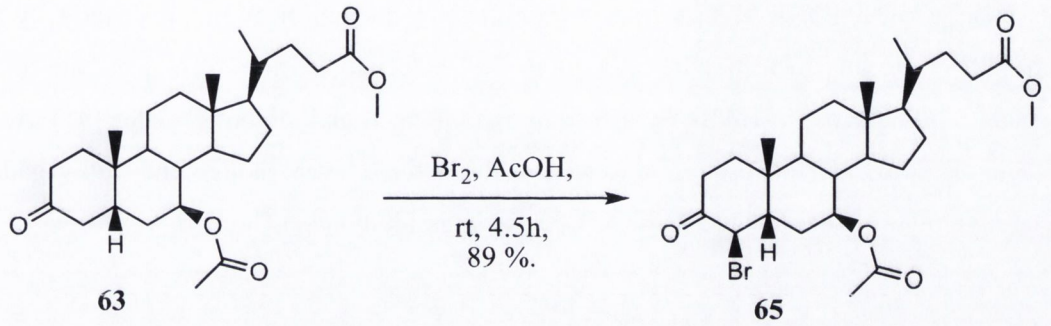

Scheme 2.16. Synthesis of 4-bromo 3-oxo derivative of UDCA-7-acetate methyl ester

2.2.11.2. Attempt for 4-azido ketone

To obtain the 4-azido derivative, we followed the procedure of Salunke *et al.* [116]. Therefore **65** was treated with five equivalents of sodium azide (NaN_3) in anhydrous DMF and stirred for 2 d at 40 °C. The reaction was not successful, thus it was repeated, without success again *(Scheme 2.17.)*. Although there are some precedents for this reaction in the literature in similar chemical environment, we could not carry out this substitution successfully.

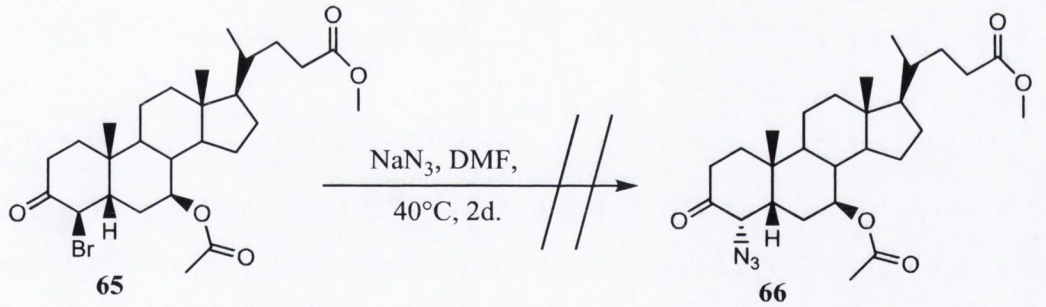

Scheme 2.17. Experiment for 3-azido ketone derivative

At the same time when this chemistry was being performed, a study appeared in *J. Med. Chem.* which indicated that the 3-hydroxyl group on A-ring of bile acids does not take part in protein binding in some instances [91]. Due to this information, and our ongoing difficulties with substitution at C2 or C4, we turned our attention to the transformations of the 3-hydroxyl group.

2.3. Design and synthesis of 3-fluorescent bile acids and non-bile acid controls

2.3.1. Introduction

This change of synthetic direction was prompted by the publication of a study by Simona Tomaselli *et al.*, in which they described an NMR solution structure of adduct between a liver bile acid binding protein (BABP) and bile acid-conjugated gadolinium chelates [91]. According to their experiments, the protein was able to bind these even though the bulky gadolinium chelating units were conjugated to the bile acids *via* amide-bond at C-3.



Figure 2.3. The Bile Acid Binding Protein (BABP, described by Tomaselli et al. [91])

Additionally, various bile acid carrier pro-drug conjugates have proven that intestinal bile acid transporters can tolerate payload incorporation at position-3 [117]. With this knowledge, future synthetic work focused on the synthesis of 3-fluorescence DCA and UDCA derivatives. Various SAR surveys and QSAR models of the human apical sodium-dependent bile acid transporter (ASBT, SLC10A2) suggest that the C3-OH is tolerant of modification [118, 119].

It was decided to introduce the fluorophore on to the bile acids *via* a 3-amino group in both of the epimers (α and β). It was also planned to synthesize a control compound with the same behaviour in the fluorescent properties lacking the bile acid moiety. For labelling **4** and **7**, we initially chose

the 5(dimethylamino)naphthalene-1-sulfonyl chloride (dansyl chloride, **29**) fluorophore, which is a widely used agent to modify amino acids.

2.3.2. Design of 3-dansyl derivatives and intermediates

Schemes *2.18* and *2.19* show our planned synthetic approaches to the newly proposed UDCA and DCA dansyl derivatives. These routes involved straightforward, well established synthetic reactions in the first few steps to obtain the 3-amino derivatives with the corresponding orientations, then the coupling of fluorophore to the amino group, followed by the hydrolysis of protecting groups.

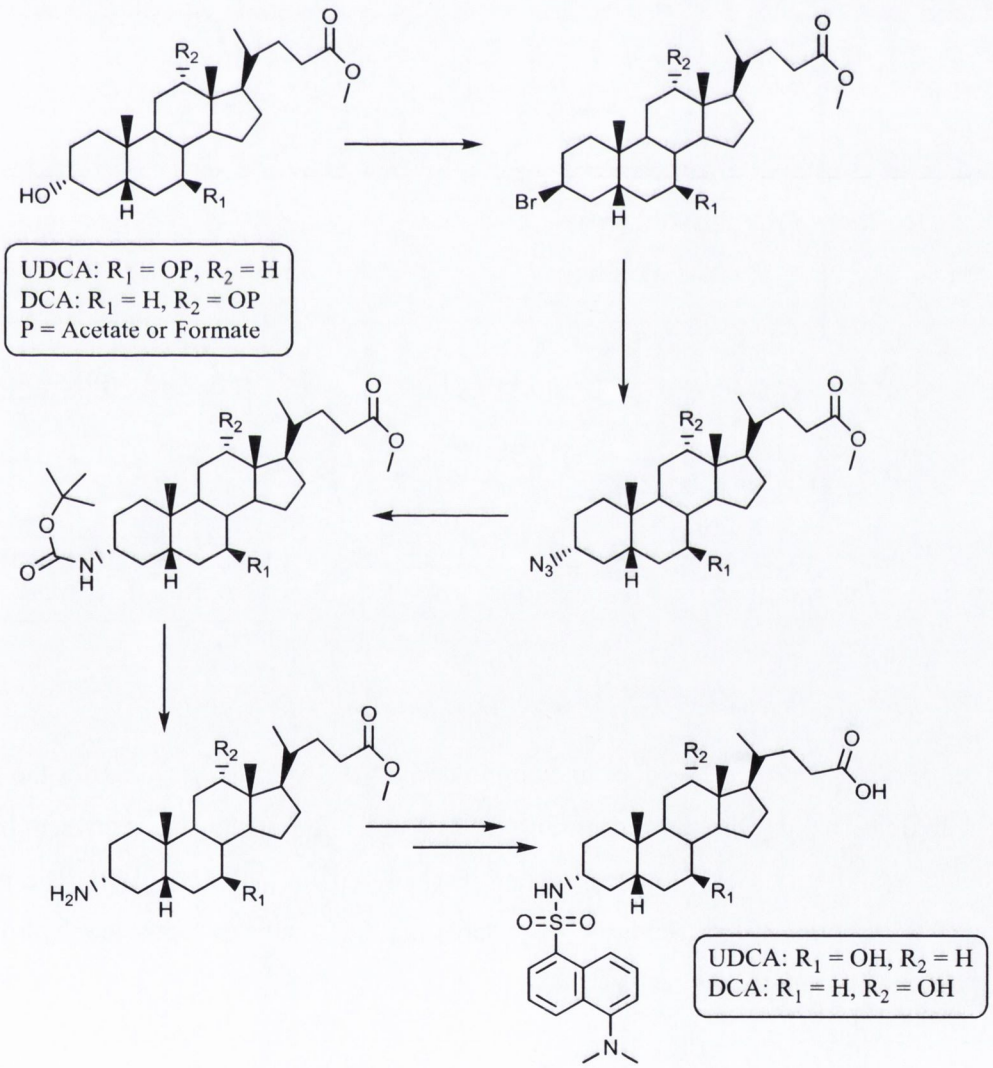

Scheme 2.18. Design of 3α-amino-dansyl derivatives

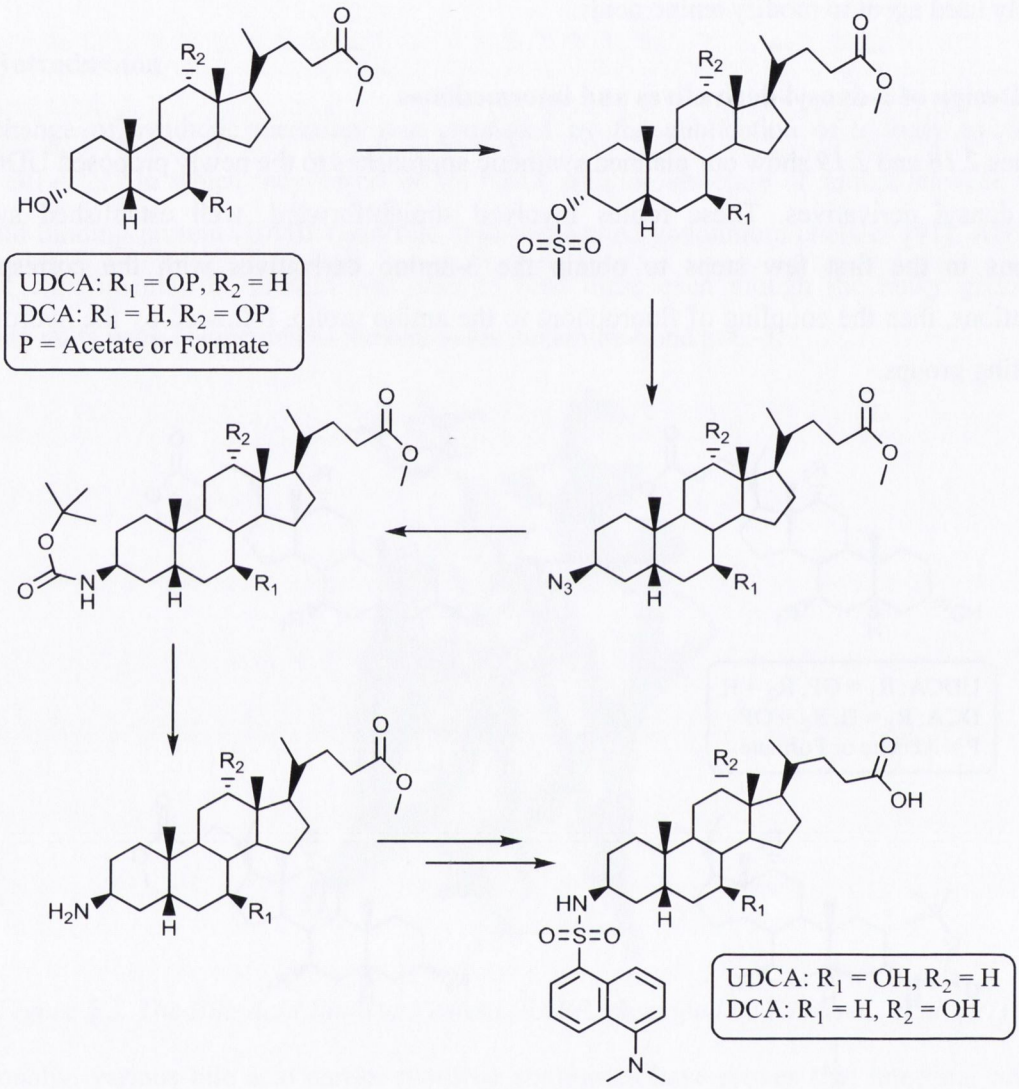

Scheme 2.19. Design of 3β-amino-dansyl derivatives

The isolation of the deprotected azido- and amino-derivatives was also required for the study of bile acid toxicity as it allowed our group to examine the relationship between bile acid hydrophobicity and toxicity on the normal oesophageal cell line HET1A [120]. The proposed compounds were synthesized from the corresponding intermediates with the hydrolysis of protecting groups. *Scheme 2.20.* represents the desired compounds.

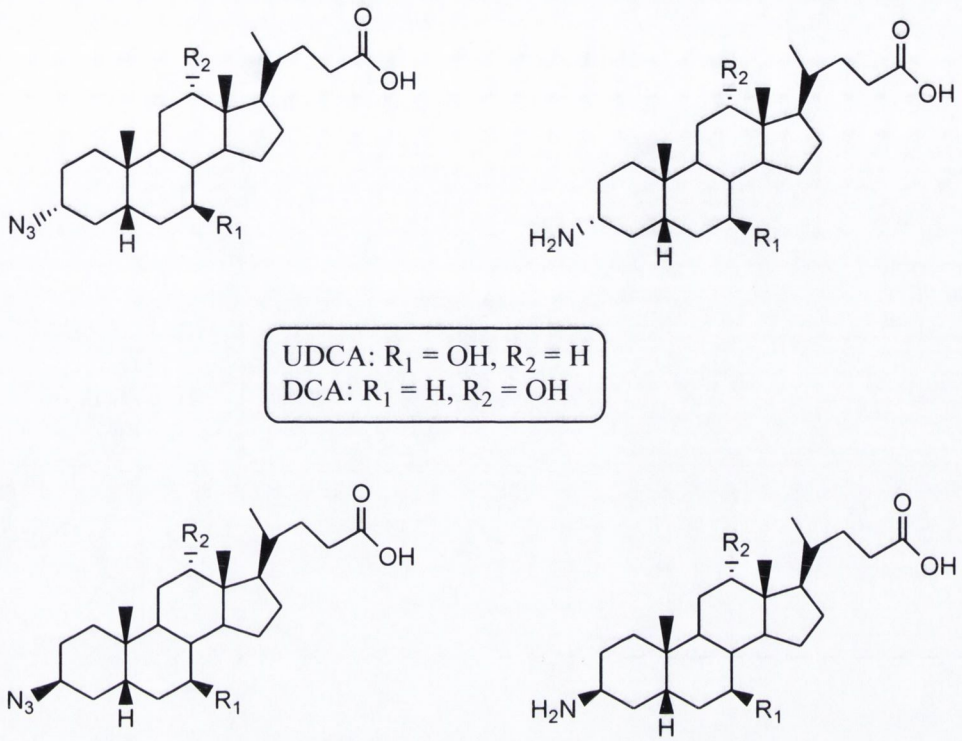

Scheme 2.20. The proposed deprotected intermediates

2.3.3. Protection of DCA (4)

For the transformations on C-3 of **4**, we needed to protect the 12-OH and carboxylic acid. A method had been developed for the protection of **7** as already described. In the present instance, the carboxylic acid was converted to methyl ester **67** under similar conditions in high yield, then the formation of diacetate **68** was carried out with Ac_2O in pyridine in the presence of 4-DMAP *(Scheme 2.21.)*.

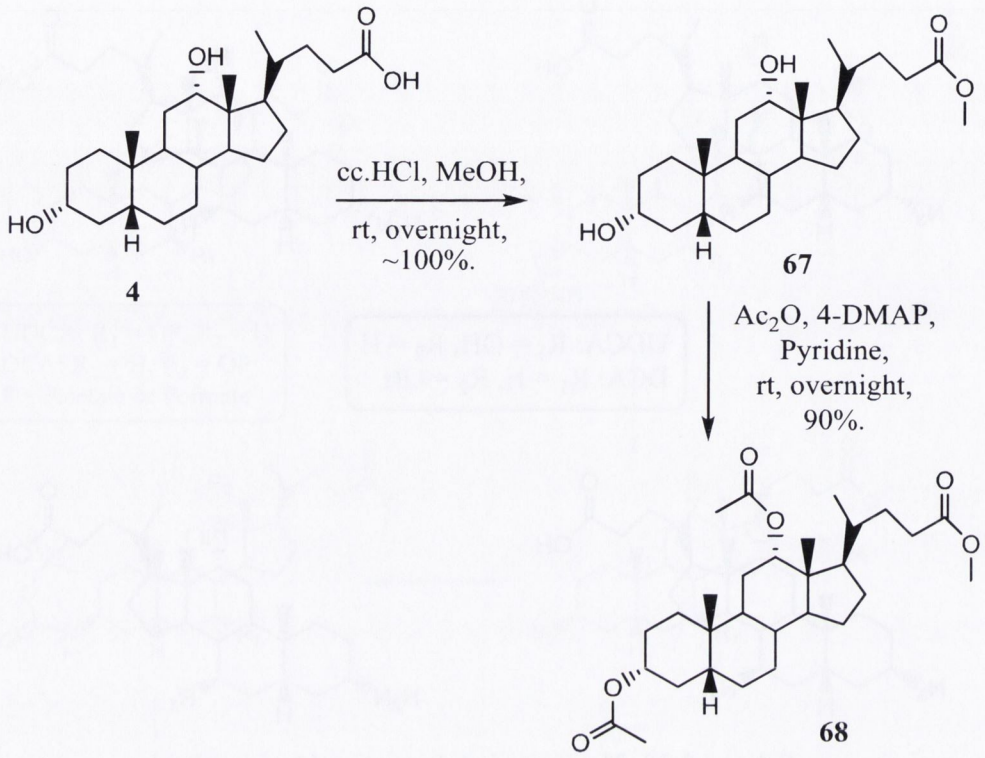

Scheme 2.21. Protection of ***4***

Previously we had used AcCl for the hydrolysis of 3-acetyl group, but in this case we tried less aggressive conditions. On the other hand, selective deprotection of 3α, 12α bile acid esters is less challenging because of the more hindered alpha (axial) orientation at position-12. MeONa is another commonly used reagent to hydrolyse esters and has the advantage that it does not convert methyl esters to acids provided an anhydrous atmosphere is maintained. Our attempt was carried out in MeOH at rt with 1.1 equivalents of MeONa. After 1 d the TLC analysis did not show the presence of **68**, thus the reaction was worked up and the crude product was purified by flash chromatography to give **69** as white foam in 87% yield, which structure was confirmed by NMR analysis (*Scheme 2.22.)*. Compound **4** and its methyl ester derivative **67** also appeared in the mixture in a few percent of the total amount.

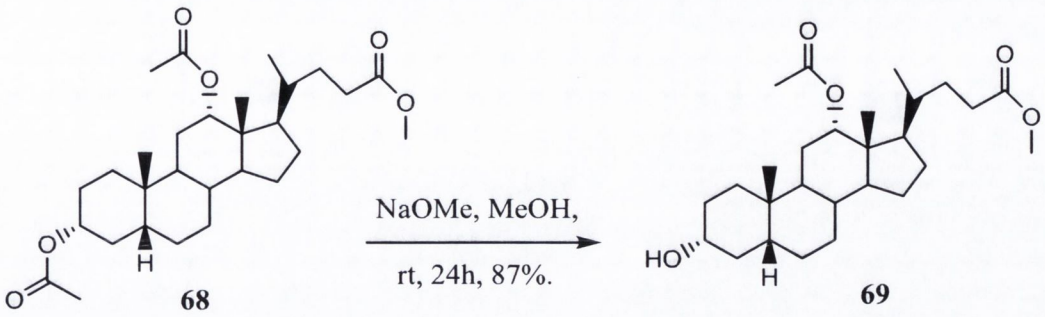

Scheme 2.22. Selective deprotection of ***68***

2.3.4. Synthesis of 3α-dansyl UDCA and 3α-dansyl DCA derivatives

It was then decided initially to develop equatorial 3α-fluorescent derivatives which would require overall replacement of the 3-OH with NH_2 with retention of configuration. There are numerous studies on the synthesis of amino derivatives from alcohol group of steroids in the literature [121-124]. The reported synthetic routes contain general reaction steps *via* bromo- and azido- or keto- and oximino-intermediates. To obtain the 3α-amino compound *via* bromo-intermediate, the alcohol first undergoes a nucleophilic substitution in a bromination reaction. This bromine is exchanged to azide in the subsequent step, and then the azide is reduced to the required amine.

2.3.4.1. Synthesis of 3β-bromo derivatives

We used NBS as a bromine source in the presence of triphenylphosphine (PPh_3), which is a good reducing agent. Using this method, the 3α-hydroxyl group is replaced by bromine *via* oxyphosphonium intermediate with inversion of configuration [125]. Compound **56** was treated with 2 equivalents of each reagent in anhydrous THF and after the disappearance of the starting material, the mixture was worked up and purified by flash chromatography to obtain **70** as colourless oil in 91% yield. The reaction starting from **69** was carried out as well under the same conditions to give **71** as product in 65% yield *(Scheme 2.23.)*.

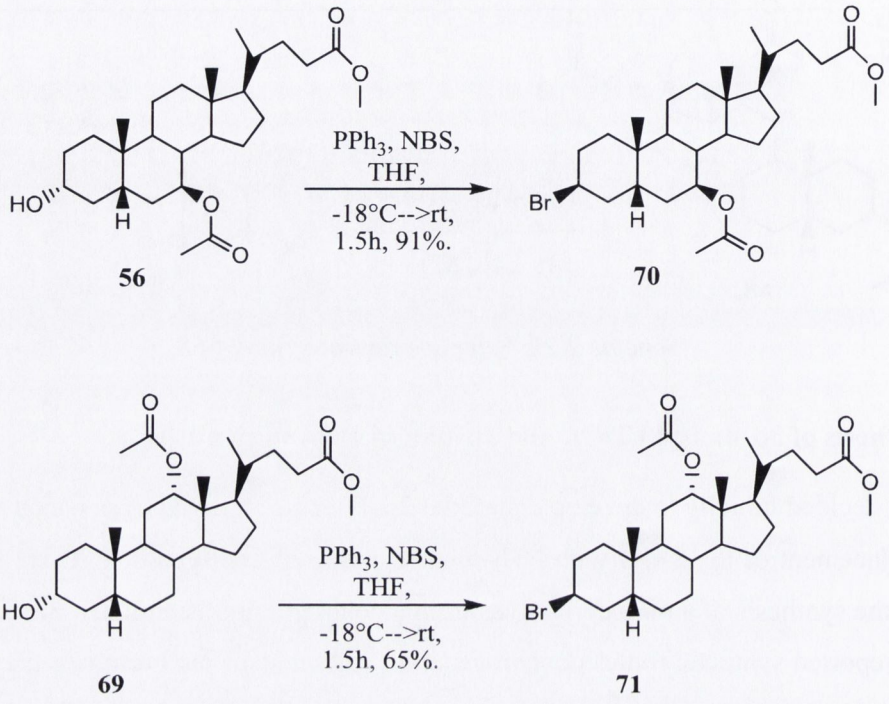

Scheme 2.23. Synthesis of 3β-bromo derivatives

2.3.4.2. Synthesis of 3α–azido derivatives

The resultant 3β-bromo derivatives were transformed to the corresponding azido intermediates in a nucleophilic SN2 substitution reaction. Most organic and inorganic azides are prepared directly or indirectly from NaN_3, which is the principal source of the azide moiety. The pseudohalogen azide anion displaces the appropriate leaving group (e.g. sulfonyl esters, I, Br) to give the azide compound. These azides were synthesized using the procedure reported by Pore *et al.* [104]. Compound **71** was treated with five equiv. of NaN_3 in DMF. The formation of the azide was followed by TLC analysis using hexane - EtOAc 3:1 as mobile phase. The difference between the R_f value of the starting material and the product seemed small, but the colour of the spots was different after development with vanillin solution, allowing us to follow the changes. The colour of **71** became dark purple under the effect of vanillin reagent, while the azide gave a yellow spot on TLC plate. After 24 h the reaction mixture was worked up and the azido compound was purified by flash chromatography to give **72** as light-yellow oil in 79% yield. 2Δ- and 3Δ-alkene derivatives also appeared in the reaction mixture as identified by NMR. The side-products can be formed due to dehydrohalogenation process mediated by the solvent. The reaction was carried

out on **70** as well under the same conditions to obtain **73** as light-yellow foam in 72% yield. The mixture of 2Δ- and 3Δ-alkenes was also isolated in 7% yield *(Scheme 2.24.)*.

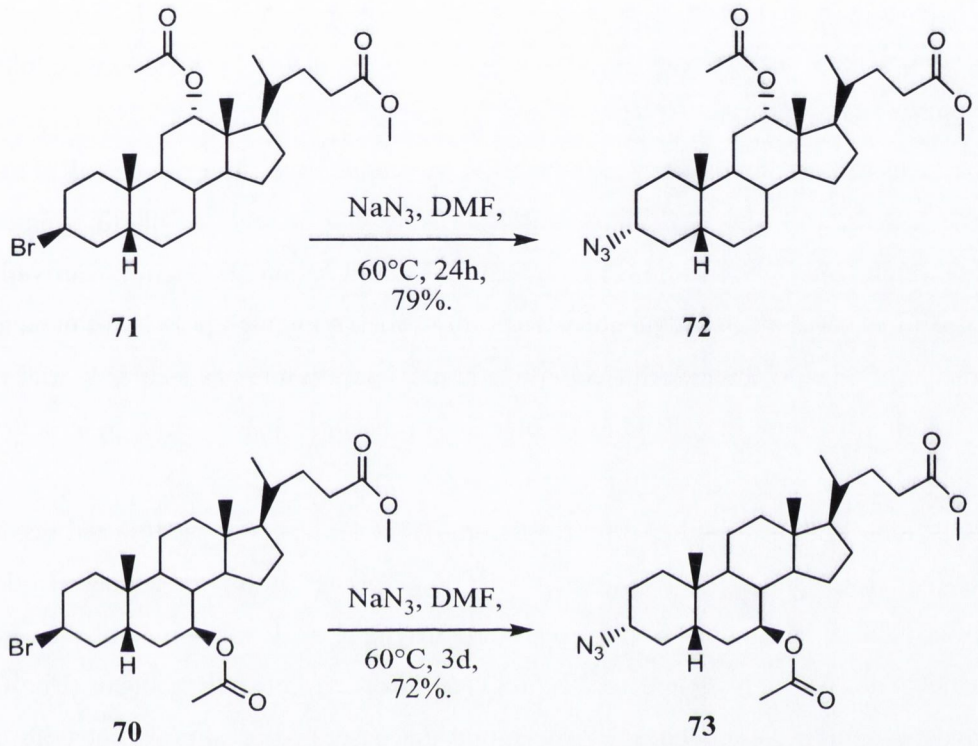

71 **72**

70 **73**

Scheme 2.24. Synthesis of 3α-azido derivatives in DMF

The presence of byproducts prompted us to try the reaction in 1,3-dimethyl-3,4,5,6-tetrahydro-2(1H)-pyrimidinone (DMPU), a solvent known to promote azide substitution reactions. Thus **71** was dissolved in DMPU and ten equiv. of NaN_3 were added to the solution. The reaction resulted in **72** in 89% yield without the formation of alkene by-products *(Scheme 2.25.)*.

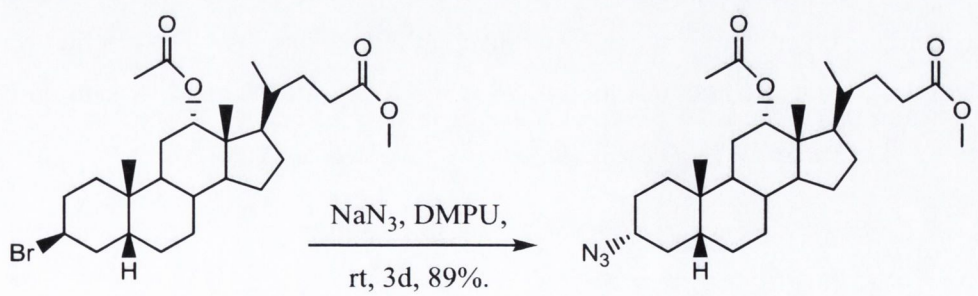

71 **72**

Scheme 2.25. Synthesis of 72 in DMPU

2.3.4.3. Reduction of 3α-azido derivatives

In the next step the azido group was reduced to amine using different conditions. Azides can be reduced to amines by hydrogenolysis or with a phosphine, such as PPh_3, in the Staudinger reaction [126]. Our attempt was carried out following the method reported by Gololobov *et al.* [127]. The authors used PPh_3 in THF and water to obtain 3-amino cholic acid derivative from the corresponding azido compound. In our case, **72** was treated with three equiv of PPh_3 under N_2 atmosphere. After 3 d, the TLC analysis did not show the presence of starting material in the reaction mixture, thus the reaction was worked up. The separation of the amino derivative **74** was not completely successful from the unreacted PPh_3, because the high polarity of the amino group made the purifying procedure with column chromatography unmanageable. It was decided to protect the amino group, in which case separation of the intermediate from by-products is more achievable.

Boc-protection of amines produced by reduction *in situ* (one-pot) is widely used because of the amine's (in)stability and the better chromatographic properties of the Boc adduct. Broderick *et al.* reported a method, in which the azido derivative of cholic acid was carbamolyated *in situ* with PtO_2 under hydrogen atmosphere in the presence of di-tert-butyl dicarbonate (Boc_2O) to give Boc-protected amino compound [128]. We used the described conditions but with a different hydrogenation catalyst. We added 1.2 equivalents of Boc_2O to the solution of **73** in EtOAc then finally 10% Pd / C, instead of the platinum catalyst, was also added. The reaction was stirred overnight under hydrogen atmosphere, after which time the TLC analysis indicated consumption of the starting material. We could detect two products on the TLC plate, which were separated by flash chromatography. The NMR analysis showed that we obtained **74** as main product in 93% yield together with 3-keto derivative **63** as by-product in a few percent. The purification of Boc-protected amino derivative was much easier than in the previous case. The reaction was repeated with **72** under the same conditions to give **75** white foam in 83% yield. A keto derivative was also formed in few percent in this attempt *(Scheme 2.26.)*.

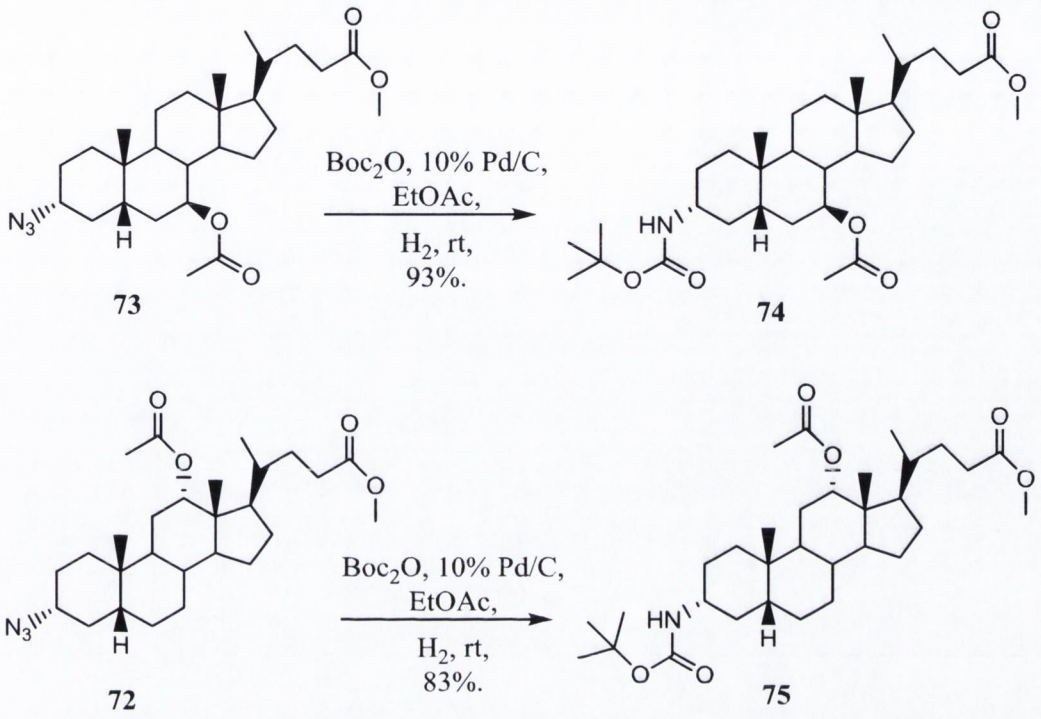

Scheme 2.26. Reduction of azide and protection in one-pot procedure

2.3.4.4. Synthesis of 3α-dansyl derivatives

To form the dansyl – amino adduct, we had to first remove the Boc-protecting group and then couple the fluorophore to the amine. Therefore, **74** was dissolved in a 1:1 mixture of TFA and DCM and stirred at rt. The reaction was complete after 4 h, the volatiles were removed and the product was dried under high vacuum. For the formation of the dansyl derivative, the intermediate was treated with 1.5 equivalents of DNSC in the presence of Et_3N following the reported method by Michael Ternon *et al.* [129]. The reaction was complete after 12 h and **76** was isolated in 82% yield (two steps from **74)** as a yellow-green foam. This synthetic approach was also applied to **75** producing the 3α-dansyl derivative **77** in 74% yield *(Scheme 2.27.)*. Unidentified fluorescent by-products were also detected in negligible amount during the reactions.

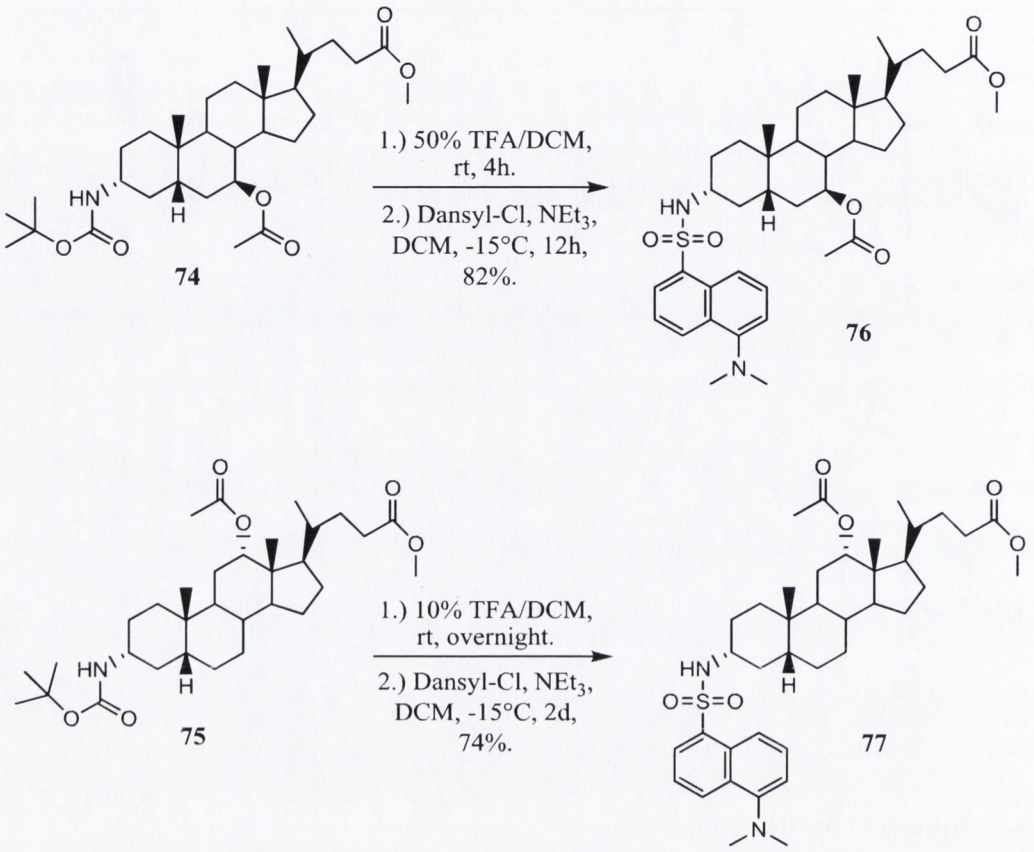

Scheme 2.27. Formation of 3-α-amino-dansyl products

2.3.4.5. Hydrolysis of 76 and 77

The hydrolysis of the acetate group and the methyl ester was attempted at pH ~ 14. Compound **76** was treated with 2M aqueous sodium hydroxide (NaOH) solution at rt and stirred for 3 d. After this time, the TLC analysis did not show any starting material in the reaction mixture and only one spot was detected as product. This compound was isolated, but the NMR analysis showed that the product contained the acetyl group at position-7. This material was treated with NaOH again and the temperature of the reaction was increased to reflux. The formation of 3α-dansyl UDCA (**78**) was followed by TLC analysis; the reaction was complete after 5 d.. The surprising lack of reactivity of the acetate group may be due to an interaction with the dansyl causing hindrance of hydroxide attack or breakdown of the resulting tetrahedral intermediate. Compound **78** was obtained as a yellow solid as product in 82% yield from **76**. The corresponding DCA adduct, **79** was obtained using similar conditions as a green-yellow solid in 82% yield *(Scheme 2.28.)*. In order to drive it to completion, this reaction was stirred at reflux for two months! The

formation of **79** was followed by TLC analysis, which showed that the hydrolysis of methyl ester was very fast, but the displacement of 12-acetate took long time. The reason is probably the orientation of 12-alcohol, which is in axial position in contrast with 7-hydroxyl coupled with supposed hindrance by the dansyl fluorophore.

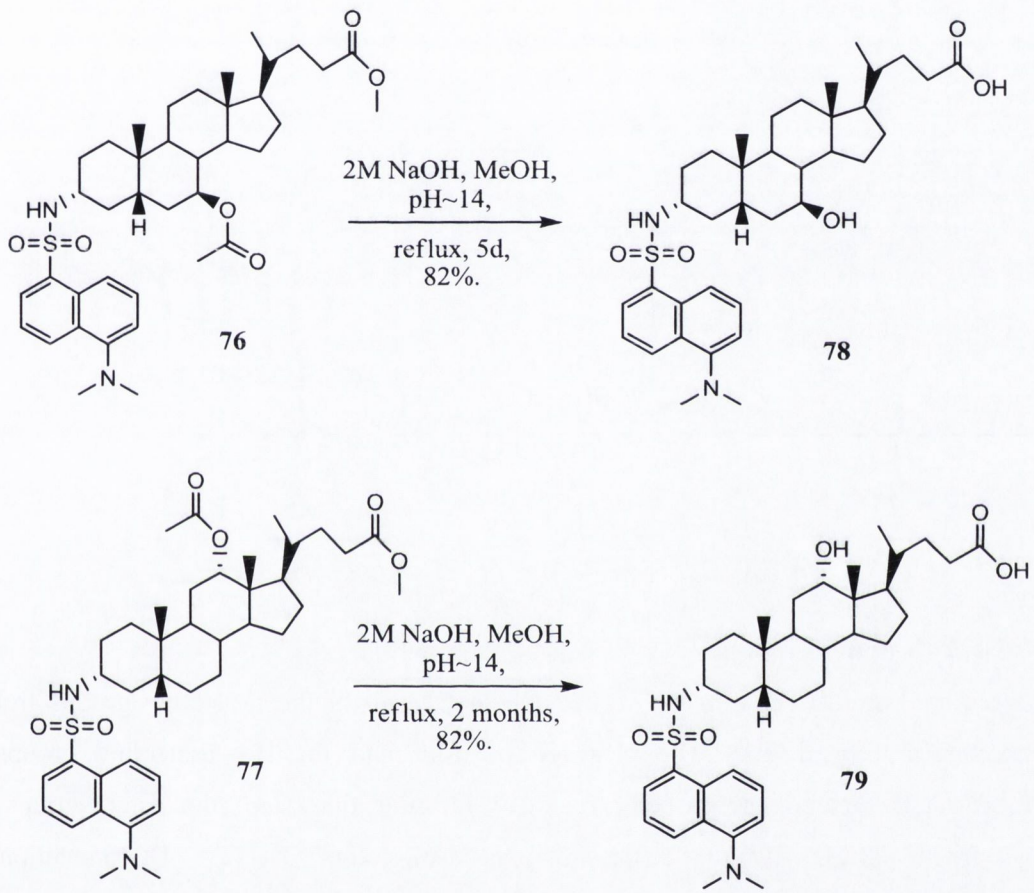

Scheme 2.28. Deprotection of 3α-amino dansyl derivatives

2.3.4.6. Hydrolysis of azido intermediates

In subsequent studies in order to examine the correlation between bile acid hydrophobicity and toxicity, we decided to synthesise azido derivatives of **4** and **7**. The hydrolysis of the protecting groups of 3α-azido UDCA **73** and DCA **72** intermediates was carried out in aqueous NaOH in MeOH as in the case of dansyl compounds. The reaction was complete after 1 d in the case of the UDCA derivative to give compound **80** as product in 99% yield. In contrast, the cleavage of protecting groups of **72** took 10 d producing **81** in 82% yield *(Scheme 2.29.)*. The longer reaction time in this case was expected but it was better than the earlier two month reaction.

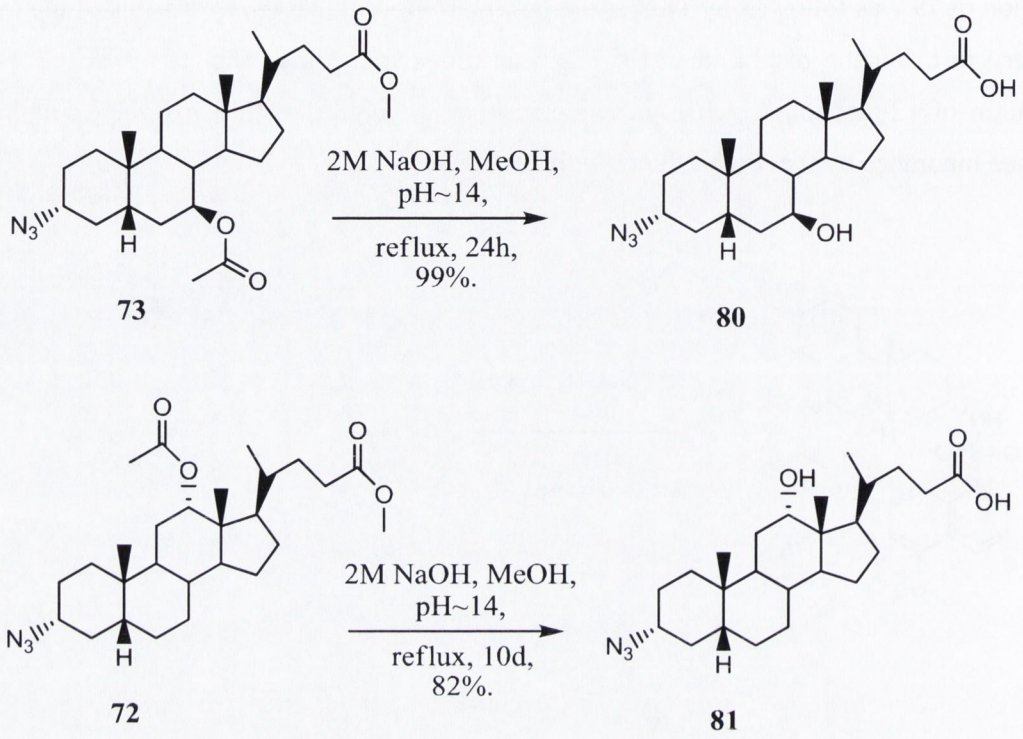

Scheme 2.29. Deprotection of 3α-azido intermediates

2.3.4.7. Deprotection of 74 and 75

For the required amino derivatives, we had to displace all of the protecting groups from the corresponding intermediates. The cleavage of ester and the Boc-protecting groups was performed using methods developed previously. In the first step, the ester groups were hydrolysed with NaOH, and then the Boc-group was displaced in 10% TFA / DCM solution. The applied method resulted in the proposed 3α-amino UDCA **82** and DCA **83** derivatives in good yields *(Scheme 2.30.)*.

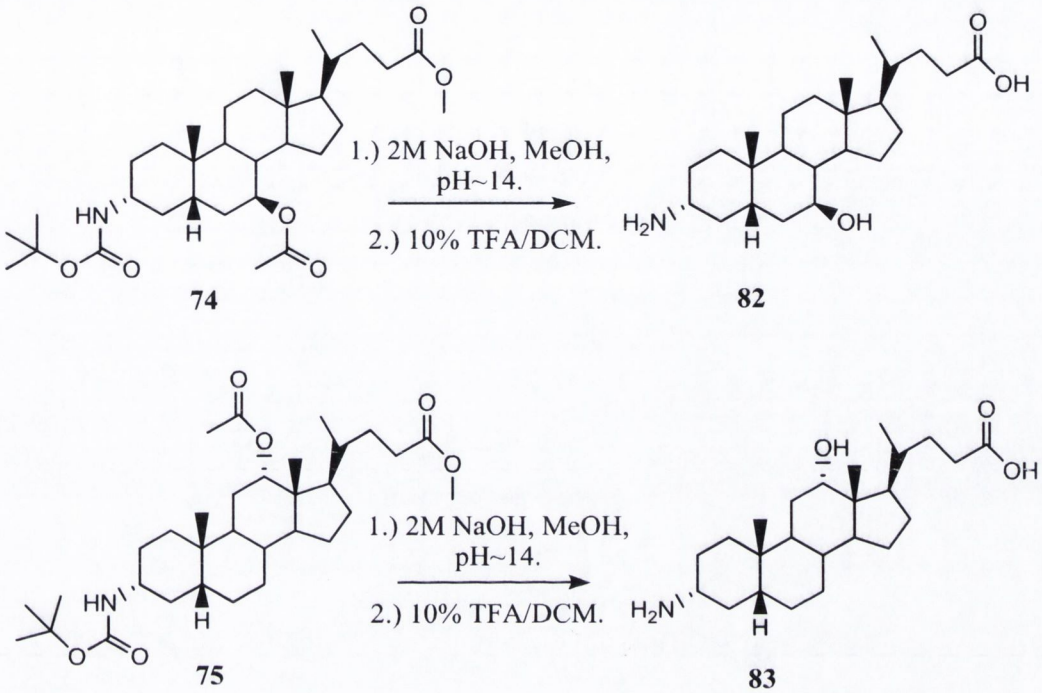

Scheme 2.30. Formation of 3α-amino derivatives

2.3.5. Synthesis of 3β-amino-dansyl UDCA and 3β-amino-dansyl DCA and hydrolysis of the protecting groups

3β-Dansyl derivatives were prepared using the same procedure for the 3α-dansyl compounds. For the configuration of β-epimers, **56** and **69** were first converted to mesylated intermediates with α–orientation. This step was then followed by the azide substitution, which resulted in β-azido derivatives causing inversion in the configuration. The intermediates and products were synthesized under the conditions described previously. In the azide reactions, DMSO was tried as solvent, but the reaction time increased significantly, thus DMPU was also used in the case of UDCA derivative. The time of the azide reactions increased significantly using the mesylate leaving group. The conditions and yields are presented in the following schemes. *Scheme 3.31* shows the synthetic route to 3β-dansyl UDCA and *Scheme 3.32* contains the steps to 3β-dansyl DCA. *Scheme 2.31.* and *Scheme 2.32.* includes the preparation of deprotected azido and amino derivatives.

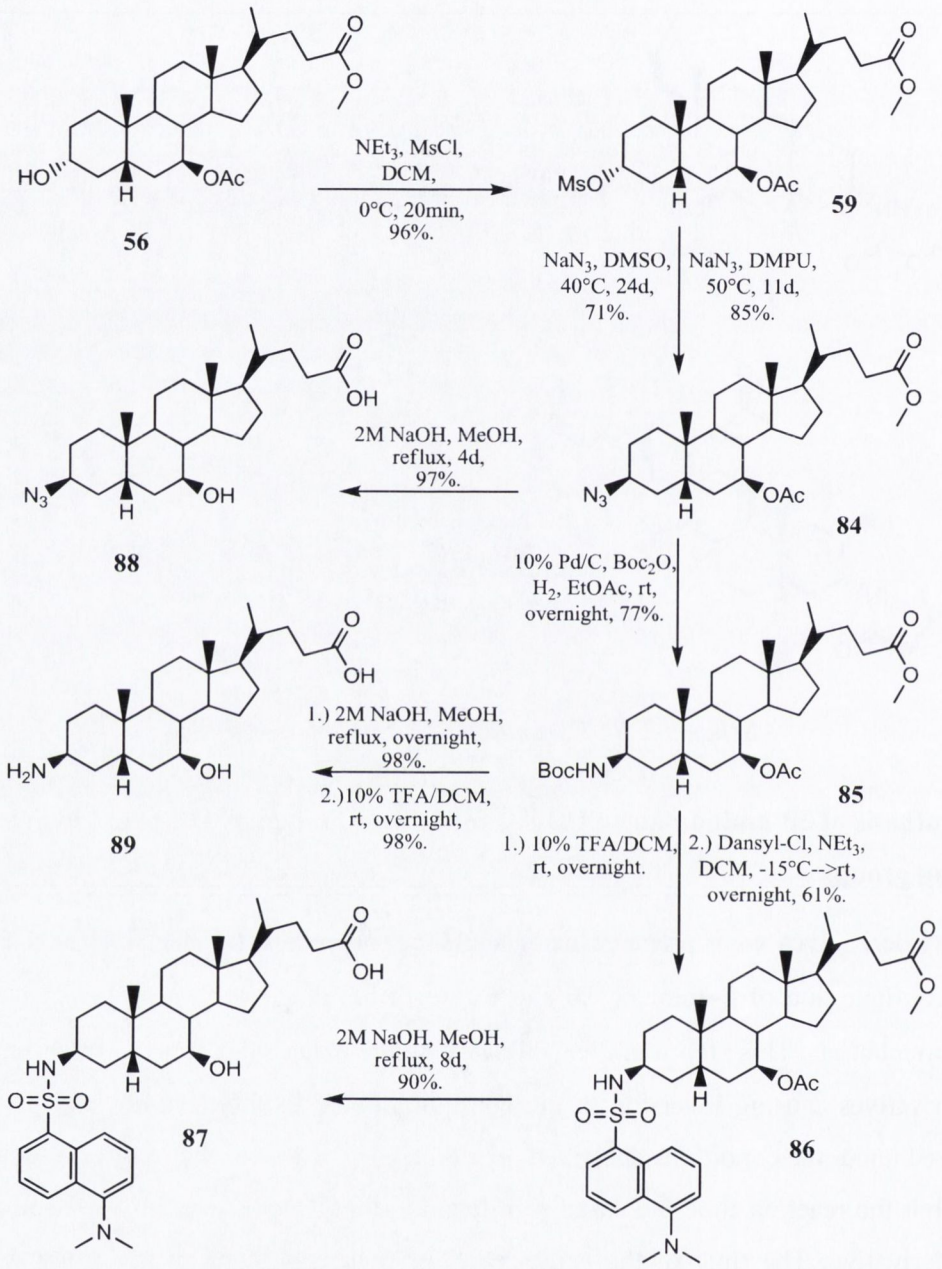

*Scheme 2.31. Synthesis of **87**, **88** and **89***

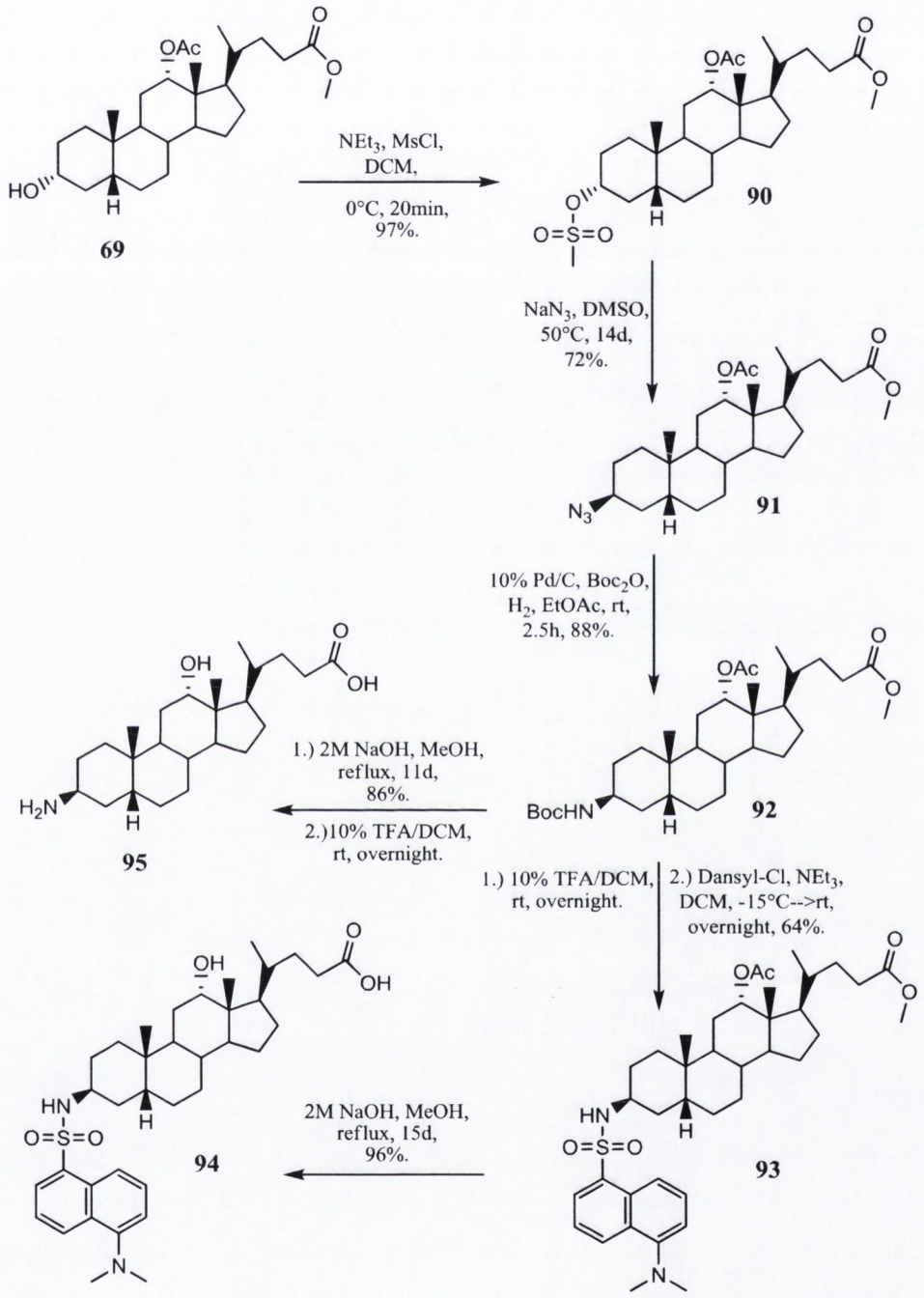

*Scheme 2.32. Synthesis of **94** and **95***

2.3.6. Design and synthesis of the dansyl control compound

It was decided to prepare a control compound which would be expected to possess similar fluorescent and lipophilicity properties to the synthesized dansyl-bile acid adducts but not the

steroidal skeleton. This could control for non-bile acidspecific effect later in cell-based experiments. Cyclohexylamine, which seemed a suitable mimic for **7** or **4** has been used for this purpose in previously reported studies in this area.

The reaction was carried out using the same method that was used to form the dansyl-amino-bile acid bond. 1.1 equivalents of dansyl chloride was added to cyclohexylamine in the presence of Et_3N at -15 °C then it was stirred at rt. The completion of the reaction was followed by TLC visualizing the spot of the product under UV light and with Dragendorf's reagent which greatly improves sensitivity in amine detection. After work-up the crude product was columned twice giving the product as a light-green foam in 95% yield *(Scheme 2.33.)*.

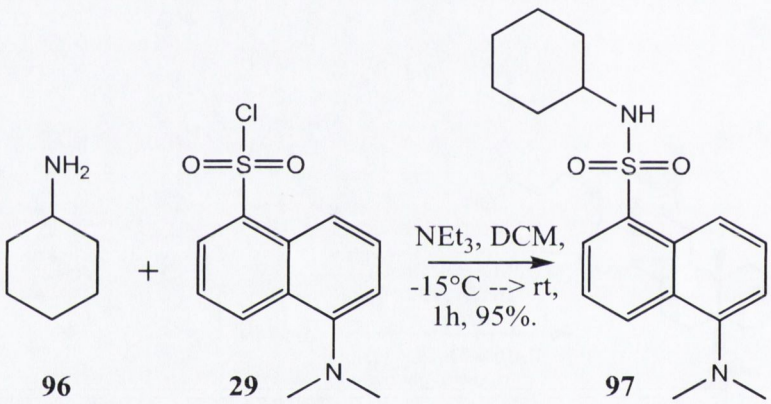

96 **29** **97**

Scheme 2.33. Synthesis of cyclohexyl-dansyl

2.3.7. Design and synthesis of 3-NBD derivatives

2.3.7.1. Introduction

As we have seen in Chapter 1 the dansyl moiety is not the only fluorophore suitable for amines. Dansyl adducts produce blue- or blue-green fluorescence, while NBD and fluorescein emit lower energy light, in the green range of the visible spectrum. It was decided to develop fluorescent bile acids which fluorescence over 500 nm as well to complement the dansyl probes. NBD-chloride is a commonly used amine sensitive fluorophore with a relatively low steric impact, which can be an advantage *via* transport processes. Its sensitivity to its environment, satisfactory quantum yield and stability make it among the most widely used reporter group in biomedical sciences [24, 39]. Yan Zhao and Zhenqi Zhong labelled 3-amino cholic acid derivative with 7-chloro-4-nitrobenzofurazan (NBD-chloride) in 3-position [130], while Schneider *et al.* reported a study

about NBD-amino cholic acid derivatives and their taurine salts introducing the fluorophore into the 3, 7 and 12 position [27]. The 3-NBD-amino derivatives of DCA and UDCA had not been reported to date.

2.3.7.2. Experiments towards synthesis of 3α-amino-NBD DCA

For the formation of NBD amino derivative we used the reported method by Zhao and Zhong [130]. The amino group of **75** was deprotected in 10% TFA / DCM in the first step, then after the removal of the Boc-group the intermediate was treated with 1.1 equivalents of NBD-chloride and 1.5 equivalents of $NaHCO_3$ in 1:1 THF / EtOH mixture. The reaction was stirred under nitrogen atmosphere to give the proposed 3α-NBD derivative **98** in 76% yield *(Scheme 2.34.)*.

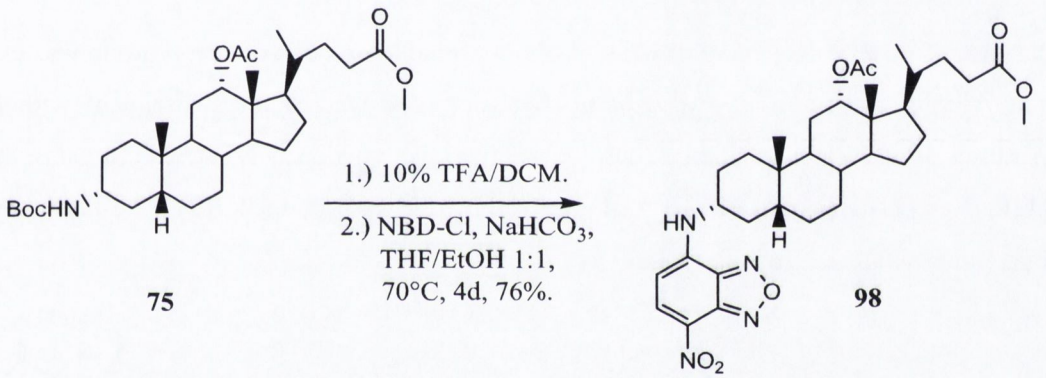

75 **98**

Scheme 2.34. Formation of 3α-amino-NBD derivative from 75

The same conditions mentioned previously in this report for the hydrolysis of the methyl and acetyl ester protecting groups were used on **98**. Compound **98** was stirred with aqueous NaOH in MeOH at reflux for 12 d, during which time the reaction was monitored by TLC. The hydrolysis of the methyl ester was quick, but before the cleavage of the acetate group could occur, the 3-amino derivative was detected on the TLC plate. At the end of the reaction we obtained the 3α-amino derivative **83** as product instead of the desired 3α-NBD compound **99** (*Scheme 2.35.*). Surprisingly the NBD – amino bond was more sensitive in basic conditions than the 12-acetyl group.

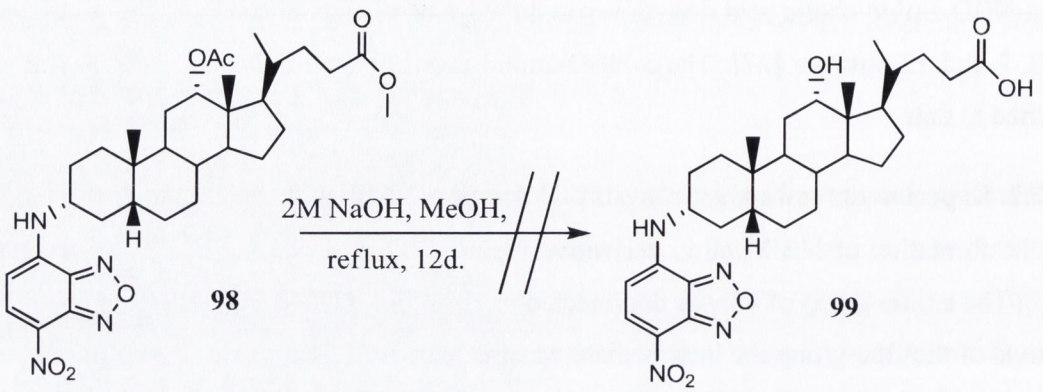

*Scheme 2.35. Experiment for deprotection of **98***

2.3.7.3. Experiments for the synthesis of 3β-amino-NBD UDCA

In the case of 3-NBD derivative of UDCA, a more rapid hydrolysis of acetyl group was expected, as the 7-group is equatorially disposed. Therefore we repeated the experiment with **85**. For preparation of the protected fluorescent intermediate the reaction was carried out using the same conditions as in the case of **75**. 3α-NBD derivative **100** was obtained after 12 d in 54% yield as orange solid *(Scheme 2.36.)*.

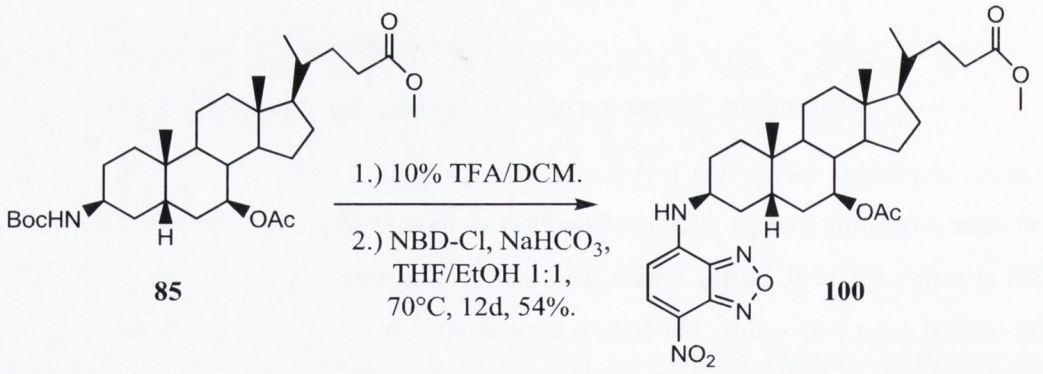

*Scheme 2.36. Formation of 3β-amino-NBD derivative from **85***

It was expected that hydrolysis of protecting groups in NBD – bile acid adduct **100** would yield the desired results using the same chemistry. Instead of the expected **101**, we obtained the 3β-amino derivative of UDCA **89**, thus we finished the experiments with acetyl protected derivatives *(Scheme 2.37.)*.

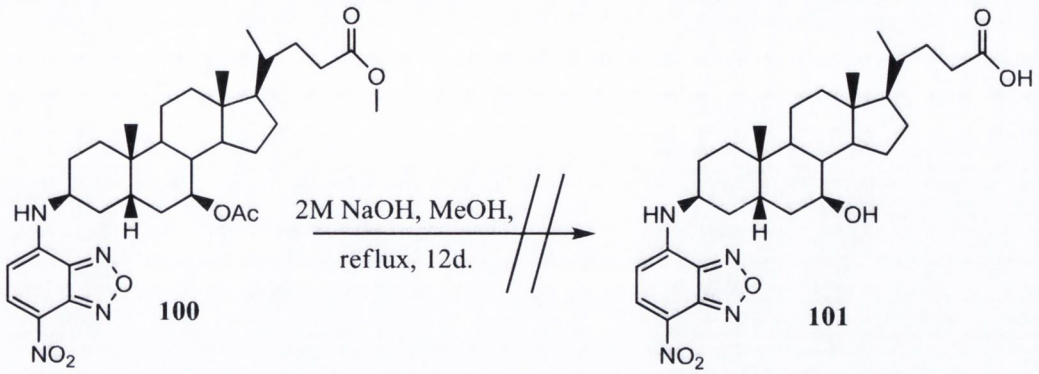

*Scheme 2.37. Experiment for deprotection of **100***

2.3.7.4. Protection of 54 and 67 with formic acid

Because of the unsuccessful deprotection experiments on **98** and **100**, an alternative protecting group for the hydroxyls was needed, one which could be removed more easily than the corresponding acetates. A commonly used protecting agent is the formyloxy group, which is about 100 times more reactive than acetate [131].

Thus, UDCA methyl ester **54** was performylated in formic acid in the presence of catalytic amount of perchloric acid [132]. The reaction resulted in two products according to TLC analysis. After separation of these compounds the NMR analysis showed that the product with higher R_f value (hexane / EtOAc 3:1, $R_f \sim 0.76$) was the required performylated derivative **102**, while the other one was also diformyloxy derivative ($R_f \sim 0.23$), but the perchloric acid cleaved the methyl group from carboxylic acid *(Scheme 2.38.)*. The formation of the free carboxylic acid can be avoided by continuously monitoring the course of the reaction. This experiment was also carried out on DCA methyl ester **67** under the same conditions. The reaction was monitored by TLC, which showed that the formation of **103** was complete after 15 min *(Scheme 2.38.)*. The diformyloxy acid was also present in the mixture, but its amount was negligible. We could obtain the performylated derivative in 83% yield in this case, while the yield of **102** was only 41% beside 49% by-product.

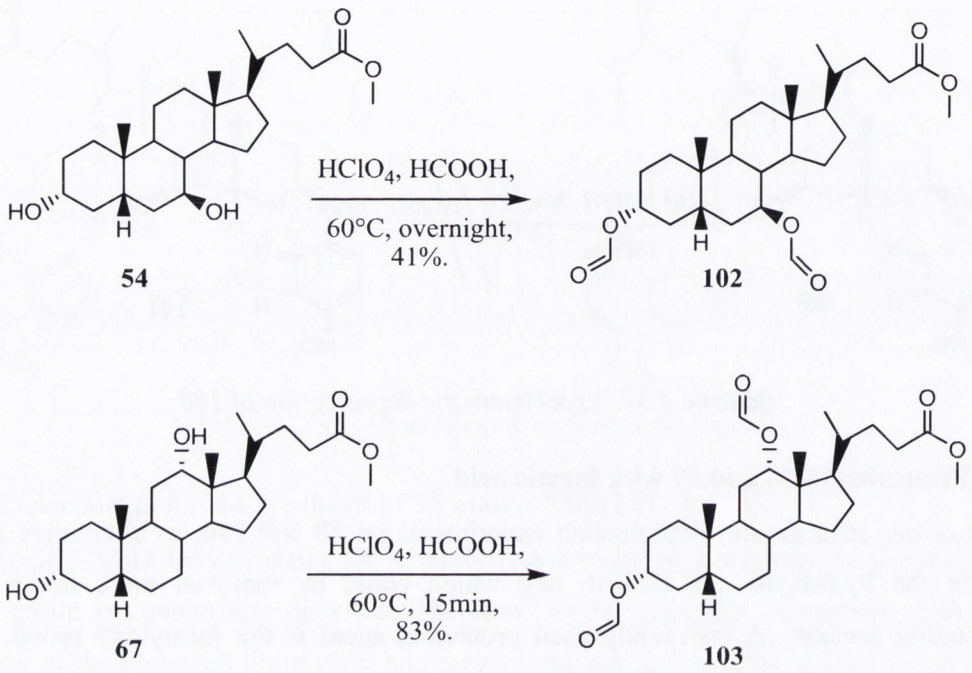

Scheme 2.38. Hydroxyl-protection with formic acid

2.3.7.5. Selective deprotection of 102 and 103

Two equiv. of aq. $NaHCO_3$ were used for preparation of selective deprotected **102** in position-3 [131]. The temperature of reaction was increased from 0 °C to rt after 1 h and stirred for 3 d. After this time, TLC analysis did not show presence of the starting material, but compound **54** appeared in the mixture. The products were separated by column chromatography to give the required product **104** in 85% yield and **54** in 15% yield *(Scheme 2.39.)*. The procedure was repeated with **103** yielding the 3α-hydroxyl DCA derivative **105** in 98% after 4 h. Because of the continuous monitoring of the reaction **67** did not appear in this case *(Scheme 2.39.)*.

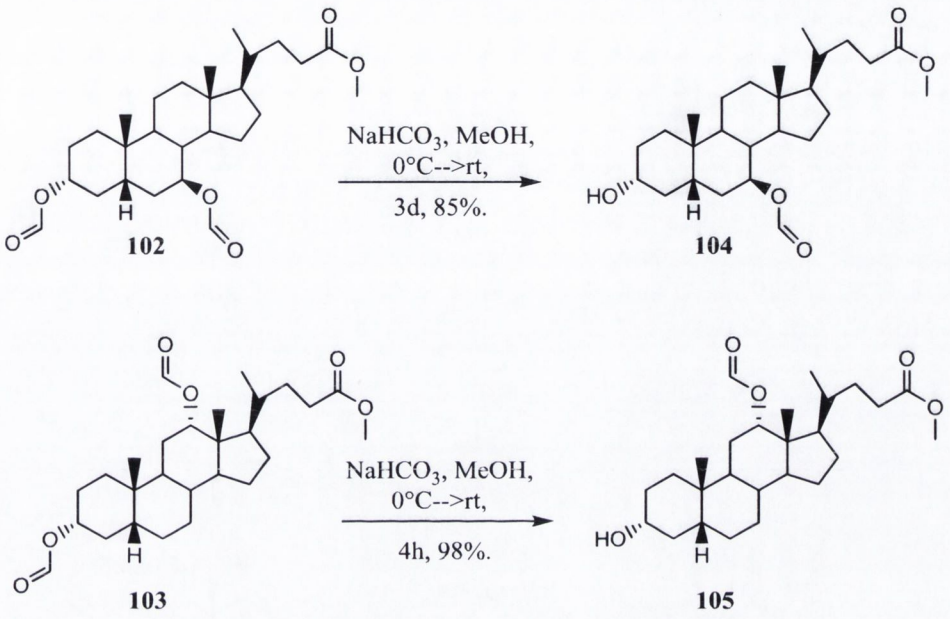

*Scheme 2.39. Selective deprotection of **102** and **103***

2.3.7.6. Preparation of 3β-NBD derivative of UDCA

The required 3β-NBD derivative was synthesized under the same conditions as in the case of acetyl protected intermediates. Thus, **104** was transformed to the corresponding mesylate **106**; this step was followed by the azide reaction to give **107,** which was reduced and protected (Boc) to afford **108**. The fluorophore was attached to the deprotected amine to afford **109** in good yield *(Scheme 2.40.)*. The isolated intermediates were determined by NMR analysis in every case.

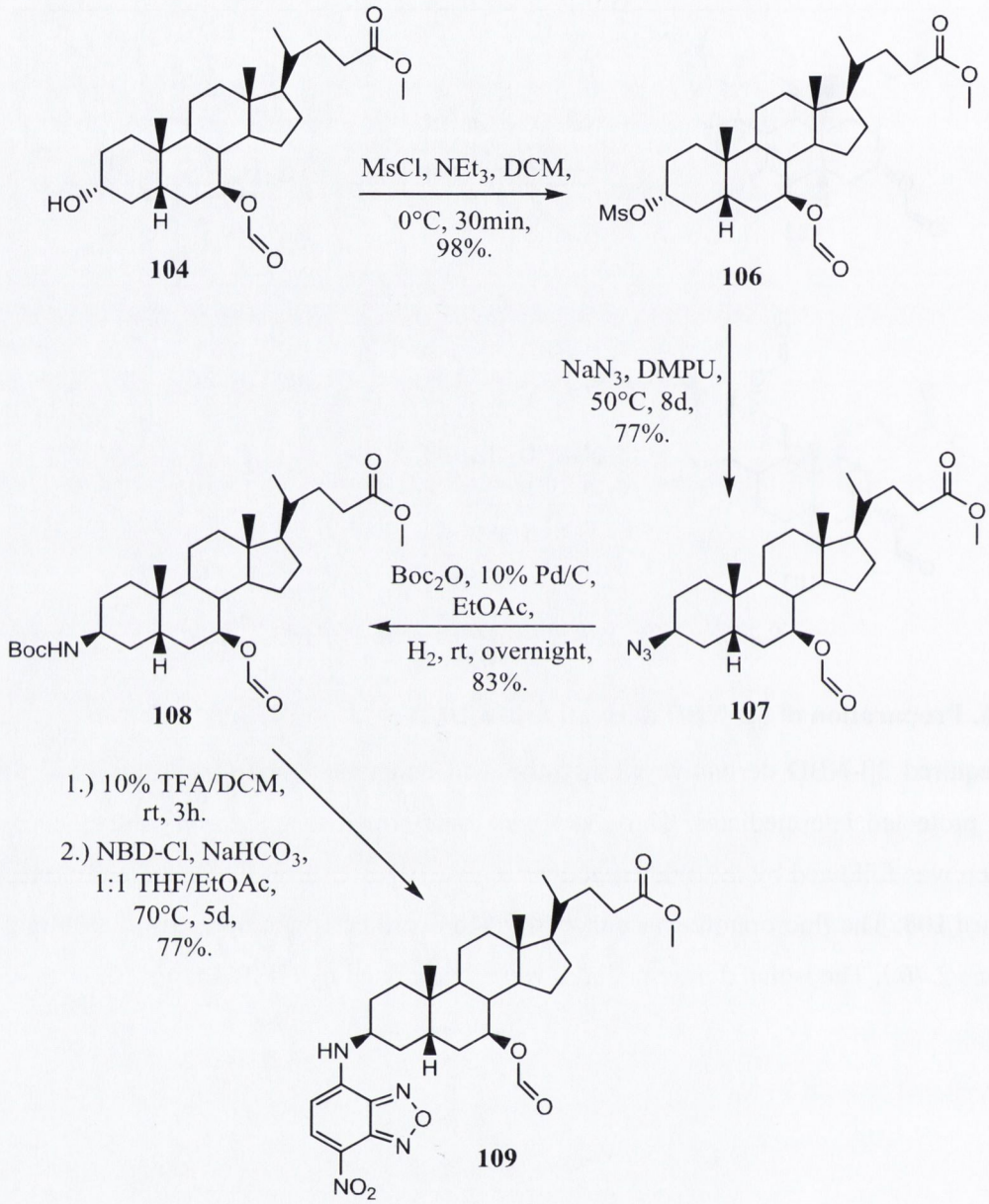

Scheme 2.40. Synthesis of 3β-NBD derivative of UDCA

2.3.7.7. Investigation into deprotection of 109

Hydrolysis of the ester groups of **109** was attempted in basic media and the formation of the required product **101** was followed by TLC analysis *(Scheme 2.41.)*. The methyl ester was cleaved after 1 d to give the 7-formyloxy intermediate, but the hydrolysis of formylated alcohol seemed very slow and the amino derivative **89** appeared at the same time as the target compound. After completion of the reaction we could hardly detect **101** over **89**. Although, during this

experiment **89** appeared to be present in larger amounts than in the case of corresponding acetyl derivative, we could not isolate sufficient product; thus, the formyl protection did not lead us to success.

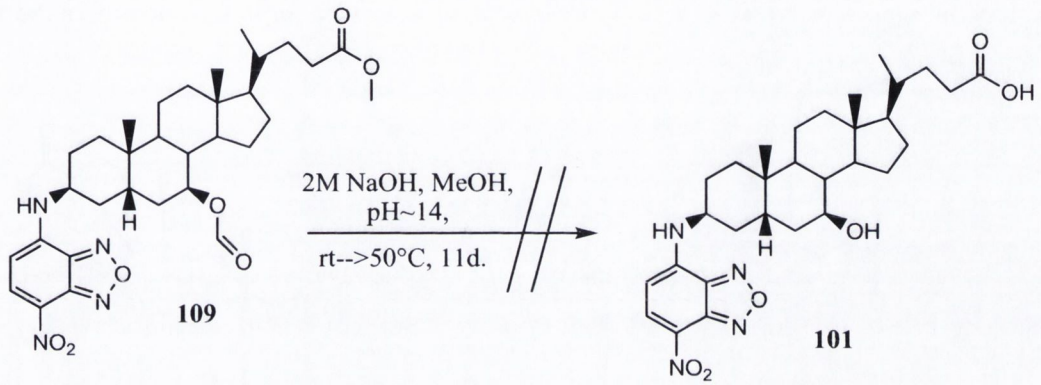

*Scheme 2.41. Experiment for deprotection of **109***

2.3.7.8. Selective deprotection of 74 and 84

Because of the unsuccessful deprotection experiments, it was necessary to find an alternative route to the required 3-NBD bile acids. The cleavage of esters can be acid- or base-catalysed. In the base-catalysed reactions, the carbon of the carbonyl group is attacked by a nucleophile (a nucleus-seeking agent, e.g. water or hydroxyl ion), leading to the cleavage of molecule into two parts. The previous experiments showed that the methyl ester was more easily hydrolysed over the acetyl or formyl groups, and the esters of 7- and 12-hydroxyls were cleaved with the NBD-group together under basic conditions. Thus the hydrolysis should be carried out before the attachment of the fluorophore and without the cleavage of the 24 methyl ester. The hydroxyl protecting group is useful during the formation of the 3-bromo- and 3-mesyl-derivatives, but after these steps it is not necessary. It was decided to try the hydrolysis on the azido- and Boc-amino-intermediates of UDCA (**84** and **74**), in the expectation that attachment of the fluorophore could be achieved selectively onto the amino group in the presence of the unprotected alcohols.

These compounds were treated with 1.3 equivalents of AcCl in MeOH and the reaction was followed by TLC using hexane / EtOAc 3:1 as mobile phase *(Scheme 2.42.)*. In the case of **74** the starting material disappeared from the mixture after 2 d to give one spot on TLC plate with very low R_f value. The crude product was sent for NMR analysis which showed that we obtained a product mixture containing 7β-acetyloxy and 7β-hydroxyderivatives in about 1:1 ratio, but did

not obtain the target compound **110**. The reaction of **84** finished after 6 d to give the expected azido compound **111** in 77% yield *(Scheme 2.42.)*. This reaction was repeated at larger scale to give the product in 98% yield after 10 d reaction time. Because of the easier detection and purification of the product it was decided to hydrolyse acetyl or formyl groups after the azide reaction in further experiments.

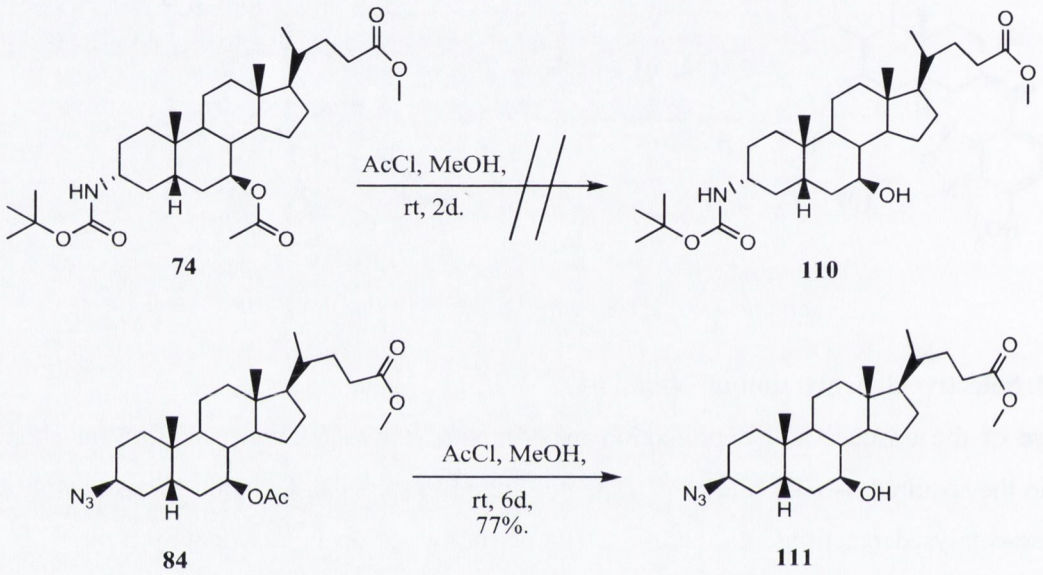

Scheme 2.43. Selective deprotection of intermediates

2.3.7.9. Synthesis of 3β-NBD, 7β-hydroxy-5β-cholanoate

The synthetic procedure to the 3β-NBD UDCA followed the previously optimized reaction steps. The selectively deprotected azido-intermediate **111** was reduced to the Boc protected amino derivative **112** and this step was followed by the coupling of the fluorophore to the bile acid *via* amino group. Compound **113** was isolated in 67% yield from **112**. *Scheme 2.43.* below describes the intermediates and conditions used.

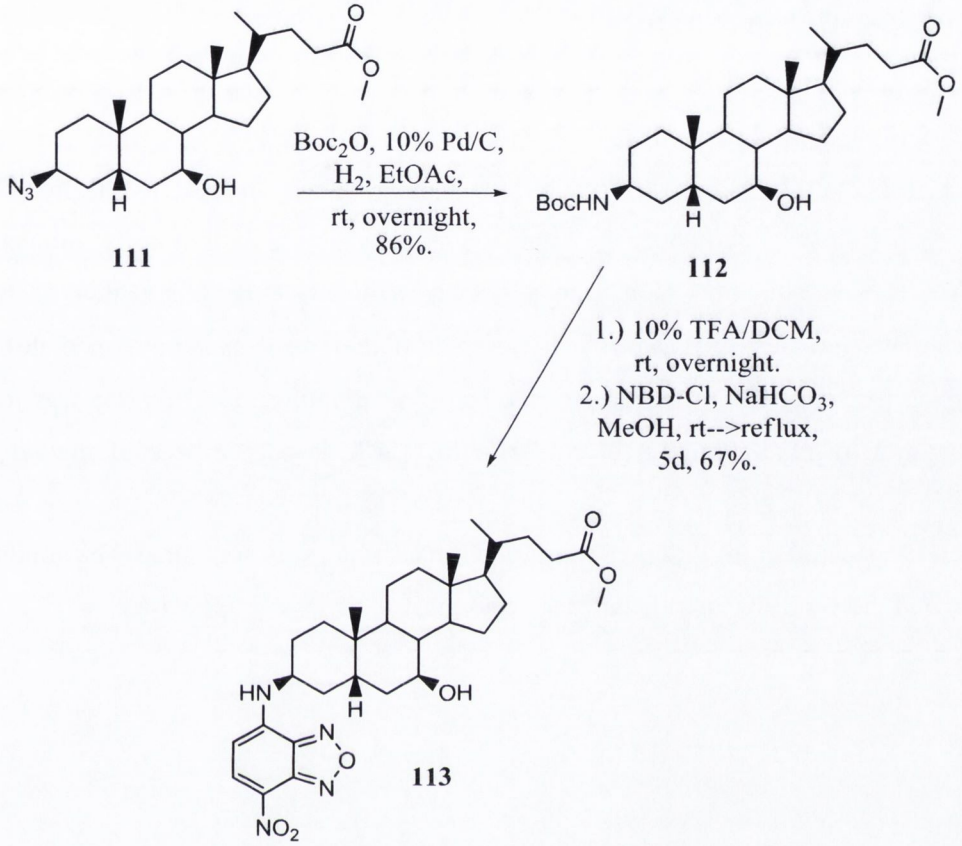

Scheme 2.43. Synthesis of 3β-amino-NBD derivative of UDCA

The hydrolysis of **113** was carried out under basic condition in MeOH at 40 °C and monitored by TLC analysis using EtOAc as mobile phase. After 3 h reaction time the deprotection was complete and the proposed product **101** was isolated in 96% yield *(Scheme 2.44.)* as orange solid. The structure of **101** was supported by NMR analysis. The 3-amino derivative was also detected in small amounts.

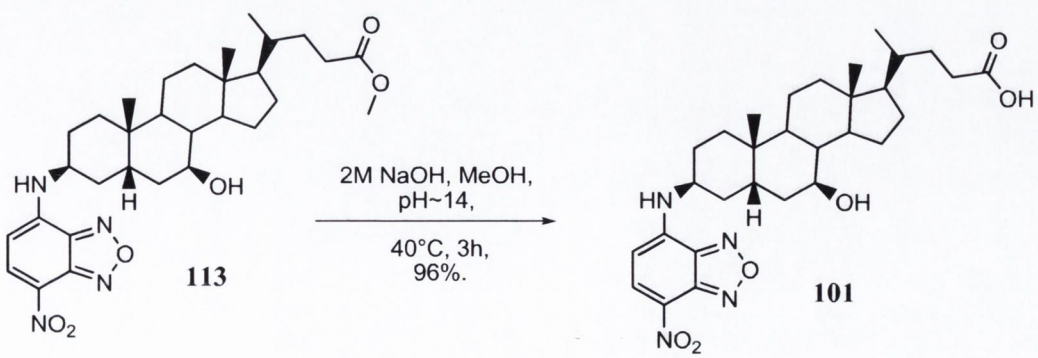

*Scheme 2.44. Hydrolysis of **113***

2.3.7.10. Synthesis of 3β-NBD DCA

For the preparation of the 3β-NBD derivative of DCA, we used the formyl protected compound **105**. To form the azido-intermediate, **105** was treated with mesyl chloride and then the mesylate **114** transformed to the required azido derivative **115** as before. The selective deprotection of the formyl group was attempted under the same conditions as in the case of acetyl protected UDCA derivative. The reaction time significantly decreased in this experiment; after 28 h the TLC analysis showed only one spot as product. We could obtain the 3β-azido intermediate**116** in 97% yield, which was reduced to the Boc protected amino derivative **117**. This step was followed by the preparation of fluorophore – bile acid adduct **118**. The hydrolysis of methyl ester was complete after 4 h to give the expected fluorescent DCA **119** in 76% yield. The 3-amino by-product also appeared in the reaction mixture, but its amount was negligible. The condition of the reactions and the yields of intermediates are presented in *Scheme 2.45.* below.

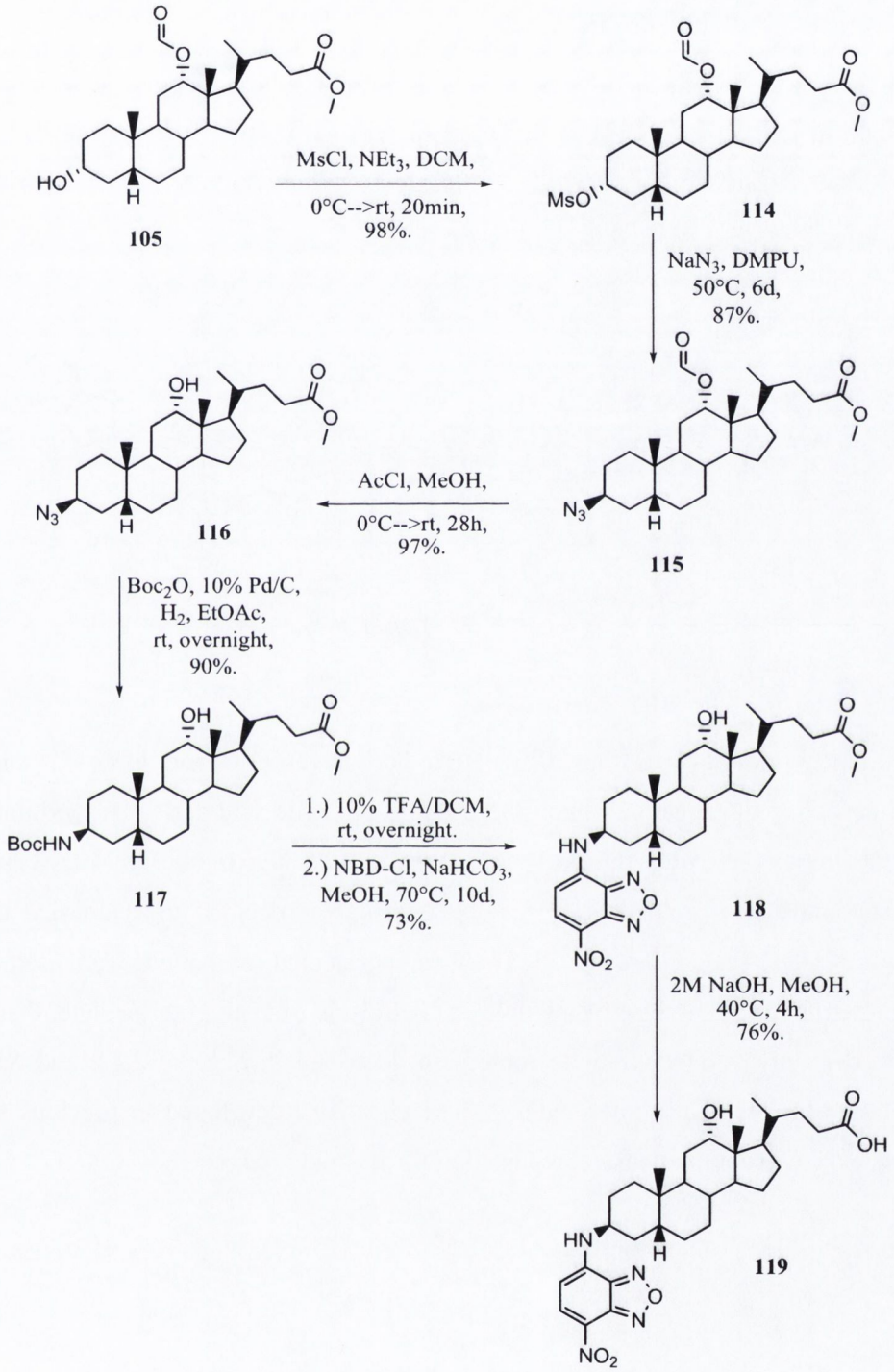

*Scheme 2.45. Synthesis of 3β-amino NBD derivative of DCA **119***

2.3.7.11. Synthesis of 3β-azido DCA derivative

The protecting groups of **115** were hydrolyzed in order to produce the missing azido-intermediate by stirring with NaOH in MeOH at rt. The reaction mixture was stirred overnight, after which time the TLC analysis did not show the starting material in the mixture. The experiment yielded the required derivative **120** in 98% yield *(Scheme 2.46.)*.

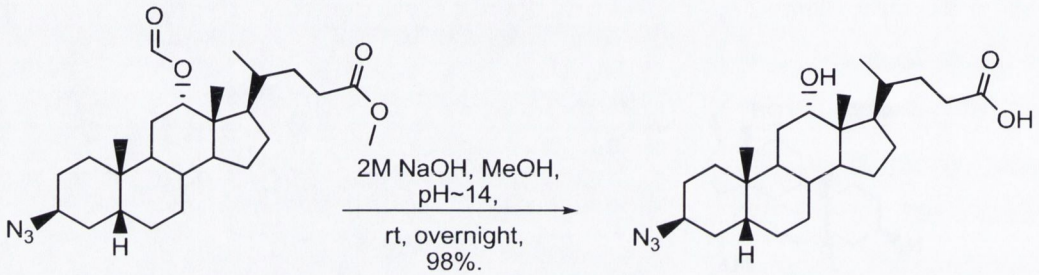

115 **120**

*Scheme 2.46. Hydrolysis of **115***

2.3.7.12. Synthesis of 3α-NBD derivatives

The preliminary biological testing of 3β-NBD derivatives (**101** and **119**) was carried out on SKGT-4 oesophageal cancer cell line. These fluorescent bile acid derivatives exhibited potential in this cell line as they were relatively non-toxic and displayed good uptake. Stability tests on these compounds also yielded good results, thus it was decided to synthesize the 3α-NBD derivatives of UDCA and DCA as well. The formyl protected compounds were used to obtain the required intermediates, because of the quicker hydrolysis of azido-intermediate, than in the case of acetate derivatives. The synthetic routes are described in *Scheme 2.47.* and *Scheme 2.48.*, which outline the steps and intermediates. The chemistry developed in previous sections was used here and so no comprehensive explanation for it is required.

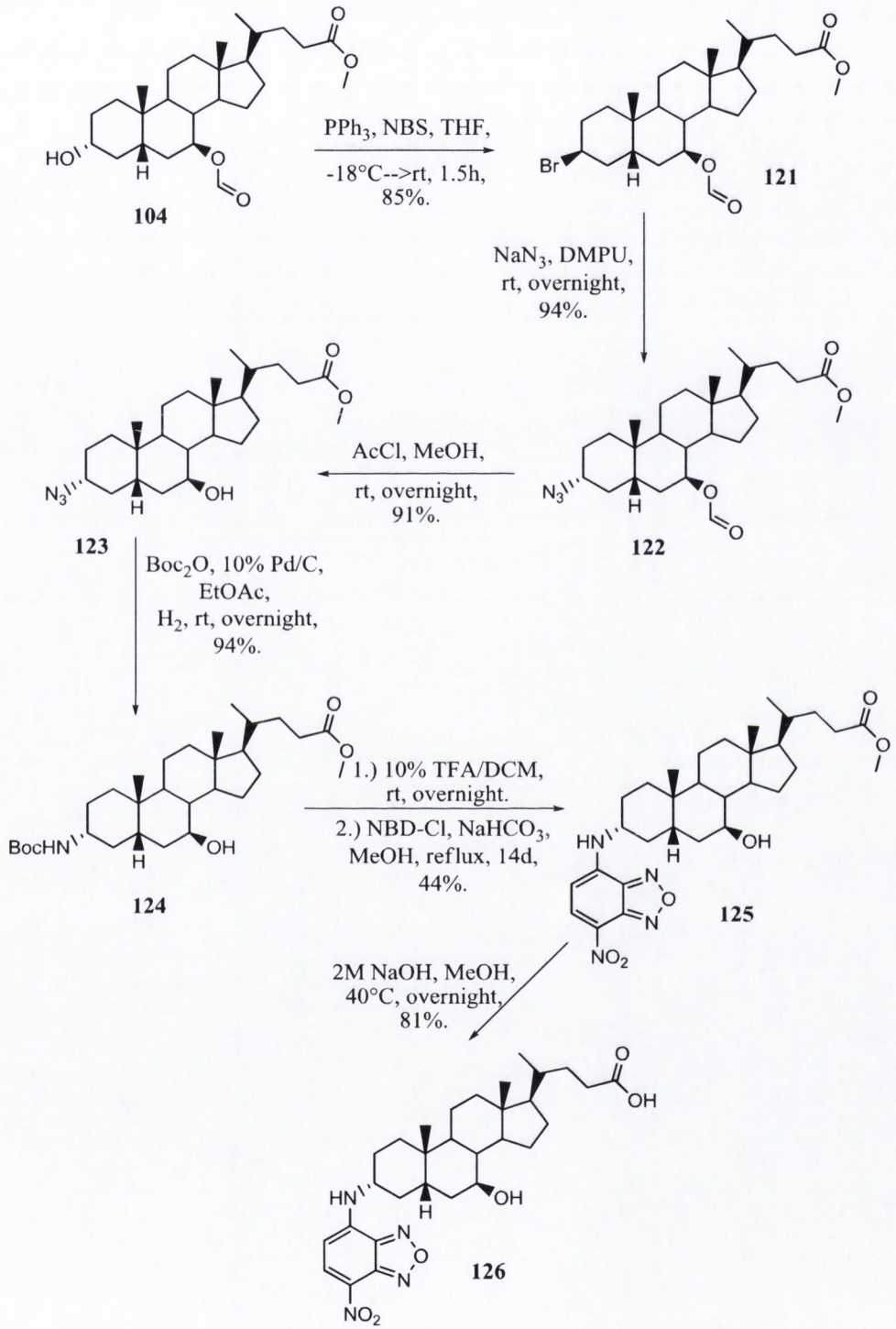

Scheme 2.47. Synthesis of 3α-amino-NBD derivative of UDCA ***126***

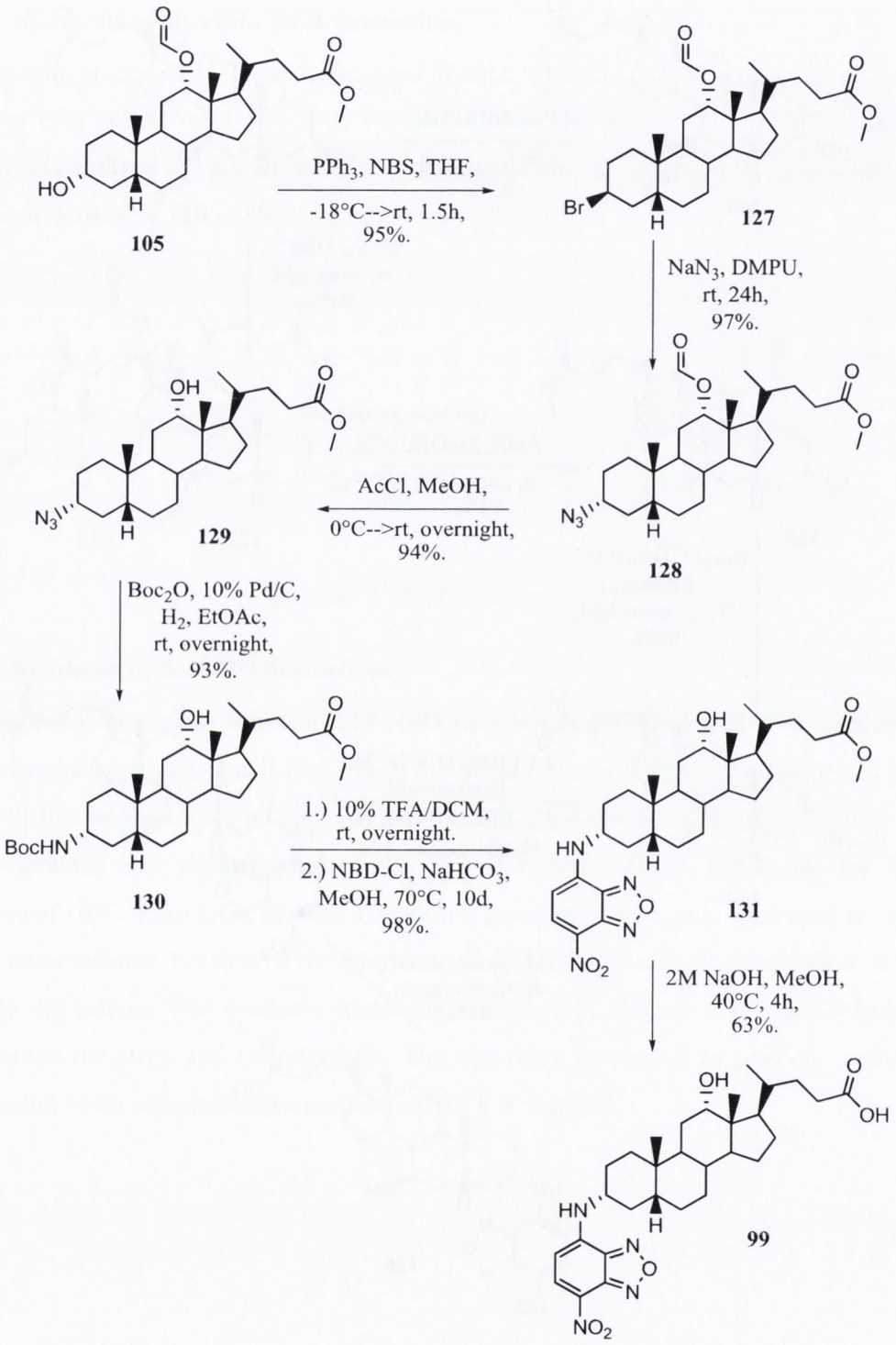

*Scheme 2.48. Synthesis of 3α-amino-NBD derivative of DCA **99***

2.4. Design and synthesis of 24-amino-NBD derivative of UDCA and cyclohexyl-NBD

2.4.1. Introduction

The rationale and synthesis of cyclohexyl-amino dansyl control compound has already been described. We subsequently felt that a control more closely mimicking the new fluorescent reporters, their mass and physicochemical properties could be obtained by abolishing the 24-carboxylic acid and introducing there a fluorescent reporter group. The synthesis route of 24-NBD compound was proposed in three steps, in which first the carboxylic acid undergoes a transformation to 24-amide, followed by the reduction of 24-carbonyl group to afford 24-amine, which is reacted with NBD-chloride in the last step. The first and second steps are based on the formation of 24-amino cholate, which was reported by Yibo Zhou *et al.* [133]. The preparation of cyclohexyl-NBD can be carried out in a single step with linking cyclohexylamine to the NBD moiety.

2.4.2. Synthesis of 24-amide

Thus in the first reaction, UDCA **7** was converted to *N*-hydrosuccinimide ester (N-HO-Su) in 10% acetonitrile / tetrahydrofuran mixture using dicyclohexylcarbodiimide (DCC) as the coupling reagent. A white solid was formed during the reaction, which was isolated to give the activated ester which was then transformed into the 24-amide **132** using aqueous ammonia solution *(Scheme 2.49.)*.

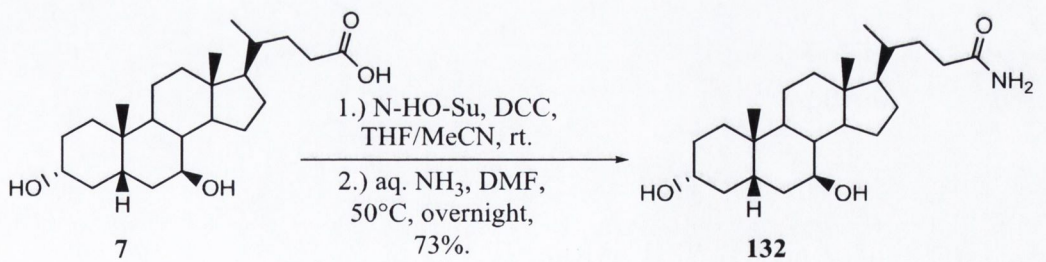

7 **132**

*Scheme 2.49. Formation of 24-amide **132***

2.4.3. Reduction of 132

In the next step, the 24-carbonyl group was reduced by lithium aluminium hydride to afford the 24-amine **133**. The reaction was carried out in THF under nitrogen atmosphere at reflux over 2 d. The Fieser-workup was used to decompose the reduction complex and excess of hydride with a calculated amount of water and 15% NaOH solution, which produced a dry granular precipitate that absorbs very little substance and is easy to filter and wash [134]. This method made the further purification easy and **133** was obtained in 61% yield *(Scheme 2.50.)*.

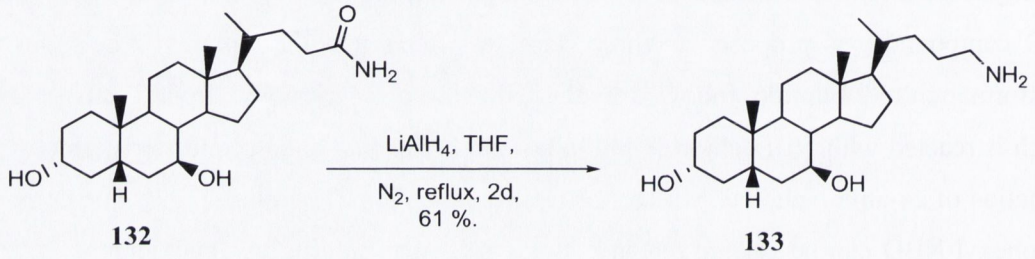

132 **133**

*Scheme 2.50. Reduction of **132***

2.4.4. Synthesis of 24-amino-NBD derivative

The formation of NBD-amino bond was carried out with the same method as earlier. The reaction was quicker on the side chain than in the case of position-3 and the attempt gave the 24-amino-NBD derivative **134** in 51% yield *(Scheme 2.51.)*.

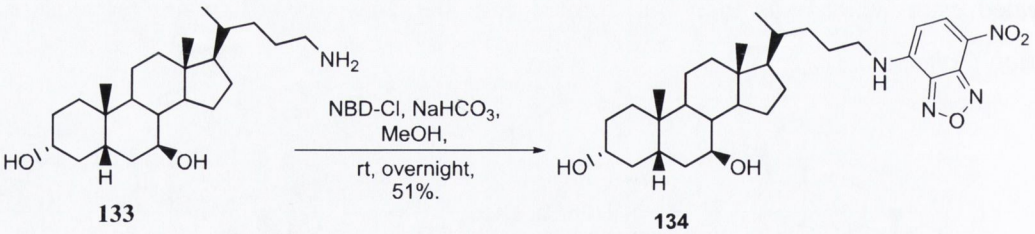

133 **134**

*Scheme 2.51. Synthesis of **134***

2.4.5. Synthesis of cyclohexyl-NBD derivative

The reaction between cyclohexylamine **96** and NBD-Cl **17** was carried out in MeOH with 1.1 equivalents of the amine. After 21 h, the TLC showed that the reaction was complete and so the reaction was worked up. The crude product was purified using column chromatography and the desired compound was obtained as an orange solid in 81% yield *(Scheme 2.52.)*.

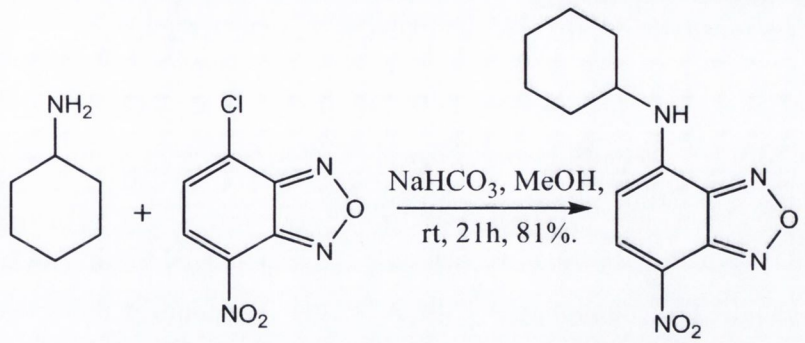

96 **17** **135**

Scheme 2.52. Synthesis of 135

2.5. Synthesis of cyclopropyl-amide derivatives of 99 and 126

2.5.1. Introduction

Studies have shown that UDCA 7 induces translocation of the GR and activates the GR in various different cell models [89, 135-137]. UDCA also can suppress NF-κB activity *via* GR activation [136] which could account for its clinical anti-inflammatory effects and corresponding observations in cell-based assays. Our research group has synthesized UDCA derivatives to study their ability to induce GR translocation in high content analysis assay using SKGT-4 cell line [138]. We reported that the cyclopropyl amide derivative of UDCA has with respect to UDCA itself significant improved potency and efficacy for the GR translocation to the nucleus, GRE transactivation and transrepression of NFkB. A mechanism for these effects has not been established. One of the major questions is whether the experimentally observed translocation is due to direct interactions between UDCA or its CPA amide and the GR, if it is downstream of cell membrane effects or if the bile acids were bound to the GR when it entered the nucleus. It seemed to the group that a 3-NBD, 24-CPA amide derivative might be useful to answer this. In experiments to be described in the next chapter, we observed that NBD bile acids do not enter the nucleus. If attachment of the CPA derivative caused nuclear fluorescence it might be an indication that the CPA was entering the nucleus on causing GR translocation, possibly by binding to it. To investigate further, we decided to synthesize the fluorescent analogue of the UDCA CPA **136** together with fluorescent DCA CPA **137**.

2.5.2. Design and synthesis of NBD labelled UDCA and DCA CPA

To prepare **136** and **137**, it was decided to use the previously synthesized 3α-NBD UDCA **126** and 3α-NBD DCA **99** as starting materials. Using this one step synthetic method and the remained samples, we can avoid the time-consuming multiple synthetic route. The amide bond was formed with the use of hydroxybenzotriazole (HOBt) and 1-[3-(Dimethylamino)propyl]-3-ethylcarbodiimide (EDC) as coupling agents. After the formation of the active esters with 1-hydroxybenztriazole, cyclopropylamine (CPA) was added to from the corresponding amides. The reaction was carried out under inert atmosphere and the products were obtained as orange solids after purification in 94% for **136** and in 90% for **137** *(Scheme 2.53.)*. The products were characterized by a combination of ^{1}H, ^{13}C NMR, IR and HR-MS.

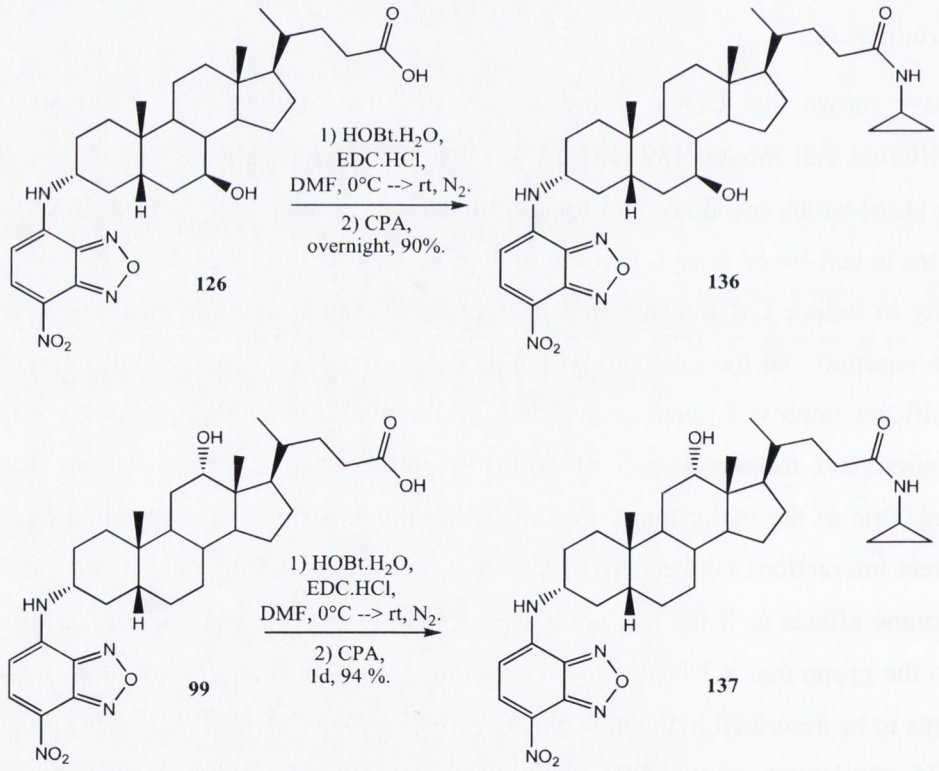

*Scheme 2.53. Synthesis of **136** and **137***

Chapter 3

Fluorescent properties and biological activity of the synthesized dansyl- and NBD-bile acid derivatives

3.1. Aims and Objectives

In this chapter we focus on the photophysical characterisation and *in vitro* behaviour of the synthesized fluorescent bile acid derivatives and control compounds *(Figure 3.1)*. Our experiments aimed to investigate the differential and opposing effects of UCDA (**7**) and DCA (**4**) on cell functionality.

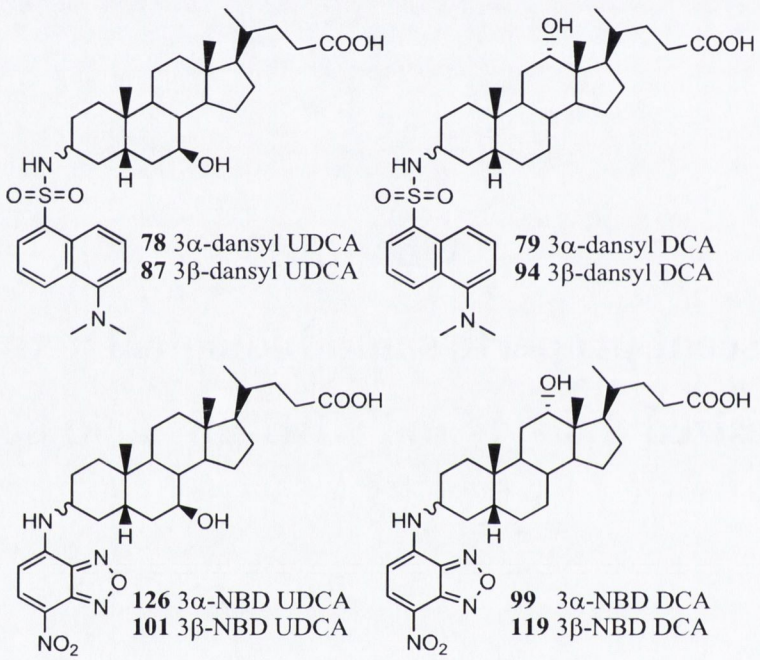

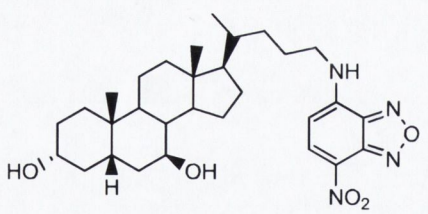

134 24-NBD UDCA

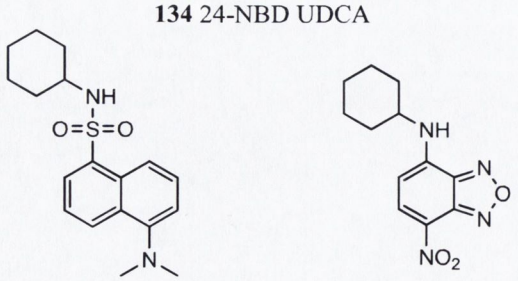

97 Cyclohexyl-dansyl **135** Cyclohexyl-NBD

Figure 3.1. The synthesized fluorescent bile acids and control compounds

To examine these fluorescent bile acids on biological assays, it is first necessary to determine their stability under similar conditions. It is also important to know their absorption and emission profile for HPLC and fluorescent measurements, which are helpful tools to quantify the observations. In the biological experiments first we intended to explore the effect of the dansyl and NBD-substituted bile acids on different cell lines using MTT assays, and then the uptake of these substances in HET1A-s. The uptake can be visualised by InCell and confocal microscopy giving additional information about the disposition of the bile acids within the cells. We intended to characterise the nature of the uptake in HET1A and Caco2 cell lines and quantify it using different techniques.

3.2. Absorption and emission study of fluorescent derivatives

3.2.1. Introduction and methods

The absorption and emission maximums of the prepared fluorescent bile acid derivatives and the control compounds were determined with the Cary 300 Scan UV-Visible spectrophotometer and SHIMADZU RF-1501 spectrofluorophotometer. EtOH was chosen for the preparation of stock solutions. The concentration of stock solutions were optimised to obtain the absorbance values between 0.2 and 1.0, thus they were prepared at 0.02 mg/ml for absorption and emission measurements of the dansyl-substituted compounds. The concentrations were chosen at 0.01 mg/ml for the absorption study for NBD derivatives, and 0.001 mg/ml for the emission measurements. The lower values of the applied concentrations are due to the high sensitivity of the NBD fluorophore, producing similar absorbance and emission intensity to the dansyl-adducts. The absorption spectra of the fluorescent bile acid derivatives and the control compounds were measured by spectrophotometer scanning by detecting the absorbance between 200 and 800 nm. The emission measurements were carried out scanning the emission wavelength between the range of 220 and 900 nm. The excitation wavelengths were chosen according to the determined absorption maxima in every case.

As discussed in Chapter 2, the 24-cyclopropyl amide derivatives of **126** and **99** were synthesized for further investigation on bile acid-glucocorticoid receptor interactions (*Figure 3.2.*).

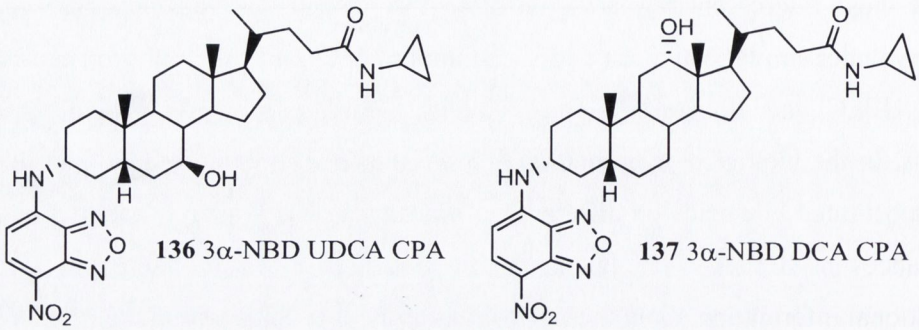

*Figure 3.2. Chemical structure of the **136** and **137***

Although this investigation and the observations are not part of this PhD work, the photophysical characterisation of **136** and **137** is discussed here as it might be interesting to compare the fluorescent properties of these amides to the carboxylic acid ones.

The obtained data from the absorbance measurements allows us to calculate the molar absorptivity constant (ε) of the fluorescent compounds with the use of the Beer-Lambert equation. This constant is a measurement of how strongly a chemical species absorbs light at a given wavelength. With the known of ε it is possible to compare the sensitivity of different fluorescent compounds.

The Beer-Lambert Law: $A = \varepsilon * c * l$

where A is absorbance, ε is the molar absorptivity (extinction coefficient, $dm^3*mol^{-1}*cm^{-1}$), c is concentration (mol/dm^3) and l is the path length (cm), which is 1 cm (cuvette width) in our measurements.

Results displaying the measurements of the fluorescent compounds are represented in the following tables and figures, with the conditions used for absorption and emission being represented in the experimental section (Chapter 5).

3.2.2. Absorption and emission measurements of the fluorescent bile acids and control compounds

The absorption measurements showed that the spectra of each dansyl-compound were similar and the substances have three absorption maxima of 218, 251 and 334–336 nm in EtOH (an example spectra showed in *Figure 3.3*). A small difference was observed between the α- and β-derivatives. In the case of **78**, **79** and **97** the third absorption maximum was at 334 nm, while the spectra showed the maxima at 336 nm in the case of 3β-dansyl derivatives (**87** and **94**). The fluorescent measurements showed that the emission maxima of each dansyl-compound were detected around 510 nm in EtOH. In the cases of **79** and **97** this value was 508 nm. The absorption and emission maxima of each compound are shown in *Table 3.1*.

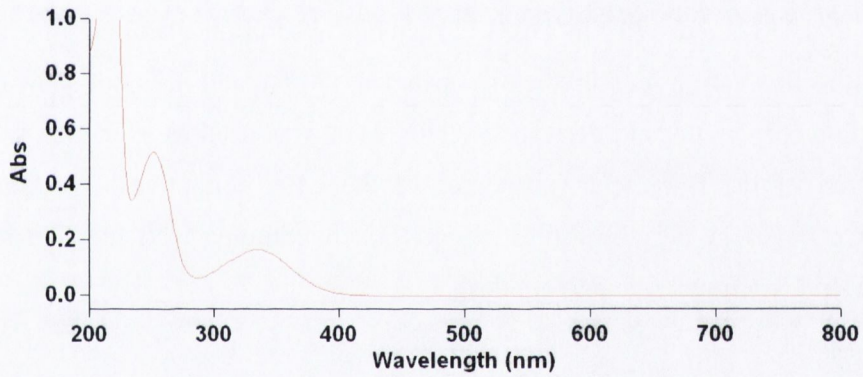

Figure 3.3. Absorption spectra of ***78*** *at the concentration of 0.02 mg/ml in* EtOH *at rt.*

The absorption spectra of 3-amino-NBD compounds (**99**, **101**, **119** and **126**), the 24-NBD UDCA (**134**) and the cyclohexyl-NBD control compounds (**135**) were also similar. As is shown in *Figure 3.4* we also detected three absorption maxima for each compound. The β -derivatives (**101** and **119**) absorbed the light at 227, 331 and 465–466 nm, while these values were red-shifted (228–231, 335 and 470 nm) in the case of **126** and **99**. Maxima of **134** and **135** were similar to the values of 3-NBD compounds. The emission study of NBD-bile acid adducts (**99**, **101**, **119**, **126** and **134**) and the cyclohexyl control (**135**) showed that the emission maxima of the compounds are detected between 530 and 540 nm, in the green range of the visible spectra. Compound **134** emits the light at lower wavelengths (526 nm) compared to the other compounds.

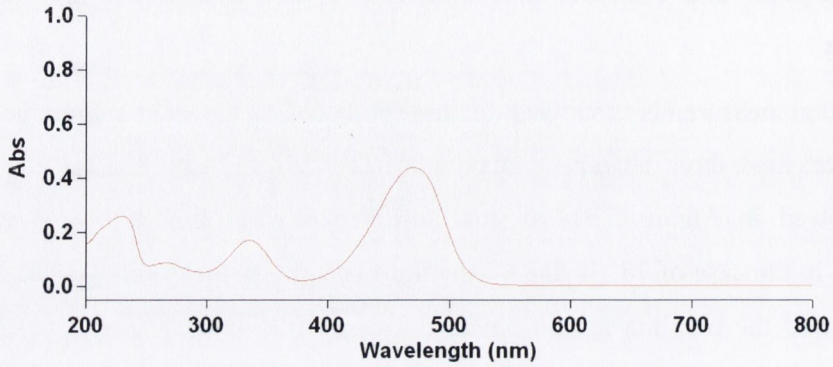

Figure 3.4. Absorption spectra of ***126*** *at the concentration of 0.01 mg/ml in* EtOH *at rt.*

In the case of CPA amides the three absorption maxima were recorded at 222, 333 and 470 nm (**136**) and 204, 337 and 470 nm (**137**). The main absorption maxima, which is the primary wavelength in fluorescent measurements appears at 470 nm and does not show difference to the corresponding carboxylic acid derivatives. This value was used as excitation wavelength in the determination of the fluorescent properties of the CPA derivatives. We could not observe significant changes in the absorption or emission maximums with the transformation of the carboxylic acid functional group to amides.

Compound	Absorption maxima - Wavelength (nm)			Emission maxima Wavelength (nm)
78 (3α-dansyl-UDCA)	218	251	**334**	**510**
87 (3β-dansyl-UDCA)	218	251	**334**	**510**
79 (3α-dansyl-DCA)	218	251	**336**	**508**
94 (3β-dansyl-DCA)	218	251	**336**	**510**
97 (Cyclohexyl-dansyl)	218	251	**334**	**508**
126 (3α-NBD-UDCA)	231	335	**470**	534
101 (3β-NBD-UDCA)	227	331	**465**	537
99 (3α-NBD-DCA)	228	335	**470**	535
119 (3β-NBD-DCA)	227	331	**466**	537
134 (24-NBD UDCA)	227	334	**466**	526
135 (Cyclohexyl-NBD)	225	334	**469**	536
136 (3α-NBD-UDCA CPA)	222	333	**470**	535
137 (3α-NBD-DCA CPA)	204	337	**470**	535

Table 3.1. Absorption and emission maxima of fluorescent bile acid derivatives and controls in EtOH at rt.

In the knowledge of the absorbance (*A*), the sample concentrations (*c*) and the cuvette width (*l*, path length) values the molar absorptivity (ε) of the fluorescent compounds were calculated (*Table 3.2.*).

Compound	Wavelength (nm)	Absorbance	ε ($dm^3*mol^{-1}*cm^{-1}$)
3α-NBD DCA **99**	470	0,462	**25626,22**
3α-NBD UDCA **126**	470	0,436	**24184,05**
3β-NBD DCA **119**	466	0,416	**23074,69**
3β-NBD UDCA **101**	465	0,438	**24294,98**
24-NBD UDCA **134**	466	0,381	**20605,70**
Cyclohexyl-NBD **135**	469	0,904	**23708,30**
3α-NBD DCA CPA **137**	470	0,335	**19896,90**
3α-NBD UDCA CPA **136**	470	0,474	**28144,22**
3α-dansyl DCA **79**	334	0,169	**5280,15**
3α-dansyl UDCA **78**	334	0,168	**5248,91**
3β-dansyl DCA **94**	336	0,142	**4436,58**
3β-dansyl UDCA **87**	336	0,152	**4749,01**
Cyclohexyl-dansyl **97**	334	0,282	**4682,70**

Table 3.2. Molar absorptivity values (ε) were calculated with the use of the Beer-Lambert equation. The table also shows the measured absorbance values at the given wavelengths.

The data clearly showed that compounds labelled with NBD absorb about five times more lights than the dansyl-adducts, which leads better fluorescent properties. The structure of the bile acids did not have impact in this value, except where the carboxylic acids were converted to amides (**136** and **137**).

3.3. Fluorescence quantum yield of the NBD derivatives

3.3.1 Introduction

When a molecule absorbs photons it goes into an excited state which can be deactivated through different competitive pathways. The process that the excited state relaxes to the ground state through photon emission is called fluorescence. Excited organic compounds also can be relaxed through phosphorescence (via triplet state), internal conversion, intersystem crossing or fluorescence quenching with a second molecule.

The quantum yield is a fluorescence process that induced by radiation and can be defined as the ratio of the number of photons emitted to the number of photons absorbed through fluorescence.

$$\Phi = \frac{Number\ of\ photons\ emitted}{Number\ of\ photons\ absorbed}$$

The maximum value of the fluorescence quantum yield can be 1.0 (100%), which means that every photon absorbed results in a photon emitted. The most reliable method to measure the fluorescence quantum yield is the comparative method developed by Williams *et al* [139], which operates with the use of well characterised standard samples with known Φ values. It is possible to determine the quantum yield directly using an "integrating sphere" as the sample compartment in the fluorimeter; this method is called the absolute method. In our experiments we applied the comparative method using the procedure provided by Jobin Yvon [140].

3.3.2 Fluorescence quantum yield measurements and results.

According to the Jobin Yvon Ltd. the measurements has to be carried out with the use of different concentrations of the sample and the cross-calibration of the standard sample with another to avoid incorrect quantum yield values. The chosen excitation wavelength has to be the same for each sample including the standards.

In our experiments 470 nm was identified as a wavelength that all samples and standards showed absorbance, and was used for the fluorescence readings as the excitation wavelength. To validate the method, two standards, fluorescein and rhodamine 6G, were cross calibrated by calculating the quantum yield of each relative to the other. The results matched the literature +/- 10%, as the quantum yield value of rhodamine 6G in EtOH is 0.95 and fluorescein in ethanolic KOH (0.01 M) is 0.925 [141].

Fluorescein: $\Phi_F = 0.922$

Rhodamine 6G: $\Phi_F = 0.953$

Fluorescein in ethanolic KOH (0.01 M) was used as the known standard and its literature quantum yield value ($\Phi_F = 0.925$) was applied to calculate the desired quantum yields for every examined products. The absorbance and emission levels in the concentration range 10 – 50 μM for five solutions of each sample and standard were obtained. The samples were prepared in EtOH, only the fluorescein standard was dissolved in ethanolic KOH (0.01 M). A slope of plotting the fluorescence intensity *vs.* absorbance was used to calculate the quantum yield for each sample using the equation:

$$\Phi_X = \Phi_{ST}\left(\frac{Grad_X}{Grad_{ST}}\right)$$

Where the Φ_X is the fluorescence quantum yield of the examined compound, the Φ_{ST} is the literature quantum yield value of the standard (fluorescein) and the $Grad_X$ and the $Grad_{ST}$ are the gradients from the plot of integrated fluorescence intensity *vs.* absorbance.

The measurements were carried out with Cary 300 Scan UV-Visible spectrophotometer and RF-1501 spectrofluorophotometer (SHIMADZU). The measured values were used to create the fluorescence intensity vs. absorbance graphs to obtain the desired $Grad_X$ values that were required for the calculation of the quantum yields. The graphs showed great linearity in every case; an example graph shown in *Figure 3.5.*

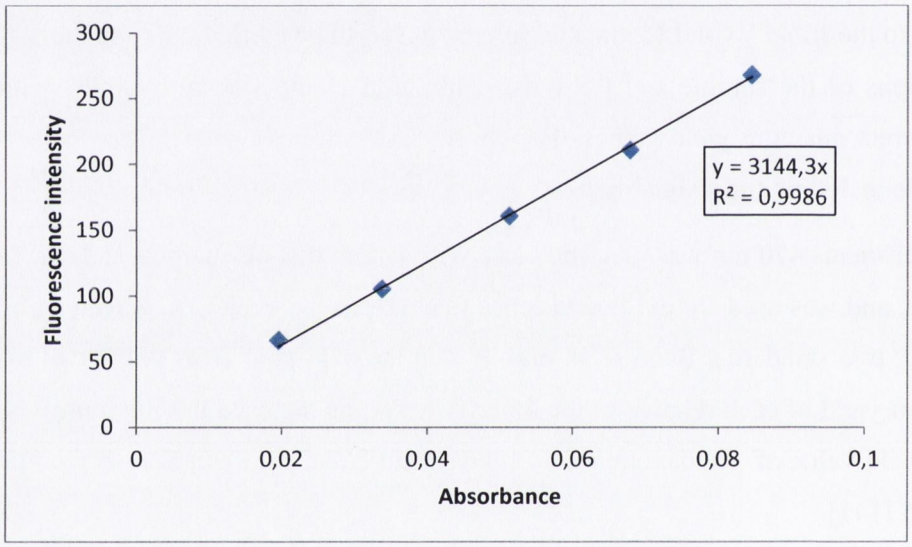

Figure 3.5. Fluorescence intensity vs. Absorbance graph of ***119*** *in* EtOH *at rt.*

Using the *y* values of the trend lines we calculated the quantum yields for each compound which are summarized in *Table 3.3.* The table shows that the NBD-compounds have low quantum yield in ethanolic environment compared to the standards. Generally we can say that the fluorescent UDCA derivatives (**101** and **126**) have higher quantum yields than the DCA ones (**99** and **119**) and the 3α-isomers of the NBD-bile acids (**99** and **126**) emit more photons than the corresponding 3β-NBD compounds (**101** and **119**). Transforming **126** and **99** to cyclopropyl amides results in lower Φ_F values in both cases, while the quantum yield for 24-NBD UDCA (**134**) is between the values of 3α- and 3β-isomers.

Sample	Φ_F
99	0.259
101	0.228
119	0.221
126	0.268
134	0.250
135	0.232
136	0.256
137	0.246
Fluorescein	0.922
Rhodamine 6G	0.953

Table 3.3. The calculated fluorescence quantum yields

3.4. Stability study of 3β-NBD UDCA (101) and 3β-NBD DCA (119)

For the biological examinations we selected two compounds to show the stability of the bile acid-amino-fluorophore bonds under physiological conditions. If the compounds lacked aqueous stability then we would have not been able to use them to investigate the trafficking of bile acids because we would have not been able to discriminate between the trafficking of the analogue and its fluorescent degradant(s). In our study we tried to represent the conditions of the used cells and follow the possible alterations. The stability of 3β-amino-NBD derivatives (**101** and **119**) was examined under physiological pH conditions (7.4) using phosphate buffer solution at 37°C. Solubility tests were carried out before starting the experiments to find the appropriate solvent ratio of acetonitrile and phosphate buffer for the preparation of the stock solutions. It was found that the 2% (**101**) and 5% (**119**) of acetonitrile in the buffer solution help avoid precipitation of the fluorescent bile acids. Results for the fluorescent compounds are shown in the following sections of this chapter and the conditions employed for HPLC analysis are discussed in the experimental section.

3.4.1. Stability study of 101

For the stability study of **101**, a stock solution was prepared at 0.01 mg/ml with 2% acetonitrile/phosphate buffer (pH = 7.4). An HPLC method was developed to explore its stability at 37°C over time. The mixture of acetonitrile and pH = 2.5 phosphate buffer was used as mobile phase with gradient method. The wavelength of detection was determined at 347 nm by

spectrophotometer analysis using the same solvent system for making the sample that used for the HPLC method. The prepared solution was run on HPLC and we could detect the main product and three impurities. The stability study was carried out in a heated sample chamber and with heated column at 37°C over 24 h with injection every hour. The analysis showed that the concentration of the main product did not show significant alteration, thus the tested compound can be regarded as stable under these conditions *(Figure 3.6.)*.

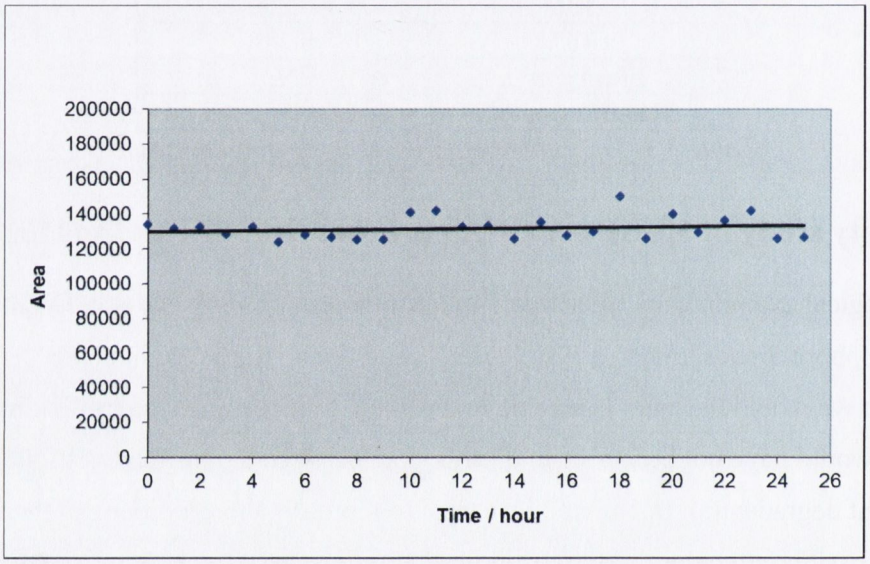

*Figure 3.6. Peak area versus time following incubation of **101** at pH 7.4 and at rt*

The deviation of the obtained data could be derived from human error during the preparation of examined samples.

3.4.2. Stability study of 119

The stock solution of **119** was prepared at 0.01 mg/ml with 5% acetonitrile/phosphate buffer (pH=7.4). The applied conditions were similar to those used in the previous experiment. The measurement was carried out as a control assay, in which we only examined the appearance of degradant(s). The test run showed only one peak on the chromatogram; other fragments did not appear at 24 h *(Figure 3.7.)* proving that these fluorescent bile acid derivatives are stable under physiological conditions.

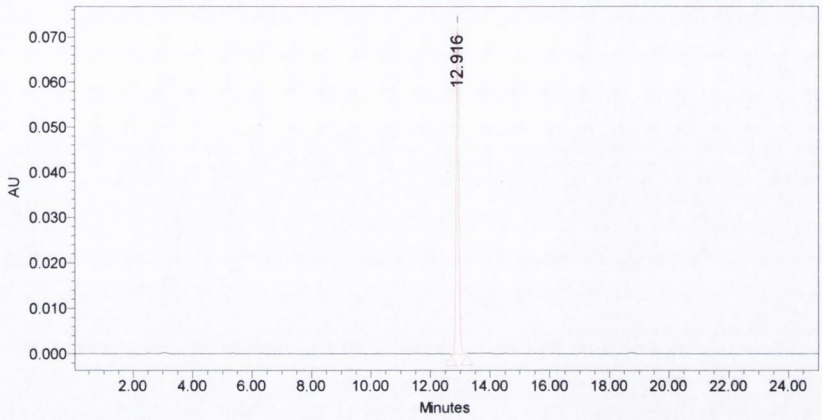

*Figure 3.7. HPLC chromatogram of **119** at T24*

3.5. Cytotoxicity of the fluorescent bile acids

After the characterization of the photophysical properties of the produced fluorescent bile acids and the determination of their stability under physiological conditions we examined their effects in live cell cultures. It was important to know the toxicity of the compounds in those cell lines in which we intended to study bile acid transport processes.

3.5.1. The MTT assay

The MTT assay is a simple method to determine the cytotoxic effect of the examined substances in live cells. It is based on the examination of enzyme activity and measured by a colorimetric assay [142]. A tetrazole derivative (3-(4,5-dimethylthiazol-2-yl)-2,5-diphenyltetrazolium bromide, MTT) is used as reagent and it is reduced to formazan by live cells forming purple crystals (*Figure 3.8.*). At the end of the experiment these crystals are dissolved in the appropriate solvent (usually DMSO) and the absorption of the solution is measured at a certain wavelength (between 500 and 600 nm) by a spectrophotometer. The correlation between the absorbance intensity and the number of live cells can be used to quantify the cytotoxicity of the examined compounds.

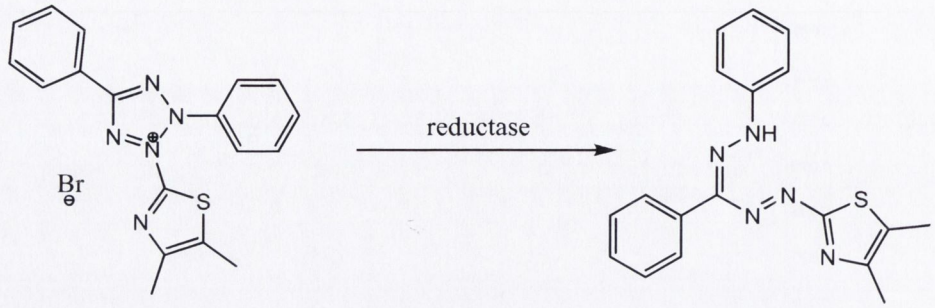

Figure 3.8. MTT is reduced to formazan by enzymes

Different derivatives of tetrazolium were developed since the method was published. The new generation of the dyes is more water soluble or gives different absorption spectra compared to the MTT reagent. With the use of XTT (2,3-bis-(2-methoxy-4-nitro-5-sulfophenyl)-2H-tetrazolium-5-carboxanilide) the final solubilisation step can be avoided, because the produced formazan derivative has a great solubility in water [143]. Another commonly used reagent is the MTS (3-(4,5-dimethylthiazol-2-yl)-5-(3-carboxymethoxyphenyl)-2-(4-sulfophenyl)-2H-tetrazolium) which has an absorbance at 490–500 nm after producing the formazan dye [144].

3.5.2. Introduction

In our experiments we applied the MTT assay to determine the cell viability after the treatment of the cells with the fluorescent bile acids. The main purpose of this project is to study the behaviour and transport of UDCA (**7**) and DCA (**4**) in normal oesophageal (HET1A) cells, thus we focused mainly on this cell line. Additionally, we examined the cytotoxic effect of the fluorescent compounds in other cell cultures, such as the oesophageal adenocarcinoma cells (SKGT4) and the hepatocarcinoma (HUH7) cell line. The stock solutions of the bile acid derivatives were prepared in DMSO which was diluted to the required concentration with supplement free medium. We treated the cells with the bile acid derivatives using four different concentrations (0.1–100 μM) and quantified the cell viability after 4 and 24 h. The cell viability was calculated to the control vehicles, which were treated with the same amount of DMSO (1%) that were used for the treatment with the compounds.

3.5.3. Cytotoxicity of the parent bile acids

DCA (**4**) and UDCA (**7**) cause opposing effects in vivo and in cell suspensions. DCA (**4**) causes DNA fragmentation, oxidative stress, Golgi fragmentation and apoptosis, while UDCA (**7**) has cytoprotective, immunomodulatory, anti-inflammatory and anti-apoptotic effects [145, 146]. In general, UDCA's (**7**) effects oppose those of DCA (**4**) [147-149]. In our experiments we examined the cytotoxicity of **4** and **7** in the 100–500 μM concentration range with the use of three different cell lines (HET1A, SKGT4, and HUH7). The stock solutions (DMSO) were diluted to the required concentration with supplement free medium and incubated for 24 h, while control wells were treated with 1% DMSO to use these data for the calculation of cell viability. Every experiment was carried out as duplicates and repeated three times to obtain 6 data for each sample.

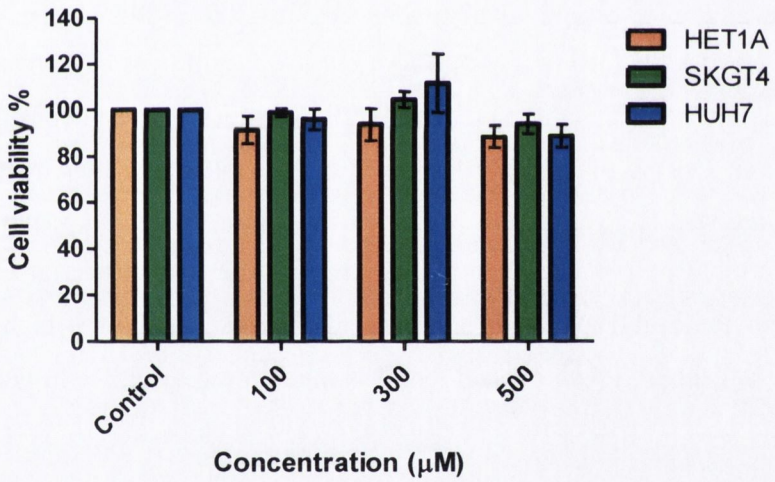

Figure 3.9. The effect of 7 on different cell lines at 37°C and 24 h

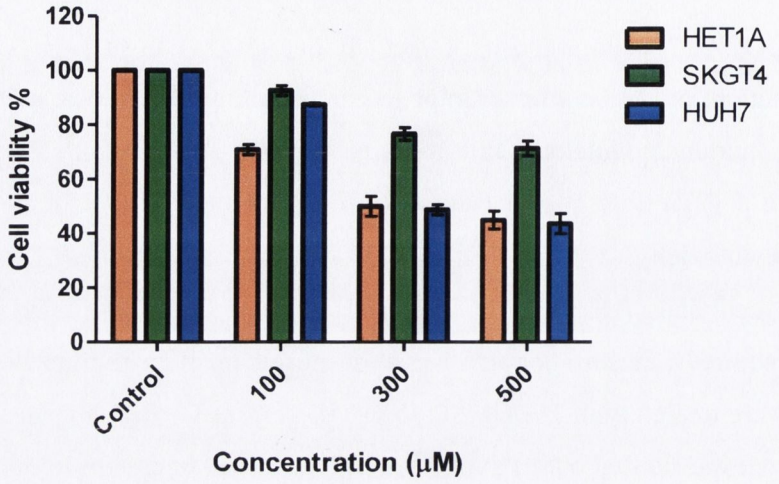

*Figure 3.10. The effect of **4** on different cell lines at 37°C and 24 h*

As is shown in *Figure 3.9.*, **7** had no significant effects on the applied cells. The toxicity of this tertiary bile acid was higher using it at 500 μM, but it was still over 80% in each case. However the effect of **7** at 300 μM was salient in HUH7 cells, it is not significant considering the standard error of the mean. On the other hand **4** showed high cytotoxicity after treating the cells with similar concentrations. The results are presented in *Figure 3.10.* Compound **4** appeared to be more toxic in normal oesophagus then in oesophageal adenocarcinoma at each concentration, while it was not toxic at 100 μM in the case of HUH7s, but it was highly toxic at higher concentrations. In general, it can be said that **4** is much more cytotoxic in the applied cell lines than **7**.

3.5.4. Cytotoxicity of the NBD compounds in different cell lines

To examine the effects of the NBD-attached bile acid derivatives in HET1As, SKGT4s and HUH7s, the cells were incubated with 100 nM, 1 μM, 10 μM and 100 μM of test compounds for 4 and 24 h. The incorporation of the NBD group decreased the solubility of the bile acids, thus the 100 μM was the highest concentration that we could use in these experiments. One of the aims of the toxicity tests was to determine the optimal concentration that could be used later in confocal experiments and transport attempts, in which the compounds stay in the live cell environment for relatively long time. It is also useful to compare the effect of the different isomers to each other and compare the obtained results with the relevant cell lines. On the other

hand these examinations are important steps to prove that the modified bile acids mimic their parents.

The obtained results showed that NBD compounds were not toxic up to 10 μM after 4 h and up to 1 μM after 24 h. Compound **134** proved to be the least toxic, while **99** the most cytotoxic compound. The biggest contrast was found between the 3α-NBD DCA (**99**) and UDCA (**126**) derivatives at higher concentrations after 4 h, but all of the 3-NBD bile acids showed high cytotoxicity after 24 h incubation. In general we can say that the lack of carboxylic acid group of the controls leads to the disappearance of cytotoxic effect on normal oesophageal cells. It also follows from the results that the NBD group does not have any effect on HET1As itself, but together with the bile acid moiety - UDCA in this case - the substance stimulates the cell growth (*Figure 3.11.*).

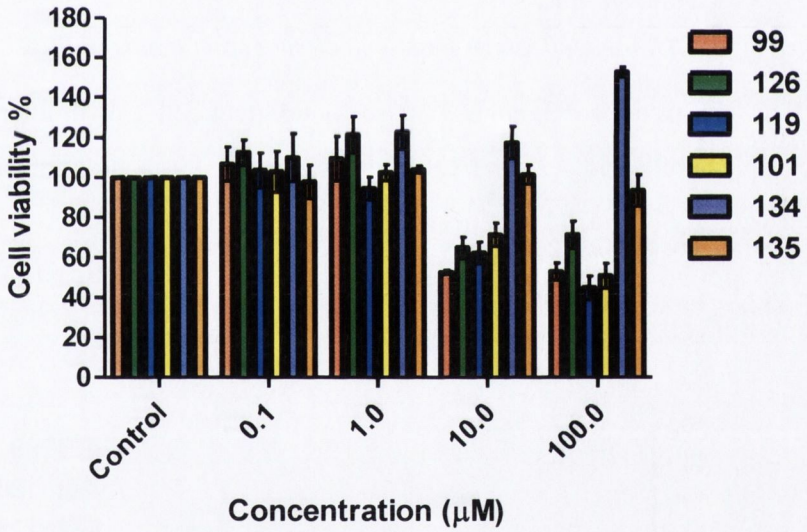

Figure 3.11. Cytotoxic effects of the prepared NBD-compounds in HET1As at 24 h

The toxicity tests were repeated with oesophageal adenocarcinoma (SKGT4) cell line using similar conditions as in the case of HET1As. The results showed that NBD-substituted bile acids and the control compound are not toxic in SKGT4s; they have rather cell growth stimulating effect in high concentration (*Figure 3.12.*). Compared to the results obtained from HET-1As we can establish that the 3α-NBD bile acids (**99** and **126**), which were the most toxic substances in the previous cell line cause opposite effects in the adenocarcinoma cells.

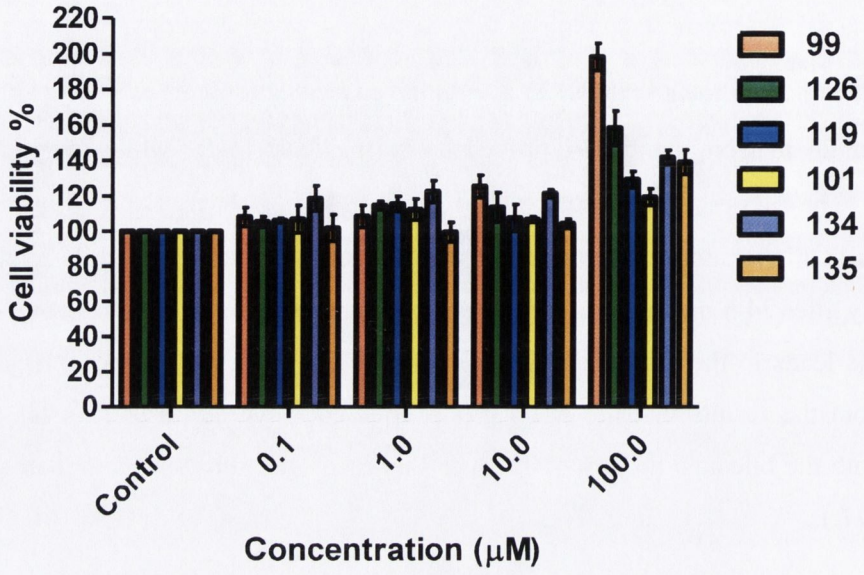

Figure 3.12. Cytotoxic effects of NBD-substituted compounds in SKGT4s at 4 h.

By treating HUH7s with the compounds we also found great cell growth after 4 h, mainly with the use of the 3αNBD bile acids (**99** and **126**). The examined substances did not cause significant changes in cell viability between the concentration range of 0.1 –10 μM. At these conditions the cell survival was around 100% in every case and the most cytotoxic 3α-NBD UDCA (**126**) did not resulted in lower cell viability than 80% (*Figure 3.13.*).

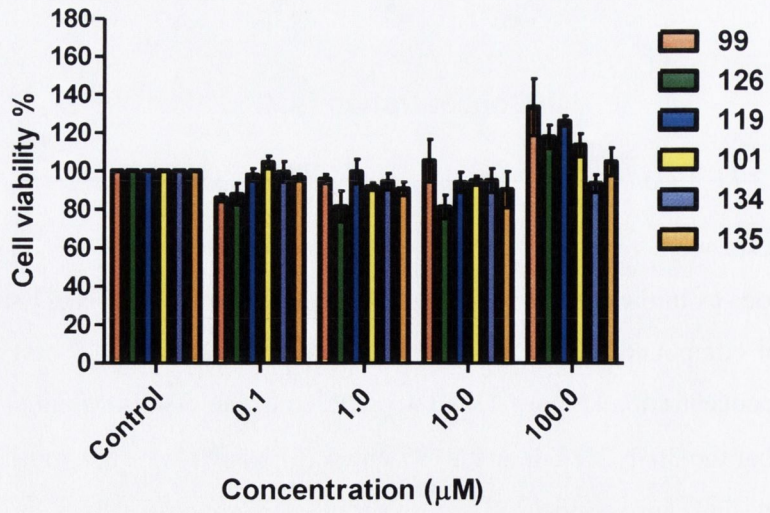

Figure 3.13. Cytotoxic effects of NBD-substituted compounds on HUH7 cell line at 24 h.

3.5.5. Cytotoxicity of the dansyl compounds in different cell lines

The toxicity tests of the dansyl-bile acid adducts (**78**, **79**, **87** and **94**) was carried out under similar conditions as used by the NBD compounds. Only the 3α-dansyl DCA (**79**) showed cytotoxic effects at 4 h in HET1As, but only at higher concentrations. Up to 1 μM the dansyl-compounds proved to be not toxic at 24 h. It can be seen in *Figure 3.14.* that the examined fluorescent molecules were toxic only at higher concentration after a long incubation time. Consistent with the results following testing of the NBD derivatives, it appears that the 3α orientation produces more toxic bile acid derivatives. As shown later, by RPHPLC retention/capacity factor, the α compounds are more lipophilic than the β compounds [120]. It is possible that this relative hydrophobicity is an influential factor in determining the cellular toxicity. Alternatively, as also shown later, the relative toxicity could be due to relative cellular access, which differs between α and β -substituted compounds.

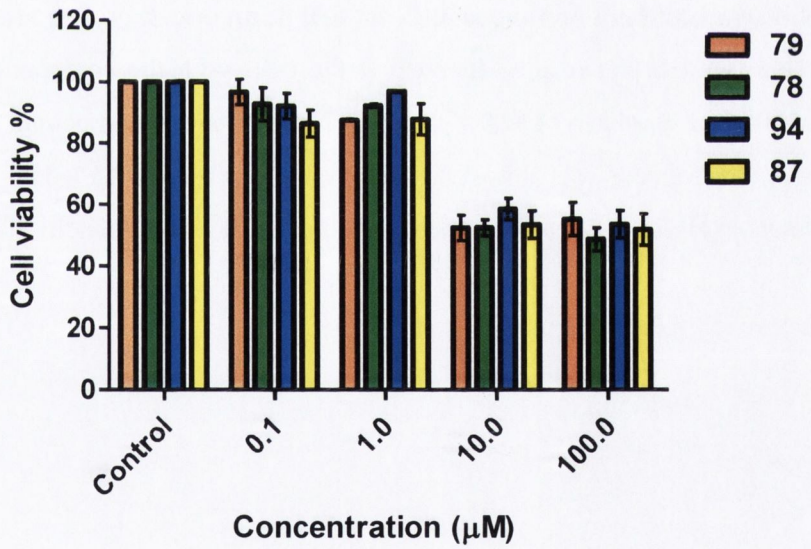

Figure 3.14. The effect of 3-dansyl bile acids on HET1As viability at 24 h.

Repeating the experiments with SKGT4 cell lines we found that the compounds showed toxicity only at 100 μM after 24 h, but this effect was not significant (*Figure 3.15.*). There was no difference between the effects of UDCA and DCA derivatives, neither the α- and β -epimers.

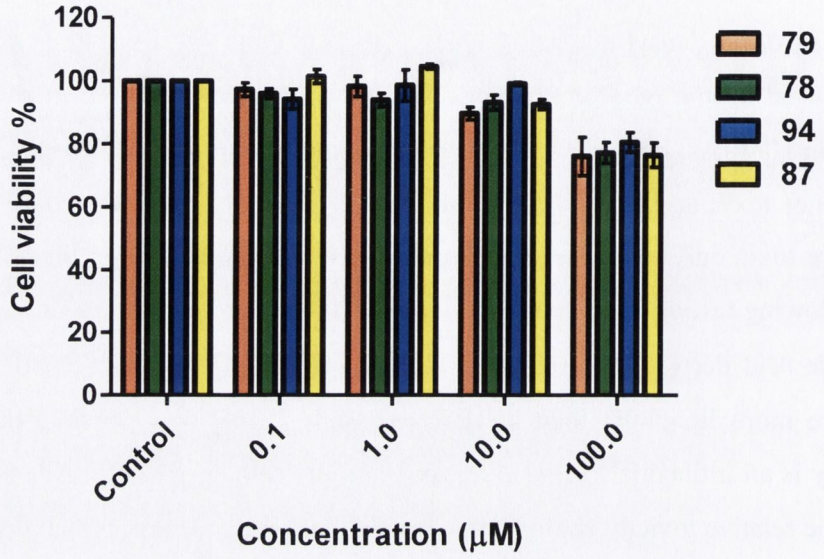

Figure 3.15. Cytotoxic effects of dansyl-bile acids in SKGT4s at 24 h.

Using HUH7 cells we could not observe significant cell death or cell growth after 4 h and there was no observable trend in the results. Incubating the cells with the compounds for 24 h the analysis showed that the 3α-dansyl DCA (**79**) is the most cytotoxic compound. Using it at 100 μM the number of the live cells was almost halved after 24 h (*Figure 3.16.*). This value is similar that we could detect in HET1As with the same compound using similar conditions.

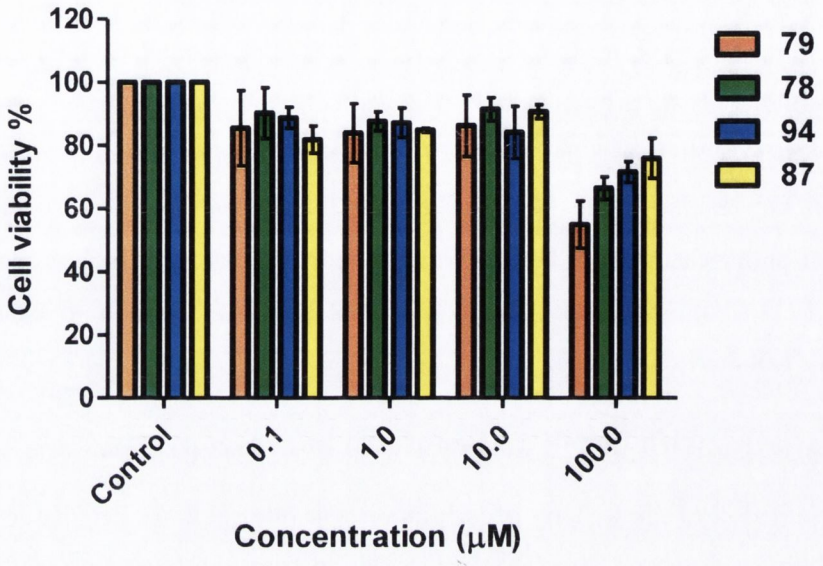

Figure 3.16. Cytotoxic effects of 3-dansyl bile acids on HUH7 cell line at 24 h.

3.5.6. Conclusion

The cytotoxicity tests of the NBD-substituted derivatives in HET1As, SKGT4s and HUH7s showed that these compounds are not toxic at lower concentrations and they can be used for other experiments without damaging the cells. Opposite effects were detected at high concentration applying normal and cancer cell lines. The 3-NBD bile acids proved to be toxic in normal cells and showed similar effects to the parents, while in the two different cancer cell lines the presence of the NBD group has changed the toxicity of the compounds. While DCA (**4**) showed great toxicity in HUH7s at 300 and 500 μM, it stimulated cell growth at 100 μM with the presence of the NBD fluorophore on the bile acid. In the case of UDCA compounds the NBD group at position-3 made the steroid toxic in normal oesophageal cells, while the effects on other cell lines were similar to the DCA derivatives. The substance behaved opposite attaching the fluorophore to the side chain (Compound **134**). It stimulated the cell growth using HET1As, while it had no intensive effects in cancer cells. The cyclohexyl-NBD control compound (**135**) did not show extraordinary influence in either case, it had a minimal cell proliferation effect in cancer cell types.

Using dansyl-fluorophore to label bile acids gave different toxicity results. The 3-modified bile acids did not show cytotoxic effects after 4 h at any concentration and in any cell lines except the

3α-dansyl DCA (**79**) in HET1As. It caused decreased cell concentrations at 10 and 100 μM, while others had no effects in these circumstances. Incubation the cells with 10 and 100 μM of the fluorescent bile acids for 24 h resulted in halved cell count using normal oesophageal cells, while in the cancer cells only the highest concentration showed minimal toxicity effects. Compared with the results of the NBD-substituted substances there were no observable cell proliferations in either cases. Both fluorophore proved to be toxic at higher concentration and only after 24 h incubation; hence these compounds are good enough to examine transport processes in live cell environment.

3.6. Uptake studies with in cell and confocal microscopy

After the determination of the toxicity of the fluorescent bile acids we decided to examine them in the live cell environment and track their distribution from the beginning of the treatment of HET1As. The HET1A cell line is not known to express a BA transporter and therefore considered impermeable to bile acid conjugates. In the following experiments we used High Content Screening (In Cell Analyzer) and Laser Scanning Confocal Microscopy to obtain information about the behavior of the fluorescently tagged bile acids. These techniques make it possible to determine the location of the compounds in the cell membrane or within the cells at different time points.

3.6.1. Introduction

To carry out the experiments 96 glass well plates were used and thirty thousand cells were incubated in each well for 24 h before the treatment with the fluorescent bile acids. During the tests the cells were not fixed, we followed the transport processes in live cell environment. The stock solutions of the fluorescent compounds (DMSO) were diluted to the required concentration with supplement free medium and freshly prepared before the treatment by every experiment. The nucleus of cells was stained in almost every experiment before addition of the compounds. The NDB-derivatives give green fluorescent signal in aqueous environment, thus in these cases we used the blue HOECHST 33342 nucleus dye. Before the examination of the blue fluorescent dansyl-bile acids the nuclei were stained with the DRAQ5 dye, which emits the light in the red range of the electromagnetic spectra. The optimal concentration of 1 μM of the NBD- substituted bile acids and the control compound was determined at which these substances are not toxic

longer timepoints and the quality of the fluorescence proved to be satisfactory to take images. In the case of dansyl-derivatives 10 μM proved to be the most useful in consideration of the weaker sensitivity of the fluorophore.

3.6.2. Disposition of NBD-bile acids within live cell environment

To date there is no evidence that normal oesophageal cells (HET1A) have bile acid transport proteins, thus the first goal of these experiments was to examine the location of the fluorescent bile acids in the live cell environment. We wanted to find first whether these modified bile acids accumulate in the cell membrane or they enter into the cells. To answer this question the GE In Cell Analyzer 1000 instrument was used first, which is a high content microscope based screening platform capable of large scale objective analysis of fluorescently labelled cells using automated image acquisition, data management and multi-parametric analysis.

In the first experiment oesophageal cells were treated with 24-NBD UDCA (**134**) and the 3-modified UDCA and DCA derivatives (**99**, **101**, **119** and **126**) then images were taken after several minutes of treatment (*Figure 3.17.*). The compounds were added to the cells in three different concentrations first (100 nM, 1 μM and 10 μM) to determine which one is optimal for fluorescent microscopy. We found that with the use of 100 nM the fluorescence signal was too weak, while the other two applied concentrations proved to be suitable. It was decided to use the fluorescent bile acids at 1 μM concentration in later experiments considering these findings and the earlier results of toxicity tests.

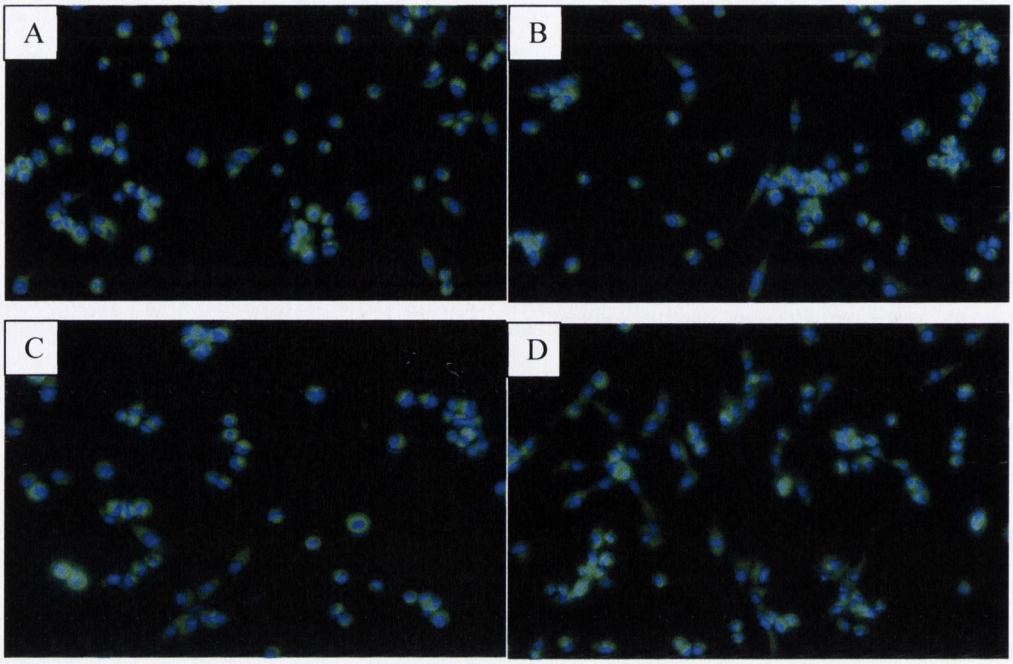

Figure 3.17. Fluorescent bile acids (green) in HET1A cells at 1 μM at 5 min; the cells were stained by Hoechst (blue) to identify the nuclei. A: 3α-NBD DCA ***99****, B: 3β-NBD DCA* ***119****, C: 3α-NBD UDCA* ***126****, D: 24-NBD UDCA* ***134****.*

The In Cell tests showed that the cells became fluorescent; hence the fluorescent bile acids came into contact with the applied cell line. Using this equipment it was not possible to decide whether the compounds entered into the cytoplasm or they just covered the surface of the cells, therefore further examinations were required to determine the quality of interaction between the cells and the modified bile acids.

3.6.3. Examination of NBD-bile acids using confocal microscopy

To answer the above question it was decided to use confocal microscope that is capable to view inside the cells to take high quality images. The practical advantage of the technology is that the microscope is able to scan a thin section of the sample and with scanning many thin sections it is possible to build up a three-dimensional image of the examined sample. This technology was used in the following experiments to help us understand the nature and behavior of bile acids in HET1As.

In the next experiments HET1A cells were treated with 1 μM of the NBD-bile acids (**99**, **101**, **119**, **126** and **134**) and the control compound (**135**) and the transport of them were followed up to 30 min by confocal microscope. The experiments showed that every fluorescent derivative entered into the cytoplasm region independently of the structure of the molecule (*Figure 3.18.*). It was also observed that the examined compounds formed spheres in the cytoplasm which could be appear as vesicles or as the compound attached to lysosomes, liposomes or endosomes. It is known that bile acids form micelles when their concentration is higher in the cytoplasm, than the critical micellar concentration (CMC). In this case it can be excluded because the control produced similar spheres without having a bile acid moiety in its structure.

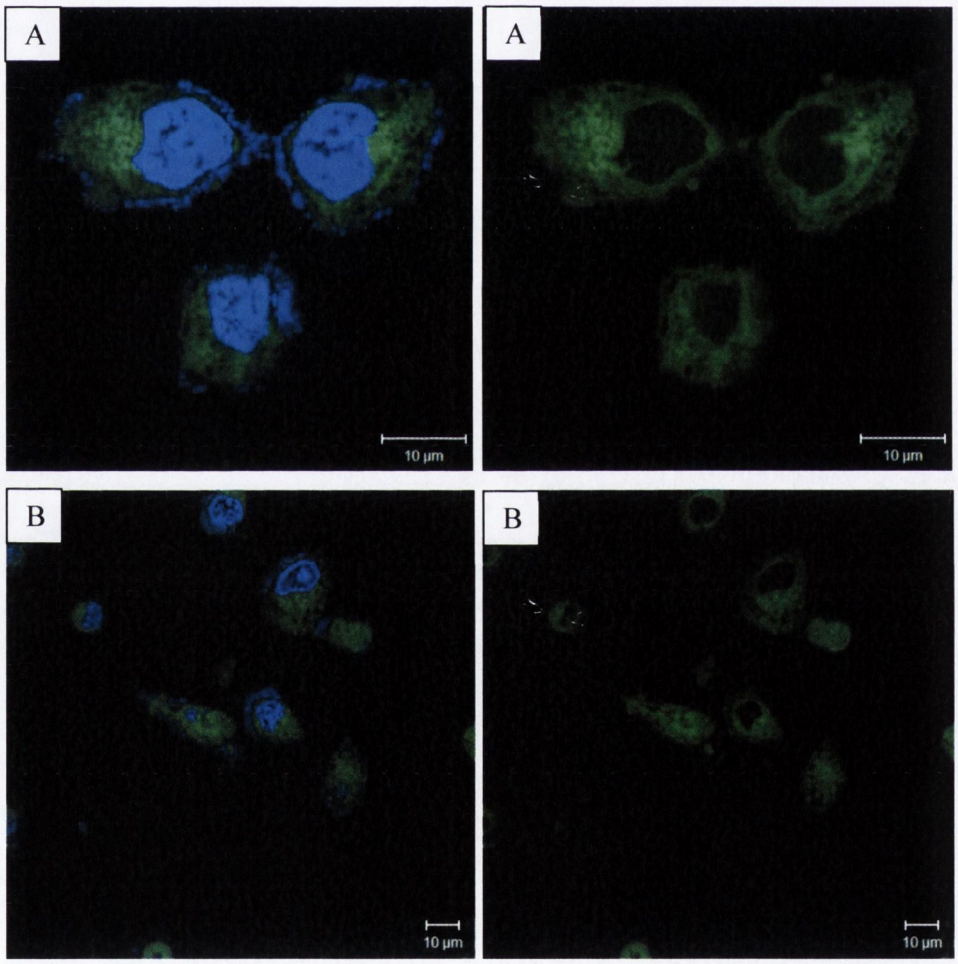

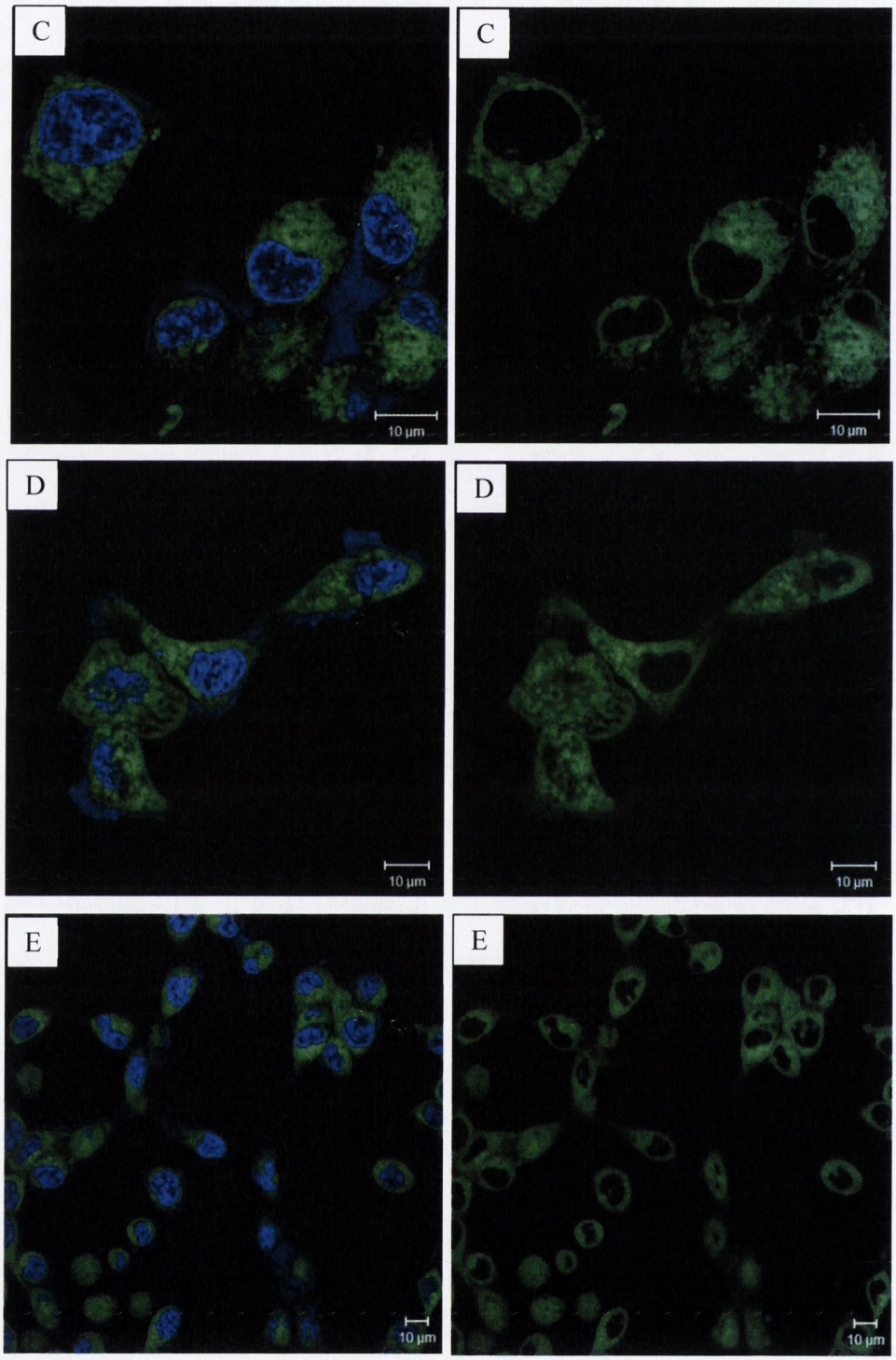
C
10 µm
C
10 µm
D
10 µm
D
10 µm
E
10 µm
E
10 µm

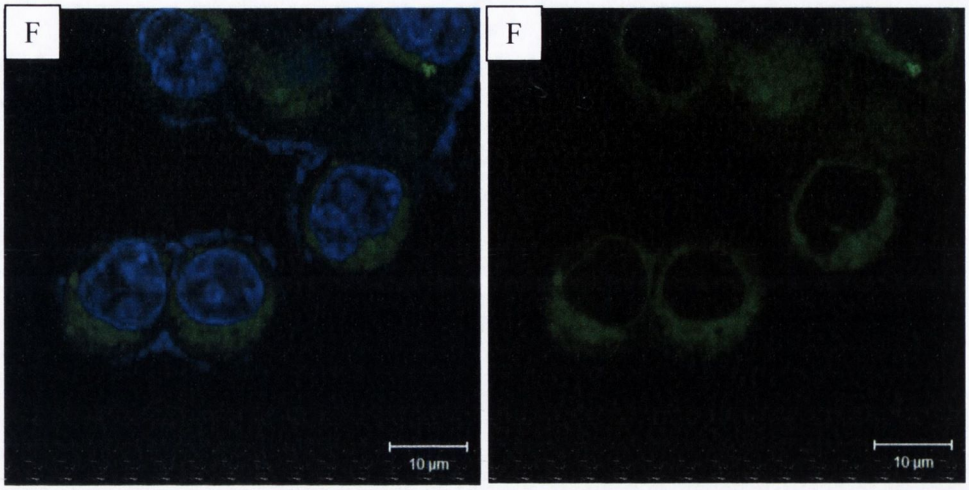

*Figure 3.18. The NBD-bile acids and the control compound in HET1As at 1 µM after several minutes. Left: The cells were stained by Hoechst (blue) to identify the nuclei. Right: The blue fluorescent signal is turned off (by LSM Image Browser software) showing that the fluorescent bile acids (green) did not penetrate into the nuclei of cells. A: 3α-NBD UDCA **126**, B: 3β-NBD UDCA **101**, C: 3α-NBD DCA **99**, D: 3β-NBD DCA **119**, E: 24-NBD UDCA **134**, F: Cyclohexyl-NBD **135**.*

The wells were scanned from bottom to top and images were taken in the centre of the cells. HET1As took bile acid derivatives up quickly; we could observe strong fluorescent signal after 1–2 min after addition. The intensity of the fluorescence increased quickly after several minutes, and then it did not change over the 30 min test time. It was not possible to quantify the fluorescence intensity using confocal microscopy, but we could detect much weaker fluorescent signalin the case of the control compound (**135**) than in the case of the NBD-bile acid adducts. This observation suggests to us that the uptake of the control compound was not so significant; hence its transport process may have occurred differently. To prove this assumption it is necessary to quantify the examined compounds in the cells.

3.6.4. The presence of the NBD derivatives in HET1A cells after 4 h

In the next step we examined the intracellular transport of the compounds. The HET1A cells were treated with the NBD-derivatives and incubated for 4 h after which time the distribution of the fluorescent bile acids was examined using the confocal microscope. We could observe similar behavior in each case and we found that the fluorescence bile acids accumulated around the

nucleus and also appeared in the nuclear membrane (*Figure 3.19.*). After this longer incubation time the fluorescent compounds were not seen throughout the cytoplasm and a transport process was observed to the nucleus or nucleus-related organelles, despite the green fluorescent signal did not appear in the nucleus. The formation of "vesicles" was seen again and appeared to be part of the transport process. Much less fluorescence could be detected after 4 h, than in the previous short time experiments. It can be concluded that these substances rapidly enter cells and accumulate around the nucleus through a slower intracellular distribution process. However the presence of the compounds in the cytoplasm was not so intensive than earlier and the direction of the transport pointed to the nucleus, the nuclear transport did not achieve.

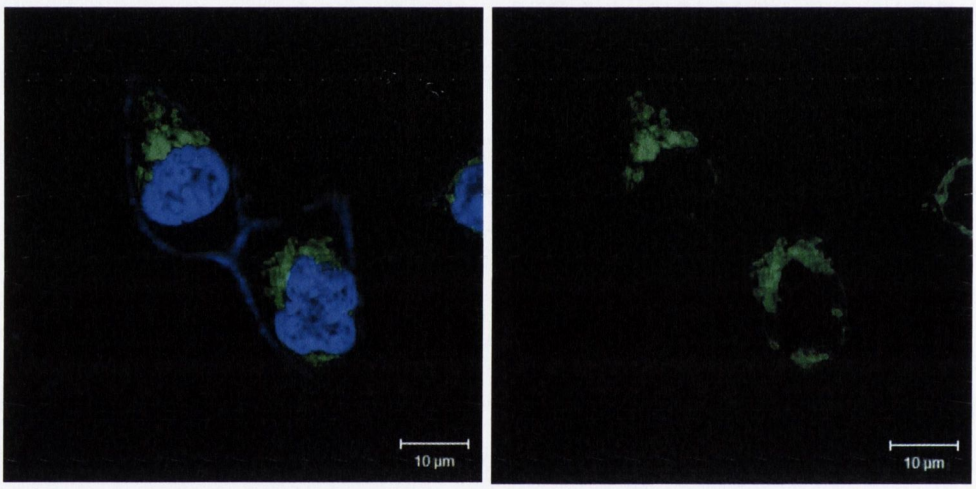

*Figure 3.19. Compound **99** (green) in HET1A cells at 1 µM after 4 h (The blue signal identifies the nuclei on the left, while this signal is turned off on the right by the LSM Image Browser software).*

3.6.5. Experiments for inhibiting the vesicular transport process

As we seen in the previous experiments the NBD-derivatives formed "vesicles" in the cytoplasmic region. To support or refute this allegation it was decided to use inhibitors to study the behavior of the compounds in the cytoplasm while vesicular transport. One of the commonly used inhibitors is primaquine ((*RS*)-*N*-(6-methoxyquinolin-8-yl)pentane-1,4-diamine), which blocks the transport process by inhibiting the formation of transport vesicles [150]. Another possible way to inhibit vesicular transport is the use of cytochalasin D inhibitor, which prevents the actin-involved movements in the cells, thus blocks the movement of transport vesicles [151].

The first test was carried out incubating the cells with 300 μM of primaquine for 30 min before the addition of the two selected fluorescent bile acids (**126** and **99**). The confocal images were taken after several min of the treatment using the confocal microscope. The experiments yielded similar observations as earlier, the tested fluorescent bile acids were taken up by the cells quickly and the circles were formed again in the cytoplasmic region in every case showing that these spheres are not vesicles.

In the second test the 3-NBD bile acids (**126** and **99**), the 24-NBD UDCA (**134**) and the control compound (**135**) were added to the pretreated oesophageal cells (3 μM) cytochalasin D and the uptake processes were followed up to 1 h. During the experiments the compounds behaved similarly to the previous tests. The use of inhibitor did not prevent the formation of fluorescent rings in the cytoplasm, it was no difference observed to the normal uptake studies. It can be concluded that these modified bile acids did not enter into the cells with vesicular transport and the formed spheres are not transport vesicles.

3.6.6. Competition experiments

To study the nature of bile acid uptake of HET1A cells it was decided to examine the effect of co- and pretreatment on the observed uptake process. Treating the cells with high concentration of DCA (**4**) and UDCA (**7**) before adding the fluorescent derivatives might change the behavior of these compounds. This experiment would indicate that the compounds are being actively taken up by the same transporter. The compounds in high concentration might activate directly or indirectly the transport proteins in the cells which are involved in the transport processes of the examined compounds. On the other hand the bile acids might downregulate these transporters causing reduced uptake of the fluorescent derivatives.

In our experiments three NBD-bile acid derivatives (Compounds **126**, **99** and **134**) were selected for the competition against the parent bile acids. Different cases were studied and the cells were treated with **4** and **7** (500 μM) in the tests. First, 1 h pretreatment was analysed before the addition of the fluorescent bile acids, then we examined the effect of **7** and **4** with addition to the cells in the same time with the NBD-bile acid adducts. Hence, 1 h pretreated cells with **7** and **4** were treated with 1 μM of **126**, **99** and **134** and monitored using confocal microscope. Pretreatment of the cells with this high concentration of **4** resulted in significant amount of cell

death after 1 h incubation, but the experiments could be carried out successfully. Analyzing the confocal images we could not observe any difference compared to the normal uptake processes. The fluorescent bile acids were taken up by HET1As quickly after the addition and "vesicles" were also present in the cytoplasm. The co-treatment experiments resulted in similar observations. It can be concluded that applying high concentrations of **7** or **4** for pre- or co-treatment did not prevent the uptake of the fluorescently labeled bile acids, but it was not possible to quantify the difference in the volume of up taken compounds using this instrument.

3.6.7. Examination of the relationship between the NBD derivatives and the Golgi apparatus

During this part of the work we tried organelle dyes to explore the relationship between the compounds and the Golgi apparatus. Fortunately, many types of dyes are available in the market and different methods were worked out to apply these substrates. In the experiments first we tried to stain the organelle using fixed cells. Fixing the cells stops the intracellular transport processes and preserves the current conditions of the cells. This method allows the opportunity to analyze the results regardless of the elapsed time after the treatment. It is also possible to stain the organelles in live cells, which guarantees similar uptake process during the experiment. This method is more difficult to carry out, but it gives more realistic indication of the transport of the fluorescent bile acids in the cells and makes it possible to study its process instead of only single stages.

3.6.7.1. Organelle staining in fixed cells

To fix the cells we tried three different solutions to see which one could be used in co-staining experiments. Ten thousand HET1A cells were seeded into each well of a 96 well plate, then, after 24 h incubation, the cells were treated with **99** and incubated for 15 min. The supernatant was then removed and the fixing procedure was carried out adding 4% of paraformaldehyde solution (in PBS) for 15 min, ice cold MeOH (-20°C) for 5 min or ice cold acetone (-20°C) for 5 min. These supernatant solutions were then removed from the wells and the cells were washed with PBS twice and incubated for 24 h in this buffer solution. The fixed cells were examined under confocal microscope to analyze the effect of the treatment on the cells. It was found that the membranes of the cells were damaged using acetone and the rest of the compound was diffused into the extracellular region, thus we disregarded the use of this solvent in further investigations.

The cells fixed with MeOH also seemed unhealthy, so this method was not adequate for the co-staining experiments either. Analyzing the cells fixed with 4% PFA we found that the distribution of the fluorescently labeled bile acid remained similar to the live cell experiments and the quantity of the compound in the cells was appropriate for imaging.

In the knowledge of these results we decided to examine the co-staining on the PFA fixed cells using the GM130 antibody to investigate the relationship between bile acids and the Golgi apparatus. The Golgi complex is localized in the perinuclear region of most eukaryotic cells and is involved in processing, transporting and sorting of intracellular proteins. GM130 is a member of the golgin family of Golgi autoantigens [152]. It is a cytoplasmic protein, which localizes mostly to the *cis*-Golgi network (CGN) and binds to the Golgi membranes [153]. The staining procedure was carried out according to the protocol described in the experimental section (Chapter 5). We also stained the nucleus with the HOECHST dye during the experiment. The stained and fixed cells were then examined by confocal microscopy. It was found that the fluorescent signal of **99** was only slightly detected. To understand the failure of the experiment we reassessed that our staining approach. To mark the Golgi apparatus with the antigen it is necessary to permeabilise the cell membrane, because the fixing procedure stops the transport processes. This step is followed by the incubation of the cells with primary and secondary antibodies and during this procedure the cells are washed with PBS several times. During these steps the fluorescent compounds were partially washed out through the permeabilised cell membrane from the cytoplasm and the distribution of the remaining compounds was changed within the cells. Without the permeabilisation step, the organelle staining is not possible, because the antibodies are not able to pass through the cell membrane. On the other hand the application of this step creates the condition for the passive diffusion, thereby causing diffusion of the bile acids from the intracellular region. The fluorescently labeled compounds might bind to transport proteins or the Golgi apparatus weakly in the cytoplasm, thus the "washing out" procedure is possible. To solve this problem we could treat the cells with the bile acids after the Golgi staining, but this would not represent the original uptake process, however the cells would be "filled up" with the compounds due to passive diffusion through a now porous membrane. Because we cannot guarantee the original distribution of the fluorescent bile acids in the cytoplasmic region the fixing method is not suitable for different organelle staining.

3.6.7.2. Organelle staining in live cells

To stain the Golgi apparatus in the live cell environment we chose the red fluorescent Human Golgi-resident enzyme (*N*-acetylgalactosaminyltransferase 2, CellLight®) [154]. Thirty thousand cells were seeded into the wells of a 96 glass well plate and the cells were incubated the appropriate amount of Golgi marker for 16 h, after which time **126** or **99** was added to the wells at 1 μM and the uptake process was followed by confocal microscopy. The confocal images were taken from the zero time of the addition of compounds up to 30 min. The fluorescent bile acids were taken up quickly by HET1As and the green fluorescent signal could be detected in the whole cytoplasmic region. *Figure 3.20.* shows the cells before treatment (left) and after 30 min of treatment (right) with 3α-NBD DCA (**99**).

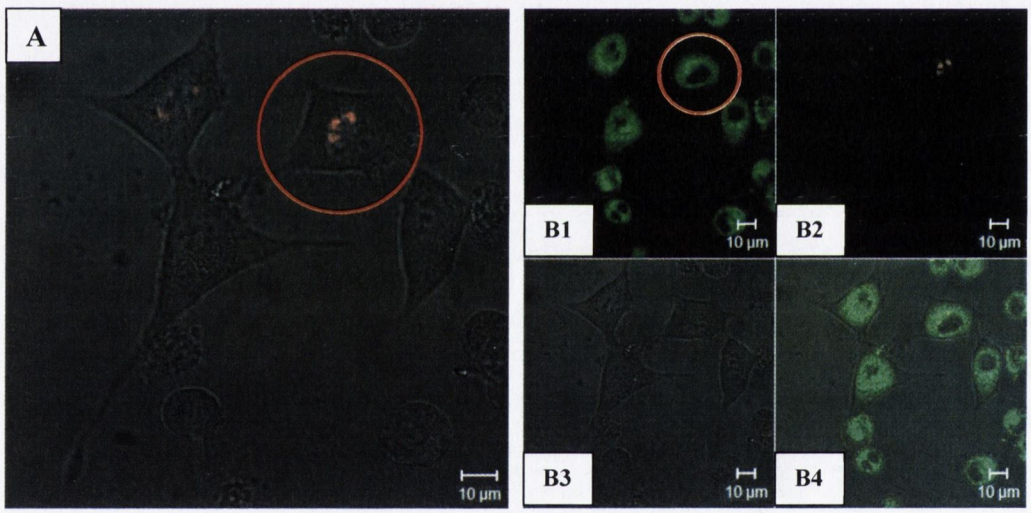

*Figure 3.20. A: HET1A cells were incubated with the Golgi marker for 16 h after which time the Golgi apparatus gave orange fluorescent signal. B1-4:Cells treated with the green fluorescent **99** at 1 μM. The confocal image shows the distribution of **99** at 30 min. (B1: Compound **99** (green), B2: Golgi marker (red), B3: Background, B4: Background+**99**+Golgi marker. The different fluorescent signals were turned off by LSM Image Browser software.)*

As can be seen the Golgi apparatus is located beside the nucleus. We found that addition of 1 μM fluorescent DCA did not cause Golgi fragmentation after 30 min. The bile acid gave a stronger fluorescent signal where the Golgi apparatus was located; it was accumulated around or within the Golgi. This accumulation could be observed after several min of incubation. The effect of treating the cells with the corresponding UDCA analog (**126**) was unclear. Lower levels of

accumulation was detected in the Golgi apparatus after 11 min and strong fluorescent signal was also detected around the nucleus. We observed a higher contrast between the green fluorescent signal of Golgi and its environment after 24 min of addition (*Figure 3.21.*). Analyzing the confocal images it can be concluded that **99** accumulates in the stained organelle quicker than its UDCA analog, but it cannot be stated that the compounds are targeted the Golgi apparatus only. Further studies are required with live cell dyes to determine which organelles are involved in bile acid uptake.

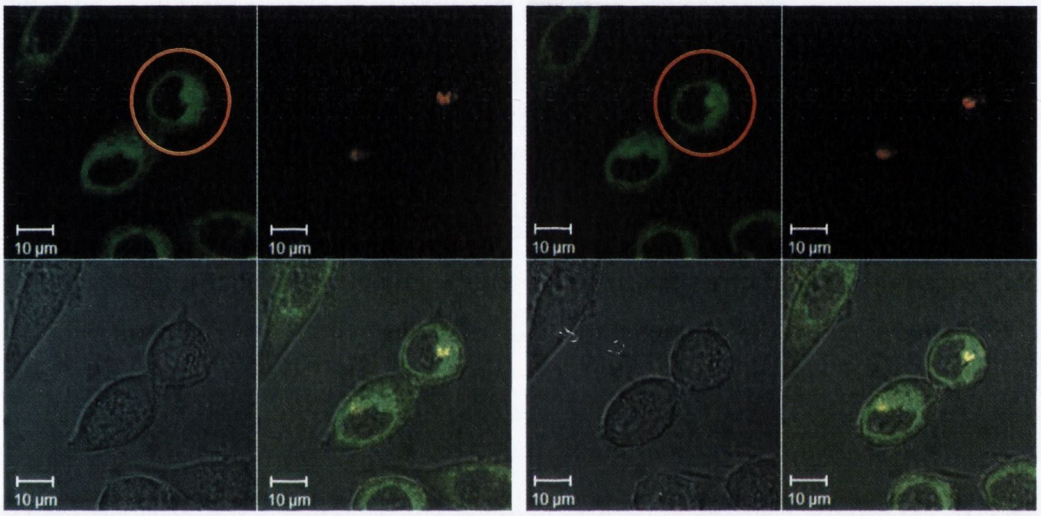

*Figure 3.21. Left: 3α-NBD UDCA (**126**) accumulated in the cytoplasm after 11 min. Right: The same cells after 24 min. The images are splitted into four parts by LSM Image Browser software showing the different fluorescent signals and background individually or together. The red circle shows the accumulation of **126** in the Golgi apparatus of the Het1A cell.*

3.6.8. Examination of the uptake of dansyl bile acids using confocal microscopy

As described above the NBD- substituted bile acids entered into oesophageal cells after 1–2 min of the addition and dispersed throughout the cytoplasm. We repeated the experiments with the dansyl analogues (**78**, **79**, **87** and **94**) to see if the structure of the fluorophore influences the uptake of the compounds. We used a higher concentration of dansyl compounds than NBD because of their lower emission properties (which could influence their relative distribution). In these experiments HET1A cells were treated with 10 µM of the dansyl bile acids and the distribution was followed up to 4 h by confocal microscope. The dansyl analogues were also transported through the cell membrane quickly and accumulated in the cytoplasmic compartment.

We could not observe a similar distribution of vesicles in the cytoplasm as we observed previously with the NBD compounds.

3.6.8.1. Uptake study of 3α-dansyl UDCA (78)

The uptake of **78** was studied after different incubation times from 0 min up to 4 h. Compound **78** entered into the oesophageal cells quickly, but the transport process was not within the confines of the cytoplasmic region. The dansyl-UDCA analog was also transported through the nuclear membrane because the blue fluorescent signal was also observed in the nucleus. Before the addition of the compound into the well the nuclei were stained with Draq5 dye which emitts red light.

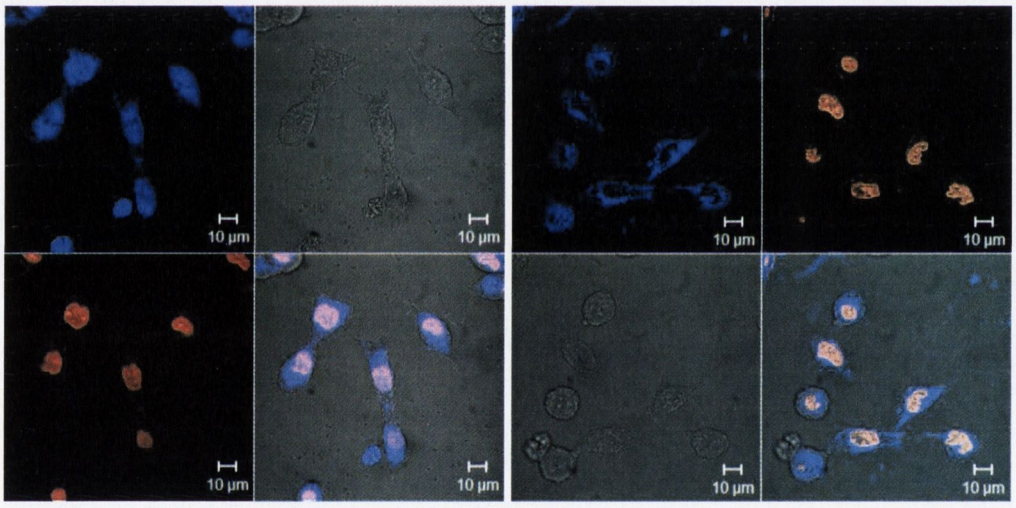

*Figure 3.22. Uptake of **78** (blue) by HET1As at 10 µM after 40 min (on the left) and after 4 h (on the right) incubation. The red fluorescent signal identifies the nuclei (Draq 5). The images are splitted into four parts by LSM Image Browser software showing the different fluorescent signals and background individually or together.*

The difference between the NBD and dansyl moiety resulted in distinct intracellular transport. It can be clearly seen in *Figure 3.22* that the dansyl bile acid also entered into the nuclear region after 40 min and accumulated more in the nucleoli. This nuclear transport implicitly occurs later than the appearance of the compound in the cytoplasm. The effect was detected after 20–30 min of the addition. Examining the presence of compound **78** after 4 h incubation in the cells we found that it decreased significantly. Initially we thought the effect may have occurred because of the breakdown of the dansyl moiety by unidentified enzymes. The confocal image showed that

compound **78** was still present in the cytoplasm (mainly around the nuclei), but it was not detected in the nucleoplasm.

In the next step we examined the effect of high concentration of bile acids on the transport and distribution events. The cells were pretreated for 1 h or co-treated with 500 μM **4** or **7** before the addition of the dansyl substituted UDCA. It was found that co-treatment with **4** changed the intracellular distribution. In contrast to the normal uptake of compound **78** we could observe significant blue fluorescent signals from the nuclear region even after 10 min (*Figure 3.23.*).

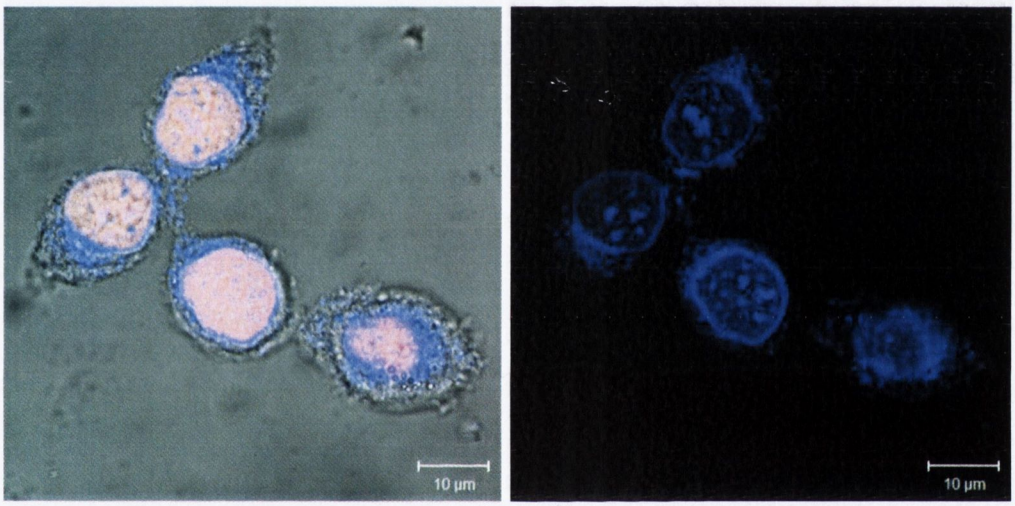

*Figure 3.23. Effect of co-treatment with DCA (**4**) (500 μM) for 10 min on the distribution of **78**. Image on the left shows the distribution of **78** and the Draq 5 nucleus dye (red) in the cells, while image on the right shows only the fluorescent signal of the bile acid derivative **78**.*

The dansyl bile acid accumulated more in the nucleolus and significant presence was also observed around the nuclei with the formation of a bright "ring" in the confocal image. Analyzing the images it seems that compound **78** binds to the nuclear membrane probably due to the mechanism of the nuclear transport process. The use of **4** at a high concentration resulted in the upregulation of nuclear transport or at least the intensity of nuclear membrane signal.

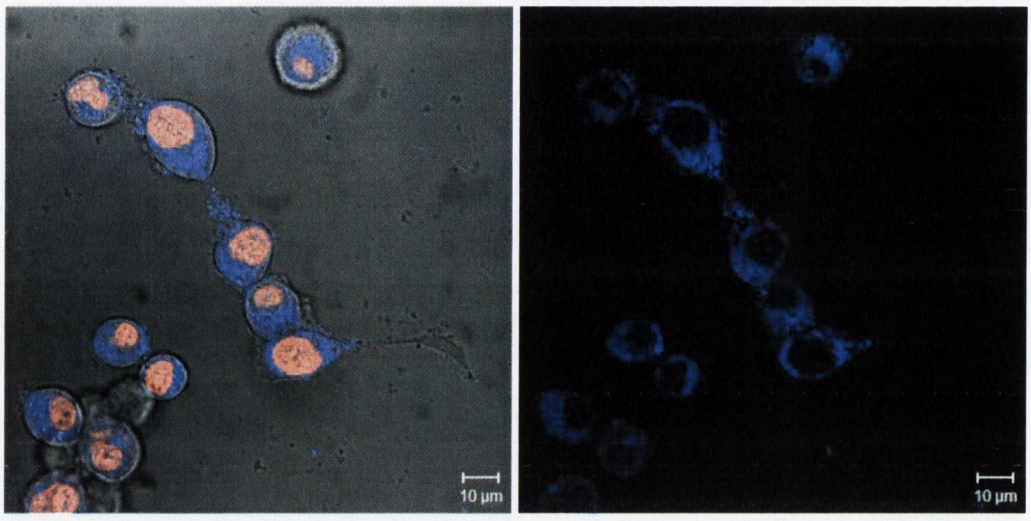

Figure 3.24. Confocal images following co-treatment of **78** *with 500 µM UDCA (7) in HET1As at 25 min. Image on the left shows the distribution of the blue bile acid derivative and the Draq 5 nucleus dye (red) in the cells, while image on the right shows only the fluorescent signal of the bile acid derivative.*

On repeating the experiment with **7** at 500 µM we found the opposite effect. The uptake was monitored up to 40 min during which time the dansyl analog was not observed in the nuclear region (*Figure 3.24.*). The accumulation of the dansyl bile acid was not seen in the nuclear membrane either which allows us to conclude that the use of **7** blocks the nuclear transport.

The pretreatment with the high concentration **4** resulted in similar observations to the co-treatment. The accumulation of compound **78** in the nuclear membrane and in the nuclei/nucleoli was observed after a relatively short time. By contrast, the 1 h pretreatment with **7** caused an opposite effect to co-treatment. We found a significant amount of dansyl UDCA in the nuclear region, mainly in the nucleolus, but the compound **78** cannot be seen in the nuclear membrane (*Figure 3.25.*).

It can be concluded from these experiments that **4** and **7** regulates the nuclear transport of bile acids in oesophageal cells. In the presence of **4** in the cells, the nuclear membrane is much more involved in the transport process than it is with the saturation of cells with **7**. However the mechanism of these effects is not known. These experiments also provide an indirect evidence of the uptake of bile acids by oesophagus due to changing the transport of other compartment such as dansyl UDCA in this case.

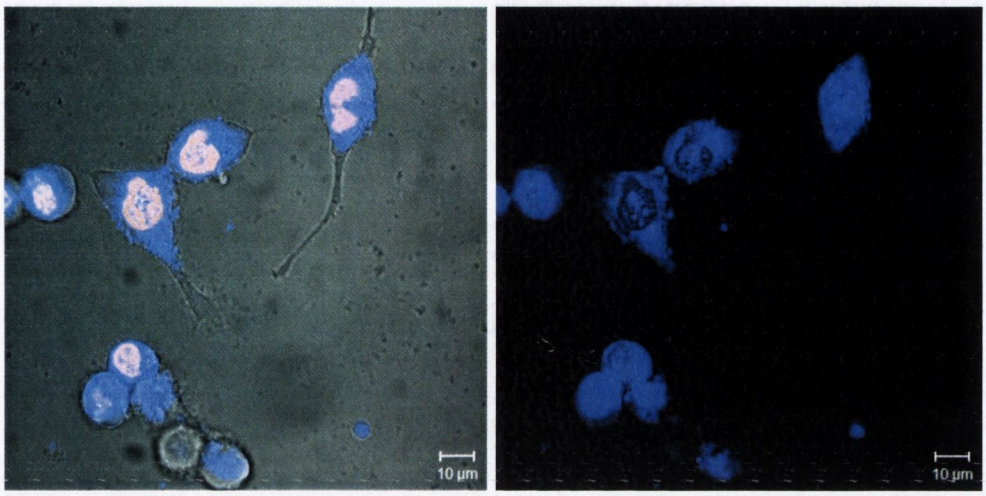

Figure 3.25. Uptake of ***78*** *in 1 h 7 pretreated HET1As. The confocal image was taken after 15 min of addition. Left: the distribution of the blue bile acid derivative and the Draq 5 nucleus dye (red) in the cells. Right: the fluorescent signal of the bile acid derivative in the same cells.*

3.6.8.2. Uptake study of 3α-dansyl DCA (79)

Similar tests were carried out to assess the uptake of **79**. The process was also monitored up to 4 h by confocal microscopy. It was found that the compounds entered into the cytoplasm quickly and accumulated around the nuclei. It can be seen in *Figure 3.26.* that the nuclear transport was not as prominent as observed in the case of the UDCA analogue. The dansyl bile acid could be also found in the nucleolus of the cells, but the nucleoplasm did not fluoresce. The nuclear membrane was well marked and gave a sharp borderline between the nucleoplasm and cytoplasm. As in the case of the **78** the appearance of the fluorescent signal significantly decreased in the cells after 4 h, while it totally dissapeared in the nuclear region.

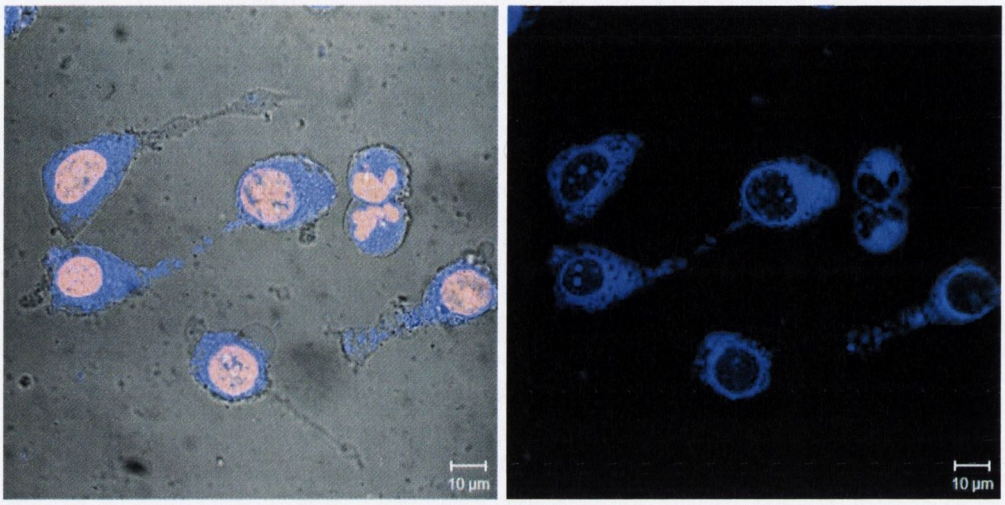

Figure 3.26. Uptake of compound **79** *(10 µM) in HET1As. The confocal image was taken after 55 min. Left: the distribution of the blue bile acid derivative and the Draq 5 nucleus dye (red) in the cells. Right: the fluorescent signal of the bile acid derivative in the same cells.*

Competition experiments were repeated in this instance using **4** and **7** at 500 µM. Co-treatment with **4** did not result in significant effects on nuclear transport. Compound **79** appeared strongly in the nuclear membrane and we could detect less in the cytoplasm. The experiment with **7** showed stronger appearance of the fluorescent bile acid in the cytoplasmic region and less in nucleolus regions, while the strong accumulation of it was not observed in the nuclear membrane. Pretreatment experiments with the secondary and tertiary bile acids resulted opposing observations. Compound **4** promoted the nuclear transport processes, while **7** down-regulated or blocked it. These findings could connect to the fact that **7** has cytoprotective effects, while **4** acts the opposite way.

3.6.8.3. Uptake study of the 3β-dansyl bile acids (87 and 94)

We also examined the 3β-epimers (**87** and **94**) of the dansyl bile acids under similar conditions as described above. The uptake of compound **87** was monitored over 3 h and a strong fluorescence signal was detected in the nuclei even after this time. In contrast to the other dansyl-bile acids, the presence of this derivative in the nuclear region remained significant after a longer incubation time. Both the nucleoplasm and the nucleoli were involved in the distribution of the substance within the cells as well as the cytoplasm (*Figure 3.27.*).

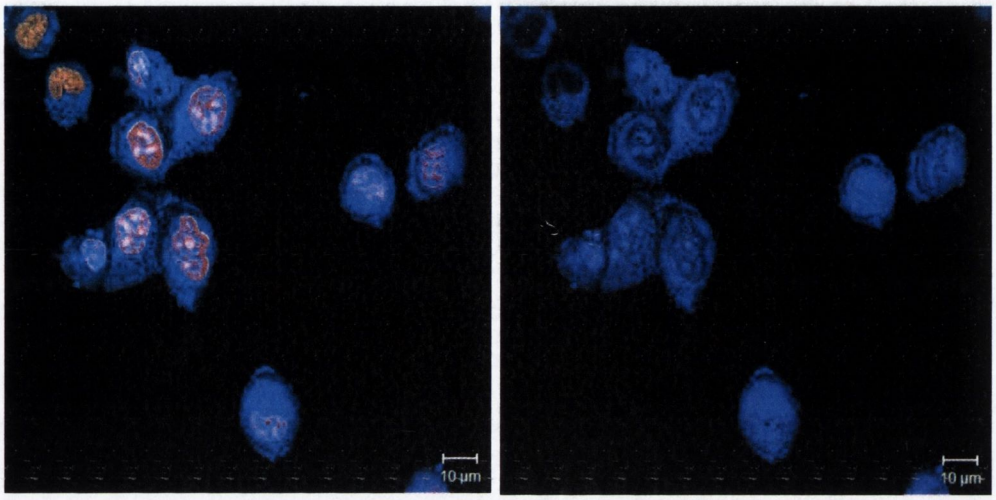

Figure 3.27. Uptake of 10 µM compound ***87*** *(blue) in HET1As. The confocal image was taken 3 h after addition. Left: the distribution of the blue bile acid derivative and the Draq 5 nucleus dye (red) in the cells. Right: the fluorescent signal of the bile acid derivative in the same cells.*

Testing compound **87** in competition experiments we could observe similar trends as earlier. Compound **4** pre- and co-treatment resulted in the accumulation of the dansyl UDCA in the nuclear membrane at high concentrations, but it did not prevent its entry into the nucleoplasm or nucleoli. Greater levels of transport were detected in response to 500 µM of **7** detected (*Figure 3.28.*) in pre- and co-treated oesophageal cells. The nuclear membrane was not involved noticably in the accumulation of **87** in the cells. The DCA analogue (**94**) of this fluorescent bile acid showed similar properties, but less was observed in the nucleoplasmic region. Nuclear transport observed in a similar manner, when treated with **4** and **7**

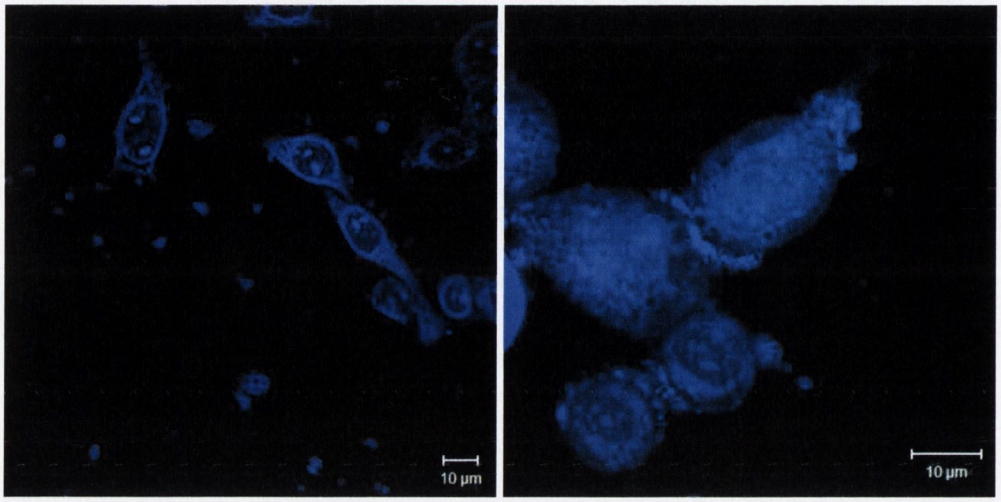

Figure 3.28. Uptake of 10µM of compound ***87*** *(blue) in pretreated HET1As with 500 µM* ***4*** *(on the left) and 7 (on the right). Images were taken after 15-20 min of addition of Compound* ***87****.*

3.6.9. Effect of cytochalasin D on intracellular distribution of the fluorescent bile acids

As we mentioned above, the use of cytochalasin D inhibits actin-related intracellular transport. The 3-dansyl bile acids were tested following pretreatment of oesophageal cells with 3 µM cytochalasin D and the uptake process monitored over 30 min. Cytochalasin D treatment markedly decreased nuclear distribution of the compounds. It did not affect the diffusion of the bile acid derivatives into the cytoplasm, but it significantly decreased their transport into the nuclear region (*Figure 3.29.*). This effect suggests that nuclear transport may be mediated by an actin-dependent process or that cytochalasin D inhibits nuclear or other intracellular transporters.

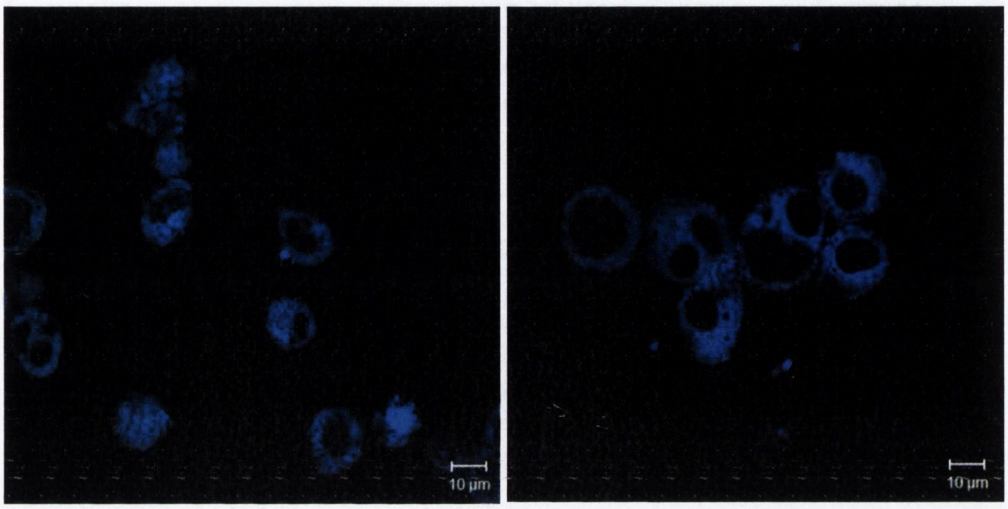

Figure 3.29. ***Left****: The uptake of 10 µM* ***78*** *(blue, 30 min) by HET1As pretreated with 3 µM cytochalasin D.* ***Right****: The uptake of 10 µM* ***79*** *(blue, 40 min) by HET1As pretreated with 3 µM cytochalasin D.*

3.7. Examination of stability and uptake of the fluorescently labelled bile acids in HET1A cell line by HPLC.

As we shown above, the NBD-bile acid adducts are stable at physiological pH over 24 h. To examine the stability of the NBD- and dansyl- substituted compounds in the live cell environment it was decided to develop a method for quality and quantity measurements. The idea based on the observations obained by the confocal studies was that the fluorescent bile acids entered into the cells and they were taken up quickly. Flow cytometry is a commonly used technique for cellular fluorescent events [155], but it relies on the fluorescent probe being stable during the experiments. To avoid the possibility that the fluorescent bile acids could be damaged by intracellular processes we decided to measure their stability in the cellular environment whereas before we had measured it in buffer.

3.7.1. Development of the HPLC method.

In the first step the composition of mobile phase, the flow rate and injection volume were examined to achieve short retention times with good detection by UV. It was found that that the water/1% pH=3.0 ammonium formate buffer/acetonitrile (15:10:75) mixture ratio was appropriate as mobile phase for the measurements and that it was possible to perform it in

isocratic mode. The pH value of this solvent composition was 3.58 which might have changed the fluorescence properties of the compounds. To obtain higher sensitivity on the UV and fluorescent detectors we determined the absorption and emission maxima of the compounds at pH = 3.58. The samples for the measurements were prepared in 20 μM for the NBD compounds and 0.02 mg/ml in the case of dansyl compounds. The absorption spectra were recorded by Cary 300 Scan UV-Visible spectrophotometer scanning and detecting the absorbance between 200 and 800 nm, and then the fluorescent measurements were taken using the SHIMADZU RF-1501 spectrofluorophotometer. The excitation wavelengths were chosen according to the absorption maximum for each compound.

The absorbance and emission values were red-shifted at pH = 3.58 compared to the values measured in EtOH. However the difference was not substantial we used these values for excitation and detection wavelengths in the HPLC measurements.

In the next step of the HPLC method, development series of solutions of the compounds were injected in different concentrations to obtain calibration curves, which gave information about the concentration range that can be detected reliably using a linearity assumption. In our system both fluorescence and UV detection were applied, but the measurements focused on the fluorescence signal. In the case of each NBD or dansyl bile acid derivative the samples were measured in nine different concentrations from 10 nM to 10 μM (10 nM, 50 nM 100 nM, 250 nM, 500 nM, 750 nM, 1 μM, 5 μM, 10 μM). Every concentration was run three times and the average peak area was calculated. The results showed linear relation between the concentration and peak areas. In a few cases the 10 μM was too high for detection, because of the sensitivity of the fluorophore. The compounds were used in our biological assays at 1 μM (NBDs) and 10 μM (dansyls); hence the correlation has to be linear in that range. *Figure 3.30.* and *Figure 3.31.* show sample calibration curves obtained from these experiments.

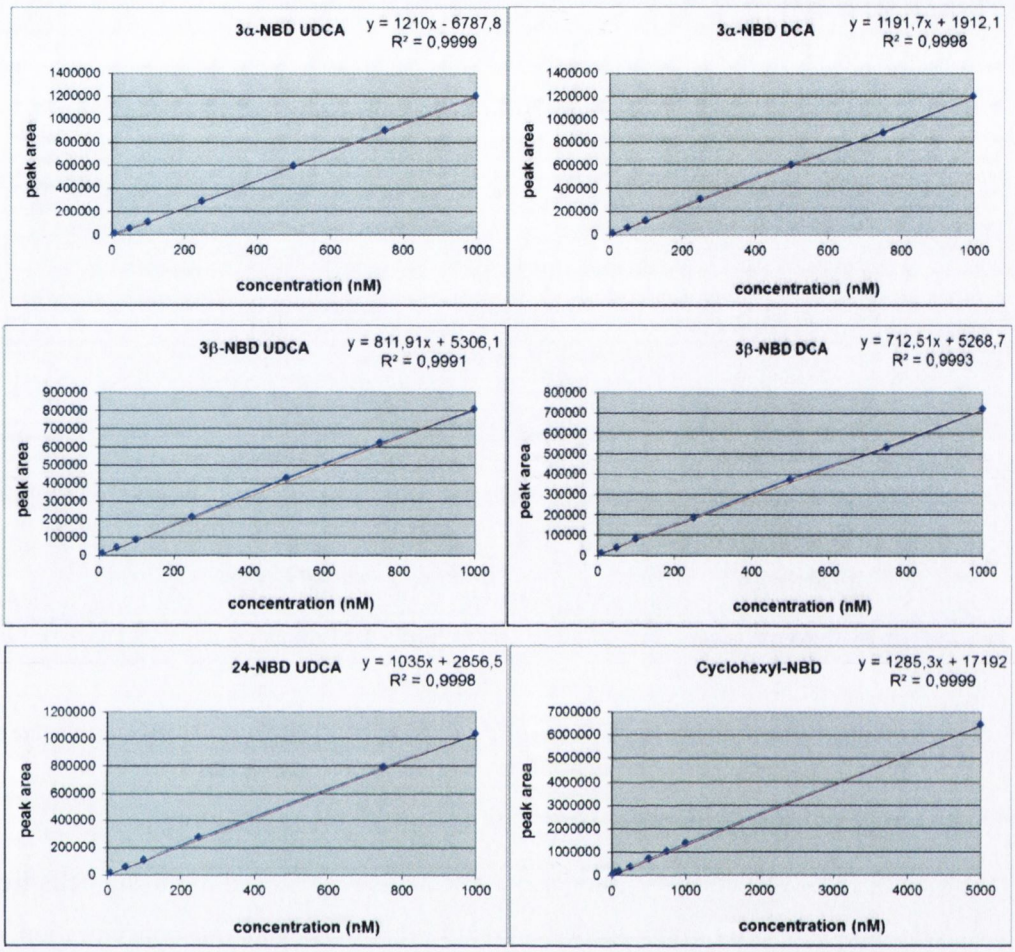

Figure 3.30. Calibration curves of the NBD-bile acids and Cyclohexyl-NBD. Concentration versus peak area at rt.

The results showed that the analytical method is useful to determine the concentration of fluorescent derivatives in biological samples between 10 nM and 5 μM in the case of NBD compounds. The analysis of the dansyls resulted in linear curve in the examined concentration range. The lower sensitivity of the dansyl fluorophore led to the detection of the higher concentrations, thus the method is appropriate to measure biological samples treated with 10 μM of the fluorescently labeled bile acids. The UV method allows mass analysis of the possible alterations of NBD bile acids on LC-MS system.

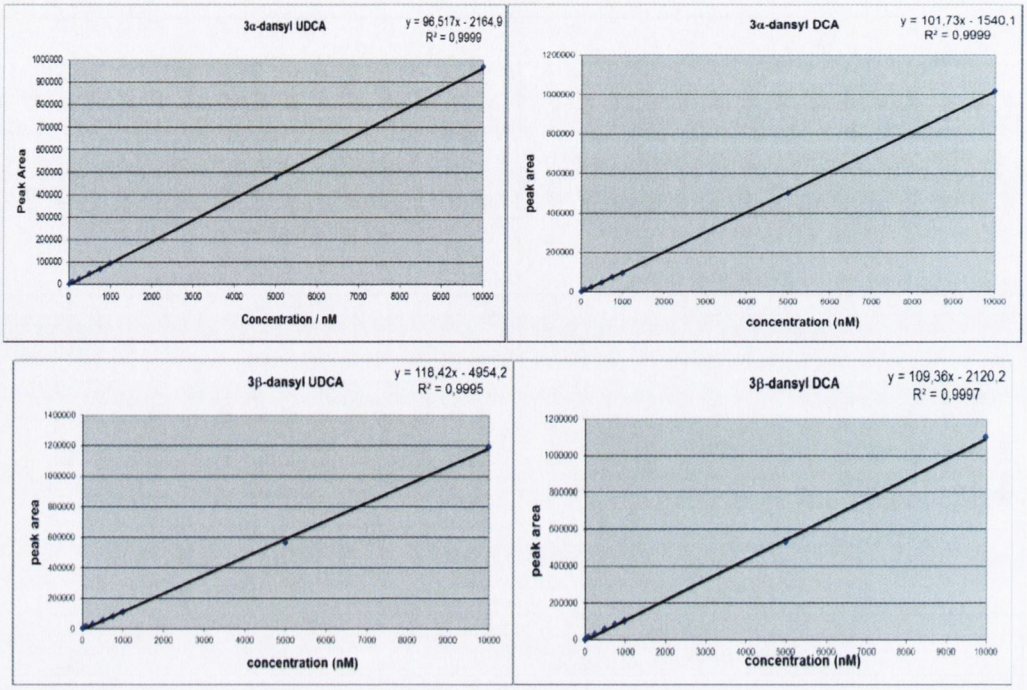

Figure 3.31. Calibration curves of the dansyl-bile acids. Concentration versus peak area at rt.

3.7. 2. Stability study of the fluorescent compounds in live cell environment.

The examination of the stability of the fluorescent bile acids was carried out using cells from the esopahgeal cell line. The cells were seeded into 48 well plate and the concentration of the compounds was measured after a 0.5 and 24 h in the supernatant and within the cells. Eighty thousand cells in 250 μl medium were placed into each well and incubated for 24 h before the treatment. The cells were then incubated with 1 μM of the NBD- or 10 μM of dansyl-derivatives for 0.5 and 24 h, after which time the supernatant was collected for measurements. It was followed by the damage of the cell membranes using 250 μl NP 40 lysis buffer for 15 min. This buffer solution was also collected into eppendorfs from the wells and stored at – 20°C until the HPLC measurements. Each compound was tested three times. The HPLC samples were prepared by adding 250 μl acetonitrile to each samples to make up the volume of the sample to 500 μl, thus the solution contained acetonitrile and aqueous supernatant or lysis buffer about 1:1 ratio. This combination is similar to that used as mobile phase during the measurements. After the addition of the acetonitrile the samples were centrifuged for 10 min at 10,000 RPM to eluate the bigger compartments of the cell residues and to precipitate the proteins from the samples which might cause damage to the column. The prepared samples were then measured according to the

previously developed HPLC method and the results were calculated using external reference standard controls. The control samples were taken from the original solutions which were given to the cells and went through the similar work up procedure as the biological samples. This protocol makes the method more reliable and help avoid dilution failures. The medium and cell lysate samples were run on HPLC using 470 nm and 540 nm for excitation and emission wavelengths in the case of NBD-derivatives, while these values were 335 nm and 517 nm for the dansyl compounds. Measuring the concentration of the compounds in the medium and in the cells makes it possible to compare total concentration to the initial concentration, which provides information on the stability of the fluorescently labelled bile acids in live cell environment. Additionally, **136** and **137** were examined using similar conditions. The results are shown in the following Figures. *Figure 3.32.* summarizes the obtained medium and cells lysate concentration values after 0.5 and 24 h.

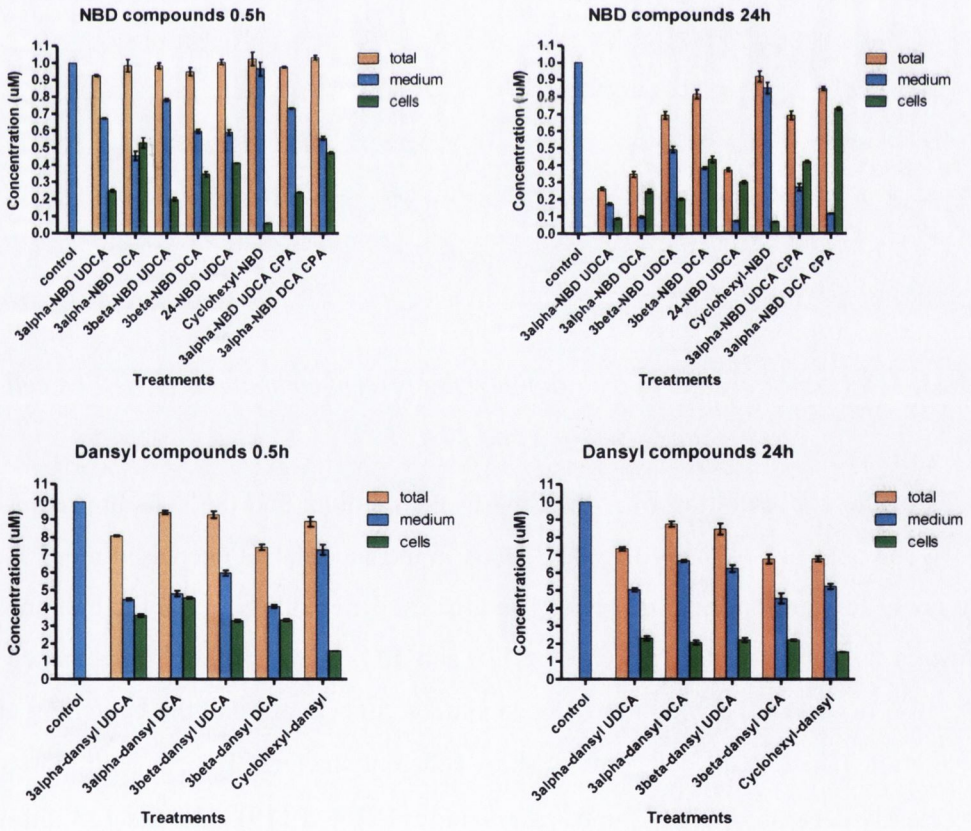

Figure 3.32. Stability of fluorescent compounds in HET1A cell line after 0.5 and 24 h.

Analyzing the total concentration bars it can be seen that both the NBD and dansyl derivatives are stable in live cell environment following short incubation time (<30 min) (*Figure 3.33.*). The concentration of NBD compounds was significantly reduced at 24 h. The greatest loss was observed in the case of the 3α derivatives and compound **134**. In these cases the concentration dropped to between 20 and 40%. Surprisingly the carboxylic modified CPA derivatives proved to be more stable than their parents with concentration maintained in the region 70 – 80%. The 3β-NBD bile acids did not disappear to the same extent over this period with 70–80% still present. Unequivocally **135** proved to be the most stable substance (~ 90%) during the experiments. The dansyl substituted compounds were generally more stable than the corresponding NBD compounds.

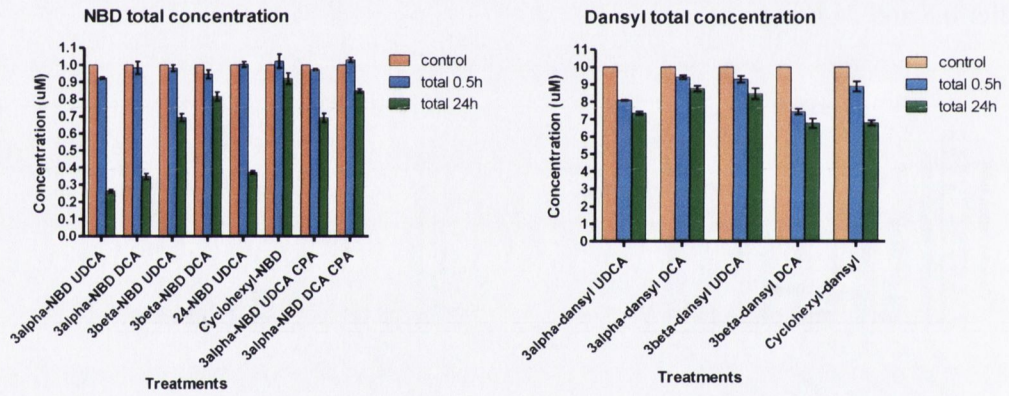

Figure 3.33. Total concentration of the examined fluorescent compounds in HET1A cell line at 0.5 and 24 h.

The changes of the concentration over the time in the medium and the cells are represented in *Figure 3.34.* The presence of the NBD compounds in the supernatant decreased more and less in every case going forward on the time scale. The greatest difference between the half an hour and one day results were observed in the case of **126** and **134**, in which the disappearance reached more than 50%. In contrast, compound **135** had similar concentration at the beginning and 24 h. The concentration values in the cells did not show coherent changes. The concentration of the 3α derivatives clearly decreased, while the β -compounds (**101** and **119**), **134** and **135** did not show significant changes. The presence of the CPA coupled 3α-NBD bile acids increased the intracellular region conversely. It is clear from these results that the compounds were degraded in

the cells over the time and the loss was recovered by the cellular uptake from the supernatant. It can be also stated that the control compound did not take part significantly in the transport, thus its degradation was not observed. The CPA amides (**136** and **137**) also seemed to avoid the degradation; hence their concentration in the cells could decrease.

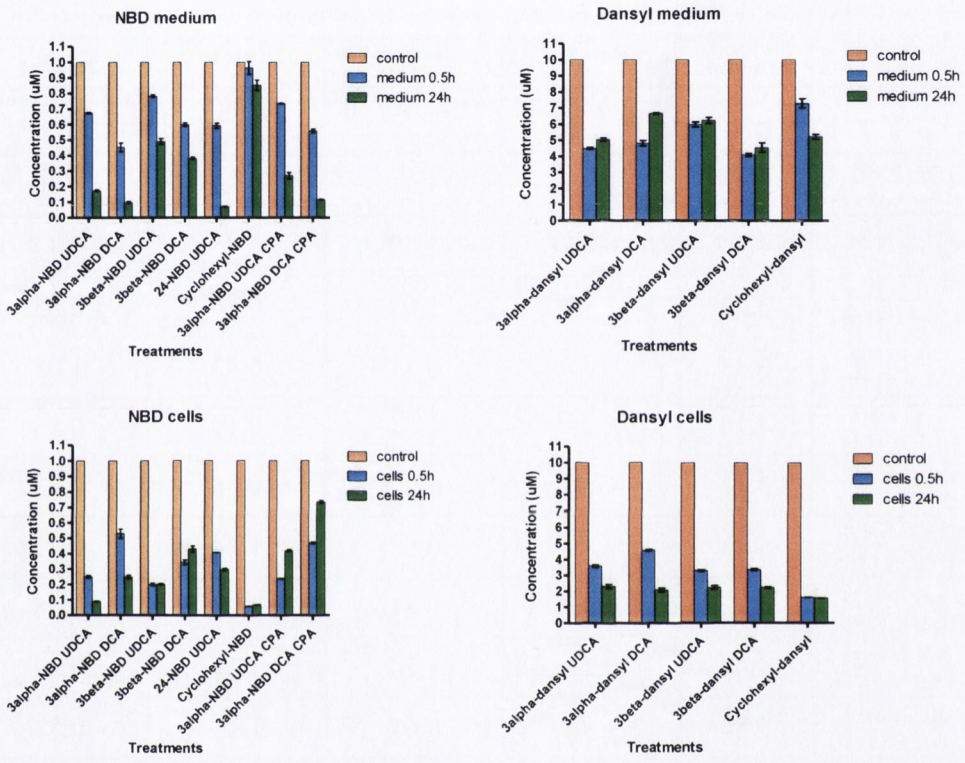

Figure 3.34. The presence of the fluorescent molecules in medium and cell lysate at 0.5 and 24 h.

The changes of the concentration of the dansyl-derivatives developed in similar way. The initial medium concentration of the dansyl-bile acids increased over the time, while it was dropped within the cells. These changes were not significant, but it refers that the quick uptake of these bile acids induced the reverse transport of the compounds. The control molecule was taken up at higher concentration than the appropriate NBD-derivative, but it was not affected by the previous process. These observations can be expressed by calculating the rate of concentrations according to different criteria. These values are presented in *Table 3.4.* together with the retention time of the compounds. The retention times correlated to the hydrophobicity of the fluorescent bile acids. Compound **79** produced long retention, which might come from the formation of intermolecular

secondary bonds, which make the molecule bulkier according to the MOE (Molecular Operating Environment program from Chemical Computing Group, Montreal, Canada) examinations. The energy minimizing test resulted in a bulky molecule where the dansyl group flexed under the steroid nucleus. This increased hydrophobicity resulted in longer retention time on the reverse-phase HPLC column.

Compound	Retention time (min)	Rate of concentration Medium/Cell 24 h	Rate of concentration Medium/Cell 0.5 h	Rate of concentration Medium 24h/0.5h	Rate of concentration Cell 24h/0.5h
3α–NBD UDCA (126)	**4.00**	1.86	1.81	0.37	0.36
3α–NBD DCA (99)	**7.45**	0.47	0.49	0.45	0.47
3β–NBD UDCA (101)	**3.69**	1.93	2.04	0.80	0.85
3β–NBD DCA (119)	**5.35**	0.57	0.71	0.83	1.05
24-NBD UDCA (134)	**4.20**	0.28	1.21	0.19	0.83
Cyclohexyl-NBD (135)	**3.11**	33.41	16.47	0.88	0.43
3α-dansyl UDCA (78)	**6.43**	2.59	0.68	1.84	0.49
3α-dansyl DCA (79)	**15.65**	2.44	0.41	2.29	0.38
3β-dansyl UDCA (87)	**4.67**	3.24	1.20	1.31	0.49
3β-dansyl DCA (94)	**5.86**	1.82	0.67	1.41	0.52

Table 3.4. Retention time and concentration ratio values derived from the HPLC measurements.

3.7. 3. Uptake of 3α-dansyl bile acids (78 and 79).

After the examination of the stability of the fluorescent compounds it was decided to follow their uptake in the 0–60 min time interval using HPLC for quantitation. Usually, in this kind of experiment, fluorescent readings are used. The coupled chromatographic step in our case provided reassurance that the fluorescent signal was derived from the intact probe. The 3α-dansyl bile acids (**78** and **79**) were selected along with **97** because of their better stability and interesting intracellular distribution properties. The experiment was carried out at 37°C and repeated at 4°C. It is known that the active transport processes, which are protein mediated, are significantly slower at 4°C, and that transport under such conditions can be attributed exclusively to passive

diffusion. This experiment could therefore determine whether active transport is significantly involved in the cellular uptake of the fluorescent bile acids (and by extension by the parent native free bile acids). The cells were treated with test compounds at 10 μM and every measurement was repeated three times. In the case of the 4°C assays the well plate was placed onto ice and the freshly prepared stock solutions were also cooled down before addition. The uptake was stopped after 0.5, 1, 5, 10, 30 and 60 min with the removal of the supernatant and the cells were lysed for 15 min. The medium and cell lysate samples were collected and stored at – 20°C until the HPLC measurements.

Figure 3.35. presents sample data from these transport experiments. The concentration of the compounds in the cells increased over the time, with corresponding smaller amounts present in the supernatant. The difference between the extent of the uptake at 37 and 4°C was significant using dansyl-bile acids, while it was similar in the case of the control. The black curves in the graphs being the difference between the amounts at 37 and 4°C reflect the extent of active transport.

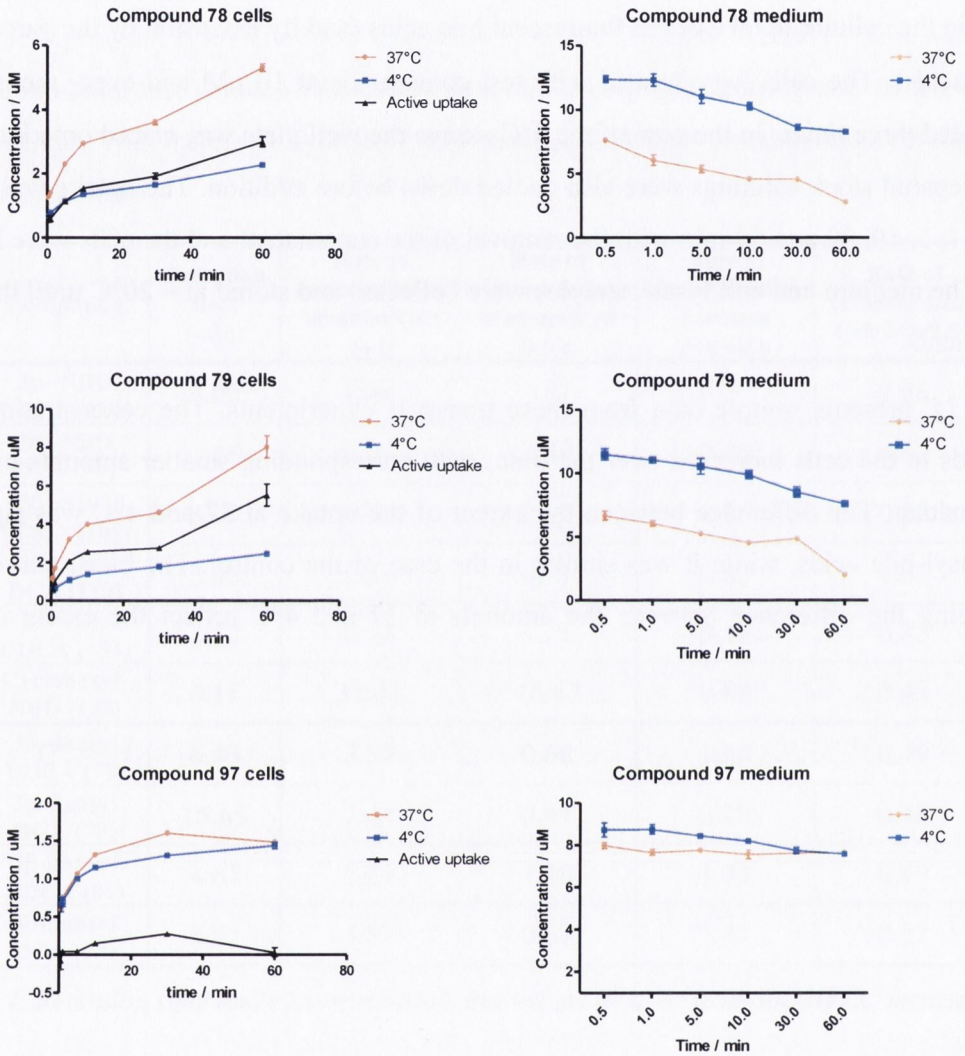

*Figure 3.35. Concentration of compounds **78**, **79** and **97** in lysed HET1A cells at 37 and 4°C.*

The data clearly show that the bile acid derivatives enter into the oesophageal cells through an active transport process. This is the first evidence that we are aware of that there is a functionally active transport process for bile acids in HET1A cells. Its importance is that it shows that where bile acids are present in refluxate in a gastro-oesophageal reflux disease (GORD) patient, the oesophageal epithelium could efficiently take up the incident bile acids. Since bile acids are known to induce a variety of biochemical changes within oesophageal cells in cell culture studies [156-159], the suggestion is that similar changes could happen in vivo.

3.7. 4. The uptake of 3α-dansyl bile acids (78 and 79) in competition experiments.

In order to prove that the active transport that was described in the previous section is relevant to the native bile acids, and that the attachment of the fluorophore does not make the bile acids better transporter substrates, we next repeated the transport experiments with native (parent) bile acids present. The other reason for doing this was to try to explain some of the observations we had made in the confocal experiments with co- or pre- treatment with bile acids. In those experiments we showed that co- or pretreatment of the cell suspensions with native bile acids altered the distribution of the fluorescent compounds. The extent of uptake of 3α-dansyl bile acids was examined in initial competition experiments at the 0.5 h time point following pre- or co-treatment with 100 μM and 300 μM **7** or **4**. Co-treatment with **78** was also examined. Control measurements were carried out at 37 and 4°C in order to estimate the extent of active uptake. In the case of the fluorescent UDCA derivative (**78**) pre- and co-treatment with 300 μM DCA, co-treatment with the same amount of **7** or co-treatment with the fluorescent DCA analogue (**79**) were examined. The results of the measurements are shown in *Figure 3.36.*

The total concentration of the compounds, estimated by summing the supernatant and cell lysate concentration, gave a constant value of 10 μM; thus, degradation did not occur over the experiments. Since the cell compartment was lysed before analysis with an equal volume of buffer to the volume of supernatant in the experiment, there is no suggestion that the total concentration under these circumstances should have been the same as the added concentration, yet it was. This must represent a considerable concentration of the probe substance in the cellular compartment from the supernatant during the 30 min incubation. In these experiments there was firstly a significantly higher intracellular concentration at 30 min at 37°C than at 4°C and correspondingly lower and higher amounts respectively in the supernatant compartment (*Figure 3.36.*). This was consistent with the earlier findings while studying the progress of uptake over 30 min. Co-treatment with **4** decreased the intracellular concentration at 37°C to that observed at 4°C indicating that it blocked active transport of **78**. This can be understood in terms of effective competition for the same transporter at higher substrate concentration (and possibly better K_m). Co-treatment of with **7** also attenuated the 37°C concentration but not by as much as co-treatment with **4**. Remarkably, pretreatment with **4** (300 μM) did not block active transport, rather it increased it. Finally for **78**, co-treatment with fluorescent DCA attenuated active uptake but not

by as much as co-treatment with the native bile acid. The peculiar effect of pretreatment versus co-treatment will be discussed below following consideration of results where this behaviour was more exaggerated. Dansyl DCA (**79**) was transported actively as observed by the significant difference in concentration intracellularly between the 4 and 37°C treatments. Co-treatment with **7** or **4** (100-300 μM) had no effect on the extent of this. Either the native bile acids are not transported by a similar process or they are not as effectively transported by a similar process (higher K_m). Pretreatment effects with dansyl DCA (**79**) were similar to those observed with the UDCA analogue. Pretreatment with **7** or **4** at 100-300 μM significantly increased the extent of active transport (at least the intracellular concentration – it was not measured at 4°C under these conditions). There was a corresponding decrease in the observed supernatant concentration and in all cases pleasing evidence of analytical precision through consistent total concentration and variance between wells. In conclusion the active transport of the dansyl compounds is facilitated or in some way upregulated by pretreatment of the cells with the native bile acids. The significance of this lies in the potential for exposure of the oesophagus to bile acids to promote intracellular accumulation of bile acids with consequent cellular damage. This is a type of feedback mechanism, which has not been observed in the oesophagus previously. There is an obvious need to identify the transporter mediating effects observed here. The likely candidates for bile acids transport ASBT and OATP are not believed to be present in the epithelium of the oesophagus and the finding of functional activity mediated by one of these or a homologous protein would be significant. ASBT expression and distribution is known to be under bile acid control in other tissues. Thus in the gall bladder, there is evidence that activation of the recently discovered bile acids G-protein coupled receptor TGR5 causes translocation of ASBT to the cell surface from storage vessels [160]. These events are coupled to movements of Ca^{2+} inter- and intra-cellularly. However functional aspects of these changes have yet to be characterised and TGR5 is not believed to be expressed in oesophageal cells. In intestinal cells, activation of PKC by DCA causes decreases in ASBT expression which should decrease bile acid uptake capacity. Much remains to be done in elucidating the mechanism and significance of the present findings in the context of oesophageal disease and the inflammation-Barrett's-cancer progression.

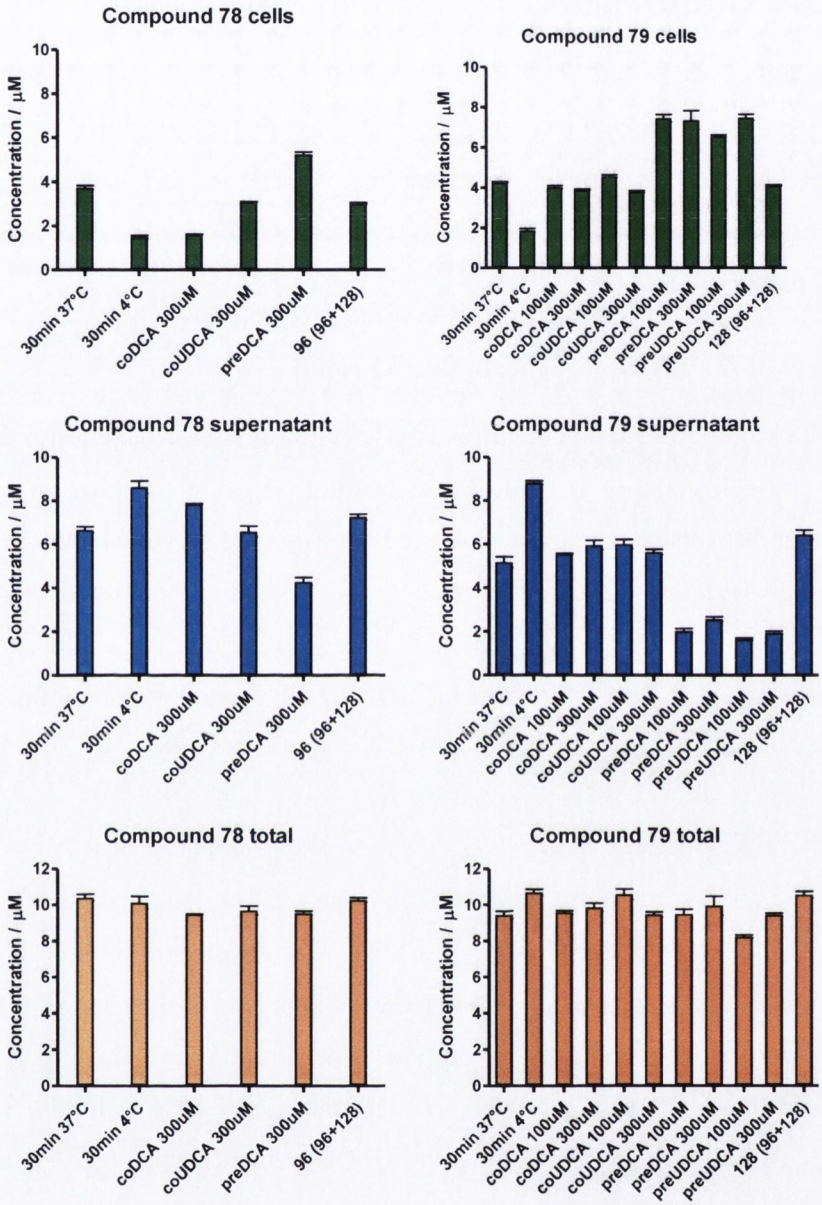

*Figure 3.36. Competition experiments of 3α-dansyl UDCA **78** and 3α-dansyl DCA **79** in HET1A cell line at 30 min. The graphs show the concentration of the tested compounds in the treated cells (green bars), in the medium (blue bars), while the overall concentrations are showed in the last graphs (red bars).*

3.8. The uptake of NBD-bile acids by Caco-2 cell line.

To examine the suitability of the NBD-bile acids for investigating the disposition of the bile acids in intestinal cells, the compounds were also studied using colorectal cancer Caco-2 cells. These have several relevant bile acid transporters including organic anion-transporting peptides [161-163]. This part of the work was carried out by postgrad colleague Johanna Salomon. Johanna used functional monolayers of Caco-2 cells.

3.8.1. Cytotxicity of the NBD-bile acids in Caco-2 cell line.

To determine the kinetics of the uptake process it was necessary to characterise the effect of the NBD-bile acids on cell viability as we had previously done using oesophageal and liver cancer cell lines. The viability measurements were carried out using the previously described MTT assay and the compounds were monitored up to 100 min by incubating them over Caco-2 monolayers using different concentrations (1–100 μM). Analysing the results we could conclude that the tested fluorescent bile acids did not affect the cells under these conditions, thus the uptake of them could be examined.

3.8.2. The bicinchoninic assay.

To standardize the results in the uptake studies first the total protein amount of cell layers were determined by bicinchoninic assay (BCA), which was developed by the Pierce Chemical Company [164]. This assay is based on two reactions which lead to the change of solution colour from green to purple in proportion to protein concentration and then it is measured by colorimetric techniques. The test is carried out with the use of BCA solution. The stock BCA solution is a highly alkaline solution containing five ingredients as bicinchoninic acid, sodium carbonate, sodium bicarbonate, sodium tartrate and cupric sulfate pentahydrate. Adding this solution to the test samples first the Cu^{2+} ions from the cupric sulfate is reduced to Cu^{+} ions by the peptide bond of proteins (this reaction is highly temperature dependent). The amount of Cu^{2+} reduced is proportional to the amount of protein present in the test sample. In the second step each formed Cu^{+} ion reacts with two bicinchoninic acid molecules to form purple chelates which strongly absorb light at a wavelength of 562 nm. The amount of protein present in the cells was quantified by measuring the absorption spectra and comparing to standards with known protein

concentration. After the determination of the amount of protein in the Caco-2 cell layers the results of bile acid uptake were expressed in nmol / mg protein concentration.

3.8.3. Examination of NBD-bile acid uptake in Caco-2 cell line.

To study the time-course of uptake of the 3-NBD bile acid derivatives (**99**, **101**,**119** and **126**) they were incubated over Caco-2 monolayers at 10 μM and studied at 37 and 4°C up to 90 min by measuring the fluorescence intensity. The rate of the active uptake was calculated then as the difference between the fluorescence measured at 37 and 4°C. The results are represented in *Figure 3.37.*

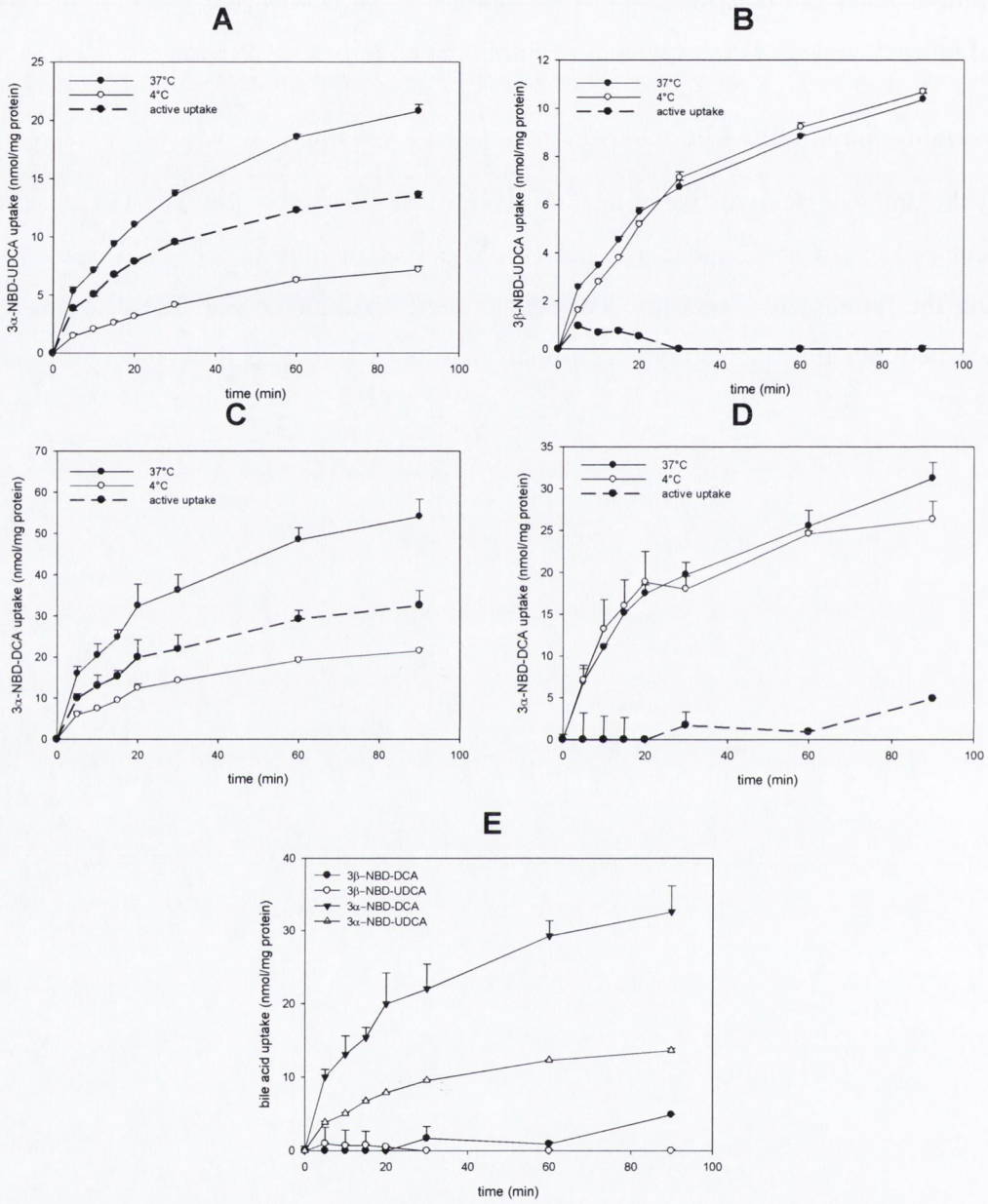

*Figure 3.37. Time course of NBD-bile acid uptake into Caco-2 cells. The uptake was studied for 90 min at 37°C and 4°C. Graphs A-D show the time-dependent rate of bile acid uptake at different temperatures (A: 3α-NBD UDCA **126**, B: 3β-NBD UDCA **101**, C: 3α-NBD DCA **99** and D: 3β-NBD DCA **119**). The rate of the active uptake was calculated as the difference between the fluorescence measured at 37 and 4°C (dashed curves). Graph E shows the rate of active uptake of the four different bile acid derivatives (**99**, **101**,**119** and **126**).*

The analysis showed that intracellular concentration was increased due to a time-dependent manner in every case. The difference between the uptake in the 37 and 4°C experiments was not significant in the case of the 3β-derivatives (**101** and **119**), indicating that these compounds were taken up by passive diffusion (*Figure 3.37. B and D*). In contrast, the uptake of the α-analogues (**126** and **99**) showed strong dependency on temperature, indicating that their entry into the cells is substantially mediated by active transport at 37°C. The highest rate of uptake was observed in the case of 3α-NBD DCA **99**, but it did not exceed 30% of the total concentration after 60 min. It is clearly seen from the results that the nature of fluorescent bile acid uptake strongly depends on the structure of the bile acid moiety. The 3α-isomers which have the same orientation of functional groups at 3- and 7- or 12-positions as the parents were taken up by active process which indicates that the ligand orientation (at C-3) has huge impact in protein binding. Changing this orientation resulted in significantly decreased bile acid uptake.

To characterise the kinetic of the active transport the 3α-NBD bile acids were incubated at 1–100 μM at 37 and 4°C for 20 min. The active transport values were then calculated (as the difference between the fluorescence measured at 37 and 4 °C) before performing kinetic analysis. The results showed that the concentration-dependent uptake of the compounds was saturable in Caco-2 monolayers (*Figure 3.38. A and B*). The uptake followed the Michaelis-Menten kinetics [165]. The graphical representation of the transport kinetics was analysed by an Eadie-Hofstee transformation [166], resulted in a single straight line for both tested substances (*Figure 3.38. C*). The Eadie–Hofstee diagram is a graphical representation of enzyme kinetics in which reaction velocity is plotted as a function of the velocity vs. substrate concentration ratio. The graph suggested that the uptake of these fluorescent bile acids was mediated by a single transporter site in Caco-2s. The results allowed us to estimate the maximum rate (V_{max}) of the uptake as the y-intercept of the obtained curves. The Michaelis-Menten constant (K_M), which is the substrate concentration at which the uptake rate is half of V_{max}, was also determined for both tested compounds from the slope of the curves. Hence, the Michaelis-Menten constants and the maximum uptake rates were estimated to be K_m = 28.20±7.45 μM and V_{max} = 1.81±0.20 nmol/(mg protein*min) for 3α-NBD DCA (**99**) and K_m = 42.27±12.98 μM and V_{max} = 2.84±0.41 nmol/(mg protein*min) for 3α-NBD UDCA (**126**).

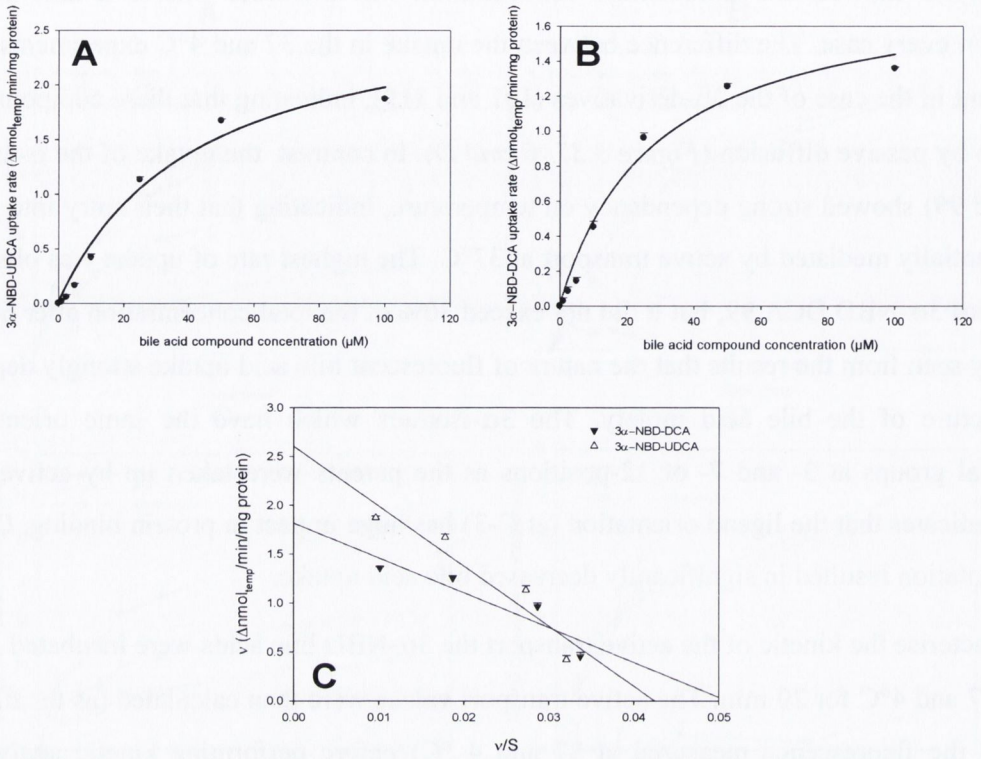

*Figure 3.38. Concentration dependence of 3α-NBD bile acids uptake by Caco-2 cell monolayers (Graph A: 3α-NBD UDCA **126**, graph B: 3α-NBD DCA **99**). Uptake of bile acid compounds was measured for 20 min at 37°C and 4°C. Graph C: The graphical representation of the transport kinetics (by an Eadie-Hofstee transformation) for both tested substances (**99** and **126**).*

The above tests were repeated incubating 24-NBD UDCA **134** and Cyclohexyl-NBD **135** over Caco-2 monolayers. However the fluorescent UDCA control showed some active transport process, the rate of the uptake did not exceed over 10% after 90 min (*Figure 3.39. C*). The result shows the importance of carboxylic acid group in the protein binding. Without this functional group the uptake of fluorescent UDCA derivative **134** significantly decreased in contrast to the 3α-labelled UDCA compound (**126**). The tests with Cyclohexyl-NBD **135** showed clearly that its uptake is due to passive diffusion in Caco-2 cells providing the importance of the presence of bile acid moiety in the active transport process in the case of NBD-bile acid uptakes (*Figure 3.39. B*).

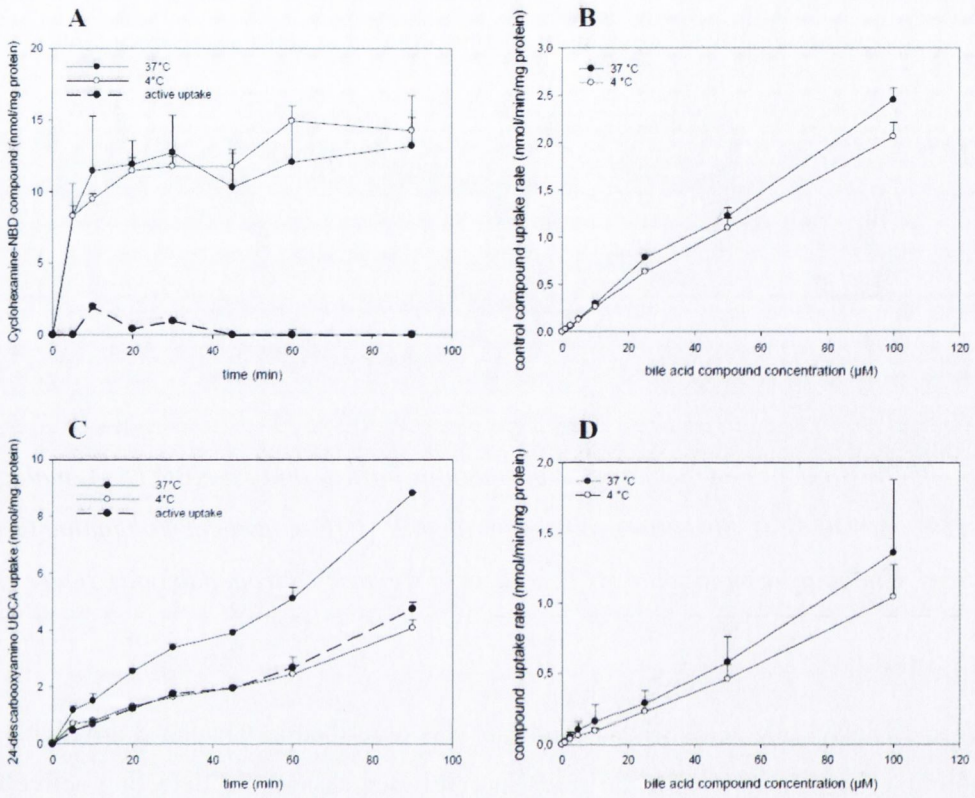

Figure 3.39. Uptake profile of the control fluorophore substances into Caco-2 cell monolayers at 37 and 4°C (Time-dependent: 10 µM, up to 90 min; Concentration-dependent: 1–100 µM, 20 min). A: Time-dependent uptake of Cyclohexyl-NBD ***135****; B: Uptake of* ***135*** *after 20 min using different concentrations.; C: Time-dependent uptake of 24-NBD UDCA* ***134****; B: Uptake of* ***134*** *after 20 min using different concentrations.*

The observed diastereoselectivity in the uptake process of the examined fluorescent bile acids is unprecedented in the bile acid literature. Possible explanations include a steric clash between the β-group and the binding pocket of the transporter protein. On the other hand, the equatorial H-bond donor in the natural bile acid mimicked by the α-NH in the corresponding NBD analogue might have a strong impact on the formation of the substrate-transporter bond. The energy minimized structures obtained from conformational analysis (using MOE software) show the ability of the NBD N-H to mimic the 3-OH group of the parents (*Figure 3.40.*). The similar

spatial arrangement of the 3-NH and 3-OH bonds might result analogous behaviour in the formation of secondary chemical bonds with carrier proteins in cellular environment.

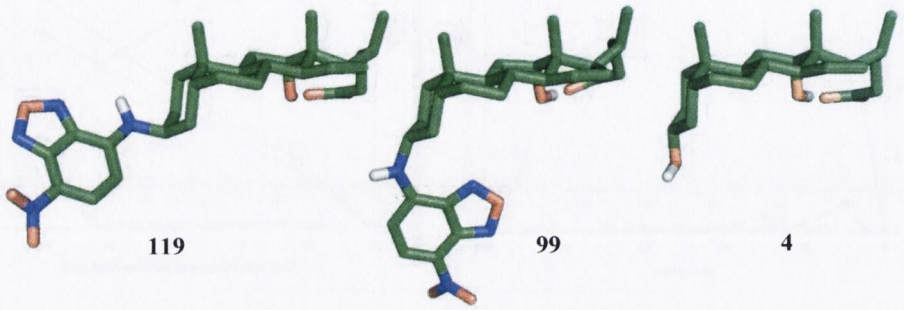

*Figure 3.40. Overlaid minimum energy conformations for 3α- and 3β-NBD DCA analogues (**99** and **119**) and DCA (**4**). Structures were generated in MOE (Chemical Computing Group, Montreal, Canada) by modification of cholic acid **4** extracted from pdb code 2QO4 [167].*

3.9. Conclusions

The NBD and Dansyl bile acids whose synthesis was described in Chapter 2 are highly suitable for determining the disposition of bile acids in cell-based assays, for detecting active transport processes affecting bile acids and for investigating the many questions about these compounds. The work shows that oesophageal cells have the capacity to actively take up bile acids and that this is positively regulated by bile acid exposure. Meanwhile work of colleagues demonstrates that the transport of these compounds is sensitive to the orientation of the fluorescent reporter group. The work described here can only be the beginnings of investigations with these fascinating substances which are now in widespread use in numerous laboratories interested in anionic transport, the oesophagus and the effects of bile acids.

Chapter 4

Design and synthesis of highly cytotoxic bile acids

4.1. Introduction

Exposure to bile acids produces changes in cell viability and proliferation that have implications in intestinal disorders, in hepatic disease and in cancer promotion in the gut and oesophagus. For example, the rise in incidence of oesophageal cancer is attributed to increased incidence of gastroesophageal reflux which brings bile acids from the stomach into contact with the oesophageal epithelium [168-170]. In the colon, increased exposure to byproducts of bile acids is thought to contribute to cancer development [171]. Paradoxically, here and in the oesophagus, bile acids may be contributing to tumour promotion by inducing apoptosis in normal cells, leading to the formation of populations of a cell phenotype resistant to cell death [172-176]. Meanwhile, fibrotic disorders of the bile duct, which causes obstruction and accumulation of bile acids in the liver leads to liver failure and death through a mechanism thought to involve hepatocyte apoptosis [177, 178]. The importance of these processes to health and disease has led to extensive study into mechanisms of bile acid effects on cell viability. Much of the focus has been on the pro-apoptotic effects of the so-called hydrophobic bile acids, LCA (**5**), DCA (**4**) and CDCA (**3**) and their glycine conjugates [179]. There is a widespread belief that the toxic effects of these compounds observed at >100 μM in cell-based assays is due to their hydrophobicity and explicitly or implicitly their tendency to form micelles [180]. A bile acid micelle could recruit plasma membrane lipids into a mixed micelle thereby disrupting the membrane integrity, leading to leakage and lysis. This undoubtedly occurs at high bile acids concentrations where the effects are similar to those observed with non-bile acid detergents such as Triton X [181]. However **3** and **4** can cause cell death at concentrations far below their CMC, making it difficult to believe that detergency is significantly involved. This is one of the problems in bile acid research, that cellular effects can be attributed to different mechanisms depending on bile acid concentration. Furthermore, non-bile acid detergents (again like Triton X) are also observed to cause cell death at concentrations significantly below their CMC (and expected lytic effects) [181]. These necrotic/detergency effects could be collectively termed non-specific effects in order to distinguish them from signalling events due to specific binding of bile acids with protein targets that could precipitate apoptotic processes. Apoptosis (programmed cell death) may occur through one or more parallel, and possibly independent processes termed *extrinsic* (involving cell surface death receptor proteins); *intrinsic* (mitochondrial leakage) or ER stress (which can be linked to the first two) [182-184]. A further kind of process, *autophagy* or self-catabolism of the cell may

be observed in some instances upon exposure to bile acids. A further complication at least in terms of classification relates to the possibility that extrinsic apoptosis can be triggered by non-specific membrane perturbations leading to activation/translocation of death receptors. A nice opportunity arose recently to experimentally separate specific from non-specific apoptotic contributions from bile acids. Katona *et al.* reported the synthesis of enantiomeric bile acid pairs of **5**, **4** and **3**. As expected **5**, **4** and **3** had the same experimental CMC values as their enantiomeric partners (*ent* LCA, *ent* DCA, *ent* CDCA) [100]. Critically, while the substances all caused apoptosis in a colon cancer cell line, the naturally occurring stereoisomers were more cytotoxic than their isomers. This tells us that at least some of the apoptotic features of bile acids are due to stereospecific interaction with protein receptors. However, these crucial findings do not appear to have altered the common tendency to hypothesise that the pro-apoptotic effects of hydrophobic bile acids is due to their hydrophobicity. This is also consistent with the observation that some polar bile acids e.g. UDCA (**7**), are relatively non-toxic [185]. Indeed as observed earlier in this work, pre-treatment of a variety of cell types with **7** can protect cells from the apoptotic influence of hydrophobic bile acids, such as **4**. Indeed, for many workers this explains and validates the use of **7** in treatment and prevention of liver failure in biliary duct disorders and cirrhosis. There are a number of possible explanations for these effects including activation by **7** of pro-survival pathways that could oppose the death signalling of the hydrophobic bile acids. However there is also a widespread belief that **7** acts by displacing the hydrophobic bile acid pool, or by making it more polar. Either way, this observation that **7** and other polar bile acids are less cytotoxic acts to reinforce the idea that hydrophobic bile acids act through a hydrophobic effect in causing cell death. Indeed the work of Martinez, showed that in colon cancer cell lines, cytotoxicity in a group of 26 naturally occurring bile acids and conjugates, correlated with hydrophobicity as reflected in reverse phase HPLC retention (the correlation amounted to the observation that only **4** and **3**, caused extensive cell death and these are relatively hydrophobic) [173]. Other publications from the Martinez group asserted that cytotoxicity is related to hydrophobicity through non-specific membrane mediated effects on survival signalling (PKC activation/translocation) [185]. Working in this laboratory R Sharma took a slightly different approach to investigating this problem [120]. Sharma produced an extended library of bile acids deliberately enriched with new members of widely differing physicochemical properties. The effect of these on cell viability of the normal oesophageal cell line HET1A was assessed at a bile

acid concentration of 500 μM using the MTT assay. Lipophilicity was assessed using a RPTLC method with post-chromatographic derivatisation (the compounds were difficult to detect by conventional UV/RI/HPLC). Unexpectedly, in this work, there was a good correlation between cytotoxicity and lipophilicity (r^2>0.6). This turned out to be particularly strong in subsets of compounds with similar functional groups (r^2>0.95). The only evidence for a specific effect in this study was that the toxicity of the prototypical toxic bile acids was not well predicted by these correlations indicating that in these cases there were additional effects. At the time the work was conducted it was not believed that the oesophageal cell line was capable of actively transporting bile acids. Therefore Sharma also studied the relationship between cell viability and lipophilicity in a cancer cell line of hepatic origin, which was expected to express bile acid transporters. In a surprising contrast to the oesophageal cell line experiments, cell viability of the HUH7 cell on exposure to bile acids at 500 μM for 24 hours was independent of bile acid lipophilicity. The study concluded that lipophilicity is a necessary but not sufficient property for bile acids to exhibit cytotoxicity. Notably from a drug discovery perspective, some of the analogues exhibited marked toxicity when tested at low concentration while some exhibited divergent activity towards normal and cancer cells which suggested promise for the development of chemotherapeutic agents. Of note was the higher toxicity of 3-azides of UDCA over DCA (**120**) analogues even though these showed the expected difference in polarity. Another interesting feature was the toxicity of the primary amides of UDCA and DCA (**138**) relative to the corresponding free acids.

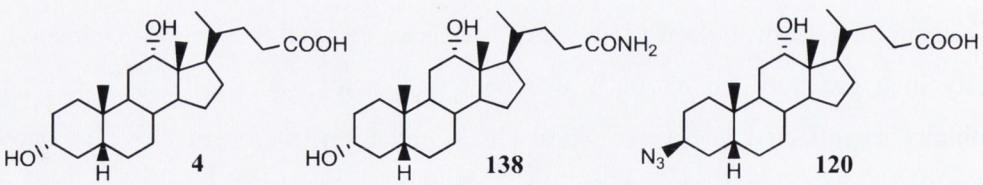

EC_{50} 257 μM EC_{50} 39 μM EC_{50} 97 μM

*Figure 4.1. EC_{50} values for the inhibition of HET1A (normal oesophageal) cell viability by DCA (**4**) and its 24-amido (**138**) and 3-azido (**120**) analogues [120]*

It is appropriate here to survey some of the general context of the work described in this Chapter and especially previous attempts to design bile acid-based cytotoxic/anti-microbial agents. There has been only a small amount or work reported in this area featuring extensive biochemical

characterization of a relatively small number of compounds. The effect of some amino acid and amino acid ester conjugates of UDCA and CDCA (**139–141**) was studied using an extensive range of cancer cell types including hepatic, breast cancer, leukemia, prostate cancer, stomach cancer, cervical and colon cancer cell lines [186-189]. CDCA amino acid conjugates have exhibited an anti-cancer effect on malignant glioblastoma cell lines U-118MG, U-87MG, T98G, and U-373M. Some of these conjugates exhibited promising effects in subsequent *in vivo* models of malignancy and in murine models of obesity [190].

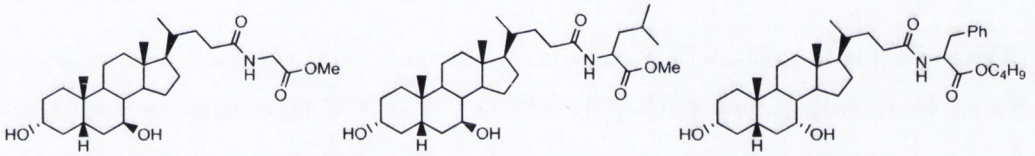

139 **140** **141**

*Figure 4.2. Examples for amino acid ester conjugates of UDCA (**139–140**) and amino acid conjugate of CDCA (**141**)* [187-190]

More recently Kihel *et al.* studied the proapoptotic effects of piperazinyl analogues of LCA (**142**) and CDCA (**143**) [191]. These were reported to cause cell death in a multiple myeloma cell line with an LD50 of 8.5 μM [192].

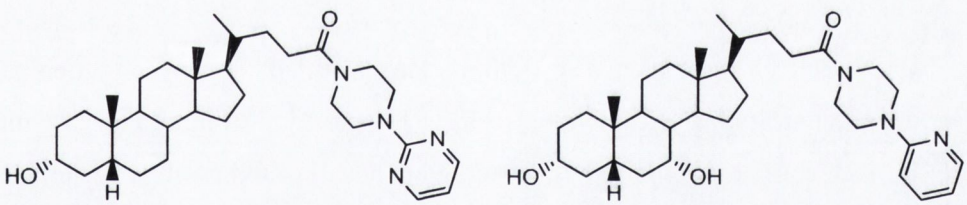

142 **143**

*Figure 4.3. Piperazinyl analogues of LCA (**142**) and CDCA (**143**) reported by Kihel et al. [191]*

These drug design efforts described above, which target proapoptotic pathways, can be distinguished from bile acid analogues that have been deliberately designed to exhibit increased amphiphlicity and tendency to self-organization in solution [193]. Such compounds cause cell death mainly through necrosis. Although these have limited scope for therapeutically relevant selectivity or effective distribution *in vivo* they can make effective anti-microbial agents. Examples in this more extensive line of research include analogues (**144** and **145**) featuring

hydrophobic side chains that act through membrane disruption causing fungal and bacterial cell death [194, 195].

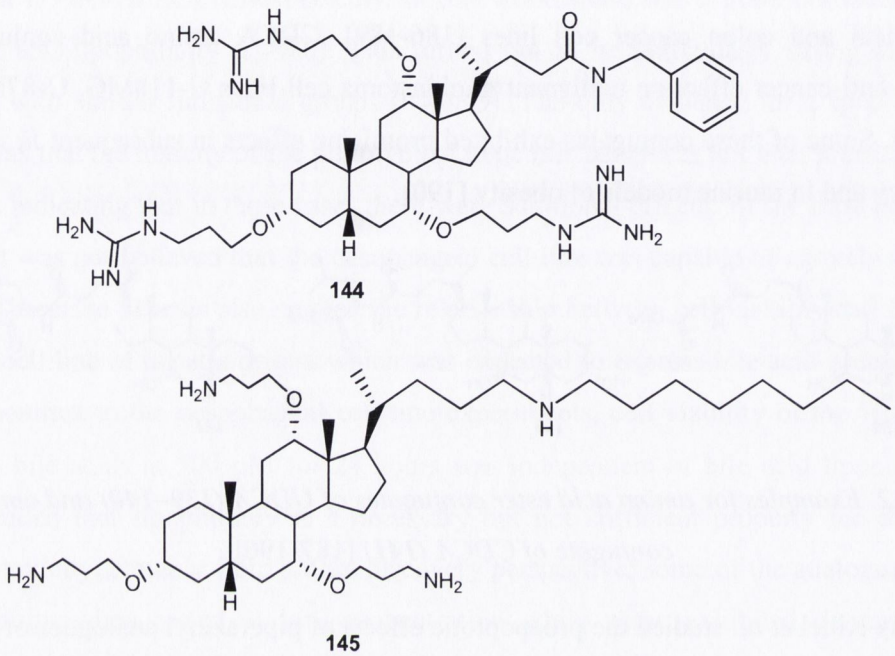

Figure 4.4. Cholic acid analogues conjugated with hydrophobic side chains designed by Savage et al. [194, 195]

A separate line of research associated with Bellini's lab identified simpler non-amphipathic bile acid analogues with interesting antimicrobial effects [196-199]. 3-Amino and 24-amido DCA analogues (**146–148**) caused pronounced effects on gram negative and positive bacteria as well as fungi at concentrations in the low micromolar range [197, 198]. The molecular mechanism of action of these compounds is unclear; however they appear to be designed to act through receptor mediated rather than membrane dependent effects. There are no reports on their activity in human normal or malignant cells.

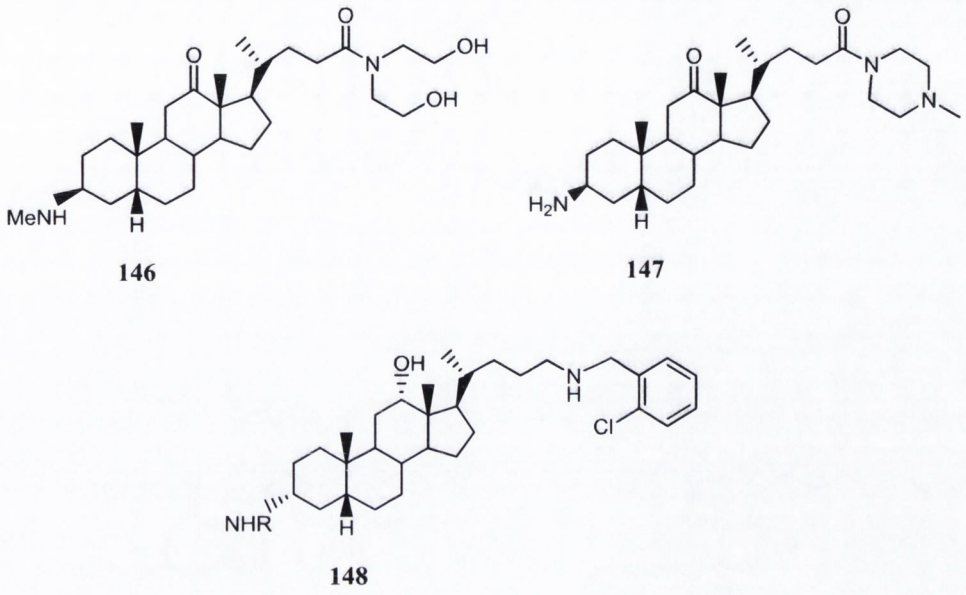

Figure 4.5. 3-amino and 24-amido DCA derivatives prepared by Bellini et al. [197, 198]

This survey prompted us to wonder what would happen if functional group features that endowed bile acids with toxicity in our work could be incorporated into a single molecule; for example could toxicity be amplified if analogues could be designed to feature both a primary amide and 3-azido group. This might reveal more insights into the structural requirements for toxicity effects but it could also lead to agents with cytotoxic potency approaching a useful level especially if it could be coupled to some selectivity. Potential clinical applications might also follow if such compounds would be capable of surmounting chemotherapeutic resistance. Therefore, the purpose of the work in described in this Chapter, was to prepare and study new bile acids integrating structural features of bile acids that were associated with inhibition of cell viability in previous work from our lab. In this process we produced several highly potent new bile acids. We conducted some preliminary investigations into the mechanism of action of these substances in order to characterize apoptosis versus necrosis and to try to define some of the pathways involved. In all we prepared and studied 23 new bile acids starting from LCA (**5**), DCA (**4**), and CDCA (**3**) featuring 3-alpha and beta azido groups with optional further substitution at C-24 with parallel amides.

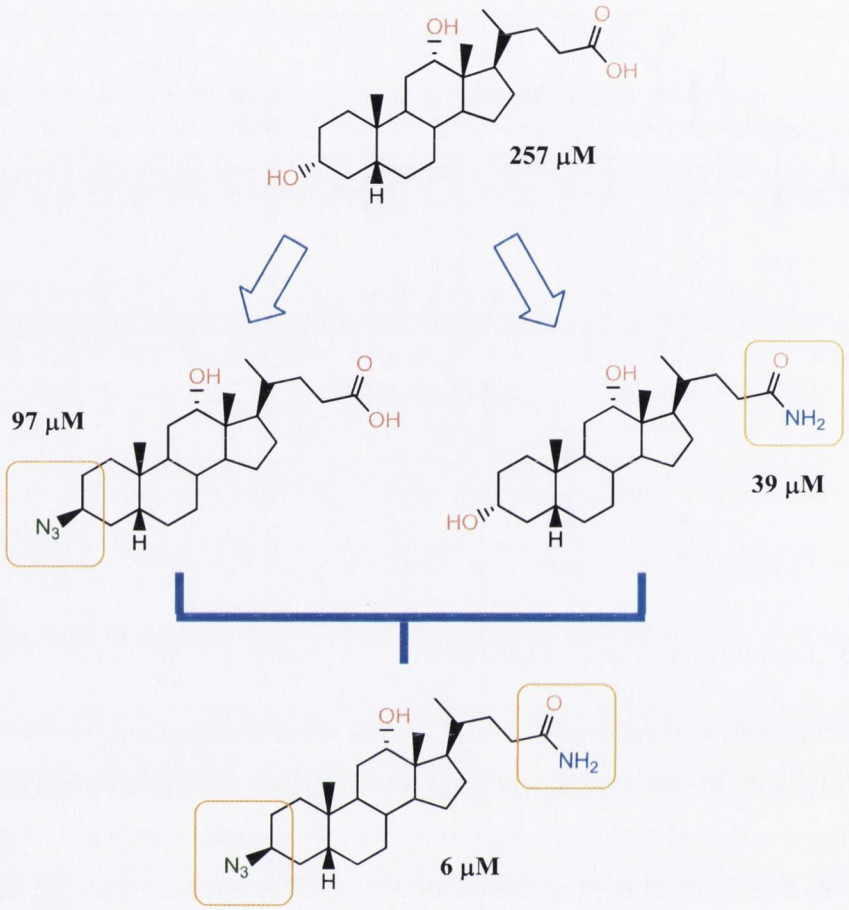

Figure 4.6. Design/exploration strategy for cytotoxic bile acids builds on earlier work on single modifications to DCA (Concentration values represent IC50)

4.2. Synthetic chemistry

4.2.1. Synthesis of 3β-azido CDCA derivatives

In this work, analogous libraries of test compounds were prepared from DCA (**4**), CDCA (**3**) and LCA (**5**). To obtain the 3β-azido compound we followed the synthetic way that was introduced in Chapter 2. In the first step the carboxylic acid was protected in MeOH followed by protection of the 3- and 7-hydroxyls by 4-DMAP catalysed acetylation with Ac_2O. To carry out transformations on the A-ring, the removal of 3-acetate was required. For the regioselective deprotection AcCl was added dropwise to the diacetate compound in MeOH yielding the product in 91% (*Scheme 4.1.*).

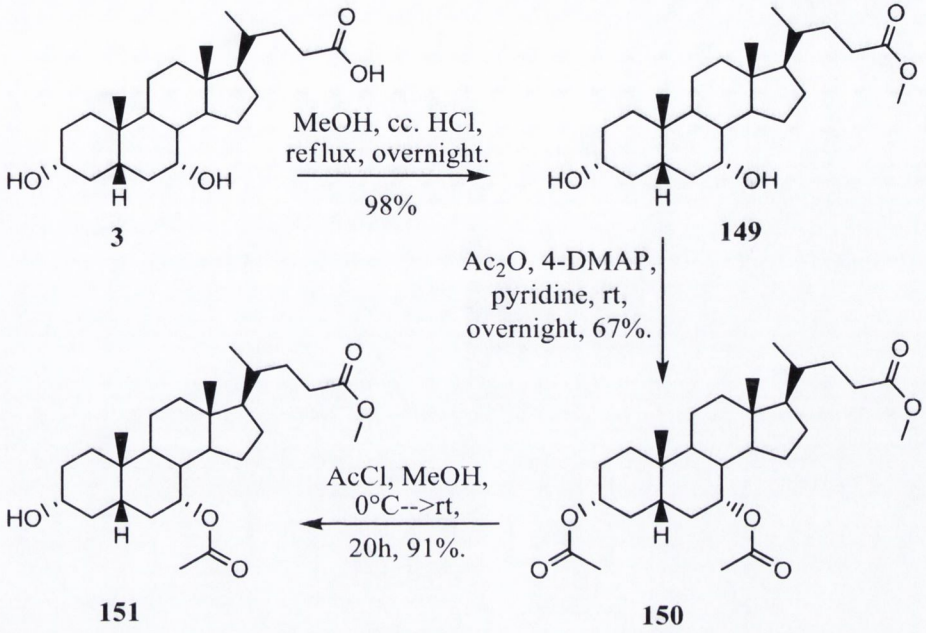

3 **149** **151** **150**

Scheme 4.1. Regioselective protection of ***3***

Compound **151** containing a free hydroxyl at position-3 was then reacted with MsCl in the presence of Et_3N. This mesylate group was then replaced with azide *via* a direct nucleophilic S_N2 substitution in the following step resulting in reverse orientation at C-3 (*Scheme 4.2.*).

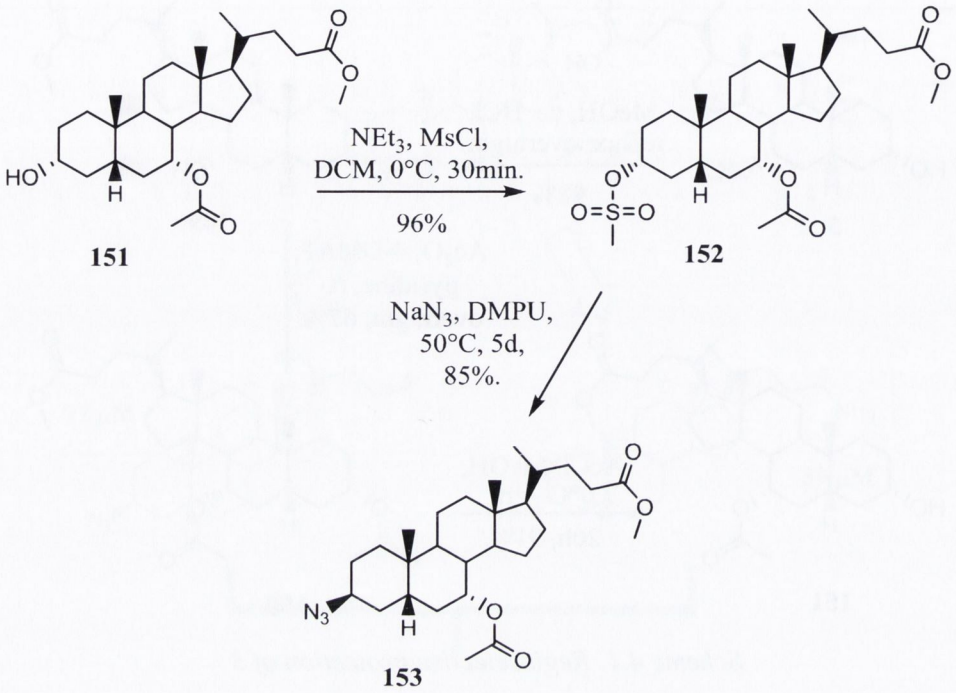

*Scheme 4.2. Formation of 3β-azide from **151**.*

To deprotect **153** at positions 7 and 24 we attempted hydrolysis under basic conditions. The hydrolysis of methyl ester was quick, but the 7-acetate resisted hydrolysis even at higher concentration of the base. The desired compound appeared in few percent contaminated with 3β-azido, 7α-acetate (**154**) was isolated as principal product (*Scheme 4.3.*). It was decided to accomplish the transformations at C-24 using this small amount of material.

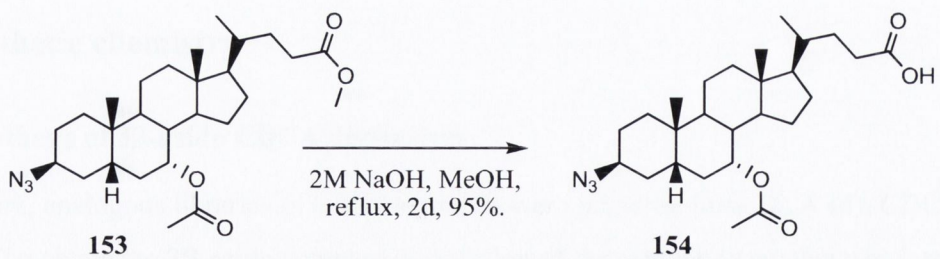

*Scheme 4.3. De-esterification of **153** at C-24*

There are different possible ways to obtain an amide from carboxylic acid. The key step in these reactions is the activation of the carbonyl group (e.g. esterification, acyl chloride formation) before coupling with the appropriate amine. The formation of 24-amide was carried out with the formation of active ester from the carboxylic acid which accepts nucleophilic attack easily by

amines. Hence, compound **154** was reacted with N-OH-Su using DCC as coupling agent, then ammonium solution was added to the intermediate to afford **155**. The reaction resulted in good yield after purification (*Scheme 4.4.*).

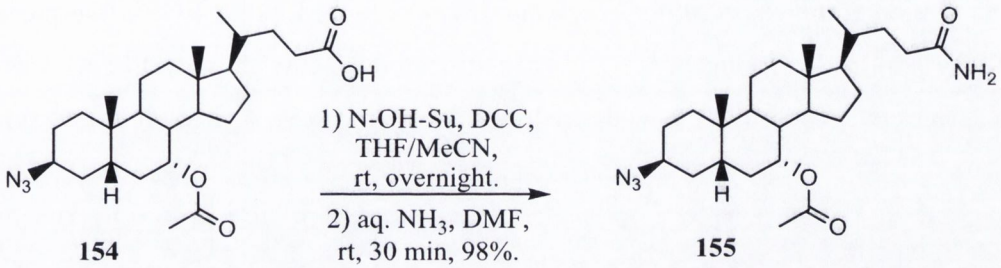

*Scheme 4.4. Synthesis of **155***

Compound **154** was also used as starting material to prepare the 24-cyclopropyl amide. As in the case of the NBD-bile acid CPA compounds we used HOBt and EDC to activate the carboxylic acid. Using this method we avoided the isolation of the active ester. The reaction was carried out in DMF at 0 °C and the formation of the intermediate was monitored by TLC analysis using ninhydrin. When the transformation was complete, the amine was added dropwise into the mixture which was stirred to rt overnight. The formation of the intermediate occurred quickly at 0 °C, thus CPA was added after 10 min. The product (**156**) was afforded in 43% yield (*Scheme 4.5.*).

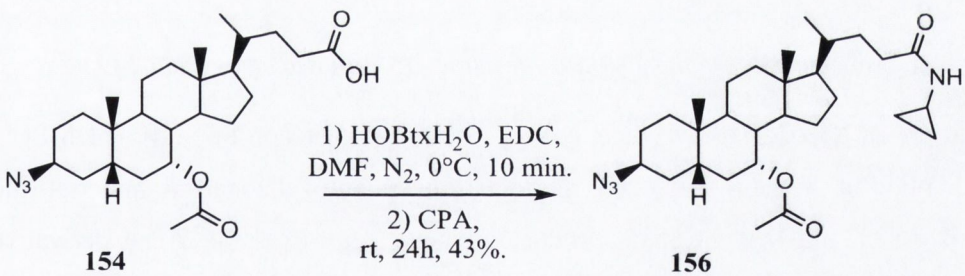

*Scheme 4.5. Synthesis of **156***

4.2.2. Experiments to afford 7β-azido CDCA

In an attempt to afford the 7β-azide, the 3-hydroxyl had to be protected regioselectively. The A-ring tends to be the most reactive of the steroid ring system, being the most open. Hence, the esterified CDCA (**149**) was reacted with Ac_2O using pyridine as catalyst. The reaction was carried out under controlled conditions producing **157** in 76% yield (*Scheme 4.6.*).

To form the azido compound the 7-hydroxyl needed to be activated for azide substitution, thus MsCl was reacted with **157**. The formation of the 7α-mesylate proved difficult with the use of the previously described method (MsCl, Et_3N), thus a different synthetic approach was carried out to obtain the desired compound [200]. Compound **157** was treated with MsCl in the presence of pyridine in DCM at low temperature and then di-isopropyl ethylamine (DIPEA) was added dropwise. This approach produced the desired substance (**158**) in 98% yield (*Scheme 4.6.*).

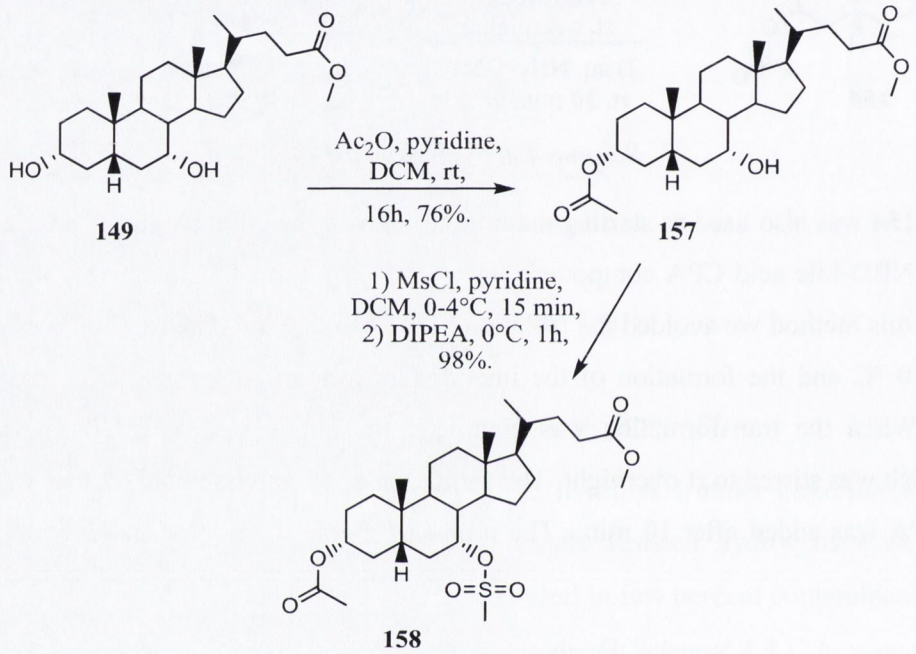

*Scheme 4.6. Synthesis of 7α-mesylate (**158**) in two steps from **149***

The formation of 7β-azide using NaN_3 promoted by the polar aprotic solvent DMPU was the proposed method in the next step. After the total conversion of the starting material (monitored by TLC) it was found that the main product of the reaction was the 7-ene derivative (**159**). Competition between elimination and substitution is a well-established feature of SN2 substitution in steroids (*Scheme 4.7.*). It may have been surmountable in our case but the product alkene appeared to be an interesting compound from a toxicity perspective being endowed with some of the physicochemical features we expected of the azide.

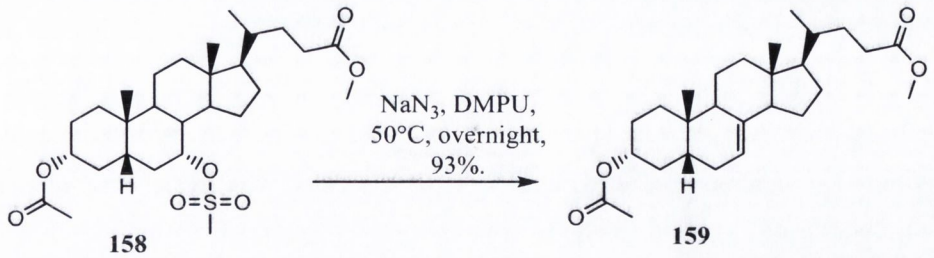

*Scheme 4.7. The formation of 7-ene derivative (**159**) in azide reaction*

Analogous approaches were followed to obtain the 24-amido and 24-cyclopropylamido compounds as in the case of 7α-acetate. Compound **159** was deprotected at C-3 and 24 then the deesterified carboxylic acid (**160**) was activated by N-OH-Su or HOBt monohydrate in the presence of coupling agent. In the final step of the synthesis the appropriate amine was reacted with the intermediate to afford compound **161** and **162** in 93 and 90% yield (*Scheme 4.8.*).

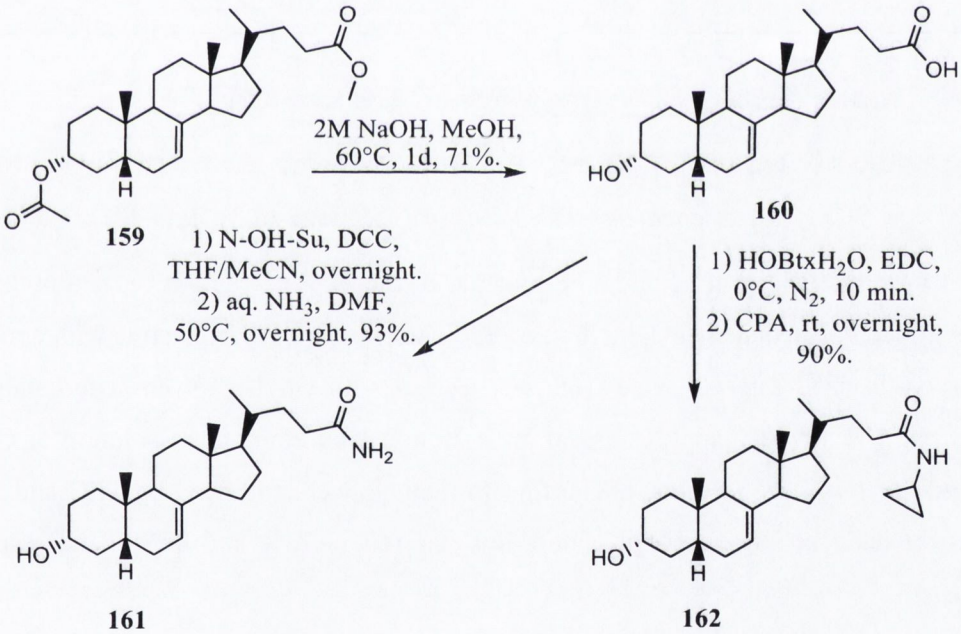

Scheme 4.8. Synthesis of 24-amido compounds

4.2.3. Synthesis of 3β-azido, 7α-hydroxyl CDCA derivatives

Because of the earlier failure in the cleavage of 7-acetate group of **153** we decided to introduce the azide to the A-ring without protecting the 7-hydroxyl. Hence, the 3-hydroxyl of the 24-esterified CDCA (**149**) was converted to mesylate under controlled reaction conditions using stoichiometric amount of MsCl in the presence of two equivalents of Et_3N. The reaction was

carried out at 0 °C and the mixture was worked up immediately after completing the addition of the reagent. The required compound (**163**) was obtained in 93% yield and its structure was proved by ^{1}H and ^{13}C NMR, IR and HR-MS. Compound **163** was then used in the azide reaction giving **164** after purification in 76% yield. The methyl ester was hydrolyzed at pH~14 (2M NaOH) yielding the free carboxylic acid (**165**) in 34% (*Scheme 4.9.*).

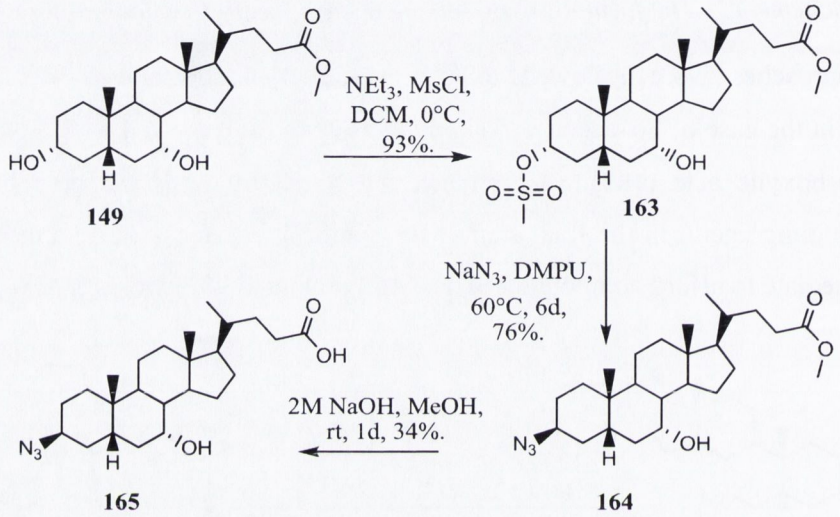

*Scheme 4.9. Synthesis of **165** from **149***

Because of the low yield in the amidation reaction of the 7-acetyl derivative, it was decided to form anhydride intermediate using ethyl chloroformate, which is more reactive with amines than the earlier synthesized esters. Hence, **165** was reacted with ethyl chloroformate catalysed the reaction with Et_3N at 10 °C in 1,3-dioxane then 10 min later ammonium solution or CPA was added slowly to form the C-N bond. The transformations were followed by TLC and after the completion of the reaction we could obtain **166** and **167** in 72% and 87% yield, respectively (*Scheme 4.10.*).

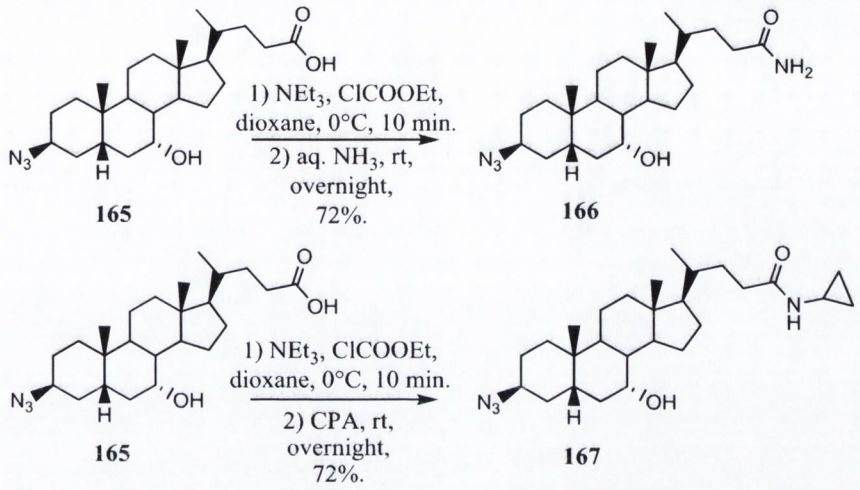

*Scheme 4.10. Synthesis of **166** and **167** from **165***

4.2.4. Synthesis of 3β-azido DCA derivatives

After the synthesis of the CDCA derivatives we turned our attention to investigation on DCA (**4**). Using **4** as starting material a panel of five amide analogues was synthesized with β-azido group on the A-ring. To obtain the 3β-azido DCA derivative (**120**) we followed the synthetic route that was described in Chapter 2. Therefore, the DCA was converted first to 24-methyl ester (**67**) then the regioselective formyl protection of the 7-alcohol was carried out in two steps. The unprotected 3-hydroxyl (**105**) was then transformed to 3β-azide (**115**) *via* 3a-mesylate (**114**), then the 12-formyl and 24-methyl esters were removed under strong basic condition. Compound **120** was obtained in 65% overall yield in six steps (*Scheme 4.11.*)

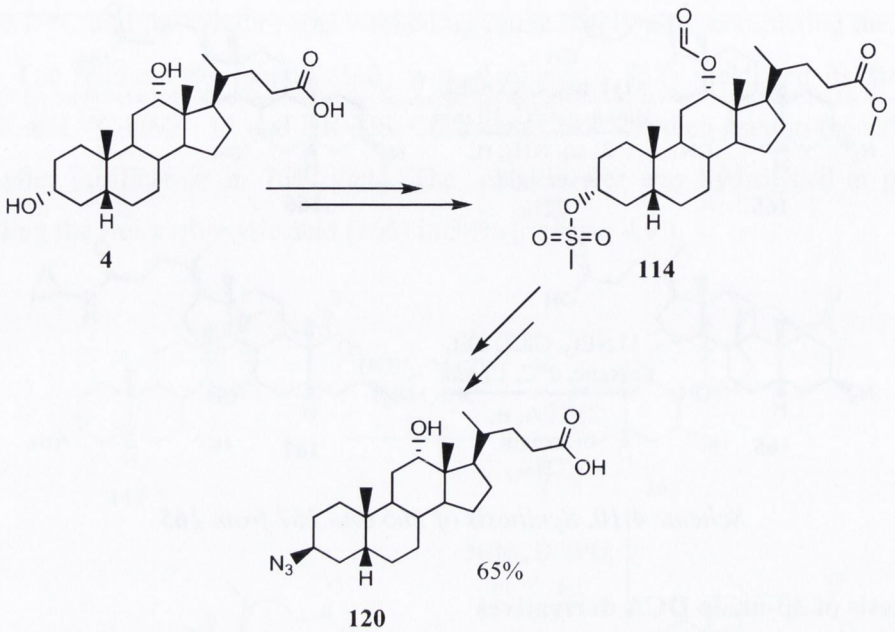

*Scheme 4.11. The synthetic route to afford compound **120***

After the hydrolysis of the 12-formyl and 24-methyl esters, the carboxylic acid was reacted with five different amines to afford 3β-azido, 24-amido (**168**), cyclopropylamido (**169**), benzylamido (**170**), cyclohexylamido (**171**) and propylamido (**172**) analogues of DCA. To obtain the 24-amido compound we used the method that form the product *via* the anhydride intermediate (*Scheme 4.10.*). Compound **120** was reacted with ethyl chloroformate in DCM in the presence of Et_3N at low temperature then after the formation of the anhydride intermediate, ammonia solution was added and stirred at rt. The reason why we decided to use this method in primary amide synthesis was that we wanted to avoid the appearance of by-products which make the separation of the strongly polar amide problematic with column chromatography. The preparation of secondary amides was carried out following the synthetic method with the use of HOBt monohydrate as described above (*Scheme 4.12.*).

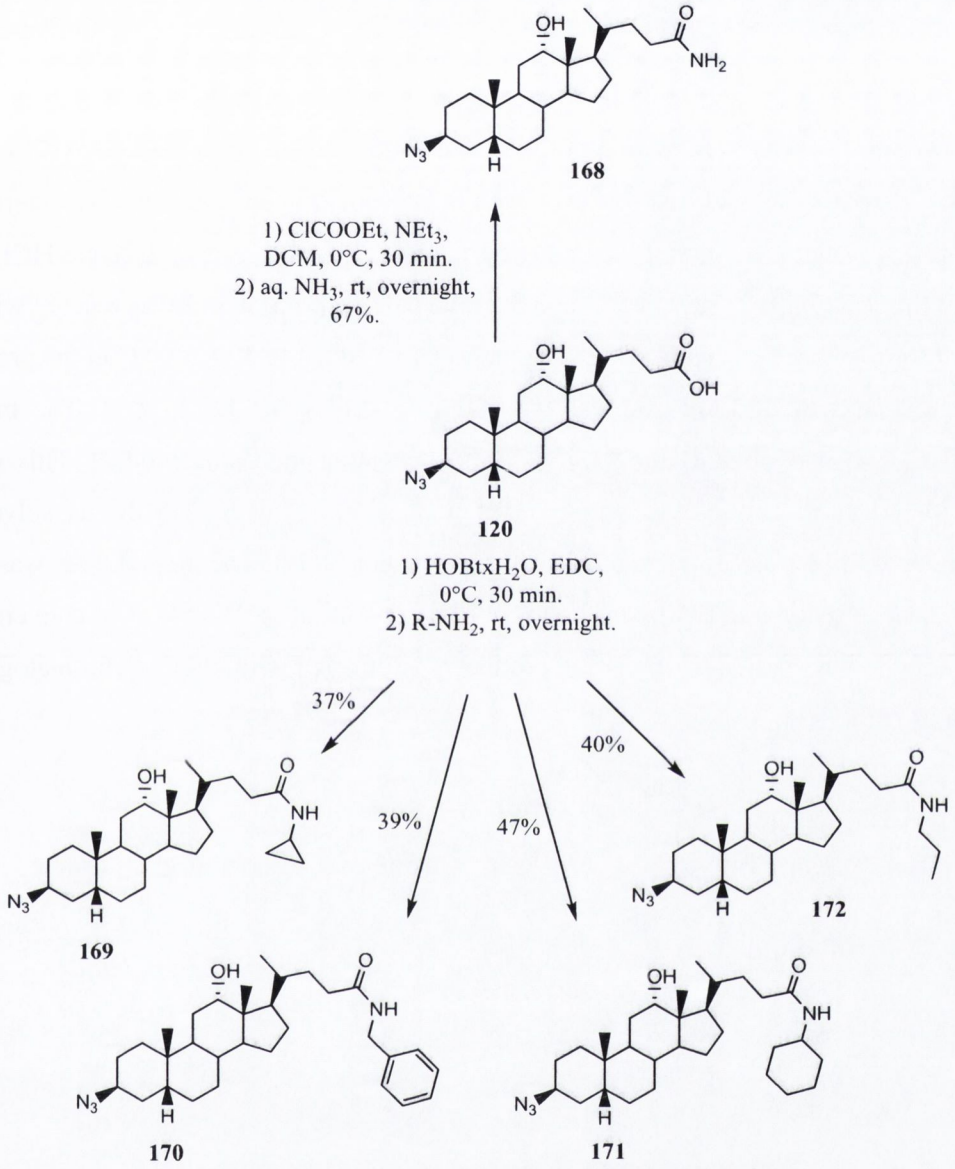

*Scheme 4.12. Preparation of 24-amides from **120***

4.2.5. Synthesis of compound 176–181

The third applied bile acid was the LCA (**5**), which is devoid of functionality on the B- and C-rings therefore presented an interesting opportunity to study the role of the B- and C-ring hydroxyls in the toxicity of bile acids. LCA is the most toxic of the common bile acids and its analogues were expected to be most toxic if lipophilicity is the most important determinant of

toxicity. Preparation of six LCA (**176 – 181**) derivatives was carried out using similar strategies as in the case of CDCA and DCA derivatives.

The synthesis of **176–181** was carried out with the formation of 3β-azido LCA (**176**) (*Scheme 4.13.*). The 24-carboxylic acid was first protected in 98% yield in an acid catalysed esterification, in which step the starting material was allowed to reflux in the presence of conc HCl solution monitoring the reaction by TLC. In the next step the 3-OH group of **173** was reacted with MsCl to prepared for displacement with azide. The reagent was added to **173** at 0 °C in the presence of stoichiometric amount of Et_3N and the reaction was stirred for 1.5 h at rt. The mesylated intermediate (**174**) was obtained in 80% yield after cleaning the crude product. This was then reacted with NaN_3 in an SN2 substitution reaction at 50 °C using DMPU as solvent. The transformation of **174** was complete after 7 d in high yield (96%). The methyl ester was cleaved then in the last step stirring **175** under strongly basic condition (pH ~ 14). The conversion was complete after 1 d at 70 °C and the crude product was purified with column chromatography to obtain **176** in 96% yield.

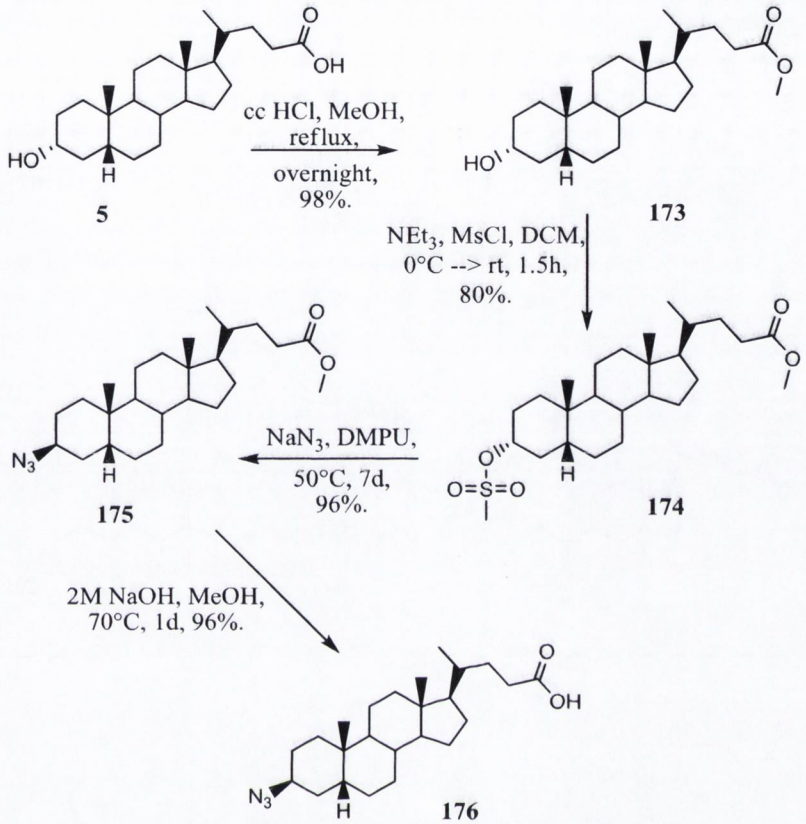

Scheme 4.13. Synthesis of ***176*** *in four steps*

The substituted LCA derivative was used in the following reactions to form the primary (**177**), cyclohexyl (**178**), propyl (**179**), CPA (**180**) and benzyl amides (**181**). To obtain **177** the carboxylic acid was converted to acid chloride was and then treated with aqueous ammonia *in situ*. Compounds **178–181** were prepared with the formation of an active ester at position-24 and then with the coupling of the organic amines. The crude products were purified by flash chromatography using a hexane/EtOAc mixture as mobile phase (gradient) and the products were obtained in good yield (*Scheme 4.14.*).

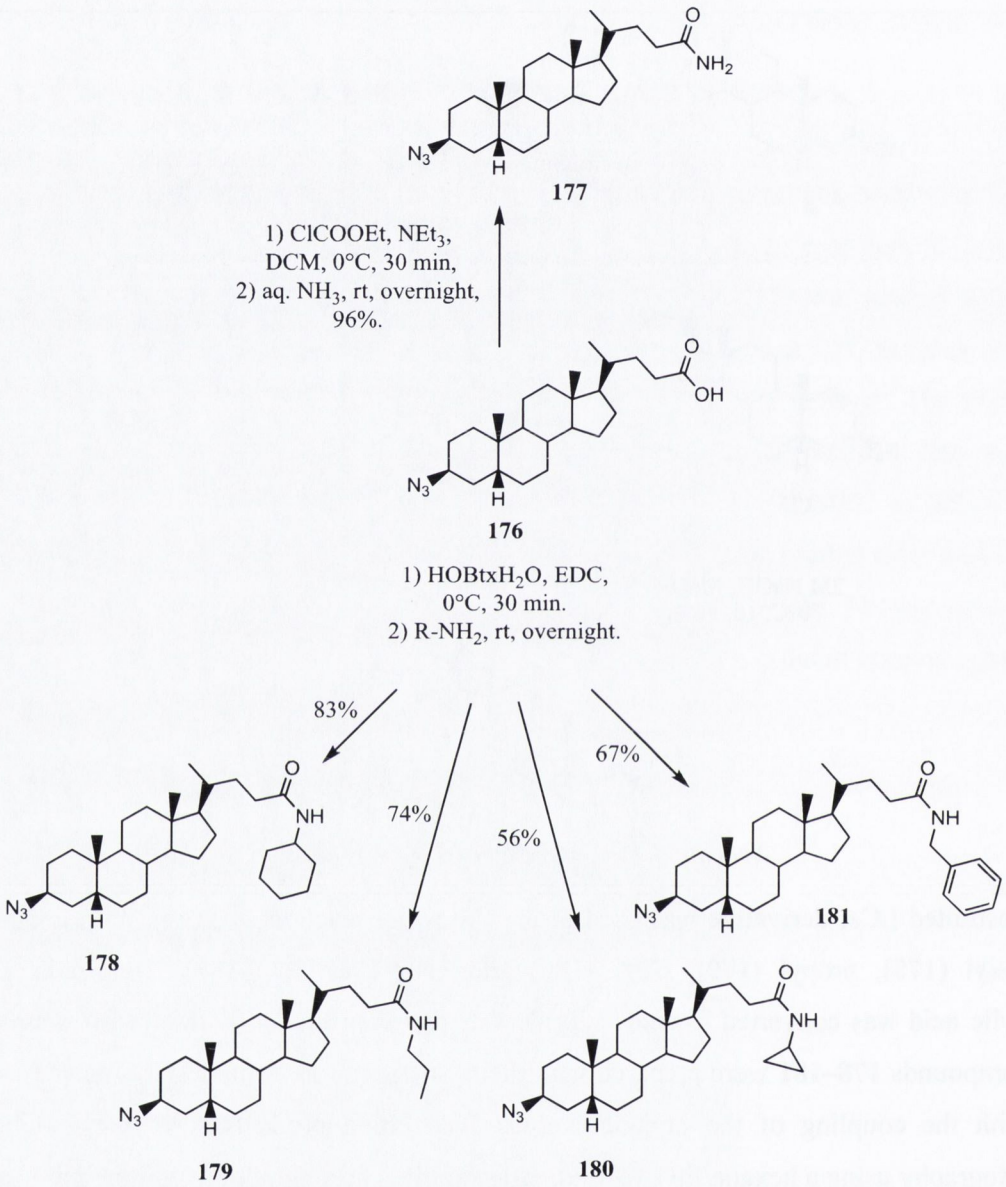

*Scheme 4.14. Synthesis of **177–181** from **176***

4.2.6. Synthesis of compound 182 and 183

For comparison in toxicity tests, the panel of compounds was expanded with the 3α-azido analogue of the 24-amido (**168**) and cyclopropylamido DCA (**169**). The amides were prepared using 3α-azido DCA (**81**) as starting material. The synthetic route to **81** started from the selectively protected DCA derivative **105** which was converted to β-bromo compound **127**. This compound was used in the azide reaction to produce 3-azide with α-orientation (**128**) which was

deesterified in the following step giving compound **81** (*Scheme 4.15.*). The same reactions were carried out earlier to synthesize the 3α-NBD DCA derivative, thus the synthetic route is described in detail in Chapter 2.

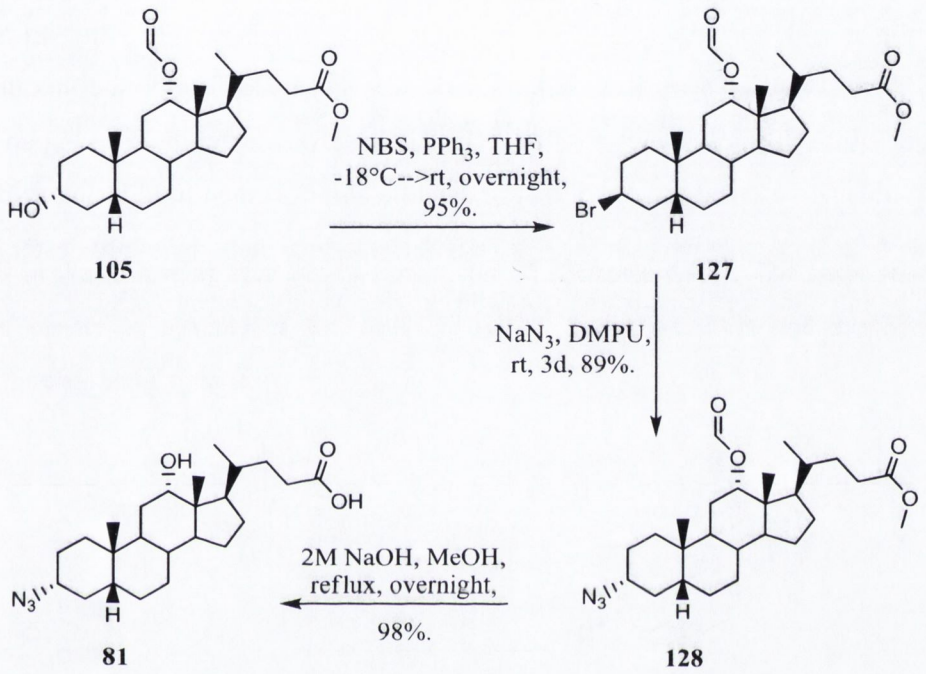

105 **127** **128** **81**

*Scheme 4.15. Preparation of **81***

The free carboxylic acid group of **81** was esterified with HOBt monohydrate in the following two reactions, then the active ester intermediate was reacted with ammonia solution or CPA producing **182** and **183** in 37% and 73% yield, respectively (*Scheme 4.16.*).

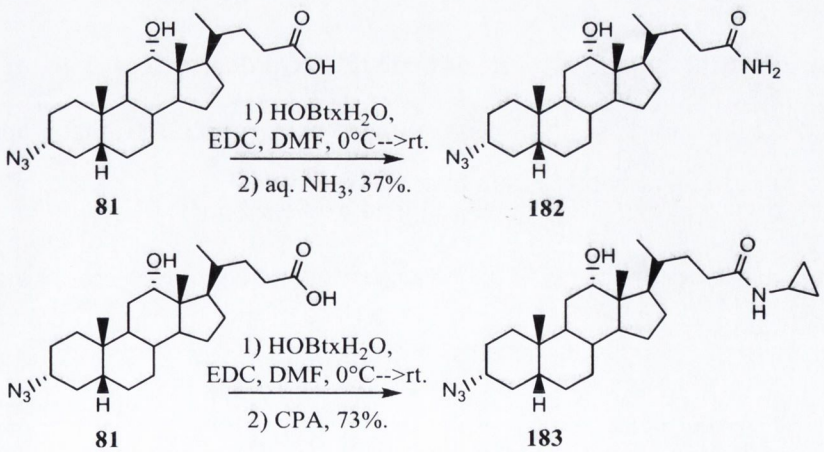

81 **182** **81** **183**

*Scheme 4.16. Synthesis of **182** and **183** from **81***

4.2.7. Synthesis of compound 186

Additionally, 3α-azido CDCA (**186**) was synthesized for comparison in biological tests by applying the Mitsunobu reaction to convert the 3-hydroxyl of CDCA to β-mesylate. Methanesulfonic acid was dissolved in anhydrous THF together with PPh_3, Et_3N and the esterified CDCA (**149**). To start the reaction DIAD was added slowly into the mixture at 0 °C. The formation of the 3β-mesylate was followed by TLC analysis. After the working up procedure the **184** was obtained as white semi-solid (15% yield). This was then used in the azide reaction yielding the 3α-azido derivative (**185**) in 79%, then, in the final step, the methyl ester group was hydrolysed to obtain the free carboxylic acid (**186**) in 88% yield (*Scheme 4.17.*).

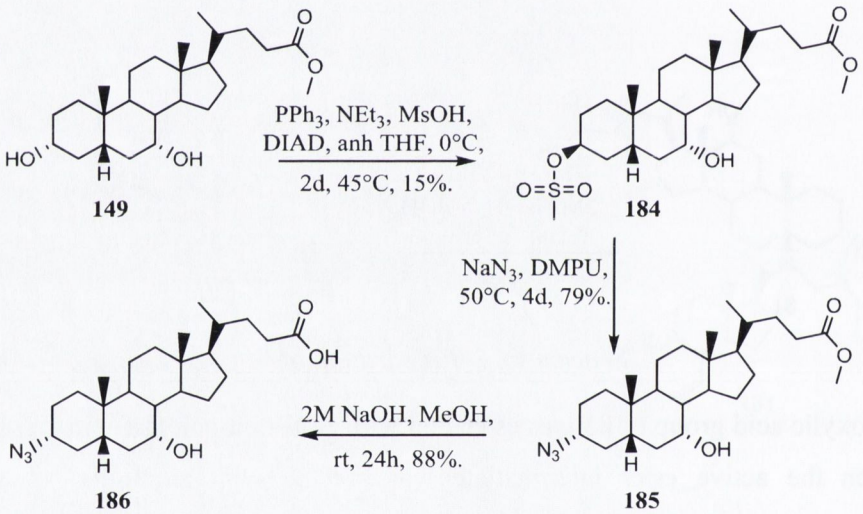

*Scheme 4.17. Synthesis of **186** from **149***

4.2.8. Summary of synthesis: a new panel of toxic bile acid derivatives

A panel of 23 new bile acid derivatives was produced using general synthetic approaches. The overall synthetic work in this Chapter is summarized in *Figure 4.6.*

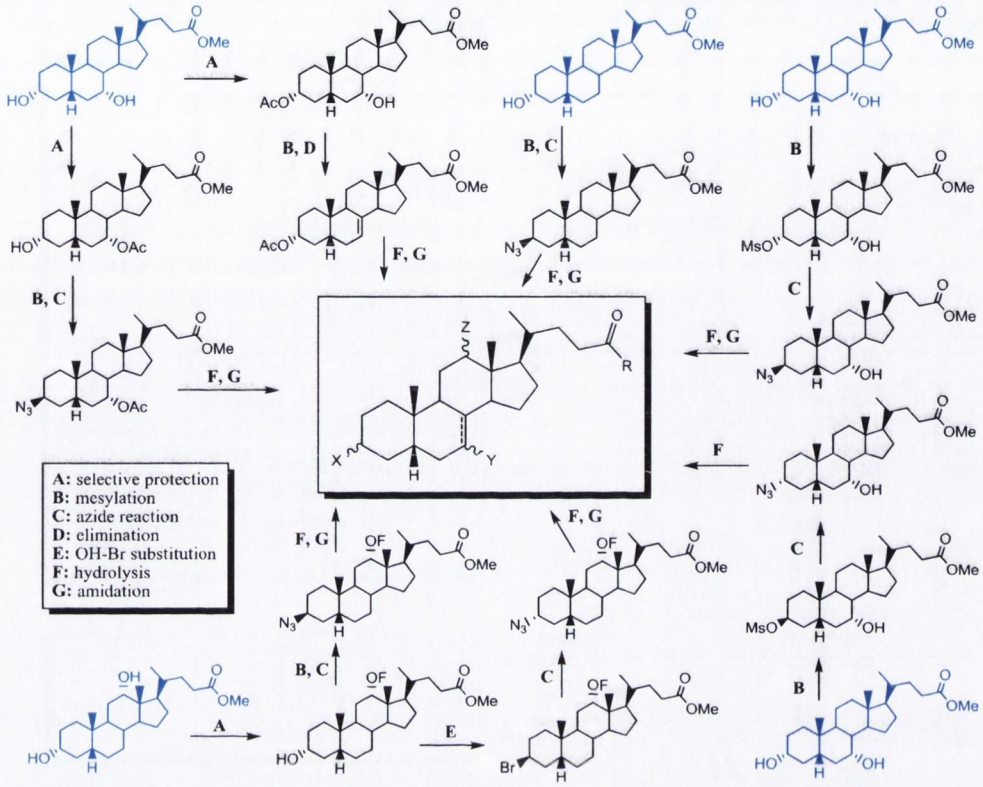

Figure 4.6. Overall synthesis of modified bile acids

We could not produce 7β-azido bile acids in sufficient quantity to permit biochemical analysis but we did produce the corresponding 7-ene and 7-acetyl derivatives of CDCA. The transformations on the B-ring can provide information about the effect of ring-hydroxyls on cell viability in different cell cultures. 3β-Azido LCA and DCA derivatives were also synthesized and amidated with several organic amines. Additionally some bile acid derivatives were produced containing the promising azido-group at C-3 with α-orientation. The synthesized CDCA, DCA and LCA derivatives are summarized in *Figure 4.7.* In the following sections we discuss the biological assays that were applied on the investigation of their cytotoxicity.

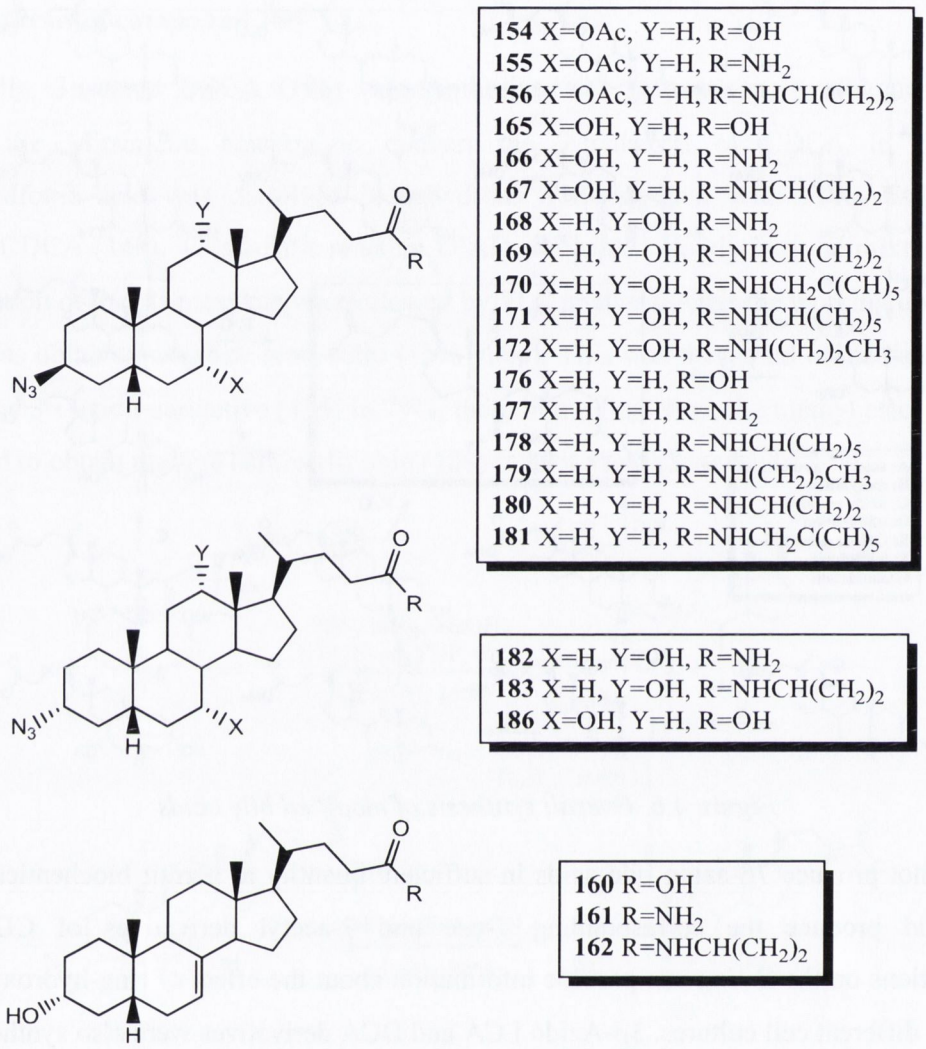

Figure 4.7. New bile acid derivatives for exploring inhibition of cell viability.

4.3. Cytotoxic bile acid effects on cell viability of Caco-2 and HT1080 cells

Human colonic epithelial cancer cells Caco-2 or fibrosarcoma HT1080 cells at 70% confluence were treated in serum free media with the compound of choice for 1 h and for 24 h. The measurements were conducted at 50 μM initially in order to survey the toxicity effects using the MTT assay. DCA, CDCA and LCA were studied as positive controls.

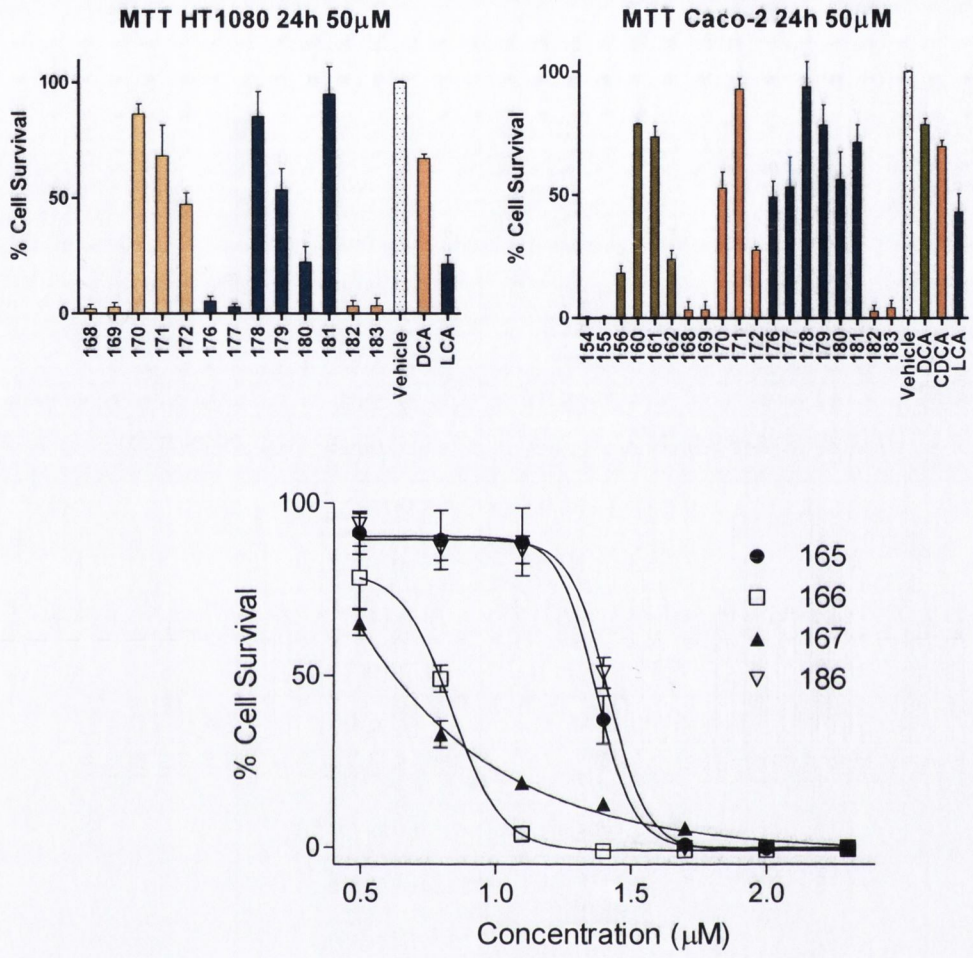

Figure 4.8. Cell viability assessment at 50 μM. Representative sigmoidal concentration response relationships are also shown for the incubation of compounds in the presence of HT1080 cells

When it became apparent that there were interesting differences in cytotoxicity and that low levels of residual viability resulted at 50 μM, we studied the effect of successively lower concentrations in order to allow estimation of a CC_{50} or EC_{50} for cell death induction or alternatively IC_{50} values for inhibition of cell viability. This data is presented in Table 4.1. This was also performed for the control compounds. These yielded values in the expected range with LCA being more toxic than DCA and CDCA in both cell lines.

IC_{50} (95% confidence interval, μM)		
Compound	**Caco–2**	**HT1080**
154	15.6 (13.4–17.6)	Nd
155	5.5 (5.2–5.8)	Nd
156	6.2 (2.1–13.2)	Nd
160	>100	Nd
161	>100	Nd
162	9.5 (4.8–18.9)	Nd
165	40.3 (28.3–57)	23.6 (20.5–27)
166	9.8 (8.1–11.9)	6.9 (6.2–7.6)
167	7.6 (5.6–10.8)	Non converge
168	10.7 (3.5–27)	3.6 (1.6–8.3)
169	6.3 (2.5–15)	1.9 (0.8–4.5)
170	>1 mM	>500
171	>1 mM	>100
172	6.3 (2.5–16)	60% @ 50
176	>250	21.3 (10.5–45)
177	>500	13.1 (12.4–13.8)
178	>1 mM	>1 mM
179	>1 mM	50% @ 100
180	>100	>100
181	>100	>100
182	12.6 (11.2–14.2)	10.0 (8.0–12.1)
183	2.3 (0.75–7.3)	5.7 (4.4–7.4)
186	43.7 (34–56)	26.2 (24.5–27.8)
DCA	80.3 (49.2–131)	110.0 (70.2–171)
CDCA	106.0 (98.3–122.6)	130.1 (80.7–210)
LCA	56.0 (37.3–84.3)	23.0 (15–35.5)

Table 4.1. IC_{50} values for analogues on cell viability of Caco-2 and HT1070 cells at 24 h

The following observations may be made about the analogues: The 3-β azide 7-acetates derived from CDCA (**154–156**) were significantly more toxic than CDCA itself; the amides (-NH and CPA) were more toxic than the β-azide with carboxylic acid side chain (5.5/6.2 versus 15.6 μM). Unexpectedly, given their enhanced lipophilicity over the parent CDCA, the alkenes **160–161** were not toxic <100 μM apart from **162** which was toxic to Caco-2 cells at IC_{50} 9.8 μM. This may represent some selectivity for one cancer cell type over the other. The 3β- azides derived from DCA **168** and **169** were among the most toxic in the panel and it seems the most toxic bile acids ever identified. The CPA amide of DCA 3β–azide produced an IC_{50} of 1.9 μM at 24 h in the HT1080 cell line; the primary amide exhibited an IC_{50} of 3.6 μM in the same cell line. The toxicity of the two compounds towards the Caco-2 line was only marginally lower. The influence of the amide structure on the toxicity in this series was highlighted by the relative lack of effect of the cyclohexyl and benzyl amido azides (**170**, **171**). The corresponding n-propyl amide (**172**) was toxic towards the Caco-2 cell line but not the HT1080. Unexpectedly the LCA series 176–181 were not especially toxic to the Caco-2 cell line at <100 μM and were only as toxic as the parent towards the HT1080 cell line in the case of the **176**, **177**. Finally α–azido analogues of CDCA were studied (**182**, **183**). The primary amide (**182**) possessed similar toxicity to the corresponding acetoxy compound (**155**) and the DCA primary amide (**168**). Overall this work, which is ongoing, indicates that it will be possible to produce compounds with submicromolar potency towards cancer cell lines by increasing diversity in this chemistry. The alpha and beta azides may be useful to maintain because of their apparent tendency to impart toxicity, their stability and potential reactivity in click type reactions. The data indicate that the toxicity may be specific because small change in structure- for example between amides, had a large effect on toxicity and because the LCA amides, were least toxic despite being the most lipophilic. Another reason for suggesting that the effects were specific is that in some instances there was markedly divergent toxicity between the two cancer cell lines (e.g. **171**, **172**, **176**, **and 177**).

4.4. Cell Viability - Flow Cytometry

Bile acid induced cell death is attributed to necrotic effects at higher concentration and to apoptotic events at lower concentration [201]. Since necrotic effects are non-specific in origin and difficult to control, it was of interest to determine the relative amounts of necrosis and apoptosis induced by selected compounds from the bile acid panel. In this work we used a

straightforward protocol employing flow cytometry. Apoptosis was detected by the signature presence of phosphatidylserine (PS) on the cell surface, necrotic cells by the permeability to the ionic propidium iodide (PI). Early apoptotic cells are therefore positive for annexin V which binds PS but not permeable to PI; late apoptotic effects are positive for annexin V and PI permeable. Meanwhile, necrotic cells become permeable to PI without being positive to annexin V. Live/healthy cells are not positive for either annexin V or PI. The protocol therefore provides an indication of the relative contributions of apoptotic and necrotic effects to the reduced viability observed in the MTT assay. Since this was the first time this type of work was conducted in our bile acid group, we also looked at effects of DCA (**4**) and LCA (**5**) as controls and to see the effects of their synthetic manipulation on cellular effects. The experiments were carried out with the supervision of Dr Shona Harmon from our research group.

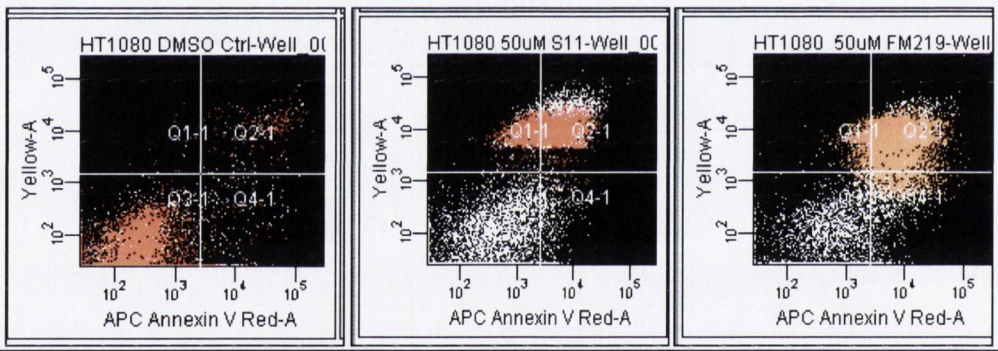

Control, HT1080	HT1080 treated with **172**, 24 h	HT1080 treated with **177**, 24 h
Q1 Necrotic - 0.2%	Q1 Necrotic -18.3%	Q1 Necrotic -24.3%
Q2 Late apoptosis – 2.5%	Q2 Late Apoptosis – 44.2%	Q3 Alive – 32.6%
Q3 Alive – 95.1%	Q3 Alive – 33.8%	Q3 Alive – 32.6%
Q4 Early apoptosis – 2.2%	Q4 Early Apoptosis – 3.6%	Q4 Early Apoptosis – 7.8%

Figure 4.9. Cell Death representative - apoptosis/necrosis

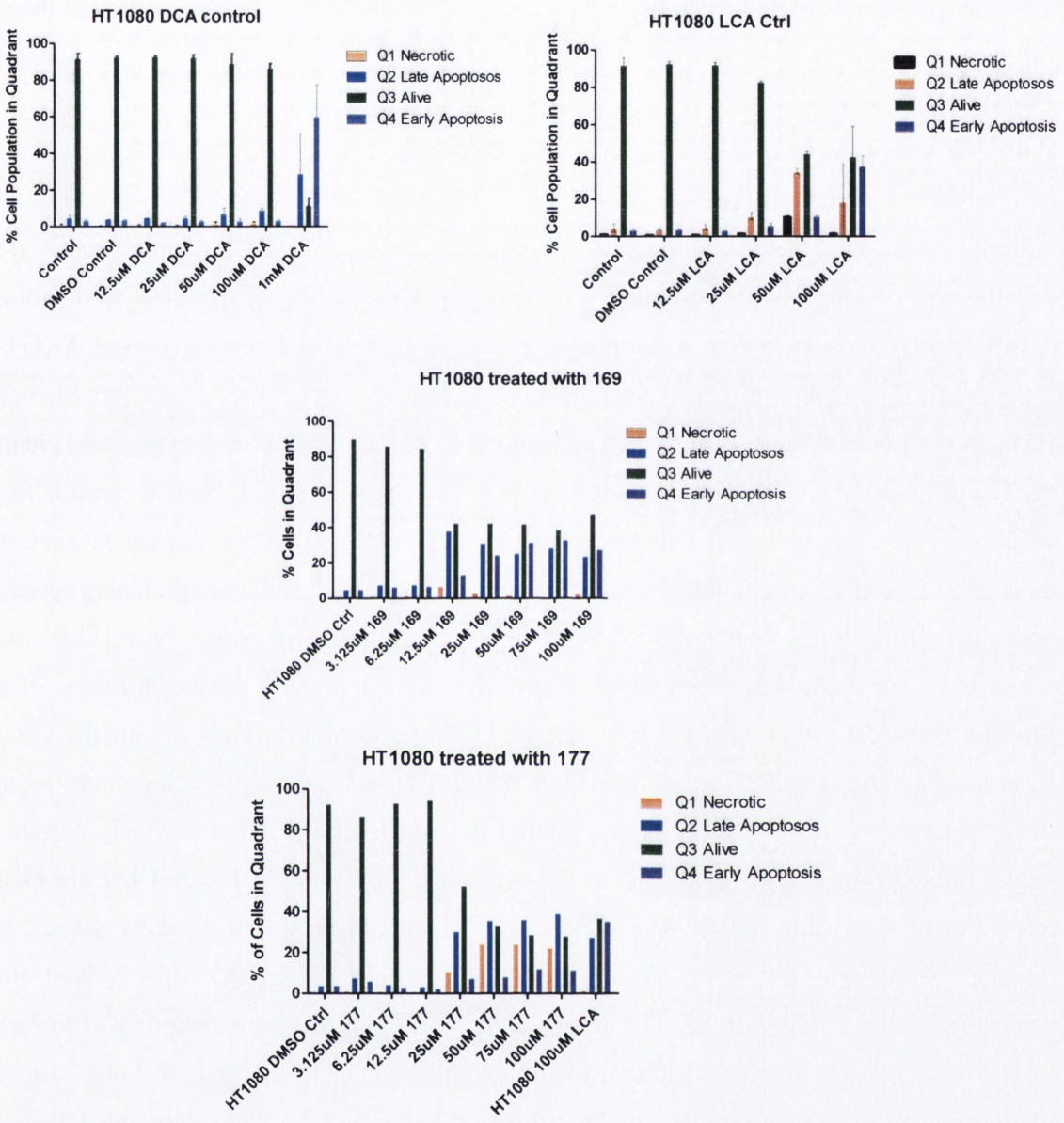

Figure 4.10. Flow Cytometry analysis: comparison of analogues and parent bile acids

Surprisingly, necrosis was not a prominent feature of the FACS analysis of cell populations treated with high concentrations of DCA (**4**) or LCA (**5**), though there were some signs of necrosis in populations treated with **5** (50–100 μM). We were pleased to discover that compound **169**, which is analysed in more detail later in this Chapter, induced cell death almost exclusively through apoptosis. By contrast compound **177**, which is related to **5** caused significant amounts

of necrosis. The data which were collected for a range of the new derivatives proved that the cell viability reductions observed previously with the MTT assay were generally due to apoptosis (rather than necrosis).

4.5. Cell viability effects on oesophageal normal and cancer cells

In order to evaluate the therapeutic potential of the above observations, cell viability studies were continued with a range of oesophageal cell types representing the progression from normal (HET1A/HEEC), through Barrett's oesophagus (GohTRT) to adenocarcinoma (OE-33, SKGT4). The results of this work, which was undertaken at St James's Institute for Molecular Medicine (IMM) by Ms Sinead Phipps, is presented in *Figure 4.11* classified according to bile acid chemo-type. The dysplastic SKGT4 cells are highly resistant to a wide variety of cytotoxic insults [202] whereas the normal oesophageal cells are sensitive [159] and this is reflected in the data set; this is a common feature of cancer cells relative to normal and one of the ongoing problems besetting cancer chemotherapeutics. In this context however we can make the following observations about the results in the oesophageal cell types. Generally, the cytotoxicity potency/efficacy of the compound panel paralleled what we saw already with cells from a different origin- the Caco-2 cells from colon and HT1080 fibrosarcoma cells. This might indicate that the compounds through specific or non-specific mechanisms cause apoptosis through similar systems widely present in cells. Of promise however, is that some of the compounds for example **176** and **182** are highly cytotoxic to SKGT4 cells. *Table 4.2* presents the IC_{50} for cell death induction by several key compounds comparing the highly sensitive primary oesophageal HEEC cells derived from oesophageal biopsy tissue with SKGT4 cells. Future work with these compounds will focus on their effects on cancer cell types that are resistance to chemotherapeutics and on studies directed at their mechanism of action. One of the reasons for this will be to explore the effects of additional chemical signals on inducing selective cell death in cancer cell lines.

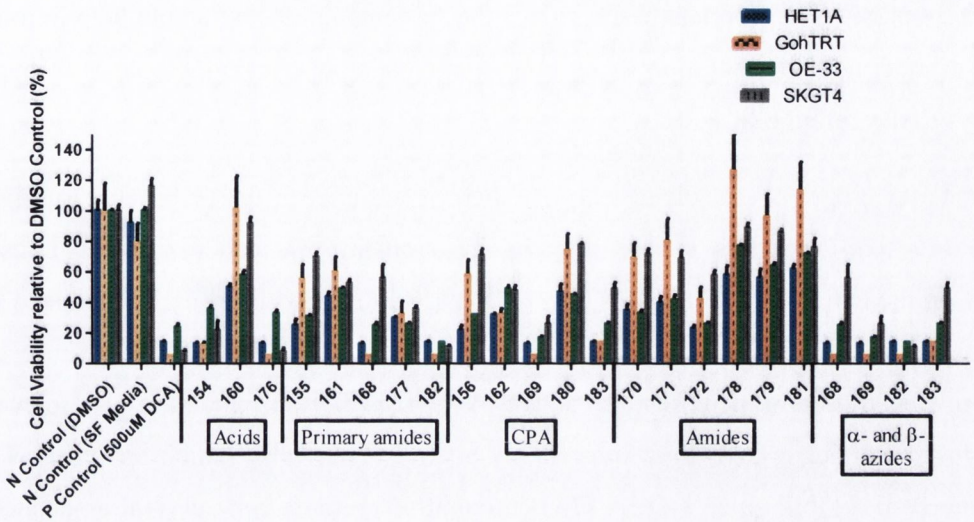

Figure 4.11. Effects on cell viability following treatment with bile acid derivatives for 24 h at 25 μM

	IC_{50} (95% confidence interval, μM)	
Compound	**HEEC**	**OE-33**
168	25.17	25.68 (24.31 – 27.11)
169	14.09 (11.46 – 17.31)	14.73 (12.12 – 17.91)
182	14.73 (6.736 – 32.21)	18.44
183	16.14 (14.15 – 18.40)	13.27 (7.153 – 24.38)
DCA (**4**)	216.2 (163.4 – 286)	391.7
LCA (**5**)	12.76 (10.31 – 15.79)	59.02 (26.59 – 131)

Table 4.2. IC_{50} values (μM) of bile acid derivatives at 24 h in oesophageal normal (HEEC) and adenocarcinoma (OE-33)

4.6. Preliminary mechanistic studies in the toxic bile acid 169

Apoptosis or programmed cell death is an essential physiological process in humans (Figure 4.12). One of the reasons for the intense study of this phenomenon and attempts to manipulate it pharmacologically is its dysregulation in cancer. Tumour cells are characterised by an ability to block or surmount normal signals instructing them to die. Apoptosis is also a part of the underlying pathophysiology of neurodegenerative disorders, in heart disease and in the context of bile acids in hepatic disorders [203-205]. Some consideration of the mechanisms of bile acid

induced apoptosis is appropriate here to place the findings in context and to help introduce some work we undertook to determine if the new compounds are causing apoptosis through similar pathways to the parent bile acids.

Cells undergo programmed suicide because there is a signal to die or because survival signals become blocked. Apoptotic signals may be from outside the cell (extrinsic), transduced by proteins on the cell surface or signals may be from within the cell primarily mediated by effects on the mitochondria (intrinsic) [206]. There are other pathways that could cause cell death including ER stress and increases in reactive oxygen species and these are also relevant to bile acid induced cell death [207-209]. Importantly bile acids may also inhibit apoptosis. This is one of the mechanisms by which UDCA (**7**) is thought to promote cell survival associated with its clinical hepatoprotective effects. Mechanisms of bile acid induced apoptosis and protection are well reviewed in Rodrigues [210].

4.6.1. Extrinsic pathways and bile acids

Death receptors, which are located on the plasma membrane/cell surface, belong to the tumour necrosis factor (TNF) receptor super-family, including TNF receptors, CD95/Fas, TRAIL (TNF related apoptosis inducing ligand receptor) and death receptors 3 and 6 [211-213]. Ligand binding causes activation of caspase-8 which triggers a proteolytic cascade leading to phagocytosis [214]. In some cell types, externally triggered cell death is dependent on amplification by mitochondrial events [206]. Thus caspase-8 cleaves Bid leading to activation of Bax and Bak. Toxic bile acids have been shown to cause cell death through Fas and TRAIL-dependent pathways, with caspase-8 activation [211]. These extrinsic effects are not well understood at a molecular level. There is a lack of evidence that bile acids interact directly with the death receptors. It seems more likely that there is an indirect effect either through stimulation of transport of death receptors through the Golgi apparatus, which may or may not be specific, or through non-specific membrane effects causing death receptor translocation/oligomerization.

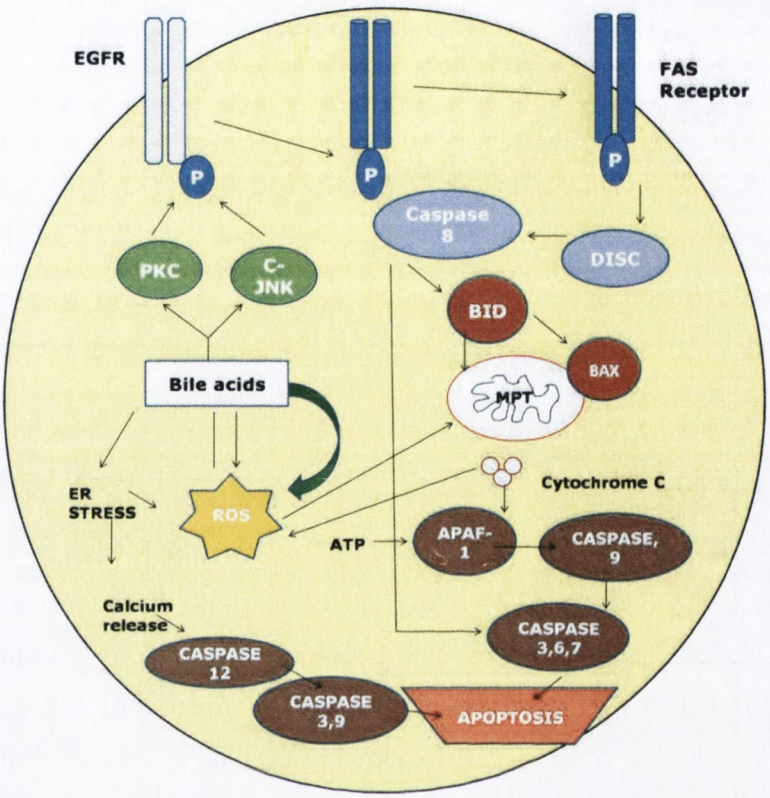

Figure 4.12. Apoptosis pathways relevant to bile acids- induced cell death The extrinsic pathway involves activation of caspase-8 and the intrinsic pathway involves induction of intracellular stresses principally arising in the mitochondria. BAs can also increase production of reactive oxygen species (ROS) and induce apoptosis through ER stress. Image adapted from [208, 215].

4.6.2. Mitochondrial/intrinsic pathways of apoptosis and bile acids

The intrinsic pathway of apoptosis is also caspase dependent but it is triggered by interactions between mitochondrial and cytoplasmic proteins leading to loss of mitochondrial membrane integrity and potential [216]. The key players in this pathway are proteins belonging to the Bcl-2 family which can be either pro- or anti-apoptotic [217]. Bcl-2, Bcl-xL and Bcl-w are anti-apoptotic members of this family [218]. They are found in the mitochondrial membrane which they help to maintain. Internal death signals cause activation of pro-apoptotic Bcl-2 members, Bax and Bak. These bind to anti-apoptotic members embedded in the mitochondrial membrane increasing mitochondrial permeability and the release of cytochrome c. This binds Apaf-1 in the

cytoplasm causing the formation of the evolving apoptosome which binds to and activates procaspase-9 [219]. This precipitates the caspase cascade and associated proteolytic activities (caspase 3- and -7) leading to digestion of structural proteins and degradation of chromosomal DNA [220]. As shown in *Figure 4.12* above, there is considerable interconnectedness between the intrinsic and extrinsic pathways. Yet another apoptotic pathway, which is important in neurones, involves release of apoptosis initiating factor (AIF) directly from the mitochondria. This binds directly to DNA causing apoptosis [216]. This process, which is caspase independent, is not associated with bile acids.

4.6.3. ER stress and bile acids

Bile acids can induce ER stress [221], leading to Ca^{2+} release (the ER is a major storage site for cellular calcium) [222]. This leads to activation of caspase 12 and eventually executioner caspases. There is also evidence of cross talk between ER stress and mitochondrial (intrinsic) processes that are mediated by Ca^{2+} fluctuations and/or formation of reactive oxygen species (ROS) [223, 224]. The latter are elevated following cellular exposure to bile acids but it is unclear whether this is consequence of mitochondrial damage (release of cytochrome c) or if it is a cause of mitochondrial damage [208].

In summary bile acids cause cell death in multiple cell types in a concentration dependent manner [208]. Some of the features of this include migration and activation of death receptors, release of cytochrome c and activation of executioner caspases [215]. These processes may be due to specific or non-specific effects or a combination; depending on bile acid concentration (e.g. high concentrations may causes necrosis). Another feature of bile acid induced cellular injury is the high level of ROS [225]. It is surprising that so far, no direct interacting partner has been identified as the agent mediating this array of effects. The importance of this apart from scientific interest lies in its relevance to induction of gastro-oesophageal-hepatic injury by bile acids and it potential chemoprevention. One of the interesting things to emerge from the present work is that bile acid toxicity can be amplified considerably by simple modification resulting in potency levels more consistent with protein binding and specific effects. It may present an opportunity to isolate specific effects and identify the elusive bile acid interacting partners. In completing this phase of the work we decided to ask (or begin to ask) a more straightforward question: are the novel cytotoxic agents, which exhibit far greater potency, inducing cell death through a similar

mechanism to the parent bile acids? It struck us that an interesting approach to this problem would be to look at the pattern of apoptotic proteins expressed in one of our cell models following exposure to DCA (**4**) or one of its azido analogues at concentrations where we had detected significant apoptosis. A commercial kit available from R&D systems allows estimation by immunoblot of amounts of selected apoptotic proteins in cellular media. The measurements were undertaken by Dr Shona Harmon from the Gilmer group. Accordingly HT1080 cells were treated with either DCA (400 μm) or **169** (10 μM for 24 h or 25 μM for 1 h). Using the R&D apoptosis kit the relative amounts of a selection of proteins were measured by densitometry; the resulting immunoblots are presented in *Figure 4.13* and densitometry analysis in *Figure 4.14*.

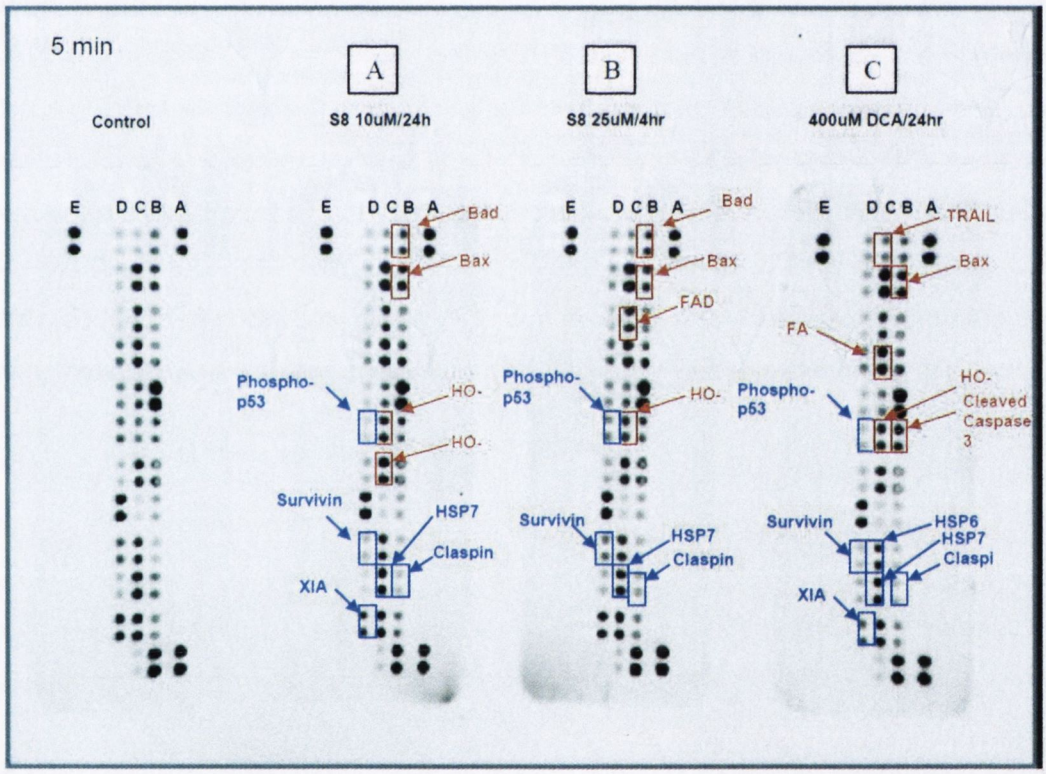

Figure 4.13. Immunoblots of cell lysates following treatment of HT1080 cells with ***169*** *(10/25 μM for 4/24 h, A and B) or DCA (400 μM for 24 h, C). Increases in protein concentration relative to control or highlighted in red; decreases in blue.*

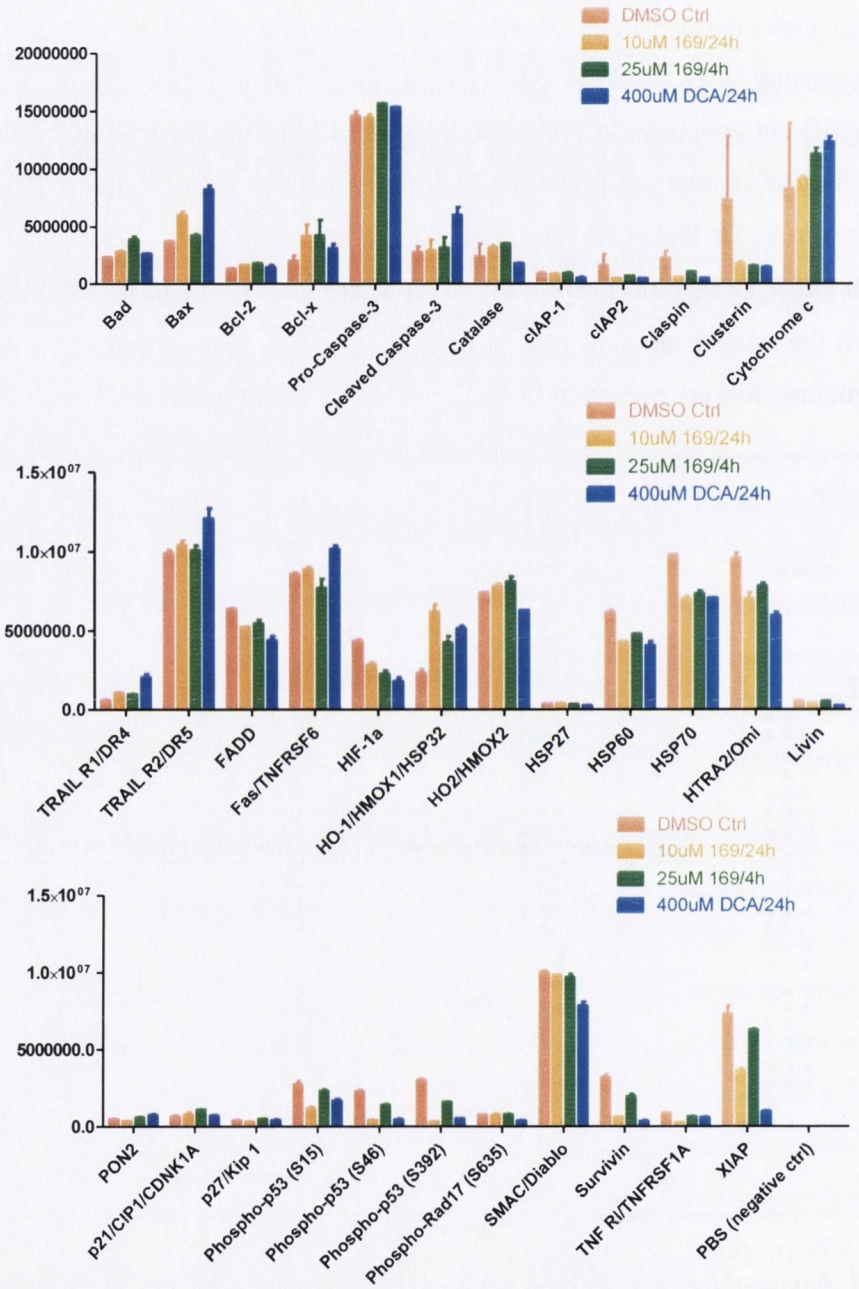

Figure 4.14. Densitometry analysis following treatment of HT1080 cells with ***169*** *(10/25 μM for 4/24 h) or* ***4*** *(400 μM for 24 h).*

Notable changes in protein expression included members of the BCL2 family: increased BAD levels with **169** at 4 h but not 24 h; BAX increases with **169** at 24 h but not 4 h and bile acid DAX increases with DCA (**4**) at 24 h; Bcl-xl increases with **169** at 4 and 24 h but not with DCA; no overall changes in caspase 3 but significant increases of activated caspase 3 with DCA treatment; large increases in TRAIL/R1DR4 with DCA (no increases in R2/DR5), moderate increases with **169** at 4 and 24 h; reductions in claspin and survivin with all three treatments; decreases of FADD with all three; substantial decreases in XIAP; similar effects on P53 phospho forms; significant decreases in HIF-1a.

Overall the data did not suggest different relative contributions from intrinsic and extrinsic pathways between **169** and DCA (400 μM, 24 h). It indicates that DCA mediated cell death at this concentration level is substantially driven by apoptotic processes (e.g. high levels of the active form of the executioner caspase-3) and finally it suggests that **169** and DCA trigger similar apoptotic pathways at 10/25 and 400 μM respectively. The relatively high potency of **169** in this context suggests that its interactions are specific and although its binding partner is unidentified the study indicates that it would be a good ligand for commencing studies into this important problem.

Chapter 5

Experimental

5.1. Chapter 2

5.1.1. General synthetic methods

All chemicals were purchased from Sigma-Aldrich (Dublin, Ireland), except where stated. All the reactions were monitored using TLC. Uncorrected melting points were measured on a Stuart Apparatus. Infra-red (IR) spectra were performed on a Perkin Elmer FT-IR Paragon 1000 spectrometer. ^{1}H and ^{13}C nuclear magnetic resonance (NMR) spectra were recorded at 27°C on a Brucker DPX 400 spectrometer (400.13MHz, ^{1}H; 100.61MHz, ^{13}C). Coupling constants are reported in Hertz. For ^{1}H-NMR assignments, chemical shifts are reported: shift value (number of protons, description of absorption, coupling constant(s) where applicable). Electrospray ionization mass spectrometry (ESI-MS) was performed in the positive ion mode on a liquid chromatography time-of-flight mass spectrometer (Micromass LCT, Waters Ltd., Manchester, UK). The samples were introduced into the ion source by an LC system (Waters Alliance 2795, Waters Corporation, USA) in acetonitrile:water (60:40% v/v) at 200 µl/min. The capillary voltage of the mass spectrometer was at 3 kV. The sample cone (de-clustering) voltage was set at 40 V. For exact mass determination, the instrument was externally calibrated for the mass range m/z 100 to m/z 1000. A lock (reference) mass (m/z 556.2771) was used. Mass measurement accuracies of $< \pm 5$ ppm were obtained. Compound purity/homogeneity was confirmed using a combination of NMR, TLC and HPLC.

5.1.2. Methods for TLC visualization

Different methods were used to visualize the spots on the developed TLC plates depending on the chemical structure of the compounds. UV light was applied in those cases where the examined molecules were UV-active such as the fluorescent bile acid derivatives. For the visualization of the non-UV-active substances we used different TLC dips as vanillin, ninhydrine or the Dragendorff's reagent. To analyze the developed TLC plates first they were sprayed with the appropriate dip and then heated until the appearance of the stained spots.

Vanillin: general stain giving purple spots for alcohols and carboxylic acids. Recipe: 15 g vanillin was dissolved in 250 ml EtOH, then 2.5 ml concentrated sulphuric acid was added and mixed. The solution was stored in brown glass container (light-sensitive).

Ninhydrin: Excellent stain for amines, amides and amino acids giving yellow spots after heating. Recipe: 1.5 g ninhydrin was dissolved in 100 ml *n*-butanol and then 3.0 ml of acetic acid was added to the mixture.

Dargendorff's reagent: This reagent was used to visualize nitrogenous compounds giving orange spots after heating. Recipe: Solution A was prepared with bismuth nitrate (1.7 g) in 100 ml water /acetic acid (4:1) mixture. To prepare Solution B 40 g potassium iodide was dissolved in 100 ml of water and then 5-5 ml of Solution A and B were mixed and diluted with 20 ml acetic acid and 70 ml water to obtain the Dargendorff's reagent.

5.1.3. Synthesis

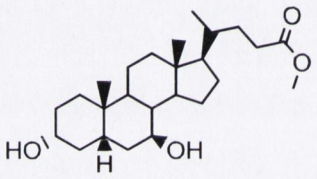

54

To a solution of UDCA (2 g, 5.1 mmol) in MeOH (40 ml) was added HCl (37%, 0.22 ml, 2.5 mmol) and stirred at reflux. The formation of the UDCA methyl ester was followed by TLC analysis and after completion of the reaction the solvent was removed *in vacuo*. The residue was dissolved in EtOAc (100 ml) and washed with water (2 × 100 ml) and brine (1 × 100 ml). The organic phase was dried over $MgSO_4$, filtered and the solvent was removed under reduced pressure to give a white, odourless solid (1.9 g, 91%). mp 152-154°C [226]; ^{1}H-NMR (400 MHz, Acetone-d_6): δ 3.62 (s, 3H, -O-CH_3), 3.50 (m, 2H, 3β-H, 7α-H), 0.98 (d, 3H, J = 6.52 Hz, 21-CH_3), 0.96 (s, 3H, 19-CH_3), 0.71 (s, 3H, 18-CH_3). ^{13}C-NMR ppm (100 MHz, Acetone-d_6): δ 174.52 (C=O, 24-C), 71.42 (CH, 3-C), 71.10 (CH, 7-C), 51.47 (CH_3, O$\underline{C}H_3$). IR_{vmax} (KBr): 3466.17, 2935.06, 2861.90 and 1711.48 cm^{-1}. HRMS: Found: $(M\text{-}Na)^+$ = 429.2960, calculated for $C_{25}H_{42}O_4Na$ = 429.2981.

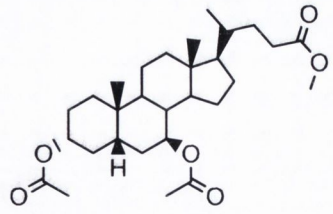

55

24-Methyl 3α, 7β-Dihydroxy-5β-cholanoate (4 g, 9.8 mmol) and 4-DMAP (240 mg, 2.0 mmol) were dissolved in anhydrous pyridine (50 ml) and Ac_2O (27.9 ml, 295.1 mmol) was added to the solution at rt and stirred overnight. Then the reaction mixture was poured into water (200 ml), extracted with EtOAc/hexane 1:1 (3 × 100 ml) and the organic phase was combined and washed with 1 N HCl solution (100 ml), water (100 ml) and brine (100 ml), dried over $MgSO_4$, filtered and the solvent was removed *in vacuo*. The resulting orange semi-solid was passed through silica gel to give the title compound as a white odourless foam (4.3 g, 89%). ^{1}H-NMR (400 MHz, $CDCl_3$): δ 4.77 (6, 1H, J_1 = 5.52 Hz, J_2 = 5.02 Hz, 7α-H), 4.68 (m, 1H, 3β-H), 3.68 (s, 3H, -O-CH_3), 2.04 (s, 3H, 3-C=OCH_3), 2.00 (s, 3H, 7-C=OCH_3), 0.98 (s, 3H, 19-CH_3), 0.94 (d, 3H, J = 6.53 Hz, 21-CH_3), 0.69 (s, 3H, 18-CH_3). ^{13}C-NMR ppm (100 MHz, $CDCl_3$): δ 174.52 and 174.41 (2C=O, 3-C=OCH_3 and 7-C=OCH_3), 170.43 (C=O, 24-C), 73.39 and 73.36 (2CH, 3-C and 7-C), 51.33 (CH_3, OCH_3), 21.65 (CH_3, 7-OC=OCH_3), 21.01 (CH_3, 3-OC=OCH_3). IR_{vmax} (KBr): 3446.52, 2951.05, 2873.46, 1736.99 and 1240.13 cm^{-1}. HRMS: Found: $(M\text{-}Na)^+$ = 513.3176, calculated for $C_{29}H_{46}O_6Na$ = 513.3192.

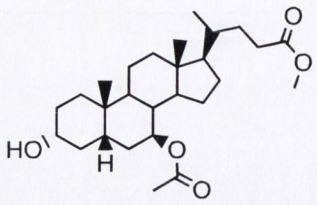

56

To a solution of 24-methyl 3α, 7β-diacetoxy-5β-cholanoate (4.2 g, 8.5 mmol) in anhydrous MeOH (60 ml) was added dropwise AcCl (0.79 ml, 11.1 mmol) at 0 °C. The mixture was allowed to warm to rt with stirring. Saturated $NaHCO_3$ was added to pH ~ 10–12 when all the starting material was reacted it was then extracted with EtOAc (3 × 100 ml). The organic phase was washed with water (2 × 100 ml), dried over $MgSO_4$, filtered and the solvent was removed *in vacuo*. The product was purified by flash chromatography using hexane/EtOAc 3:1 as mobile phase furnishing the title compound as a white solid (2.9 g, 75%). ^{1}H-NMR δ (400 MHz, CD_3OD): δ 4.79 (6, 1H, J_1 = 5.02 Hz, J_2 = 6.03 Hz, J_3 = 4.51 Hz, 7α-H), 3.66 (s, 3H, -O-CH_3), 3.51 (m, 1H, 3β-H), 1.98 (s, 3H, 7-C=OCH_3), 1.00 (s, 3H, 19-CH_3), 0.97 (d, 3H, J = 6.52 Hz, 21-CH_3), 0.73 (s, 3H, 18-CH_3). ^{13}C-NMR ppm (100 MHz, CD_3OD): δ 176.35 (C=O, 7-O<u>C</u>=OCH_3), 172.53 (C=O, 24-C), 75.30 (CH, 7-C), 71.93 (CH, 3-C), 52.00 (CH_3, O<u>C</u>H_3), 21.79 (CH_3, 7-C=O<u>C</u>H_3). IR_{vmax} (KBr): 3441.75, 2946.96, 2870.64, 1736.34 and 1247.36 cm^{-1}. HRMS: Found: $(M\text{-}Na)^+$ = 471.3095, calculated for $C_{27}H_{44}O_5Na$ = 471.3086.

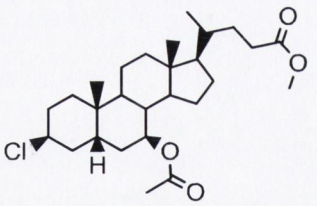

57

To a solution of **56** (0.250 g, 0.557 mmol) in pyridine (15 ml) was added phosphoryl chloride (0.28 ml, 3.065 mmol) and stirred at 40 °C for 18 h after which time TLC analysis showed the reaction was complete. The mixture was cooled to rt and poured into a mixture of ice and 1 M aqueous HCl (100 ml). The resulting mixture was extracted with EtOAc (3 × 100 ml) and washed with water (50 ml) and saturated $NaHCO_3$ (50 ml). The solvent was removed under reduced pressure and the crude product was cleaned by flash chromatography using 5% EtOAc in hexane to give product as a light yellow oil (0.154 g, 64%). ^{1}H-NMR (400 MHz, $CDCl_3$): δ 4.71 (m, 1H, 7α-H), 4.56 (s, 1H, 3α-H), 3.68 (s, 3H, -O-CH_3), 2.01 (s, 3H, 7-C=OCH_3), 1.05 (s, 3H, 19-CH_3),

0.94 (d, 3H, J = 6.25 Hz, 21-CH_3), 0.70 (s, 3H, 18-CH_3). ^{13}C-NMR ppm ($CDCl_3$): δ 174.82 (C=O, 24-C), 170.82 (C=O, 7-OC=OCH_3), 73.92 (CH, 7-C), 51.64 (CH_3, OCH_3), 21.98 (CH_3, 7-C=OCH_3).

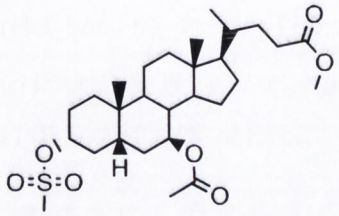

59

To a solution of **56** (1 g) and Et_3N (0.34 ml) in anhydrous DCM (30 ml) was added MsCl (0.26 ml in 10 ml anhydrous DCM) dropwise at 0 °C and stirred for 20 min, after which time TLC analysis showed the reaction was complete. Then, cooled water (50 ml) was added to the mixture, which was separated and the aqueous phase extracted with DCM (2 × 40 ml). The organic phase was washed with brine (100 ml), dried over $MgSO_4$, filtered and the solvent removed under reduced pressure to give product as a colourless oil (1.115 g, 95%). ^{1}H-NMR (400 MHz, $CDCl_3$): δ 4.77 (m, 1H, 7α-H), 4.62 (m, 1H, 3β-H), 3.68 (s, 3H, -O-CH_3), 3.02 (s, 3H, -OSO_2CH_3), 2.00 (s, 3H, 7-C=OCH_3), 0.99 (s, 3H, 19-CH_3), 0.94 (d, 3H, J = 6.02 Hz, 21-CH_3), 0.69 (s, 3H, 18-CH_3). ^{13}C-NMR ppm (100 MHz, $CDCl_3$): δ 174.82 (C=O, 24-C), 170.70 (C=O, 7-OC=OCH_3), 81.72 (CH, 3-C), 73.42 (CH, 7-C), 52.68 (CH_3, -OSO_2CH_3), 51.64 (CH_3, OCH_3), 21.92 (CH_3, 7-C=OCH_3). IR_{vmax} (DCM): 3436.82, 2950.45, 2873.89, 1729.45, 1646.30 and 1173.83 cm^{-1}. HRMS: Found: $(M\text{-}Na)^+$ = 549.2858, calculated for $C_{28}H_{46}O_7SNa$ = 549.2862.

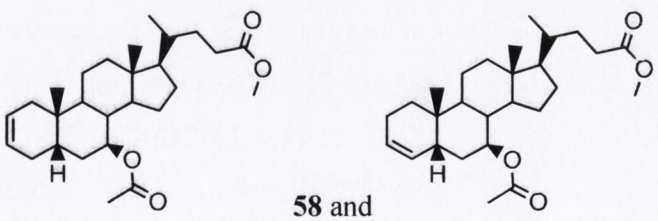

58 and **60**

Compound **59** (0.241 g, 0.458 mmol) was dissolved in dry DMF (20 ml) and treated with LiBr (0.159 g, 1.833 mmol) at rt. The reaction was followed by TLC (hexane/EtOAc 5:1). After 4 d the temperature of reaction was increased to 60 °C and DBU (0.2 ml, 1.374 mmol) was added into the mixture and stirred for 1 d at this temperature after which time the TLC analysis did not show the presence of starting material. 1 M aqueous HCl (100 ml) was added to the mixture and

extracted with EtOAc (3 × 100 ml), then the organic phase was washed with std. $NaHCO_3$ (100 ml) and brine (100 ml). The solvent was removed under reduced pressure and the crude product was cleaned by flash chromatography using 10% EtOAc in hexane as mobile phase to give colourless oil as product (0.123 g, 64%). The mixture was used in the following step without separation of the products. ^{1}H-NMR (400 MHz, $CDCl_3$): δ 5.66 and 5.59 (m, 1H, 2-H and 4-H), 5.52 (m, 1H, 3-H), 4.86 and 4.56 (m, 1H, 7α-H), 3.67 (s, 3H, -O-CH_3), 2.01 (s, 3H, 7-C=OCH_3), 1.03 (d, 3H, J = 9.79 Hz, 19-CH_3), 0.93 (dd, 3H, J_1 = 2.76 Hz, J_2 = 3.51 Hz, 21-CH_3), 0.70 (s, 3H, 18-CH_3).

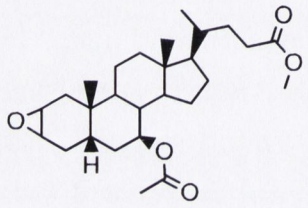
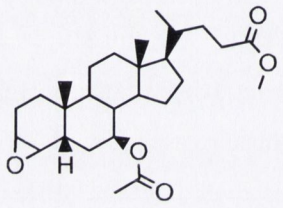

61 and **62**

A mixture of **58** and **60** (0.095 g, 0.221 mmol) was dissolved in DCM (10 ml) when *m*-chloroperbenzoic acid (*m*-CPBA, 0.099 g in 5 ml DCM) was added dropwise at 0 °C. The mixture was allowed to stir up to rt. After 4.5 h TLC analysis did not show the presence of starting material, thus the mixture was washed with sat. $NaHCO_3$ (3 × 50 ml), dried over $MgSO_4$, filtered and the solvent removed under reduced pressure. The crude product was purified by flash colum chromatography using 10% EtOAc in hexane as mobile phase to give product mixture in 26% yield. The spectroscopic analysis showed high number of different products, thus the product was not used in further reactions.

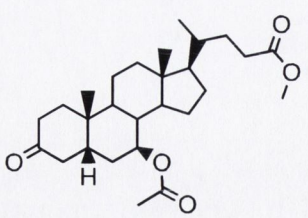

63

To the solution of **56** (0.2 g, 0.446 mmol) in DCM (15 ml) was added pyridinium chlorochromate (PCC, 0.115 g, 0.535 mmol) with stirring at rt overnight, after which time the TLC analysis showed that the reaction was complete. EtOAc (50 ml) was added to the mixture and the combinated organic phase was washed with water (3 × 50 ml) and brine (50 ml), dried over

$MgSO_4$, filtered and the solvent was removed under reduced pressure to yield product as white solid (0.186 g, 93%). Compound **63** was used without further purification in the next reaction step. ^{1}H-NMR (400 MHz, $CDCl_3$): δ 4.80 (sex, 1H, J_1 = 5.27 Hz, J_2 = 5.52 Hz, J_3 = 5.02 Hz, 7α-H), 3.68 (s, 3H, -O-CH_3), 2.02 (s, 3H, 7-C=OCH_3), 1.09 (s, 3H, 19-CH_3), 0.95 (d, 3H, J = 6.27 Hz, 21-CH_3), 0.73 (s, 3H, 18-CH_3). ^{13}C-NMR ppm (100 MHz, $CDCl_3$): δ 211.91 (C=O, 3-C), 175.11 (C=O, 24-C), 171.01 (C=O, 7-OC=OCH_3), 73.41 (CH, 7-C), 51.96 (CH_3, OCH_3), 22.20 (CH_3, 7-C=OCH_3).

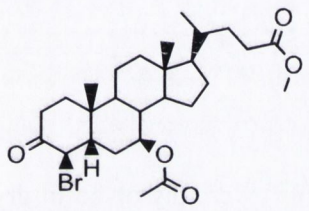

65

To the solution of **63** (0.100 g, 0.224 mmol) in glacial acetic acid (10 ml) was added bromine (0.03 ml in 10 ml gl. AcOH, 0.605 mmol) dropwise at rt . The mixture was stirred for 4.5 h. Then the reaction mixture was poured into aqueous $Na_2S_2O_3$ (50 ml) and extracted with EtOAc (3 × 50 ml). The organic phase was washed with water (50 ml) and brine (50 ml) and the solvent was removed under reduced pressure. The crude product was purified by flash column chromatography (15% EtOAc / hexane) to yield product as a white solid (0.105 g, 89%). ^{1}H-NMR (400 MHz, $CDCl_3$): δ 4.89 (d, 1H, J = 12.55 Hz, 4α-H), 4.81 (m, 1H, 7α-H), 3.68 (s, 3H, -O-CH_3), 2.03 (s, 3H, 7-C=OCH_3), 1.15 (s, 3H, 19-CH_3), 0.94 (d, 3H, J = 6.52 Hz, 21-CH_3), 0.73 (s, 3H, 18-CH_3). ^{13}C-NMR ppm (100 MHz, $CDCl_3$): δ 201.34 (C=O, 3-C), 174.77 (C=O, 24-C), 170.42 (C=O, 7-OC=OCH_3), 71.77 (CH, 7-C), 51.67 (CH_3, OCH_3), 21.84 (CH_3, 7-C=OCH_3).

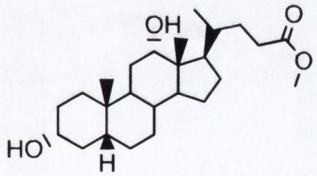

67

To a solution of **4** (5 g, 12.736 mmol) in MeOH (50 ml) was added HCl (32%, 0.63 ml, 6.368 mmol) and the reaction stirred at reflux. The formation of the DCA methyl ester was monitored via TLC analysis and after the reaction went to completion the solvent was removed under reduced pressure to give a white foam (5.18 g, 100%). ^{1}H-NMR (400 MHz, $CDCl_3$): δ 3.96 (s,

1H, 12β-H), 3.65 (s, 3H, -O-CH_3), 3.60 (m, 1H, 3β-H), 0.96 (d, 3H, J = 6.28 Hz, 21-CH_3), 0.89 (s, 3H, 19-CH_3), 0.66 (s, 3H, 18-CH_3). ^{13}C-NMR ppm (100 MHz, $CDCl_3$): δ 174.87 (C=O, 24-C), 73.27 (CH, 12-C), 71.93 (CH, 3-C), 51.65 (CH_3, O<u>C</u>H_3). IR_{vmax} (KBr): 3425.33, 2937.43, 2864.51 and 1740.96 cm^{-1}. HRMS: Found: $(M-Na)^+$ = 429.2984, calculated for $C_{25}H_{42}O_4Na$ = 429.2981.

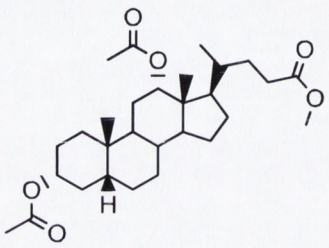

68

Compound **67** (364 mg, 0.895 mmol) and 4-DMAP (22 mg, 0.179 mmol) were dissolved in dry pyridine (15 ml) and Ac_2O (2.5 ml, 26.857 mmol) was added to the solution at rt and stirred overnight. Then the reaction mixture was poured into cooled 1 M HCl solution (100 ml), extracted with EtOAc (3 × 50 ml) and the organic phase was washed with water (100 ml) and brine (100 ml), dried over $MgSO_4$, filtered and the solvent was removed *in vacuo* to give a white odourless foam (394 mg, 90%). This was used without further purification in the next reaction step.^{1}H-NMR (400 MHz, $CDCl_3$): δ 5.10 (s, 1H, 12β-H), 4.72 (m, 1H, 3β-H), 3.68 (s, 3H, -O-CH_3), 2.12 (s, 3H, 12-C=OCH_3) 2.05 (s, 3H, 3-C=OCH_3), 0.92 (s, 3H, 19-CH_3), 0.83 (d, 3H, J = 6.53 Hz, 21-CH_3), 0.74 (s, 3H, 18-CH_3). ^{13}C-NMR ppm (100 MHz, $CDCl_3$): δ 174.78 (C=O, 24-C), 170.74 and 170.65 (2C=O, 3-<u>C</u>=OCH_3 and 12-<u>C</u>=OCH_3), 76.03 (CH, 12-C), 74.34 (CH, 3-C), 51.67 (CH_3, O<u>C</u>H_3).

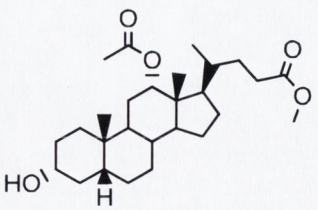

69

To a solution of **68** (1.96 g, 3.994 mmol) in dry MeOH (10 ml) was added MeONa (237 mg, 4.394 mmol) at rt and stirred for 24 h. The reaction mixture was poured into 2 M HCl solution (50 ml) and extracted with EtOAc (3 × 500 ml). The organic phase was washed with water (2 ×

100 ml) and brine (100 ml), dried over $MgSO_4$, filtered and the solvent removed under reduced pressure. The crude product was purified by flash chromatography using 30% EtOAc in hexanes as mobile phase. The title compound was obtained as a white foam (1.56 g, 87%). ^{1}H-NMR (400 MHz, $CDCl_3$): δ 5.09 (s, 1H, 12β-H), 3.68 (s, 3H, -O-CH_3), 3.64 (m, 1H, 3β-H), 2.10 (s, 3H, 12-C=OCH_3), 0.91 (s, 3H, 19-CH_3), 0.82 (d, 3H, J = 6.27 Hz, 21-CH_3), 0.73 (s, 3H, 18-CH_3). ^{13}C-NMR ppm (100 MHz, $CDCl_3$): δ 174.79 (C=O, 24-C), 170.79 (C=O, 12-C=OCH_3), 76.07 (CH, 12-C), 71.85 (CH, 3-C), 51.66 (CH_3, OCH_3). IR_{vmax} (KBr): 3441.20, 2937.47, 2865.80, 1738.85 and 1246.22 cm^{-1}. HRMS: Found: $(M\text{-}Na)^+$ = 471.3080, calculated for $C_{27}H_{44}O_5Na$ = 471.3086.

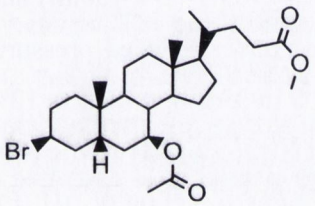

70

PPh_3 (0.170 g) was added to a stirred solution of **56** (0.145 g) in anhydrous THF (15 ml) and the mixture cooled to -18 °C. NBS (NBS) (0.115 g) was added dropwise to the reaction mixture which was allowed to warm to rt. After 1.5 h, when TLC analysis showed no more starting material present, the reaction mixture was poured into water (50 ml) and extracted with EtOAc (3 × 50 ml). The organic phase was dried over $MgSO_4$, filtered and the solvent was evaporated under reduced pressure. The product was separated by flash chromatography, using hexane-EtOAc 3:1 as mobile phase to yield colourless oil (0.151 g, 91%). ^{1}H-NMR (400 MHz, $CDCl_3$): δ 4.76 (s, 1H, 3α-H), 4.69 (m, 1H, 7α-H), 3.67 (s, 3H, -O-CH_3), 2.00 (s, 3H, 7-C=OCH_3), 1.06 (s, 3H, 19-CH_3), 0.93 (d, 3H, J = 6.53 Hz, 21-CH_3), 0.69 (s, 3H, 18-CH_3). ^{13}C-NMR ppm (100 MHz, $CDCl_3$): δ 174.83 (C=O, 24-C), 170.81 (C=O, 7-OC=OCH_3), 74.01 (CH, 7-C), 51.64 (CH_3, OCH_3), 21.97 (CH_3, 7-C=OCH_3). IR_{vmax} (DCM): 3435.54, 2948.89, 1729.41, 1646.49 and 1243.23 cm^{-1}. HRMS: Found: $(M\text{-}Na)^+$ = 533.2249, calculated for $C_{27}H_{43}BrO_4Na$ = 533.2242.

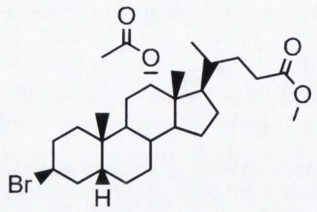

71

PPh_3 (0.821g) was added to a stirred solution of **69** (1.035 g) in anhydrous THF (40 ml) and the mixture was cooled to -18 °C. NBS (1.210 g) was added in three parts to the reaction mixture over 1 h and it was allowed to warm to rt. After 1.5 h, when TLC analysis showed no more starting material present, the reaction mixture was poured into 1 M HCl solution (150 ml) and extracted with EtOAc (3 × 100 ml). The organic phase was washed with water (2 × 100ml) and brine (100ml), dried over $MgSO_4$, filtered and the solvent evaporated under reduced pressure. The product was separated by flash chromatography twice, using 30% EtOAc first then 0–12% EtOAc in hexane as mobile phase to yield colourless semi-solid (0.766 g, 65%). ^{1}H-NMR (400 MHz, $CDCl_3$): δ 5.10 (s, 1H, 12β-H), 4.80 (s, 1H, 3α-H), 3.68 (s, 3H, -O-CH_3), 2.09 (s, 3H, 12-C=OCH_3), 1.00 (s, 3H, 19-CH_3), 0.83 (d, 3H, J = 6.28 Hz, 21-CH_3), 0.75 (s, 3H, 18-CH_3). ^{13}C-NMR ppm (100 MHz, $CDCl_3$): δ 175.07 (C=O, 24-C), 170.85 (C=O, 12-OC=OCH_3), 76.41 (CH, 12-C), 51.97 (CH_3, OCH_3), 21.78 (CH_3, 12-C=OCH_3). IR_{vmax} (KBr): 3444.74, 2940.49, 2873.22, 1736.69 and 1245.03 cm^{-1}. HRMS: Found: $(M\text{-}Na)^+$ = 533.2252, calculated for $C_{27}H_{43}BrO_4Na$ = 533.2242.

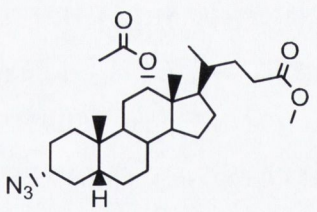

72

To a stirred solution of **71** (0.712 g) in DMPU (20 ml) was added 10 equivalents NaN_3 (0.904 g) at rt. The mixture was stirred for 4 d then poured into water (100 ml) and extracted with EtOAc (3 × 50 ml). The organic phase was washed with brine (100 ml), dried over $MgSO_4$, filtered and the solvent was evaporated in vacuum. The product was separated on a flash column using 0-12% EtOAc in hexane as mobile phase to yield light yellow oil as product (0.589 g, 89%). ^{1}H-NMR (400 MHz, $CDCl_3$): δ 5.09 (s, 1H, 12β-H), 3.68 (s, 3H, -O-CH_3), 3.29 (m, 1H, 3β-H), 2.11 (s, 3H, 12-C=OCH_3), 0.92 (s, 3H, 19-CH_3), 0.83 (d, 3H, J = 6.53 Hz, 21-CH_3), 0.74 (s, 3H, 18-CH_3).

^{13}C-NMR ppm (100 MHz, $CDCl_3$): δ 175.07 (C=O, 24-C), 171.04 (C=O, 12-OC=OCH_3), 76.27 (CH, 12-C), 61.41 (CH, 3-C), 51.98 (CH_3, OCH_3), 21.79 (CH_3, 12-C=OCH_3). IR_{vmax} (DCM): 2941.42, 2867.23, 2091.28, 1738.46 and 1245.13 cm^{-1}. HRMS: Found: $(M-Na)^+$ = 496.3168, calculated for $C_{27}H_{43}N_3O_4Na$ = 496.3151.

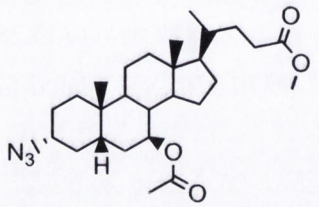

73

To a stirred solution of **70** (1.876 g) in anhydrous DMF (40 ml) was added 5 equivalents NaN_3 (1.192 g) at 60 °C. The mixture was stirred overnight then poured into sat. $NaHCO_3$ (150 ml) and extracted with EtOAc (3 × 100 ml). The organic phase was washed with brine (200 ml), dried over $MgSO_4$, filtered and the solvent was evaporated *in vacuo*. The product was separated on a flash column (hexane/EtOAc 9:1) to yield orange foam (1.258 g, 72%). ^{1}H-NMR (400 MHz, $CDCl_3$): δ 4.76 (sex, 1H, J_1 = 5.52 Hz, J_2 = 5.53 Hz, J_3 = 5.01 Hz, 7α-H), 3.68 (s, 3H, -O-CH_3), 3.28 (m, 1H, 3β-H), 2.00 (s, 3H, 7-C=OCH_3), 0.99 (s, 3H, 19-CH_3), 0.94 (d, 3H, J = 6.53 Hz, 21-CH_3), 0.69 (s, 3H, 18-CH_3). ^{13}C-NMR ppm (100 Mhz, $CDCl_3$): δ 174.52 (C=O, 24-C), 170.40 (C=O, 7-OC=OCH_3), 73.31 (CH, 7-C), 60.58 (CH, 3-C), 51.32 (CH_3, OCH_3), 21.63 (CH_3, 7-C=OCH_3). IR_{vmax} (KBr): 3430.05, 2929.21, 2871.64, 2099.67, 1745.61, 1722.74, 1256.74 and 1164.61 cm^{-1}. HRMS: Found: $(M-Na)^+$ = 496.3159, calculated for $C_{27}H_{43}N_3O_4Na$ = 496.3151.

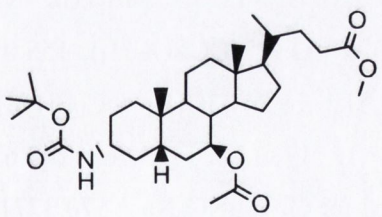

74

The solution of **73** (0.855 g) and Boc_2O (0.473 g) in EtOAc (10 ml) was added to a pre-reduced 10% Pd/C in EtOAc (10 ml) under hydrogen at rt. The reaction mixture was stirred overnight (TLC: hexane/EtOAc 3:1) then it was filtered on a celite pad. The celite was washed with EtOAc (3 × 10 ml) and the organic phase was removed *in vacuo*. The product was purified by flash chromatography (mobile phase: 15% EtOAc in hexanes) to yield product as a white foam (0.915

g, 93%). ^{1}H-NMR (400 MHz, $CDCl_3$): δ 4.76 (m, 1H, 7α-H), 4.42 (s, 1H, 3-NH), 3.68 (s, 3H, -O-CH_3), 3.41 (br. s, 1H, 3β-H), 2.00 (s, 3H, 7-C=OCH_3), 1.45 (s, 9H, -OC(CH_3)$_3$), 0.98 (s, 3H, 19-CH_3), 0.94 (d, 3H, *J* = 6.28 Hz, 21-CH_3), 0.69 (s, 3H, 18-CH_3). ^{13}C-NMR ppm (100 MHz, $CDCl_3$): δ 174.84 (C=O, 24-C), 170.79 (C=O, 7-OC=OCH_3), 155.34 (C=O, 3-NHC=OOC(CH_3)$_3$), 79.21 (C, -O<u>C</u>(CH_3)$_3$), 73.80 (CH, 7-C), 51.64 (CH_3, OCH_3), 28.56 (3CH_3, -OC(<u>C</u>H_3)$_3$), 21.98 (CH_3, 7-C=OCH_3). IR_{vmax} (KBr): 3391.31, 2949.10, 2872.09, 1735.28, 1366.04, 1246.92, 1169.40 and 1022.30 cm^{-1}. HRMS: Found: $(M\text{-}Na)^+$ = 570.3765, calculated for $C_{32}H_{53}NO_6Na$ = 570.3771.

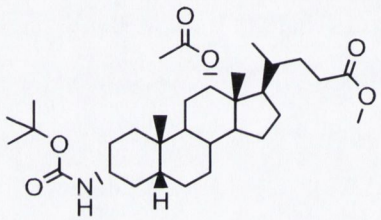

75

The solution of **72** (0.460 g) and Boc_2O (0.255 g) in EtOAc (10 ml) was added to a pre-reduced 10% Pd/C (~50 mg) in EtOAc (10 ml) under hydrogen at rt. The reaction mixture was stirred overnight (TLC: hexane/EtOAc 3:1) then the Pd/C was filtered out on a celite pad. The celite was washed with EtOAc (3 × 10 ml) and the organic phase was removed in vacuum. The product was cleaned by flash chromatography (mobile phase: 0–12% EtOAc in hexanes) to yield a white foam as product (0.441 g, 83%). ^{1}H-NMR (400 MHz, $CDCl_3$): δ 5.09 (s, 1H, 12β-H), 4.43 (br s, 1H, 3-NH), 3.68 (s, 3H, -O-CH_3), 3.41 (br. s, 1H, 3β-H), 2.10 (s, 3H, 12-C=OCH_3), 1.46 (s, 9H, -OC(CH_3)$_3$), 0.91 (s, 3H, 19-CH_3), 0.82 (d, 3H, *J* = 6.02 Hz, 21-CH_3), 0.73 (s, 3H, 18-CH_3). ^{13}C-NMR ppm (100 MHz, $CDCl_3$): δ 174.46 (C=O, 24-C), 170.25 (C=O, 12-OC=OCH_3), 155.07 (C=O, 3-NHC=OOC(CH_3)$_3$), 75.76 (CH, 12-C), 51.34 (CH_3, OCH_3), 28.25 (3CH_3, -OC(<u>C</u>H_3)$_3$), 21.22 (CH_3, 12-C=OCH_3). IR_{vmax} (KBr): 3392.89, 2935.53, 2867.18, 1739.25, 1713.76, 1245.67 and 1171.61 cm^{-1}. HRMS: Found: $(M\text{-}Na)^+$ = 570.3792, calculated for $C_{32}H_{53}NO_6Na$ = 570.3771.

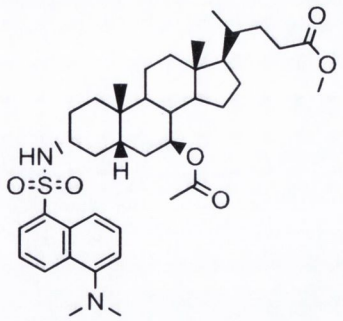

76

Compound **74** (0.3 g) was dissolved in 50% TFA/DCM (20 ml) and stirred for 4 h at rt (followed by TLC analysis using hexane/EtOAc 3:1 as mobile phase) then the solvent was removed *in vacuo* using toluene (2 × 40 ml) to evaporate water. The crude product (0.289 g) was dissolved in anhydrous DCM (10 ml) then the mixture was cooled to -15 °C. The solution of dansyl chloride (0.208 g) and Et_3N (0.21 ml) in DCM (10 ml) was added dropwise to the mixture and stirred overnight at rt then it was poured into brine (50 ml) and extracted with DCM (3 × 40 ml). The dried organic phase (over Na_2SO_4) was evaporated in vacuum and the crude product was purified by flash chromatography using 20% EtOAc in hexane as mobile phase to yield the product as yellow-green foam (0.308 g, 82%). ^{1}H-NMR (400 MHz, $CDCl_3$): δ 8.64 (s, 1H, aromatic-H), 8.35 (d, 1H, J = 8.32 Hz, aromatic-H), 8.30 (d, 1H, J = 7.34 Hz, aromatic-H), 7.60 (m, 2H, aromatic-H), 7.30 (s, 1H, aromatic-H), 4.61 (m, 2H, 7α-H and 3-NH), 3.68 (s, 3H, -O-CH_3), 3.08 (m, 1H, 3β-H), 2.98 (s, 6H, -N(CH_3)$_2$), 1.96 (s, 3H, 7-C=OCH_3), 0.91 (d, 6H, 21-CH_3 and 19-CH_3), 0.65 (s, 3H, 18-CH_3). ^{13}C-NMR ppm (100 MHz, $CDCl_3$): δ 175.14 (C=O, 24-C), 171.01 (C=O, 7-OC=OCH_3), 136.38 (C, aromatic-C), 130.44 (CH, aromatic-C), 130.00 (CH, aromatic-C), 129.85 (CH, aromatic-C), 128.66 (C, aromatic-C), 124.15 (C, aromatic-C), 116.07 (C, aromatic-C), 72.95 (CH, 7-C), 51.96 (CH_3, OCH_3), 22.24 (CH_3, 7-C=OCH_3). IR_{vmax} (KBr): 3441.86, 2947.13, 2870.72, 1733.85, 1250.25, 1161.51, 1145.55, 790.82, 627.75 and 571.00 cm^{-1}. HRMS: Found: $(M-H)^+$ = 681.3932, calculated for $C_{39}H_{57}N_2O_6S$ = 681.3937.

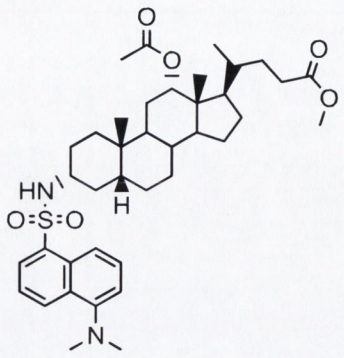

77

Compound **75** (0.150 g) was dissolved in 10% TFA/DCM (20 ml) and stirred overnight at rt (followed by TLC analysis using hexane/EtOAc 3:1 as mobile phase) then the solvent was removed under reduced pressure using toluene (3 × 40 ml) to evaporate water. The crude product was dissolved in anhydrous DCM (10 ml) then the mixture was cooled to -15 °C. The solution of dansyl chloride (0.109 g) and Et_3N (0.14 ml) in DCM (10 ml) was added dropwise to the mixture and stirred for 2 d at rt then it was poured into brine (100 ml) and extracted with DCM (3 × 50 ml). The dried organic phase (over Na_2SO_4) was evaporated in vacuum and the crude product was purified by flash chromatography using 20% EtOAc in hexane as mobile phase to yield the product as light-green foam (0.168 g, 74%). ^{1}H-NMR (400 MHz, $CDCl_3$): δ 8.66 (br s, 1H, aromatic-H), 8.34 (s, 1H, aromatic-H), 8.30 (d, 1H, J = 6.78 Hz, aromatic-H), 7.59 (m, 2H, aromatic-H), 7.29 (s, 1H, aromatic-H), 5.03 (s, 1H, 12β-H), 4.67 (d, 1H, 3-NH), 3.68 (s, 3H, -O-CH_3), 3.08 (m, 1H, 3β-H), 2.99 (s, 6H, -N(CH_3)$_2$), 2.01 (s, 3H, 12-C=OCH_3), 0.82 (d, 6H, 21-CH_3 and 19-CH_3), 0.69 (s, 3H, 18-CH_3). ^{13}C-NMR ppm (100 MHz, $CDCl_3$): δ 175.06 (C=O, 24-C), 170.86 (C=O, 12-OC=OCH_3), 136.40 (C, aromatic-C), 130.51 (CH, aromatic-C), 130.04 (CH, aromatic-C), 129.92 (C, aromatic-C), 128.49 (CH, aromatic-C), 124.10 (CH, aromatic-C), 116.00 (CH, aromatic-C), 76.24 (CH, 12-C), 51.96 (CH_3, OCH_3), 21.73 (CH_3, 12-C=OCH_3). IR_{vmax} (KBr): 3441.97, 2939.73, 2866.74, 1736.22, 1246.60, 1144.62, 790.79, 631.37 and 571.06 cm^{-1}. HRMS: Found: $(M\text{-}Na)^+$ = 703.3748, calculated for $C_{39}H_{56}N_2O_6SNa$ = 703.3757.

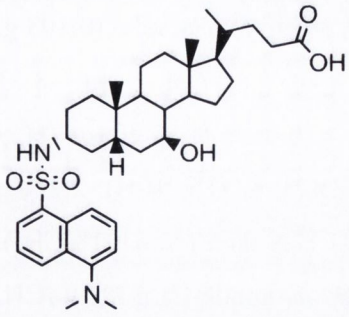

78

Compound **76** (0.274 g) in MeOH (20 ml) was stirred with 2 M NaOH solution (pH~14) at reflux for 5 d. At that point TLC analysis showed the reaction was completion. The mixture was poured into 1 M HCl solution and extracted with EtOAc (3 × 50 ml). The organic layer was washed with water (2 × 100 ml) and brine (100 ml), dried over Na_2SO_4, filtered and the solvent was removed under reduced pressure to give the product as a light yellow solid (0.207 g, 82%). Mp: 101-102 °C (novel compound). ^{1}H-NMR (400 MHz, $CDCl_3$): δ 8.62 (s, 1H, aromatic-H), 8.30 (d, 2H, aromatic-H), 7.59 (t, 2H, aromatic-H), 7.28 (s, 1H, aromatic-H), 5.00 (s, 1H, 3-NH), 3.43 (br. s, 1H, 7α-H), 3.07 (m, 1H, 3β-H), 2.96 (s, 6H, -N(CH_3)$_2$), 0.94 (t, 6H, 21-CH_3 and 19-CH_3), 0.64 (s, 3H, 18-CH_3). ^{13}C-NMR ppm (100 MHz, $CDCl_3$): δ 179.31 (C=O, 24-C), 136.00 (C, aromatic-C), 130.16 (C, aromatic-C), 129.69 (aromatic-C), 129.51 (aromatic-C), 128.25 (aromatic-C), 123.61 (aromatic-C), 71.28 (CH, 7-C). IR_{vmax} (KBr): 3443.11, 2929.76, 2865.67, 1709.10, 1454.60, 1310.26, 1143.98, 789.93, 630.02 and 571.31 cm^{-1}. HRMS: Found: $(M-H)^+$ = 625.3677, calculated for $C_{36}H_{53}N_2O_5S$ = 625.3675.

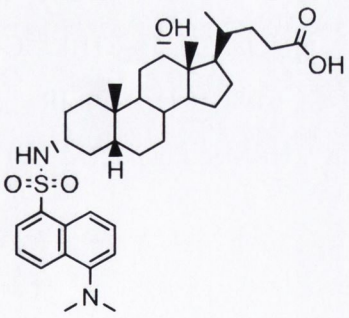

79

Compound **77** (0.135 g) in MeOH (15 ml) was stirred with 2 M NaOH solution (pH~14) at reflux for 4 d. At that point TLC analysis showed that the reaction was complete, the mixture was poured into 2 M HCl solution (50 ml) and extracted with EtOAc (3 × 50 ml). The organic layer was washed with water (2 × 100 ml) and brine (100 ml), dried over Na_2SO_4, filtered and the

solvent was removed under reduced pressure to give the product as a green-yellow solid (0.103 g, 82%). Mp: 101-102 °C (novel compound). ^{1}H-NMR (400 MHz, $CDCl_3$): δ 8.57 (d, 1H, J = 8.53 Hz, aromatic-H), 8.29 (t, 2H, aromatic-H), 7.56 (q, 2H, J = 8.03 Hz, aromatic-H), 7.20 (d, 1H, J = 7.53 Hz, aromatic-H), 5.06 (s, 1H, 3-NH), 3.96 (s, 1H, 12β-H), 3.12 (m, 1H, 3β-H), 2.92 (s, 6H, -N(CH_3)$_2$), 0.98 (d, 3H, J = 6.03 Hz, 21-CH_3), 0.83 (s, 3H, 19-CH_3), 0.65 (s, 3H, 18-CH_3). ^{13}C-NMR ppm (100 MHz, $CDCl_3$): δ 179.56 (C=O, 24-C), 136.22 (C, aromatic-C), 130.19 (CH, aromatic-C), 129.80 (C, aromatic-C), 129.72 (CH, aromatic-C), 129.33 (CH, aromatic-C), 128.30 (C, aromatic-C), 123.44 (CH, aromatic-C), 115.35 (CH, aromatic-C), 73.44 (CH, 12-C). IR_{vmax} (KBr): 3447.17, 2937.74, 2865.69, 1708.91, 1452.64, 1309.32, 1143.45, 790.16, 631.38, 571.91 and 585.12 cm^{-1}. HRMS: Found: $(M-H)^+$ = 625.3683, calculated for $C_{36}H_{53}N_2O_5S$ = 625.3675.

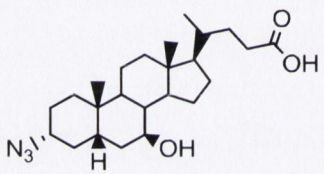

80

To a solution of **73** (0.150 g) in MeOH (15 ml) was added 2 M NaOH solution to pH~14 and stirred at reflux for 1 d, when TLC analysis showed the hydrolysis was complete. Then the reaction mixture was poured into 1 M HCl solution (50 ml) and extracted with EtOAc (3 × 50 ml). The organic layer was washed with water (2 × 100 ml) and brine (100 ml), dried over Na_2SO_4, filtered and the solvent was removed under reduced pressure to give the product as a light yellow solid (0.131 g, 99%).^{1}H-NMR (400 MHz, $CDCl_3$): δ 3.60 (m, 1H, 7α-H), 3.30 (m, 1H, 3β-H), 0.98 (s, 3H, 19-CH_3), 0.96 (d, 3H, J = 6.53 Hz, 21-CH_3), 0.69 (s, 3H, 18-CH_3). ^{13}C-NMR ppm (100 MHz, $CDCl_3$): δ 180.19 (C=O, 24-C), 71.68 (CH, 7-C), 61.30 (CH, 3-C). IR_{vmax} (KBr): 3375.06, 2934.00, 2867.03, 2093.18, 1690.57 and 1255.27 cm^{-1}. HRMS: Found: $(M-Na)^+$ = 440.2896, calculated for $C_{24}H_{39}N_3O_3Na$ = 440.2889.

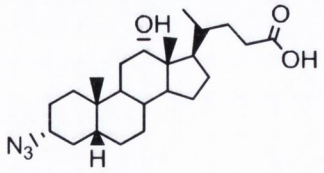

81

To a solution of **72** (0.101 g) in MeOH (10 ml) was added 2 M NaOH solution to pH~14 and stirred at reflux for 10 d, when TLC analysis showed the hydrolysis was complete. Then the reaction mixture was poured into 1 M HCl solution (50 ml) and extracted with EtOAc (3 × 50 ml). The organic layer was washed with water (2 × 100 ml) and brine (100 ml), dried over Na_2SO_4, filtered and the solvent was removed under reduced pressure to give the product as a light-brown solid (0.074 g, 82%). Mp: 88 °C [120]. ^{1}H-NMR (400 MHz, $CDCl_3$): δ 4.01 (s, 1H, 12β-H), 3.35 (m, 1H, 3β-H), 1.01 (d, 3H, J = 6.03 Hz, 21-CH_3), 0.94 (s, 3H, 19-CH_3), 0.70 (s, 3H, 18-CH_3). ^{13}C-NMR ppm (100 MHz, $CDCl_3$): δ 179.80 (C=O, 24-C), 73.29 (CH, 12-C), 61.40 (CH, 3-C). IR_{vmax} (KBr): 3440.00, 2941.49, 2866.14, 2090.46, 1709.85, 1679.00 and 1246.00 cm^{-1}. HRMS: Found: $(M\text{-}Na)^+$ = 440.2878, calculated for $C_{24}H_{39}N_3O_3Na$ = 440.2889.

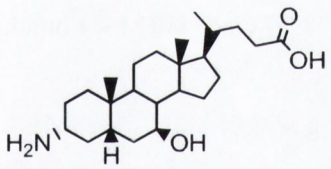

82

Compound **74** (0.200 g) was dissolved in MeOH (15 ml) and treated with 2 M aqueous NaOH at pH~14. The reaction was complete after 12 h, poured into 1 M HCl (50 ml) and extracted with EtOAc (3 × 50 ml). The organic phase was washed with water (2 × 100 ml) and brine (100 ml), dried over Na_2SO_4 and the solvent was removed under reduced pressure. The crude product (0.153 g) was dissolved in 10% TFA/DCM (20 ml) and stirred at rt for 1 d. The solvent was removed under reduced pressure after completing the reaction. Water was removed under reduced pressure as an azeotrope with toluene (2 × 30 ml) then the product was recrystallised from hexane to yield light brown solid (0.176 g). Mp: 190 °C (novel compound). ^{1}H-NMR (400 MHz, CD_3OD): 5.01 (m, 1H, 7α-H), 3.12 (br. s, 1H, 3β-H), 1.08 (s, 3H, 19-CH_3), 0.98 (d, 3H, J = 6.52 Hz, 21-CH_3), 0.76 (s, 3H, 18-CH_3). ^{13}C-NMR ppm (100 MHz, CD_3OD): δ 178.06 (C=O, 24-C), 80.46 (CH, 7-C). IR_{vmax} (KBr): 3427.76, 2955.18, 1779.26, 1677.28 and 1179.31 cm^{-1}. HRMS: Found: $(M\text{-}H)^+$ = 392.3178, calculated for $C_{24}H_{42}NO_3$ = 392.3165.

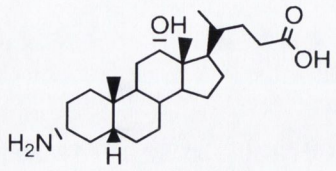

83

Compound **75** (0.150 g) was dissolved in MeOH (15 ml) and treated with 2 M aqueous NaOH at pH~14. The reaction was complete after 2 d, poured into 1 M HCl (50 ml) and extracted with EtOAc (3 × 50 ml). The organic phase was washed with water (2 × 100 ml) and brine (100 ml), dried over Na_2SO_4 and the solvent was removed under reduced pressure. The crude product (0.112 g) was dissolved in 10% TFA/DCM (20 ml) and stirred at rt for 1 d. The solvent was removed under reduced pressure after completing the reaction. Water was removed under reduced pressure as an azeotrope with toluene (2 × 30 ml) then the product was recrystallised from hexane to yield light brown solid (0.116 g). Mp: 215 °C. ^{1}H-NMR (400 MHz, CD_3OD): δ 4.02 (s, 1H, 12β-H), 3.12 (m, 1H, 3β-H), 1.04 (d, 3H, J = 6.52 Hz, 21-CH_3), 1.00 (s, 3H, 19-CH_3), 0.75 (s, 3H, 18-CH_3). ^{13}C-NMR ppm (100 MHz, CD_3OD): δ 177.97 (C=O, 24-C), 73.55 (CH, 12-C). IR_{vmax} (KBr): 3428.31, 2942.23, 2869.65, 1676.69 and 1198.73 cm^{-1}. HRMS: Found: $(M-H)^+$ = 392.3150, calculated for $C_{24}H_{42}NO_3$ = 392.3165.

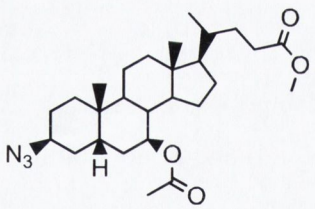

84

Compound **59** (0.705 g) and NaN_3 (0.870 g) in DMPU (20 ml) were stirred at 50 °C for 11 d (TLC hexane : EtOAc 3:1) then poured into water (50 ml) and extracted with EtOAc (3 × 50 ml). The organic phase was washed with brine (100 ml) dried over $MgSO_4$, filtered and the solvent was removed under reduced pressure to give the crude product as yellow oil. This was purified by flash chromatography using 5% then 10% EtOAc in hexane as mobile phase to yield white solid as product (0.537 g, 85%). ^{1}H-NMR (400MHz, $CDCl_3$): δ 4.74 (m, 1H, 7α-H), 3.95 (s, 1H, 3α-H), 3.68 (s, 3H, -O-CH_3), 2.00 (s, 3H, 7-C=OCH_3), 1.01 (s, 3H, 19-CH_3), 0.93 (d, 3H, J = 6.53 Hz, 21-CH_3), 0.69 (s, 3H, 18-CH_3). ^{13}C-NMR ppm (100 MHz, $CDCl_3$): δ 174.52 (C=O, 24-C), 170.52 (C=O, 7-OC=OCH_3), 73.47 (CH, 7-C), 57.94 (CH, 3-C), 51.33 (CH_3, OCH_3), 21.65 (CH_3,

7-C=OCH_3). IR_{vmax} (DCM): 3445.10, 2946.85, 2871.37, 2102.43, 1736.79 and 1248.22 cm^{-1}. HRMS: Found: $(M\text{-}Na)^+$ = 496.3164, calculated for $C_{27}H_{43}N_3O_4Na$ = 496.3151.

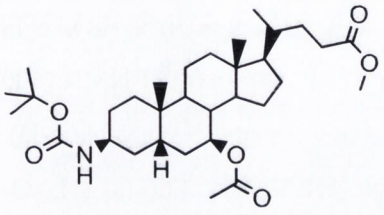

85

The solution of **84** (0.754 g) and Boc_2O (0.417 g) in EtOAc (10 ml) was added to a pre-reduced 10% Pd/C in EtOAc (10 ml) under hydrogen at rt. The reaction mixture was stirred overnight (TLC: hexane/EtOAc 3:1) then it was filtered on a celite pad. The celite was washed with EtOAc (3 × 10 ml) and the organic phase was removed in vacuum. The product was cleaned by flash chromatography (mobile phase: 15% EtOAc in hexanes) to yield a white foam as product (0.672 g, 77%). ^{1}H-NMR (400 MHz, $CDCl_3$): δ 4.75 (m, 2H, 7α-H and 3-NH), 3.88 (br s, 1H, 3α-H), 3.67 (s, 3H, -O-CH_3), 1.99 (s, 3H, 7-C=OCH_3), 1.45 (s, 9H, -$OC(CH_3)_3$), 1.00 (s, 3H, 19-CH_3), 0.93 (d, 3H, J = 6.53 Hz, 21-CH_3), 0.69 (s, 3H, 18-CH_3). ^{13}C-NMR ppm (100 MHz, $CDCl_3$): δ 175.15 (C=O, 24-C), 171.04 (C=O, 7-OC=OCH_3), 74.12 (CH, 7-C), 51.95 (CH_3, OCH_3), 28.85 ($3CH_3$, -$OC(\underline{C}H_3)_3$), 22.28 (CH_3, 7-C=OCH_3). IR_{vmax} (KBr): 3391.26, 2949.62, 2871.50, 1730.05, 1365.69, 1245.20, 1170.09 and 1021.06 cm^{-1}. HRMS: Found: $(M\text{-}Na)^+$ = 570.3760, calculated for $C_{32}H_{53}NO_6Na$ = 570.3771.

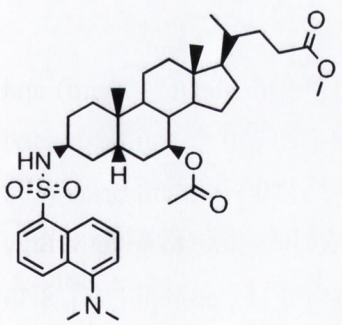

86

Compound **85** (0.327 g) was dissolved in 10% TFA/DCM (20 ml) and stirred at rt overnight (followed by TLC analysis using hexane/EtOAc 3:1 as mobile phase) then the solvent was removed under reduced pressure. The residual water was removed as an azeotrope with toluene (2 × 30 ml) and 0.150 g from the crude product was dissolved in anhydrous DCM (10 ml) then

the mixture was cooled to -15 °C. The solution of dansyl-chloride (0.108 g) and Et_3N (0.14 ml) in DCM (10 ml) was added dropwise to the mixture and stirred overnight at rt then it was poured into brine (50 ml) and extracted with DCM (3 × 40 ml). The dried organic phase (over Na_2SO_4) was evaporated in vacuum and the crude product was flash columned using 20% EtOAc in hexane as mobile phase to yield the product as yellow-green foam (0.140 g, 61%). ^{1}H-NMR (400 MHz, $CDCl_3$): δ 8.61 (s, 1H, aromatic-H), 8.29 (t, 2H, aromatic-H), 7.58 (m, 2H, aromatic-H), 7.24 (s, 1H, aromatic-H), 4.98 (d, 1H, J = 6.02 Hz, 3-NH), 4.55 (m, 1H, 7α-H), 3.66 (s, 3H, -O-CH_3), 3.47 (s, 1H, 3α-H), 2.94 (s, 6H, -N(CH_3)$_2$), 1.94 (s, 3H, 7-C=OCH_3), 0.89 (d, 6H, 21-CH_3 and 19-CH_3), 0.63 (s, 3H, 18-CH_3). ^{13}C-NMR ppm (100 MHz, $CDCl_3$): δ 174.81 (C=O, 24-C), 170.65 (C=O, 7-OC=OCH_3), 129.98 (CH, aromatic-C), 129.68 (CH, aromatic-C), 128.37 (CH, aromatic-C), 73.55 (CH, 7-C), 51.63 (CH_3, OCH_3), 21.89 (CH_3, 7-C=OCH_3). IR_{vmax} (KBr): 3440.62, 2946.79, 2870.23, 1730.24, 1244.69, 1143.06 and 791.11 cm^{-1}. HRMS: Found: $(M-H)^+$ = 681.3929, calculated for $C_{39}H_{57}N_2O_6S$ = 681.3937.

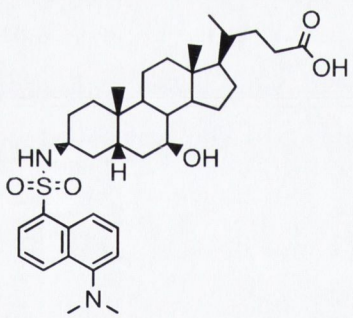

87

Compound **86** (0.116 g) was treated with 2 M aqueous NaOH at pH~14 in MeOH (20 ml) and stirred at reflux. The reaction was complete after 8 d, poured into 1 M HCl (50 ml) and extracted with EtOAc (3 × 50 ml). The organic phase was washed with water (2 × 100 ml) and brine (100 ml), dried over Na_2SO_4 and the solvent was removed under reduced pressure to give yellow solids as product (0.096 g, 90%). ^{1}H-NMR (400 MHz, $CDCl_3$): δ 8.64 (s, 1H, aromatic-H), 8.36 (s, 1H, aromatic-H), 8.30 (d, 1H, J = 7.03 Hz, aromatic-H), 7.58 (m, 2H, aromatic-H), 7.28 (s, 1H, aromatic-H), 5.16 (d, 1H, 3-NH), 3.51 (s, 1H, 3α-H), 3.35 (m, 1H, 7α-H), 2.97 (s, 6H, -N(CH_3)$_2$), 0.91 (d, 3H, J = 6.52 Hz, 21-CH_3), 0.84 (s, 3H, 19-CH_3), 0.63 (s, 3H, 18-CH_3). ^{13}C-NMR ppm (100 MHz, $CDCl_3$): 179.37 (C=O, 24-C), 129.89 (CH, aromatic-C), 129.72 (CH,

aromatic-C), 128.31 (CH, aromatic-C), 115.56 (CH, aromatic-C), 71.23 (CH, 7-C). IR_{vmax} (KBr): 3448.51, 2934.80, 2867.25, 1709.69, 1141.98 and 790.59 cm^{-1}. HRMS: Found: $(M-H)^+$ = 625.3655, calculated for $C_{36}H_{53}N_2O_5S$ = 625.3675.

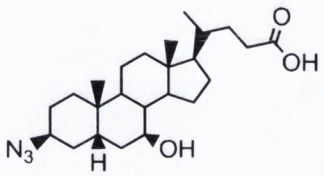

88

To a solution of **84** (0.150 g) in MeOH (15 ml) was added 2 M NaOH solution to pH~14 and stirred at reflux for 1 d, when TLC analysis showed the hydrolysis was complete. Then the reaction mixture was poured into 1 M HCl solution (50 ml) and extracted with EtOAc (3 × 50 ml). The organic layer was washed with water (2 × 100 ml) and brine (100 ml), dried over Na_2SO_4, filtered and the solvent was removed under reduced pressure to give the product as a white solid (0.129 g, 97%). ^{1}H-NMR (400 MHz, $CDCl_3$): δ 3.93 (s, 1H, 3α-H), 3.55 (m, 1H, 7α-H), 1.00 (s, 3H, 19-CH_3), 0.96 (d, 3H, J = 6.02 Hz, 21-CH_3), 0.70 (s, 3H, 18-CH_3). ^{13}C-NMR ppm (100 MHz, $CDCl_3$): 179.81 (C=O, 24-C), 71.54 (CH, 7-C), 58.42 (CH, 3-C). IR_{vmax} (KBr): 3330.87, 2929.30, 2867.30, 2103.92, 1687.49 and 1243.05 cm^{-1}. HRMS: Found: $(M)^-$ = 416.2913, calculated for $C_{24}H_{38}N_3O_3$ = 416.2913.

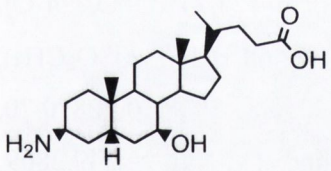

89

Compound **85** (0.150 g) was dissolved in MeOH (15 ml) and treated with 2 M aqueous NaOH at pH~14. The reaction was complete after 2 d, poured into 1 M HCl (50 ml) and extracted with EtOAc (3 × 50 ml). The organic phase was washed with water (2 × 100 ml) and brine (100 ml), dried over Na_2SO_4 and the solvent was removed under reduced pressure. The crude product (0.140 g) was dissolved in 10% TFA/DCM (20 ml) and stirred at rt overnight. The solvent was removed under reduced pressure after completing the reaction. Water was removed under reduced pressure as an azeotrope with toluene (2 × 30 ml) to yield light brown solid (0.108 g, 98%). Mp: 128 °C (novel compound). ^{1}H-NMR (400 MHz, MeOD): δ 5.02 (s, 1H, 7α-H), 3.48

(br s, 3H, NH_2 and 3α-H), 1.06 (s, 3H, 19-CH_3), 0.98 (d, 3H, J = 6.52 Hz, 21-CH_3), 0.74 (s, 3H, 18-CH_3). ^{13}C-NMR ppm (100 MHz, MeOD): δ 176.28 (C=O, 24-C), 78.62 (CH, 7-C). IR_{vmax} (KBr): 3427.48, 2950.53, 1778.22, 1675.52, 1203.55 and 1176.30cm^{-1}. HRMS: Found: $(M-H)^+$ = 392.3158, calculated for $C_{24}H_{42}NO_3$ = 392.3165.

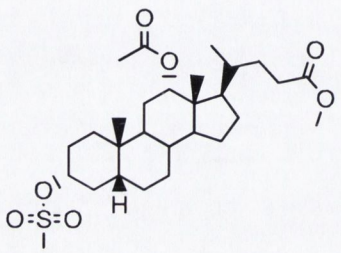

90

To a solution of **69** (0.485 g) and Et_3N (0.17 ml) in anhydrous DCM (15 ml) was added methane sulfonyl chloride (0.13 ml in 10 ml anhydrous DCM) dropwise at 0 °C and stirred for 20 min, after which time TLC analysis showed the reaction was complete. Then cooled water (40 ml) was added to the mixture, it was separated and the aqueous phase was extracted with DCM (3 × 40 ml). The organic phase was washed with brine (100 ml), dried over $MgSO_4$, filtered and the solvent was removed under reduced pressure to give colourless oil as product (0.554 g, 97%). ^{1}H-NMR (400 MHz, $CDCl_3$): δ 5.09 (s, 1H, 12β-H), 4.62 (m, 1H, 3β-H), 3.68 (s, 3H, -O-CH_3), 3.02 (s, 3H, -OSO_2CH_3), 2.12 (s, 3H, 12-C=OCH_3), 0.92 (s, 3H, 19-CH_3), 0.82 (d, 3H, J = 6.52 Hz, 21-CH_3), 0.73 (s, 3H, 18-CH_3). ^{13}C-NMR ppm (100 MHz, $CDCl_3$): δ 174.74 (C=O, 24-C), 170.68 (C=O, 12-OC=OCH_3), 83.00 (CH, 3-C), 75.89 (CH, 12-C), 52.68 (CH_3, -OSO_2CH_3), 51.66 (CH_3, OCH_3), 21.53 (CH_3, 12-C=OCH_3). IR_{vmax} (DCM): 3435.88, 3948.10, 2870.70, 1733.40, 1644.45, 1373.33, 1248.52 and 1174.20 cm^{-1}. HRMS: Found: $(M-Na)^+$ = 549.2869, calculated for $C_{28}H_{46}O_7SNa$ = 549.2862.

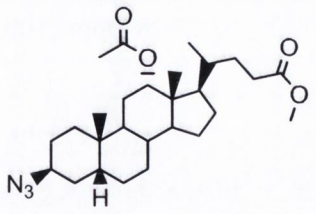

91

Compound **90** (0.554 g) and NaN_3 (1.026 g) in DMSO (20 ml) were stirred at 50 °C for 15 d (TLC hexane : EtOAc 3:1) then poured into water (100 ml) and extracted with EtOAc (3 × 50 ml). The organic phase was washed with brine (100 ml) dried over $MgSO_4$, filtered and the solvent was removed under reduced pressure to give the crude product as yellow oil. This was purified by column chromatography using 5% then 10% EtOAc in hexane as mobile phase to yield light-yellow oil as product (0.356 g, 72%). ^{1}H-NMR (400 MHz, $CDCl_3$): δ 5.10 (s, 1H, 12β-H), 3.96 (s, 1H, 3α-H), 3.67 (s, 3H, -O-CH_3), 2.09 (s, 3H, 12-C=OCH_3), 0.94 (s, 3H, 19-CH_3), 0.82 (d, 3H, J = 6.52 Hz, 21-CH_3), 0.74 (s, 3H, 18-CH_3). ^{13}C-NMR ppm (100 MHz, $CDCl_3$): δ 175.08 (C=O, 24-C), 170.85 (C=O, 12-OC=OCH_3), 76.41 (CH, 12-C), 59.01 (CH, 3-C), 51.98 (CH_3, OCH_3), 21.78 (CH_3, 12-C=OCH_3). IR_{vmax} (DCM): 3447.97, 2938.74, 2872.81, 2102.14, 1737.52 and 1245.87 cm^{-1}. HRMS: Found: $(M\text{-}Na)^+$ = 496.3139, calculated for $C_{27}H_{43}N_3O_4Na$ = 496.3151.

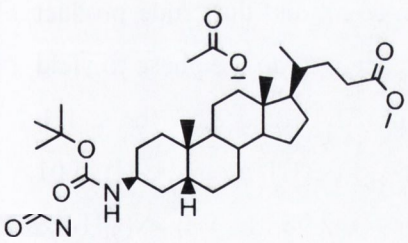

92

The solution of **91** (0.309 g) and Boc_2O (0.171 g) in EtOAc (10 ml) was added to a pre-reduced 10% Pd/C (~50 mg) in EtOAc (10 ml) under hydrogen at rt. The reaction mixture was stirred overnight (TLC: hexane/EtOAc 3:1) then it was filtered on a celite pad. The celite was washed with EtOAc (3 × 10 ml) and the organic phase was removed in vacuum. The product was cleaned by flash chromatography (mobile phase: 15% EtOAc in hexane) to yield a white foam as product (0.314 g, 88%). ^{1}H-NMR (400 MHz, $CDCl_3$): δ 5.09 (s, 1H, 12β-H), 4.85 (br s, 1H, 3-NH), 3.90 (br s, 1H, 3α-H), 3.67 (s, 3H, -O-CH_3), 2.09 (s, 3H, 12-C=OCH_3), 1.46 (s, 9H, -OC(CH_3)$_3$), 0.94

(s, 3H, 19-CH_3), 0.82 (d, 3H, J = 6.52 Hz, 21-CH_3), 0.74 (s, 3H, 18-CH_3). ^{13}C-NMR ppm (100 MHz, $CDCl_3$): δ 175.08 (C=O, 24-C), 170.95 (C=O, 12-OC=OCH_3), 76.34 (CH, 12-C), 51.97 (CH_3, OCH_3), 28.90 (3CH_3, -OC(CH_3)$_3$), 21.78 (CH_3, 12-C=OCH_3). IR_{vmax} (KBr): 3400.49, 2934.05, 2869.02, 1738.63, 1713.61, 1245.37, 1171.24 and 1021.99 cm^{-1}. HRMS: Found: $(M-Na)^+$ = 570.3763, calculated for $C_{32}H_{53}NO_6Na$ = 570.3771.

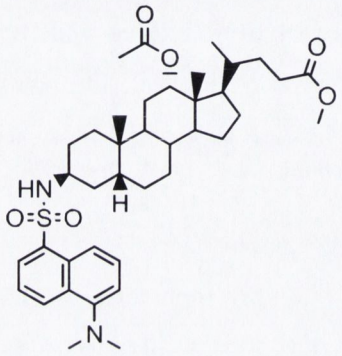

93

Compound **92** (0.281 g) was dissolved in 10% TFA/DCM (20 ml) and stirred at rt overnight (followed by TLC analysis using hexane/EtOAc 3:1 as mobile phase) then the solvent was removed in vacuum using toluene (2 × 40 ml) to evaporate water. 0.200 g from the crude product was dissolved in anhydrous DCM (20 ml) then the mixture was cooled to -15 °C. The solution of dansyl-chloride (0.145 g) and Et_3N (0.19 ml) in DCM (10 ml) was added dropwise to the mixture and stirred overnight at rt then it was poured into brine (100 ml) and extracted with DCM (3 × 50 ml). The dried organic phase (over Na_2SO_4) was evaporated in vacuum and the crude product was purified by column chromatography using 0–15% EtOAc in hexane as mobile phase to yield the product as orange foam (0.139 g, 64%). ^{1}H-NMR (400 MHz, $CDCl_3$): δ 8.63 (br s, 1H, aromatic-H), 8.30 (m, 2H, aromatic-H), 7.60 (t, 2H, aromatic-H), 7.28 (s, 1H, aromatic-H), 5.01 (d, 2H, 12β-H and 3-NH), 3.66 (s, 3H, -O-CH_3), 3.54 (m, 1H, 3α-H), 2.96 (m, 6H, -N(CH_3)$_2$), 2.01 (s, 3H, 12-C=OCH_3), 0.80 (s, 3H, 19-CH_3), 0.78 (d, 3H, *J* = 6.03 Hz, 21-CH_3), 0.68 (s, 3H, 18-CH_3). ^{13}C-NMR ppm (100 MHz, $CDCl_3$): δ 174.73 (C=O, 24-C), 170.49 (C=O, 12-OC=OCH_3), 135.67 (C, aromatic-C), 130.26 (CH, aromatic-C), 129.88 (CH, aromatic-C), 129.72 (CH, aromatic-C), 128.32 (CH, aromatic-C), 123.65 (C, aromatic-C), 115.48 (C, aromatic-C), 75.95 (CH, 12-C), 51.64 (CH_3, OCH_3), 21.38 (CH_3, 12-C=OCH_3). IR_{vmax} (KBr): 3441.72, 2929.04, 2868.87, 1736.68, 1246.69, 1143.49 and 790.74 cm^{-1}. HRMS: Found: $(M-H)^+$ = 681.3937, calculated for $C_{39}H_{57}N_2O_6S$ = 681.3937.

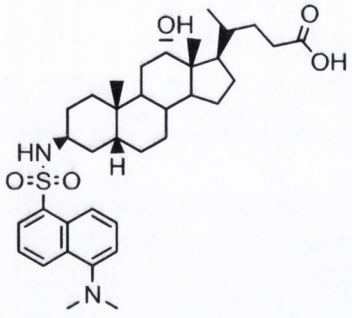

94

Compound **93** (0.111 g) was treated with 2 M aqueous NaOH at pH~14 in MeOH (15 ml) and stirred at reflux. The reaction was complete after 15 d, poured into 1 M HCl (50 ml) and extracted with EtOAc (3 × 50 ml). The organic phase was washed with water (2 × 100 ml) and brine (100 ml), dried over Na_2SO_4 and the solvent was removed under reduced pressure to give yellow solids as product (0.099 g, 96%). Mp: 110 °C (novel compound). ^{1}H-NMR (400 MHz, $CDCl_3$): δ 8.68 (br s, 1H, aromatic-H), 8.41 (br s, 1H, aromatic-H), 8.30 (d, 1H, J = 7.02 Hz, aromatic-H), 7.60 (t, 2H, aromatic-H), 7.28 (s, 1H, aromatic-H), 5.13 (s, 1H, 3-NH), 3.93 (s, 1H, 12β-H), 3.54 (s, 1H, 3α-H), 3.01 (m, 6H, -N(CH_3)$_2$), 0.95 (d, 3H, J = 6.03 Hz, 21-CH_3), 0.82 (s, 3H, 19-CH_3), 0.63 (s, 3H, 18-CH_3). ^{13}C-NMR ppm (100 MHz, $CDCl_3$): δ 179.33 (C=O, 24-C), 129.95 (CH, aromatic-C), 129.75 (C, aromatic-C), 128.15 (CH, aromatic-C), 73.23 (CH, 12-C). IR_{vmax} (KBr): 3439.05, 2929.49, 2865.96, 1710.30, 1141.83, 790.51, 624.98 and 570.94 cm^{-1}. HRMS: Found: $(M-H)^+$ = 625.3668, calculated for $C_{36}H_{53}N_2O_5S$ = 625.3675.

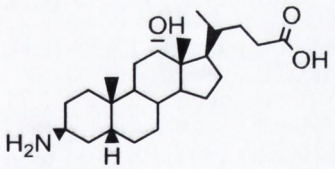

95

Compound **92** (0.95 g) was dissolved in MeOH (15 ml) and treated with 2 M aqueous NaOH at pH~14. The reaction was complete after 11 d, poured into 1 M HCl (50 ml) and extracted with EtOAc (3 × 50 ml). The organic phase was washed with water (2 × 100 ml) and brine (100 ml), dried over Na_2SO_4 and the solvent was removed under reduced pressure. The crude product was dissolved in 10% TFA/DCM (20 ml) and stirred at rt for overnight. The solvent was removed under reduced pressure after completing the reaction. Water was removed under reduced pressure as an azeotrope with toluene (2 × 30 ml) to yield light brown solid (0.088 g). ^{1}H-NMR (400

MHz, MeOD): δ 4.00 (s, 1H, 12β-H), 3.49 (br s, 3H, NH_2 and 3α-H), 1.03 (s, 3H, 19-CH_3), 0.86 (d, 3H, J = 6.44 Hz, 21-CH_3), 0.74 (s, 3H, 18-CH_3). ^{13}C-NMR ppm (100 MHz, MeOD): δ 175.95 (C=O, 24-C), 72.03 (CH, 12-C). IR_{vmax} (KBr): 3434.78, 2945.98, 1780.51, 1679.59 and 1171.29 cm^{-1}. HRMS: Found: $(M-H)^+$ = 392.3162, calculated for $C_{24}H_{42}NO_3$ = 392.3165.

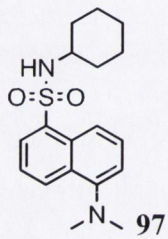

97

To a solution of cyclohexylamine (0.12 ml) and Et_3N (0.42 ml) in anhydrous DCM (10 ml) was added DNSC (0.300 g in 10 ml anh. DCM) dropwise at -15 °C and stirred at rt overnight. Reaction completion was monitored by TLC using hexane : EtOAc (3 : 1) as mobile phase, then the mixture was poured into 0.5 M HCl solution (100 ml) and extracted with EtOAc (3 × 50 ml). The organic phase was dried over Na_2SO_4, filtered and the solvent was removed under reduced pressure. The crude product was purified by column chromatography (2×) using hexane : EtOAc (3 :1) as mobile phase to obtain the product as light green foam (0.318 g, 95%). ^{1}H-NMR (400 MHz, $CDCl_3$): δ 8.58 (d, 1H, J = 8.03 Hz, aromatic-H), 8.31 (d, 2H, J = 7.53 Hz, aromatic-H), 7.57 (m, 2H, aromatic-H), 4.72 (d, 1H, J = 7.53 Hz, aromatic-H) 3.13 (s, 1H, cyclohexyl), 2.92 (s, 6H, $N(CH_3)_2$), 1.66-1.04 (m, 10H, cyclohexyl). ^{13}C-NMR ppm (100 MHz, $CDCl_3$): δ 136.11 (C, aromatic), 130.31 (CH, aromatic), 129.89 (C, aromatic), 129.70 (C, aromatic), 129.43 (CH, aromatic), 128.31 (CH, aromatic), 123.42 (CH, aromatic), 119.06 (C, aromatic), 115.25 (CH, aromatic), 52.94 (CH, cyclohexyl), 34.00 (CH_2, cyclohexyl), 25.21 (CH_2, cyclohexyl), 24.71 (CH_2, cyclohexyl). IR_{vmax} (KBr): 3291.68, 2933.45, 2854.36, 1575.12, 1452.76, 1318.86, 1141.83, 1072.92, 789.59, 628.24 and 580.32 cm^{-1}. HRMS: Found: $(M-H)^+$ = 333.1626, calculated for $C_{18}H_{25}N_2O_2S$ = 333.1637.

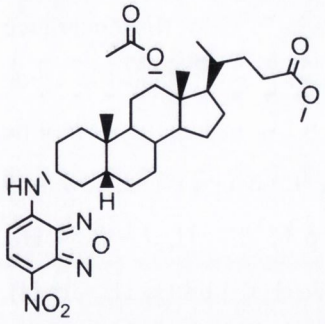

98

$NaHCO_3$ (0.070 g) and NBD-Cl (0.123 g) were added to a solution of deprotected **75** (0.250 g) in THF/EtOH 1:1 (20 ml) and stirred at 70 °C for 4 d. The completion of reaction was followed by TLC analysis using hexane/EtOAc 3:1 as mobile phase. Then the solvent was removed under reduced pressure and the crude product was purified on flash column using 20-40% EtOAc in hexane as mobile phase to give orange foam as product (0.260 g, 76%). Mp: 226 °C (novel compound). ^{1}H-NMR (400 MHz, $CDCl_3$): δ 8.51 (d, 1H, J = 7.83 Hz, aromatic-H), 6.21 (d, 2H, J = 8.81 Hz, aromatic-H and 3-NH), 5.12 (s, 1H, 12β-H), 3.68 (s, 4H, 3β-H, -O-CH_3), 2.13 (s, 3H, 12-OC=OCH_3), 1.01 (s, 3H, 19-CH_3), 0.83 (d, 3H, J = 5.87 Hz, 21-CH_3), 0.76 (s, 3H, 18-CH_3). ^{13}C-NMR ppm (100 MHz, $CDCl_3$): δ 174.74 (C=O, 24-C), 170.62 (C=O, 12-O<u>C</u>=OCH_3), 144.50 (C, aromatic-C), 144.12 (C, aromatic-C), 142.92 (C, aromatic-C), 136.70 (CH, aromatic-C), 123.78 (C, aromatic-C), 98.76 (CH, aromatic-C), 75.94 (CH, 12-C), 51.68 (CH_3, OCH_3), 21.59 (CH_3, 12-OC=O<u>C</u>H_3). IR_{vmax} (KBr): 3317.64, 2929.68, 2867.43, 1736.51, 1579.27, 1307.06 and 1254.54 cm^{-1}. HRMS: Found: $(M\text{-}Na)^+$ = 633.3276, calculated for $C_{33}H_{46}N_4O_7Na$ = 633.3264.

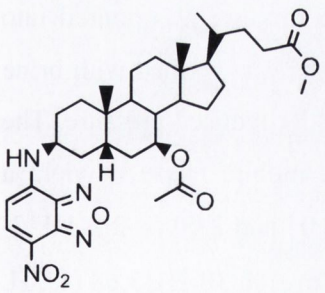

100

Compound **85** (0.327 g) was dissolved in 10% TFA/DCM (20 ml) and stirred at rt overnight (followed by TLC analysis using hexane/EtOAc 3:1 as mobile phase) then the solvent was removed in vacuum using toluene (2 × 40 ml) to evaporate water. 0.176 g from the crude product was dissolved in THF/EtOH 1:1 (20 ml) and NBD chloride (0.086 g) and $NaHCO_3$ ($NaHCO_3$)

(0.049 g) were added and stirred at 70 °C. The reaction was monitored via TLC for disappearance of the free amine. After 11 d the solvent was evaporated under reduced pressure and the crude product was purified twice on flash column using 25% then 20% of EtOAc in hexane as mobile phase to afford the product as orange solid (0.129 g, 54%). ^{1}H-NMR (400 MHz, $CDCl_3$): δ 8.49 (d, 1H, J = 8.53 Hz, aromatic-H), 6.35 (d, 1H, J = 7.03 Hz, 3-NH), 6.17 (d, 1H, J = 8.54 Hz, aromatic-H), 4.76 (sex, 1H, J_1 = 5.27 Hz, J_2 = 5.77 Hz, J_3 = 4.77 Hz, 7α-H), 4.08 (s, 1H, 3α-H), 3.66 (s, 3H, -O-CH_3), 1.99 (s, 3H, 7-OC=OCH_3), 1.07 (s, 3H, 19-CH_3), 0.92 (d, 3H, J = 6.28 Hz, 21-CH_3), 0.69 (s, 3H, 18-CH_3). ^{13}C-NMR ppm (100 MHz, $CDCl_3$): δ 174.79 (C=O, 24-C), 170.86 (C=O, 7-O<u>C</u>=OCH_3), 144.60 (C, aromatic-C), 144.06 (C, aromatic-C), 142.079 (C, aromatic-C), 136.58 (CH, aromatic-C), 124.17 (C, aromatic-C), 99.11 (CH, aromatic-C), 73.42 (CH, 7-C) 51.65 (CH_3, OCH_3), 21.92 (CH_3, 7-OC=O<u>C</u>H_3). IR_{vmax} (KBr): 3416.48, 2947.90, 2870.89, 1728.40, 1573.47, 1307.46 and 1246.87 cm^{-1}. HRMS: Found: $(M-Na)^+$ = 633.3258, calculated for $C_{33}H_{46}N_4O_7Na$ = 633.3264.

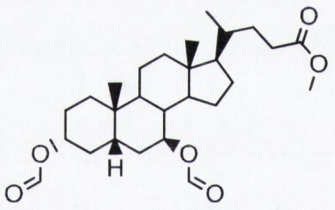

102

To a stirred solution of **54** (1.867 g, 4.591 mmol) in formic acid (10 ml) was added 3 drops of perchloric acid at 40 °C and the reaction was heated to 60 °C for 20 min, after which time TLC analysis showed reaction to be complete (Hexane/EtOAc 3 : 1). The mixture was poured into water (75 ml) and extracted with EtOAc (3 × 50 ml). The organic phase was washed with brine (100 ml), dried over $MgSO_4$, filtered and the solvent was removed under reduced pressure. The product was purified on silica gel using 20% EtOAc in hexane as mobile phase to yield a colourless semi-solid (1.87 g, 88%). ^{1}H-NMR (400 MHz, $CDCl_3$): δ 8.04 and 8.00 (s, 2 x 1H, 3- and 7-OC=O<u>H</u>), 4.91 (sex, 1H, J_1 = 5.27 Hz, J_2 = 5.52 Hz7α-H), 4.83 (m, 1H, 3β-H), 3.68 (s, 3H, -O-CH_3), 1.01 (s, 3H, 19-CH_3), 0.97 (d, 3H, J = 6.27 Hz, 21-CH_3), 0.70 (s, 3H, 18-CH_3). ^{13}C-NMR ppm (100 MHz, $CDCl_3$): δ 174.80 (C=O, 24-C), 161.14 and 160.76 (2C=O, 3-O<u>C</u>=OH and 7-O<u>C</u>=OH), 73.74 and 73.52 (2CH, 3-C and 7-C), 51.64 (CH_3, O<u>C</u>H_3). IR_{vmax} (KBr): 3436.73,

2950.85, 2873.88, 1721.86 and 1181.66 cm^{-1}. HRMS: Found: $(M-Na)^+$ = 485.2892, calculated for $C_{27}H_{42}O_6Na$ = 485.2879.

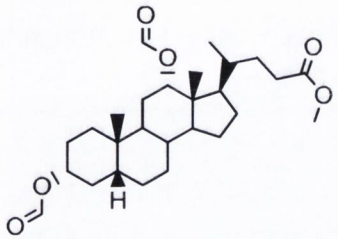

103

To a stirred solution of **67** (2.01 g, 4.943 mmol) in formic acid (15 ml) was added 3 drops of perchloric acid at 40 °C and the reaction was heated to 60 °C for 20 min, after which time TLC analysis showed reaction to be complete (Hexane/EtOAc 3 : 1). The mixture was poured into water (75 ml) and extracted with EtOAc (3 × 50 ml). The organic phase was washed with brine (100 ml), dried over $MgSO_4$, filtered and the solvent was removed under reduced pressure. The product was purified on silica gel using 25% EtOAc in hexanes as mobile phase to yield a white foam (1.959 g, 86%). ^{1}H-NMR (400 MHz, $CDCl_3$): δ 8.15 (s, 1H, 12-OC=OH), 8.04 (s, 1H, 3-OC=OH), 5.26 (s, 1H, 12β-H), 4.85 (m, 1H, 3β-H), 3.67 (s, 3H, -O-CH_3), 0.94 (s, 3H, 19-CH_3), 0.85 (d, 3H, J = 6.84 Hz, 21-CH_3), 0.75 (s, 3H, 18-CH_3). ^{13}C-NMR ppm (100 MHz, $CDCl_3$): δ 174.39 (C=O, 24-C), 160.50 and 160.39 (2C=O, 3-C=OCH_3 and 12-C=OCH_3), 75.80 (CH, 12-C), 73.91 (CH, 3-C), 51.34 (CH_3, OCH_3). IR_{vmax} (KBr): 3431.01, 2949.54, 2870.45, 1721.42 and 1176.03 cm^{-1}. HRMS: Found: $(M-Na)^+$ = 485.2881, calculated for $C_{27}H_{42}O_6Na$ = 485.2879.

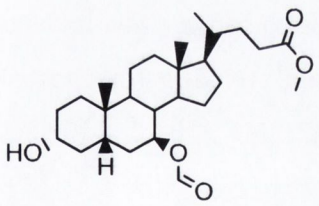

104

To a solution of **102** (3.93 g, 8.491 mmol) in MeOH (100 ml) was added 2 equivalents $NaHCO_3$ (1.427 g, 16.983 mmol) in three parts at 0 °C and allowed to warm to rt. After 2.5 h, when TLC analysis showed no more starting material present, the mixture was poured into water (200 ml) and extracted with EtOAc (3 × 100 ml). The organic phase was washed with brine (200 ml), dried over $MgSO_4$, filtered and the solvent was removed under reduced pressure to give the product as white foam (3.48 g, 94%). ^{1}H-NMR (400 MHz, $CDCl_3$): δ 8.00 (s, 1H, 7-OC=OH), 4.91 (sex,

1H, J_1 = 5.02 Hz, J_2 = 5.52 Hz, 7α-H), 3.68 (s, 3H, -O-CH_3), 3.60 (m, 1H, 3β-H), 0.98 (s, 3H, 19-CH_3), 0.93 (d, 3H, J = 6.53 Hz, 21-CH_3), 0.69 (s, 3H, 18-CH_3). ^{13}C-NMR ppm (100 MHz, $CDCl_3$): δ 174.84 (C=O, 24-C), 161.20 (C=O, 7-O<u>C</u>=OH), 74.09 (CH, 7-C), 71.38 (CH, 3-C), 51.65 (CH_3, O<u>C</u>H_3). IR_{vmax} (DCM): 3420.26, 2935.92, 2870.91, 1721.55 and 1187.93 cm^{-1}. HRMS: Found: $(M\text{-}Na)^+$ = 457.2942, calculated for $C_{26}H_{42}O_5Na$ = 457.2930.

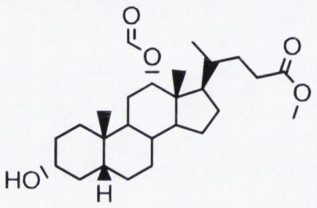

105

To a solution of **103** (0.887 g, 1.918 mmol) in MeOH (50 ml) was added 2 equivalents $NaHCO_3$ (0.322 g, 3.835 mmol) in three parts at 0 °C and allowed to warm to rt. After 1.5 h, when TLC analysis showed no more starting material present, the mixture was poured into water (150 ml) and extracted with EtOAc (3 × 75 ml). The organic phase was washed with brine (100 ml), dried over $MgSO_4$, filtered and the solvent was removed under reduced pressure to give the product as white foam (0.814 g, 98%). ^{1}H-NMR (400 MHz, $CDCl_3$): δ 8.13 (s, 1H, 12-OC=OH), 5.25 (s, 1H, 12β-H), 3.67 (s, 3H, -O-CH_3), 3.64 (m, 1H, 3β-H), 0.92 (s, 3H, 19-CH_3), 0.85 (d, 3H, J = 6.03 Hz, 21-CH_3), 0.75 (s, 3H, 18-CH_3). ^{13}C-NMR ppm (100 MHz, $CDCl_3$): δ 174.75 (C=O, 24-C), 160.80 (C=O, 12-<u>C</u>=OCH_3), 76.14 (CH, 12-C), 71.79 (CH, 3-C), 51.66 (CH_3, O<u>C</u>H_3). IR_{vmax} (KBr): 3436.90, 2937.01, 2865.77, 1720.95 and 1179.34 cm^{-1}. HRMS: Found: $(M\text{-}Na)^+$ = 457.2910, calculated for $C_{26}H_{42}O_5Na$ = 457.2930.

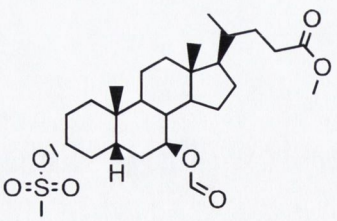

106

The solution of Et_3N (0.1 ml) and methane sulfonyl chloride (0.08 ml) in anhydrous DCM (5 ml) was added dropwise to the stirred solution of **104** (0.286 g) in anhydrous DCM (20 ml) at 0 °C and allowed to warm to rt. After 20 min when TLC analysis showed the reaction was complete the mixture was poured into water (100 ml) and extracted with DCM (3 × 50 ml). The organic

phase was dried over $MgSO_4$ then removed under reduced pressure to give the product as colourless semi-solid (0.330 g, 98%). ^{1}H-NMR (400 MHz, $CDCl_3$): δ 7.99 (s, 1H, 7-OC=O<u>H</u>), 4.91 (sex, 1H, J_1 = 5.02 Hz, J_2 = 5.52, Hz, 7α-H), 4.62 (m, 1H, 3β-H), 3.68 (s, 3H, -O-CH_3), 3.02 (s, 3H, -OSO_2CH_3), 1.00 (s, 3H, 19-CH_3), 0.94 (d, 3H, J = 6.02 Hz, 21-CH_3), 0.69 (s, 3H, 18-CH_3). ^{13}C-NMR ppm (100 MHz, $CDCl_3$): δ 175.12 (C=O, 24-C), 161.41 (C=O, 7-O<u>C</u>=OH), 81.89 (CH, 3-C), 73.83 (CH, 7-C), 53.00 (CH_3, OSO_2CH_3), 51.97 (CH_3, O<u>C</u>H_3). IR_{vmax} (KBr): 3438.55, 2952.63, 2874.54, 1718.71, 1354.77, 1174.23, 929.55 and 527.59 cm^{-1}. HRMS: Found: $(M\text{-}K)^+$ = 551.2451, calculated for $C_{27}H_{47}O_7SK$ = 551.2445.

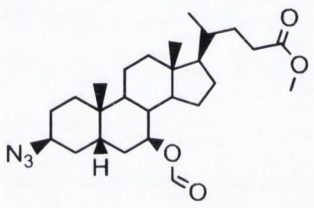

107

NaN_3 (0.387 g) was added to the stirred solution of **106** (0.306 g) in DMPU (15 ml) at 50 °C and the reaction was monitored via TLC (Hexane/EtOAc 5:1). After 8 d the mixture was partitioned between water and EtOAc. The organic phase was retrieved and dried over Na_2SO_4. The crude product was purified by column chromatography using 15% EtOAc in hexane as mobile phase to yield white solid as product (0.211 g, 77%). ^{1}H-NMR (400 MHz, $CDCl_3$): δ 8.00 (s, 1H, 7-OC=O<u>H</u>), 4.89 (m, 1H, 7α-H), 3.96 (m, 1H, 3α-H), 3.68 (s, 3H, -O-CH_3), 1.02 (s, 3H, 19-CH_3), 0.94 (d, 3H, J = 6.53 Hz, 21-CH_3), 0.70 (s, 3H, 18-CH_3). ^{13}C-NMR ppm (100 MHz, $CDCl_3$): δ 174.50 (C=O, 24-C), 160.90 (C=O, 7-O<u>C</u>=OH), 73.56 (CH, 7-C), 57.87 (CH, 3-C), 51.34 (CH_3, O<u>C</u>H_3). IR_{vmax} (KBr): 3422.62, 2946.08, 2884.65, 2111.22, 1737.16 and 1188.73 cm^{-1}. HRMS: Found: $(M\text{-}Na)^+$ = 482.3002, calculated for $C_{26}H_{41}N_3O_4Na$ = 482.2995.

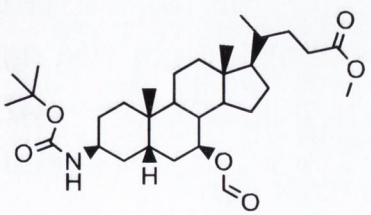

108

To a pre-reduced 10% Pd/C (~50 mg) in EtOAc (10 ml) was added the solution of **107** (0.178 g) and Boc_2O (0.101 g) in EtOAc (10 ml) under H_2 at rt and stirred overnight, then the Pd/C was

filtered out on a celite pad and the solvent was removed under reduced pressure. The yield colourless oil was purified on a flash column using 20-25% EtOAc in hexane as mobile phase to afford white foam as product (0.171 g, 83%). ^{1}H-NMR (400 MHz, $CDCl_3$): δ 7.99 (s, 1H, 7-OC=O<u>H</u>), 4.89 (m, 1H, 7α-H), 4.77 (br s, 1H, 3-NH), 3.89 (br s, 1H, 3α-H), 3.67 (s, 3H, -O-CH_3), 1.46 (s, 9H, -OC(CH_3)$_3$), 1.01 (s, 3H, 19-CH_3), 0.93 (d, 3H, *J* = 6.02 Hz, 21-CH_3), 0.69 (s, 3H, 18-CH_3). ^{13}C-NMR ppm (100 MHz, $CDCl_3$): 175.15 (C=O, 24-C), 161.48 (C=O, 7-OC=OH), 74.29 (CH, 7-C), 51.97 (CH_3, OCH_3), 28.89 ($3CH_3$, -OC(<u>C</u>H_3)$_3$). IR_{vmax} (KBr): 3402.77, 2948.72, 2872.00, 1719.75 and 1171.86 cm^{-1}. HRMS: Found: $(M\text{-}Na)^+$ = 556.3632, calculated for $C_{31}H_{51}NO_6Na$ = 556.3614.

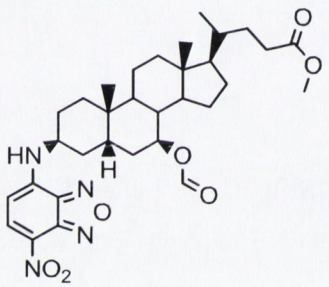

109

Compound **108** (0.170 g) was stirred in 10% TFA/DCM (20 ml) at rt until there was no Boc-protected compound present (monitored by TLC), then the solvent was removed and the residue dried under reduced pressure to give light brown solid as crude product. This was dissolved in THF/EtOH 1:1 (20 ml) then $NaHCO_3$ (0.053 g) and NBD chloride (0.092 g) were added to the solution and stirred at 70 °C for 5 d (monitored by TLC using hexane/EtOAc 1:1 as mobile phase). After this time the solvent was removed under reduced pressure and the product was separated by column chromatography (30-40% EtOAc in hexane as mobile phase) to give orange solid as product (0.142 g, 77%). ^{1}H-NMR (400 MHz, $CDCl_3$): δ 8.50 (d, 1H, *J* = 8.54 Hz, aromatic-H), 8.00 (s, 1H, 7-OC=O<u>H</u>), 6.37 (d, 1H, *J* = 7.02 Hz, 3-NH), 6.20 (d, 1H, *J* = 8.53 Hz, aromatic-H), 4.93 (m, 1H, 7α-H), 4.11 (s 1H, 3α-H), 3.68 (s, 3H, -O-CH_3), 1.10 (s, 3H, 19-CH_3), 0.95 (d, 3H, *J* = 6.53 Hz, 21-CH_3), 0.72 (s, 3H, 18-CH_3). IR_{vmax} (KBr): 3415.45, 2947.42, 2871.14, 1718.05, 1573.39, 1449.51, 1307.37, 1252.98, 1176.34 and 596.86 cm^{-1}. HRMS: Found: $(M\text{-}Na)^+$ = 619.3123, calculated for $C_{32}H_{44}N_4O_4Na$ = 619.3108.

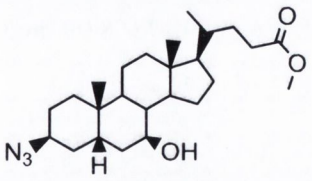

111

To a stirred solution of **84** (0.308 g) in anhydrous MeOH (30 ml) was added AcCl (0.06 ml in 5 ml anhydrous MeOH) dropwise at 0 °C and allowed to warm to rt. The reaction was monitored by TLC until there was no starting material present. Then the mixture was partitioned between saturated $NaHCO_3$ and EtOAc. The organic phase was washed with water (2 × 100 ml) and brine (100 ml), dried over Na_2SO_4, filtered and the solvent was removed under reduced pressure to give the product as light yellow semi-solid (0.273 g, 97%). ^{1}H-NMR (400 MHz, $CDCl_3$): δ 3.93 (s, 1H, 3α-H), 3.68 (s, 3H, -O-CH_3), 3.55 (m, 1H, 7α-H), 0.99 (s, 3H, 19-CH_3), 0.95 (d, 3H, J = 6.52 Hz, 21-CH_3), 0.69 (s, 3H, 18-CH_3). ^{13}C-NMR ppm (100 MHz, $CDCl_3$): δ 17.86 (C=O, 24-C), 71.48 (CH, 7-C), 58.42 (CH, 3-C), 51.66 (CH_3, OCH_3). IR_{vmax} (DCM): 3431.06, 2935.49, 2866.03, 2103.17 and 1739.37 cm^{-1}. HRMS: Found: $(M\text{-}Na)^+$ = 454.3051, calculated for $C_{25}H_{41}N_3O_3Na$ = 454.3046.

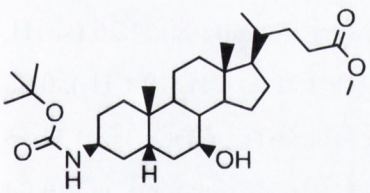

112

To a pre-reduced 10% Pd/C (~50 mg) in EtOAc (10 ml) was added the solution of **111** (0.273 g) and Boc_2O (0.166 g) in EtOAc (5 ml) under H_2 at rt and stirred overnight. Then the Pd/C was filtered out on a celite pad and the solvent was removed under reduced pressure. The crude product was cleaned on a flash column using 25% EtOAc in hexane as mobile phase to afford white foam as product (0.276 g, 86%). ^{1}H-NMR (400 MHz, $CDCl_3$): δ 4.83 (d, 1H, J = 7.03 Hz, 3-NH), 3.88 (br s, 1H, 3α-H), 3.68 (s, 3H, -O-CH_3), 3.56 (br s, 1H, 7α-H), 1.46 (s, 9H, -$OC(CH_3)_3$), 0.99 (s, 3H, 19-CH_3), 0.94 (d, 3H, J = 6.53 Hz, 21-CH_3), 0.69 (s, 3H, 18-CH_3). ^{13}C-NMR ppm (100 MHz, $CDCl_3$): δ 174.86 (C=O, 24-C), 71.41 (CH, 7-C), 51.66 (CH_3, OCH_3),

28.59 ($3CH_3$, -OC($\underline{C}H_3$)$_3$). IR_{vmax} (KBr): 3457.49, 2932.95, 2865.84, 1698.40, 1168.99 and 1021.60 cm^{-1}. HRMS: Found: $(M\text{-}Na)^+$ = 528.3685, calculated for $C_{30}H_{51}NO_5Na$ = 528.3665.

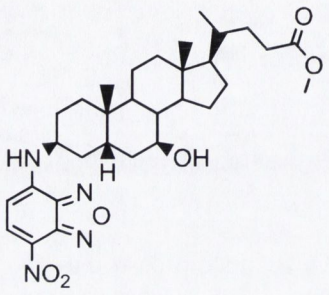

113

Compound **112** (0.269 g) was stirred in 10% TFA/DCM (20 ml) at rt until there was no Boc-protected compound present. Then the solvent was removed and the residue dried under reduced pressure to give light brown solid as crude product. This was dissolved in MeOH (20 ml) then $NaHCO_3$ (0.112 g) and NBD chloride (0.117 g) were added to the solution and stirred at 70 °C for 5 d (monitored by TLC using hexane/EtOAc 1:1 as mobile phase). After this time the mixture was poured into brine (70 ml) and extracted with EtOAc (3 × 60 ml). The collected organic phase was dried over Na_2SO_4, filtered and the solvent was removed under reduced pressure then the product was purified by column chromatography (50% EtOAc in hexane as mobile phase) to give orange solid as product (0.202 g, 67%). ^{1}H-NMR (400 MHz, $CDCl_3$): δ 8.51 (d, 1H, J = 9.03 Hz, aromatic-H), 6.42 (d, 1H, J = 7.03 Hz, 3-NH), 6.19 (d, 1H, J = 8.53 Hz, aromatic-H), 4.26 (s, 1H, 7β-OH), 4.10 (s, 1H, 3α-H), 3.69 (s, 3H, -O-CH_3), 3.61 (s, 1H, 7α-H), 1.10 (s, 3H, 19-CH_3), 0.96 (d, 3H, J = 6.52 Hz, 21-CH_3), 0.71 (s, 3H, 18-CH_3). ^{13}C-NMR ppm (100 MHz, $CDCl_3$): δ 175.15 (C=O, 24-C), 144.86 (C, aromatic-C), 144.36 (C, aromatic-C), 143.21 (C, aromatic-C), 136.94 (CH, aromatic-C), 124.29 (C, aromatic-C), 99.30 (CH, aromatic-C), 71.58 (CH, 7-C) 52.00 (CH_3, OCH_3). IR_{vmax} (KBr): 3404.92, 2932.39, 2865.09, 1736.45, 1574.72, 1307.25 and 1265.61 cm^{-1}. HRMS: Found: $(M\text{-}Na)^+$ = 591.3157, calculated for $C_{31}H_{44}N_4O_6Na$ = 591.3159.

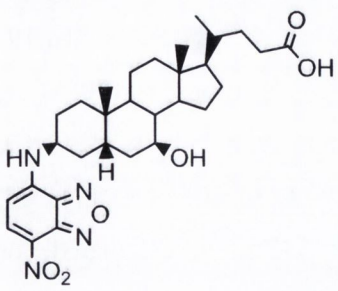

101

The hydrolysis of **113** (0.200 g) was carried out in MeOH (20 ml) with 2 M NaOH at pH~14 at 40 °C for 3 h. The mixture was poured into 2 M HCl (50 ml) and extracted with EtOAc (3 × 50 ml). The crude product was purified by flash chromatography using DCM / MeOH 9:1 as mobile phase to give orange solid as product (0.188 g, 96%). Mp: 208 – 210 °C (novel compound). ^{1}H-NMR (400 MHz, DMSO-d_6): 11.92 (br. s, 1H, acid), 9.03 (br. s, 1H, 7β-OH), 8.49 (s, 1H, aromatic-H), 6.68 (s, 1H, 3-NH), 6.37 (br. s, 1H, aromatic-H), 3.32 (s, 1H, 7α-H), 0.95 (s, 3H, 19-CH_3), 0.89 (d, 3H, J = 6.42 Hz, 21-CH_3), 0.63 (s, 3H, 18-CH_3). ^{13}C-NMR ppm (100 MHz, DMSO-d_6): 174.88 (C=O, 24-C), 144.45 (C, aromatic-C), 137.66 (C, aromatic-C), 137.59 (C, aromatic-C), 120.90 (C, aromatic-C), 100.09 (CH, aromatic-C), 69.35 (CH, 7-C). IR_{vmax} (KBr): 3413.89, 2931.04, 2865.99, 1574.58, 1307.39 and 1250.03 cm^{-1}. HRMS: Found: $(M\text{-}Na)^+$ = 577.3031, calculated for $C_{30}H_{42}N_4O_6Na$ = 577.3002.

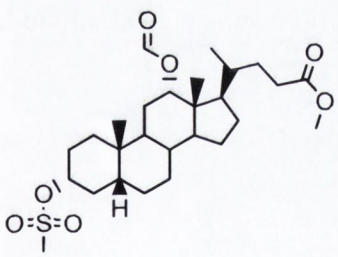

114

The solution of Et_3N (0.1 ml) and methane sulfonyl chloride (0.15 ml) in anhydrous DCM (5 ml) was added dropwise to the stirred solution of **105** (0.279 g) in anhydrous DCM (20 ml) at 0 °C and allowed to warm to rt. After 20 min when TLC analysis showed the reaction was complete the mixture was poured into water (50 ml) and extracted with DCM (3 × 50 ml). The organic phase was dried over $MgSO_4$ then removed under reduced pressure to give the product as colourless oil (0.322 g, 98%). ^{1}H-NMR (400 MHz, $CDCl_3$): δ 8.15 (s, 1H, 12-OC=O<u>H</u>), 5.26 (s,

1H, 12β-H), 4.63 (m, 1H, 3β-H), 3.67 (s, 3H, -O-CH_3), 3.01 (s, 3H, -OSO_2CH_3), 0.93 (s, 3H, 19-CH_3), 0.85 (d, 3H, J = 6.03 Hz, 21-CH_3), 0.75 (s, 3H, 18-CH_3). ^{13}C-NMR ppm (100 MHz, $CDCl_3$): δ 174.69 (C=O, 24-C), 160.71 (C=O, 12-O<u>C</u>=OH), 82.79 (CH, 3-C), 75.97 (CH, 12-C), 52.67 (CH_3, OSO_2CH_3), 51.66 (CH_3, O<u>C</u>H_3). IR_{vmax} (DCM): 2947.01, 2871.16, 1717.89, 1353.88, 1174.09 and 932.87 cm^{-1}. HRMS: Found: $(M\text{-}Na)^+$ = 535.2710, calculated for $C_{27}H_{44}O_7SNa$ = 535.2705.

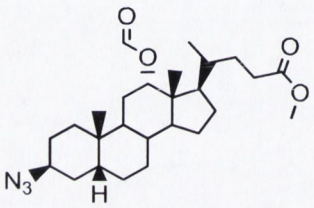

115

NaN_3 (0.408 g) was added to the stirred solution of **114** (0.322 g) in DMPU (20 ml) at 50 °C and the reaction was monitored via TLC (hexane/EtOAc 5:1). After 6 d the mixture was partitioned between water and EtOAc. The organic phase was retrieved and dried over Na_2SO_4. The crude product was purified by column chromatography using 20% EtOAc in hexane as mobile phase to yield colourless oil as product (0.253 g, 87%). ^{1}H-NMR (400 MHz, $CDCl_3$): δ 8.13 (s, 1H, 12-OC=O<u>H</u>), 5.26 (s, 1H, 12β-H), 3.95 (s, 1H, 3α-H), 3.67 (s, 3H, -O-CH_3), 0.95 (s, 3H, 19-CH_3), 0.85 (d, 3H, J = 6.52 Hz, 21-CH_3), 0.76 (s, 3H, 18-CH_3). ^{13}C-NMR ppm (100 MHz, $CDCl_3$): δ 174.39 (C=O, 24-C), 160.37 (C=O, 12-O<u>C</u>=OH), 76.00 (CH, 12-C), 58.35 (CH, 3-C), 51.35 (CH_3, O<u>C</u>H_3). IR_{vmax} (DCM): 2938.73, 2872.92, 2101.83, 1738.92, 1720.86 and 1171.43 cm^{-1}. HRMS: Found: $(M\text{-}Na)^+$ = 482.2974, calculated for $C_{26}H_{41}N_3O_4Na$ = 482.2995.

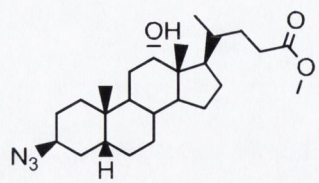

116

To a stirred solution of **115** (0.322 g) in anhydrous MeOH (30 ml) was added AcCl (0.07 ml in 5 ml anhydrous MeOH) dropwise at 0 °C and allowed to warm to rt. The reaction was monitored via TLC until there was no starting material present. Then the mixture was partitioned between saturated $NaHCO_3$ and EtOAc. The organic phase was washed with water (2 × 100 ml) and brine (100 ml), dried over Na_2SO_4, filtered and the solvent was removed under reduced pressure to give

the product as yellow semi-solid (0.294 g, 97%). ^{1}H-NMR (400 MHz, $CDCl_3$): δ 4.01 (s, 1H, 12β-H), 3.97 (s, 1H, 3α-H), 3.68 (s, 3H, -O-CH_3), 0.99 (d, 3H, J = 5.87 Hz, 21-CH_3), 0.96 (s, 3H, 19-CH_3), 0.70 (s, 3H, 18-CH_3). ^{13}C-NMR ppm (100 MHz, $CDCl_3$): δ 174.51 (C=O, 24-C), 73.00 (CH, 12-C), 58.52 (CH, 3-C), 51.36 (CH_3, O$\underline{C}H_3$). IR_{vmax} (KBr): 3528.85, 2932.82, 2093.51, 1725.62, 1449.91, 1312.94 and 1196.78 cm^{-1}. HRMS: Found: $(M-Na)^+$ = 454.3052, calculated for $C_{25}H_{41}N_3O_3Na$ = 454.3046.

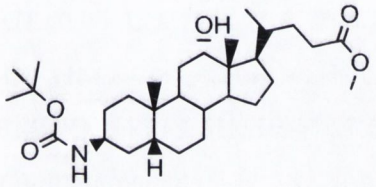

117

To a pre-reduced 10% Pd/C (~50 mg) in EtOAc (10 ml) was added the solution of **116** (0.245 g) and Boc_2O (0.149 g) in EtOAc (5 ml) and stirred under H_2 at rt. The reaction mixture was stirred overnight (TLC: hexane/EtOAc 3:1) then it was filtered on a celite pad. The celite was washed with EtOAc (3 × 10 ml) and the organic phase was removed in vacuum. The product was purified by flash chromatography (mobile phase: 30% EtOAc in hexane) to yield a white foam as product (0.260 g, 90%). ^{1}H-NMR (400 MHz, $CDCl_3$): 4.84 (br s, 1H, 3-NH), 4.00 (s, 1H, 12β-H), 3.92 (br s, 1H, 3α-H), 3.68 (s, 3H, -O-CH_3), 1.46 (s, 9H, -OC(CH_3)$_3$), 0.99 (d, 3H, *J* = 6.02 Hz, 21-CH_3), 0.96 (s, 3H, 19-CH_3), 0.69 (s, 3H, 18-CH_3). ^{13}C-NMR ppm (100 MHz, $CDCl_3$): δ 174.54 (C=O, 24-C), 72.97 (CH, 12-C), 51.34 (CH_3, OCH_3), 28.29 ($3CH_3$, -OC($\underline{C}H_3$)$_3$). IR_{vmax} (KBr): 3459.32, 2937.54, 2865.92, 1698.37 and 1171.03 cm^{-1}. HRMS: Found: $(M-Na)^+$ = 528.3654, calculated for $C_{30}H_{51}NO_5Na$ = 528.3665.

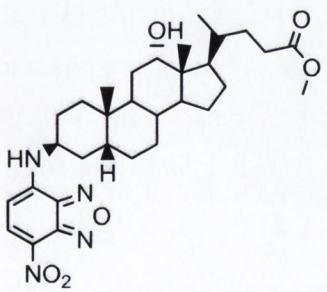

118

Compound **117** (0.259 g) was stirred in 10% TFA/DCM (20 ml) at rt until there was no Boc-protected compound present. Then the solvent was removed and the residue dried under reduced

pressure to give light brown solid as crude product. This was dissolved in MeOH (20 ml) then $NaHCO_3$ (0.130 g) and NBD chloride (0.112 g) were added to the solution and stirred at 70 °C for 10 d (monitored by TLC using hexane/EtOAc 1:1 as mobile phase). After this time the mixture was poured into brine (50 ml) and extracted with EtOAc (3 × 50 ml). The collected organic phase was dried over Na_2SO_4, filtered and the solvent was removed under reduced pressure then the product was purified by column chromatography (50% EtOAc in hexane as mobile phase) to give orange solid as product (0.213 g, 73%). ^{1}H-NMR (400 MHz, $CDCl_3$): δ 8.49 (d, 1H, J = 9.04 Hz, aromatic-H), 6.47 (d, 1H, J = 7.03 Hz, 3-NH), 6.19 (d, 1H, J = 9.04 Hz, aromatic-H), 4.26 (s, 1H, 12α-OH), 4.12 (s, 1H, 3α-H), 4.05 (s, 1H, 12β-H), 3.69 (s, 4H, -O-CH_3), 1.03 (s, 3H, 19-CH_3), 1.00 (d, 3H, J = 6.53 Hz, 21-CH_3), 0.72 (s, 3H, 18-CH_3). ^{13}C-NMR ppm (100 MHz, $CDCl_3$): δ 175.10 (C=O, 24-C), 144.88 (C, aromatic-C), 143.30 (C, aromatic-C), 137.07 (CH, aromatic-C), 134.40 (C, aromatic-C), 124.07 (C, aromatic-C), 104.33 (CH, aromatic-C), 73.53 (CH, 12-C), 52.01 (CH_3, OCH_3). IR_{vmax} (KBr): 3538.32, 3408.93, 2943.25, 2864.97, 1736.80, 1574.32, 1336.49 and 1314.61 cm^{-1}. HRMS: Found: $(M\text{-}Na)^+$ = 591.3163, calculated for $C_{31}H_{44}N_4O_6Na$ = 591.3159.

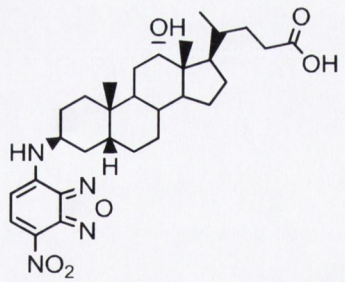

119

The hydrolysis of **118** (0.205 g) was carried out in MeOH (20 ml) with 2 M NaOH at pH~14 at 40 °C for 4 h. The mixture was poured into 2 M HCl (50 ml) and extracted with EtOAc (3 × 50 ml). The crude product was purified by column chromatography using EtOAc as mobile phase to afford the product as orange solid (0.152 g, 76%). Mp: 216–218 °C (novel compound). ^{1}H-NMR (400 MHz, DMSO-d_6): 8.31 (d, 1H, J = 9.03 Hz, aromatic-H), 6.29 (s, 1H, aromatic-H), 4.10 (br s, 1H, 3α-OH), 3.81 (s, 1H, 12β-H), 0.93 (s, 6H, 21-CH_3 and 19-CH_3), 0.61 (s, 3H, 18-CH_3). ^{13}C-NMR ppm (100 MHz, DMSO-d_6): δ 175.27 (C=O, 24-C), 145.65 (C, aromatic-C), 144.87 (C, aromatic-C), 135.39 (CH, aromatic-C), 131.60 (C, aromatic-C), 128.66 (C, aromatic-C), 100.02 (CH, aromatic-C), 71.10 (CH, 12-C). IR_{vmax} (KBr): 3410.69, 2927.61, 2863.42, 1703.83, 1575.98

and 1310.90 cm^{-1}. HRMS: Found: $(M-Na)^+$ = 577.3019, calculated for $C_{30}H_{42}N_4O_6Na$ = 577.3002.

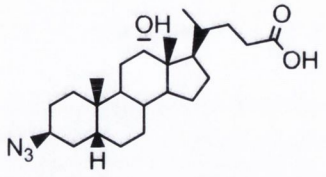

120

To a solution of **115** (0.253 g) in MeOH (20 ml) was added 2 M NaOH solution to pH~14 and stirred at reflux for 1 d, when TLC analysis (hexane/EtOAc 1:1) showed the hydrolysis was complete. Then the reaction mixture was poured into 1 M HCl solution (50 ml) and extracted with EtOAc (3 × 50 ml). The organic layer was washed with water (2 × 100 ml) and brine (100 ml), dried over Na_2SO_4, filtered and the solvent was removed under reduced pressure to give the product as a white solid (0.226 g, 98%). ^{1}H-NMR (400 MHz, $CDCl_3$): δ 4.02 (s, 1H, 12β-H), 3.97 (s, 1H, 3α-H), 1.00 (d, 3H, J = 6.52 Hz, 21-CH_3), 0.96 (s, 3H, 19-CH_3), 0.70 (s, 3H, 18-CH_3). ^{13}C-NMR ppm (100 MHz, $CDCl_3$): δ 179.94 (C=O, 24-C), 73.43 (CH, 12-C), 58.85 (CH, 3-C). IR_{vmax} (KBr): 3445.86, 2938.64, 2870.58, 2103.19, 1709.09 and 1254.81 cm^{-1}. HRMS: Found: $(M-Na)^+$ = 440.2877, calculated for $C_{24}H_{39}N_3O_3Na$ = 440.2889.

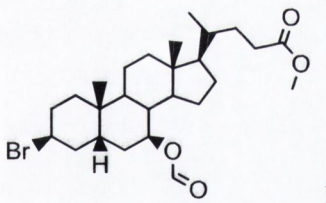

121

Triphenylphoshine (2.097 g) was added to a solution of **104** (1.738 g) in anhydrous THF (80 ml) and NBS (1.423 g) was added in 3 parts over 1 h at -18 °C then allowed to warm to rt and stirred overnight. The reaction mixture was poured into 1 M HCl solution (100 ml) and extracted with EtOAc (3 × 75 ml). The organic layer was washed with brine (x 100 ml) and after drying over $MgSO_4$ the solvent was removed under reduced pressure. The crude product was purified by flash chromatography (hexane/EtOAc 5:1) to afford the product as white foam (1.694 g, 85%). ^{1}H-NMR (400 MHz, $CDCl_3$): δ 7.99 (s, 1H, 7-OC=O<u>H</u>), 4.84 (m, 1H, 7α-H), 4.76 (s, 1H, 3α-H), 3.67 (s, 3H, -O-CH_3), 1.06 (s, 3H, 19-CH_3), 0.93 (d, 3H, J = 6.53 Hz, 21-CH_3), 0.70 (s, 3H, 18-CH_3). ^{13}C-NMR ppm (100 MHz, $CDCl_3$): δ 175.12 (C=O, 24-C), 161.50 (C=O, 7-O<u>C</u>=OH),

74.41 (CH, 7-C), 51.97 (CH_3, O<u>C</u>H_3). IR_{vmax} (DCM): 2947.48, 2871.35, 1737.49, 1719.36 and 1178.56 cm^{-1}. HRMS: Found: $(M\text{-}Na)^+$ = 519.2070, calculated for $C_{26}H_{41}BrO_3Na$ = 519.2086.

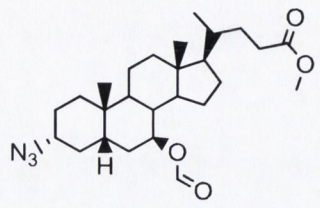

122

To a solution of **121** (1.693 g) in DMPU (50 ml) was added NaN_3 (2.212 g) at rt and stirred overnight. Then the reaction mixture was poured into water (100 ml) and extracted with EtOAc (3 × 75 ml). The organic phase was washed with brine (1 × 100 ml), dried over Na_2SO_4, filtered and the solvent was evaporated in vacuum. The crude product was purified on a flash column using hexane/EtOAc 5:1 as mobile phase to obtain the product as colourless oil (1.464 g, 94%). ^{1}H-NMR (400 MHz, $CDCl_3$): δ 8.00 (s, 1H, 7-OC=O<u>H</u>), 4.91 (sex, 1H, J_1 = 5.27 Hz, J_2 = 5.53 Hz, 7α-H), 3.68 (s, 3H, -O-CH_3), 3.30 (m, 1H, 3β-H), 1.00 (s, 3H, 19-CH_3), 0.94 (d, 3H, J = 6.52 Hz, 21-CH_3), 0.70 (s, 3H, 18-CH_3). ^{13}C-NMR ppm (100 MHz, $CDCl_3$): δ 174.81 (C=O, 24-C), 161.12 (C=O, 7-O<u>C</u>=OH), 73.76 (CH, 7-C), 60.81 (CH, 3-C), 51.64 (CH_3, O<u>C</u>H_3). IR_{vmax} (DCM): 2946.73, 2871.54, 2093.30, 1720.62, 1453.67, 1255.13 and 1187.30 cm^{-1}. HRMS: Found: $(M\text{-}Na)^+$ = 482.2998, calculated for $C_{26}H_{41}N_3O_4Na$ = 482.2995.

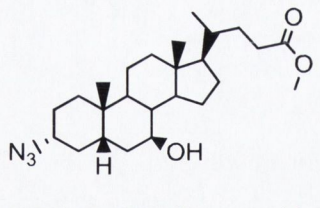

123

AcCl (0.65 ml) was added dropwise to a stirred solution of **122** (1.411 g) in anhydrous MeOH (60 ml) at 0 °C and allowed to warm to rt. After overnight the reaction mixture was poured into saturated $NaHCO_3$ (100 ml) and extracted with EtOAc (3 × 100 ml). The organic layer was dried over Na_2SO_4, filtered and the solvent was removed under reduced pressure. The crude product was purified on flash column (hexane/EtOAc 3:1) to give the product as yellow semi-solid (1.210 g, 91%). ^{1}H-NMR (400 MHz, $CDCl_3$): δ 3.69 (s, 3H, -O-CH_3), 3.60 (m, 1H, 7α-H), 3.30 (m, 1H, 3β-H), 0.98 (s, 3H, 19-CH_3), 0.95 (d, 3H, J = 6.27 Hz, 21-CH_3), 0.70 (s, 3H, 18-CH_3). ^{13}C-NMR ppm (100 MHz, $CDCl_3$): δ 174.85 (C=O, 24-C), 71.29 (CH, 7-C), 60.99 (CH, 3-C), 51.65 (CH_3,

O$\underline{C}$H$_3$). IR$_{vmax}$ (DCM): 3424.26, 2938.77, 2866.74, 2092.43, 1739.29, 1452.41, 1254.58, 1167.83 and 1022.77 cm^{-1}. HRMS: Found: (M-Na)$^+$ = 454.3057, calculated for $C_{25}H_{41}N_3O_3Na$ = 454.3046.

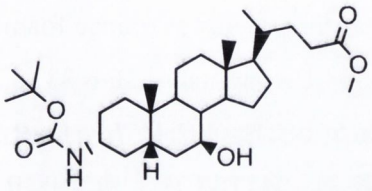

124

10% Pd/C (~100 mg) in EtOAc (30 ml) was pre-reduced under hydrogen atmosphere over 30 min then the solution of **123** (1.182 g) and Boc_2O (0.717 g) in EtOAc (20 ml) was added via syringe and stirred at rt overnight. The reaction mixture was filtered through a celite pad and washed with EtOAc (3 × 10 ml). The solvent was removed under reduced pressure and the crude product was purified by flash chromatography using 30% EtOAc in hexanes as mobile phase to yield the product as white foam (1.300 g, 94%). ^{1}H-NMR (400 MHz, $CDCl_3$): δ 4.42 (br s, 1H, 3-NH), 3.68 (s, 3H, -O-CH$_3$), 3.56 (m, 1H, 7α-H), 3.39 (br s, 1H, 3β-H), 1.45 (s, 9H, -OC(CH$_3$)$_3$), 0.96 (s, 3H, 19-CH$_3$), 0.95 (d, 3H, J = 6.27 Hz, 21-CH$_3$), 0.69 (s, 3H, 18-CH$_3$). ^{13}C-NMR ppm (100 MHz, $CDCl_3$): δ 174.85 (C=O, 24-C), 71.48 (CH, 7-C), 51.65 (CH$_3$, OCH$_3$), 28.56 (3CH$_3$, -OC($\underline{C}$H$_3$)$_3$). IR$_{vmax}$ (DCM): 3380.47, 2933.70, 1692.59 and 1170.19 cm^{-1}. HRMS: Found: (M-Na)$^+$ = 528.3669, calculated for $C_{30}H_{51}NO_5Na$ = 528.3665.

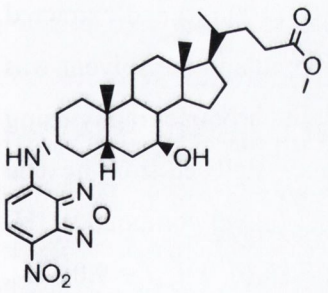

125

Compound **124** (1.265 g) was dissolved in 10% TFA/DCM (60 ml) and stirred at rt overnight (followed by TLC analysis using hexane/EtOAc 1:1 as mobile phase) then the solvent was removed in vacuum. The residue was dried under reduced pressure using toluene (3 × 100 ml). The yield foam was dissolved in MeOH (50 ml) then $NaHCO_3$ (2.102 g) and NBD chloride (0.549 g) were added to the solution. The reaction mixture was stirred vigorously for 2 weeks at

reflux; reaction completion was checked by TLC using hexane : EtOAc (50:50) as mobile phase. It was poured into brine (150 ml) and extracted with EtOAc (3 × 100 ml). The organic phase was dried over Na_2SO_4, filtered and the solvent was removed in vacuum to afford the crude product as black semi-solid. This was purified by flash column using 40-70% EtOAc in hexanes (40, 50, 60 and 70% EtOAc in 100 ml solvent mixture) as mobile phase to obtain the product as orange foam (0.622 g, 44%). ^{1}H-NMR (400 MHz, $CDCl_3$): δ 8.49 (d, 1H, J = 8.54 Hz, aromatic-H), 6.88 (d, 1H, J = 7.53 Hz, 3-NH), 6.19 (d, 1H, J = 9.04 Hz, aromatic-H), 3.67 (s, 5H, -O-CH_3, 7α-H, 3β-H), 1.08 (s, 3H, 19-CH_3), 0.95 (d, 3H, J = 6.03 Hz, 21-CH_3), 0.72 (s, 3H, 18-CH_3). ^{13}C-NMR ppm (100 MHz, $CDCl_3$): δ 174.44 (C=O, 24-C), 144.16 (C, aromatic-C), 143.87 (C, aromatic-C), 136.48 (CH, aromatic-C), 123.07 (C, aromatic-C), 71.14 (CH, 7-C), 51.35 (CH_3, OCH_3). IR_{vmax} (KBr): 3402.60, 2933.80, 2867.01, 1733.12, 1579.17 and 1304.77 cm^{-1}. HRMS: Found: $(M\text{-}Na)^+$ = 591.3169, calculated for $C_{31}H_{44}N_4O_6Na$ = 591.3159.

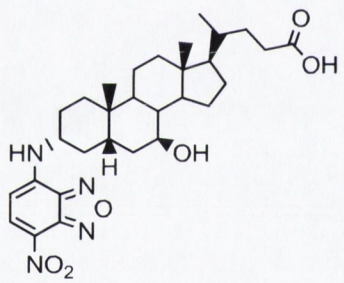

126

2 M NaOH was added to a stirred solution of **125** (0.589 g) and warmed to 40 °C. The reaction mixture was left at this temperature overnight then poured into 2 M HCl (100 ml) and extracted with EtOAc (3 × 75 ml). The organic layer was dried over Na_2SO_4, filtered and the solvent was removed under reduced pressure. The crude product was purified by flash chromatography using 2% acetic acid in EtOAc as mobile phase. The obtained product was recrystallised from hexane to give orange solid as final product (0.465 g, 81%). Mp: 148–150 °C (novel compound). ^{1}H-NMR (400 MHz, Acetone-d_6): 8.51 (d, 1H, J = 9.04 Hz, aromatic-H), 6.55 (d, 1H, J = 9.04 Hz, aromatic-H), 3.93 (br s, 1H, 7α-H), 3.51 (m, 1H, 3β-H), 1.05 (s, 3H, 19-CH_3), 0.97 (d, 3H, J = 6.53 Hz, 21-CH_3), 0.72 (s, 3H, 18-CH_3). ^{13}C-NMR ppm (100 MHz, Acetone-d_6): 175.03 (C=O, 24-C), 70.94 (CH, 7-C). IR_{vmax} (KBr): 3436.13, 2932.86, 2868.26, 1708.42, 1621.14, 1579.48 and 1304.52 cm^{-1}. HRMS: Found: $(M\text{-}Na)^+$ = 577.3005, calculated for $C_{30}H_{42}N_4O_6Na$ = 577.3002.

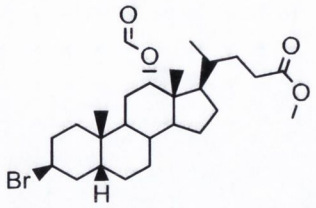

127

Triphenylphoshine (2.135 g) was added to a solution of **105** (1.769 g) in anhydrous THF (80 ml) and NBS (1.449 g) was added in 3 parts over 1 h at -18 °C then allowed to warm to rt and stirred for 1.5 h. The reaction mixture was poured into 1 M HCl solution (100 ml) and extracted with EtOAc (3 × 75 ml). The organic layer was washed with brine (2 × 100 ml) and after drying over $MgSO_4$ the solvent was removed under reduced pressure. The crude product was purified on flash column (hexane/EtOAc 5:1) to afford the product as pale white solid (1.919 g, 95%). ^{1}H-NMR (400 MHz, $CDCl_3$): δ 8.13 (s, 1H, 12-OC=OH), 5.26 (s, 1H, 12β-H), 4.79 (s, 1H, 3α-H), 3.68 (s, 3H, -O-CH_3), 1.01 (s, 3H, 19-CH_3), 0.85 (d, 3H, J = 6.52 Hz, 21-CH_3), 0.76 (s, 3H, 18-CH_3). ^{13}C-NMR ppm (100 MHz, $CDCl_3$): 174.70 (C=O, 24-C), 160.68 (C=O, 12-OC=OH), 76.29 (CH, 12-C), 51.67 (CH_3, OCH_3). IR_{vmax} (KBr): 3426.56, 2939.12, 2873.47, 1739.75, 1720.29 and 1180.89 cm^{-1}. HRMS: Found: $(M\text{-}Na)^+$ = 519.2073, calculated for $C_{26}H_{41}BrO_3Na$ = 519.2086.

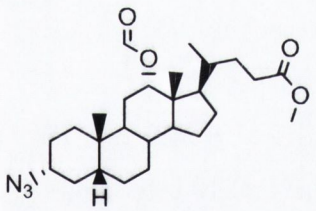

128

To a solution of **127** (1.852 g) in DMPU (50 ml) was added NaN_3 (2.420 g) at rt and stirred overnight. Then the reaction mixture was poured into water (100 ml) and extracted with EtOAc (3 × 50 ml). The organic phase was washed with brine (100 ml), dried over Na_2SO_4, filtered and the solvent was evaporated in vacuum. The crude product was purified on a flash column using hexane/EtOAc 5:1 as mobile phase to obtain the product as colourless semi-solid (1.652 g, 97%). ^{1}H-NMR (400 MHz, $CDCl_3$): δ 8.14 (s, 1H, 12-OC=OH), 5.26 (s, 1H, 12β-H), 3.67 (s, 3H, -O-CH_3), 3.34 (m, 1H, 3β-H), 0.93 (s, 3H, 19-CH_3), 0.85 (d, 3H, J = 6.03 Hz, 21-CH_3), 0.75 (s, 3H, 18-CH_3). ^{13}C-NMR ppm (100 MHz, $CDCl_3$): 174.40 (C=O, 24-C), 160.42 (C=O, 12-OC=OH), 75.70 (CH, 12-C), 60.98 (CH, 3-C), 51.34 (CH_3, OCH_3). IR_{vmax} (DCM): 2941.27, 2867.58,

2092.01, 1738.62, 1720.31, 1448.60, 1251.73 and 1177.39 cm^{-1}. HRMS: Found: $(M\text{-}Na)^+$ = 482.2995, calculated for $C_{26}H_{41}N_3O_4Na$ = 482.2995.

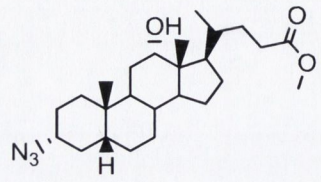

129

AcCl (0.51 ml) was added dropwise to a stirred solution of **128** (1.645 g) in anhydrous MeOH (60 ml) at 0 °C and allowed to warm to rt. After overnight the reaction mixture was poured into saturated $NaHCO_3$ (100 ml) and extracted with EtOAc (3 × 100 ml). The organic layer was dried over Na_2SO_4, filtered and the solvent was removed under reduced pressure. The product was recrystallised from diethyl ether to obtain light-yellow crystalls (1.457 g, 94%). ^{1}H-NMR (400 MHz, $CDCl_3$): δ 4.00 (s, 1H, 12β-H), 3.68 (s, 3H, -O-CH_3), 3.35 (m, 1H, 3β-H), 0.99 (d, 3H, J = 6.53 Hz, 21-CH_3), 0.94 (s, 3H, 19-CH_3), 0.69 (s, 3H, 18-CH_3). ^{13}C-NMR ppm (100 MHz, $CDCl_3$): 175.15 (C=O, 24-C), 73.50 (CH, 12-C), 61.69 (CH, 3-C), 51.97 (CH_3, O$\underline{C}H_3$). IR_{vmax} (DCM): 3524.40, 2939.82, 2866.15, 2091.49, 1739.60, 1448.24 and 1252.74 cm^{-1}. HRMS: Found: $(M\text{-}Na)^+$ = 454.3038, calculated for $C_{25}H_{41}N_3O_3Na$ = 454.3046.

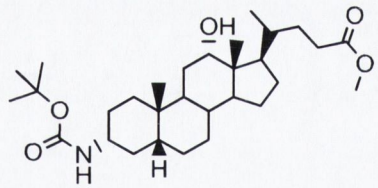

130

10% Pd/C (~100 mg) in EtOAc (30 ml) was pre-reduced under hydrogen atmosphere over 30 min then the solution of **129** (1.424 g) and Boc_2O (0.864 g) in EtOAc (20 ml) was added via syringe and stirred at rt overnight. The reaction mixture was filtered through a celite pad and washed with EtOAc (3 × 10 ml). The solvent was removed under reduced pressure and the crude product was purified by column chromatography using 30% EtOAc in hexanes as mobile phase to yield the product as white foam (1.549 g, 93%). ^{1}H-NMR (400 MHz, $CDCl_3$): δ 4.45 (br s, 1H, 3-NH), 4.00 (s, 1H, 12β-H), 3.68 (s, 3H, -O-CH_3), 3.43 (br s, 1H, 3β-H), 1.45 (s, 9H, -OC(CH_3)$_3$), 0.99 (d, 3H, J = 6.27 Hz, 21-CH_3), 0.93 (s, 3H, 19-CH_3), 0.69 (s, 3H, 18-CH_3). ^{13}C-NMR ppm (100 MHz, $CDCl_3$): δ 174.83 (C=O, 24-C), 73.30 (CH, 12-C), 51.65 (CH_3, OCH_3), 28.57 (3CH_3, -

$OC(\underline{C}H_3)_3$). IR_{vmax} (DCM): 3380.58, 2935.81, 1691.31 and 1171.11 cm^{-1}. HRMS: Found: $(M\text{-}Na)^+$ = 528.3666, calculated for $C_{30}H_{51}NO_5Na$ = 528.3665.

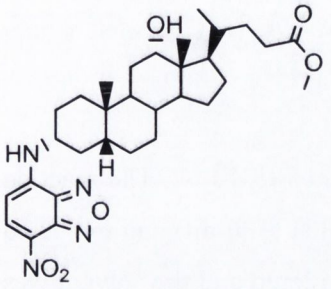

131

Compound **130** (1.524 g) was dissolved in 10% TFA/DCM (60 ml) and stirred at rt overnight (followed by TLC analysis using hexane/EtOAc 3:1 as mobile phase) then the solvent was removed in vacuum. The residue was dried under reduced pressure using toluene (3 × 100 ml). The yield foam was dissolved in MeOH (60 ml) then $NaHCO_3$ (2.533 g) and NBD chloride (0.862 g) were added to the solution. The reaction mixture was stirred vigorously for 10 d at reflux; reaction completion was checked by TLC using hexane : EtOAc (50:50) as mobile phase. It was poured into brine (100ml) and extracted with EtOAc (3 × 100 ml). The organic phase was dried over Na_2SO_4, filtered and the solvent was removed in vacuum to afford the crude product as black semi-solid. This was purified by flash column using 30-40% EtOAc in hexanes as mobile phase to obtain the product as orange foam (0.679 g, 98%). ^{1}H-NMR (400 MHz, $CDCl_3$): δ 8.46 (d, 1H, J = 8.53 Hz, aromatic-H), 6.51 (s, 1H, 3-NH), 6.17 (d, 1H, J = 8.53 Hz, aromatic-H), 4.26 (s, 1H, 12α-OH), 4.07 (s, 1H, 12β-H), 3.67 (s, 4H, 3β-H, -O-CH_3), 1.02 (s, 3H, 19-CH_3), 0.97 (d, 3H, J = 6.03 Hz, 21-CH_3), 0.71 (s, 3H, 18-CH_3). ^{13}C-NMR ppm (100 MHz, $CDCl_3$): δ 174.48 (C=O, 24-C), 144.09 (C, aromatic-C), 143.78 (C, aromatic-C), 136.50 (CH, aromatic-C), 133.78 (C, aromatic-C), 122.93 (C, aromatic-C), 103.71 (CH, aromatic-C), 72.95 (CH, 12-C), 51.36 (CH_3, OCH_3). IR_{vmax} (DCM): 3529.91, 3294.51, 2938.41, 2867.28, 1735.15, 1582.76 and 1304.42 cm^{-1}. HRMS: Found: $(M\text{-}Na)^+$ = 591.3142, calculated for $C_{31}H_{44}N_4O_6Na$ = 591.3159.

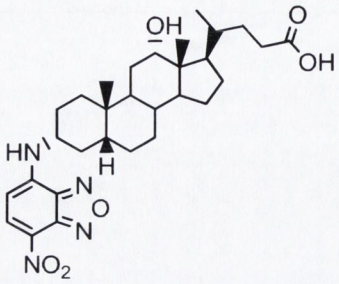

99

2 M NaOH was added to a stirred solution of **131** (1.621 g) and warmed to 40 °C. The reaction mixture was left at this temperature overnight then poured into 2 M HCl (100 ml) and extracted with EtOAc (3 × 100 ml). The organic layer was dried over Na_2SO_4, filtered and the solvent was removed under reduced pressure. The crude product was purified by flash chromatography using first 20% hexane then 2% acetic acid in EtOAc as mobile phase to yield orange solid as product (0.997 g, 63%). Mp: 225 °C (novel compound). ^{1}H-NMR (400 MHz, DMSO-d_6): 11.93 (s, 1H, 24-COOH), 9.52 (s, 1H, 3-NH), 8.47 (d, 1H, J = 8.54 Hz, aromatic-H), 6.46 (d, 1H, J = 9.04 Hz, aromatic-H), 4.25 (s, 1H, 12α-OH), 3.82 (s, 2H, 12β-H and 3β-H), 0.93 (d, 6H, J = 4.52 Hz, 21-CH_3 and 19-CH_3), 0.61 (s, 3H, 18-CH_3). ^{13}C-NMR ppm (100 MHz, DMSO-d_6): 174.98 (C=O, 24-C), 144.40 (C, aromatic-C), 144.27 (C, aromatic-C), 138.01 (CH, aromatic-C), 136.18 (C, aromatic-C), 120.06 (C, aromatic-C), 105.85 (CH, aromatic-C), 70.89 (CH, 12-C). IR_{vmax} (DCM): 3309.77, 2937.30, 2859.90, 1707.17, 1582.18 and 1304.06 cm^{-1}. HRMS: Found: $(M-Na)^+$ = 577.2999, calculated for $C_{30}H_{42}N_4O_6Na$ = 577.3002.

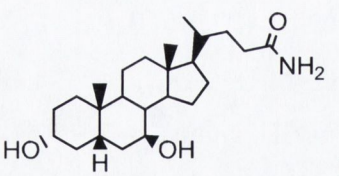

132

Compound **7** (2 g) was dissolved in anhydrous THF (50 ml) and acetonitrile (5 ml) then DCC (1.156 g) and N-Hydroxysuccinimide (0.879 g) were added to the reaction mixture at rt and stirred overnight. The reaction was followed by TLC analysis using hexane/EtOAc 1:3 as mobile phase. Then the white solid formed was filtered out and the filtrate was concentrated under reduced pressure to give the intermediate as white foam. This was dissolved in DMF (50 ml) and ammonia solution (1.42 ml, 28% in water) was added at 50 °C and stirred overnight. The reaction mixture was poured into brine (50 ml) and the precipitate was collected by suction filtration and washed with water (2 × 30 ml). The product was dried under high vacuum to give the amide as

white solid (1.536 g, 77%). ^{1}H-NMR (400 MHz, CD_3OD): δ 3.49 (m, 2H, 3β-H, 7α-H), 1.00-0.98 (d, 6H, J = 8.04 Hz, 21-CH_3, 19- CH_3), 0.73 (s, 3H, 18-CH_3). ^{13}C-NMR ppm (100 MHz, CD_3OD): δ 179.85 (C=O, 24-C), 72.10 (CH, 3-C), 71.93 (CH, 7-C). IR_{vmax} (KBr): 3334.21, 2930.22, 2853.01, 1666.65, 1627.95 and 1051.08 cm^{-1}. HRMS: Found: $(M\text{-}Na)^+$ = 414.2979, calculated for $C_{24}H_{41}NO_3Na$ = 414.2984.

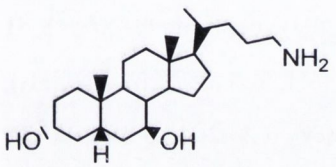

133

Compound **132** (0.723 g) was dissolved in anhydrous THF (40 ml) under N_2 and stirred. $LiAlH_4$ (18.046 ml, 1.0 M in THF) was added slowly via syringe and the mixture was heated to reflux for 2 d. When the reaction was complete (followed by TLC analysis using DCM/MeOH 4:1 + 1% NH_4OH as mobile phase) the mixture was cooled down to rt and water (2 ml), 15% NaOH solution (2 ml) and water (6 ml) again were added carefully and stirred for 2 h at this temperature. After this time the precipitate was filtered out by suction filtration and washed with EtOAc (2 × 30 ml). The organic phase was dried over Na_2SO_4, filtered and the solvent was removed under reduced pressure. The crude product was purified by flash chromatography using first 20% MeOH in DCM then 20% MeOH and 1% NH_4OH in DCM as mobile phase. The cleaned amine was dried under high vacuum to give yellow foam as product (0.427 g, 61%). ^{1}H-NMR (400 MHz, DMSO-d_6): 3.29 (m, 4H, 3β-H, 7α-H, NH_2), 0.90 (d, 3H, J = 6.53 Hz, 21-CH_3), 0.88 (s, 3H, 19-CH_3), 0.61 (s, 3H, 18-CH_3). ^{13}C-NMR ppm (100 MHz, DMSO-d_6): 69.72 (CH, 3-C), 69.46 (CH, 7-C). IR_{vmax} (KBr): 3414.21, 2932.12, 2864.40, 1659.18, 1452.94, 1374.63 and 1053.97 cm^{-1}. HRMS: Found: $(M\text{-}H)^+$ = 378.3375, calculated for $C_{24}H_{44}NO_2$ = 378.3372.

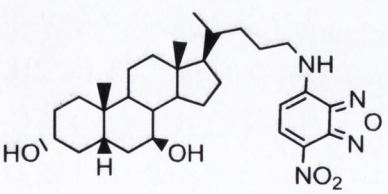

134

To a solution of **133** (0.368 g) in MeOH (30 ml) were added $NaHCO_3$ (0.123 g) and NBD chloride (0.214 g) at rt and stirred for 2 d, after which time TLC analysis showed the reaction was

complete (using DCM/MeOH 4:1 + 1% NH_4OH as mobile phase). Then the reaction mixture was poured into brine (100 ml) and extracted with EtOAc (3 × 75 ml). The organic phase was dried over Na_2SO_4, filtered and the solvent was removed under reduced pressure. The residue was purified twice by column chromatography over silica gel using 50%, 80% and 100% EtOAc in hexane as mobile phase. The product was recrystallised from diethyl ether and hexane to obtain orange solid as final compound (0.269 g, 51%). M.p.: 104-106 °C (novel compound). ^{1}H-NMR (400 MHz, $CDCl_3$): δ 8.52 (d, 1H, J = 8.77 Hz, NBD), 6.56 (s, 1H, NH), 6.21 (d, 1H, J = 8.81 Hz, NBD), 3.62 (m, 2H, 3β-H, 7α-H), 3.49 (m, 2H, 24-CH_2), 1.00 (d, 3H, J = 6.52 Hz, 21-CH_3), 0.97 (s, 3H, 19-CH_3), 0.70 (s, 3H, 18-CH_3). ^{13}C-NMR ppm (100 MHz, $CDCl_3$): δ 144.05 (C, NBD), 143.73 (C, NBD), 136.41 (CH, NBD), 123.55 (C, NBD), 98.35 (CH, NBD), 71.22 (CH, 7-C), 71.19 (CH, 3-C). IR_{vmax} (KBr): 3413.71, 2932.43, 2865.87, 1585.58, 1300.72 and 1271.70 cm^{-1}. HRMS: Found: $(M\text{-}Na)^+$ = 563.3205, calculated for $C_{30}H_{44}N_4O_5Na$ = 563.3209.

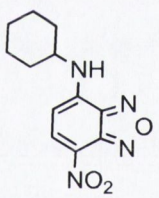

135

To a solution of NBD chloride (0.443 g) and $NaHCO_3$ (0.254 g) in MeOH (30 ml) was added cyclohexylamine (0.23 ml) at rt and stirred. Reaction completion was monitored by TLC using hexane : EtOAc (3 : 1) as mobile phase, then the mixture was poured into brine (100 ml) and extracted with EtOAc (3 × 50 ml). The organic phase was dried over Na_2SO_4, filtered and the solvent was removed under reduced pressure. The crude product was purified by column chromatography using pet ether : EtOAc (3 :1) as mobile phase to obtain the product as orange solid (0.431 g, 81%). ^{1}H-NMR (400 MHz, $CDCl_3$): δ 8.50 (d, 1H, J = 8.31 Hz, NBD), 6.26-6.20 (m, 2H, NH and NBD), 3.70 (s, 1H, cyclohexyl), 2.20 (s, 2H, cyclohexyl), 1.89 (s, 2H, cyclohexyl), 1.78 (d, 1H, cyclohexyl), 1.48 (m, 4H, cyclohexyl), 1.35 (m, 1H, cyclohexyl). ^{13}C-NMR ppm (100 MHz, $CDCl_3$): δ 144.48 (C, NBD), 144.10 (C, NBD), 143.06 (C, NBD), 136.77 (CH, NBD), 123.54 (C, NBD), 98.77 (CH, NBD), 52.99 (CH, cyclohexyl), 32.34 (CH_2, cyclohexyl), 25.33 (CH_2, cyclohexyl), 24.68 (CH_2, cyclohexyl). IR_{vmax} (KBr): 3380.11, 2929.89,

1572.27, 1493.35 and 1317.80 cm^{-1}. HRMS: Found: $(M\text{-}Na)^+$ = 285.0964, calculated for $C_{12}H_{14}N_4O_3Na$ = 285.0964.

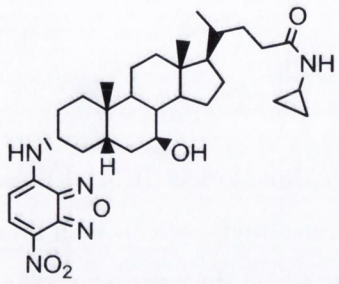

136

To a solution of **126** (0.100 g) in DMF (10 ml) were added EDC hydrochloride (0.173 g) and HOBt x H_2O (0.122 g) at 0 °C under N_2 atmosphere and stirred at rt overnight, after which time the mixture was cooled to 0 °C and cyclopropylamine (0.04 ml) was added then stirred at rt for 30 min. Reaction completion was monitored by TLC using EtOAc as mobile phase, then the mixture was poured into 1 M HCl solution (50 ml) and extracted with EtOAc (3 × 50 ml). The organic phase was dried over Na_2SO_4, filtered and the solvent was removed under reduced pressure. The crude product was purified by column chromatography using EtOAc as mobile phase to obtain the product as orange solid (0.096 g, 90%). ^{1}H-NMR (400 MHz, DMSO-d_6): 9.25 (s, 1H, 7β-OH), 8.48 (d, 1H, J = 9.04 Hz, aromatic-H), 6.49 (d, 1H, J = 9.04 Hz, aromatic-H), 3.35 (s, 1H, 7α-H), 0.94 (s, 3H, 19-CH_3), 0.89 (d, 3H, J = 5.04 Hz, 21-CH_3), 0.63 (s, 3H, 18-CH_3), 0.59 (d, 2H, J = 5.04 Hz, CPA), 0.35 (d, 2H, J = 1.76 Hz, CPA). ^{13}C-NMR ppm (100 MHz, DMSO-d_6): 173.60 (C=O, 24-C), 144.48 (C, aromatic-C), 144.22 (C, aromatic-C), 138.00 (CH, aromatic-C), 120.18 (C, aromatic-C), 99.12 (CH, aromatic-C), 69.32 (CH, 7-C), 5.63 (CH_2, CPA), 5.61 (CH_2, CPA). IR_{vmax} (KBr): 3446.50, 2932.98, 1621.50, 1580.13, 1448.87, 1300.93 and 1240.66 cm^{-1}. HRMS: Found: $(M\text{-}Na)^+$ = 616.3510, calculated for $C_{33}H_{47}N_5O_5Na$ = 616.3475.

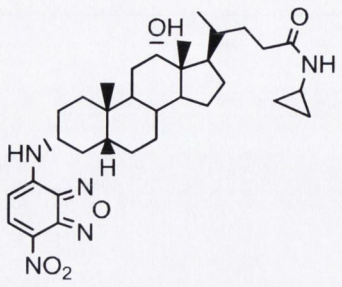

137

To a solution of **99** (0.100 g) in DMF (10 ml) were added EDC hydrochloride (0.345 g) and HOBt × H_2O (0.244 g) at 0 °C under N_2 atmosphere and stirred at rt overnight, after which time the mixture was cooled to 0 °C and cyclopropylamine (0.04 ml) was added then stirred at rt for 30 min. Reaction completion was monitored by TLC using EtOAc as mobile phase, then the mixture was poured into 1 M HCl solution (50 ml) and extracted with EtOAc (3 × 50 ml). The organic phase was dried over Na_2SO_4, filtered and the solvent was removed under reduced pressure. The crude product was purified by column chromatography using EtOAc as mobile phase to obtain the product as orange solid (0.100 g, 94%). ^{1}H-NMR (400 MHz, $CDCl_3$): δ 8.48 (d, 1H, J = 8.76 Hz, aromatic-H), 7.43 (br. s, 1H, amide bond), 6.90 (br. s, 1H, 3-NH), 6.21 (d, 1H, J = 8.52 Hz, aromatic-H), 4.04 (s, 1H, 12β-H), 1.01 (s, 3H, 19-CH_3), 0.97 (d, 3H, J = 5.52 Hz, 21-CH_3), 0.77 (d, 2H, J = 6.24 Hz, CPA), 0.70 (s, 3H, 18-CH_3), 0.51 (s, 2H, CPA). ^{13}C-NMR ppm (100 MHz, $CDCl_3$): δ 175.58 (C=O, 24-C), 150.21 (C, aromatic-C), 144.50 (C, aromatic-C), 143.52 (C, aromatic-C), 136.94 (C, aromatic-CH), 123.04 (CH, aromatic-C), 98.66 (C, aromatic-CH), 73.42 (CH, 12-C), 6.72 (CH_2, CPA), 6.70 (CH_2, CPA). IR_{vmax} (KBr): 3399.06, 2934.38, 2865.28, 1620.76, 1581.44, 1447.63, 1303.34 and 1279.23 cm^{-1}. HRMS: Found: $(M\text{-}Na)^+$ = 616.3505, calculated for $C_{33}H_{47}N_5O_5Na$ = 616.3475.

5.2. Chapter 3 Methods

5.2.1. Absorption measurements

A Cary 300 Scan UV-Visible Spectrophotometer was used to determine the absorption maxima of the fluorescent compounds at rt. The stock solutions were prepared at 0.01 mg/ml (NBDs) or 0.02 mg/ml (dansyls) in EtOH or in water/1% pH = 3.0 ammonium formate buffer/acetonitrile (15:10:75) solution at pH=3.58. Samples were scanned from 200–800 nm. Cuvette type was Hella Blue quartz 10 mm.

5.2.2. Fluorescence measurements

To obtain the fluorescence maxima the stock solutions were prepared in 0.001 mg/ml (NBDs) or 0.02 mg/ml (dansyls) in EtOH or in water/1% pH = 3.0 ammonium formate buffer/acetonitrile (15:10:75) solution at pH=3.58. The fluorescence was measured with RF-1501 Spectrofluorophotometer (SHIMADZU) at rt. The emission wavelength range was chosen between 220–900 nm, while the excitation wavelengths were chosen according to the absorption maxima of the compounds. Cuvette type was Hella Blue quartz 10 mm.

5.2.3. Fluorescence quantum yield

A Cary 300 Scan UV-Visible Spectrophotometer was used to determine the absorption maxima of **5–8** at rt. The stock solutions were prepared at 0.01 mg/ml in EtOH. Samples were scanned from 200–800 nm. Cuvette type was Hella Blue quartz 10 mm. To obtain the fluorescence maxima the stock solutions were prepared in 0.001 mg/ml in EtOH and measured with RF-1501 Spectrofluorophotometer (SHIMADZU) at rt. The emission wavelength range was chosen between 220–900 nm, while the excitation wavelength was 470 nm. Fluorescein and rhodamine 6G were cross-calibrated by calculating the quantum yield of each relative to the other. The results matched the literature +/- 10%: fluorescein Φ_F 0.922, rhodamine 6G Φ_F 0.953. The absorbance and emission levels in the concentration range 10–50 μM for five solutions of each sample and standard were obtained. (Fluorescein in ethanolic KOH (0.01 M), all other solutions in EtOH.) The slope of a plot of fluorescence intensity versus absorbance was used to calculate the quantum yield (Φ_F) for each sample using the equation: $\Phi_F = \Phi_{ST}(S_X/S_{ST})$.

5.2.4. Stability study of 3β-NBD UDCA (101) and 3β-NBD DCA (119) by HPLC

For the HPLC measurements, a WATERS Alliance system was used with 2475 Multi λ Fluorescence Detector and 2487 Dual λ Absorbance Detector controlled by EMPOWER Software. The reverse phase HPLC column was a C18 5 μm 4.6 × 250 mm from Xbridge™.

For the stability study of **101**, a stock solution was prepared in 0.01 mg / ml with 2% acetonitrile / phosphate buffer (pH = 7.4), while the stock solution of **119** was prepared at 0.01 mg/ml with 5% acetonitrile/phosphate buffer (pH=7.4). The stability study was carried out at 37 °C over 24 h with injection every hour. HPLC conditions were flow rate: 1.0 ml/min; wavelength of detection: 346 nm; injection volume: 20 μl; temperature of column and sample: 37 °C; runtime: 25 min;

gradient 0 min 50% mobile phases A and B, 0 – 10 min increase to 80% mobile phase B, 10 –20 min 80% mobile phase B, 20 – 21 min decrease to 50% mobile phase B, 21 – 25 min 50% mobile phases A and B; mobile phase A: pH = 2.5 phosphate buffer; mobile phase B: acetonitrile.

5.2.5. Cell cultures

5.2.5.1. HET1A

HET-1A is an adherent epithelial cell line derived in 1986 from human esophageal autopsy tissue of a 25 year old man. The cell line was purchased from American Type Culture Collection (ATCC, Rockville, MD). Cells were cultured in bronchial epithelial cell basal medium (Lonza Group Ltd, Switzerland) supplemented with triiodothyronine, insulin, transferrin, retinoic acid, hydrocortisone, human recombinant epidermal growth factor, epinephrine and bovine pituitary extract. Cultures were maintained at 37 °C in a humidified atmosphere containing 5% CO_2 and routinely maintained in T-75 cm^2 cell culture flasks (Nunclon, Roskilde, Denmark) in a volume of 10 ml medium. Cells were passaged twice a week (1/3 dilution). Cells were washed with Hanks balanced salt solution (HBSS) and removed from plastic surface using trypsin (1 ml, 0.05% w/v) (Gibco, Invitrogen Ltd., Paisley, UK) to form a cell suspension. The trypsin was neutralised with soya bean trypsin inhibitor (1 ml, 0.05% w/v) (Sigma-aldrich, St. Louis, MO, USA). A cell pellet was obtained by centrifuging at 1200 rpm for 3 min. The pellet was resuspended in culture media and divided into cell culture flasks for maintenance of cell stock or enumerated in the conventional way using a haemacytometer prior to use in an experiment.

5.2.5.2. SKGT4

The SKGT4 cell line, an adherent cell line derived from a well-differentiated adenocarcinoma arising in Barrett's epithelium of the distal esophagus was generously provided by Dr. David Schrump (Bethesda, MA) [227]. Cells were maintained in RPMI 1640 medium supplemented with 10% heat-inactivated fetal bovine serum (FBS) and 4 mM L-Glutamine (GIBCO, Invitrogen Ltd., Paisley, UK) at 37 °C in a humidified atmosphere containing 5% CO_2 and routinely maintained in T-75 cm^2 cell culture flasks (Nunclon, Roskilde, Denmark) in a volume of 10 ml medium. Cells were passaged three times a week (1/3 or 1/6 dilution). Cells were washed with PBS and removed from plastic surface using trypsin (2 ml, 0.05% w/v) to form a cell suspension which was diluted by adding double the volume of cell culture medium. A cell pellet was

obtained by centrifuging at 1200 rpm for 3 min. The pellet was resuspended in culture media and divided into cell culture flasks for maintenance of cell stock or enumerated in the conventional way using a haemacytometer prior to use in an experiment.

5.2.5.3. HUH7

The hepatic (HUH7) cells were maintained in DMEM medium supplemented with 10% heat-inactivated fetal bovine serum (FBS) at 37 °C in a humidified atmosphere containing 5% CO_2 and routinely maintained in T-75 cm^2 cell culture flasks (Nunclon, Roskilde, Denmark) in a volume of 10 ml medium. Cells were passaged three times a week (1/3 or 1/6 dilution). Cells were washed with PBS and removed from plastic surface using trypsin (2 ml, 0.05% w/v) to form a cell suspension which was diluted by adding double the volume of cell culture medium. A cell pellet was obtained by centrifuging at 1200 rpm for 3 min. The pellet was resuspended in culture media and divided into cell culture flasks for maintenance of cell stock or enumerated in the conventional way using a haemacytometer prior to use in an experiment.

5.2.6. The MTT assay

Cell viability was measured using the 3-[4,5-dimethylthiazol-2-yl]-2,5-diphenyltetrazolium bromide (MTT) assay. Cells were plated into 96 well plates at a concentration of 8×10^4 cells/ml (HET1A), 6×10^4 cells/ml (SKGT4) and 10×10^4 cells/ml (HUH7) in a 100 µl volume. After 24 h the cells were treated with the fluorescent bile acids at indicated concentrations for the appropriate time in supplement free medium. Control wells were treated with medium without supplements as a positive control for cell death. Vehicle control wells were treated with DMSO 1%. After 22 h cells were incubated with 20 µL of MTT solution for a further 2 h. The medium was aspirated from the wells and DMSO (100 µL) added to each well to lyse the cells. The plates were shaken for 10 min to dissolve the formazan crystals and then read on a VERSAmax Microplate Reader (Molecular Devices, Sunnyvale, CA, USA) at a wavelength of 570 nm. Cell survival rates were determined by calculating to the DMSO control.

5.2.7. InCell measurements

HET1A cells (3×10^4 cells/well) were plated into 96 well glass plate in a 200 µl volume and incubated for 24 h before treatment at 37 °C. After this time Hoechst 33342 (5 µg/ml) (blue, NBDs) dye was added to each well for 15 min to stain the nuclei. The medium was removed then

and NBD compounds were added into the wells at 1 μM (prepared in supplement free medium containing 1% of DMSO) immediately before the beginning of the measurements. Control wells were left untreated or treated with 1% DMSO as a vehicle. Images were acquired using the GE InCell Analyser 1000. Four fields of view per well were acquired using a 10 × objective for n=3 experiments.

5.2.8. Confocal measurements

5.2.8.1. Uptake study

Preparation of the samples: 3×10^4 cells (HET1A) were plated into 96 well glass plate in a 200 μl volume and incubated for 24 h before treatment at 37 °C. After this time Hoechst 33342 (5 μg/ml) (blue, NBDs) or Draq5 (1/500 dilution, red, dansyls) dyes were added to each well for 15 min to stain the nuclei. The medium was removed then and NBD compounds were added into the wells at 1 μM, while dansyls at 10 μM (prepared in supplement free medium containing 1% of DMSO) immediately before the beginning of the measurements. Control wells were left untreated or treated with 1% DMSO as a vehicle. The images were taken using a Nikon T800 confocal fluorescent microscope and analysed by the LSM Image Browser program. Original magnification ×63.

5.2.8.2. Inhibition of vesicular transport

HET1A cells (3×10^4 cells/well) were plated into 96 well glass plate in a 200 μl volume and incubated for 24 h before treatment at 37 °C. After this time the cells were treated with Primaquine (300 μM) (Sigma-Aldrich) or Cytochalasin D (3 μM) (Sigma-Aldrich) and incubated for 30 min. Hoechst 33342 (5 μg/ml) (blue, NBDs) dye was added then to each well for 15 min to stain the nuclei. The medium was removed then NBD compounds were added into the wells at 1 μM (prepared in supplement free medium containing 1% of DMSO) immediately before the beginning of the measurements. Control wells were left untreated or treated with NBDs as a vehicle. Images were acquired using the GE In Cell Analyser 1000. Four fields of view per well were acquired using a 10 × objective for n=3 experiments.

5.2.8.3. Competition experiments

Preparation of the samples: 3×10^4 cells (HET1A) were plated into 96 well glass plate in a 200 µl volume and incubated for 24 h before treatment at 37 °C. The medium was removed then and the cold bile acids were added at the appropriate concentration (prepared in supplement free medium) and incubated for 1 h (pretreatment experiments). After this time the medium was removed and Hoechst 33342 (5 µg/ml) (blue, NBDs) or Draq5 (1/500 dilution, red, dansyls) dyes were added to each well for 15 min to stain the nuclei. NBD compounds were added into the wells at 1 µM, while dansyls at 10 µM (prepared in supplement free medium containing 1% of DMSO) immediately before the beginning of the measurements. In the co-treatment experiments the cold bile acids and the fluorescent bile acids were prepared in supplement free medium containing the compartments at the appropriate concentrations. Control wells were left untreated or treated with 1% DMSO as a vehicle. The images were taken using a Nikon T800 confocal fluorescent microscope and analysed by the LSM Image Browser program. Original magnification ×63.

5.2.8.4. Organelle staining in fixed cells

After the appropriate treatment time HET1A cells were fixed with 4% paraformaldehyde and then permeabilized with 0.1% (vol/vol) Triton X-100/phosphate-buffered saline followed by blocking with 5% bovine serum albumin/phosphate-buffered saline. Cells were incubated with anti-GM130 Golgi antibody (Sigma–Aldrich Chemical Co.) and then incubated with AlexaFluor-488-conjugated secondary antibody (Invitrogen). cells were fixed with 4% paraformaldehyde/PBS (15 min) then permeabilised with 0.1% (v/v) Triton X-100/PBS (5 min) followed by blocking with 3% BSA/PBS (30 min-overnight). Cells were incubated with purified monoclonal mouse anti-glucocorticoid receptor (GR) antibody (0.5 µg/ml, 50 µl, 1 h) (BD Biosciences, San Jose, California, USA) then incubated with AlexaFluor-488-conjugated secondary antibody (80 µg/ml , 50 µl, 30 min) (Invitrogen, Carlsbad, CA, USA) protected from light. Control wells were treated similar way excluding the incubation step with the primary antibody. Finally the nuclei were stained with Hoechst 33342 (10 µg/ml, 50 µl, 15 min) (Invitrogen, Carlsbad, CA, USA) and the images were taken using a Nikon T800 confocal fluorescent microscope and analysed by the LSM Image Browser program. Original magnification ×63.

5.2.8.5. Live cell Golgi staining

HET1A cells (3×10^4 cells/well) were plated into 96 well glass plate in a 200 µl volume and incubated for 24 h before treatment at 37 °C. After this time Human Golgi-resident enzyme (*N*-acetylgalactosaminyltransferase 2, CellLight®) was added at 1×10^8 particles/ml in BEBM and incubated for 16 h. Hoechst 33342 (5 µg/ml) (blue, NBDs) dye was added then to each well for 15 min to stain the nuclei. The medium was removed then NBD compounds were added into the wells at 1 µM (prepared in supplement free medium containing 1% of DMSO) immediately before the beginning of the measurements. Control wells were left untreated or treated with 1% DMSO as a vehicle. Images were acquired using the GE In Cell Analyser 1000. Four fields of view per well were acquired using a 10 × objective for n=3 experiments.

5.2.9. Analysis of biological samples by HPLC

Preparation of the samples: 8×10^4 cells in a 250 µl volume were plated into 48 well plate and incubated for 24 h before treatments. The medium was removed then and NBD compounds were added into the wells at 1 µM, while dansyls at 10 µM (prepared in supplement free medium containing 1% of DMSO) at 37 or 4 °C. After the appropriate incubation time the medium was collected into eppendorfs and NP 40 lysis buffer was added to the cells and shaken for 15 min, after which time the lysate was also collected into eppendorfs and stored at -20 °C until the measurements.

For the HPLC measurements, WATERS Alliance system was used with 2475 Multi λ Fluorescence Detector and 2487 Dual λ Absorbance Detector controlled by EMPOWER Software. The applied column symmetry was C18 5 µm 4.6 × 250 mm from Xbridge™.

The measurement of the biological samples was carried out at rt. HPLC conditions were flow rate: 1.5 ml/min; wavelength of excitation: 470 nm (NBDs) and 335 nm (dansyls) wavelength of detection: 540 nm (NBDs), 517 nm (dansyls); injection volume: 20 µl; temperature of column and sample: rt; runtime: 20 min; isocratic water/1% pH=3.0 ammonium formate buffer/acetonitrile (15:10:75), pH=3.58.

5.2.10. Uptake studies in Caco-2 cell line

Caco-2 cells were grown to polarized monolayers on 24-well plates for 21 days, before uptake studies were performed in bicarbonated Krebs-Ringer buffer (KRB: 15 mM HEPES, 116.4 mM NaCl, 5.4 mM KCl, 0.78 mM NaH_2PO_4, 25 mM $NaHCO_3$, 1.8 mM $CaCl_2$, 0.81 mM $MgSO_4$ and 5.55 mM glucose; pH 7.4). Uptake of the fluorescent bile acid compounds (**3-6**) was studied at different time points, concentrations and temperatures. Bile acid compounds were dissolved in KRB containing 0.1% DMSO at all times.

Time-dependence of bile acid uptake including the control fluorophore substances was studied by incubating cell monolayers (at 10 μM final concentration) for up to 90 min at either 37°C or 4°C. After 5, 10, 15, 30, 45, 60 and 90 min, monolayers were washed twice with ice-cold KRB, solubilized in 1% (w/v) Triton X-100 solution and bile acid activity was measured in the cell lysate (see below). Concentration-dependence of bile acid uptake was studied at a compound concentration range of 1 to 100 μM for 20 min at 37°C and 4°C. Active uptake of bile acid compounds was calculated as the difference between the fluorescence, after exposure to **99**, **101**, **119** and **126** at 37°C and 4°C.

The fluorescence activity of the bile acids compounds was analyzed in 24-well plates using an automated plate reader (FLUOstar Optima, BMG Labtech, Offenburg, Germany) at excitation and emission wavelengths of 485 and 520 nm, respectively. The samples were diluted with KRB, where appropriate. For standardization, the total protein amount of cell layers was determined by bicinchoninic acid (BCA) assay according to the manufacturer's instructions (Pierce, Thermo Scientific, Rockford, USA).

5.2.11. Kinetics

The saturable transport of the bile acid compounds was analyzed by assuming Michaelis-Menten type carrier-mediated transport represented by the equation:

$v = V_{max} \times (S) / [(K_m + (S)]$, where (S) was [bile acid compound].

Half-saturation constant (K_m) and maximum uptake rates (V_{max}) of the bile acid compounds was calculated by this equation to the experimental profile of the uptake rate (v) versus the substrate concentration (S) using a non-linear least squares regression analysis program, WinNonlin (Pharsight, Mountain View, CA, USA).

5.2.12. Molecular modelling

The strucutres of DCA and its 3-α and -β NBD analogs were generated by *in silico* modification in MOE (Chemical Computing Group, Montreal, Canada) of cholic acid extracted from pdb code 2QO4 [167]. The bile acid models were energy minimised using Merck Molecular Force Field 94x (MMFF94x) interfaced to MOE with gradient 0.5. Then structures were further manipulated in MOE.

5.3. Chapter 4

5.3.1. Chemistry

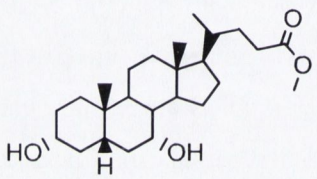

149

To a solution of CDCA (5 g, 12.7 mmol) dissolved in MeOH (94 ml), concentrated HCl (37%, 0.53 ml, 6.35 mmol) was added drop-wise using a syringe. The mixture was stirred under reflux and left overnight. The formation of the product was followed using TLC analysis. When the reaction was complete, the solvent was removed under reduced pressure giving white, odourless solid (5.07 g, 98%). ^{1}H-NMR (400 MHz, $CDCl_3$): δ 3.88 (m, 1H, 7β-H), 3.67 (s, 3H, -OCH_3), 3.5 (m, 1H, 3β-H,), 0.96 (d, 3H, 21-CH_3), 0.92 (s, 3H, 19-CH_3), 0.67 (s, 3H 18-CH_3). ^{13}C-NMR ppm (100 MHz, $CDCl_3$): δ 174.36 (C=O, 24-C), 71.76 (CH, 3-C), 68.26 (CH, 7-C), 51.09 (CH_3, O$\underline{C}H_3$). IR_{vmax} (KBr): 3424.28, 2932.36, 2866.53, 1741.25, 1447.62, 1375.42 cm^{-1}. HRMS: Found: $(M\text{-}Na)^+$ = 429.2987, calculated for $C_{25}H_{42}O_4Na$ = 429.2981.

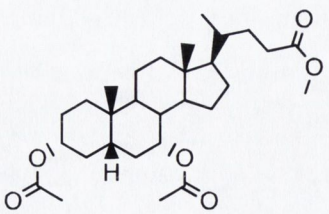

150

Compound **149** (2 g, 4.92 mmol) and 4-DMAP (120 mg, 0.98 mmol) were both dissolved in anhydrous pyridine (30 ml). Ac_2O (14 ml, 148 mmol) was added to the solution and the reaction mixture was allowed to stir overnight at rt. The mixture was poured into water (200 ml) and the

compound was extracted with EtOAc : hexane (1:1) (3 × 100 ml). The organic phases were combined and washed with 1M HCl (100 ml), water (100 ml) and brine (100 ml). The organic layer was dried over $MgSO_4$ and filtered. The solvent was removed and the semi-solid residue was purified by flash column chromatography using hexane: EtOAc (3:1) as mobile phase. white foam (67%, 1.617 g). ^{1}H-NMR (400 MHz, $CDCl_3$): δ 5.12 (m, 1H, 7β-H), 4.83 (sex, 1H, J_1 = 4.02 Hz, J_2 = 7.02 Hz, J_3= 4.52 Hz, 3β-H), 3.91 (s, 3H, -O-CH_3), 2.48 (s, 3H, 3 –C=OCH_3), 2.43 (s, 3H, 7 –C=OCH_3), 1.31 (s, 3H, 19-CH_3), 1.28 (d, 3H, J = 6.53 Hz, 21-CH_3) 0.89 (s, 3H, 18-CH_3). ^{13}C-NMR ppm (100 MHz, $CDCl_3$): 173.54 (C=O, 24-C), 169.49 and 169.28 (2C=O, 3-C=OCH_3 and 7-C=OCH_3), 73.08 and 70.15 (2CH, 3-C and 7-C), 51.08 (CH_3, OCH_3), 21.17 (CH_3, 7-OC=OCH_3), 21.06 (CH_3, 3-OC=OCH_3). IR_{vmax} (KBr): 2942.84, 2872.20, 2848.09, 1734.83, 1466.86, 1438.18, 1378.44, 1364.49, 1248.94 cm^{-1}. HRMS: Found: $(M\text{-}Na)^+$ = 513.3208, calculated for $C_{29}H_{46}O_6Na$ = 513.3192.

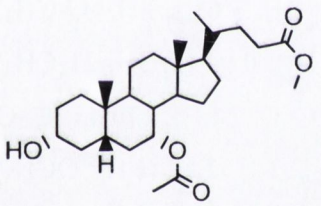

151

Compound **150** (1.55 g, 3.17 mmol) was dissolved in anhydrous MeOH (22 ml) then AcCl (0.29 ml, 4.078 mmol), dissolved in MeOH (3 ml) was added drop-wise to the reaction mixture at 0 °C. The mixture was allowed to reach rt and left stirring for 20 h then it was quenched by the addition of saturated $NaHCO_3$ (70 ml) and water. The compound was extracted using EtOAc (3 × 50 ml) the organic phase was dried over $MgSO_4$. The organic solvent was removed under reduced pressure and the product formed as a white solid (1.294 g, 91%). ^{1}H-NMR (400 MHz, $CDCl_3$): δ 4.86 (m, 1H, 7β-H), 4.12 (m, 1H, 3β-H), 3.65 (s, 3H, -O-CH_3), 1.97 (s, 3H, 7 –C=OCH_3), 0.91 (s, 3H, 19-CH_3), 0.9 (d, 3H, 21-CH_3) 0.63 (s, 3H, 18-CH_3). ^{13}C-NMR ppm (100 MHz, $CDCl_3$): δ 174.30 (C=O, 24-C), 170.23 (C=O, 7-C=OCH_3), 71.32 and 70.91 (2CH, 3-C and 7-C), 51.08 (CH_3, OCH_3), 21.21 (CH_3, 7-OC=OCH_3). HRMS: Found: $(M\text{-}Na)^+$ = 471.3084, calculated for $C_{27}H_{44}O_5Na$ = 471.3086.

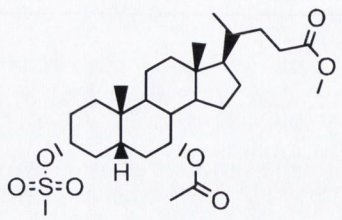

152

To a stirred solution of **151** (1.273 g, 2.84 mmol) in anhydrous DCM (38 ml) was added Et_3N (0.43 ml, 3.105 mmol). Methanesulfonyl chloride (0.331 ml, 4.276 mmol) dissolved in anhydrous DCM (12 ml) was added drop-wise to the mixture at 0 °C. The reaction mixture was stirred for 30 min, after which time TLC analysis showed that the reaction was complete, then it was quenched by cooled water (50 ml). The compound was extracted using DCM (2 × 40 ml). The organic phase was washed with brine (100 ml), dried over $MgSO_4$ and filtered. The solvent was removed using the rotary evaporator, ensuring the bath temperature was no higher than 40 °C. The flask was placed under high pressure, giving semi-solid oil as the product (1.43 g, 96%). ^{1}H-NMR (400 MHz, $CDCl_3$): δ 4.90 (m, 1H, 7β-H), 4.52 (m, 1H, 3β-H), 3.68(s, 3H, -O-CH_3), 3.02(s, 3H, -OSO_2CH_3), 2.08 (s, 3H, 7-C=OCH_3), 0.96 (s, 3H, 19-CH_3), 0.94 (d, 3H, 21-CH_3), 0.67 (s, 3H, 18-CH_3). ^{13}C-NMR ppm (100 MHz, $CDCl_3$): δ 174.69 (C=O, 24-C), 170.43 (C=O, 7-O<u>C</u>=OCH_3), 81.39 (CH, 3-C), 71.01 (CH, 7-C), 52.57 (CH_3, -OSO_2<u>C</u>H_3), 51.52 (CH_3, O<u>C</u>H_3), 21.59 (CH_3, 7-C=O<u>C</u>H_3). HRMS: Found: $(M\text{-}Na)^+$ = 549.2874, calculated for $C_{28}H_{46}O_7SNa$ = 549.2862.

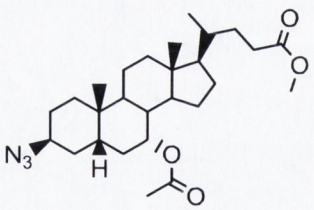

153

To a solution of **152** (1.791 g, 3.4 mmol) in DMPU, was added NaN_3 (2.21 g, 34 mmol) at 50 °C. The reaction mixture was left stirring for 5 d and then poured into distilled water (100 ml). EtOAc (3 × 100 ml) was used to extract the compound. The organic phase was washed with brine (100 ml), dried over Na_2SO_4 and filtered. The solvent was removed under reduced pressure, the residue was purified by flash column chromatography, using 25% EtOAc in hexane as mobile phase. The yield product was white foam (1.369 g, 85%). ^{1}H-NMR (400 MHz, $CDCl_3$): δ 4.89 (m, 1H, 7β-H), 3.96 (m, 1H, 3α-H), 3.67 (s, 3H, -O-CH_3), 2.05 (s, 3H, 7-C=OCH_3), 0.96

(s, 3H, 19-CH_3), 0.92 (d, 3H, 21-CH_3), 0.65 (s, 3H, 18-CH_3). ^{13}C-NMR ppm (100 MHz, $CDCl_3$): δ 174.95 (C=O, 24-C), 170.60 (C=O, 7-OC=OCH_3), 71.64 (CH, 7-C), 58.65 (CH, 3-C), 51.65 (CH_3, O$\underline{C}H_3$), 21.68 (CH_3, 7-C=O$\underline{C}H_3$). IR $_{vmax}$ (KBr): 2940.67, 2871.82, 2099.71(N_3), 1734.83, 1438.26, 1376.34, 1247.76, 1222.33 cm^{-1}.

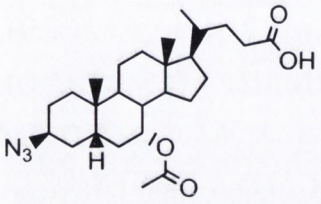

154

Compound **153** (0.78 g, 1.647 mmol) was dissolved in MeOH (10 ml) and 1M NaOH (2 ml) was added drop-wise to the solution, until pH~14 was attained. The mixture was stirred at rt. After 48 h, more aqueous NaOH (2 ml) was added and the temperature of the reaction was raised to 65 °C. The reaction was monitored using TLC analysis and once complete, the mixture was poured into 2M HCl (50 ml) and extracted using EtOAc (3 × 50ml). The organic phase was washed with water (2 × 100 ml) and brine (100 ml), dried over Na_2SO_4, filtered and the solvent removed under the high vacuum to afford the product as white foam (0.719 g, 95%). ^{1}H-NMR (400 MHz, $CDCl_3$): δ 4.91 (m, 1H, 7β-H), 3.97 (m, 1H, 3β-H), 3.33 (s, 3H, -O-CH_3), 2.05 (s, 3H, 7-C=OCH_3), 0.98 (s, 3H, 19-CH_3), 0.97 (d, 3H, 21-CH_3), 0.73 (s, 3H, 18-CH_3). IR_{vmax} (KBr): 3329.05, 2927.43, 2101.15, 1732.77 and 1247.18 cm^{-1}., HRMS: Found: $(M-H)^-$ = 458.3015, calculated for $C_{26}H_{40}N_3O_4$ = 458.3019.

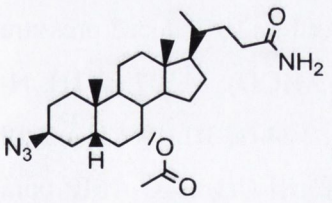

155

Compound **154** (0.15 g, 0.326 mmol) was dissolved in anhydrous THF (15 ml) and acetonitrile (1.5 ml), then N-OH-Su (0.124 g, 1.07 mmol) and DCC (0.22 g, 1.06 mmol) were added to the mixture and the reaction was left stirring overnight. The white solid formed was filtered off and the filtrate was concentrated using the rotary evaporator and placed under high vacuum. The compound was then dissolved in DMF and ammonia solution (37%, 0.054 ml) was added. The

white solid precipitated from the mixture when brine (70 ml) was added. The mixture was filtered using suction filtration. The filtrate was washed with water (2 × 30 ml) and allowed to dry in the air. Column chromatography was carried out using 50-100% EtOAc in hexane as the mobile phase. The organic solvent was removed under reduced pressure leaving behind the dried solid (0.147 g, 98%). ^{1}H-NMR (400 MHz, $CDCl_3$): δ 5.49 (s, 2H, NH_2), 4.90 (m, 1H, 7β-H), 3.93 (m, 1H, 3α-H), 2.05 (s, 3H, 7-C=OCH_3), 0.97 (s, 3H, 19-CH_3), 0.94 (d, 3H, 21-CH_3), 0.67 (s, 3H, 18-CH_3). ^{13}C-NMR ppm (100 MHz, $CDCl_3$): δ 175.5 (C=O, C=ONH_2), 169.9 (C=O, 7-C=O), 71.00 (CH, 3-C), 58.08 (CH, 7-C). IR_{vmax} (KBr): 3328.23, 2927.53, 2100.90, 1665.73 and 1247.07 cm^{-1}. HRMS: Found: $(M\text{-}Na)^+$ = 481.3153, calculated for $C_{26}H_{42}N_4O_3Na$ = 481.3155.

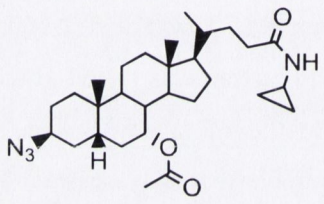

156

To a solution of **154** (0.1 g, 0.217 mmol) in anhydrous DMF (10 ml) was added HOBt monohydrate (0.044 g, 0.325 mmol) and EDC (0.047 ml, 0.26 mmol) at 0 °C under N_2 atmosphere. After 10 min, a solution of cyclopropylamine (0.023 ml, 0.322 mmol) dissolved in anhydrous DMF (0.5 ml) was added slowly to the mixture and left stirring for 24 h. Once complete, the reaction mixture was poured into brine (70 ml) and extracted using EtOAc (3 × 50 ml). The organic phase was dried over Na_2SO_4, filtered and the solvent was removed using the rotary evaporator. The crude product was purified by flash column chromatography using gradient elution (25-100% EtOAc in hexane). The solvent was removed under reduced pressure giving a white solid (0.047 g, 43%) as product. ^{1}H-NMR (400 MHz, MeOD): δ 7.07 (s, 1H, N-H), 6.3 (m, 1H, 7β-H), 5.35 (m, 1H, 3α-H), 3.47 (s, 3H, 7-OC=OCH_3), 2.34 (s, 3H, 19-CH_3), 2.19 (d, 3H, 21-CH_3), 2.07 (s, 3H, 18-CH_3), 2.08 and 1.91 (m, 2H, cyclopropyl-CH_2). ^{13}C-NMR ppm (100 MHz, MeOD): δ 174.78 (C=O, C=ONH_2), 170.16 (C=O, 7-OC=OCH_3), 71.25 (CH, 3-C), 6.49 (CH_2, cyclopropyl-CH_2). IR_{vmax} (KBr): 3429.95, 2938.13, 2100.42, 1734.02, 1651.02 and 1248.42 cm^{-1}. HRMS: Found: $(M\text{-}Na)^+$ = 521.3463, calculated for $C_{29}H_{46}N_4O_3Na$ = 521.3468.

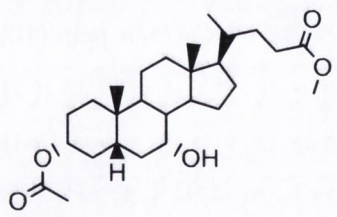

157

To a solution of **149** (2 g, 4.9 mmol) in DCM (30 ml), were added Ac_2O (3.25 ml, 34.3 mmol) and pyridine (5.97 ml, 73.8 mmol). After 16 h, TLC analysis showed that the reaction had gone to completion. EtOAc (100 ml) was added to the mixture and washed with 1M HCl (100 ml) and water (2 × 100 ml). The organic layer was collected, dried over $MgSO_4$ and filtered. The crude product was purified by flash column chromatography (Hexane: EtOAc, 3:1) and the solvent was removed under high vacuum to produce a white solid (1.668 g, 76%). ^{1}H-NMR (400 MHz, $CDCl_3$): δ 4.82 (m, 1H, 3β-H), 4.10 (1H, 7β-H), 3.91 (s, 3H, -O-CH_3), 2.26 (3H, 3-C=O-CH_3), 1.18 (d, 3H, 21-CH_3), 1.16 (s, 3H, 19-CH_3), 0.91 (s, 3H, 18-CH_3). ^{13}C-NMR ppm (100 MHz, $CDCl_3$): δ 174.33 (C=O, 24-C), 170.38 (C=O, 3-C=OCH_3) 74.28 (CH, 7-C), 68.39 (CH, 3-C), 51.44 (CH_3, OCH_3). IR_{vmax} (KBr): 3531.43, 2942.98, 2867.01, 1737.24, 1440.12, 1379.84, 1364.52, 1250.45 cm^{-1}. HRMS: Found: $(M\text{-}Na)^+$ = 471.3086, calculated for $C_{27}H_{44}O_5Na$ = 471.3086.

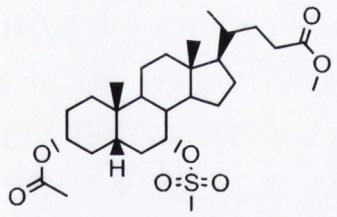

158

Compound **157** (0.5 g, 1.114 mmol) was dissolved in anhydrous DCM (15 ml) at 0-4 °C then anhydrous pyridine (0.448 ml, 5.56 mmol) and methanesulfonyl chloride (0.434 ml, 4.4 mmol) were added to the mixture and stirred for 15 min. DIPEA (0.486 ml, 2.79 mmol) dissolved in anhydrous DCM (4 ml) was added drop-wise over 15 min, with the temperature kept at 0 °C and stirred for 1 h. 0.1M aq. HCl (80 ml) was added to the mixture and the product was extracted using DCM (2 × 60 ml). The DCM layer was washed with brine (160 ml), dried using $MgSO_4$ and filtered. The solvent was removed with the rotary evaporator and the flask was placed under high pressure to dry the product (98%, 0.575 g). ^{1}H-NMR (400 MHz, $CDCl_3$): δ 4.93 (m, 1H, 7β-H), 4.612 (m,1H, 3β-H), 3.68 (s, 3H, -O-CH_3), 3.0431 (s, 3H, -OSO_2CH_3), 2.04 (s, 3H, 3-

C=OCH_3), 0.95 (s, 3H, 19-CH_3), 0.94 (d, 3H, 21-CH_3), 0.67 (s, 3H, 18-CH_3). ^{13}C-NMR ppm (100 MHz, $CDCl_3$): δ 174.25 (C=O, 24-C), 170.25 (C=O, 3-O<u>C</u>=OCH_3), 80.91 (CH, 3-C), 73.45 (CH, 7-C), 52.10 (CH_3, -OSO_2<u>C</u>H_3), 51.09 (CH_3, O<u>C</u>H_3), 21.059 (CH_3, 3-C=O<u>C</u>H_3). IR_{vmax} (DCM): 2941, 2872.23, 1732.65, 1438.06, 1367.61, 1345.53, 1248.96, 1173.61, 1138.01 cm^{-1}. HRMS: Found: $(M\text{-}Na)^+$ = 549.2850, calculated for $C_{28}H_{46}O_7SNa$ = 549.2862.

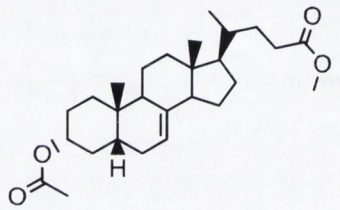

159

Compound **158** (0.617 g, 1.117 mmol) was dissolved in DMPU (17 ml) then NaN_3 (0.76 g, 11.69 mmol) was added at 50 °C. The reaction mixture was left stirring overnight and TLC analysis indicated that the reaction was complete. Brine (100 ml) was poured into the mixture and the product was extracted using EtOAc (3 × 50 ml). The organic phase was dried over Na_2SO_4, filtered and the solvent removed under reduced pressure. The crude product was purified by flash column chromatography using a gradient eluent (EtOAc 3%, followed by 6%, 9%, 12% and 15% in hexane). The yield product is white foam (0.450 g, 93%). ^{1}H-NMR (400 MHz, $CDCl_3$): δ 5.12 (m, 1H, 7-H), 4.75 (m, 1H, 3β-H), 3.68 (s, 3H, -O-CH_3), 2.04 (s, 3H, 3-C=OCH_3), 0.96 (s, 3H, 19-CH_3), 0.94 (d, 3H, 21-CH_3), 0.71 (s, 3H, 18-CH_3). ^{13}C-NMR ppm (100 MHz, $CDCl_3$): δ 174.31 (C=O, 24-C), 170.22 (C=O, 3-O<u>C</u>=OCH_3), 136.74 (quaternary C, 8-C), 114.92 (CH, 7-C), 73.23 (CH, 3-C), 51.085 (CH_3, -OCH_3), 21.02 (CH_3, 3-C=O<u>C</u>H_3). IR_{vmax} (KBr): 2952.47, 2871.89, 1730.01, 1451.58, 1437.29, 1379.29, 1362.42, 1326.88, 1311.19 cm^{-1}. HRMS: Found: $(M\text{-}Na)^+$ = 453.2959, calculated for $C_{27}H_{42}O_4Na$ = 453.2981.

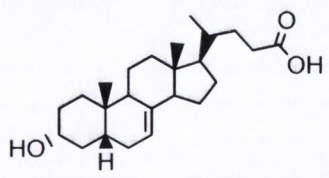

160

To a solution of **159** (0.7 g, 1.63 mmol) in MeOH (40 ml) was added 2M NaOH (2 ml) drop-wise to pH~14. The mixture was stirred at 60 °C for 1 d then it was poured into 2M HCl (50 ml) and extracted with EtOAc (3 × 50 ml). The organic phase was washed with water (2 × 100 ml) and brine (100 ml), dried over Na_2SO_4, filtered and solvent removed *in vacuo*, leaving a white solid (0.43 g, 71%). ^{1}H-NMR (400 MHz, MeOD): δ 5.14 (m, 1H, 7-H), 3.55 (m, 1H, 3β-H), 3.3 (s, 3H, -O-CH_3), 0.99 (d, 3H, 21-CH_3), 0.89 (s, 3H, 19-CH_3), 0.61 (s, 3H, 18-CH_3). IR_{vmax} (KBr): 3342.10, 2934.10, 2859.74, 1708.32, 1541.26, 1468.23, 1447.14, 1416.48, 1367.02, 1333.67, 1286.98 cm^{-1}. HRMS: Found: $(M)^-$ = 373.2757, calculated for $C_{24}H_{37}O_3$ = 373.2743.

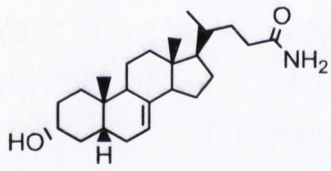

161

The protocol was analogous to that of **155** starting from compound **160** (0.15 g, 0.4 mmol) in anhydrous THF (15 ml) and acetonitrile (1.5 ml), then DCC (0.248 g, 1.2 mmol) and N-OH-Su (0.138 g, 1.19 mmol) was added. The mixture was left stirring overnight. The solid was filtered off and the filtrate was concentrated using the rotary evaporator. The product was dissolved in DMF (5 ml) and ammonia solution (37%, 0.044 ml) was added. The reaction mixture was stirred at 50 °C and left overnight, then the mixture was poured into brine (70 ml) and the precipitate collected by suction filtration. The solid collected on the filter paper was washed with distilled water (2 × 30 ml) and the solid (0.14 g, 93%) was allowed to dry. ^{1}H-NMR (400 MHz, MeOD): δ 5.78 (m, 1H, 7-H), 4.18 (m, 1H, 3β-H), 1.6 (d, 3H, 21-CH_3), 1.53 (s, 3H, 19-CH_3), 1.24 (s, 3H, 18-CH_3). ^{13}C-NMR ppm (100 MHz, $CDCl_3$): δ 179.8 (C=O, C=ONH_2), 138.68 (quaternary C, 8-C), 116.63 (CH, 7- C), 71.83 (CH, 3-C). IR_{vmax} (KBr): 3327.85, 2929.36, 1626.36 and 1576.41 cm^{-1}.HRMS: Found: $(M\text{-}Na)^+$ = 396.2874, calculated for $C_{24}H_{39}NO_2Na$ = 396.2878.

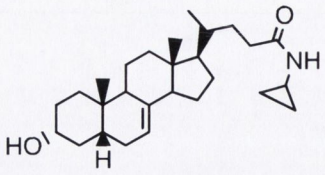

162

To a stirred solution of **160** (0.056 g, 0.15 mmol) in anhydrous DMF (10 ml) were added HOBt (0.03 g, 0.22 mmol) and EDC (0.05 ml, 0.228 mmol) at 0 °C under N_2. After 10 min, cyclopropylamine (0.016 ml, 0.22 mmol) dissolved in anhydrous DMF was added slowly and the reaction mixture was left stirring overnight. When the reaction was complete, brine (70 ml) was added to the mixture and product was extracted using EtOAc (3 × 50 ml). The organic phase was washed with brine (100 ml), dried using $NaSO_4$ and filtered. The solvent was removed under reduced pressure to give a white solid (0.053 g, 90%). ^{1}H-NMR (400 MHz, $CDCl_3$): δ 5.67 (d, 1H, N-H), 5.11 (m, 1H, 7-H), 3.63 (1H, 3β-H), 0.93 (d, 3H, 21-CH_3), 0.86 (s, 3H, 19-CH_3), 0.77 (m, 2H, cyclopropyl-CH_2), 0.54 (s, 3H, 18-CH_3), 0.49 (2H, cyclopropyl-CH_2). ^{13}C-NMR ppm (100 MHz, $CDCl_3$): δ 175.41 (C=O, C=ONH_2), 137.67 (quaternary C, 8-C), 115.86 (CH, 7- C), 71.68 (CH, 3-C), 7.06 (CH_2, cyclopropyl-$\underline{C}H_2$). IR_{vmax} (KBr): 3444.44, 2931.55 and 1663.29 cm^{-1}. HRMS: Found: $(M\text{-}Na)^+$ = 436.3178, calculated for $C_{27}H_{43}NO_2Na$ = 436.3191.

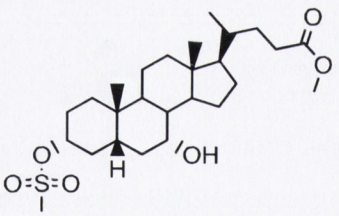

163

Compound **149** (1.177 g, 2.895 mmol) and triethyl amine (0.81 ml, 5.789 mmol) were dissolved in anhydrous DCM (20 ml) and methanesulfonyl chloride (0.27 ml, 3.473 mmol in 5 ml anh. DCM) was added drop-wise in 10 min at 0 °C, then crushed ice was added immediately and stirred. The organic phase was separated and washed with saturated $NaHCO_3$ (2 × 50 ml), water (50 ml) and brine (50 ml) then dried over $MgSO_4$, filtered and the solvent was removed under reduced pressure. The yield product: white foam (1.299 g, 93%). ^{1}H-NMR (400 MHz, $CDCl_3$): δ 4.54 (m, 1H, 3β-H), 3.87 (s, 1H, 7β-H), 3.68 (s, 3H, -O-CH_3), 3.01 (s, 3H, -SO_2-CH_3), 0.95 – 0.93 (d, 6H, 21-CH_3 and 19-CH_3), 0.67 (s, 3H, 18-CH_3). ^{13}C-NMR ppm (100 MHz, $CDCl_3$): δ 174.55 (C=O, 24-C), 82.57 (CH, 3-C), 68.73 (CH, 7-C). IR_{vmax} (KBr): 3552.50, 2942.04,

1737.27, 1348.89, 1170.76 and 926.45 cm^{-1}. HRMS: Found: $(M\text{-}Na)^+$ = 507.2758, calculated for $C_{26}H_{44}O_6SNa$ = 507.2756.

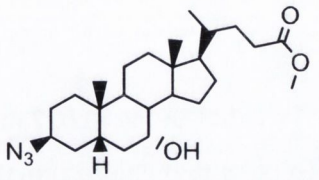

164

To a solution of **163** (1.263 g, 2.606 mmol) in DMPU was added NaN_3 (1.694 g, 26.059 mmol) and stirred at 60-65 °C until the TLC analysis showed that the reaction was complete. Then the mixture was poured into 1M HCl (100 ml) and extracted with EtOAc (3 × 50 ml). The organic layer was collected and washed with water (100 ml) and brine (100 ml), dried over Na_2SO_4, filtered and the solvent was evaporated. The crude product was purified by column chromatography using hexane : EtOAc 3:1 as mobile phase to afford colourless semi-solid as product (0.86 g, 76%). ^{1}H-NMR (400 MHz, $CDCl_3$): δ 3.92 (s, 1H, 3α-H), 3.88 (s, 1H, 7β-H), 3.68 (s, 3H, -O-CH_3), 0.95 – 0.93 (d, 6H, 19-CH_3 and 21-CH_3), 0.68 (s, 3H, 18-CH_3). ^{13}C-NMR ppm (100 MHz, $CDCl_3$): δ 175.20 (C=O, 24-C), 69.04 (CH, 7-C). IR_{vmax} (KBr): 3494.84, 2930.37, 2091.78 and 1739.85 cm^{-1}. HRMS: Found: $(M\text{-}Na)^+$ = 454.3029, calculated for $C_{25}H_{41}N_3O_3Na$ = 454.3046.

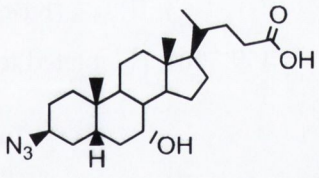

165

Compound **164** (0.84 g, 1.946 mmol) was dissolved in MeOH and stirred with 2M NaOH (pH~14) at rt overnight. The reaction mixture was then poured into 1M HCl (100 ml) and extracted with EtOAc (3 × 50 ml). The organic phase was washed with water (2 × 100 ml) and dried over Na_2SO_4. After filtration the solvent was removed to give white foam as product (0.277 g, 34%). ^{1}H-NMR (400 MHz, $CDCl_3$): δ 3.92 (s, 1H, 3α-H), 3.88 (s, 1H, 7β-H), 0.96 (d, 6H, 19-CH_3 and 21-CH_3), 0.68 (s, 3H, 18-CH_3). ^{13}C-NMR ppm (100 MHz, $CDCl_3$): δ 179.88 (C=O, 24-C), 68.50 (CH, 7-C). IR_{vmax} (KBr): 3450.29, 2927.53, 2101.43 and 1709.14 cm^{-1}. HRMS: Found: $(M)^-$ = 416.2901, calculated for $C_{24}H_{38}N_3O_3$ = 416.2913.

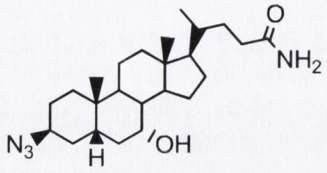

166 and 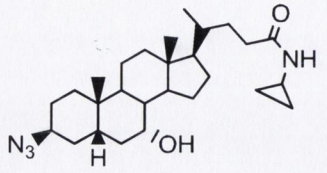

167

To a solution of **165** (0.1 g, 0.239 mmol) in dioxane (10 ml) was added triethyl amine (0.037 ml, 0.263 mmol in 2 ml dioxane) then the mixture was cooled down to 10 °C. Ethyl chloroformate (0.025 ml, 0.263 mmol) was added drop-wise, then 10 min later the amine (0.031 ml, 0.599 mmol ammonia solution or 0.042 ml, 0.599 mmol cyclopropylamine) was added drop-wise. The mixture was stirred at 10 °C additional 30 min and rt overnight, then the reaction mixture was poured into 1M HCl (50 ml) and extracted with EtOAc (3 × 50 ml). The organic phase was with water (50 ml) and brine (50 ml), dried over Na_2SO_4, filtered and the solvent was removed under reduced pressure. The residues were purified by column chromatography to afford the products.

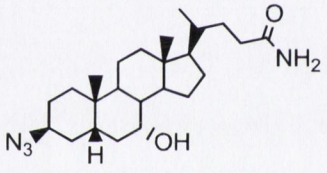

166

white foam (0.071 g, 72%). ^{1}H-NMR (400 MHz, $CDCl_3$): δ 5.88 (br s, 2H, NH_2), 3.92 (s, 1H, 3α-H), 3.87 (s, 1H, 7β-H), 0.96 (d, 6H, 21-CH_3 and 19-CH_3), 0.68 (s, 3H, 18-CH_3). ^{13}C-NMR ppm (100 MHz, $CDCl_3$): 177.10 (C=O, 24-C), 69.02 (CH, 7-C), 50.89 (CH, 3-C). IR_{vmax} (KBr): 3436.57, 2927.53, 2101.06 and 1648.37 cm^{-1}. HRMS: Found: $(M\text{-}Na)^+$ = 439.3061, calculated for $C_{24}H_{40}N_4O_2Na$ = 439.3049.

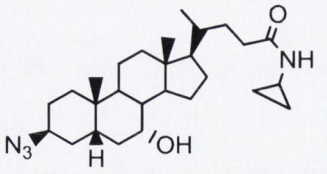

167

white foam (0.095 g, 87%). ^{1}H-NMR (400 MHz, $CDCl_3$): δ 6.11 (s, 1H, NH), 3.92 (s, 1H, 3α-H), 3.88 (s, 1H, 7β-H), 2.73 (m, 1H, CPA-CH), 0.95 (d, 6H, 21-CH_3 and 19-CH_3), 0.80 (m, 2H, CPA), 0.67 (s, 3H, 18-CH_3), 0.56 (m, 2H, CPA). ^{13}C-NMR ppm (100 MHz, $CDCl_3$): δ 176.00 (C=O, 24-C), 68.75 (CH, 7-C), 50.54 (CH, 3-C), 6.73 (2 x CH_2, CPA). IR_{vmax} (KBr): 3429.43, 2929.05, 2096.61 and 1665.91 cm^{-1}. HRMS: Found: $(M\text{-}Na)^+$ = 479.3349, calculated for $C_{27}H_{44}N_4O_2Na$ = 479.3362.

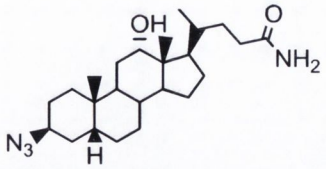

168

Compound **120** (0.150 g, 0.36 mmol) was dissolved in anhydrous DCM (13 ml) and Et_3N (3 eq, 1.1 mmol) was added at 0 °C, followed by the slow addition of ethyl chloroformate (1.2 eq, 0.43 mmol). After 30 min of stirring at 0° C, aqueous ammonia (35%, 1.2 eq, 0.43 mmol) was added. The reaction was let warm up to rt and left to stir overnight. TLC analysis confirmed the reaction had undergone completion and was mixed with 1 M HCl. This was then extracted with EtOAc (3 × 100 ml). The organic phase was collected and washed with water (100 ml) and brine (100 ml). The organic phase was dried over Na_2SO_4, filtered and the solvent removed under reduced pressure to form a white foam (Compound **8**) (0.101 g, 67%). ^{1}H-NMR (400 MHz, $CDCl_3$): δ 3.98 (s, 2H, 12β-H and 3α-H), 1.05 (d, 3H, J = 6.04 Hz, 21-CH_3), 0.97 (s, 3H, 19-CH_3), 0.73 (s, 3H, 18-CH_3). ^{13}C-NMR ppm (100 MHz, $CDCl_3$): δ 179.89 (C=O, 24-C), 74.03 (CH, 12-C), 60.22 (CH, 3-C). IR_{vmax} (KBr): 3400.40, 2937.50, 2102.52 and 1666.29 cm^{-1}. HRMS: Found: $(M\text{-}Na)^+$ = 439.3027, calculated for $C_{24}H_{40}N_4O_2Na$ = 439.3049.

General method for 24-amido DCA derivatives:

To a stirred solution of **120** (0.15 g, 0.359 mmol) in DMF (10 ml) were added HOBt monohydrate (0.243 g, 1.796 mmol) and EDC (0.32 ml, 1.796 mmol) at 0 °C and monitored by TLC. When the intermediate was formed the amine (1.2 eqv.) was added at 0 °C and stirred at rt. When the reaction was complete the mixture was poured into brine (50 ml) and extracted with EtOAc (3 × 50 ml). The organic phase was collected and dried over Na_2SO_4, filtered and the solvent was removed under reduced pressure. The crude product was purified by column chromatography using 50 – 100% EtOAc in hexane (containing 50, 60, 70, 80, 90 and 100% EtOAc in the solvent mixture) as mobile phase to give the product.

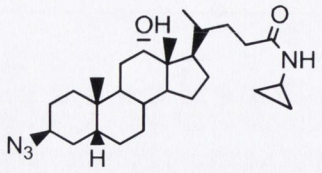

169

Light yellow foam (40 mg, 37%). ^{1}H-NMR (400 MHz, $CDCl_3$): δ 5.62 (br s, 1H, NH), 4.00 and 3.96 (d, 2H, 12β- and 3α-H), 2.70 (m, 1H, CPA-CH), 0.98 (d, 3H, J = 6.52 Hz, 21-CH_3), 0.95 (s, 3H, 19-CH_3), 0.78 (m, 2H, CPA-CH_2), 0.69 (s, 3H, 18-CH_3), 0.49 (m, 2H, CPA-CH_2). ^{13}C-NMR ppm (100 MHz, $CDCl_3$): 174.70 (C=O, 24-C), 72.99 (CH, 12-C), 58.52 (CH, 3-C), 6.46 (2 × CH_2, CPA). IR_{vmax} (KBr): 3302.59, 2937.69, 2102.59 and 1648.38 cm^{-1}. HRMS: Found: $(M\text{-}Na)^+$ = 479.3353, calculated for $C_{27}H_{44}N_4O_2Na$ = 479.3362.

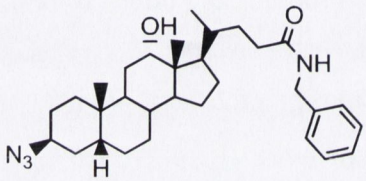

170

White foam (70 mg, 39%). ^{1}H-NMR (400 MHz, $CDCl_3$): δ 7.35 – 7.28 (m, 5H, aromatic-H), 5.78 (br s, 1H, NH), 4.46 – 4.41 (m, 2H, benzyl-CH_2), 4.00 and 3.96 (d, 2H, 12β- and 3α-H), 1.00 (d, 3H, J = 6.00 Hz, 21-CH_3), 0.96 (s, 3H, 19-CH_3), 0.69 (s, 3H, 18-CH_3). ^{13}C-NMR ppm (100 MHz, $CDCl_3$): δ 173.76 (C=O, 24-C), 138.78, 129.16, 128.29, 127.98 (aromatic carbons), 73.63 (CH, 12-C), 59.15 (CH, 3-C). IR_{vmax} (KBr): 3414.05, 2927.53, 2107.71, 1646.85 and 698.15 cm^{-1}. HRMS: Found: $(M\text{-}Na)^+$ = 529.3544, calculated for $C_{31}H_{46}N_4O_2Na$ = 529.3518.

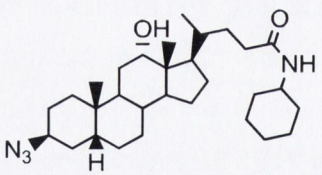

171

Light yellow foam (85 mg, 47%). ^{1}H-NMR (400 MHz, $CDCl_3$): δ 5.33 (br s, 1H, NH), 4.01 and 3.96 (d, 2H, 12β- and 3α-H), 3.77 (m, 1H, cyclohexyl-CH), 0.99 (d, 3H, J = 6.52 Hz, 21-CH_3), 0.95 (s, 3H, 19-CH_3), 0.69 (s, 3H, 18-CH_3). ^{13}C-NMR ppm (100 MHz, $CDCl_3$): 172.90 (C=O, 24-C), 73.62 (CH, 12-C), 59.16 (CH, 3-C). IR_{vmax} (KBr): 3434.18, 2932.36, 2102.19 and 1643.62 cm^{-1}. HRMS: Found: $(M\text{-}Na)^+$ = 521.3864, calculated for $C_{30}H_{50}N_4O_2Na$ = 521.3831.

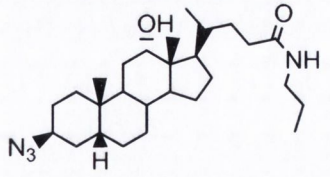

172

White foam (65 mg, 40%). ^{1}H-NMR (400 MHz, $CDCl_3$): δ 5.49 (br s, 1H, NH), 4.01 and 3.97 (d, 2H, 12β- and 3α-H), 3.25 (m, 2H, propyl-CH_2), 1.01 – 0.92 (m, 9H, 21-CH_3 + propyl-CH_3 + 21-CH_3), 0.70 (s, 3H, 18-CH_3). ^{13}C-NMR ppm (100 MHz, $CDCl_3$): 173.89 (C=O, 24-C), 73.65 (CH, 12-C), 59.17 (CH, 3-C), 41.66 (CH_2, propyl), 11.81 (CH_3, propyl). IR_{vmax} (KBr): 3425.12, 2935.22, 2102.60 and 1638.55 cm^{-1}. HRMS: Found: $(M\text{-}Na)^+$ = 481.3507, calculated for $C_{27}H_{46}N_4O_2Na$ = 481.3518.

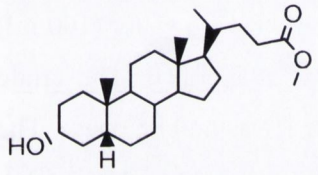

173

LCA (3 g, 7.966 mmol) was dissolved in MeOH and cc. HCl (0.34 ml, 3.983 mmol) added and the mixture was stirred at reflux. After the completion of the reaction the solvent was removed and the residue was dissolved in EtOAc (50 ml) than washed with water (50 ml) and brine (50 ml). The organic phase was dried over $MgSO_4$, filtered and the solvent was removed under reduced pressure giving a white solid as product (3.049 g, 98%) which was used without further furification in the next step.

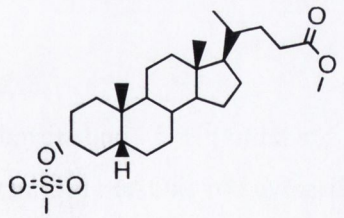

174

To the solution of **173** (3.049 g, 7.807 mmol) and triethyl amine (1.24 ml, 8.871 mmol) in anhydrous DCM (50 ml) was added the solution of mesyl chloride (0.94 ml, 12. 097 mmol) in anhydrous DCM (10 ml) drop-wise at 0 °C and stirred at rt for 1.5 h. Then the reaction mixture was washed with 1M HCl (2 × 100 ml), water (100 ml) and brine (100 ml), dried over $MgSO_4$, filtered and the solvent was removed under reduced pressure giving a white solid as product (3.01

g, 80%). ^{1}H-NMR (400 MHz, $CDCl_3$): 4.66 (m, 1H, 3β-H), 3.68 (s, 3H, -O-CH_3), 3.02 (s, 3H, -SO_2-CH_3), 0.94 (s, 3H, 19-CH_3), 0.93 (d, 3H, J = 6.52 Hz, 21-CH_3), 0.65 (s, 3H, 18-CH_3). ^{13}C-NMR ppm (100 MHz, $CDCl_3$): 174.59 (C=O, 24-C), 82.81 (CH, 3-C), 51.32 (CH_3, -O-$\underline{C}H_3$).

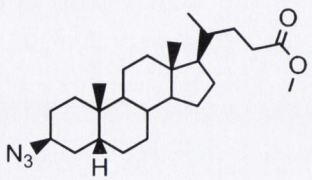

175

Compound **174** (2.88 g, 6.145 mmol) was dissolved in DMPU (40 ml) then NaN_3 (4 g, 61.447 mmol) was added to the mixture and stirred at 50 °C for 6 d after which time TLC analysis showed the reaction was comlete. The reaction mixture was poured into 1 M HCl (100 ml) and extracted with EtOAc (3 × 75 ml). The collected organic phase was washed with water (100 ml) and brine (100 ml), dried over Na_2SO_4, filtered and the solvent was evaporated. The crude product was purified by column chromatography using hexane : EtOAc 1:1 as mobile phase. The yield product was white solid (2.44 g, 96%). ^{1}H-NMR (400 MHz, $CDCl_3$): δ 3.97 (s, 1H, 3α-H), 3.68 (s, 3H, -O-CH_3), 0.96 (s, 3H, 19-CH_3), 0.93 (d, 3H, J = 6.52 Hz, 21-CH_3), 0.66 (s, 3H, 18-CH_3). ^{13}C-NMR ppm (100 MHz, $CDCl_3$): δ 175.24 (C=O, 24-C), 58.85 (CH, 3-C). IR_{vmax} (KBr): 2937.19, 2089.38 and 1734.37 cm^{-1}. HRMS: Found: $(M-Na)^+$ = 438.3078, calculated for $C_{25}H_{41}N_3O_2Na$ = 438.3096.

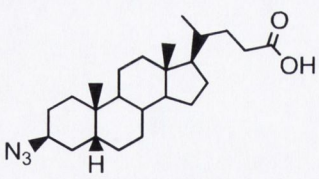

176

To a solution of **175** (2.35 g, 5.654 mmol) in MeOH was added 2M NaOH to pH~14 and stirred at reflux overnight. Then the MeOH was removed and the residue dissolved in EtOAc (100 ml) which was washed with 2M HCl (2 × 100 ml), water (100 ml) and brine (100 ml). The organic phase was then dried over Na_2SO_4, filtered and the solvent was removed under reduced pressure to afford white solid as product (2.18 g, 96%%). ^{1}H-NMR (400 MHz, $CDCl_3$): δ 3.98 (s, 1H, 3α-H), 0.97 (s, 3H, 19-CH_3), 0.95 (d, 3H, J = 6.24 Hz, 21-CH_3), 0.67 (s, 3H, 18-CH_3). ^{13}C-NMR

ppm (100 MHz, $CDCl_3$): 180.57 (C=O, 24-C), 59.24 (CH, 3-C). IR_{vmax} (KBr): 2935.93, 2102.56 and 1706.14 cm^{-1}. HRMS: Found: $(M-H)^-$ = 400.2966, calculated for $C_{24}H_{38}N_3O_2$ = 400.2964.

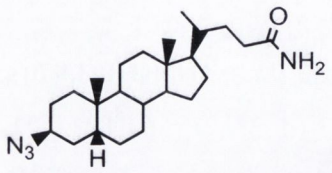

177

0.75 mmol) was added at 0 °C, followed by the slow addition of ethylchloroformate (1.2 eq, 0.3 mmol). After 30 min of stirring at 0° C, aqueous ammonia (35%, 1.2 eq, 0.3 mmol) was added. The reaction was let warm up to rt and left to stir overnight. TLC analysis confirmed the reaction had undergone completion and was mixed with 1M HCl (50 ml). This was then extracted with EtOAc (3 × 100 ml). The organic phase was collected and washed with water (100 ml) and brine (100 ml). The organic phase was dried over Na_2SO_4, filtered and the solvent removed under reduced pressure to form a white foam (0.093 g, 96%). ^{1}H-NMR (400 MHz, CD_3OD): δ 4.86 (s, 1H, 3α-H), 1.71 (s, 3H, 19-CH_3), 1.68 (d, 3H, J = 6.04 Hz, 21-CH_3), 1.42 (s, 3H, 18-CH_3). ^{13}C-NMR ppm (100 MHz, CD_3OD): δ 183.89 (C=O, 24-C). IR_{vmax} (KBr): 2927.66, 2100.82 and 1654.59 cm^{-1}. HRMS: Found: $(M-Na)^+$ = 423.3086, calculated for $C_{24}H_{40}N_4ONa$ = 423.3100.

General method for 24-amido LCA derivatives:

To a stirred solution of **176** (0.15 g, 0.374 mmol) in DMF (10 ml) were added HOBt monohydrate (0.253 g, 1.868 mmol) and EDC (0.33 ml, 1.868 mmol) at 0 °C and monitored by TLC. When the intermediate was formed the amine (1.2 eqv.) was added at 0 °C and stirred at rt.

EtOAc (3 × 50 ml). The organic phase was collected and dried over Na_2SO_4, filtered and the solvent was removed under reduced pressure. The crude product was purified by column chromatography using EtOAc : hexane 1:1 as mobile phase to give the product.

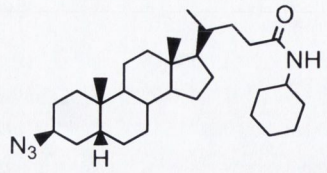

178

Light yellow foam (0.149 g, 83%). ^{1}H-NMR (400 MHz, $CDCl_3$): δ 5.33 (br s, 1H, NH), 3.97 (s, 1H, 3α-H), 3.78 (m, 1H, cyclohexyl-CH), 0.96 (s, 3H, 19-CH_3), 0.93 (d, 3H, J = 6.04 Hz, 21-CH_3), 0.65 (s, 3H, 18-CH_3). ^{13}C-NMR ppm (100 MHz, $CDCl_3$): 172.41 (C=O, 24-C), 58.60 (CH, 3-C). IR_{vmax} (KBr): 3318.76, 2930.15, 2100.76 and 1639.16 cm^{-1}. HRMS: Found: $(M\text{-}Na)^+$ = 505.3865, calculated for $C_{30}H_{50}N_4ONa$ = 505.3882.

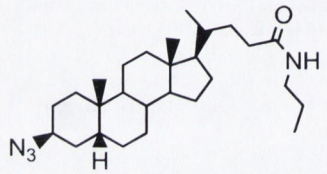

179

white foam (0.123 g, 74%). ^{1}H-NMR (400 MHz, $CDCl_3$): δ 5.49 (br s, 1H, NH), 3.96 (s, 1H, 3α-H), 3.25 (m, 2H, propyl-CH_2), 0.96 – 0.92 (m, 9H, 19-CH_3 + propyl-CH_3 + 21-CH_3), 0.65 (s, 3H, 18-CH_3). ^{13}C-NMR ppm (100 Mhz, $CDCl_3$): δ 173.35 (C=O, 24-C), 58.59 (CH, 3-C), 11.19 (CH_3, propyl). IR_{vmax} (KBr): 3278.17, 2935.82, 2101.57 and 1645.32 cm^{-1}. HRMS: Found: $(M\text{-}2H+Na)^+$ = 463.3401, calculated for $C_{27}H_{44}N_4ONa$ = 463.3413.

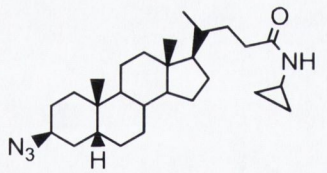

180

white foam (0.093 g, 56%). ^{1}H-NMR (400 MHz, $CDCl_3$): δ 5.65 (br s, 1H, NH), 3.97 (s, 1H, 3α-H), 2.71 (m, 1H, CPA-CH), 0.96 (s, 3H, 19-CH_3), 0.92 (d, 3H, J = 6.52 Hz, 21-CH_3), 0.78 (m, 2H, CPA-CH_2), 0.65 (s, 3H, 18-CH_3), 0.50 (m, 2H, CPA-CH_2). ^{13}C-NMR ppm (100 MHz, $CDCl_3$): 175.17 (C=O, 24-C), 58.91 (CH, 3-C), 6.77 (2 x CH_2, CPA). IR_{vmax} (KBr): 2932.36, 2102.08 and 1645.39 cm^{-1}. HRMS: Found: (M+Na) = 463.3399, calculated for $C_{27}H_{44}N_4ONa$ = 463.3413.

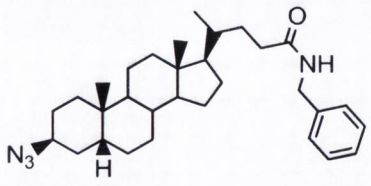

181

Light yellow foam (0.123 g, 67%). ^{1}H-NMR (400 MHz, $CDCl_3$): δ 7.37 – 7.28 (m, 5H, aromatic-H), 5.76 (br s, 1H, NH), 4.46 (d, 2H, J = 5.52 Hz, benzyl-CH_2), 3.97 (s, 1H, 3α-H), 0.97 (s, 3H, 19-CH_3), 0.94 (d, 3H, J = 6.04 Hz, 21-CH_3), 0.66 (s, 3H, 18-CH_3). ^{13}C-NMR ppm (100 MHz, $CDCl_3$): 173.50 (C=O, 24-C), 138.51, 128.83, 127.98, 127.64 (aromatic carbons), 58.90 (CH, 3-C). IR_{vmax} (KBr): 3293.28, 3065.29, 3030.69, 2932.36, 2101.90, 1644.72, 731.74 and 697.67 cm^{-1}. HRMS: Found: (M+H) = 491.3751, calculated for $C_{31}H_{47}N_4O$ = 491.3750.

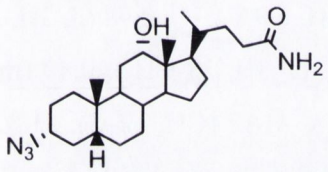

182

To a solution of **81** (0.15 g, 0.359 mmol) in DMF (10 ml) were added HOBt monohydrate (0.243 g, 1.796 mmol) and EDC (0.32 ml, 1.796 mmol) at 0 °C and stirred for 1 h. Then ammonia solution (0.023 ml, 0.431 mmol) was added to the mixture and stirred for 1 d at rt. The reaction mixture was poured into water (50 ml) and the precipitate was collected on a Buchner funnel, washed with water (3 × 20 ml) and dried on the air to yield the product as white solid (0.055 g, 37%). ^{1}H-NMR (400 MHz, Acetone-d_6): δ 3.97 (s, 1H, 12β-H), 3.43 (m, 1H, 3β-H), 1.02 (d, 3H, J = 6.52 Hz, 21-CH_3), 0.97 (s, 3H, 19-CH_3), 0.71 (s, 3H, 18-CH_3). ^{13}C-NMR ppm (100 MHz, Acetone-d_6): δ 175.62 (C=O, 24-C), 72.77 (CH, 12-C), 61.89 (CH, 3-C). IR_{vmax} (KBr): 3382.75, 2939.74, 2091.78 and 1655.26 cm^{-1}. HRMS: Found: (M+Na) = 439.3039, calculated for $C_{24}H_{40}N_4O_2Na$ = 439.3049.

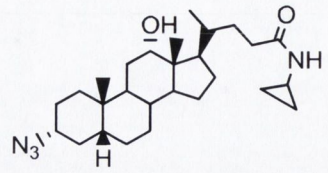

183

To a solution of **81** (0.15 g, 0.359 mmol) in DMF (10 ml) were added HOBt monohydrate (0.243 g, 1.796 mmol) and EDC (0.32 ml, 1.796 mmol) at 0 °C and stirred for 1 h. Then cyclopropyl amine (0.03 ml, 0.431 mmol) was added to the mixture and stirred for 1 d at rt. The reaction mixture was poured into brine (50 ml) and extracted with EtOAc (3 × 50 ml). The organic phase was dried over Na_2SO_4, filtered and the solvent was removed under reduced pressure. The crude product was purified twice by column chromatography using hexane : EtOAc 1:2 – 100% EtOAc as mobile phase to afford white foam as product (0.119 g, 73%). ^{1}H-NMR (400 MHz, $CDCl_3$): δ 5.66 (s, 1H, NH), 3.99 (m, 1H, 12β-H), 3.34 (s, 1H, 3β-H), 2.70 (m, 1H, CPA-CH), 0.98 (d, 3H, J = 6.00 Hz, 21-CH_3), 0.93 (s, 3H, 19-CH_3), 0.78 (m, 2H, CPA), 0.68 (s, 3H, 18-CH_3), 0.49 (m, 2H, CPA). ^{13}C-NMR ppm (100 MHz, $CDCl_3$): δ 175.04 (C=O, 24-C), 73.17 (CH, 12-C), 61.37 (CH, 3-C), 6.75 (2 × CH_2, CPA). IR_{vmax} (KBr): 3434.92, 2938.91, 2086.95 and 1650.61 cm^{-1}. HRMS: Found: (M+H) = 457.3542, calculated for $C_{27}H_{45}N_4O_2$ = 457.3543.

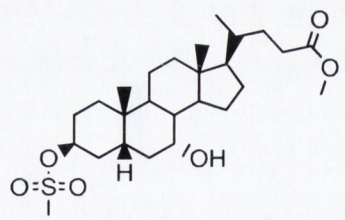

184

Compound **149** (0.8 g, 1.967 mmol) and PPh_3 (1.703 g, 6.492 mmol) were dissolved in anhydrous THF (40 ml) and cooled down to 0 °C. Et_3N (0.55 ml, 3.935 mmol) and methanesylfonic acid (0.27 ml, 4.132 mmol) were added to the mixture at this temperature. The solution was warmed to 45 °C and DIAD (1.2 ml, 6.099 mmol) was added drop-wise and the mixture was stirred until TLC analysis showed the reaction was complete. Then the solvent was removed and the residue was dissolved in EtOAc (100 ml) which was washed with 1M HCl (2 × 100 ml), water (100 ml) and brine (100 ml). After drying the organic phase over $MgSO_4$ the solvent was removed and the product was purified by column chromatography using hexane : EtOAc 3:1, 1:1 and 1:3 as mobile phase. The yield product was odourless semi-solid (0.139 g, 15%). ^{1}H-NMR (400 MHz, $CDCl_3$): δ 5.00 (m, 1H, 3α-H), 3.88 (s, 1H, 7β-H), 3.68 (s, 3H, -O-

CH_3), 3.01 (s, 3H, $-SO_2-CH_3$), 0.98 (s, 3H, 19-CH_3), 0.95 (d, 3H, J = 6.52 Hz, 21-CH_3), 0.68 (s, 3H, 18-CH_3). ^{13}C-NMR ppm (100 MHz, $CDCl_3$): δ 175.19 (C=O, 24-C), 81.22 (CH, 3-C), 68.98 (CH, 7-C). IR_{vmax} (KBr): 3448.15, 2939.07, 1737.73, 1351.28, 1173.17 and 901.12 cm^{-1}. HRMS: Found: $(M-Na)^+$ = 507.2690, calculated for $C_{26}H_{44}O_6SNa$ = 507.2756.

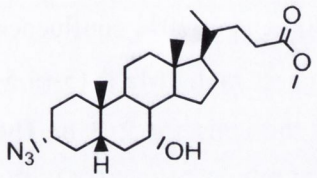

185

Compound **184** (0.139 g, 0.287 mmol) was dissolved in DMPU (30 ml) then NaN_3 (0.187 g, 2.869 mmol) was added and stirred at 50 °C until TLC analysis showed the conversion of starting material was 100%. Then the reaction mixture was quenched with 1M HCl (50 ml) and extracted with EtOAc (3 × 50 ml). The organic layer was collected and washed with water (2 × 100 ml) and brine (100 ml), dried over Na_2SO_4, filtered and the solvent was removed under reduced pressure. The product was purified by column chromatography using hexane : EtOAc 3:1 as mobile phase to afford yellow semi-solid (0.098 g, 79%). ^{1}H-NMR δ (400 MHz, $CDCl_3$): 3.87 (s, 1H, 7β-H), 3.68 (s, 3H, -O-CH_3), 3.16 (s, 1H, 3β-H), 0.95 (d, 6H, 21-CH_3 and 19-CH_3), 0.67 (s, 3H, 18-CH_3). ^{13}C-NMR ppm (100 MHz, $CDCl_3$): δ 174.88 (C=O, 24-C), 68.44 (CH, 7-C). IR_{vmax} (KBr): 3516.06, 2934.95, 2086.95 and 1721.20 cm^{-1}. HRMS: Found: $(M-Na)^+$ = 454.3040, calculated for $C_{25}H_{41}N_3O_3Na$ = 454.3046.

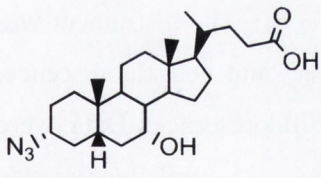

186

To a solution of **185** (0.098 g, 0.228 mmol) in MeOH (20 ml) was added 2M NaOH to pH~14 and stirred at rt for 1 d. Then the excess NaOH was neutralised with 1M HCl solution (100 ml) and the mixture was extracted with EtOAc (3 × 50 ml). The organic phase was washed with water (2 × 100 ml) and brine (100 ml), dried over Na_2SO_4, filtered and the solvent was removed under reduced pressure to give white foam as product (0.084 g, 88%). ^{1}H-NMR (400 MHz, $CDCl_3$): δ 3.88 (s, 1H, 7β-H), 3.17 (s, 1H, 3β-H), 0.96 (d, 3H, J = 6.56 Hz, 21-CH_3), 0.93 (s, 3H,

19-CH_3), 0.68 (s, 3H, 18-CH_3). ^{13}C-NMR ppm (100 MHz, $CDCl_3$): δ 180.24 (C=O, 24-C), 68.84 (CH, 7-C). IR_{vmax} (KBr): 3447.49, 2932.08, 2086.95 and 1708.59 cm^{-1}. HRMS: Found: $(M)^-$ = 416.2914, calculated for $C_{24}H_{38}N_3O_3$ = 416.2913.

5.3.2. MTT assay

Human colonic epithelial cancer cells Caco-2 or fibrosarcoma HT1080 cells at 70% confluence were treated in serum free media with compound of choice for 1 h / 24 h. MTT (3-(4,5-Dimethylthiazol-2-yl)-2,5-diphenyltetrazolium bromide was added to the cells for 2–3 h. The media was removed from the cells and a solubilisation solution (usually DMSO) was added to the cells to dissolve the insoluble formazan into a purple coloured solution. The absorbance of this was quantified at a 600 nm. Compounds were assessed in triplicate across the range 100 nm- 1 mM. Resultant concentration effects curves were transformed and analyzed using PRISM4.

5.3.3. Flow cytometry

Annexin V flow cytometry assay. Cells were grown to 80% Confluence in T25 flasks and treated with Aspirin/ST0702 for 24 h in serum free medium, control cells were treated only with vehicle in serum free media for 24hrs. Following 24 h treatment cells were removed from T25 flasks and washed with 1X Binding Buffer, before being resuspended in 100ml of 1X binding buffer. 20ml of these cells were stained using 5 ml Annexin V-FITC and 5ml propidium iodide and incubated at rt for 15 min in the dark. Following incubation, samples were diluted in 1X binding Buffer and analyzed within 5 min using a BD FACSArray (BD Biosciences, Oxford, UK). Flow cytometry was performed on double stained cell samples (CaCo-2 and HT1080 cells). The instrument was set up to measure the size (forward scatter), granularity (side scatter) and cell fluorescence. Antibody binding was measured by analyzing individual cells for fluorescence. Data were analyzed using BD FACS Array software and expressed as a percentage of control fluorescence in arbitrary units. Cells in late stages of apoptosis or those already dead have lost PM integrity and are permeable to PI whereas Annexin V binds to cells in early apoptosis and continues to be bound through cell death. Thus cells in earyl stage of apoptosis will be Annexin V positive and PI negative (in Q4), cells in late stage of apoptosis (in Q2) or Annexin V Positive and PI positive and finally already dead (in Q1). Healthy cells are Annexin V and PI negative (in Q3).

References

1. Jean-Louis, S., Akare, S., Ali, M.A., Mash, E.A., Jr., Meuillet, E., and Martinez, J.D., *Deoxycholic acid induces intracellular signaling through membrane perturbations.* J. Biol. Chem., 2006. 281(21): p. 14948-60.

2. Mukhopadhyay, S. and Maitra, U., *Chemistry and biology of bile acids.* Cur. Sci., 2004. 87(12): p. 1666-1683.

3. Roda, A., Hofmann, A.F., and Mysels, K.J., *The influence of bile salt structure on self-association in aqueous solutions.* J. Biol. Chem., 1983. 258: p. 6362-6370.

4. F., H.A. and Hagey, L.R., *Bile acids: chemistry, pathochemistry, biology, pathobiology, and therapeutics.* Cell. Mol. Life Sci., 2008. 65: p. 2461-2483.

5. Danielson, H., Nair, P.P., and Kritchevsky, D., *The Bile Acids: Chemistry, Physiology and Metabolism.* Plenum Press, New York, 1973. 2: p. 1-32.

6. Hofmann, A.F. and Arias, I.M., *The Liver: Biology and Pathology.* Raven Press, New York, 1994. 3rd edn: p. 677.

7. Hofmann, A.F., *Bile Acids: The Good, the Bad, and the Ugly.* News Physiol. Sci., 1999. 14: p. 24-29.

8. Falany, C.N., Johnson, M.R., Barnes, S., and Diasio, R.B., *Glycine and taurine conjugation of bile acids by a single enzyme. Molecular cloning and expression of human liver bile acid CoA:amino acid N-acyltransferase.* J. Biol. Chem., 1994. 269: p. 19375-19379.

9. Hofmann, A.F., *The continuing importance of bile acids in liver and intestinal disease.* Arch. Intern. Med., 1999. 159(22): p. 2647-58.

10. Hofmann, A.F., *The enterohepatic circulation of bile acids.* Handbook of Physiology, 1989: p. 567-596.

11. Bernstein, H., Bernstein, C., Payne, C.M., Dvorakova, K., and Garewal, H., *Bile acids as carcinogens in human gastrointestinal cancers.* Mut. Res./Reviews in Mut. Res., 2005. 589(1): p. 47-65.

12. Spivey, J.R., Bronk, S.F., and Gores, G.J., *Glycochenodeoxycholate-induced lethal hepatocellular injury in rat hepatocytes. Role of ATP depletion and cytosolic free calcium.* J. Clin. Invest., 1993. 92(1): p. 17-24.

13. Heuman, D.M., Pandak, W.M., Hylemon, P.B., and Vlahcevic, Z.R., *Conjugates of ursodeoxycholate protect against cytotoxicity of more hydrophobic bile salts: in vitro studies in rat hepatocytes and human erythrocytes.* Hepatology, 1991. 14(5): p. 920-926.

14. Quist, R.G., Ton-Nu, H.T., Lillienau, J., Hofmann, A.F., and Barrett, K.E., *Activation of mast cells by bile acids.* Gastroenterology, 1991. 101(2): p. 446-456.

15. Ota, S., Tsukahara, H., Terano, A., Hata, Y., Hiraishi, H., Mutoh, H., and Sugimoto, T., *Protective effect of tauroursodeoxycholate against chenodeoxycholate-induced damage to cultured rabbit gastric cells.* Dig. Dis. Sci., 1991. 36(4): p. 409-416.

16. Scholmerich, J., Becher, M.S., Schmidt, K., Schubert, R., Kremer, B., Feldhaus, S., and Gerok, W., *Influence of hydroxylation and conjugation of bile salts on their membrane-damaging properties--studies on isolated hepatocytes and lipid membrane vesicles.* Hepatology, 1984. 4: p. 661-666.

17. Hofmann, A.F., *Cholestatic liver disease: pathophysiology and therapeutic options.* Liver, 2002. 22(2): p. 14-19.

18. Paumgartner, G., *Medical treatment of cholestatic liver diseases: From pathobiology to pharmacological targets.* World J. Gastroenterol., 2006. 12(28): p. 4445-4451.

19. Nigro, N.D. and Campbell, R.L., *The bile acids: Physiology and Metabolism.* Plenum Press, New York, 1976. 3: p. 155-168.

20. Cook, J.W., Kennaway, E.L., and Kennaway, N.M., *Production of Tumours in Mice by Deoxycholic Acid.* Nature, 1945. 145: p. 627.

21. Debruyne, P.R., Bruyneel, E.A., Li, X., Zimber, A., Gespach, C., and Mareel, M.M., *The role of bile acids in carcinogenesis.* Mutat. Res., 2001. 480-481: p. 359-69.

22. Thompson, M.B., *Bile acids in the assessment of hepatocellular function.* Toxicol. Pathol., 1996. 24(1): p. 62-71.

23. Watanabe, Y. and Imai, K., *High-performance liquid chromatography and sensitive detection of amino acids derivatized with 7-fluoro-4-nitrobenzo-2-oxa-1,3-diazole.* Anal. Biochem., 1981. 116(2): p. 471-472.

24. Ghosh, P.B. and Whitehouse, M.W., *7-Chloro-4-nitrobenzo-2-oxa-1,3-diazole: a New Fluorigenic Reagent for Amino Acids and other Amines.* Biochem. J., 1968. 108(1): p. 155-156.

25. Boulton, A.J., Ghosh, P.B., and Katritzky, A.R., *Heterocyclic rearrangements. Part V. Rearrangement of 4-arylazo-and 4-nitroso-benzofuroxans: new syntheses of the benzotriazole and benzofurazan ring systems.* J. Chem. Soc. B, 1966: p. 1004-1011.

26. Di Nunno, L., Florio, S., and Todesco, P.E., *Qxidation of Substituted Anilines to Nitroso-compounds.* J. Chem. Soc. C, 1970(10): p. 1425-1428

27. Schneider, S., Schramm, U., Schreyer, A., Buscher, H.P., Gerok, W., and Kurz, G., *Fluorescent derivatives of bile salts. 1. Synthesis and properties of NBD-amino derivatives of bile salts.* J. Lipid Res., 1991. 32: p. 1755-1767.

28. Rohacova, J., Marin, M.L., Martinez-Romero, A., Diaz, L., O'Connor, J.E., Gomez-Lechon, M.J., Donato, M.T., Castell, J.V., and Miranda, M.A., *Fluorescent benzofurazan-*

cholic acid conjugates for in vitro assessment of bile acid uptake and its modulation by drugs. Chem. Med. Chem., 2009. 4(3): p. 466-72.

29. Zhao, Y. and Zhong, Z., *Oligomeric Cholates: Amphiphilic Foldamers with Nanometer-Sized Hydrophilic Cavities.* J. Am. Chem. Soc., 2005(127): p. 17894-17901.

30. Maglova, L.M., Jackson, A.M., Meng, X.J., Carruth, M.W., Schteingart, C.D., Ton-Nu, H.T., Hofmann, A.F., and Weinman, S.A., *Transport characteristics of three fluorescent conjugated bile acid analogs in isolated rat hepatocytes and couplets.* Hepatology, 1995. 22(2): p. 637-47.

31. Holzinger, F., Schteingart, C.D., Ton-Nu, H.T., Eming, S.A., Monte, M.J., Hagey, L.R., and Hofmann, A.F., *Fluorescent bile acid derivatives: relationship between chemical structure and hepatic and intestinal transport in the rat.* Hepatology, 1997. 26(5): p. 1263-71.

32. Yamaguchi, H., Okada, M., Akitaya, S., Ohara, H., Mikkaichi, T., Ishikawa, H., Sato, M., Matsuura, M., Saga, T., Unno, M., Abe, T., Mano, N., Hishinuma, T., and Goto, J., *Transport of fluorescent chenodeoxycholic acid via the human organic anion transporters OATP1B1 and OATP1B3.* J. Lipid Res., 2006. 47(6): p. 1196-202.

33. Nicolaou, M., Andress, E.J., Zolnerciks, J.K., Dixon, P.H., Williamson, C., and Linton, K.J., *Canalicular ABC transporters and liver disease.* J. Pathol., 2012. 226(2): p. 300-15.

34. Kemp, S., Theodoulou, F.L., and Wanders, R.J., *Mammalian peroxisomal ABC transporters: from endogenous substrates to pathology and clinical significance.* Br. J. Pharmacol., 2011. 164(7): p. 1753-66.

35. Stieger, B. and Geier, A., *Genetic variations of bile salt transporters as predisposing factors for drug-induced cholestasis, intrahepatic cholestasis of pregnancy and therapeutic response of viral hepatitis.* Expert Opin. Drug Metab. Toxicol., 2011. 7(4): p. 411-25.

36. Bajor, A., G., G.P., and Abrahamsson, H., *Bile acids: short and long term effects in the intestine.* Scand. J. Gastroenterol. , 2010. 45(6): p. 645-64.

37. Dawson, P.A., *Role of the intestinal bile acid transporters in bile acid and drug disposition.* Handb. Exp. Pharmacol., 2011(201): p. 169-203.

38. Schramm, U., Fricker, G., Buscher, H.P., Gerok, W., and Kurz, G., *Fluorescent derivatives of bile salts. III. Uptake of 7 beta-NBD-NCT into isolated hepatocytes by the transport systems for cholyltaurine.* J. Lipid Res., 1993. 34(5): p. 741-57.

39. Schramm, U., Dietrich, A., Schneider, S., Buscher, H.P., Gerok, W., and Kurz, G., *Fluorescent derivatives of bile salts. II. Suitability of NBD-amino derivatives of bile salts for the study of biological transport.* J. Lipid Res., 1991. 32(11): p. 1769-79.

40. Schwab, D., Stieger, B., Hagenbuch, B., Meier, P.J., Gerok, W., and Kurz, G., *Uptake of 3 alpha, 7 alpha, 12 alpha-trihydroxy-24-nor-5 beta-cholan-23-sulfonate into isolated rat hepatocytes by three transport systems.* J. Lipid Res., 1997. 38(5): p. 935-48.

41. Rohacova, J., Marin, M.L., and Miranda, M.A., *Complexes between fluorescent cholic acid derivatives and human serum albumin. a photophysical approach to investigate the binding behavior.* J. Phys. Chem. B., 2010. 114(13): p. 4710-6.

42. Kida, M., Mano, Y., Ueno, Y., Kobayashi, K., Goto, J., Ishii, M., and Shimosegawa, T., *Vectorial transport of bile acids in immortalized mouse bile duct cells.* Hepatol. Res., 2003. 27(2): p. 151-157.

43. Yamaguchi, H., Kobayashi, M., Okada, M., Takeuchi, T., Unno, M., Abe, T., Goto, J., Hishinuma, T., and Mano, N., *Rapid screening of antineoplastic candidates for the human organic anion transporter OATP1B3 substrates using fluorescent probes.* Cancer Lett., 2008. 260(1-2): p. 163-9.

44. A., B., Wring, S.A., Coop, A., and Polli, J.E., *Influence of charge and steric bulk in the C-24 region on the interaction of bile acids with human apical sodium-dependent bile acid transporter.* Mol. Pharm., 2006. 3(3): p. 282-92.

45. Holzinger, F., Schteingart, C.D., Ton-Nu, H.T., Cerre, C., Steinbach, J.H., Yeh, H.Z., and Hofmann, A.F., *Transport of fluorescent bile acids by the isolated perfused rat liver: kinetics, sequestration, and mobilization.* Hepatology, 1998. 28(2): p. 510-20.

46. Murray, J.W., Thosani, A.J., Wang, P., and Wolkoff, A.W., *Heterogeneous accumulation of fluorescent bile acids in primary rat hepatocytes does not correlate with their homogenous expression of ntcp.* Am. J. Physiol. Gastrointest. Liver Physiol., 2011. 301(1): p. G60-8.

47. Mita, S., Suzuki, H., Akita, H., Hayashi, H., Onuki, R., Hofmann, A.F., and Sugiyama, Y., *Inhibition of bile acid transport across Na+/taurocholate cotransporting polypeptide (SLC10A1) and bile salt export pump (ABCB 11)-coexpressing LLC-PK1 cells by cholestasis-inducing drugs.* Drug Metab. Dispos., 2006. 34(9): p. 1575-81.

48. Gautam, A., Ng, O.C., Strazzabosco, M., and Boyer, J.L., *Quantitative assessment of canalicular bile formation in isolated hepatocyte couplets using microscopic optical planimetry.* J. Clin. Invest., 1989. 83(2): p. 565-73.

49. Grüne, S., Meng, X.J., and Weinman, S.A., *cAMP stimulates fluorescent bile acid uptake into hepatocytes by membrane hyperpolarization.* Am. J. Physiol., 1996. 270(2 Pt 1): p. G339-46.

50. Weber, G., *Polarization of the Fluorescence of Macromolecules 2. Fluorescent conjugates of ovalbumin and bovine serum albumin.* Biochem. J., 1952. 51(2): p. 155-167.

51. Crawford, J.M., Lin, Y.J., Teicher, B.A., Narciso, J.P., and Gollan, J.L., *Physical and biological properties of fluorescent dansylated bile salt derivatives: the role of steroid ring hydroxylation.* Biochim. Biophys. Acta, 1991. 1085(2): p. 223-34.

52. Rohacova, J., Marin, M.L., Martinez-Romero, A., O'Connor, J.E., Gomez-Lechon, M.J., Donato, M.T., Castell, J.V., and Miranda, M.A., *Synthesis of new, UV-photoactive dansyl derivatives for flow cytometric studies on bile acid uptake.* Org. Biomol. Chem., 2009. 7(23): p. 4973-80.

53. Rohacova, J., Sastre, G., Marin, M.L., and Miranda, M.A., *Dansyl Labeling To Modulate the Relative Affinity of Bile Acids for the Binding Sites of Human Serum Albumin.* J. Phys. Chem. B., 2011.

54. http://upload.wikimedia.org/wikipedia/en/8/8a/Fluorescein_spectra.jpg.

55. Giepmans, B.N.G., Adams, S.R., Ellisman, M.H., and Tsien, R.Y., *The Fluorescent Toolbox for Assessing Protein Location and Function.* Science, 2006. 312(5771): p. 217-224.

56. Sjoback, R., Nygren, J., and Kubista, M., *Absorption and Fluorescence Properties of Fluorescein.* Spectrochim. Acta. A, 1995. 51:7-7.

57. D., M., G., M., and A., S., *Fluorescein as a model molecular calculator with reset capability.* Nature Materials, 2005. 10: p. 768-71.

58. Delon, A., Usson, Y., Derouard, J., Biben, T., and Souchier, C., *Continuous photobleaching in vesicles and living cells: a measure of diffusion and compartmentation.* Biophys. J. , 2006. 90: p. 2548-2562.

59. Song, L., Hennink, E.J., Young, I.T., and Tanke, H.J., *Photobleaching kinetics of fluorescein in quantitative fluorescence microscopy.* Biophys. J., 1995. 68: p. 2588-2600.

60. Song, L., van Gijlswijk, R.P., Young, I.T., and Tanke, H.J., *Influence of fluorochrome labeling density on the photobleaching kinetics of fluorescein in microscopy.* Cytometry, 1997. 27: p. 213-223.

61. Sherman, I.A. and Fisher, M.M., *Hepatic transport of fluorescent molecules: in vivo studies using intravital TV microscopy.* Hepatology, 1986. 6(3): p. 444-9.

62. Schteingart, C.D., Eming, S., Ton-Nu, H.T., Crombie, D.L., and Hofmann, A.F., *Synthesis, structure and transport properties of fluorescent derivatives of bile acids. In: Paumgartner G, Gerok W, Stiehl A, eds. Bile acids and the hepatobiliary system.* London: Kluwer Academic, 1992: p. 177-183.

63. Kitamura, T., Gatmaitan, Z., and Arias, I.M., *Serial quantitative image analysis and confocal microscopy of hepatic uptake, intracellular distribution and biliary secretion of a fluorescent bile acid analog in rat hepatocyte doublets.* Hepatology, 1990. 12(6): p. 1358-64.

64. Briz, O., el-Mir, M.Y., Bravo, P., Villanueva, G.R., and Marin, J.J., *Fetal excretion of the fluorescent bile acid derivative cholylglycylamido-fluorescein (FITC-GC) by the rat placenta-maternal liver tandem.* Placenta, 1998. 19(1): p. 119-26.

65. Mills, C.O., Rahman, K., Coleman, R., and Elias, E., *Cholyl-lysylfluorescein: synthesis, biliary excretion in vivo and during single-pass perfusion of isolated perfused rat liver.* Biochim. Biophys. Acta., 1991. 1115(2): p. 151-6.

66. Mills, C.O., Iqbal, S., and Elias, E., *Synthesis and biliary excretion of tyrosine-conjugated bile salts in Wistar rats.* Biochim. Biophys. Acta., 1986. 876(3): p. 667-76.

67. Mills, C.O., Milkiewicz, P., Saraswat, V., and Elias, E., *Cholyllysyl fluroscein and related lysyl fluorescein conjugated bile acid analogues.* Yale J. Biol. Med., 1997. 70(4): p. 447-57.

68. Mills, C.O., Milkiewicz, P., Molloy, D.P., Baxter, D.J., and Elias, E., *Synthesis, physical and biological properties of lithocholyl-lysyl-fluorescein: a fluorescent monohydroxy bile salt analogue with cholestatic properties.* Biochim. Biophys. Acta, 1997. 1336(3): p. 485-96.

69. Roda, A., Minutello, A., Angellotti, M.A., and Fini, A., *Bile acid structure-activity relationship: evaluation of bile acid lipophilicity using 1-octanol/water partition coefficient and reverse phase HPLC.* J. Lipid Res., 1990. 31(8): p. 1433-43.

70. Jean-Louis, S., Akare, S., Ali, M.A., Mash, E.A.J., Meuillet, E., and Martinez, J.D., *Deoxycholic acid induces intracellular signaling through membrane perturbations.* J. Biol. Chem., 2006. 281(21): p. 14948-60.

71. Han, K.C., Kim, J.H., Kim, K.H., Kim, E.E., Seo, J.H., and Yang, E.G., *Identification of farnesoid X receptor modulators by a fluorescence polarization-based interaction assay.* Anal. Biochem., 2010. 398(2): p. 185-90.

72. Rohacova, J., Marin, M.L., Martinez-Romero, A., O'Connor, J.E., Gomez-Lechon, M.J., Donato, M.T., Castell, J.V., and Miranda, M.A., *Photophysical characterization and flow cytometry applications of cholylamidofluorescein, a fluorescent bile acid scaffold.* Photochem. Photobiol. Sci., 2008. 7(7): p. 860-6.

73. Liu, X., LeCluyse, E.L., Brouwer, K.R., Gan, L.-S.L., Lemasters, J.J., Stieger, B., Meier, P.J., and Brouwer, K.L.R., *Biliary excretion in primary rat hepatocytes cultured in a collagen-sandwich configuration.* Am. J. Physiol. Gastrointest. Liver Physiol., 1999. 277: p. G12-G21.

74. Martinez-Becerra, P., Briz, O., Romero, M.R., Macias, R.I., Perez, M.J., Sancho-Mateo, C., Lostao, M.P., Fernandez-Abalos, J.M., and Marin, J.J., *Further characterization of the electrogenicity and pH sensitivity of the human organic anion-transporting polypeptides OATP1B1 and OATP1B3.* Mol. Pharmacol., 2011. 79(3): p. 596-607.

75. de Waart, D.R., Hausler, S., Vlaming, M.L., Kunne, C., Hanggi, E., Gruss, H.J., Oude Elferink, R.P., and Stieger, B., *Hepatic transport mechanisms of cholyl-L-lysyl-fluorescein.* J. Pharmacol. Exp. Ther., 2010. 334(1): p. 78-86.

76. Baxter, D.J., Rahman, K., Bushell, A.J., Mills, C.O., Elias, E., and Billington, D., *Biliary lipid output by isolated perfused rat livers in response to cholyl-lysylfluorescein.* Biochim. Biophys. Acta, 1995. 1256(3): p. 374-80.

77. Milkiewicz, P., Baiocchi, L., Mills, C.O., Ahmed, M., Khalaf, H., Keogh, A., Baker, J., and Elias, E., *Plasma clearance of cholyl-lysyl-fluorescein: a pilot study in humans.* J. Hepatol., 1997. 27(6): p. 1106-9.

78. Milkiewicz, P., Saksena, S., Cardenas, T., Mills, C.O., and Elias, E., *Plasma elimination of cholyl-lysyl-fluorescein (CLF): a pilot study in patients with liver cirrhosis.* Liver, 2000. 20(4): p. 330-4.

79. Milkiewicz, P., Mills, C.O., Hubscher, S.G., Cardenas, R., Cardenas, T., Williams, A., and Elias, E., *Visualization of the transport of primary and secondary bile acids across liver tissue in rats: in vivo study with fluorescent bile acids.* J. Hepatol., 2001. 34(1): p. 4-10.

80. Oddi, A., Mills, C.O., Custureri, F., Di Nicola, V., Elias, E., and Di Matteo, G., *Intraoperative biliary tree imaging with cholyl-lysyl-fluorescein: an experimental study in the rabbit.* Surg. Laparosc. Endosc., 1996. 6(3): p. 198-200.

81. Bravo, P., Bender, V., and Cassio, D., *Efficient in vitro vectorial transport of a fluorescent conjugated bile acid analogue by polarized hepatic hybrid WIF-B and WIF-B9 cells.* Hepatology, 1998. 27(2): p. 576-83.

82. Wilton, J.C., Matthews, G.M., Burgoyne, R.D., Mills, C.O., Chipman, J.K., and Coleman, R., *Fluorescent choleretic and cholestatic bile salts take different paths across the hepatocyte: transcytosis of glycolithocholate leads to an extensive redistribution of annexin II.* J. Cell. Biol. , 1994. 127(2): p. 401-10.

83. Yamaguchi, K., Murai, T., Yabuuchi, H., Hui, S.P., and Kurosawa, T., *Measurement of bile salt export pump transport activities using a fluorescent bile acid derivative.* Drug Metab. Pharmacokinet., 2010. 25(2): p. 214-9.

84. Fang, L., Chan, W.H., He, Y.B., Kwong, D.W., and Lee, A.W., *Fluorescent anion sensor derived from cholic acid: the use of flexible side chain.* J. Org. Chem., 2005. 70(19): p. 7640-6.

85. Wang, H., Chan, W.H., and Lee, A.W., *Cholic acid-based fluorescent probes for enantioselective recognition of trifunctional amino acids.* Org. Biomol. Chem., 2008. 6(5): p. 929-34.

86. Wang, H. and Chan, W.H., *A cholic acid-based fluorescent chemosenor for the detection of ATP.* Org. Biomol. Chem., 2008. 6(1): p. 162-8.

87. Liu, S.Y., Fang, L., He, Y.B., Chan, W.H., Yeung, K.T., Cheng, Y.K., and Yang, R.H., *Cholic-acid-based fluorescent sensor for dicarboxylates and acidic amino acids in aqueous solutions.* Org. Lett., 2005. 7(26): p. 5825-8.

88. Weitzel, C., Stark, D., Kullmann, F., Scholmerich, J., Holstege, A., and Falk, W., *Ursodeoxycholic acid induced activation of the glucocorticoid receptor in primary rat hepatocytes.* Eur. J. Gastroenterol. Hepatol., 2005. 17(2): p. 169-77.

89. Tanaka, H. and Makino, I., *Ursodeoxycholic acid-dependent activation of the glucocorticoid receptor.* Biochem. Biophys. Res. Com., 1992. 188(2): p. 942-948.

90. Keely, S.J., Scharl, M.M., Bertelsen, L.S., Hagey, L.R., Barrett, K.E., and Hofmann, A.F., *Bile acid-induced secretion in polarized monolayers of T84 colonic epithelial cells: structure-activity relationships.* Am. J. Physiol. - Gastrointest. Liver Physiol., 2007. 292(1): p. G290-G297.

91. Tomaselli, S., Zanzoni, S., Ragona, L., Gianolio, E., Aime, S., Assfalg, M., and Molinari, H., *Solution Structure of the Supramolecular Adduct between a Liver Cytosolic Bile Acid Binding Protein and a Bile Acid-Based Gadolinium(III)-Chelate, a Potential Hepatospecific Magnetic Resonance Imaging Contrast Agent.* J. Med. Chem., 2008. 51(21): p. 6782-6792.

92. Kramer, W., Wess, G., Neckermann, G., Schubert, G., Fink, J., Girbig, F., Gutjahr, U., Kowalewski, S., Baringhaus, K.H., and Böger, G., *Intestinal absorption of peptides by coupling to bile acids.* J. Biol. Chem., 1994. 269(14): p. 10621-10627.

93. Swaan, P.W., Hillgren, K.M., Szoka, F.C., Jr., and Oie, S., *Enhanced transepithelial transport of peptides by conjugation to cholic acid.* Bioconjug. Chem., 1997. 8(4): p. 520-5.

94. Bhat, L., Jandeleit, B., Dias, T.M., Moors, T.L., and Gallop, M.A., *Synthesis and biological evaluation of novel steroidal pyrazoles as substrates for bile acid transporters.* Bioorg. Med. Chem. Lett., 2005. 15(1): p. 85-7.

95. Bonar-Law, R.P., *Synthesis of macrocycles from steroidal starting materials.*, 1989, University of Dublin: Dublin.

96. Kritchevsky, D., Poli, G., Scolastico, C., and Sirtori, C.R., *Novel derivatives of 3 alpha,7 alpha-dihydroxy-5 beta-cholan-24-oic acid (chenodeoxycholic acid) and 3 alpha,7 beta-dihydroxy-5 beta-cholan-24-oic acid (ursodeoxycholic acid).* Steroids, 1986. 47(1): p. 41-8.

97. Wess, G., Kramer, W., Bartmann, W., Enhsen, A., Glombik, H., Müllner, S., Bock, K., Dries, A., Kleine, H., and Schmitt, W., *Modified bile acids: preparation of 7α,12α-dihydroxy-3β- and 7α,12α-dihydroxy-3α-(2-hydroxyethoxy)-5β-cholanic acid and their biological activity.* Tetrahedron Letters, 1992. 33(2): p. 195-198.

98. Gouin, S. and Zhu, X.X., *Synthesis of 3 alpha- and 3 beta-dimers from selected bile acids.* Steroids, 1996. 61(11): p. 664-9.

99. Fieser, L.F. and Rajagopalan, S., *Oxidation of Steroids. III. Selective Oxidations and Acylations in the Bile Acid Series1.* Journal of the American Chemical Society, 1950. 72(12): p. 5530-5536.

100. Katona, B.W., Cummins, C.L., Ferguson, A.D., Li, T., Schmidt, D.R., Mangelsdorf, D.J., and Covey, D.F., *Synthesis, Characterization, and Receptor Interaction Profiles of Enantiomeric Bile Acids.* J. Med. Chem., 2007. 50(24): p. 6048-6058.

101. Dias, R.J., Ramachandra, R., *1977.* Synth. Commun., Studies directed toward synthesis of quassinoids. 3. Selective hydrolysis of 3-alpha-acetate functional-group of cholic-acid derivatives. 7: p. 293-297.

102. Yanuka, Y. and Halperin, G., *Stereospecific bromination of methyl 3.alpha.,7.alpha.-diacetoxy-12-oxocholanate, catalyzed by boron trifluoride.* J. Org. Chem., 1973. 38(15): p. 2587-2590.

103. Alvarez-Manzaneda, E., Chahboun, R., Barranco, I., Cabrera, E., Alvarez, E., Lara, A., Alvarez-Manzaneda, R., Hmamouchi, M., and Es-Samti, H., *Diastereoselective routes towards the austrodorane skeleton based on pinacol rearrangement: synthesis of (+)-austrodoral and (+)-austrodoric acid.* Tetrahedron, 2007. 63(48): p. 11943-11951.

104. Pore, V.S., Aher, N.G., Kumar, M., and Shukla, P.K., *Design and synthesis of fluconazole/bile acid conjugate using click reaction.* Tetrahedron, 2006. 62(48): p. 11178-11186.

105. Hirota, H., Yokoyama, A., Miyaji, K., Nakamura, T., and Takahashi, T., *Synthetic studies on quassinoids: Total synthesis of (±)-amarolide.* Tetrahedron Letters, 1987. 28(4): p. 435-438.

106. Santos, G.A., Murray, A.P., Pujol, C.A., Damonte, E.B., and Maier, M.S., *Synthesis and antiviral activity of sulfated and acetylated derivatives of 2beta,3alpha-dihydroxy-5alpha-cholestane.* Steroids, 2003. 68(2): p. 125-32.

107. Holysz, R.P., *Preparation and Dehydrohalogenation of 4-Halo-3-ketosteroids.* Journal of the American Chemical Society, 1953. 75(18): p. 4432-4437.

108. Prileschajew, N., *Oxydation ungesättigter Verbindungen mittels organischer Superoxyde.* Ber. Dtsch. Chem. Ges., 1909. 42(4): p. 4811-4815.

109. Bartlett, P.D., *Recent Work on the Mechanisms of Peroxide Reactions.* Rec. Chem. Prog., 1950. 11(47).

110. Comin, M.J., Elhalem, E., and Rodriguez, J.B., *Cerium ammonium nitrate: a new catalyst for regioselective protection of glycols.* Tetrahedron, 2004. 60(51): p. 11851-11860.

111. Corey, E.J. and Suggs, J.W., *Pyridinium chlorochromate. An efficient reagent for oxidation of primary and secondary alcohols to carbonyl compounds.* Tetrahedron Letters, 1975. 16(31): p. 2647-2650.

112. Shimizu, Y., Mitsuhashi, H., and Caspi, E., *A new practical synthesis of 1-dehydro-3-keto steroids of the A/B cis series.* Tetrahedron Letters, 1966. 7(34): p. 4113-4116.

113. Demir, A.S., Sabol, M.R., Jeganathan, A., Dolence, E.K., Watt, D.S., and Moldowan, J.M., *Synthesis of biological markers in fossil fuels 5. A synthesis of 5α-cholan-24-oic acid.* Org. Prep. Proc. Int., 1987. 19(2-3): p. 197-208.

114. Opsenica, D., Pocsfalvi, G., Milhous, W.K., and Solaja, B.A., *Antimalarial peroxides: the first intramolecular 1,2,4,5-tetraoxane.* J. Serb. Chem. Soc., 2002. 67(7): p. 465–471.

115. Iida, T., Momose, T., Chang, F.C., and Nambara, T., *Potential Bile Acid Metabolites. XI. : Syntheses of Stereoisomeric 7, 12-Dihydroxy-5α-cholanic Acids.* Chem. & Pharm. Bulletin, 1986. 34(5): p. 1934-8.

116. Salunke, D.B., Hazra, B.G., Gonnade, R.G., Bhadbhade, M.M., and Pore, V.S., *An efficient method for the synthesis of methyl 11α-amino-3α,7α-diacetoxy-12-oxo-5β-cholan-24-oate.* Tetrahedron, 2005. 61(14): p. 3605-3612.

117. Balakrishnan, A. and Polli, J.E., *Apical Sodium Dependent Bile Acid Transporter (ASBT, SLC10A2): A Potential Prodrug Target.* Mol. Pharm., 2006. 3(3): p. 223-230.

118. Zheng, X., Ekins, S., Raufman, J.-P., and Polli, J.E., *Computational Models for Drug Inhibition of the Human Apical Sodium-Dependent Bile Acid Transporter.* Mol. Pharm., 2009. 6(5): p. 1591-1603.

119. Hu, N.J., Iwata, S., Cameron, A.D., and Drew, D., *Crystal structure of a bacterial homologue of the bile acid sodium symporter ASBT.* Nature, 2011. 478(7369): p. 408-11.

120. Sharma, R., Majer, F., Peta, V.K., Wang, J., Keaveney, R., Kelleher, D., Long, A., and Gilmer, J.F., *Bile acid toxicity structure–activity relationships: Correlations between cell viability and lipophilicity in a panel of new and known bile acids using an oesophageal cell line (HET-1A).* Bioorg. Med. Chem., 2010. 18(18): p. 6886-6895.

121. Boonyarattanakalin, S., Martin, S.E., Sun, Q., and Peterson, B.R., *A Synthetic Mimic of Human Fc Receptors: Defined Chemical Modification of Cell Surfaces Enables Efficient Endocytic Uptake of Human Immunoglobulin-G.* J. Am. Chem. Soc., 2006. 128(35): p. 11463-11470.

122. Sugandhi, E.W., Slebodnick, C., Falkinham Ill, J.O., and Gandour, R.D., *Synthesis and antimicrobial evaluation of water-soluble, dendritic derivatives of epimeric 5α-cholestan-3-amines and 5α-cholestan-3-yl aminoethanoates.* Steroids, 2007. 72(8): p. 615-626.

123. del Amo, V., Bhattarai, K.M., Nissinen, M., Rissanen, K., Pérez-Payán, M.N., and Davis, A.P., *A Short Synthesis of Methyl 3α,7α,12α-Triaminocholanoate, the 'Triaza-Analogue' of Methyl Cholate.* Synlett, 2005. 2005(EFirst): p. 1319,1321.

124. Bhattarai, K.M., del Amo, V., Magro, G., Sisson, A.L., Joos, J.-B., Charmant, J.P.H., Kantacha, A., and Davis, A.P., *The "triamino-analogue" of methyl allocholate; a rigid, functionalised scaffold for supramolecular chemistry.* Chem. Commun., 2006(22): p. 2335-2337.

125. Castro, B.R., *Replacement of Alcoholic Hydroxyl Groups by Halogens and Other Nucleophiles via Oxyphosphonium Intermediates*, in *Organic Reactions*. 2004. p. 1–162.

126. Staudinger, H. and Meyer, J., *Über neue organische Phosphorverbindungen III. Phosphinmethylenderivate und Phosphinimine.* Helv. Chim. Acta, 1919. 2(1): p. 635-646.

127. Gololobov, Y.G., Zhmurova, I.N., and Kasukhin, L.F., *Sixty years of Staudinger reaction.* Tetrahedron, 1981. 37(3): p. 437-472.

128. Broderick, S., Davis, A.P., and Williams, R.P., *The "triamino-analogue" of methyl cholate; a facial amphiphile and scaffold with potential for combinatorial and molecular recognition chemistry.* Tetrahedron Letters, 1998. 39(33): p. 6083-6086.

129. Ternon, M., José Díaz-Mochón, J., Belsom, A., and Bradley, M., *Dendrimers and combinatorial chemistry—tools for fluorescent enhancement in protease assays.* Tetrahedron, 2004. 60(39): p. 8721-8728.

130. Zhao, Y. and Zhong, Z., *Oligomeric Cholates: Amphiphilic Foldamers with Nanometer-Sized Hydrophilic Cavities.* J. Am. Chem. Soc., 2005. 127(50): p. 17894-17901.

131. Bhattarai, K.M., *Synthesis of a series of organic soluble cholaphanes.*, 1995, University of Dublin: Dublin.

132. Tsemg, K.-Y. and Klein, P.D., *Formylated bile acids: Improved synthesis, properties, and partial deformylation.* Steroids, 1977. 29(5): p. 635-648.

133. Zhou, Y., Ryu, E.-H., Zhao, Y., and Woo, L.K., *Solvent-Responsive Metalloporphyrins: Binding and Catalysis.* Organometallics, 2006. 26(2): p. 358-364.

134. Micovic, V. and Mihailovic, M., *The Reduction of Acid Amides with Lithium Aluminum Hydride.* J. Org. Chem., 1953. 18(9): p. 1190-1200.

135. Weitzel, C., Stark, D., Kullmann, F., Schölmerich, J., Holstege, A., and Falk, W., *Ursodeoxycholic acid induced activation of the glucocorticoid receptor in primary rat hepatocytes.* Eur. J. Gastroenterol. Hepatol., 2005. 17(2): p. 169-177.

136. Miura, T., Ouchida, R., Yoshikawa, N., Okamoto, K., Makino, Y., Nakamura, T., Morimoto, C., Makino, I., and Tanaka, H., *Functional modulation of the glucocorticoid*

receptor and suppression of NF-kappaB-dependent transcription by ursodeoxycholic acid. J. Biol. Chem., 2001. 276: p. 47371–47378.

137. Tanaka, H., Makino, Y., Miura, T., Hirano, F., Okamoto, K., Komura, K., Sato, Y., and Makino, I., *Ligand-independent activation of the glucocorticoid receptor by ursodeoxycholic acid. Repression of IFN-gamma-induced MHC class II gene expression via a glucocorticoid receptor-dependent pathway.* J. Immunol., 1996. 156(4): p. 1601-1608.

138. Sharma, R., Prichard, D., Majer, F., Byrne, A.-M., Kelleher, D., Long, A., and Gilmer, J.F., *Ursodeoxycholic Acid Amides As Novel Glucocorticoid Receptor Modulators.* J. Med. Chem., 2010. 54(1): p. 122-130.

139. Williams, A.T.R., Winfield, S.A., and Miller, J.N., *Relative fluorescence quantum yields using a computer-controlled luminescence spectrometer.* Analyst, 1983. 108(1290).

140. Inc., H.J.Y., *A Guide to Recording Fluorescence Quantum Yields.* http://www.jobinyvon.com/usadivisions/Fluorescence/applications/quantumyieldstrad.pdf .

141. Magde, D., Wong, R., and Seybold, P.G., *Fluorescence Quantum Yields and Their Relation to Lifetimes of Rhodamine 6G and Fluorescein in Nine Solvents: Improved Absolute Standards for Quantum Yields¶.* Photochem. Photobiol., 2002. 75(4): p. 327-334.

142. Mosmann, T., *Rapid colorimetric assay for cellular growth and survival: application to proliferation and cytotoxicity assays.* J. Immunol. Meth., 1983. 65(1-2): p. 55-63.

143. Roehm, N.W., Rodgers, G.H., Hatfield, S.M., and Glasebrook, A.L., *An improved colorimetric assay for cell proliferation and viability utilizing the tetrazolium salt XTT.* J. Immunol. Meth., 1991. 142(2): p. 257-265.

144. Cory, A.H., Owen, T.C., Barltrop, J.A., and Cory, J.G., *Use of an aqueous soluble tetrazolium/formazan assay for cell growth assays in culture.* Cancer Communications, 1991. 3(7): p. 207-12.

145. Payne, C.M., Crowley-Skillicorn, C., Bernstein, C., Holubec, H., Moyer, M.P., and Bernstein, H., *Hydrophobic Bile Acid-Induced Micronuclei Formation, Mitotic Perturbations, and Decreases in Spindle Checkpoint Proteins: Relevance to Genomic Instability in Colon Carcinogenesis.* Nutrition and Cancer, 2010. 62(6): p. 825-840.

146. Zhou, Y., Doyen, R., and Lichtenberger, L.M., *The role of membrane cholesterol in determining bile acid cytotoxicity and cytoprotection of ursodeoxycholic acid.* Biochim. Biophys. Acta (BBA) - Biomembranes, 2009. 1788(2): p. 507-513.

acids: regulation of apoptosis by ursodeoxycholic acid. Journal of Lipid Research, 2009. 50(9): p. 1721-1734.

148. Rodrigues, C.M.P. and Steer, C.J., *The therapeutic effects of ursodeoxycholic acid as an anti-apoptotic agent.* Expert Opinion on Investigational Drugs, 2001. 10(7): p. 1243-1253.

149. Sola, S., Aranha, M.M., Steer, C.J., and Rodrigues, C.M.P., *Game and players: mitochondrial apoptosis and the therapeutic potential of ursodeoxycholic acid.* Curr. Issues Mol. Biol., 2007. 9(2): p. 123-38.

150. Hiebsch, R.R., Raub, T.J., and Wattenberg, B.W., *Primaquine blocks transport by inhibiting the formation of functional transport vesicles. Studies in a cell-free assay of protein transport through the Golgi apparatus.* J. Biol. Chem., 1991. 266(30): p. 20323-20328.

151. Cooper, J.A., *Effects of cytochalasin and phalloidin on actin.* J. Cell. Biol., 1987. 105(4): p. 1473-8.

152. Chan, E.K.L. and Fritzler, M.J., *Golgins: coiled-coil-rich proteins associated with the Golgi Complex.* Electronic Journal of Biotech., 1998. 1(2).

153. Nakamura, N., Rabouille, C., Watson, R., Nilsson, T., Hui, N., Slusarewicz, P., Kreis, T.E., and Warren, G., *Characterization of a cis-Golgi matrix protein, GM130.* J. Cell Biol., 1995. 131(6): p. 1715-1726.

154. Storrie, B., White, J., Rottger, S., Stelzer, E.H., Suganuma, T., and Nilsson, T., *Recycling of golgi-resident glycosyltransferases through the ER reveals a novel pathway and provides an explanation for nocodazole-induced Golgi scattering.* J. Cell Biol., 1998. 143(6): p. 1505-21.

155. Loken, M.R., *Immunofluorescence Techniques in Flow Cytometry and Sorting (2nd ed.).* Wiley, 1990: p. 341–53.

156. Jenkins, G.J., D'Souza, F.R., Suzen, S.H., Eltahir, Z.S., James, S.A., Parry, J.M., Griffiths, P.A., and Baxter, J.N., *Deoxycholic acid at neutral and acid pH, is genotoxic to oesophageal cells through the induction of ROS: The potential role of anti-oxidants in Barrett's oesophagus.* Carcinogenesis, 2007. 28(1): p. 136-42.

157. Dvorak, K., Payne, C.M., Chavarria, M., Ramsey, L., Dvorakova, B., Bernstein, H., Holubec, H., Sampliner, R.E., Guy, N., Condon, A., Bernstein, C., Green, S.B., Prasad, A., and Garewal, H.S., *Bile acids in combination with low pH induce oxidative stress and oxidative DNA damage: relevance to the pathogenesis of Barrett's oesophagus.* Gut, 2007. 56(6): p. 763-71.

158. Guy, N.C., Garewal, H., Holubec, H., Bernstein, H., Payne, C.M., Bernstein, C., Bhattacharyya, A.K., and Dvorak, K., *A novel dietary-related model of esophagitis and Barrett's esophagus, a premalignant lesion.* Nutr. Cancer, 2007. 59(2): p. 217-27.

159. Jolly, A.J., Wild, C.P., and Hardie, L.J., *Acid and bile salts induce DNA damage in human oesophageal cell lines.* Mutagenesis, 2004. 19(4): p. 319-24.

160. Keitel, V., Cupisti, K., Ullmer, C., Knoefel, W.T., Kubitz, R., and Haussinger, D., *The membrane-bound bile acid receptor TGR5 is localized in the epithelium of human gallbladders.* Hepatology, 2009. 50(3): p. 861-70.

161. Hayeshi, R., Hilgendorf, C., Artursson, P., Augustijns, P., Brodin, B., Dehertogh, P., Fisher, K., Fossati, L., Hovenkamp, E., Korjamo, T., Masungi, C., Maubon, N., Mols, R., Mullertz, A., Monkkonen, J., O'Driscoll, C., Oppers-Tiemissen, H.M., Ragnarsson, E.G., Rooseboom, M., and Ungell, A.L., *Comparison of drug transporter gene expression and functionality in Caco-2 cells from 10 different laboratories.* Eur. J. Pharm. Sci., 2008. 35(5): p. 383-96.

162. Sun, H., Chow, E.C., Liu, S., Du, Y., and Pang, K.S., *The Caco-2 cell monolayer: usefulness and limitations.* Expert Opin. Drug Metab. Toxicol., 2008. 4(4): p. 395-411.

163. Ahlin, G., Hilgendorf, C., Karlsson, J., Szigyarto, C.A., Uhlen, M., and Artursson, P., *Endogenous gene and protein expression of drug-transporting proteins in cell lines routinely used in drug discovery programs.* Drug Metab. Dispos., 2009. 37(12): p. 2275-83.

164. Smith, P.K., Krohn, R.I., Hermanson, G.T., Mallia, A.K., Gartner, F.H., Provenzano, M.D., Fujimoto, E.K., Goeke, N.M., Olson, B.J., and Klenk, D.C., *Measurement of protein using bicinchoninic acid.* Anal. Biochem., 1985. 150(1): p. 76-85.

165. Johnson, K.A. and Goody, R.S., *The Original Michaelis Constant: Translation of the 1913 Michaelis–Menten Paper.* Biochemistry, 2011. 50(39): p. 8264-8269.

166. Hofstee, B.H., *Non-inverted versus inverted plots in enzyme kinetics.* Nature, 1959. 184: p. 1296-8.

167. Capaldi, S., Guariento, M., Saccomani, G., Fessas, D., Perduca, M., and Monaco, H.L., *A single amino acid mutation in zebrafish (Danio rerio) liver bile acid-binding protein can change the stoichiometry of ligand binding.* J. Biol. Chem., 2007. 282(42): p. 31008-18.

168. Sato, T., Miwa, K., Sahara, H., Segawa, M., and Hattori, T., *The sequential model of Barrett's esophagus and adenocarcinoma induced by duodeno-esophageal reflux without exogenous carcinogens.* Anticancer Res., 2002. 22(1A): p. 39-44.

169. Miwa, K., Sahara, H., Segawa, M., Kinami, S., Sato, T., Miyazaki, I., and Hattori, T., *Reflux of duodenal or gastro-duodenal contents induces esophageal carcinoma in rats.* Int. J. Cancer, 1996. 67(2): p. 269-74.

170. Fein, M., Peters, J.H., Chandrasoma, P., Ireland, A.P., Oberg, S., Ritter, M.P., Bremner, C.G., Hagen, J.A., and DeMeester, T.R., *Duodenoesophageal reflux induces esophageal adenocarcinoma without exogenous carcinogen.* J. Gastrointest. Surg., 1998. 2(3): p. 260-8.

171. Hill, M.J., *Bile flow and colon cancer.* Mutat. Res., 1990. 238(3): p. 313-20.

172. Powell, A.A., LaRue, J.M., Batta, A.K., and Martinez, J.D., *Bile acid hydrophobicity is correlated with induction of apoptosis and/or growth arrest in HCT116 cells.* Biochem. J., 2001. 356(Pt 2): p. 481-6.

173. Martinez, J.D., Stratagoules, E.D., LaRue, J.M., Powell, A.A., Gause, P.R., Craven, M.T., Payne, C.M., Powell, M.B., Gerner, E.W., and Earnest, D.L., *Different bile acids exhibit distinct biological effects: the tumor promoter deoxycholic acid induces apoptosis and the chemopreventive agent ursodeoxycholic acid inhibits cell proliferation.* Nutr. Cancer, 1998. 31(2): p. 111-118.

174. Tsuchiya, S., Tsuji, M., Morio, Y., and Oguchi, K., *Involvement of endoplasmic reticulum in glycochenodeoxycholic acid-induced apoptosis in rat hepatocytes.* Toxicol. Lett., 2006. 166(2): p. 140-9.

175. Benz, C., Angermuller, S., Otto, G., Sauer, P., Stremmel, W., and Stiehl, A., *Effect of tauroursodeoxycholic acid on bile acid-induced apoptosis in primary human hepatocytes.* Eur. J. Clin. Invest., 2000. 30(3): p. 203-9.

176. Faubion, W.A., Guicciardi, M.E., Miyoshi, H., Bronk, S.F., Roberts, P.J., Svingen, P.A., Kaufmann, S.H., and Gores, G.J., *Toxic bile salts induce rodent hepatocyte apoptosis via direct activation of Fas.* J. Clin. Invest., 1999. 103(1): p. 137-45.

177. Yerushalmi, B., Dahl, R., Devereaux, M.W., Gumpricht, E., and Sokol, R.J., *Bile acid-induced rat hepatocyte apoptosis is inhibited by antioxidants and blockers of the mitochondrial permeability transition.* Hepatology, 2001. 33(3): p. 616-26.

178. Kwo, P., Patel, T., Bronk, S.F., and Gores, G.J., *Nuclear serine protease activity contributes to bile acid-induced apoptosis in hepatocytes.* Am. J. Physiol., 1995. 268(4 Pt 1): p. G613-21.

179. Zhang, R., Gong, J., Wang, H., and Wang, L., *Bile salts inhibit growth and induce apoptosis of culture human normal esophageal mucosal epithelial cells.* World J. Gastroenterol., 2005. 11(41): p. 6466-71.

180. Katona, B.W., Rath, N.P., Anant, S., Stenson, W.F., and Covey, D.F., *Enantiomeric deoxycholic acid: total synthesis, characterization, and preliminary toxicity toward colon cancer cell lines.* J. Org. Chem., 2007. 72(24): p. 9298-307.

181. Koley, D. and Bard, A.J., *Triton X-100 concentration effects on membrane permeability of a single HeLa cell by scanning electrochemical microscopy (SECM).* Proc. Natl. Acad. Sci., 2010. 107(39): p. 16783-16787.

182. Patel, T. and Gores, G.J., *Inhibition of bile-salt-induced hepatocyte apoptosis by the antioxidant lazaroid U83836E.* Toxicol. Appl. Pharmacol., 1997. 142(1): p. 116-22.

183. Gumpricht, E., Dahl, R., Devereaux, M.W., and Sokol, R.J., *Beta-carotene prevents bile acid-induced cytotoxicity in the rat hepatocyte: Evidence for an antioxidant and anti-apoptotic role of beta-carotene in vitro.* Pediatr. Res., 2004. 55(5): p. 814-21.

184. Tan, K.P., Yang, M., and Ito, S., *Activation of nuclear factor (erythroid-2 like) factor 2 by toxic bile acids provokes adaptive defense responses to enhance cell survival at the emergence of oxidative stress.* Mol. Pharmacol., 2007. 72(5): p. 1380-90.

185. Im, E. and Martinez, J.D., *Ursodeoxycholic acid (UDCA) can inhibit deoxycholic acid (DCA)-induced apoptosis via modulation of EGFR/Raf-1/ERK signaling in human colon cancer cells.* J. Nutr., 2004. 134(2): p. 483-6.

186. Park, Y.H., Kim, J.A., Baek, J.H., Jung, E.J., Kim, T.H., Suh, H., Park, M.H., and Kim, K.W., *Induction of apoptosis in HepG2 human hepatocellular carcinoma cells by a novel derivative of ursodeoxycholic acid (UDCA).* Arch. Pharm. Res., 1997. 20(1): p. 29-33.

187. Park, S.E., Lee, S.W., Hossain, M.A., Kim, M.Y., Kim, M.N., Ahn, E.Y., Park, Y.C., Suh, H., Kim, G.Y., Choi, Y.H., and Kim, N.D., *A chenodeoxycholic derivative, HS-1200, induces apoptosis and cell cycle modulation via Egr-1 gene expression control on human hepatoma cells.* Cancer Lett., 2008. 270(1): p. 77-86.

188. Im, E.O., Choi, Y.H., Paik, K.J., Suh, H., Jin, Y., Kim, K.W., Yoo, Y.H., and Kim, N.D., *Novel bile acid derivatives induce apoptosis via a p53-independent pathway in human breast carcinoma cells.* Cancer Lett., 2001. 163(1): p. 83-93.

189. Choi, Y.H., Im, E.O., Suh, H., Jin, Y., Yoo, Y.H., and Kim, N.D., *Apoptosis and modulation of cell cycle control by synthetic derivatives of ursodeoxycholic acid and chenodeoxycholic acid in human prostate cancer cells.* Cancer Lett., 2003. 199(2): p. 157-67.

190. Yee, S.B., Yeo, W.J., Park, B.S., Kim, J.Y., Baek, S.J., Kim, Y.C., Seo, S.Y., Lee, S.H., Kim, J.H., Suh, H., Kim, N.D., Lim, Y.J., and Yoo, Y.H., *Synthetic chenodeoxycholic acid derivatives inhibit glioblastoma multiform tumor growth in vitro and in vivo.* Int. J. Oncol., 2005. 27(3): p. 653-659.

191. El Kihel, L., Clement, M., Bazin, M.A., Descamps, G., Khalid, M., and Rault, S., *New lithocholic and chenodeoxycholic piperazinylcarboxamides with antiproliferative and pro-apoptotic effects on human cancer cell lines.* Bioorg. Med. Chem., 2008. 16(18): p. 8737-44.

192. Brossard, D., El Kihel, L., Clement, M., Sebbahi, W., Khalid, M., Roussakis, C., and Rault, S., *Synthesis of bile acid derivatives and in vitro cytotoxic activity with pro-apoptotic process on multiple myeloma (KMS-11), glioblastoma multiforme (GBM), and colonic carcinoma (HCT-116) human cell lines.* Eur. J. Med. Chem., 2010. 45(7): p. 2912-2918.

193. Vatmurge, N.S., Hazra, B.G., Pore, V.S., Shirazi, F., Chavan, P.S., and Deshpande, M.V., *Synthesis and antimicrobial activity of beta-lactam-bile acid conjugates linked via triazole.* Bioorg. Med. Chem. Lett., 2008. 18(6): p. 2043-7.

194. Savage, P.B. and Li, C., *Cholic acid derivatives: novel antimicrobials.* Expert Opin. Investig. Drugs, 2000. 9(2): p. 263-72.

195. Lai, X.Z., Feng, Y., Pollard, J., Chin, J.N., Rybak, M.J., Bucki, R., Epand, R.F., Epand, R.M., and Savage, P.B., *Ceragenins: cholic acid-based mimics of antimicrobial peptides.* Acc. Chem. Res., 2008. 41(10): p. 1233-40.

196. Bellini, A.M., Vertuani, G., Quaglio, M.P., and Cavazzini, G., *[Bile acid derivatives with antimicrobial activity].* Farmaco Sci., 1979. 34(11): p. 967-78.

197. Bellini, A.M., Quaglio, M.P., Mencini, E., Guarneri, M., Cavazzini, G., and Fini, A., *Antimicrobial activity of basic cholane derivatives, VIII.* Arch. Pharm. (Weinheim), 1989. 322(12): p. 879-83.

198. Bellini, A.M., Mencini, E., Quaglio, M.P., Guarneri, M., and Fini, A., *Antimicrobial activity of basic cholane derivatives. Part IX.* Arch. Pharm. (Weinheim), 1990. 323(4): p. 201-5.

199. Cavazzini, G., Bellini, A.M., Quaglio, M.P., and Guarneri, M., *[Antibacterial activity of cholane derivatives. III. Amidie and amine derivatives of cholic, desoxycholic, chenodesoxycholic and ursodesoxycholic acids].* Nuovi Ann. Ig. Microbiol., 1982. 33(2-3): p. 419-33.

200. Dumic, M., Filic, D., Vinkovic, M., Jamnicky, B., and Kamenar, B., *1-Sulfonyl-1a,2,6,6a-tetrahydro-1H,4H-[1,3]-dioxepino[5,6-b]azirines: A novel class of fused dioxepins, potent hypoglycemic agents.* Tetrahedron Letters, 1993. 34(22): p. 3639-3642.

201. Tsagarakis, N.J., Drygiannakis, I., Batistakis, A.G., Kolios, G., and Kouroumalis, E.A., *A concentration-dependent effect of ursodeoxycholate on apoptosis and caspases activities of HepG2 hepatocellular carcinoma cells.* Eur. J. Pharmacol., 2010. 640(1-3): p. 1-7.

202. Kim, S.J., Chung, M.J., Kim, J.S., Kim, B., Park, W.H., Kim, S.H., Kim, S.Z., Lee, J.S., and Kim, S.M., *Deciphering the role of paclitaxel in the SKGT4 human esophageal adenocarcinoma cell line.* Int. J. Oncol., 2011. 39(6): p. 1587-91.

203. Lefebvre, P., Cariou, B., Lien, F., Kuipers, F., and Staels, B., *Role of bile acids and bile acid receptors in metabolic regulation.* Physiol. Rev., 2009. 89(1): p. 147-91.

204. Jaeschke, H., Gores, G.J., Cederbaum, A.I., Hinson, J.A., Pessayre, D., and Lemasters, J.J., *Mechanisms of hepatotoxicity.* Toxicol. Sci., 2002. 65(2): p. 166-76.

205. von Haehling, S., Schefold, J.C., Jankowska, E.A., Springer, J., Vazir, A., Kalra, P.R., Sandek, A., Fauler, G., Stojakovic, T., Trauner, M., Ponikowski, P., Volk, H.D., Doehner, W., Coats, A.J., Poole-Wilson, P.A., and Anker, S.D., *Ursodeoxycholic acid in patients with chronic heart failure: a double-blind, randomized, placebo-controlled, crossover trial.* J. Am. Coll. Cardiol., 2012. 59(6): p. 585-92.

206. Henry-Mowatt, J., Dive, C., Martinou, J.C., and James, D., *Role of mitochondrial membrane permeabilization in apoptosis and cancer.* Oncogene, 2004. 23(16): p. 2850-60.

207. Kim, I., Xu, W., and Reed, J.C., *Cell death and endoplasmic reticulum stress: disease relevance and therapeutic opportunities.* Nat. Rev. Drug Discov., 2008. 7(12): p. 1013-30.

208. Perez, M.J. and Briz, O., *Bile-acid-induced cell injury and protection.* World J. Gastroenterol., 2009. 15(14): p. 1677-89.

209. Malhi, H., Guicciardi, M.E., and Gores, G.J., *Hepatocyte death: a clear and present danger.* Physiol. Rev., 2010. 90(3): p. 1165-94.

210. Amaral, J.D., Viana, R.J.S., Ramalho, R.M., Steer, C.J., and Rodrigues, C.M.P., *Thematic Review Series: Bile Acids: Bile acids: regulation of apoptosis by ursodeoxycholic acid* J. Lipid Res., 2009. 50(9): p. 1721-1734.

211. Guicciardi, M.E. and Gores, G.J., *Life and death by death receptors.* FASEB J., 2009. 23(6): p. 1625-37.

212. Schutze, S., Tchikov, V., and Schneider-Brachert, W., *Regulation of TNFR1 and CD95 signalling by receptor compartmentalization.* Nat. Rev. Mol. Cell Biol., 2008. 9(8): p. 655-62.

213. Herbein, G. and O'Brien, W.A., *Tumor necrosis factor (TNF)-alpha and TNF receptors in viral pathogenesis.* Proc. Soc. Exp. Biol. Med., 2000. 223(3): p. 241-57.

214. Nagata, S., *Fas ligand-induced apoptosis.* Annu. Rev. Genet., 1999. 33: p. 29-55.

215. Fulda, S. and Debatin, K.M., *Caspase Activation in Cancer Therapy.* In: Madame Curie Bioscience Database [Internet]. Austin (TX): Landes Bioscience, 2000.

216. Elmore, S., *Apoptosis: A Review of Programmed Cell Death.* Toxicologic Pathology, 2007. 35(4): p. 495-516.

217. Youle, R.J. and Strasser, A., *The BCL-2 protein family: opposing activities that mediate cell death.* Nat. Rev. Mol. Cell Biol., 2008. 9(1): p. 47-59.

218. Ayllon, V., Cayla, X., Garcia, A., Fleischer, A., and Rebollo, A., *The anti-apoptotic molecules Bcl-xL and Bcl-w target protein phosphatase 1alpha to Bad.* Eur. J. Immunol., 2002. 32(7): p. 1847-55.

219. Belizário, J.E., Alves, J., Occhiucci, J.M., Garay-Malpartida, M., and Sesso, A., *A mechanistic view of mitochondrial death decision pores.* Brazilian Journal of Medical and Biological Research, 2007. 40: p. 1011-1024.

220. Zheng, T.S., Schlosser, S.F., Dao, T., Hingorani, R., Crispe, I.N., Boyer, J.L., and Flavell, R.A., *Caspase-3 controls both cytoplasmic and nuclear events associated with Fas-mediated apoptosis in vivo.* Proc. Nat. Ac. Sci., 1998. 95(23): p. 13618-13623.

221. M., P.C., Crowley-Weber, C.L., Dvorak, K., Bernstein, C., Bernstein, H., Holubec, H., Crowley, C., and Garewal, H., *Mitochondrial perturbation attenuates bile acid-induced cytotoxicity.* Cell Biol. Toxicol., 2005. 21(5-6): p. 215-31.

222. Bernstein, H., Payne, C.M., Bernstein, C., Schneider, J., Beard, S.E., and Crowley, C.L., *Activation of the promoters of genes associated with DNA damage, oxidative stress, ER stress and protein malfolding by the bile salt, deoxycholate.* Toxicol. Lett., 1999. 108(1): p. 37-46.

223. Hotamisligil, G.S., *Endoplasmic Reticulum Stress and the Inflammatory Basis of Metabolic Disease.* Cell. Biol. Toxicol., 2010. 140(6): p. 900–917.

224. Simon, H.U., Haj-Yehia, A., and Levi-Schaffer, F., *Role of reactive oxygen species (ROS) in apoptosis induction.* Apoptosis, 2000. 5(5): p. 415-418.

225. Lee, T.-Y., Chen, F.-Y., Chang, H.-H., and Lin, H.-C., *The effect of capillarisin on glycochenodeoxycholic acid-induced apoptosis and heme oxygenase-1 in rat primary hepatocytes.* Mol.Cell. Biochem., 2009. 325(1): p. 53-59.

226. Huang, L., Zhu, H., Xu, X., Zhang, C., and Shen, Y.-M., *Synthesis and characterization of organometallic rhenium(I) and technetium(I) bile acid complexes.* J. Org. Chem., 2009. 694(20): p. 3247-3253.

227. Altorki, N., Schwartz, G.K., Blundell, M., Davis, B.M., Kelsen, D.P., and Albino, A.P., *Characterization of cell lines established from human gastric-esophageal adenocarcinomas. Biologic phenotype and invasion potential.* Cancer, 1993. 72(3): p. 649-57.

Appendix

Copy of Publication

Author's personal copy

Bioorganic & Medicinal Chemistry 20 (2012) 1767–1778

Contents lists available at SciVerse ScienceDirect

Bioorganic & Medicinal Chemistry

journal homepage: www.elsevier.com/locate/bmc

New fluorescent bile acids: Synthesis, chemical characterization, and disastereoselective uptake by Caco-2 cells of 3-deoxy 3-NBD-amino deoxycholic and ursodeoxycholic acid

Ferenc Májer [a], Johanna J. Salomon [a], Ruchika Sharma [a], Simona V. Etzbach [a], Mohd Nadzri Mohd Najib [a], Ray Keaveny [a], Aideen Long [b], Jun Wang [a], Carsten Ehrhardt [a], John F. Gilmer [a,*]

[a] School of Pharmacy and Pharmaceutical Sciences, Trinity College Dublin, Panoz Institute, Dublin 2, Ireland
[b] Cell Signalling, Institute of Molecular Medicine, Trinity Centre for Health Science, St. James's Hospital, Dublin 8, Ireland

ARTICLE INFO

Article history:
Received 4 November 2011
Revised 23 December 2011
Accepted 2 January 2012
Available online 12 January 2012

Keywords:
NBD label
Ursodeoxycholic acid
Deoxycholic acid
Bile acid transporter
OATP
Stereoselective

ABSTRACT

Deoxycholic acid (DCA), a secondary bile acid (BA), and ursodeoxycholic acid (UDCA), a tertiary BA, cause opposing effects in vivo and in cell suspensions. Fluorescent analogues of DCA and UDCA could help investigate important questions about their cellular interactions and distribution.

We have prepared a set of isomeric 3α- and 3β-amino analogues of UDCA and DCA and derivatised these with the discrete fluorophore, 4-nitrobenzo-2-oxa-1,3-diazol (NBD), forming the corresponding four fluorescent adducts. These absorb in the range 465–470 nm and fluoresce at approx. 535 nm.

In order to determine the ability of the new fluorescent bile acids to mimic the parents, their uptake was studied using monolayers of Caco-2 cells, which are known to express multiple proteins of the organic anion-transporting peptide (OATP) subfamily of transporters. Cellular uptake was monitored over time at 4 and 37 °C to distinguish between passive and active transport.

All four BA analogues were taken up but in a strikingly stereo- and structure-specific manner, suggesting highly discriminatory interactions with transporter protein(s). The α-analogues of DCA and to a lesser extent UDCA were actively transported, whereas the β-analogues were not. The active transport process was saturable, with Michaelis–Menten constants for 3α-NBD DCA (**5**) being $K_m = 42.27 \pm 12.98$ μM and $V_{max} = 2.8 \pm 0.4$ nmol/(mg protein*min) and for 3α-NBD UDCA (**3**) $K_m = 28.20 \pm 7.45$ μM and $V_{max} = 1.8 \pm 0.2$ nmol/(mg protein*min). These fluorescent bile acids are promising agents for investigating questions of bile acid biology and for detection of bile acids and related organic anion transport processes.

© 2012 Elsevier Ltd. All rights reserved.

1. Introduction

The secondary bile acid (BA), deoxycholic acid (DCA, **1** Fig. 1) is a putative promoter of intestinal carcinogenesis. DCA causes DNA fragmentation, oxidative stress, Golgi fragmentation and apoptosis.[1] Conversely, the clinically used ursodeoxycholic acid (UDCA, **2** Fig. 1) is cytoprotective, immunomodulatory, anti-inflammatory and anti-apoptotic.[2] In general, UDCA's effects oppose those of DCA.[3–5] For example, pre-treatment with UDCA can prevent DCA induced apoptosis and Golgi fragmentation in colon cancer cells.[6]

The divergent cellular effects of DCA and UDCA have been widely investigated and there has been progress in characterising some of the molecular mechanisms involved.[7–10] However, new tools and strategies are required to investigate direct cellular interactions of the compounds, their uptake and distribution. Fluorescent steroid analogues can prove useful for this kind of problem. Such compounds may also be used to probe interacting proteins and related cellular transport mechanisms.

The 4-nitrobenzo-2-oxa-1,3-diazole (NBD) group is a particularly useful reporter group in this context because of its relatively low steric impact, its sensitivity to its environment, satisfactory quantum yield and stability.[11,12] In the BA field, the synthesis and chemical characterisation of 3-,7- and 12-α- and β-NBD analogues of cholic acid (CA, Fig. 1a) and their tauro conjugates have been reported, followed by comprehensive studies of their uptake and hepatic metabolism in vitro and in rats.[12–14] Recently, the 3- and 7-amino NBD analogues of CA were studied as uptake probes for flow cytometry in isolated rat hepatocytes.[15] NBD-labelled 24-lysyl conjugates of UDCA (Fig. 1a) and DCA have been studied as substrates for hepatic[16] and intestinal transport proteins.[17] Other investigations into (tauro)-UDCA have employed the UDCA 7-NBD analogue.[5,18,19]

Astonishingly, the 3-deoxy 3-NBD-amino derivatives of DCA and UDCA have not been reported to date. Placement of the fluorescent reporter group at C-3 appears to us to be optimal for exploring the disposition of UDCA and DCA because this preserves

* Corresponding author. Tel.: +353 1 896 2795; fax: +353 1 896 2793.
E-mail address: gilmerjf@tcd.ie (J.F. Gilmer).

0968-0896/$ - see front matter © 2012 Elsevier Ltd. All rights reserved.
doi:10.1016/j.bmc.2012.01.002

Author's personal copy

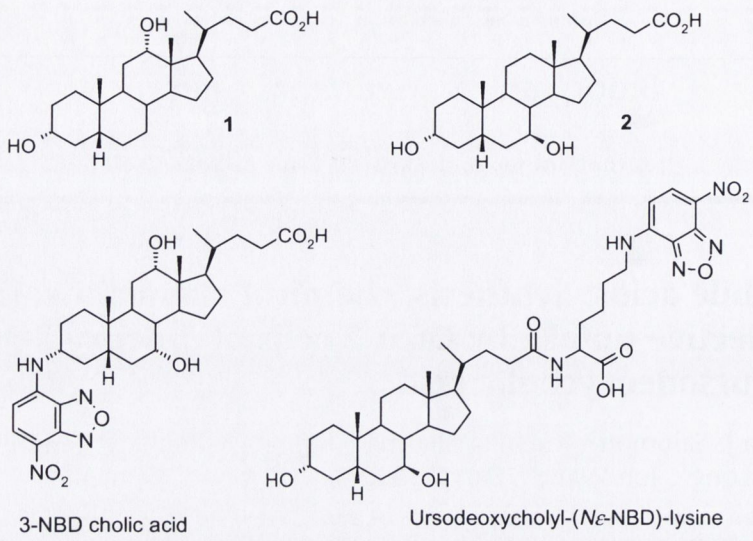

Figure 1a. Structures of bile acids UDCA (**1**) and DCA (**2**) along with fluorescent analogues of cholic acid and UDCA that have been studied previously.

the 7- and 12-OH groups that account for the differing chemical and biological properties of the parent compounds. Importantly, C-3 modification also preserves the characteristic free bile acid side chain. Structural studies probing the interaction of UDCA with cognate proteins would also support incorporation of a reporter group at the BA C3. In the 3.0 Å crystal structure of human type III 3α-hydroxysteroid dehydrogenase (HSD)/bile acid binding protein (AKR1C2) complexed with NADP(+) and UDCA anion, the carboxylate group of UDCA was modelled in the oxyanion hole, deep in the protein with the 3-OH solvent exposed (11513593, PDB 1 ihi). The liver cytosolic bile acid binding protein (BABP) binds BAs in a similar fashion, which led to the elegant design of diagnostic compounds elaborated at C-3 with gadolinium binding EDTA groups.[20] Additionally, various SAR surveys and QSAR models of the human apical sodium-dependent bile acid transporter (ASBT, SLC10A2) suggest that the C3-OH is tolerant of modification.[21,22] Finally, various bile acid carrier pro-drug conjugates have proven that intestinal bile acid transporters can tolerate payload incorporation at C-3.[23]

We have synthesised isomeric 3-deoxy 3-NBD-amino derivatives of UDCA and DCA (Fig. 1b) as probes for studying the distribution of these important steroids. A control compound lacking the steroidal nucleus (**7**) was also prepared to detect non-specific effects. In order to assess the suitability of the new analogues for investigating the disposition of the parent BAs, we have studied their uptake into polarised monolayers of intestinal epithelial Caco-2 cells. The Caco-2 cell line exhibits many of the features of the normal intestinal epithelium including expression of various BA transporter proteins, such as the sodium-dependent bile acid transporter (ASBT) and various members of the organic anion-transporting peptide (OATP) subfamily.[24,25] Caco-2 cells are therefore routinely used for assessing bile acid uptake and transport[26] and they are considered a suitable model for preliminary assessment of the NBD analogues as surrogates of DCA and UDCA.

The uptake of the DCA and UDCA 3-NBD compounds **3** and **5** was strikingly structure and stereo-specific. The DCA α-analogue was sufficiently rapidly taken up to suggest general applicability in the detection of active transport processes with significant practical advantages over experimental set-ups utilising radiolabelled substrates.

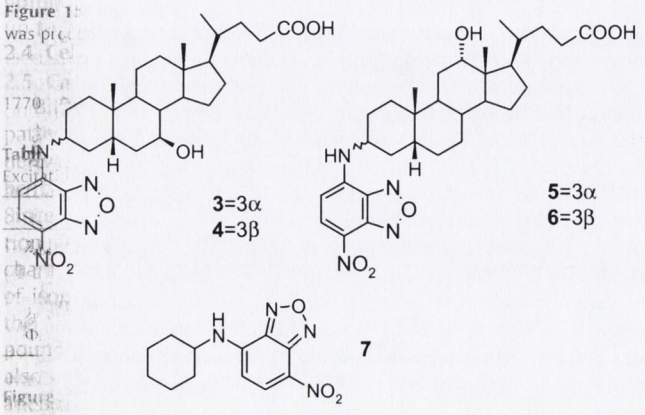

Figure 1b. New NBD analogues of UDCA and DCA **3**–**6**; cyclohexylamine-NBD **7** was produced as a non-bile acid fluorescent control.

2. Results/Discussion

2.1. Chemistry

The NBD compounds (**3**–**6**) were produced as shown in Scheme 1 by formation of the appropriate azides, reduction and displacement of NBD chloride. The orthogonally protected formate-methyl esters of UDCA and DCA (**8**, **9**) were obtained in three steps from the parent bile acids. In order to produce the β-NBD compounds, these were first converted to the corresponding 3-α mesylates (**10** and **11**), followed by SN2 substitution to give the β-azides. In early experiments the 3-amino-NBD group was found to be labile to conditions required to remove the formyl protection. Therefore, the formate esters were selectively removed (acetyl chloride in dry MeOH) at the azide stage to yield **12**, **13**. The α-azides were reduced and BOC-protected in situ followed by purification by flash chromatography. The BOC protection was removed, the NBD introduced and finally the 24-ester groups hydrolysed to give **4** and **6**.

The α-compounds **3**, **5** required amine introduction at C-3 with retention of configuration. After several unsuccessful attempts with introduction of methanesulfonate, we turned to bromide and generated 3-βbromides **14**, **15** using a mixture of $P(Ph_3)_3$ and *N*-bromosuccinimide in THF at low temperature. Azide displacement of the β-bromides producing **16**, **17** was faster than the displacement of the α-mesylates in the 3-β series (**10**, **11**). The

Author's personal copy

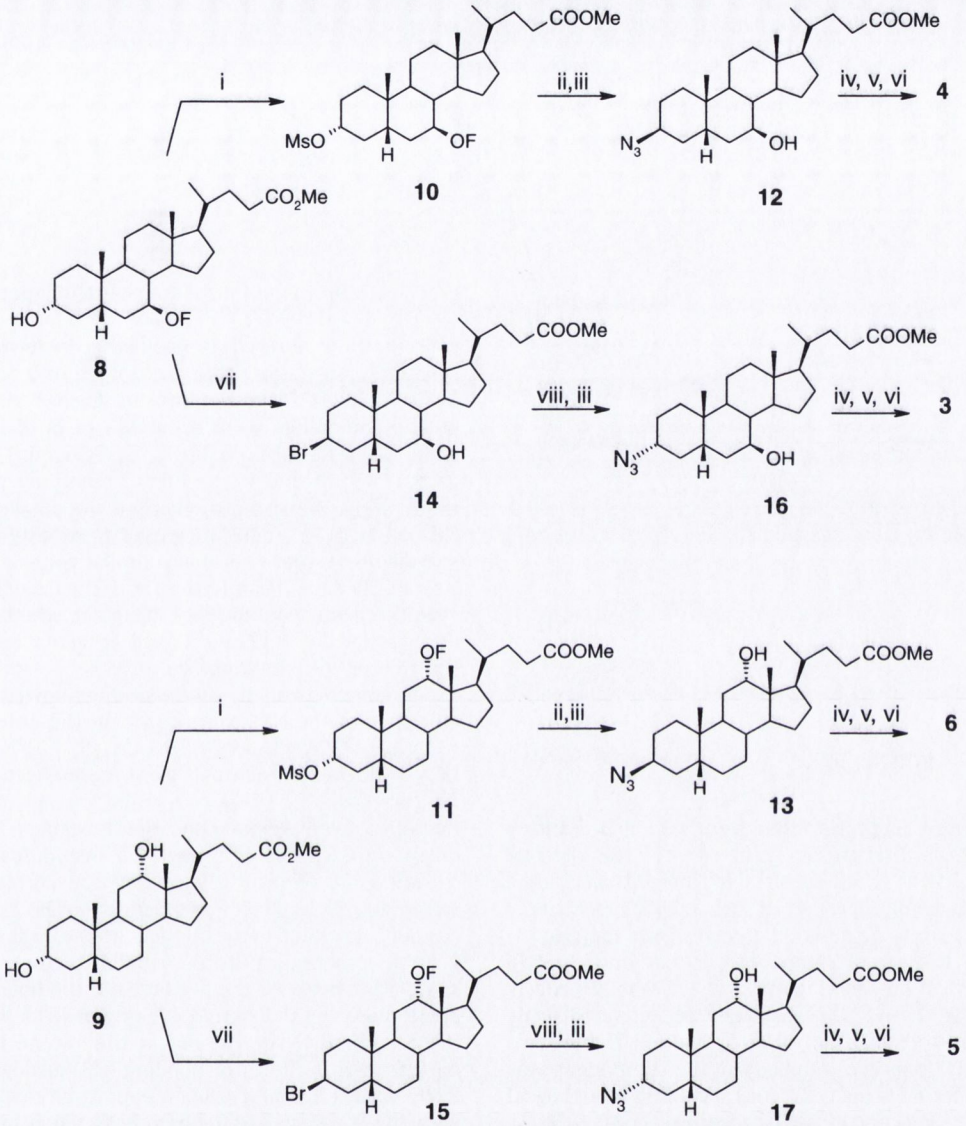

Scheme 1. Synthesis of UDCA and DCA NBD analogues **3–6**. Reagents and conditions: (i) MsCl, NEt_3, DCM, 0 °C, 20 min; (ii) NaN_3, DMPU, 50 °C, 6–8 d; (iii) AcCl, an. MeOH, 0 °C to rt, overnight; (iv) 10% Pd/C, $(BOC)_2O$, H_2, EtOAc, rt, overnight; (v) (a) 10% TFA/DCM, rt, overnight (b) NBD-Cl, $NaHCO_3$, MeOH, reflux, 5–14 d; (vi) 2 M NaOH/MeOH (pH~14), 40 °C, 4 h; (vii) $P(Ph_3)_3$, NBS, THF, −18 °C to rt, 1.5 h; (viii) NaN_3, DMPU, rt, overnight.

route to the α-NBD compounds was otherwise similar to that used to generate the β-compounds with regioselective deformylation, reduction, BOC protection and purification, de-BOC, NBD formation and de-esterification. Amino analogues of cholic acid and their NBD derivatives have been produced by stereoselective reduction of the corresponding oximes. The current approach is longer but it is clean, high yielding and the SN2 substitution provides stereochemical control. The NBD derivative of cyclohexylamine was obtained by direct treatment of the amine with NBD chloride. The NBD compounds were bright orange crystalline solids, pure by HPLC (>98%) and their structure confirmed by HRMS/NMR.

2.2. Stability and physicochemical characterisation

The stability of 3β–NBD UDCA was assessed in pH 7.4 buffer (37 °C) using HPLC to monitor remaining compound as a function of time. There was no change in the LC-fluorescence peak area over 24 h under these conditions showing that the 3-NBD group was stable. The same HPLC method could also be used to assess lipophilicity. The β-compounds (calculated capacity factor (k') for 3β-NBD-DCA was 7.3 and for 3β-NBD-UDCA 5.1) were more polar than the corresponding α-compounds (k' for 3α-NBD-DCA was 10.8 and for 3α-NBD-UDCA 5.6). As expected the DCA analogues were more hydrophobic than the corresponding UDCA analogues.

2.3. Photo/physical characterization

The UV/Vis absorption spectra of **3–6** measured in ethanol solution exhibited maxima at 228, 335 and 470 nm (Table 1). The β-compounds were red-shifted relative to the α-compounds by around 5 nm (Fig. 2). The fluorescence emission spectra for 3–6 exhibited maxima at λ_{Em} 537 nm with a 2–3 nm blue shift for the α-isomers (λ_{Em} was recorded using an λ_{abs} of 470 nm). These values were not affected by oxygen exposure. They are broadly in agreement with previously reported fluorescence values for dipolic acid NBD derivatives.[13,15]

Author's personal copy

Table 1
Excitation/emission characteristics of 3-amino-NBD derivatives of UDCA and DCA. Quantum yields (ΦF) were estimated relative to fluorescein in 0.01 KOH ($\Phi F_{ST} = 0.925$)

	3 (3α-NBD-UDCA)	**4** (3β-NBD-UDCA)	**5** (3α-NBD-DCA)	**6** (3β-NBD-DCA)	**7** Cyclohexyl amine-NBD
λ_{abs} (nm)	231	227	228	227	225
	335	331	335	331	334
	470	465	470	466	469
λ_{Em} (nm)	534	537	535	537	536
ΦF	0.268	0.228	0.259	0.221	0.232

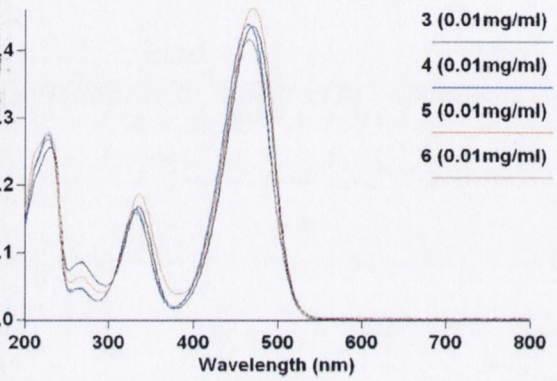

Figure 2. UV–Vis spectra overlaid of **3**–**6** acquired in EtOH at 0.01 mg/ml overlaid.

2.4. Cell viability

Bile acids can cause apoptosis through intrinsic and extrinsic pathways and necrosis through detergent effects.[8] The effect of derivatising the bile acids is not predictable though toxicity may be related to physicochemical properties such as hydrophobicity.[10] Since the NBD-bile acids were designed to investigate the disposition and uptake of the parent compounds, it was important to characterise their effect on cell viability. The cell viability effects of isomeric NBD-BAs (1–100 μM) was therefore measured using the MTT assay after incubating Caco-2 monolayers with the compounds for up to 100 min. The cytoxicity of the compounds was also assessed in other relevant cells lines including oesophageal adenocarcinoma (SKGT-4) and hepatic cancer cell lines (HUH-7). Compounds **3**–**6** did not affect cell viability in any of these cell lines up to 24 h up to 100 μM.

2.5. Caco-2 uptake

The time-course of uptake of **3**–**6** (10 μM) into Caco-2 cell mondiayers was studied at 37 °C (which included contributions from active and passive uptake) and at 4 °C (which reflects only passive diffusion) (Fig. 2). In general, uptake increased in a time-dependent manner for up to 60 min. Differences in uptake of the β compounds (**4** and **6**) between 37 and 4 °C were not significant ($P = 0.12$ and $P = 0.25$ for **4** and **6**, respectively) (Fig. 2B and D). The β compounds were therefore taken up exclusively through passive diffusion at 37 °C. In contrast, uptake of the α -compounds **3** and **5** at 37 °C was significantly higher ($P < 0.01$) to that at 4 °C (Fig. 2A and C). The passive component did not exceed 30% of the total uptake in either case.

The active transport of **3** and **5** was then kinetically characterised. Cells were incubated for 20 min with the compounds at concentrations ranging from 1 to 100 μM at 37 °C and 4 °C. The obtained values at 4 °C were subtracted from total uptake at 37 °C, before performing kinetic analysis. The concentration-dependent uptake of the bile acid compounds, **3** and **5** was clearly saturable (Fig. 3A and B). An Eadie-Hofstee transformation (i.e., a graphical representation of transport kinetics in which reaction velocity is plotted as a function of the velocity (v) versus substrate concentration ratio (v/[S]) obtained a single straight line for both substrates, suggesting that the uptake of **3** and **5** was mediated by a single transporter site in Caco-2 cells (Fig. 3C). The kinetic parameters were estimated to be $K_m = 42.27 \pm 12.98$ μM and $V_{max} = 2.8 \pm 0.4$ nmol/(mg protein∗min) for **3** and $K_m = 28.20 \pm 7.45$ μM and $V_{max} = 1.8 \pm 0.2$ nmol/(mg protein∗min) for **5**, respectively. We also characterised the uptake of the cyclohexyl-NBD adduct (**7**), a substance used previously to control for non-specific fluorescent effects in a similar context (Fig. 4). Compound **7** established rapid equilibrium with the Caco-2 cells (Fig. 5), however, there was no difference in uptake whether the experiments were carried out at 37 or 4 °C, indicating that only passive diffusion contributed to cellular uptake.

The time-dependent uptake studies allowed ranking the uptake efficiency of the NBD compounds in the order 3α-NBD-DCA (**5**) >3α-NBD-UDCA (**3**) >3β-NBD-DCA (**6**) >3β-NBD-UDCA (**4**). The DCA analogues in each pair were more effectively taken up than the corresponding UDCA compound, possibly due to their greater hydrophobicity. Remarkably, the β-isomers in each case were taken up exclusively through passive diffusion, whereas both α-compounds were mostly actively transported. This peculiar diastereoselective exclusion of a fluorescent BA from active transport has not been noted in the bile acid literature as far as we are aware. Possible reasons for the observed diastereoselectivity include: (i) a steric clash between the β-group and the boundary of the pocket accommodating the steroidal A ring or (ii) a high dependence on the equatorial H-bond donor in the natural bile acid mimicked by the α-NH in the corresponding NBD analogue. This seems less likely since a loss of a H-bond opportunity would reduce binding enthalpy as reflected in the pseudo K_m value, rather than exclusion as observed. Representative low energy conformers for the DCA isomers appear in Figure 5 along with a model of DCA. Whatever its cause, the exclusion of 3β-analogues is relevant to the design of bile acid pro-drug conjugates as well as inhibitors and substrates for bile acid transporters.

The Caco-2 cell line has been used to assess the permeability of various bile acid pro-drug conjugates and it exhibits active uptake of sterically bulky 24-side chain peptide conjugates.[27]

The high diastereoselectivity of the process as well as the Eadie-Hofstee transformation suggest that the active transport process was mediated by a single transporter site. Bile acids are transported via several transport proteins such as NTCP (SLC10A1), ASBT (SLC10A2), BSEP (ABCB11), OSTα/OSTβ and OATP.[28,29] Of these, NTCP, ASBT and BSEP are reported to be inconsistently expressed in the Caco-2 literature.[30,31] Moreover, the free bile acids were not substrates for hASBT-transfected MDCK cells, although they inhibited hASBT translocation of taurocholate with low μM potency.[32] The presence of the basolateral transporters OSTα and OSTβ in Caco-2 cells was recently demonstrated by Ming et al. on mRNA level.[33] Several groups have shown numerous OATP transporters to be expressed in Caco-2 cells particularly OATP2A1, OATP4A1 and OATP2B1.[24,31,34] OATP2B1 is highly expressed in the apical cell membrane, making the transporter the most likely candidate for the uptake observed in Caco-2 cells in the present study.

Author's personal copy

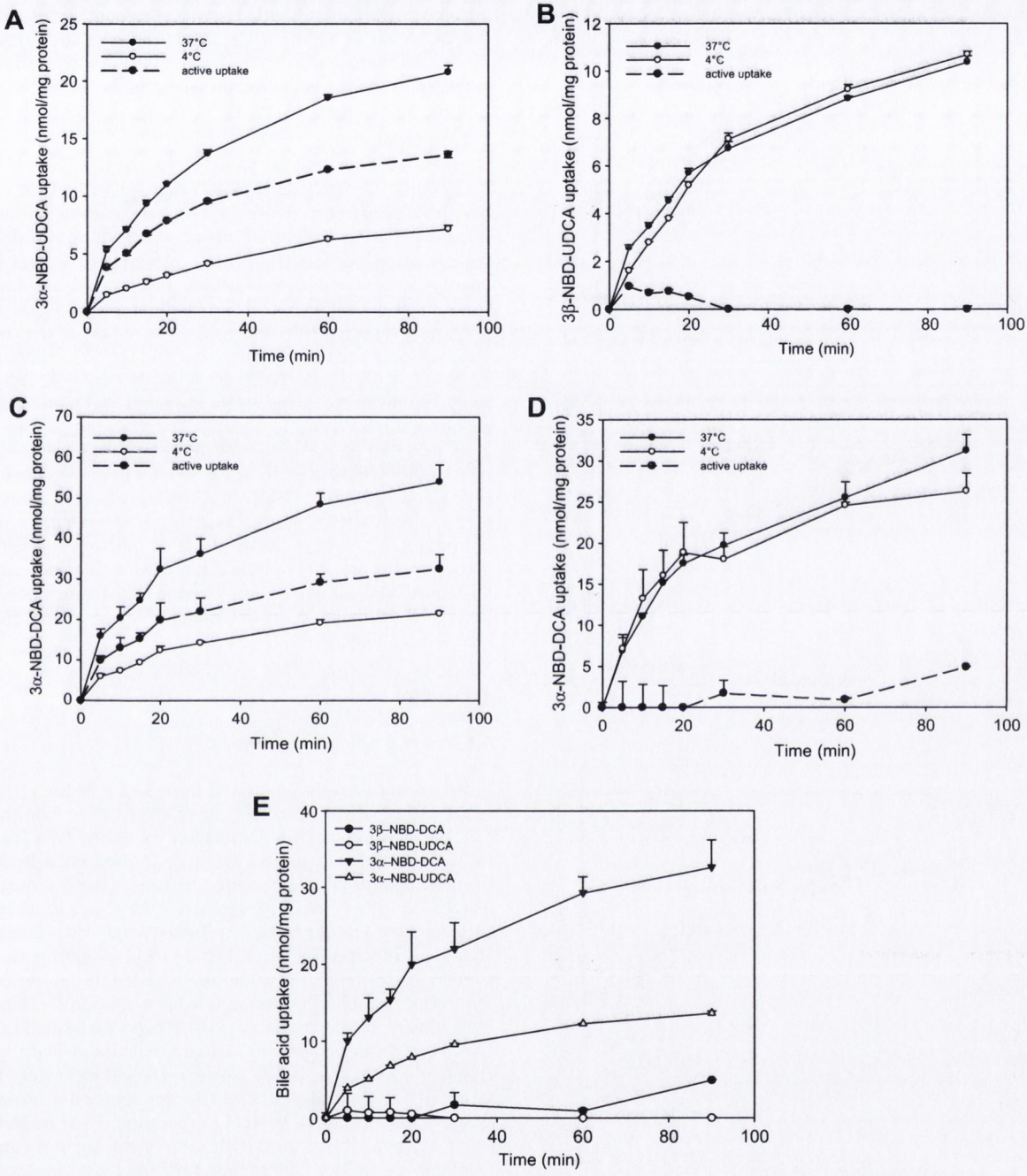

Figure 3. Time course of bile acid (**3**, **4**, **5** and **6**) uptake into Caco-2 cell monolayers. Uptake of **3** (**A**), **4** (**B**), **5** (**C**) and **6** (**D**) was studied for 90 min at 37 °C (●) and 4 °C (○). The active uptake rate of bile acid compounds (10 μM) was estimated from the difference between the fluorescence after exposure to **3**, **4**, **5** and **6** at 37 °C and 4 °C (**E**). Data represent mean ± SD ($n = 3$).

Previously, OATP2B1 was found to be expressed in the jejunal epithelium and has been described to mediate uptake of taurocholate with a K_m of 72 μM, which is in the same order of magnitude as observed here.[35]

The use of aminoNBD bile acids as fluorescent tools goes back almost 20 years to the synthesis, characterisation, distribution and metabolism of 3-, 7- and 12-aminoNBD analogues of CA.[12–14] In an interesting re-exploration of some of these compounds, Rohacova *et al.* reported that 3α, 3β, 7α and 7β NBD CA accumulate in freshly isolated rat hepatocytes in a manner that was transporter mediated, because uptake was markedly attenuated by troglitazone, an inhibitor of hepatic NCTP and OATP.[15] While 3α NBD CA was efficiently taken up, all of the isomers underwent active transport. The same group recently reported on some transport characteristics of a series of 3- and 7α/β CA dansyl analogues in hepatocytes.[36] In this series the 7α- and β compounds appeared to be taken up to similar extents, and, although there was a marked difference in extent of uptake of the 3-isomers, there was still significant active uptake of the 3β-analogue.

Analogues of chenodeoxycholic acid (CDCA), CA, UDCA, DCA and lithocholic acid incorporating a 24-(Nε-NBD)lysine were reported to be transported via OATP1B1 and OATP1B3-expressing

Author's personal copy

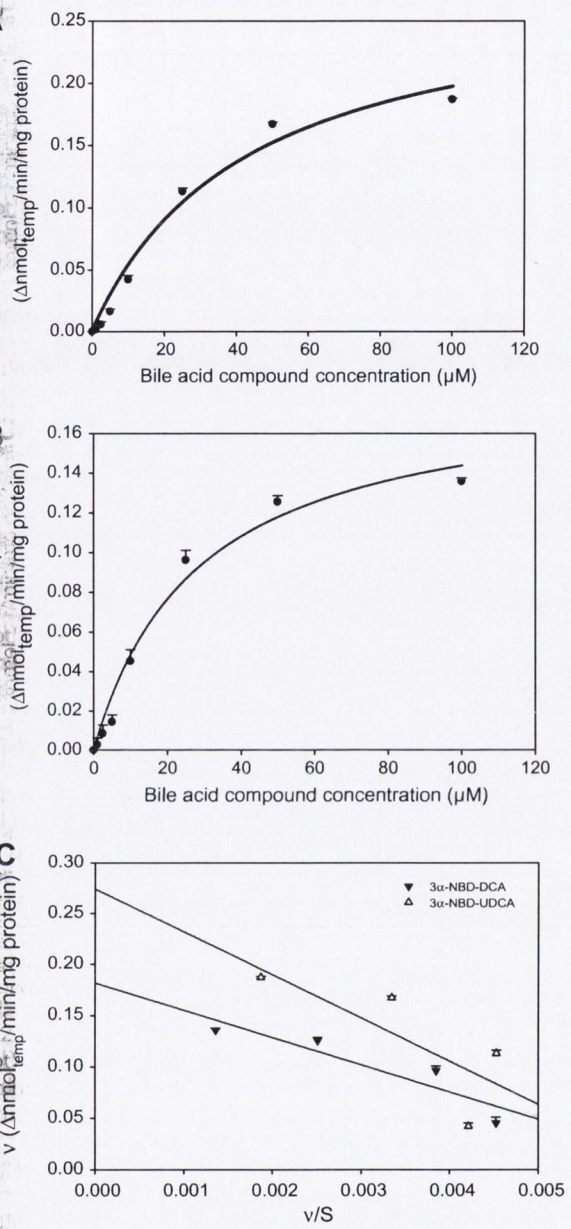

Figure 4. Concentration dependence of **3** and **5** uptake by Caco-2 cell monolayers. Uptake of bile acid compounds **3** (**A**) and **5** (**B**) was measured for 20 min at 37 °C and 4 °C. Active uptake of bile acid compounds was calculated as the difference between the fluorescence after exposure to **3** and **5** at 37 °C and 4 °C. Data represent mean ± SD ($n = 3$). Eadie-Hofstee transformations of the data (**C**): v, uptake rate; S, bile acid compound concentration. In Caco-2 monolayers, one single transporter site was identified for the uptake of both NBD bile acid compounds. Data are represented as mean ± SD, ($n = 3$).

HepG2 cells. The CDCA analogue was most efficiently transported by both OATP subtypes with K_m values one order of magnitude lower than observed in the present study for the 3α NBD compounds.[16] Fluorescent-lysyl analogues should properly be considered as reporters for the corresponding bile acid glycine conjugates since the terminal acid group is similarly placed with respect to the steroidal scaffold. In these compounds the pentyl-*N*ε-NBD reporter group replaces one of the hydrogen atoms on the glycyl methylene carbon. This arrangement, which substantially increases mass and steric bulk, produces high affinity substrates for OATPs (and ASBTs) but this kind of reporter is not suitable for investigating mechanistic questions related to unconjugated bile acids. It is important to note in this context that free DCA and UDCA possess chemical properties such as size, polarity and pK_a that are distinct from their glycine and tauro conjugates and they cause different biological effects.[8]

3. Conclusions

3α- and 3β-deoxy NBD-amino derivatives of DCA and UDCA have been prepared as fluorescent probes for investigating the contrasting effects of the parent bile acid compounds for detection of organic anion-transporting peptide mediated processes. The compounds possess adequate aqueous stability and are non-toxic in several cell lines. They have similar fluorescent characteristics to previously reported NBD analogues. The uptake of the compounds was strikingly diastereospecific; whereas the 3α-compounds taken up by active transport, the 3β-compounds were not. Eadie-Hofstee analysis indicated that the active transport was mediated by a single protein. However, to identify the transporter site which is mainly mediating the uptake of fluorescent bile acids, further uptake studies would need to be carried out in relevant heterologous expression systems. 3α-NBD DCA warrants further study as a tool for functional activity studies associated with organic anion transporter proteins. The specificity of the interactions suggests that the α-compounds are able to mimic the natural bile acid parents. The 3α-UDCA/DCA pair will be employed to investigate mechanistic aspects of the functional antagonism exhibited by these compounds in intestinal biology.

4. Experimental

4.1. General synthetic methods

All chemicals were purchased from Sigma-Aldrich (Dublin, Ireland), except where stated. All the reactions were monitored using TLC. Uncorrected melting points were measured on a Stuart Apparatus. Infra-red (IR) spectra were performed on a Perkin Elmer FT–IR Paragon 1000 spectrometer. ^{1}H and ^{13}C nuclear magnetic resonance (NMR) spectra were recorded at 27 °C on a Brucker DPX 400 spectrometer (400.13 MHz, ^{1}H; 100.61 MHz, ^{13}C). Coupling constants are reported in Hertz. For ^{1}H NMR assignments, chemical shifts are reported: shift value (number of protons, description of absorption, coupling constant(s) where applicable). Electrospray ionization mass spectrometry (ESI-MS) was performed in the positive ion mode on a liquid chromatography time-of-flight mass spectrometer (Micromass LCT, Waters Ltd, Manchester, UK). The samples were introduced into the ion source by an LC system (Waters Alliance 2795, Waters Corporation, USA) in MeCN:water (60:40% v/v) at 200 μl/min. The capillary voltage of the mass spectrometer was at 3 kV. The sample cone (de-clustering) voltage was set at 40 V. For exact mass determination, the instrument was externally calibrated for the mass range m/z 100 to 1000. A lock (reference) mass (m/z 556.2771) was used. Mass measurement accuracies of <±5 ppm were obtained. Compound purity/homogeneity was confirmed using a combination of NMR, TLC and HPLC.

4.1.1. 24-Methyl 3α-(methylsulfonyl)oxy, 7β-formyloxy-5β-cholanoate (10)

A solution of triethylamine (0.1 ml) and methanesulfonyl chloride (0.08 ml) in anhydrous DCM (5 ml) was added dropwise to a stirred solution of **8** (0.286 g) in anhydrous DCM (20 ml) at 0 °C and the mixture allowed to warm to rt. After 20 min, when TLC analysis showed the reaction was complete, the mixture was poured into water (100 ml) and extracted with DCM (3 × 50 ml). The organic phase was dried over $MgSO_4$ then removed under reduced pressure to give the product as colourless semi-solid (0.330 g, 98%). ^{1}H

Author's personal copy

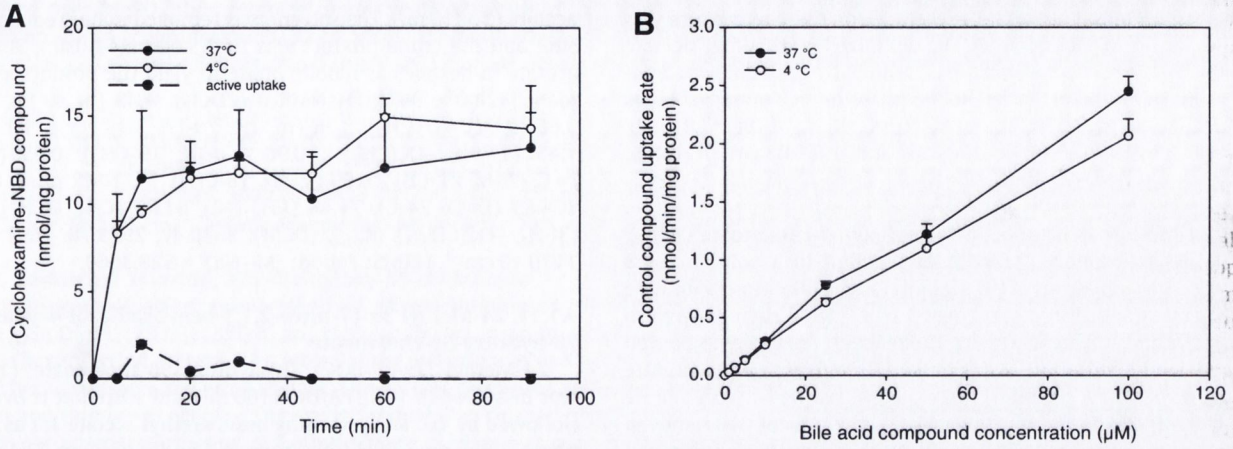

Figure 5. Uptake of the cyclohexamine NBD adduct (**7**) into Caco-2 cell monolayers was studied for 90 min at 37 °C (●) and 4 °C (○). The active component was estimated from the difference between fluorescence levels after exposure at 37 °C and 4 °C. Panel B shows concentration dependent uptake of **7** by Caco-2 cell monolayers. Uptake was measured for 20 min at 37 °C and 4 °C. Data are represented as mean ± SD, (n = 3).

NMR δ ($CDCl_3$): 7.99 (s, 1H, 7-OC=O*H*), 4.91 (6, 1H, J_1 = 5.02 Hz, J_2 = 5.52 Hz, 7α-H), 4.62 (m, 1H, 3β-H), 3.68 (s, 3H, –O–CH_3), 3.02 (s, 3H, –OSO_2CH_3), 1.00 (s, 3H, 19-CH_3), 0.94 (d, 3H, J = 6.02 Hz, 21-CH_3), 0.69 (s, 3H, 18-CH_3). ^{13}C NMR ppm ($CDCl_3$): 175.12 (C=O, 24-C), 161.41 (C=O, 7-OC=OH), 81.89 (CH, 3-C), 73.83 (CH, 7-C), 53.00 (CH_3, OSO_2CH_3), 51.97 (CH_3, OCH_3). IR_{vmax} (KBr): 3438.55, 2952.63, 2874.54, 1718.71, 1354.77, 1174.23, 929.55 and 527.59 cm^{-1}. HRMS: Found: $(M-K)^+$ = 551.2451.

4.1.2. 24-Methyl 3β-azido, 7β-formyloxy-5β-cholanoate

Sodium azide (0.387 g) was added to a stirred solution of **10** (0.306 g) in DMPU (15 ml) at 50 °C and the reaction was monitored by TLC (hexane/ethyl acetate 5:1). After 8 d the mixture was partitioned between water and ethyl acetate. The organic phase was retrieved and dried over Na_2SO_4. The crude product was cleaned by column chromatography using 15% ethyl acetate in hexane as mobile phase to yield white solid as product (0.211 g, 77%). ^{1}H NMR δ ($CDCl_3$): 8.00 (s, 1H, 7-OC=O*H*), 4.89 (m, 1H, 7α-H), 3.96 (m, 1H, 3α-H), 3.68 (s, 3H, –O–CH_3), 1.02 (s, 3H, 19-CH_3), 0.94 (d, 3H, J = 6.53 Hz, 21-CH_3), 0.70 (s, 3H, 18-CH_3). ^{13}C NMR ppm ($CDCl_3$): 174.50 (C=O, 24-C), 160.90 (C=O, 7-OC=OH), 73.56 (CH, 7-C), 57.87 (CH, 3-C), 51.34 (CH_3, OCH_3). IR_{vmax} (KBr): 3422.62, 2946.08, 2884.65, 2111.22, 1737.16 and 1188.73 cm^{-1}. HRMS: Found: $(M-Na)^+$ = 482.3002.

4.1.3. 24-Methyl 3β-azido, 7β-hydroxy-5β-cholanoate (12)

To a stirred solution of 24-methyl 3β-azido, 7β-formyloxy-5β-cholanoate (0.308 g) in anhydrous MeOH (30 ml) was added acetyl chloride (0.06 ml in 5 ml anhydrous MeOH) dropwise at 0 °C and allowed to warm to rt. The reaction was monitored by TLC until there was no starting material present. Then, the mixture was partitioned between saturated aq. $NaHCO_3$ and ethyl acetate. The organic phase was washed with water (2 × 100 ml) and brine (1 × 100 ml), dried over Na_2SO_4, filtered and the solvent removed under reduced pressure to give the product as light yellow semi-solid (0.273 g, 97%). ^{1}H NMR δ ($CDCl_3$): 3.93 (s, 1H, 3α-H), 3.68 (s, 3H, –O–CH_3), 3.55 (m, 1H, 7α-H), 0.99 (s, 3H, 19-CH_3), 0.95 (d, 3H, J = 6.52 Hz, 21-CH_3), 0.69 (s, 3H, 18-CH_3). ^{13}C NMR ppm ($CDCl_3$): 17.86 (C=O, 24-C), 71.48 (CH, 7-C), 58.42 (CH, 3-C), 51.66 (CH_3, OCH_3). IR_{vmax} (DCM): 3431.06, 2935.49, 2866.03, 2103.17 and 1739.37 cm^{-1}. HRMS: Found: $(M-Na)^+$ = 454.3051.

4.1.4. 24-Methyl 3β-(*N*-BOC), 7β-hydroxy-5β-cholanoate

To a pre-reduced suspension of 10% Pd/C (~50 mg) in ethyl acetate (10 ml) was added a solution of **12** (0.273 g) and di-*tert*-butyl dicarbonate (0.166 g) in ethyl acetate (5 ml) under H_2 at rt and stirred overnight. Then the Pd/C was filtered out on a celite pad and the solvent was removed under reduced pressure. The crude product was cleaned on a flash column using 25% ethyl acetate in hexane as mobile phase to afford title compound as a white foam (0.276 g, 86%). ^{1}H NMR δ ($CDCl_3$): 4.83 (d, 1H, J = 7.03 Hz, 3-NH), 3.88 (br s, 1H, 3α-H), 3.68 (s, 3H, –O–CH_3), 3.56 (br s, 1H, 7α-H), 1.46 (s, 9H, –$OC(CH_3)_3$), 0.99 (s, 3H, 19-CH_3), 0.94 (d, 3H, J = 6.53 Hz, 21-CH_3), 0.69 (s, 3H, 18-CH_3). ^{13}C NMR ppm ($CDCl_3$): 174.86 (C=O, 24-C), 71.41 (CH, 7-C), 51.66 (CH_3, OCH_3), 28.59 ($3CH_3$, -$OC(CH_3)_3$). IR_{vmax} (KBr): 3457.49, 2932.95, 2865.84, 1698.40, 1168.99 and 1021.60 cm^{-1}. HRMS: Found: $(M-Na)^+$ = 528.3685.

4.1.5. 24-Methyl 3β-(7-nitro-2,1,3-benzoxadiazol-4-yl)amino, 7β-hydroxy-5β-cholanoate

24-Methyl 3β-(*N*-BOC), 7β-hydroxy-5β-cholanoate (0.269 g) was stirred in 10% TFA/DCM (20 ml) at rt until there was no BOC-protected compound evident by TLC. The solvent was removed and the residue dried under reduced pressure to give a light brown solid crude product. This was dissolved in MeOH (20 ml) then sodium bicarbonate (0.112 g) and NBD chloride (0.1 g) were added and the solution stirred at 70 °C for 5 d (monitored by TLC using hexane/ethyl acetate 1:1 as mobile phase). After this time the mixture was poured into brine (70 ml) and extracted with ethyl acetate (3 × 60 ml). The collected organic phase was dried over Na_2SO_4, filtered and the solvent was removed under reduced pressure then the product was separated by column chromatography (50% ethyl acetate in hexane as mobile phase) to give orange solid as product (0.202 g, 67%). ^{1}H NMR δ ($CDCl_3$): 8.51 (d, 1H, J = 9.03 Hz, aromatic-H), 6.42 (d, 1H, J = 7.03 Hz, 3-NH), 6.19 (d, 1H, J = 8.53 Hz, aromatic-H), 4.26 (s, 1H, 7β-OH), 4.10 (s, 1H, 3α-H), 3.69 (s, 3H, –O–CH_3), 3.61 (s, 1H, 7α-H), 1.10 (s, 3H, 19-CH_3), 0.96 (d, 3H, J = 6.52 Hz, 21-CH_3), 0.71 (s, 3H, 18-CH_3). ^{13}C NMR ppm ($CDCl_3$): 175.15 (C=O, 24-C), 144.86 (C, aromatic-C), 144.66 (C, aromatic-C), 143.21 (C, aromatic-C), 136.94 (CH, aromatic-C), 124.29 (C, aromatic-C), 99.30 (CH, aromatic-C), 71.58 (CH, 7-C), 52.00 (CH_3, OCH_3). IR_{vmax} (KBr): 3404.92, 2932.39, 2865.84, 1736.45, 1574.72, 1307.25 and 1265.61 cm^{-1}. HRMS: Found: $(M-Na)^+$ = 591.3157.

4.1.6. 3β-(7-nitro-2,1,3-benzoxadiazol-4-yl)amino, 7β-hydroxy-5β-cholanoic acid (4)

24-Methyl 3β-(7-nitro-2,1,3-benzoxadiazol-4-yl)amino, 7β-hydroxy-5β-cholanoate (0.2 g) was dissolved in a mixture of Me

Author's personal copy

and 2 M NaOH (pH ~14) at 40 °C for 3 h. The mixture was poured into 2 M HCl (50 ml) and extracted with ethyl acetate (3 × 50 ml). The crude product was cleaned by flash chromatography using DCM/MeOH 9:1 as mobile phase to give orange solid as product (0.188 g, 96%). Mp: 208–210 °C. IR_{vmax} (KBr): 3413.89, 2931.04, 2865.99, 1574.58, 1307.39 and 1250.03 cm^{-1}. HRMS: Found: $(M-Na)^+ = 577.3031$.

4.1.7. 24-Methyl 3β-bromo, 7β-formyloxy-5β-cholanoate (14)

Triphenylphosphine (2.097 g) was added to a solution of **8** (1.738 g) in anhydrous THF (80 ml) and *N*-bromosuccinimide (1.423 g) was added in 3 parts over 1 h at −18 °C then allowed to warm to rt and stirred overnight. The reaction mixture was poured into 1 M HCl solution (100 ml) and extracted with ethyl acetate (3 × 75 ml). The organic layer was washed with brine (1 × 100 ml) and after drying over $MgSO_4$ the solvent was removed under reduced pressure. The crude product was flash columned (hexane/ethyl acetate 5:1) to afford the product as white foam (1.694 g, 85%). ^1H NMR δ ($CDCl_3$): 7.99 (s, 1H, 7-OC=O*H*), 4.84 (m, 1H, 7α-H), 4.76 (s, 1H, 3α-H), 3.67 (s, 3H, –O–CH_3), 1.06 (s, 3H, 19-CH_3), 0.93 (d, 3H, J = 6.53 Hz, 21-CH_3), 0.70 (s, 3H, 18-CH_3). ^{13}C NMR ppm ($CDCl_3$): 175.12 (C=O, 24-C), 161.50 (C=O, 7-OC=OH), 74.41 (CH, 7-C), 51.97 (CH_3, OCH_3). IR_{vmax} (DCM): 2947.48, 2871.35, 1737.49, 1719.36 and 1178.56 cm^{-1}. HRMS: Found: $(M-Na)^+ = 519.2070$.

4.1.8. 24-Methyl 3α-azido, 7β-formyloxy-5β-cholanoate

To a solution of **14** (1.693 g) in DMPU (50 ml) was added sodium azide (2.21 g) at rt and stirred overnight. Then the reaction mixture was poured into water (100 ml) and extracted with ethyl acetate (3 × 75 ml). The organic phase was washed with brine (1 × 100 ml), dried over Na_2SO_4, filtered and the solvent was evaporated in vacuum. The crude product was cleaned on a flash column using hexane/ethyl acetate 5:1 as mobile phase to obtain the product as colourless oil (1.464 g, 94%). ^1H NMR δ ($CDCl_3$): 8.09 (s, 1H, 7-OC=O*H*), 4.91 (6, 1H, J_1 = 5.27 Hz, J_2 = 5.53 Hz, 7α-H), 3.68 (s, 3H, –O–CH_3), 3.30 (m, 1H, 3β-H), 1.00 (s, 3H, 19-CH_3), 0.94 (d, 3H, J = 6.52 Hz, 21-CH_3), 0.70 (s, 3H, 18-CH_3). ^{13}C NMR ppm ($CDCl_3$): 174.81 (C=O, 24-C), 161.12 (C=O, 7-OC=OH), 78.76 (CH, 7-C), 60.81 (CH, 3-C), 51.64 (CH_3, OCH_3). IR_{vmax} (DCM): 2946.73, 2871.54, 2093.30, 1720.62, 1453.67, 1255.13 and 1187.30 cm^{-1}. HRMS: Found: $(M-Na)^+ = 482.2998$.

4.1.9. 24-Methyl 3α-azido, 7β-hydroxy-5β-cholanoate (16)

Acetyl chloride (0.65 ml) was added dropwise to a stirred solution of 24-methyl 3α-azido, 7β-formyloxy-5β-cholanoate (1.411 g) in anhydrous MeOH (60 ml) at 0 °C and allowed to warm to rt. After overnight the reaction mixture was poured into saturated $NaHCO_3$ (100 ml) and extracted with ethyl acetate (3 × 100 ml). The organic layer was dried over Na_2SO_4, filtered and the solvent was removed under reduced pressure. The crude product was cleaned on flash column (hexane/ethyl acetate 3:1) to give the product as yellow semi-solid (1.210 g, 91%). ^1H NMR δ ($CDCl_3$): 3.69 (s, 3H, –O–CH_3), 3.60 (m, 1H, 7α-H), 3.30 (m, 1H, 3β-H), 0.98 (s, 3H, 19-CH_3), 0.95 (d, 3H, J = 6.27 Hz, 21-CH_3), 0.70 (s, 3H, 18-CH_3). ^{13}C NMR ppm ($CDCl_3$): 174.85 (C=O, 24-C), 71.29 (CH, 7-C), 60.99 (CH, 3-C), 51.65 (CH_3, OCH_3). IR_{vmax} (DCM): 3424.26, 2938.77, 2866.74, 2092.43, 1739.29, 1452.41, 1254.58, 1167.83 and 1022.77 cm^{-1}. HRMS: Found: $(M-Na)^+ = 454.3057$.

4.1.10. 24-Methyl 3α-(*N*-BOC), 7β-hydroxy-5β-cholanoate

Pd/C (~100 mg) in ethyl acetate (30 ml) was pre-reduced under H_2 atmosphere over 30 min then a solution of **16** (1.182 g) and di-tert-butyl dicarbonate (0.717 g) in ethyl acetate (20 ml) was added via syringe and the mixture stirred at rt overnight. The reaction mixture was filtered through a celite pad and washed with ethyl acetate (3 × 10 ml). The solvent was removed under reduced pressure and the crude product was flash columned using 30% ethyl acetate in hexanes as mobile phase to yield the product as white foam (1.300 g, 94%). ^1H NMR δ ($CDCl_3$): 4.42 (br s, 1H, 3-NH), 3.68 (s, 3H, –O–CH_3), 3.56 (m, 1H, 7α-H), 3.39 (br s, 1H, 3β-H), 1.45 (s, 9H, -OC(CH_3)$_3$), 0.96 (s, 3H, 19-CH_3), 0.95 (d, 3H, J = 6.27 Hz, 21-CH_3), 0.69 (s, 3H, 18-CH_3). ^{13}C NMR ppm ($CDCl_3$): 174.85 (C=O, 24-C), 71.48 (CH, 7-C), 51.65 (CH_3, OCH_3), 28.56 ($3CH_3$, –OC(CH_3)$_3$). IR_{vmax} (DCM): 3380.47, 2933.70, 1692.59 and 1170.19 cm^{-1}. HRMS: Found: $(M-Na)^+ = 528.3669$.

4.1.11. 24-Methyl 3α-(7-nitro-2,1,3-benzoxadiazol-4-yl)amino, 7β-hydroxy-5β-cholanoate

24-Methyl 3α-(*N*-BOC), 7β-hydroxy-5β-cholanoate (1.265 g) was dissolved in 10% TFA/DCM (60 ml) and stirred at rt overnight (followed by TLC analysis using hexane/ethyl acetate 1:1 as mobile phase) then, the solvent was removed under vacuum. The residue was further dried by successive evaporation of toluene (3 × 100 ml). The yield foam was dissolved in MeOH (50 ml) then $NaHCO_3$ (2.102 g) and NBD chloride (0.549 g) were added to the solution. The reaction mixture was stirred vigorously for 2 weeks at reflux; reaction completion was checked by TLC using hexane:ethyl acetate (50:50) as mobile phase. It was poured into brine (150 ml) and extracted with ethyl acetate (3 × 100 ml). The organic phase was dried over Na_2SO_4, filtered and the solvent was removed in vacuum to afford the crude product as black semi-solid. This was purified with flash column using 40–70% ethyl acetate in hexanes as mobile phase to obtain the product as orange foam (0.622 g, 44%). ^1H NMR δ ($CDCl_3$): 8.49 (d, 1H, J = 8.54 Hz, aromatic-H), 6.88 (d, 1H, J = 7.53 Hz, 3-NH), 6.19 (d, 1H, J = 9.04 Hz, aromatic-H), 3.67 (s, 5H, –O–CH_3, 7α-H, 3β-H), 1.08 (s, 3H, 19-CH_3), 0.95 (d, 3H, J = 6.03 Hz, 21-CH_3), 0.72 (s, 3H, 18-CH_3). ^{13}C NMR ppm ($CDCl_3$): 174.44 (C=O, 24-C), 144.16 (C, aromatic-C), 143.87 (C, aromatic-C), 136.48 (CH, aromatic-C), 123.07 (C, aromatic-C), 71.14 (CH, 7-C), 51.35 (CH_3, OCH_3). IR_{vmax} (KBr): 3402.60, 2933.80, 2867.01, 1733.12, 1579.17 and 1304.77 cm^{-1}. HRMS: Found: $(M-Na)^+ = 591.3169$.

4.1.12. 3α-(7-nitro-2,1,3-benzoxadiazol-4-yl)amino, 7β-hydroxy-5β-cholanoate (3)

NaOH (2 M) was added to a stirred methanolic solution of 24-methyl 3α-(7-nitro-2,1,3-benzoxadiazol-4-yl)amino, 7β-hydroxy-5β-cholanoate (0.589 g) and the mixture warmed to 40 °C. The reaction mixture was left at this temperature overnight then poured into 2 M HCl (100 ml) and extracted with ethyl acetate (3 × 75 ml). The organic layer was dried over Na_2SO_4, filtered and the solvent was removed under reduced pressure. The crude product was purified by flash chromatography using 2% acetic acid in ethyl acetate as mobile phase. The product was recrystallised from hexane to give orange solid as final product (0.465 g, 81%). Mp: 148–150 °C. ^1H NMR δ (acetone-d_6): 8.51 (d, 1H, J = 9.04 Hz, aromatic-H), 6.55 (d, 1H, J = 9.04 Hz, aromatic-H), 3.93 (br s, 1H, 7α-H), 3.51 (m, 1H, 3β-H), 1.05 (s, 3H, 19-CH_3), 0.97 (d, 3H, J = 6.53 Hz, 21-CH_3), 0.72 (s, 3H, 18-CH_3). ^{13}C NMR ppm (acetone-d_6): 175.03 (C=O, 24-C), 70.94 (CH, 7-C). IR_{vmax} (KBr): 3436.13, 2932.86, 2868.26, 1708.42, 1621.14, 1579.48 and 1304.52 cm^{-1}. HRMS: Found: $(M-Na)^+ = 577.3005$.

4.1.13. 24-Methyl 3α-(methylsulfonyl)oxy, 12α-formyloxy-5β-cholanoate (11)

The solution of triethylamine (0.1 ml) and methanesulfonyl chloride (0.15 ml) in anhydrous DCM (5 ml) was added drop-wise to a stirred solution of **9** (0.279 g) in anhydrous DCM (20 ml) at 0 °C and allowed to warm to rt. After 20 min when TLC analysis showed the reaction was complete the mixture was poured into H_2O (50 ml) and extracted with DCM (3 × 50 ml). The organic phase

Author's personal copy

was dried over $MgSO_4$ then removed under reduced pressure to give the product as colourless oil (0.322 g, 98%). ^{1}H NMR δ ($CDCl_3$): 8.15 (s, 1H, 12-OC=O*H*), 5.26 (s, 1H, 12β-H), 4.63 (m, 1H, 3β-H), 3.67 (s, 3H, –O–CH_3), 3.01 (s, 3H, -OSO_2CH_3), 0.93 (s, 3H, 19-CH_3), 0.85 (d, 3H, J = 6.03 Hz, 21-CH_3), 0.75 (s, 3H, 18-CH_3). ^{13}C NMR ppm ($CDCl_3$): 174.69 (C=O, 24-C), 160.71 (C=O, 12-OC=OH), 82.79 (CH, 3-C), 75.97 (CH, 12-C), 52.67 (CH_3, OSO_2CH_3), 51.66 (CH_3, OCH_3). IR_{vmax} (DCM): 2947.01, 2871.16, 1717.89, 1353.88, 1174.09 and 932.87 cm^{-1}. HRMS: Found: $(M-Na)^+$ = 535.2710.

4.1.14. 24-Methyl 3β-azido, 12α-formyloxy-5β-cholanoate

Sodium azide (0.408 g) was added to a stirred solution of **11** (0.322 g) in DMPU (20 ml) at 50 °C and the reaction was monitored by TLC (hexane:ethyl acetate 5:1). After 6 d the mixture was partitioned between water and ethyl acetate. The organic phase was retrieved and dried over Na_2SO_4. The crude product was cleaned by column chromatography using 20% ethyl acetate in hexane as mobile phase to yield colourless oil as product (0.253 g, 87%). ^{1}H NMR δ ($CDCl_3$): 8.13 (s, 1H, 12-OC=O*H*), 5.26 (s, 1H, 12β-H), 3.95 (s, 1H, 3α-H), 3.67 (s, 3H, –O–CH_3), 0.95 (s, 3H, 19-CH_3), 0.85 (d, 3H, J = 6.52 Hz, 21-CH_3), 0.76 (s, 3H, 18-CH_3). ^{13}C NMR ppm ($CDCl_3$): 174.39 (C=O, 24-C), 160.37 (C=O, 12-OC=OH), 76.00 (CH, 12-C), 58.35 (CH, 3-C), 51.35 (CH_3, OCH_3). IR_{vmax} (DCM): 2938.73, 2872.92, 2101.83, 1738.92, 1720.86 and 1171.43 cm^{-1}. HRMS: Found: $(M-Na)^+$ = 482.2974.

4.1.15. 24-Methyl 3β-azido, 12α-hydroxy-5β-cholanoate (13)

To a stirred solution of 24-methyl 3β-azido, 12α-formyloxy-5β-cholanoate (0.322 g) in anhydrous MeOH (30 ml) was added acetyl chloride (0.07 ml in 5 ml anhydrous MeOH) dropwise at 0 °C and allowed to warm to rt. The reaction was monitored by TLC until there was no starting material present. Then the mixture was partitioned between saturated $NaHCO_3$ and ethyl acetate. The organic phase was washed with water (2 × 100 ml) and brine (100 ml), dried over Na_2SO_4, filtered and the solvent removed under reduced pressure to give the product as yellow semi-solid (0.294 g, 97%). ^{1}H NMR δ ($CDCl_3$): 4.01 (s, 1H, 12β-H), 3.97 (s, 1H, 3α-H), 3.68 (s, 3H, –O–CH_3), 0.99 (d, 3H, J = 5.87 Hz, 21-CH_3), 0.96 (s, 3H, 19-CH_3), 0.70 (s, 3H, 18-CH_3). ^{13}C NMR ppm ($CDCl_3$): 174.51 (C=O, 24-C), 73.00 (CH, 12-C), 58.52 (CH, 3-C), 51.36 (CH_3, OCH_3). IR_{vmax} (KBr): 3528.85, 2932.82, 2093.51, 1725.62, 1449.91, 1312.94 and 1196.78 cm^{-1}. HRMS: Found: $(M-Na)^+$ = 454.3052.

4.1.16. 24-Methyl 3β-(*N*-BOC), 12α-hydroxy-5β-cholanoate

To a pre-reduced suspension of 10% Pd/C (~50 mg) in ethyl acetate (10 ml) was added a solution of **13** (0.245 g) and di-*tert*-butyl dicarbonate (0.149 g) in ethyl acetate (5 ml) and stirred under H_2 at rt. The reaction mixture was stirred overnight (TLC: hexane:ethyl acetate 3:1) then it was filtered on a celite pad. The celite was washed with ethyl acetate (3 × 10 ml) and the organic phase was removed in vacuum. The product was cleaned by flash chromatography (mobile phase: 30% ethyl acetate in hexane) to yield a white foam as product (0.260 g, 90%). ^{1}H NMR δ ($CDCl_3$): 4.84 (br s, 1H, 3-NH), 4.00 (s, 1H, 12β-H), 3.92 (br s, 1H, 3α-H), 3.68 (s, 3H, –O–CH_3), 1.46 (s, 9H, –OC(CH_3)$_3$), 0.99 (d, 3H, J = 6.02 Hz, 21-CH_3), 0.96 (s, 3H, 19-CH_3), 0.69 (s, 3H, 18-CH_3). ^{13}C NMR ppm ($CDCl_3$): 174.54 (C=O, 24-C), 72.97 (CH, 12-C), 51.34 (CH_3, OCH_3), 28.29 (3CH_3, –OC(CH_3)$_3$). IR_{vmax} (KBr): 3459.32, 2937.54, 2865.92, 1698.37 and 1171.03 cm^{-1}. HRMS: Found: $(M-Na)^+$ = 528.3654.

4.1.17. 24-Methyl 3β-(7-nitro-2,1,3-benzoxadiazol-4-yl)amino, 12α-hydroxy-5β-cholanoate

24-Methyl 3β-(*N*-BOC), 12α-hydroxy-5β-cholanoate (0.259 g) was stirred in 10% TFA/DCM (20 ml) at rt until there was no BOC-protected compound present. Then the solvent was removed and the residue dried under reduced pressure to give light brown solid as crude product. This was dissolved in MeOH (20 ml) then $NaHCO_3$ (0.130 g) and NBD chloride (0.112 g) were added to the solution and stirred at 70 °C for 10 d (monitored by TLC using hexane/ethyl acetate 1:1 as mobile phase). After this time the mixture was poured into brine (50 ml) and extracted with ethyl acetate (3 × 50 ml). The collected organic phase was dried over Na_2SO_4, filtered and the solvent was removed under reduced pressure then the product was separated by column chromatography (50% ethyl acetate in hexane as mobile phase) to give orange solid as product (0.213 g, 73%). ^{1}H NMR δ ($CDCl_3$): 8.49 (d, 1H, J = 9.04 Hz, aromatic-H), 6.47 (d, 1H, J = 7.03 Hz, 3-NH), 6.19 (d, 1H, J = 9.04 Hz, aromatic-H), 4.26 (s, 1H, 12α-OH), 4.12 (s, 1H, 3α-H), 4.05 (s, 1H, 12β-H), 3.69 (s, 4H, –O–CH_3), 1.03 (s, 3H, 19-CH_3), 1.00 (d, 3H, J = 6.53 Hz, 21-CH_3), 0.72 (s, 3H, 18-CH_3). ^{13}C NMR ppm ($CDCl_3$): 175.10 (C=O, 24-C), 144.88 (C, aromatic-C), 143.30 (C, aromatic-C), 137.07 (CH, aromatic-C), 134.40 (C, aromatic-C), 124.07 (C, aromatic-C), 104.33 (CH, aromatic-C), 73.53 (CH, 12-C), 52.01 (CH_3, OCH_3). IR_{vmax} (KBr): 3538.32, 3408.93, 2943.25, 2864.07, 1736.80, 1574.32, 1336.49 and 1314.61 cm^{-1}. HRMS: Found: $(M-Na)^+$ = 591.3163.

4.1.18. 3β-(7-nitro-2,1,3-benzoxadiazol-4-yl)amino, 12α-hydroxy-5β-cholanoate (6)

The hydrolysis of 24-methyl 3β-(7-nitro-2,1,3-benzoxadiazol-4-yl)amino, 12α-hydroxy-5β-cholanoate (0.205 g) was carried out in MeOH (20 ml) with 2 M NaOH at pH ~14 at 40 °C for 4 h. The mixture was poured into 2 M HCl (50 ml) and extracted with ethyl acetate (3 × 50 ml). The crude product was purified by column chromatography using ethyl acetate as mobile phase to afford the product as orange solid (0.152 g, 76%). Mp: 216–218 °C. ^{1}H NMR δ (DMSO-d_6): 8.31 (d, 1H, J = 9.03 Hz, aromatic-H), 6.29 (s, 1H, aromatic-H), 4.10 (br s, 1H, 3α-OH), 3.81 (s, 1H, 12β-H), 0.93 (s, 6H, 21-CH_3 and 19-CH_3), 0.61 (s, 3H, 18-CH_3). ^{13}C NMR ppm (DMSO-d_6): 175.27 (C=O, 24-C), 145.65 (C, aromatic-C), 144.97 (C, aromatic-C), 135.39 (CH, aromatic-C), 131.60 (C, aromatic-C), 128.66 (C, aromatic-C), 100.02 (CH, aromatic-C), 71.10 (CH, 12-C). IR_{vmax} (KBr): 3410.69, 2927.61, 2863.42, 1703.83, 1575.98 and 1310.90 cm^{-1}. HRMS: Found: $(M-Na)^+$ = 577.3019.

4.1.19. 24-Methyl 3β-bromo, 12α-formyloxy-5β-cholanoate

Triphenylphosphine (2.135 g) was added to a solution of (1.769 g) in anhydrous THF (80 ml) and *N*-bromosuccinimide (1.449 g) was added in 3 parts over 1 h at −18 °C then allowed to warm to rt and stirred for 1.5 h. The reaction mixture was poured into 1 M HCl solution (100 ml) and extracted with ethyl acetate (3 × 75 ml). The organic layer was washed with brine (2 × 100 ml) and after drying over $MgSO_4$ the solvent was removed under reduced pressure. The crude product was flash columned (hexane:ethyl acetate 5:1) to afford the product as pale white solid (1.919 g, 95%). ^{1}H NMR δ ($CDCl_3$): 8.13 (s, 1H, 12-OC=O*H*), 5.26 (s, 1H, 12β-H), 4.79 (s, 1H, 3α-H), 3.68 (s, 3H, –O–CH_3), 1.01 (s, 3H, 19-CH_3), 0.85 (d, 3H, J = 6.52 Hz, 21-CH_3), 0.76 (s, 3H, 18-CH_3). ^{13}C NMR ppm ($CDCl_3$): 174.70 (C=O, 24-C), 160.68 (C=O, 12-OC=OH), 76.29 (CH, 12-C), 51.67 (CH_3, OCH_3). IR_{vmax} (KBr): 3426.56, 2939.12, 2873.47, 1739.75, 1720.29 and 1180.89 cm^{-1}. HRMS: Found: $(M-Na)^+$ = 519.2073.

4.1.20. 24-Methyl 3α-azido, 12α-formyloxy-5β-cholanoate

To a solution of **15** (1.852 g) in DMPU (50 ml) was added sodium azide (2.420 g) at rt and stirred overnight. Then the reaction mixture was poured into water (100 ml) and extracted with ethyl acetate (3 × 50 ml). The organic phase was washed with brine (100 ml), dried over Na_2SO_4, filtered and the solvent was evaporated in vacuum. The crude product was cleaned on a flash column using hexane:ethyl acetate 5:1 as mobile phase to obtain the product as colourless semi-solid (1.652 g, 97%). ^{1}H NMR δ ($CDCl_3$):

Author's personal copy

(m, 1H, 12-OC=O*H*), 5.26 (s, 1H, 12β-H), 3.67 (s, 3H, –O–CH_3), 3.34 (m, 1H, 3β-H), 0.93 (s, 3H, 19-CH_3), 0.85 (d, 3H, J = 6.03 Hz, 21-CH_3), 0.75 (s, 3H, 18-CH_3). ^{13}C NMR ppm ($CDCl_3$): 174.40 (C=O, 24-C), 160.42 (C=O, 12-OC=OH), 75.70 (CH, 12-C), 60.98 (CH, 3-C), 51.34 (CH_3, OCH_3). IR_{vmax} (DCM): 2941.27, 2867.58, 2092.01, 1738.62, 1720.31, 1448.60, 1251.73 and 1177.39 cm^{-1}. HRMS: Found: $(M-Na)^+$ = 482.2995.

4.1.21. 24-Methyl 3α-azido, 12α-hydroxy-5β-cholanoate (17)

Acetyl chloride (0.51 ml) was added drop-wise to a stirred solution of 24-methyl 3α-azido, 12α-formyloxy-5β-cholanoate (1.645 g) in anhydrous MeOH (60 ml) at 0 °C and allowed to warm to rt. After overnight stirring, the reaction mixture was poured into saturated $NaHCO_3$ (100 ml) and extracted with ethyl acetate (3 × 100 ml). The organic layer was dried over Na_2SO_4, filtered and the solvent was removed under reduced pressure. The product was recrystallised from diethyl ether to obtain light-yellow crystals (1.457 g, 94%). ^{1}H NMR δ ($CDCl_3$): 4.00 (s, 1H, 12β-H), 3.68 (s, 3H, –O–CH_3), 3.35 (m, 1H, 3β-H), 0.99 (d, 3H, J = 6.53 Hz, 21-CH_3), 0.94 (s, 3H, 19-CH_3), 0.69 (s, 3H, 18-CH_3). ^{13}C NMR ppm ($CDCl_3$): 175.15 (C=O, 24-C), 73.50 (CH, 12-C), 61.69 (CH, 3-C), 51.97 (CH_3, OCH_3). IR_{vmax} (DCM): 3524.40, 2939.82, 2866.15, 2091.49, 1739.60, 1448.24 and 1252.74 cm^{-1}. HRMS: Found: $(M-Na)^+$ = 454.3038.

4.1.22. 24-Methyl 3α-(*N*-BOC), 12α-hydroxy-5β-cholanoate

A suspension of 10% Pd/C (~100 mg) in ethyl acetate (30 ml) was pre-reduced under hydrogen atmosphere over 30 min then the solution of **17** (1.424 g) and di-*tert*-butyl dicarbonate (0.864 g) in ethyl acetate (20 ml) was added via syringe and stirred at rt overnight. The reaction mixture was filtered through a celite pad and washed with ethyl acetate (3 × 10 ml). The solvent was removed under reduced pressure and the crude product was flash columned using 30% ethyl acetate in hexanes as mobile phase to yield the product as white foam (1.549 g, 93%). ^{1}H NMR δ ($CDCl_3$): 4.45 (br s, 1H, 3-NH), 4.00 (s, 1H, 12β-H), 3.68 (s, 3H, –O–CH_3), 3.43 (br s, 1H, 3β-H), 1.45 (s, 9H, -OC(CH_3)$_3$), 0.99 (d, 3H, J = 6.27 Hz, 21-CH_3), 0.93 (s, 3H, 19-CH_3), 0.69 (s, 3H, 18-CH_3). ^{13}C NMR ppm ($CDCl_3$): 174.83 (C=O, 24-C), 73.30 (CH, 12-C), 51.65 (CH_3, OCH_3), 28.57 (3CH_3, -OC(CH_3)$_3$). IR_{vmax} (DCM): 3380.58, 2935.81, 1691.31 and 1171.11 cm^{-1}. HRMS: Found: $(M-Na)^+$ = 528.3666.

4.1.23. 24-Methyl 3α-(7-nitro-2,1,3-benzoxadiazol-4-yl)amino, 12α-hydroxy-5β-cholanoate

24-Methyl 3α-(*N*-BOC), 12α-hydroxy-5β-cholanoate (1.524 g) was dissolved in 10% TFA/DCM (60 ml) and stirred at rt overnight (followed by TLC analysis using hexane:ethyl acetate 3:1 as mobile phase) then the solvent was removed in vacuum. The residue was dried under reduced pressure using toluene (3 × 100 ml). The yield foam was dissolved in MeOH (60 ml) then $NaHCO_3$ (2.533 g) and NBD chloride (0.862 g) were added to the solution. The reaction mixture was stirred vigorously for 10 d at reflux; reaction completion was checked by TLC using hexane:ethyl acetate (50:50) as mobile phase. It was poured into brine (100 ml) and extracted with ethyl acetate (3 × 100 ml). The organic phase was dried over Na_2SO_4, filtered and the solvent was removed in vacuum to afford the crude product as black semi-solid. This was purified with flash column using 30–40% ethyl acetate in hexane as mobile phase to obtain the product as orange foam (0.679 g, 98%). ^{1}H NMR δ ($CDCl_3$): 8.46 (d, 1H, J = 8.53 Hz, aromatic-H), 6.51 (s, 1H, 3-NH), 6.17 (d, 1H, J = 8.53 Hz, aromatic-H), 4.26 (s, 1H, 12α-OH), 4.07 (s, 1H, 12β-H), 3.67 (s, 4H, 3β-H, –O–CH_3), 1.02 (s, 3H, 19-CH_3), 0.97 (d, 3H, J = 6.03 Hz, 21-CH_3), 0.71 (s, 3H, 18-CH_3). ^{13}C NMR ppm ($CDCl_3$): 174.48 (C=O, 24-C), 144.09 (C, aromatic-C), 143.78 (C, aromatic-C), 136.50 (CH, aromatic-C), 133.78 (C, aromatic-C), 122.93 (C, aromatic-C), 103.71 (CH, aromatic-C), 72.95 (CH, 12-C), 51.36 (CH_3, OCH_3). IR_{vmax} (DCM): 3529.91, 3294.51, 2938.41, 2867.28, 1735.15, 1582.76 and 1304.42 cm^{-1}. HRMS: Found: $(M-Na)^+$ = 591.3142.

4.1.24. 3α-(7-nitro-2,1,3-benzoxadiazol-4-yl)amino, 12α-hydroxy-5β-cholanoate (5)

Methyl 3α-(7-nitro-2,1,3-benzoxadiazol-4-yl)amino, 12α-hydroxy-5β-cholanoate (1.621 g) was dissolved in a mixture of methanol and aq. NaOH (2 M) and the mixture warmed to 40 °C. The reaction mixture was left at this temperature overnight then poured into 2 M HCl (100 ml) and extracted with ethyl acetate (3 × 100 ml). The organic layer was dried over Na_2SO_4, filtered and the solvent was removed under reduced pressure. The crude product was flash columned using first 20% hexane then 2% acetic acid in ethyl acetate as mobile phase to yield orange solid as product (0.997 g, 63%). Mp: 225 °C. ^{1}H NMR δ (DMSO): 11.93 (s, 1H, 24-COOH), 9.52 (s, 1H, 3-NH), 8.47 (d, 1H, J = 8.54 Hz, aromatic-H), 6.46 (d, 1H, J = 9.04 Hz, aromatic-H), 4.25 (s, 1H, 12α-OH), 3.82 (s, 2H, 12β-H and 3β-H), 0.93 (d, 6H, J = 4.52 Hz, 21-CH_3 and 19-CH_3), 0.61 (s, 3H, 18-CH_3). ^{13}C NMR ppm (DMSO): 174.98 (C=O, 24-C), 144.40 (C, aromatic-C), 144.27 (C, aromatic-C), 138.01 (CH, aromatic-C), 136.18 (C, aromatic-C), 120.06 (C, aromatic-C), 105.85 (CH, aromatic-C), 70.89 (CH, 12-C). IR_{vmax} (DCM): 3309.77, 2937.30, 2859.90, 1707.17, 1582.18 and 1304.06 cm^{-1}. HRMS: Found: $(M-Na)^+$ = 577.2999.

4.2. Stability and physiochemical characterisation

For the HPLC measurements, a WATERS Alliance system was used with 2475 Multi λ Fluorescence Detector and 2487 Dual λ Absorbance Detector controlled by EMPOWER Software. The applied column symmetry was C18 5 μm 4.6 × 250 mm from Xbridge™. For the stability study of **4**, a stock solution was prepared in 0.01 mg/ml concentration with 2% MeCN/phosphate buffer (pH = 7.4). The stability study was carried out at 37 °C over 24 h with injection every h. HPLC conditions were flow rate: 1.0 ml/min; wavelength of detection: 346 nm; injection volume: 20 μl; temperature of column and sample: 37 °C; runtime: 25 min; gradient 0 min 50% mobile phases A and B, 0–10 min increase to 80% mobile phase B, 10–20 min 80% mobile phase B, 20–21 min decrease to 50% mobile phase B, 21–25 min 50% mobile phases A and B; mobile phase A: pH = 2.5 phosphate buffer; mobile phase B: MeCN.

To assess lipophilicity of **3**–**6** the samples were prepared (1 μM) in MeCN/water 75:15. HPLC conditions were flow rate: 1.5 ml/min; wavelength of detection: 335 nm (absorbance detector); wavelength of excitation: 470 nm, wavelength of detection: 535 nm (fluorescence detector); injection volume: 20 μl; temperature of column and sample: rt; runtime: 10 min; mobile phase: isocratic–water/1% pH = 3.0 ammonium formate buffer/MeCH (15:10:75).

4.3. Photophysical characterisation

A Cary 300 Scan UV–Visible Spectrophotometer was used to determine the absorption maxima of **3**–**6**. The stock solutions were prepared at 0.01 mg/ml in EtOH. Samples were scanned from 200–800 nm. Cuvette type was Hella Blue quartz 10 mm. To obtain the fluorescence maxima the stock solutions were prepared in 0.001 mg/ml concentration in ethanol and measured with RF-1501 Spectrofluorophotometer (SHIMADZU). The emission wavelength range was chosen between 220–900 nm, while the excitation wavelength was 470 nm. Fluorescein and rhodamine 6G, were cross calibrated by calculating the quantum yield of each relative to the other. The results matched the literature ±10%: fluorescein Φ*F* 0.922, rhodamine 6G Φ*F* 0.953. The absorbance and

Author's personal copy

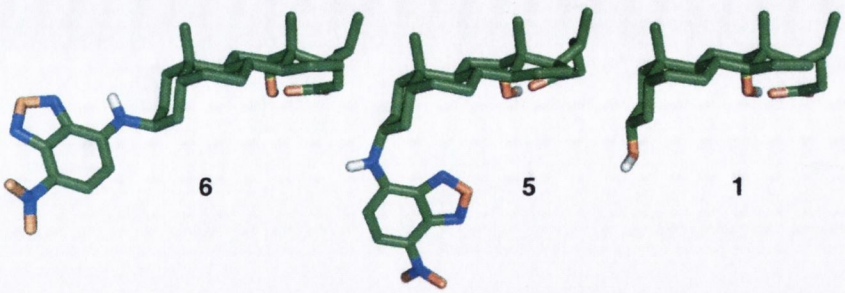

Figure 6. Minimum energy conformations for DCA-3-α and β analogues **5** and **6** and DCA. These were generated by modifying a model of CA (pdb code 2QO4) in MOE and energy minimising with MMFF94x (this approach predicts a H-bond between the acid chain and 12α-OH). The picture shows the different orientations available to the 3-NH in the two configurations. In the α-orientation, the NH may mimic the OH group of the parent bile acid in H-bond donation capacity.

emission levels in the concentration range 10–50 μM for five solutions of each sample and standard were obtained. (Fluorescein in ethanolic KOH (0.01 M), all other solutions in EtOH.) The slope of a plot of fluorescence intensity versus absorbance was used to calculate the quantum yield (ΦF) for each sample using the equation: $\Phi F = \Phi_{ST}(S_x/S_{ST})$.

4.4. Uptake studies

Caco-2 cells were grown to polarised monolayers on 24-well plates for 21 d, before uptake studies were performed in bicarbonated Krebs-Ringer buffer (KRB: 15 mM HEPES, 116.4 mM NaCl, 5.4 mM KCl, 0.78 mM NaH_2PO_4, 25 mM $NaHCO_3$, 1.8 mM $CaCl_2$, 0.81 mM $MgSO_4$ and 5.55 mM glucose; pH 7.4). Uptake of the fluorescent bile acid compounds (**3–6**) was studied at different time points, concentrations and temperatures. Solutions of bile acid compounds were prepared using KRB containing 0.1% DMSO at all times.

Time-dependence of bile acid uptake was studied by incubating cell monolayers (at 10 μM) for up to 90 min at either 37 or 4 °C. After 5, 10, 15, 30, 45, 60 and 90 min, monolayers were washed twice with ice-cold KRB, solubilised in 1% (w/v) Triton X-100 solution and bile acid activity was measured in the cell lysate (see below). Concentration-dependence of bile acid uptake was studied at a compound concentration range of 1–100 μM for 20 min at 37 °C and 4 °C. Active uptake of bile acid compounds was calculated as the difference between the fluorescence, after exposure to compounds **3–6** at 37 °C and 4 °C.

The fluorescence activity of the bile acids compounds was analysed in 24-well plates using an automated plate reader (FLUOstar Optima, BMG Labtech, Offenburg, Germany) at excitation and emission wavelengths of 485 and 520 nm, respectively. The samples were diluted with KRB, where appropriate. For standardization, the total protein amount of cell layers was determined by bicinchoninic acid (BCA) assay according to the manufacturer's instructions (Pierce, Thermo Scientific, Rockford, USA).

4.5. Uptake kinetics

The saturable uptake of the bile acid compounds was analysed by assuming Michaelis–Menten type carrier-mediated transport represented by the equation:

$$v = V_{max} \times (S)/[(K_m + (S)]$$

where (S) was [bile acid compound].

Half-saturation constant (K_m) and maximum uptake rates (V_{max}) of the bile acid compounds was calculated by this equation to the experimental profile of the uptake rate (v) versus the substrate concentration (S) using a non-linear least squares regression analysis program, WinNonlin (Pharsight, Mountain View, CA, USA).

4.6. Molecular modelling

The structures of DCA and its 3-α and -β NBD analogues were generated by in silico modification in MOE (Chemical Computing Group, Montreal, Canada) of cholic acid extracted from pdb code 2QO4[37] The bile acid models were energy minimised using Merck Molecular Force Field 94x (MMFF94x) interfaced to MOE with gradient 0.5. Then structures were further manipulated in MOE and the picture in Figure 6 generated using the programme PyMOL.

4.7. Statistical analysis

All uptake studies were performed in triplicate. Results were expressed as mean ± SD, were compared using one-way analysis of variance (ANOVA) followed by Student–Newman–Keuls post hoc test. P <0.05 was considered as significant.

Acknowledgments

This study has been funded in by the Irish Health Research Board (TRA/2007/11) and through a Strategic Research Cluster grant (07/SRC/B1154) under the National Development Plan co-funded by EU Structural Funds and Science Foundation Ireland.

References and notes

1. Payne, C. M.; Crowley-Skillicorn, C.; Bernstein, C.; Holubec, H.; Moyer, M. P.; Bernstein, H. *Nutr. Cancer* **2011**, *62*, 825.
2. Zhou, Y.; Doyen, R.; Lichtenberger, L. M. *Biochim. Biophys. Acta.* **2009**, *1788*, 507.
3. Amaral, J. D.; Viana, R. J.; Ramalho, R. M.; Steer, C. J.; Rodrigues, C. M. *J. Lipid Res.* **2009**, *50*, 1721.
4. Rodrigues, C. M.; Steer, C. J. *Expert Opin. Investig. Drugs.* **2001**, *10*, 1243.
5. Sola, S.; Aranha, M. M.; Steer, C. J.; Rodrigues, C. M. *Curr. Issues Mol. Biol.* **2007**, *9*, 123–138.
6. Byrne, A. M.; Foran, E.; Sharma, R.; Davies, A.; Mahon, C.; O'Sullivan, J.; O'Donoghue, D.; Kelleher, D.; Long, A. *Carcinogenesis* **2010**, *31*, 737.
7. Hofmann, A. F. *Arch. Intern. Med.* **1999**, *159*, 2647.
8. Hofmann, A. F.; Hagey, L. R. *Cell Mol. Life Sci.* **2008**, *65*, 2461.
9. Sharma, R.; Long, A.; Gilmer, J. F. *Curr. Med. Chem.* **2011**, *18*, 4029.
10. Sharma, R.; Majer, F.; Peta, V. K.; Wang, J.; Keaveney, R.; Kelleher, D.; Long, A.; Gilmer, J. F. *Bioorg. Med. Chem.* **2010**, *18*, 6886.
11. Ghosh, P. B.; Whitehouse, M. W. *Biochem. J.* **1968**, *108*, 155.
12. Schramm, U.; Dietrich, A.; Schneider, S.; Buscher, H. P.; Gerok, W.; Kurz, G. *J. Lipid Res.* **1991**, *32*, 1769.
13. Schneider, S.; Schramm, U.; Schreyer, A.; Buscher, H. P.; Gerok, W.; Kurz, G. *J. Lipid Res.* **1991**, *32*, 1755.
14. Schramm, U.; Fricker, G.; Buscher, H. P.; Gerok, W.; Kurz, G. *J. Lipid Res.* **1993**, *34*, 741.
15. Rohacova, J.; Marin, M. L.; Martinez-Romero, A.; Diaz, L.; O'Connor, J. E.; Gomez-Lechon, M. J.; Donato, M. T.; Castell, J. V.; Miranda, M. A. *ChemMedChem* **2009**, *4*, 466.
16. Yamaguchi, H.; Okada, M.; Akitaya, S.; Ohara, H.; Mikkaichi, T.; Ishikawa, H.; Sato, M.; Matsuura, M.; Saga, T.; Unno, M.; Abe, T.; Mano, N.; Hishinuma, T.; Goto, J. *J. Lipid Res.* **2006**, *47*, 1196.
17. Holzinger, F.; Schteingart, C. D.; Ton-Nu, H. T.; Eming, S. A.; Monte, M. J.; Hagey, L. R.; Hofmann, A. F. *Hepatology* **1997**, *26*, 1263.
18. Sola, S.; Amaral, J. D.; Castro, R. E.; Ramalho, R. M.; Borralho, P. M.; Kren, B. T.; Tanaka, H.; Steer, C. J.; Rodrigues, C. M. *Hepatology* **2005**, *42*, 925.

Author's personal copy

19. Sola, S.; Castro, R. E.; Kren, B. T.; Steer, C. J.; Rodrigues, C. M. *Biochemistry* **2004**, *43*, 8429.
20. Assfalg, M.; Gianolio, E.; Zanzoni, S.; Tomaselli, S.; Russo, V. L.; Cabella, C.; Ragona, L.; Aime, S.; Molinari, H. *J. Med. Chem.* **2007**, *50*, 5257.
21. Zheng, X.; Ekins, S.; Raufman, J. P.; Polli, J. E. *Mol. Pharm.* **2009**, *6*, 1591.
22. Hu, N. J.; Iwata, S.; Cameron, A. D.; Drew, D. *Nature* **2011**, *478*, 408.
23. Balakrishnan, A.; Polli, J. E. *Mol. Pharm.* **2006**, *3*, 223.
24. Endter, S.; Francombe, D.; Ehrhardt, C.; Gumbleton, M. *J. Pharm. Pharmacol.* **2009**, *61*, 583.
25. Alrefai, W. A.; Sarwar, Z.; Tyagi, S.; Saksena, S.; Dudeja, P. K.; Gill, R. K. *Am. J. Physiol. Gastrointest. Liver Physiol.* **2005**, *288*, G978.
26. Geyer, J.; Wilke, T.; Petzinger, E. *Naunyn. Schmiedebergs Arch. Pharmacol.* **2006**, *372*, 413.
27. Swaan, P. W.; Hillgren, K. M.; Szoka, F. C., Jr.; Oie, S. *Bioconjug. Chem.* **1997**, *8*, 520.
28. Klaassen, C. D.; Aleksunes, L. M. *Pharmacol. Rev.* **2010**, *62*, 1.
29. Hagenbuch, B.; Gui, C. *Xenobiotica* **2008**, *38*, 778.
30. Hilgendorf, C.; Ahlin, G.; Seithel, A.; Artursson, P.; Ungell, A. L.; Karlsson, J. *Drug Metab. Dispos.* **2007**, *35*, 1333.
31. Sai, Y.; Kaneko, Y.; Ito, S.; Mitsuoka, K.; Kato, Y.; Tamai, I.; Artursson, P.; Tsuji, A. *Drug Metab. Dispos.* **2006**, *34*, 1423.
32. Balakrishnan, A.; Wring, S. A.; Polli, J. E. *Pharm. Res.* **2006**, *23*, 1451.
33. Ming, X.; Knight, B. M.; Thakker, D. R. *Mol. Pharm.* **2011**, *8*, 1677.
34. Tamai, I.; Nezu, J.; Uchino, H.; Sai, Y.; Oku, A.; Shimane, M.; Tsuji, A. *Biochem Biophys. Res. Commun.* **2000**, *273*, 251.
35. Nozawa, T.; Kobayashi, D.; Imai, K.; Nezu, J.; Tsuji, A.; Tamai, I. *J. Pharmacol. Exp. Ther.* **2003**, *306*, 703.
36. Rohacova, J.; Marin, M. L.; Martinez-Romero, A.; O'Connor, J. E.; Gomez-Lechon, M. J.; Donato, M. T.; Castell, J. V.; Miranda, M. A. *Org. Biomol. Chem.* **2009**, *7*, 4973.
37. Capaldi, S.; Guariento, M.; Saccomani, G.; Fessas, D.; Perduca, M.; Monaco, H. L. *J. Biol. Chem.* **2007**, *282*, 31008.